


# ASSESSMENT OF ENVIRONMENTAL FACTOR EFFECTS ON FATIGUE AND HEALING PERFORMANCE OF ASPHALT MIXTURES

*by*

**Ahmed Ibrahim Ahmed Aljubory**

**Thesis submitted to the University of Nottingham for the degree of Doctor of Philosophy**

**Department of Civil Engineering**

**Nottingham Transportation Engineering Centre (NTEC)**

**September 2018**

*Dedicated To My*

# *Wife*

# *Daughters*

# *and*

# *Son*

## Abstract

Oxidative ageing and moisture damage can be an example of time-dependent environmental conditions affecting the durability of bituminous mixtures simultaneously. Ageing may excessively increase the stiffness modulus and moisture damage may excessively decrease it causing different types of distresses such as cracking and rutting. Consequently, this thesis set out to investigate and understand the individual and combined effects of moisture damage and/or ageing on fatigue and healing performance of asphalt mixtures.

The experimental programme to achieve this aim was applied to asphalt mixtures exposed to moisture conditioning and/or ageing as following:
Part One: Measuring the indirect tensile stiffness modulus (ITSM) and dynamic complex modulus $|E^*|$ using the Nottingham Asphalt Tester (NAT) and Four-Point Bending (4-PB) machine respectively. The Ageing Index (AI), Index of Retained Stiffness Modulus (IRSM), and $|E^*|_{index}$ were determined to assess the effect of these environmental conditions. Part Two: Characterising the fatigue behaviour using the 4-PB test and the developed indirect tensile fatigue test (ITFT) in the constant strain method. The traditional approach ($N_{f50}$), ASTM D-7460 method, and Arizona State University (ASU) method were applied to analyse these fatigue testing results. Part Three: Assessing the healing performance using the ITFT and 4-PB test. The Healing Index (HI) and Healing Ratio (HR) were determined to evaluate the effect of rest periods.

Limestone aggregate from Tunstead quarry was used in a continuously graded dense bitumen macadam (DBM) asphalt mixture. Different air voids content, testing temperatures, binder penetration grades, binder content and time of loading were also investigated. In addition, the British Board of Agrément (BBA-Thin Surfacing: A.2) and BS EN 12697-12: 2008 procedures were individually used to induce the moisture damage in asphalt mixtures. AASHTO P-2002 was also used for simulating the short and long-term oven ageing (STOA and LTOA).

The results of IRSM and $|E^*|_{index}$ indicated that no significant moisture damage issue has arisen from using both water sensitivity methods, even when the moisture conditioning was applied to specimens after ageing. Limestone

aggregate may play the important role in these results as a non-susceptible aggregate to moisture damage.

In addition, the results of modified ITFT showed a general behaviour that, the stiffer the asphalt mixture the better the fatigue performance. This stiffening might motivate the elastic properties of the bitumen to dominate and increase the ability of asphalt mixtures to recover their original shape during the 0.4-second rest period following the 0.1-second load application. Therefore this might generally result in a longer fatigue life. It was also found by using the 4-PB test that moisture conditioning and ageing reduced slightly the fatigue life of asphalt mixtures. However, both have less effect at 10 than at 20°C. The fatigue life of aged mixtures has improved at 10 and 20°C when aged asphalt mixtures have been exposed to moisture conditioning. This conditioning could increase the flexibility of aged specimens and the increased flexibility might increase the fatigue life.

Furthermore, it was possible to apply uniform and non-uniform rest periods between the repeated loadings by means of 4-PB and ITFT. The modified ITFT showed an increase in the number of cycles to failure due to applying random rest periods regardless of mixture circumstances. Additionally, the moisture conditioning of control mixtures had less effect on the potential of damage recovery than ageing and ageing combined with moisture as determined by the 4-PB healing tests. Moisture conditioning could increase the flexibility of control mixtures and this flexibility might contribute to more recovery. Healing tests of 100 loading cycles (10 seconds) followed by 100 rest cycles (10 seconds) induced a slight damage and therefore showed the best healing indices at all circumstances. It may indicate that the less the fatigue damage, the greater the opportunity to heal the cracking during the applied rest periods.

A statistical model was developed based on the ITFT results to predict the number of cycles to failure by incorporating the combined effects of ageing and moisture conditions applied to asphalt mixtures of different parameters.

Finally, it is recommended as a future work to assess the combined influence of moisture damage and ageing using different types of aggregate.

## Acknowledgment

First and foremost, all praise and glory are due to "ALLAH" the Almighty, who gave me the opportunity, the health, the patience and the power to accomplish this research.

I wish to extend my appreciation, gratitude and sincere thanks to Professor Gordon Airey, the main supervisor of this study, for his guidance, continuous support, sound advice, kind help and endless encouragement throughout the period of this research. Further, I would like to extend my thanks to my co-supervisor Dr James Grenfell, for his trust, invaluable assistance, advice and guidance. Their knowledge and experience in this field encouraged me to do my best.

I would like to acknowledge and extend my sincere thanks to Mr Andrew Dawson for reviewing my thesis and his valuable insights during the course of this work.

I also acknowledge the tremendous help and advice from Dr Cinzia Maggiore, senior asset management consultant at Jacobs and from Dr Cocurullo Andrea, former research fellow at Nottingham Transportation Engineering Centre.

Special thanks also go to all technicians in the laboratory of Nottingham Transportation Engineering Centre, Richard, Martyn, Jon, Lawrence, Laura, Matthew, and Antony for providing necessary laboratory services and creating an efficient work environment.

I owe my loving thanks to my wife, Rasha, my daughters; Reem and Yasmeen, and my little boy, Ayoub for their love, patience, encourage and support. My loving thanks are due to my mother, her supplication and moral encouragement made things easier. Many thanks are due to my brothers, my sister, and my wife's family for their loving support.

My warm thanks are due to the best friend, Hamid Alacash, for his kind and sincere helps throughout the research period. Further, I would like to express my sincere thanks to Ahmed Nassar for his continual encouragement and honest

friendships over the years of the study. Special thanks go to the current and former colleagues, researchers, and staff at Nottingham Transportation Engineering Centre (NTEC) with whom I shared my enjoyable moments and experiences.

My sincere thanks are due to the Ministry of Higher Education and Scientific Research/Republic of Iraq, Mustansiriya University at Baghdad and Iraqi Cultural Attaché at London for awarding me a scholarship to study in the UK, their financial support is highly appreciated.

Finally, thank you very much for all of you and for all the others who I did not mention.

*Ahmed Aljubory*
*September 2018*

## Declaration

I declare that the contents and the work described in this thesis were performed at the University of Nottingham, Faculty of Engineering from August 2014 to September 2018. I hereby certify that this thesis is my own and has not been submitted in whole or in part to any other university or any other educational association for a higher degree.

**Ahmed Ibrahim Ahmed Aljubory**
**Nottingham, 2018**

We declare that the contents and the work described in this thesis were performed at the University of Nottingham, Faculty of Engineering from August 2014 to September 2018 under our supervision.

**Gordon Airey**
Professor of Pavement Engineering Materials, and Director of the Nottingham Transportation Engineering Centre (NTEC), Faculty of Engineering

**Dr James Grenfell**
Research Officer at Nottingham Transportation Engineering Centre (NTEC), Faculty of Engineering

## List of Contents

Abstract ..... I
Acknowledgment ..... III
Declaration ..... V
List of Contents ..... VI
List of Figures ..... XII
List of Tables ..... XXII
Chapter One: Introduction ..... 1
1.1 Background ..... 1
1.2 Fatigue behaviour of asphalt concrete pavement ..... 4
1.3 Fatigue failure criteria and analysis methods ..... 6
1.4 Problem statement ..... 7
1.5 Objectives of study ..... 9
1.6 Scope of study ..... 10
Chapter Two: Review of Literature ..... 12
2.1 Fatigue phenomenon of asphalt pavement structures ..... 12
2.2 Fundamental approaches of fatigue behaviour ..... 17
2.2.1 Phenomenological approach ..... 17
2.2.2 The fracture mechanics approach ..... 22
2.2.3 Dissipated energy approach ..... 24
2.3 Laboratory fatigue testing methods ..... 25
2.3.1 Flexural fatigue tests ..... 27
2.3.2 Direct tension test ..... 28
2.3.3 Tension/compression test ..... 29
2.3.4 Diametral test ..... 29
2.3.5 Triaxial test ..... 30
2.3.6 Wheel-tracking test ..... 31
2.4 Healing phenomenon in asphalt mixtures ..... 32

2.5 Factors affecting fatigue performance of asphalt paving mixtures ..... 34
2.5.1 Rest period ..... 34
2.5.2 Binder content ..... 39
2.5.3 Binder type and hardness ..... 41
2.5.4 Air voids content ..... 42
2.5.5 Compaction efforts ..... 42
2.5.6 Environmental conditions ..... 43
2.5.6.1 Moisture ..... 44
2.5.6.2 Ageing ..... 45
2.5.6.3 Temperature ..... 47
2.6 Summary ..... 49
Chapter Three: Materials and Testing Methodology ..... 50
3.1 Introduction ..... 50
3.2 Materials ..... 50
3.2.1 Bitumen ..... 50
3.2.2 Aggregate ..... 50
3.3 Fabrication of test specimens ..... 51
3.3.1 Mixing and compaction ..... 51
3.3.2 Cutting and trimming of test specimens ..... 51
3.3.3 Volumetric properties ..... 52
3.3.4 Storage ..... 53
3.4 Preparation of testing conditions ..... 54
3.4.1 Ageing conditions ..... 55
3.4.2 Short-term oven ageing (STOA) ..... 55
3.4.3 Long-term oven ageing (LTOA) ..... 56
3.4.4 Moisture conditioning ..... 59
3.5 Testing methods ..... 63
3.5.1 Main tests ..... 63

3.5.2 Supplementary tests ..... 63
Chapter Four: Evaluation of Environmental Effects on Stiffness Modulus of Asphalt Mixtures ..... 65
4.1 Introduction ..... 65
4.2 Plan of Chapter Four ..... 66
4.3 Testing methods ..... 67
4.3.1 Indirect Tensile Stiffness Modulus Test (ITSM) ..... 67
4.3.1.1 Test description ..... 67
4.3.2 Fourier Transform Infrared Spectroscopy (FTIR) ..... 69
4.4. Investigated variables ..... 71
4.5 ITSM results ..... 73
4.5.1 Effect of air voids content and testing temperature on ageing ..... 73
4.5.2 Effect of binder grades on ageing ..... 78
4.5.3 Effect of binder contents on ageing ..... 84
4.6 Individual and combined effects of moisture and ageing ..... 87
4.7 Index of Retained Stiffness Modulus (IRSM) results ..... 89
4.7.1 Effect of testing temperatures on IRSM ..... 89
4.7.2 Effect of binder grades on IRSM ..... 91
4.7.3 Effect of binder contents on IRSM ..... 100
4.8 Summary ..... 101
Chapter Five: Evaluation of Physical and Rheological Properties of Neat and Recovered Binders ..... 105
5.1 Introduction ..... 105
5.2 Bitumen recovery method ..... 105
5.3 Rheological properties ..... 107
5.3.1 Dynamic Shear Rheometer (DSR) ..... 107
5.3.2 Master curve for complex shear modulus and Phase angle ..... 110
5.3.3 Dynamic Mechanical Analysis (DMA) ..... 111
5.3.4 Shear Complex Modulus Index (SCMI) ..... 117

5.4 Physical properties ..... 121
5.4.1 Penetration test ..... 121
5.4.2 Ring and Ball Softening Point test ..... 121
5.5 Summary ..... 123
Chapter Six: Evaluation of Environmental Effects on Dynamic Modulus of Asphalt Mixtures ..... 125
6.1 Introduction ..... 125
6.2 Complex Modulus Test |E*| ..... 126
6.3 Master curve for the complex modulus |E*| and Phase angles δ (°) ... 132
6.4 Discussion of complex modulus |E*| and Phase angles δ (°) results ... 132
6.5 Summary ..... 144
Chapter Seven: Evaluation of Environmental Factor Effects on Fatigue Performance of Asphalt Mixtures using the Modified ITFT ..... 145
7.1 Introduction ..... 145
7.2 Calculation of maximum tensile strain ($\varepsilon_0$) ..... 146
7.3 ITFT in controlled strain method ..... 149
7.4 Investigated mixture parameters and testing conditions ..... 155
7.5 Possible fatigue analysis methods for ITFT ..... 157
7.5.1 The phenomenological approach ($N_{f50}$) ..... 157
7.5.2 Hysteresis loop distortion ..... 157
7.5.3 Rowe and ASU methods ..... 163
7.6 Results of ITFT in constant strain method ..... 172
7.6.1 Effect of air voids ..... 173
7.6.2 Effect of testing temperatures ..... 178
7.6.3 Effect of binder grades ..... 182
7.6.4 Effect of binder content ..... 187
7.7 Effect of individual and combined environmental factors effect ..... 190
7.8 Statistical Model ..... 205
7.9 Summary ..... 212

Chapter Eight: Evaluation of Environmental Factor Effects on Fatigue Performance of Asphalt Mixtures using the Four-Point Bending Test ..... 215
8.1 Introduction ..... 215
8.2 Four-point bending (4-PB) test ..... 216
8.3 Assessment of fatigue failure point ..... 219
8.4 Test results ..... 221
8.4.1 Effect of air voids content ..... 221
8.4.2 Effect of testing temperature ..... 223
8.4.3 Effect of moisture conditioning ..... 226
8.4.4 Effect of ageing ..... 230
8.4.5 Combined effect of ageing and moisture conditioning ..... 233
8.5 Effect of fatigue analysis methods ..... 235
8.6 Effect of binder penetration grades ..... 238
8.7 Effect of fatigue testing method ..... 238
8.8 Summary ..... 241
Chapter Nine: Evaluation of Environmental Factor Effects on Healing Susceptibility of Asphalt Mixtures using the 4-PB Test and ITFT ..... 243
9.1 Introduction ..... 243
9.2 Healing tests ..... 244
9.3 Healing tests using the 4-PB machine ..... 245
9.3.1 Results of healing tests using the 4-PB machine ..... 248
9.4 Healing tests using the modified ITFT ..... 262
9.4.1 Results of healing tests using the modified ITFT ..... 264
9.5 Summary ..... 269
Chapter Ten: Summary of Ageing and Moisture Damage Indices ..... 271
10.1 Introduction ..... 271
10.2 Effect of ageing ..... 271
10.2.1 ITSM results ..... 271
10.2.2 $|E^*|$ results ..... 272

10.3 Effect of Moisture ..... 275
10.3.1 ITSM results ..... 275
10.3.2 |E*| results ..... 276
10.4 Combined effect of ageing and moisture conditioning..... 279
10.4.1 ITSM results ..... 279
10.4.2 |E*| results ..... 279
Chapter Eleven: Conclusions and Recommendations for Future Works ..... 284
11.1 Summary ..... 284
11.2 Conclusions ..... 285
11.2.1 Effect of moisture conditioning and ageing on stiffness moduli . 285
11.2.2 Effect of moisture conditioning and ageing on fatigue failure .... 286
11.2.3 Effect of moisture conditioning and ageing on healing potential 287
11.3 Further work..... 288
11.3.1 In terms of mixtures variables..... 288
11.3.2 In terms of testing conditions..... 288
11.3.3 In terms of rest periods..... 288
11.3.4 In terms of testing methods..... 289
11.3.5 In terms of analysis methods ..... 289
11.4 Implications for future practice ..... 290
11.4.1 Implications for laboratory practice..... 290
11.4.2 Implications regarding in-site behaviour ..... 291
References ..... 292
Appendix..... A-1
A-1: Sample of hysteresis loops progress of ITFT. ..... A-1
A-2: Calculations of Chi-Square Goodness-of-Fit Test..... A-4
A-3: Testing profile for |E*| test using the 4-PB machine. .....A-12
A-4: Testing profile for healing test using the 4-PB machine. .....A-13

## List of Figures

Figure 1.1: Crack pattern developed with deflectometer flexural fatigue tester, (Jimenez, 1972).....3

Figure 1.2: Fatigue cracking (www.pavementinteractive.org).....3

Figure 1.3: Fatigue cracking showing the beginning of a pothole (www.pavementinteractive.org).....4

Figure 1.4: Schematic of fatigue cracking mechanism (Priest and Timm, 2006).....4

Figure 1.5: Diagrammatic illustration of Ni + Np (Lytton et al., 1993).....6

Figure 1.6: Failure criteria in controlled stress and controlled strain fatigue tests (Baburamani, 1999).....7

Figure 1.7: Outline of Thesis.....11

Figure 2.1: Tensile strain in asphalt layer caused by moving wheel .....13

Figure 2.2: S-N relationship (www.pavementinteractive.org).....13

Figure 2.3: Bottom-up cracking: .....16

Figure 2.4: Top-down cracking: (a) Field observation in the pavement (b) Field core drilled from the crack (www.pavementinteractive.org).....16

Figure 2.5: (S-N) method - relation between fatigue life (Nf) and applied stress (σt) or strain (εt).....18

Figure 2.6: Modulus variation during a fatigue test. (Estimation of asphalt concrete fatigue curves – A damage theory approach).....23

Figure 2.7: A stress-strain hysteresis loop (one loading cycle), controlled-strain testing (Shen and Carpenter, 2007).....24

Figure 2.8: Commonly used fatigue test arrangements (Zeiada, 2012).....26

Figure 2.9: Rest times between vehicle's axles passing over the pavement (Zeiada, 2012).....34

Figure 2.10: Fatigue tests (a) Discontinuous loading and (b) Intermittent loading (Zeiada, 2012).....35

Figure 3.1: Gradation curve for 14mm DBM mixtures. ..... 51
Figure 3.2: Mixing, compacting, and sawing or coring for prismatic beam or core specimens. ..... 53
Figure 3.3: Coring and trimming procedure for ITSM and ITFT tests. ..... 54
Figure 3.4: Sawing and trimming procedure for 4PB tests. ..... 54
Figure 3.5: Short Term Oven Ageing (STOA) of loose mixture at 135˚C..... 56
Figure 3.6: Cages for core specimens. ..... 57
Figure 3.7: Cages for prismatic beam specimens..... 57
Figure 3.8: LTOA for compacted core specimens at 85˚C for 120 hours. ..... 58
Figure 3.9: LTOA for compacted beam specimens at 85˚C for 120 hours. ..... 58
Figure 3.10: Applied vacuum to core specimens..... 61
Figure 3.11: Applied vacuum to prismatic beam specimens. ..... 61
Figure 3.12: Flow chart of testing methodology..... 64

Figure 4.1: Indirect Tensile Stiffness Modulus Test (ITSM). ..... 69
Figure 4.2: Example of FTIR absorbance spectrum for an aged binder sample (Hofko et al., 2018)..... 71
Figure 4.3: Effect testing temperature and air voids content on ITSM of 14mm DBM manufactured with 40/60 Pen and 5% binder content. ..... 75
Figure 4.4: FTIR absorbance graph..... 76
Figure 4.5: Effect of testing temperature and air voids content on the Ageing Index of 14mm DBM manufactured with 40/60 Pen and 5% binder content. ..... 78
Figure 4.6: Effect of binder grades on ITSM of 14mm DBM at 10˚C and different air voids content. ..... 79
Figure 4.7: Effect of binder grades on ITSM of 14mm DBM at 20˚C and different air voids content. ..... 80
Figure 4.8: Effect of binder grades on the Ageing Index ($ITSM_{LTOA}/ITSM_{STOA}$) of 14mm DBM at different testing temperatures and air voids content. ..... 82

Figure 4.9: FTIR absorbance graph shows the effect of binder grades on ageing in terms of sulfoxide (S=O) and carbonyl (C=O) components at wave numbers; 1030 and 1700 respectively. ..... 83

Figure 4.10: Effect of binder grades on the increment of carbonyl component. ..... 84

Figure 4.11: Effect of binder contents on ITSM of 14mm DBM at 10˚C. ..... 85

Figure 4.12: Effect of binder contents on ITSM of 14mm DBM at 20˚C. ..... 85

Figure 4.13: Effect of binder contents on the Ageing Index of 14mm DBM at different testing temperatures and air voids content. ..... 86

Figure 4.14: IRSM of 14mm DBM with 40/60 Pen using BS EN method. ..... 90

Figure 4.15: IRSM of 14mm DBM with 40/60 Pen using BBA method. ..... 91

Figure 4.16: IRSM of control 14mm DBM with different binder grades (Individual effect of moisture damage). ..... 94

Figure 4.17: IRSM of LTOA 14mm DBM with different binder grades (combined effect of moisture and ageing). ..... 94

Figure 4.18: IRSM 14mm DBM with different binder grades (Individual effect of moisture damage). ..... 95

Figure 4.19: IRSM of LTOA 14mm DBM with different binder grades (combined effect of moisture and ageing). ..... 95

Figure 4.20: FTIR absorbance graph of asphalt binders recovered from mixtures of 40/60 Pen exposed to ageing and/or moisture damage. ..... 97

Figure 4.21: FTIR absorbance graph of asphalt binders recovered from mixtures of 100/150 Pen exposed to ageing and/or moisture damage. ..... 98

Figure 4.22: Effect of ageing and/or moisture damage on the increment of carbonyl component of asphalt binders recovered from mixtures of 40/60 Pen. ..... 99

Figure 4.23: Effect of ageing and moisture damage on the increment of carbonyl component of asphalt binders recovered from mixtures of 100/150 Pen..... 99

Figure 4.24: IRSM of 14mm DBM with different binder contents..... 100

Figure 5.1: CVO - ADS Rheometer (AASHTO T-315). ..... 107
Figure 5.2: The DSR testing configuration (Subhy, 2017). ..... 108
Figure 5.3: Dynamic Shear Rheometer (DSR) apparatus and specimens set up. ..... 110
Figure 5.4: Master curves for the shear complex modulus ($G^*$) at 20˚C reference temperature (RT) - effect of ageing and moisture conditions. ..... 113
Figure 5.5: Master curves for phase angles (δ) at 20˚C reference temperature (RT) - effect of ageing and moisture conditions. ..... 114
Figure 5.6: Black diagram curves - effect of ageing and moisture conditions. ..... 116
Figure 5.7: Shear complex modulus index (SCMI) at 20˚C of recovered binders from mixtures manufactured with 40/60 Pen and 100/150 Pen and exposed to ageing and moisture conditions. ..... 118
Figure 5.8: Effect of ageing and moisture conditions on isochrones plot at 10Hz. ..... 119
Figure 5.9: Samples of WLF fitting of the shift factors aT for the production of master curves. ..... 120

Figure 6.1: Typical sinusoidal wave during the complex modulus test. ..... 127
Figure 6.2: Representation of complex modulus (Airey, 1997). ..... 128
Figure 6.3: Basic principles of 4- point bending (BS EN 12697-26: 2012). .. 130
Figure 6.4: Check test of the damage during the dynamic modulus. ..... 131
Figure 6.5: Master curves for $|E^*|$ at 20˚C reference temperature (RT) - effect of ageing and moisture conditions. ..... 134
Figure 6.6: Master curves for δ at reference temperature 20˚C (RT) - effect of ageing and moisture conditions. ..... 135
Figure 6.7: $|E^*|_{index}$ of mixtures manufactured with 40/60 Pen - effect of ageing and moisture conditions. ..... 136
Figure 6.8: $|E^*|$ index of mixtures manufactured with 100/150 Pen - effect of ageing and moisture conditions. ..... 137

Figure 6.9: Black diagrams at 20˚C reference temperature (RT) - effect of ageing and moisture conditions. ..... 140
Figure 6.10: Cole – Cole diagram - effect of ageing and moisture conditions. ..... 141
Figure 6.11: Isochrones plot for mixtures manufactured with 40/60 Pen - effect of ageing and moisture conditions. ..... 142
Figure 6.12: Isochrones plot for mixtures manufactured with 100/150 Pen - effect of ageing and moisture conditions. ..... 143

Figure 7.1: Initial strain calculation using ITFT EN 12697-24:2004. ..... 148
Figure 7.2: Calculation of strain amplitude according to EN 12697-26:2004. ..... 148
Figure 7.3: Initial strain (Resilient) calculation based on EN 12697-24:2012 – constant stress method. ..... 149
Figure 7.4: Set up of LVDTs in ITFT controlled strain method. ..... 151
Figure 7.5: A single pulse of ITFT in constant strain method. ..... 151
Figure 7.6: Inputs (red box) and outputs (green boxes) of modified ITFT software. ..... 152
Figure 7.7: Failure in strain control mode (at 40% of initial stiffness). ..... 152
Figure 7.8: Cracks at 50% of initial stiffness of wet asphalt mixture specimen of 10/20 Pen and 6.3% air voids content. ..... 153
Figure 7.9: Cracks at 50% of initial stiffness along the vertical plane of dry asphalt mixture specimen of 40/60 Pen and 12.7% air voids content. ..... 154
Figure 7.10: Fatigue life from constant stress and strain methods using ITFT. ..... 155
Figure 7.11: Stress-Strain Hysteresis Loop through the Progress of Fatigue Failure (Alkhateeb and Shenoy, 2004). ..... 158
Figure 7.12: Dissipated energy for a bending test and the ITFT (Maggiore, 2014). ..... 159
Figure 7.13: Calculation of Dissipated Energy (Maggiore, 2014). ..... 159

Figure 7.14: Sample of hysteresis loop for a single pulse in ITFT at cycle 50th – asphalt mixture specimen of 40/60 Pen. ..... 160

Figure 7. 15: Sample of hysteresis loop for a single pulse in ITFT at cycle 50th – asphalt mixture specimen of 100/150 Pen. ..... 160

Figure 7.16: Sample of hysteresis loop for a single pulse in ITFT at cycle 50th – asphalt mixture specimen of 10/20 Pen. ..... 161

Figure 7.17: Sample of hysteresis loops progress of ITFT at 400 με and 20˚C. ..... 162

Figure 7.18: The reduction of initial stiffness and HLI progress. ..... 163

Figure 7.19: Fatigue analysis method for ITFT of 40/60 Pen asphalt mixture..... 164

Figure 7.20: Fatigue analysis method for ITFT of 100/150 Pen asphalt mixture..... 164

Figure 7.21: Fatigue analysis methods for ITFT of 40/60 Pen asphalt mixture..... 166

Figure 7.22: Fatigue analysis methods for ITFT of 100/150 Pen asphalt mixture..... 166

Figure 7.23: Fatigue analysis methods for ITFT of 10/20 Pen asphalt mixture..... 167

Figure 7. 24: Original X-ray images (left) and Binary images of air voids (right). ..... 170

Figure 7.25: Air voids variation along the height of asphalt mixture specimen. ..... 171

Figure 7.26: Variation of stiffness modulus and air voids content in ITFT.... 171

Figure 7.27: Stiffness ratio vs. damage parameter from X-ray CT and ITFT. ..... 172

Figure 7.28: Effect of air voids content on fatigue characterisation at 10˚C. ..... 175

Figure 7.29: Effect of air voids content on fatigue characterisation at 20˚C. ..... 175

Figure 7.30: Effect of air voids content on fatigue characterisation at 20˚C. ..... 176

Figure 7.31: Effect of air voids content on fatigue characterisation at 20˚C. ..... 176
Figure 7.32: Effect of air voids content on fatigue characterisation at 20˚C. ..... 177
Figure 7.33: Effect of air voids content on fatigue characterisation at 20˚C. ..... 177
Figure 7.34: Effect of testing temperature on fatigue characterisation at 4% air voids content. ..... 179
Figure 7.35: Effect of testing temperature on fatigue characterisation at 8% air voids content. ..... 179
Figure 7.36: Effect of testing temperature on fatigue characterisation at 12% air voids content. ..... 180
Figure 7.37: Effect of testing temperature on fatigue characterisation of LTOA dry mixtures. ..... 180
Figure 7.38: Effect of testing temperature on fatigue characterisation of control wet mixtures. ..... 181
Figure 7.39: Effect of testing temperature on fatigue characterisation of LTOA wet mixtures. ..... 181
Figure 7.40: Effect of binder grades on fatigue characterisation in dry conditions. ..... 184
Figure 7.41: Effect of binder grades on fatigue characterisation in wet conditions. ..... 184
Figure 7.42: Effect of binder grades on fatigue characterisation in wet conditions. ..... 185
Figure 7.43: Effect of binder grades on fatigue characterisation in dry conditions. ..... 185
Figure 7.44: Effect of binder grades on fatigue characterisation of LTOA mixtures in wet conditions - BS EN method. ..... 186
Figure 7.45: Effect of binder grades on fatigue characterisation in wet conditions - BBA method. ..... 186
Figure 7.46: Effect of binder contents on fatigue characterisation in dry condition. ..... 188

Figure 7.47: Effect of binder contents on fatigue characterisation in wet conditions. ..... 188
Figure 7.48: Effect of binder contents on fatigue characterisation in dry condition. ..... 189
Figure 7.49: Effect of binder contents on fatigue characterisation in wet conditions. ..... 189
Figure 7.50: Effect of environmental factors on fatigue characterisation at 10˚C. ..... 192
Figure 7.51: Effect of environmental factors on fatigue characterisation at 20˚C. ..... 192
Figure 7. 52: Effect of environmental factors on fatigue characterisation at 20˚C. ..... 193
Figure 7. 53: Horizontal and vertical deformations of 40/60 Pen asphalt mixtures at different conditions. ..... 193
Figure 7.54: Effect of environmental factors on stiffness deterioration of 40/60 Pen asphalt mixtures. ..... 194
Figure 7. 55: Number of cycles to failure by traditional approach Nf50. ..... 196
Figure 7. 56: Number of cycles to failure by the ASU method. ..... 196
Figure 7. 57: Effect of environmental factors on fatigue characterisation at 20˚C. ..... 198
Figure 7. 58: Effect of environmental factors on fatigue characterisation at 20˚C. ..... 198
Figure 7.59: Effect of environmental factors on fatigue characterisation at 20˚C. ..... 199
Figure 7.60: Effect of environmental factors on fatigue characterisation at 20˚C. ..... 199
Figure 7.61: Effect of environmental factors on fatigue characterisation at 20˚C. ..... 200
Figure 7.62: Effect of environmental factors on fatigue characterisation at 20˚C. ..... 200
Figure 7.63: Determination of $\varepsilon 10^6$ from WÖHLER (or S-N) curve. ..... 201

Figure 7.64: Examples of scatter diagrams with different values of correlation coefficient (ρ). ..... 206
Figure 7.65: Number of cycles to failure ($N_f$) versus applied strain. ..... 206
Figure 7.66: Number of cycles to failure ($N_f$) versus stiffness modulus. ..... 207
Figure7.67: Number of cycles to failure ($N_f$) versus air voids content. ..... 207
Figure 7.68: Number of cycles to failure ($N_f$) versus testing temperatures. . 208
Figure 7.69: The predicted and observed number of cycles to failure ($N_f$). .. 212

Figure 8.1: Commonly used fatigue test arrangements (Thom, 2006). ..... 216
Figure 8.2: 4-PB equipment at the University of Nottingham (Maggiore, 2014). ..... 216
Figure 8.3: Samples of typical fatigue tests using the 4PB machine. ..... 218
Figure 8.4: Normalised complex modulus × cycles versus loading cycles (ASTM D7460-10). ..... 220
Figure 8.5: A comparison of phenomenological approach, Nf50 and Normalised complex modulus × cycles versus loading cycles. ..... 220
Figure 8.6: Effect of air voids content on fatigue life at 10°C – dry condition. ..... 222
Figure 8.7: Effect of air voids content on fatigue life at 20°C – dry condition. ..... 222
Figure 8.8: Effect testing temperature on fatigue life of dry control mixtures (6% air voids content). ..... 224
Figure 8.9: Effect of testing temperature on fatigue life of dry control mixtures (12% air voids content). ..... 224
Figure 8.10: Effect of testing temperature on fatigue life of immersed control mixtures (12% air voids content). ..... 225
Figure 8.11: Effect of testing temperature on fatigue life of dry aged mixtures (12% air voids content). ..... 225
Figure 8.12: Effect of testing temperature on fatigue life of wet aged mixtures (12% air voids content). ..... 226

Figure 8.13: Moisture conditioning effect on fatigue life of control mixture at 10°C. ..... 227
Figure 8.14: Moisture conditioning effect on fatigue life of control mixture at 20°C. ..... 227
Figure 8.15: Moisture conditioning effect on fatigue life of control mixture at 20°C – ASTM D 7460. ..... 228
Figure 8.16: Moisture conditioning effect on fatigue life of aged mixtures at 10°C. ..... 229
Figure 8.17: Moisture conditioning effect on fatigue life of aged mixtures at 20°C. ..... 229
Figure 8.18: Moisture conditioning effect on fatigue life of aged mixtures at 20°C. ..... 230
Figure 8.19: Ageing (LTOA) effect on fatigue life at 10°C. ..... 231
Figure 8.20: Ageing (LTOA) effect on fatigue life at 20°C. ..... 232
Figure 8.21: Ageing (LTOA) effect on fatigue life at 20°C – ASTM D 7460. .. 232
Figure 8.22: Combined effect of moisture and ageing on fatigue life at 10°C. ..... 234
Figure 8.23: Combined effect of moisture and ageing on fatigue life at 20°C. ..... 234
Figure 8.24: Combined effect of moisture and ageing on fatigue life at 20°C – ASTM D 7460. ..... 235
Figure 8.25: A comparison of phenomenological (Nf50) and ASTM D 7460 fatigue analysis methods. ..... 237
Figure 8.26: A comparison between 4PB and ITFT for dry control mixtures. ..... 239
Figure 8.27: A comparison between 4PB and ITFT for wet control mixtures. ..... 239
Figure 8.28: A comparison between 4PB and ITFT for dry aged mixtures. ... 240
Figure 8.29: A comparison between 4PB and ITFT for wet aged mixtures. .. 240

Figure 9.1: A typical curve of stiffness ratio versus application of loading cycles for tests with and without rest period (Mamlouk et al., 2012). ..... 244

Figure 9.2: Effect of short loading time on initial stiffness modulus. ..... 246

Figure 9.3: Test A versus test B of different air voids content mixtures. ..... 249

Figure 9.4: Test A versus test C of different air voids content mixtures. ..... 250

Figure 9.5: Test A versus test D of different air voids content mixtures. ..... 250

Figure 9.6: Effect of different loading and rest period times on healing ratio of control asphalt mixtures exposed to moisture conditioning. ..... 254

Figure 9.7: Effect of moisture conditioning and/or ageing on fatigue damage recovery using tests B versus A configurations. ..... 256

Figure 9.8: Effect of moisture conditioning on fatigue damage recovery using tests B versus A configurations. ..... 258

Figure 9.9: Samples of healing tests for combined conditions (aged and moisture conditioned asphalt mixtures) ..... 260

Figure 9.10: Examples of beam fatigue test results using haversine deflection-control with and without rest periods (Mamlouk et al., 2012). .... 261

Figure 9.11: Schematic of loading in stages; I, II, III of fatigue test (Soltani and Anderson, 2005). ..... 262

Figure 9.12: LVDT's setting in the healing test. ..... 264

Figure 9.13: Effect of random rest periods on stiffness degradations of unaged mixtures. ..... 267

Figure 9.14: Effect of random rest periods on stiffness degradations of LTOA mixtures. ..... 268

## List of Tables

Table 3.1: Testing conditions. ..... 62

Table 4.1: Summary of investigated variables. ..... 72

Table 4.2: Error bars of the average values of ITSM results (Five samples were tested to find the average) presented in Figure 4.3. ..... 75

Table 4.3: Errors of the average values of ITSM results presented in Figures 4.5 and 4.6. ..... 81

Table 4.4: Ageing Index for all tested parameters and conditions. ..... 86

Table 4.5: Summary of investigated mixture variables and conditions. ..... 88

Table 4.6: Summary of moisture damage results (IRSM results). ..... 101

Table 5.1: Details of recovered binders for DSR test. ..... 111

Table 5.2: Needle penetration test results and Ageing Index (AI). ..... 122

Table 5.3: Ring and Ball Softening Point temperatures and the Softening Point Increment (ΔS). ..... 123

Table 6.1: Key of basic principles of 4- point bending shown in Figure 5.3.. 130

Table 6.2: Summary of investigated mixture conditions for complex modulus tests. ..... 131

Table 7.1: Summary of the main investigated parameters (One specimen was used at each strain level to find the number of cycles to failure). ..... 156

Table 7.2: Results of test of significance (ANOVA test – single factor method) for the effect of air voids content on fatigue performance of asphalt mixtures. ..... 174

Table 7.3: Results of test of significance (ANOVA test – single factor method) for the effect of testing temperature on fatigue performance of asphalt mixtures. ..... 178

Table 7.4: Results of test of significance (ANOVA test – single factor method) for the effect of binder grades on fatigue performance of asphalt mixtures. ..... 183

Table 7.5: Number of cycles to failure of 40/60 Pen mixtures exposed to different testing conditions using $N_{f50}$ and the ASU methods with ANOVA test results. ..... 195

Table 7.6: Fatigue relationships for asphalt mixtures exposed to different testing conditions. ..... 203

Table 7.7: Fatigue parameters of asphalt mixture exposed to different testing conditions. ..... 204

Table 7.8: Spearman and Pearson correlation coefficients. ..... 209

Table 7.9: Effect of using different parameters on the change of $R^2$. ..... 209

Table 7.10: Chi-square goodness of fit test results. ..... 212

Table 8.1: Dimensions of prismatic beam specimens, BS EN 12697 24:2012..... 217

Table 8.2: Summary of investigated mixture conditions for fatigue test by 4PB (Two replicates were used to find the number of cycles to failure)..... 217

Table 8.3: Ageing Index..... 233

Table 8.4: A comparison of phenomenological ($N_{f50}$) and ASTM D 7460 fatigue analysis methods..... 237

Table 9.1: Summary of investigated mixture conditions for healing test by 4PB (One or two replicates were used to find HR and HI). ..... 247

Table 9.2: Summary of loading time and rest time combinations chosen for healing tests using the 4-PB machine. ..... 247

Table 9.3: Effect of air voids on HR and HI results..... 251

Table 9.4: Ranking of compound-loading test conditions of different loading and rest period times based on HR and HI..... 254

Table 9.5: A summary of healing test results. ..... 257

Table 9.6: Loading times and rest times (Maggiore, 2014). ..... 263

Table 9.7: HR and HI indices of healing test by ITFT..... 265

Table 9.8: Random number of loading cycles and random number of rest period cycles as resulted from the test..... 266

Table 10.1: Summary of Ageing Index (AI) results using the ITSM (The average of five replications was used to measure the ITSM). ..... 272

Table 10.2: Summary of Ageing Index ($|E^*|_{A\text{-index}}$) results using $|E^*|$ test (The average of two replications was used to measure $|E^*|$). ..... 274

Table 10.3: Summary of IRSM results using ITSM (The average of five replications was used to measure the ITSM). ..... 277

Table 10.4: Summary of $|E^*|_{MD\text{-}index}$ results using $|E^*|$ test (The average of two replications was used to measure $|E^*|$). ..... 278

Table 10.5: Summary of AI + IRSM results using ITSM (The average of five replications was used to measure the ITSM). ..... 281

Table 10.6: Summary of AI + IRSM results using $|E^*|$ test (The average of two replications was used to measure $|E^*|$). ..... 282

Table 10.7: Comparison between the individual effect of ageing and the combined effect of ageing and moisture. ..... 283

# Chapter One: Introduction

## 1.1 Background

An asphalt pavement is a multi-layered structure designed to withstand the in-place repetitions of different traffic loadings and prevailing environmental conditions. Asphalt pavements tend to deteriorate with time and traffic loadings because of the chemical composition and viscoelastic properties of asphalt binders utilised in manufacturing asphalt paving mixtures. This deterioration typically takes place in different types of distresses such as rutting, fatigue cracking, moisture damage, and low temperature cracking (Arambula and Kutay, 2009).

One of the principal distresses that affect flexible pavement structures is fatigue cracking which has a significant importance in the design and performance of asphalt roads (Baburamani, 1999, Di Benedetto et al., 2003, Miller and Bellinger, 2003). Fatigue cracking is a phenomenon which takes place in pavements due to repeated stresses or strains resulting from the repetitive applications of traffic loadings. The capability of asphalt mixtures to withstand these repetitive deflections is characterised as fatigue resistance. Fatigue cracking resistance is defined as the ability of these mixtures to resist the frequent traffic loadings under the prevailing environmental conditions without early failure being induced or substantial cracking (Baburamani, 1999, Maggiore, 2014).

The proper design of asphalt concrete pavements requires sufficient structural layers thicknesses and selecting the appropriate materials to ensure that repeated stresses or strains will not cause fatigue cracking. Since Hveem's investigation in 1955, the fatigue distress of asphalt pavements has had a great significance and considerable attention on this problem not only through field studies but also through laboratory studies have been undertaken by many agencies (Yu and Zou, 2013). Fatigue failure was evidenced by cracking as described by Hveem. Hveem found that a correlation between the observations of fatigue cracking and the measured repeated deflections that the pavement must experience with each passing wheel (Hveem, 1955). Hveem also reported the need for considering and evaluating flexural fatigue characteristics of

asphalt concrete mixtures. Figure 1.1 shows a sample of crack pattern developed with the deflectometer flexural fatigue tester designed later by Jimenez (Jimenez, 1972).

The initiation and propagation of fatigue cracking typically occurs in areas of the pavement exposed to repeated traffic loadings such as the wheel paths. In the beginning, fatigue cracking takes place as hairline cracks, which with additional traffic applications grow and interconnect developing patterns of alligator skin or chicken wire cracking forms shown in Figure 1.2. If these cracking are left without observation and maintenance, pieces of the affected pavement surface could detach under more traffic loadings and the distress progresses more into further detrimental circumstance such as potholes as shown in Figure 1.3 (Miller and Bellinger, 2003).

In theory, as a vehicle passes over a point within a pavement section, a tensile stress is generated at the bottom of the asphalt layer. If the resulting tensile stress exceeds the tensile capacity of the in-service material, damage and eventually fatigue cracking will occur. Moreover, when in-service materials are subjected to repeated load applications and different environmental conditions at a level which induces stresses generally exceeding the tensile strength capacity of these materials, these cracks will gradually propagate toward the surface of the pavement as shown in Figure 1.4 (Chiangmai, 2010).

Proper design should make sure that an in-service pavement structure endures during the whole design period as adequately fatigue-resistant material. Therefore the number of load applications at a specific stress or strain to which in-service pavement structural layer can experience before failure is characterised as the fatigue life. This life is affected by different parameters; first, properties of the mixture such as type and content of asphalt binder, air voids content, and aggregate grading and type. Second, testing conditions; temperature, mode of loadings, rate of loading (frequency), the applied stress or strain during the tests, the type of test method, and rest periods between repeated loadings (Monismith et al., 1994, Baburamani, 1999, Huang, 2007).

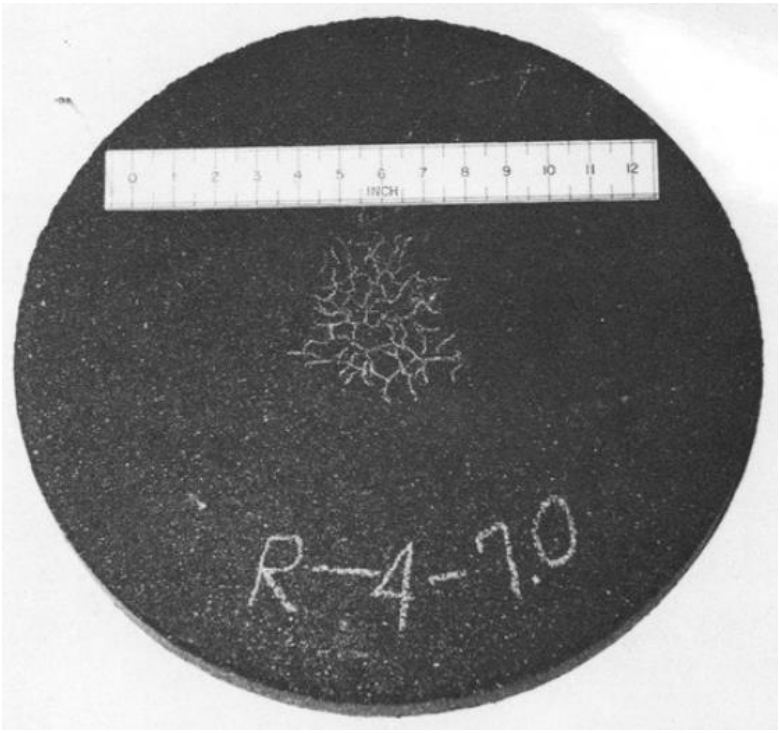



Figure 1.1: Crack pattern developed with deflectometer flexural fatigue tester, (Jimenez, 1972).



Figure 1.2: Fatigue cracking (www.pavementinteractive.org).



Figure 1.3: Fatigue cracking showing the beginning of a pothole (www.pavementinteractive.org).

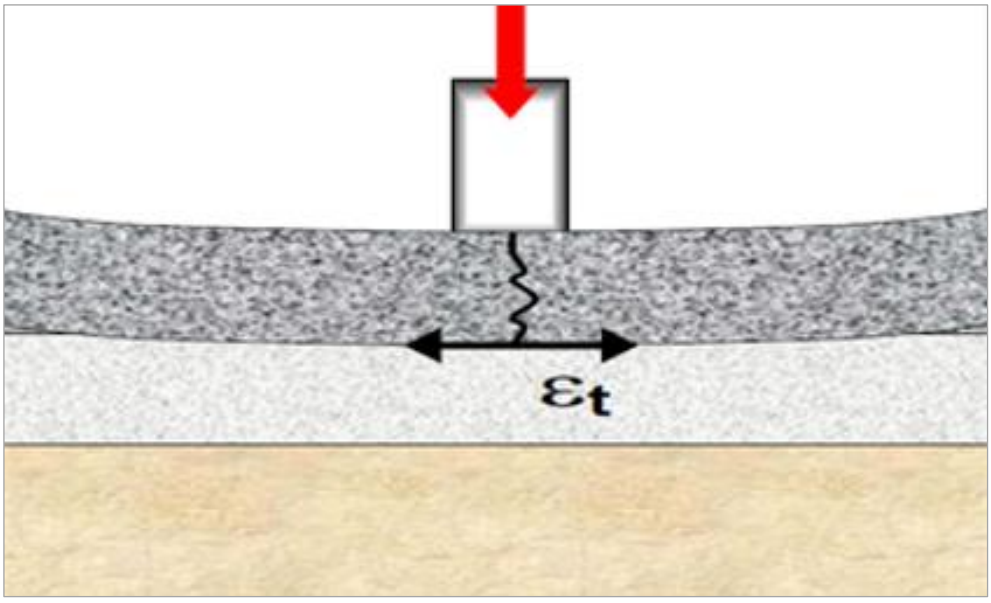



Figure 1.4: Schematic of fatigue cracking mechanism (Priest and Timm, 2006).

## 1.2 Fatigue behaviour of asphalt concrete pavement

The fatigue behaviour of asphalt concrete pavements has been studied for a number of decades to understand this complicated phenomenon. Recently, studies have been developed to improve the correlation of fatigue results to the real fatigue behaviour occurring in asphalt pavements. The major goal of these studies is to investigate and predict the fatigue behaviour of in-service pavements in an attempt to prevent this principal form of distress, which can induce more serious structural damage (Chiangmai, 2010).

The fatigue characterisation of asphalt mixtures is considered a fundamental component of asphalt pavement structural design and analysis to ensure adequate fatigue performance of the in-site pavement. Therefore it is important to take into account the complex nature of asphalt mixture. This mixture is a heterogeneous complex composite material of anisotropic behaviour consisting of air, binder and aggregate. It ages with time and heals during the rest periods between repetitive traffic applications (Walubita, 2006).

Fatigue of bituminous materials is recognised as a complex failure mechanism. This mechanism includes crack initiation and propagation, and crack healing. The fatigue failure can be described as an initiation of minor hairline cracks, followed by the development of these micro cracks into wider macroscopic cracks, which coalesce together to form a network of cracks. In the final stage these macroscopic cracks propagate through the thickness of the pavement inducing the loss of pavement structural integrity. In this circumstance, the cracked pavement has already induced a pothole as an example of the final stage of fatigue failure (Soenen et al., 2003). Consequently, the development and propagation of fatigue cracks inside a pavement structure can be categorised into two major phases: pre-localisation and post-localisation. In general, pre localisation is manifested by the initiation and propagation of micro-cracks, and post failure represents the formation and propagation of macro-cracks (Zhang et al., 2013).

Figure 1.5 simply illustrates that Ni, which is micro-crack initiation stage, is defined as the number of load applications required to initiate a tiny micro crack of 7.5 mm in length. While Np is associated with the propagation of the 7.5 mm micro-crack through the entire asphalt layer thickness. Furthermore, Figure 1.5 clearly illustrates why Np is a function of the entire layer thickness (d). Thus, to adequately characterise the fatigue resistance, both Ni and Np must be determined (Lytton et al., 1993). The fatigue life can be equal to the total of Ni and Np if the laboratory to field shift factors are not considered (Walubita et al., 2012).

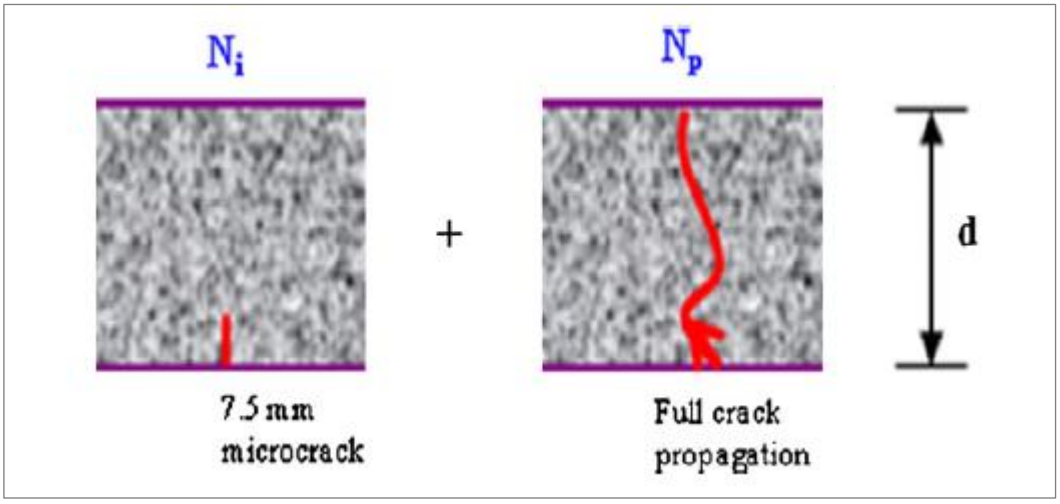



Figure 1.5: Diagrammatic illustration of Ni + Np (Lytton et al., 1993).

Huang et al., 2007 indicated that although the general theories of fatigue behaviour might be understood, experiments have failed to clarify how these theories could be used to make responsible and applicable quantitative predictions. In spite of recommended mathematical models for fatigue life prediction of asphalt mix such as Shell Model (Shell 1978), Asphalt Institute Model (Asphalt Institute 1981) and SHRP Model (SHRP 1994 a and b), these traditional models were found to either produce poor predictions or lack generality. In addition, these models associate the fatigue life with the modulus of asphalt mixtures which needs to be measured experimentally and therefore they are difficult to implement.

### 1.3 Fatigue failure criteria and analysis methods

Different fatigue criteria depend on the mode of loading used to determine the number of load cycles to failure from laboratory tests as shown in Figure 1.6. First, for a controlled-strain test, a specific percent reduction of initial stiffness can be specified to end the test. Second, for a controlled-stress test, either the specimen experiences a 100% increase in the strain compared to the initial strain to terminate the test or complete failure (fracture) of the specimen (Bhasin et al., 2009).

Historically, the traditional phenomenological approach has typically been used to predict the fatigue failure of asphalt paving mixtures (Monismith et al., 1994, Daniel et al., 2004, Ghuzlan and Carpenter, 2003). Moreover, Baburamani,

1999, Liang and Zhou, 1997, Ghuzlan and Carpenter, 2003 reported that the mechanistic approach based on fracture mechanics can also be used to investigate the fatigue failure of asphalt pavement structures and mixtures. In addition, many researchers applied different dissipated energy approaches as a fundamental method to describe the fatigue behaviour of asphalt mixtures (Van Dijk, 1975, Van Dijk and Visser, 1977, Hopman et al., 1989; Pronk and Hopman, 1990; Pronk, 1995, Rowe, 1993 and 1996, Shen and Carpenter, 2007).

Finally, it is agreed that a shift factor needs to be applied to the laboratory fatigue test results regardless the method used to predict the number of cycles to failure. This shift factor allows taking into consideration the effects of actual load distribution in the pavement structure, rest periods between repeated loadings, the lateral distribution of traffic loads, the variation of the in service pavement temperature, and oxidative ageing of binder (Soenen et al., 2003).

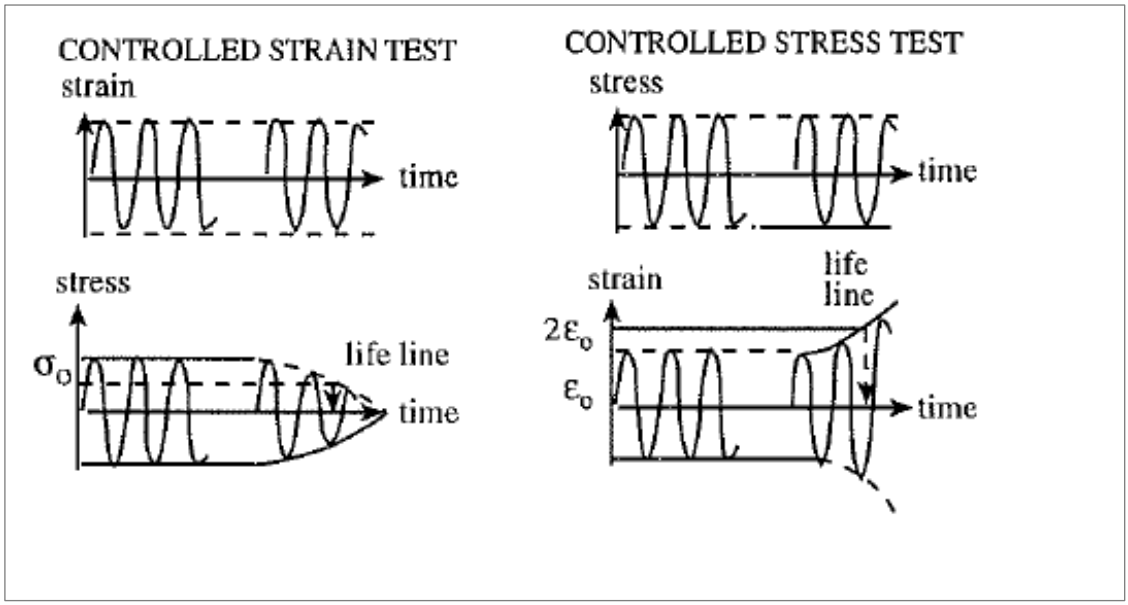



Figure 1.6: Failure criteria in controlled stress and controlled strain fatigue tests (Baburamani, 1999).

### 1.4 Problem statement

In fact, the pavement structure will be exposed to the influence of multiple parameters, which affects their performance simultaneously. These parameters include mixture variables, weather conditions, and types and rates of uniform and wander traffic loadings. Over time pavements deteriorate due to the

damaging effect of these conditions and variables and therefore they eventually require maintenance or rehabilitation.

Oxidative ageing and moisture damage are the time-dependent primary environmental factors affecting the durability of bituminous paving mixtures. Age hardening of the bituminous binder is manifested as an increase in the stiffness modulus contributing to serious pavement distresses such as fatigue and thermal cracking (Chen and Huang, 2000, Woo et al., 2008). At the same time, the pavement will be exposed to another destructive environmental factor, moisture damage. Moisture damage is generally identified as a loss of adhesion (stripping or adhesive failure) between the bitumen and aggregate interface and/or loss of cohesion (cohesive failure) in the asphalt mixture. Both mechanisms can lead to stiffness reduction of asphalt mixtures resulting in serious distresses of asphalt pavement such rutting and in turn the complete deterioration of pavement structure (Airey and Choi, 2002, Zaumanis et al., 2017).

Accordingly, the asphalt mixture will age and stiffen excessively due to oxidation but at the same time will become softer due to the detrimental effect of water. In combination with different repeated loadings and time of loadings, and temperature variations, the excessive stiffness increase due to ageing and the stiffness reduction due to moisture induced damage can lead to the complete deterioration of pavement structure.

Previous studies have not satisfactorily considered the combined effect of damaging environmental factors such as ageing and moisture damage which can simultaneously affect the structure of asphalt pavements. Few studies; Mehrara and Khodaii, 2015 and López and Miró, 2016 combined the effect of ageing and moisture damage on fatigue performance of asphalt mixtures. However, López and Miró, 2016 considered the effect of water in the standard condition. Mehrara and Khodaii, 2015 also investigated the effect of these factors on healing performance of these mixtures.

Consequently, it is seriously required to understand the combined influence of these time-dependent damaging environmental circumstances on the stiffness

modulus and in turn on the fatigue and healing susceptibility of asphalt mixtures. In particular, if they are combined with other important factors such as temperature variations, rate of loading, mixture parameters, and different testing methods.

### 1.5 Objectives of study

This study sets out to explore the fatigue and healing phenomenon of asphalt paving materials. In particular, the aim of this research project is to develop an understanding of the way in which the moisture damage and/or ageing affect the fatigue and healing performance of the asphalt mixture.

The research programme to achieve this aim has been divided into main and supplementary areas. First, the main area involves an extensive laboratory investigation of the influence of moisture damage and/or ageing on the stiffness modulus, fatigue characterisation and healing performance. In this part, the effects of important parameters which are supposed to be related to moisture damage and ageing such as air voids content, testing temperature, binder penetration grades, and time of loading (frequency) and in turn affect the stiffness modulus and fatigue performance are investigated. In fact, measuring the stiffness and complex moduli of asphalt mixtures are considered in this study for their influence on the fatigue resistance of these mixtures. Secondly, supplementary tests are used on the neat and recovered binders to investigate their physical and rheological properties before and after the exposure of asphalt mixtures to moisture damage and/or ageing.

The overall objectives of the project are to:

1. Evaluate the individual and combined influences of moisture damage and ageing on the stiffness and complex moduli of 14mm DBM (Dense Bitumen Macadam) asphalt mixtures using the Nottingham Asphalt Tester (NAT) and four-point bending (4-PB) machine respectively.
2. Characterise the fatigue behaviour of asphalt mixtures which are exposed to moisture damage and/or ageing in the presence of other parameters stated earlier using 4-PB test and the Indirect Tensile Fatigue Test (ITFT) in controlled strain method.

3. Assess the healing performance of asphalt mixtures which are exposed to moisture damage and/or ageing using the ITFT and 4-PB testing methods. These methods are used to insert uniform and non-uniform (or random) rest periods between different repeated loadings in order to observe the influence of the investigated environmental factors on the potential recovery of tested mixtures.
4. Examine the effect of the applied environmental conditions (moisture conditioning and ageing) on the different bitumen binders by comparison between the physical and rheological properties of binders recovered from mixtures which are exposed to moisture conditioning and/or ageing and those properties of neat binders.

## 1.6 Scope of study

The scope of this thesis consists of a literature review, a methodology chapter which is then followed by seven chapters focusing on the objectives of this study, and finally a chapter summarising the final conclusions and recommendations for future research works.

The literature review in Chapter Two summarises the main findings with regard to the fundamental approaches explaining fatigue cracking phenomenon of asphalt mixtures. Particular attention is also given to the main factors affecting this phenomenon. Chapter Three simply presents the methodology to achieve the testing programme of this research. The testing programme is divided in this research work into main and supplementary tests. Chapters Four to Nine display the main and supplementary testing results. Chapter Ten summarises the results of ageing and moisture damage indices. The main tests are also grouped into three parts, the first one is concerned with stiffness and dynamic moduli measurements by the NAT and 4PB machine and the results are presented in Chapters Four and Six respectively. The second group deals with two different fatigue testing methods, indirect tension (ITFT) and flexural (4PB). Chapter Seven and Eight display the discussion and results of both fatigue tests respectively. In the third part, the non-standard healing study is conducted by ITFT and 4PB test and Chapter Nine shows the discussion and findings of this part. Chapter Five summarises the results of supplementary tests in an attempt to understand better some unexplained results collected in Chapter Four.

Finally, the outline of this thesis is presented in Figure 1.7.

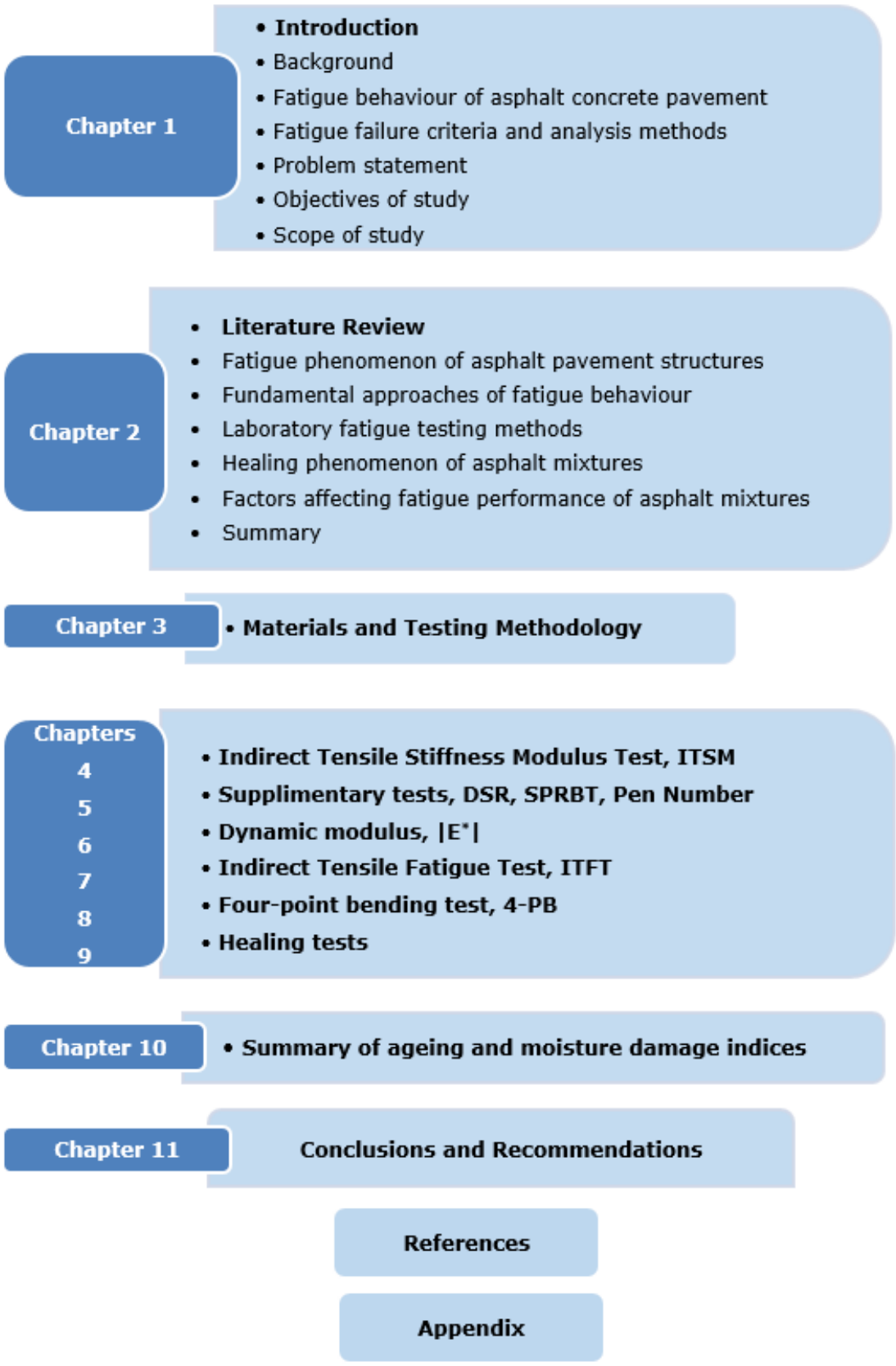



Figure 1.7: Outline of Thesis.

# Chapter Two: Review of Literature

The outline of this chapter is to review literature with regard to the fatigue and healing of asphalt paving materials which can contribute to more understanding of this phenomenon. This literature involves six sections; the first three parts describe the fatigue phenomenon, fundamental approaches of fatigue behaviour, and laboratory fatigue testing methods of asphalt paving mixtures. Further, section four discusses the healing phenomenon. The most important factors affecting fatigue and healing of asphalt mixtures; rest period, binder content, binder grade, air voids content, compaction efforts, and environmental factors; water, aging, and temperature, are discussed in section five. Finally, part six presents the summary.

## 2.1 Fatigue phenomenon of asphalt pavement structures

Asphalt pavement infrastructures provide important services to the public. Therefore, it is important to assess and maintain these infrastructures from any possible damages may adversely affect these critical services.

Fatigue cracking is one of the most important detrimental distresses affecting the performance of asphalt pavements. This phenomenon takes place in asphalt roads due to repeated strains or stresses resulting from the repetitive applications of traffic loadings as shown in Figure 2.1. Incidentally, fatigue characteristics are important not only to roadways but also to many other structures and machines. Wöhler, 1860 was the first researcher who investigated the characterisation of fatigue behaviour of steam engine axles under repeated loading by conducting a systematic rotating bending experiment. In Wöhler's study, the S-N relationship (The relationship between stress or strain and number of cycles to failure) shown in Figure 2.2 was established as the foundation for fatigue studies. Since then, it is recognised as the most widely used basic fatigue characteristic relationship and engineers continuously investigated the cyclic-load effects on the characterisation of fatigue behaviour. (Shen and Carpenter, 2007, Yamamoto, 2013). In addition, Ghuzlan and Carpenter, 2003 also indicated that Hveem was one of the former investigators who stated that fatigue failure resulted from repetitive loadings on asphalt pavements constructed over layers of considerably resilient soils.

Hveem concluded that there is a relationship between the repetitive deflections that result with each passing load on pavement from one side and crack observations and fatigue failures on the other side.

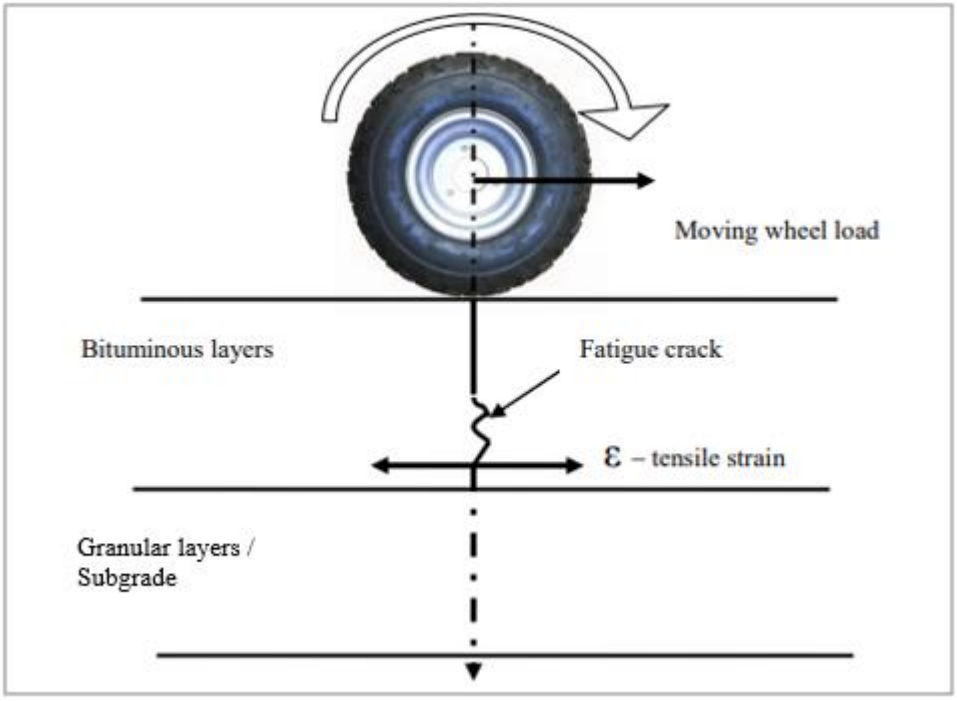



Figure 2.1: Tensile strain in asphalt layer caused by moving wheel (Vieira et al., 2012).

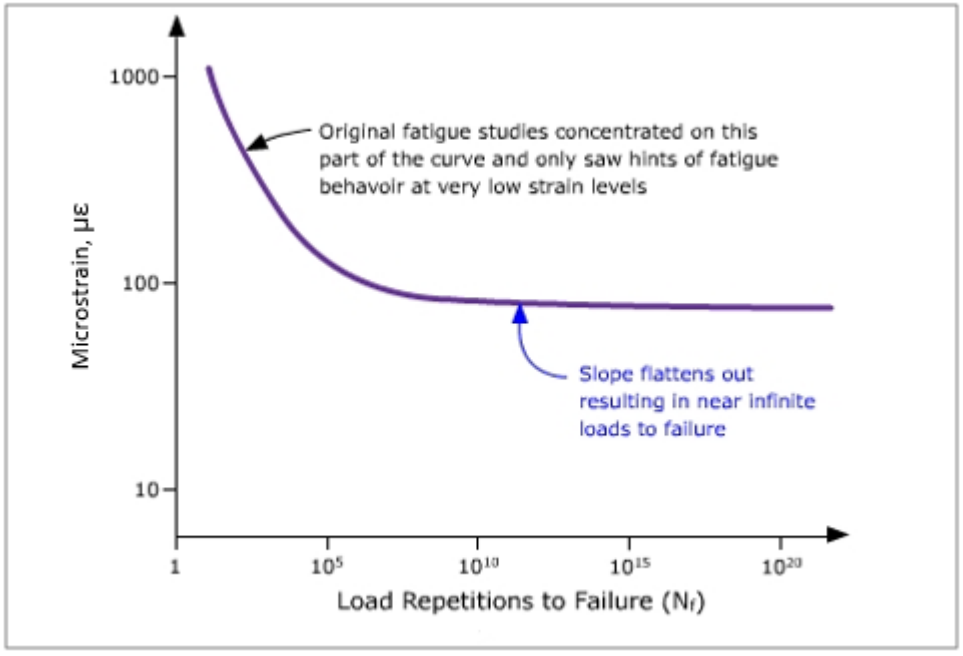



Figure 2.2: S-N relationship (www.pavementinteractive.org).

Fatigue failure traditionally occurs due to the local tensile strains resulting from repetitive applications of traffic loads moving over the asphalt pavement. This failure is often thought to start when a cracking initiates at the bottom of the bituminous layers where the tensile bending stresses are the greatest and propagates through the complete thickness of the pavement to the surface. This is referred to as bottom-up fatigue cracking as shown in Figure 2.3. In general, with the increase of load repetitions, failure turns out to be visible after an evolution of two stages which have been identified in the fatigue failure growth; crack initiation and crack propagation.

However, a substantial focus on the opposite, top-down fatigue cracking shown in Figure 2.4 has gained increased attention in recent years. Different studies have been conducted to prevent or mitigate and rehabilitate this controversial distress. However, the understanding of top-down cracking is still in need of further investigations. No agreements have been reached to explain the reason of this type of cracking. This can be probably attributed to the fact that it has been reported in pavements with thin or thick asphalt layer and stiff or soft base, in regions of different climate, in forms of interconnected or longitudinal cracking, and outside or within of wheel paths (Wu, 2016).

Many factors have been reported could cause top-down cracking (TDC), including; mixture properties, pavement structure, climate, and traffic loads (Wu, 2016). First, with regard to mixture properties, it was found that high air voids content resulting from gap graded mix or segregation of mix in the field allow for water to remain in the pavement inducing moisture damage, and hence, increases the potential of TDC (Malan et al. 1989, Baladi et al. 2003, Harmelink et al. 2008). Second, relating to pavement structure, a premature longitudinal cracking was observed in thick asphalt layers or stiff bases coarse (Molenaar et al. 1984, Uhlmeyer et al. 2000, Wen and Ramme 2008). Loss of bond between asphalt reinforcements is also one of causes for TDC (Dauzats and Linder 1982, Metcalf et al. 1998). Third, age hardenings at the top of asphalt surface layers and hot climate increase the potential of this cracking in the field (Rolt 2000, Pellinen et al. 2004). Moreover, the potential opportunity of TDC occurrence in asphalt pavement increases by temperature changes which affect the stress relaxation of pavement inducing thermal fatigue (Dauzats and Rampal

1987, Roque and Ruth 1990). Finally, it was observed that fatigue cracking in the pavement surface may occur due to the residual stress (Hugo and Kennedy, 1985). Groenendijk 1998 also indicated that considerable stress/strain resulting at the pavement surface from horizontal shear stresses in the tyre-pavement interface is one of the possible reasons of TDC.



(a)



(b)

Figure 2.3: Bottom-up cracking:
(a) Field observations at pavement surface (b) Field observations in cross-section (http://eng.auburn.edu/research/centers/ncat/).







(a) (b)

Figure 2.4: Top-down cracking: (a) Field observation in the pavement (b) Field core drilled from the crack (www.pavementinteractive.org).

## 2.2 Fundamental approaches of fatigue behaviour

It is important to precisely understand the fatigue behaviour of asphalt mixtures to ensure a good structural pavement design and an accurate in-service pavement performance (Di Benedetto et al., 2003). In order to understand this behaviour, the approaches to describe the fatigue failure of these mixtures must be identified. In general, the traditional phenomenological approach has historically been used to evaluate the fatigue performance of asphalt paving mixtures. Due to asphalt industries move towards producing more reliable design methods by using mechanistic and performance basis, fundamental approaches have been developed to evaluate and improve the understanding of fatigue failure of asphalt materials (Daniel et al., 2004).

It is reported that intensive laboratory investigations have been carried out to study the influence of repetitive traffic loadings on the fatigue performance of asphalt pavement structures. It is also reported that fatigue properties can be derived thorough these laboratory testing and the phenomenological method or fracture mechanics-based approach can be used to describe the development of fatigue distress (Aglan and Figueroa, 1993, Liang and Zhou, 1997, Baburamani, 1999, Ghuzlan and Carpenter, 2003). In the same perspective, Shen and Carpenter, 2007, Tarefder et al., 2013, Maggiore, 2014 indicated that many researchers used the dissipated energy approach as a fundamental method to describe and characterise the fatigue behaviour of Hot Mix Asphalt (HMA).
The following sections present the three main approaches used to characterise the fatigue behaviour of asphalt mixtures.

### 2.2.1 Phenomenological approach

The phenomenological approach or the S-N approach (stress-number of cycles to failure) assesses the fatigue life by plotting the stress or strain at the bottom of asphalt concrete layers at the initial load cycles versus load cycles number to failure as presented in Figure 2.5 (Baburamani, 1999, Ghuzlan and Carpenter, 2003, Diab et al., 2013). Baburamani (1999) also indicated that the assessment of fatigue performance is dependent on conducting fatigue testing at different stress/strain levels and the relationship between the initial strains versus the number of cycles has been used to predict the fatigue life. Furthermore, Ghuzlan

and Carpenter, 2003 and Zeiada, 2012 indicated that S-N approach is widely used in conventional asphalt pavement design and analysis based on the simple relationship of cumulative damage (D), Miner's (1945) linear law. The cumulative damage is determined as the ratio of the predicted (actual) number of traffic load repetitions (n) to the allowable (maximum) number of load repetitions (N) as shown in Equation 2.1. In theory, fatigue damage should occur at an accumulated damage value of 1.0. If a normal distribution is assumed to be applicable for the damage ratio computed, some failure level as a percentage of area cracked can be calculated and checked with in-service performance.

$$D = \sum_{i=1}^{T} \frac{n_i}{N_i} \qquad 2.1$$

Where:

D = damage.

T = total number of periods.

$n_i$ = actual traffic for period i.

Ni = allowable failure repetitions under conditions prevailing in period i.

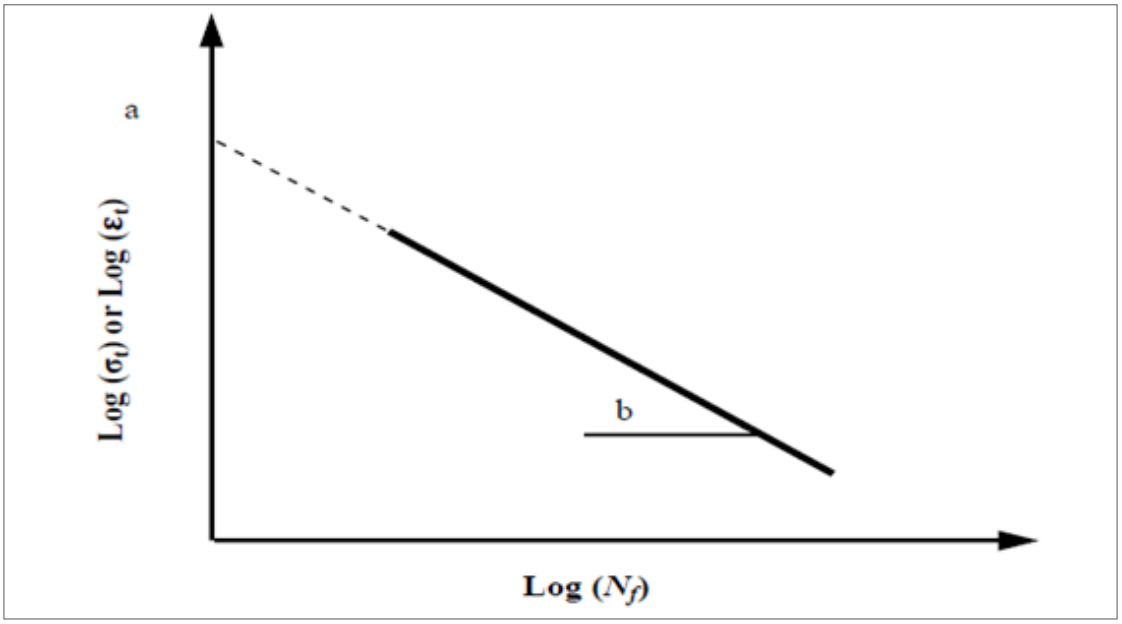



Figure 2.5: (S-N) method - relation between fatigue life ($N_f$) and applied stress (σt) or strain ($\varepsilon_t$).

Ghuzlan and Carpenter, 2003 also referred to the importance of failure criterion definitions of this approach to interpret the results of fatigue tests and in turn assess the fatigue life properly. This interpretation of fatigue test results is dependent on the mode of loading. In the controlled strain test, failure is defined at a specific percentage of asphalt mix stiffness reduction; in general a 50% stiffness reduction is used. In contrast, in controlled stress test, failure is typically defined as the fracture of the specimen. Tarefder et al., 2013 also indicated that the fatigue failure in traditional approach is defined according to American Association of State Highway Transportation Officials (AASHTO) as the number of cycles at which a reduction of 50% in the initial stiffness of investigated material occurs ($N_{f\,50}$).

Pell, 1967 demonstrated that results from fatigue test can be formulated by introducing the familiar relationship of S-N approach through experimental constants characterise the fatigue response of asphalt pavement. The relationship between the number of cycles to failure ($N_f$) and the more important parameter for fatigue cracking, tensile strain or stress can be presented into the following:

$$N_f = a\left(\frac{1}{\varepsilon_t}\right)^b \qquad 2.2$$

Where:

$N_f$ = number of cycles to failure,

$\varepsilon_t$ = induced strain, and

a and b = regression constants (the intercept and the slope of the fatigue line respectively).

Furthermore, Monismith et al., 1985 indicated that the most general used form to predict the fatigue life is a function of two parameters; the tensile strain and mix stiffness. Therefore, the basic for developing most fatigue characterisation models was proposed and presented in the following form including both parameters.

$$N_f = a(\varepsilon_t)^b(S_o)^c \qquad 2.3$$

Where:

$N_f$ = Allowable number of load applications to prevent fatigue cracking of asphalt layer,
$\varepsilon_t$ = Tensile strain at the bottom of the asphalt layer expressed in microstrain,
$S_o$ = Stiffness modulus of the asphalt material in MPa,
a, b, c = Regression constants determined from laboratory fatigue tests.

Al-Qadi et al., 2003 indicated that according to the Asphalt Institute, the values of a, b, and c are equal to 0.0796, 3.291, and 0.854, respectively while for Shell, a, b, and c are equal to 0.0685, 5.671, and 2.363, respectively.

In the same perspective, Finn et al., 1986 found that fatigue behaviour is influenced by the modulus of the HMA besides strain. It was quantified some of the temperature variations which can affect HMA fatigue performance by introducing the dynamic stiffness modulus in the fatigue characterisation forms to overcome some limitations of these models. It was recommended to consider the following relations to predict the number of load repetitions to produce 10 and 45% fatigue cracking of wheel tracks, respectively.

$$Log\left(N_f\right) = 15.947 - 3.291\log(\varepsilon) - 0.854log(E) \quad 2.4$$

$$Log\left(N_f\right) = 16.086 - 3.291\log(\varepsilon) - 0.854log(E) \quad 2.5$$

Where:
$N_f$ = Allowable number of load repetitions required to cause either 10 or 45% fatigue cracking in wheel tracks,
$\varepsilon$ = Tensile strain at the bottom of the HMA layer expressed in microstrain,
E = Stiffness modulus of the asphalt layer expressed in MPa.

Aglan and Figueroa, 1993 stated that although the traditional approach has some limitations, its simplicity contributed to its wide adaptation. From a structural design perspective, this approach does not specify the number of cycles for each stage of cracks; initiation and propagation where the relative magnitude of each one is very important. In addition, the constants a and b are definitely regression constants and many variables can affect them and in turn affect fatigue response, such as test temperatures, mode of loading, and rate

of loading. Consequently, they are not considered material constants. Similarly, Liang and Zhou, 1997, stated that the two main approaches, phenomenological and the fracture mechanics approaches, cannot accurately reflect the main material properties through the used regression constants. However, Ghuzlan and Carpenter, 2003 concluded that the values of these regression constants, (a) and (b) influenced by a number of parameters including mixtures properties, loading modes and test conditions. It was found that asphalt content, testing temperature and mode of loading showed a significant influence on (a) and (b) relationship without taking into account the effect of rest period. On the other hand, air voids levels, type of asphalt and aggregate gradations had insignificant effect on (a) and (b) relationship. Moreover, it was concluded that there is a reliable relationship between them which might be useful in the structural pavement design. It was also reported that the values of fatigue coefficients (a) and (b) vary from a model to another. Typically, the range of b value varies between 3 and 6 while there are wide different values for a.

Furthermore, Diab et al., 2013 evaluated the effect of hydrated lime (HL) on the response of phenomenological approach parameters of HMA; (a) and (b). Firstly, it was concluded that parameter (a) increased with adding HL to HMA, while parameter (b) seems to be insensitive to mixture type; control mixture and modified mixture by HL. Additionally, it was found that both fatigue parameters of HL modified mixtures are highly correlated and in the different conditions. Finally, it was concluded that parameters (a) and (b) could be considered material constants at low loading frequencies (up to 10Hz) while they could not be considered material parameters for different testing temperatures.

Finally, Abojaradeh (2013) indicated that the traditional fatigue failure approaches are based on a simple correlation between the accumulated tensile strain in the specimen and the number of load cycles to failure. The criteria to identify the failure have depended on arbitrary measures such as 50 percent reduction of material stiffness. Therefore, this traditional approach does not unify the onset of fatigue failure by using different modes of loading.

### 2.2.2 The fracture mechanics approach

The fatigue behaviour of asphalt concrete mixtures can be described as a process of damage through the principles of fracture mechanics. It was indicated that the following three stages are considered for the fatigue life to develop in this approach; (1) Crack initiation, (2) Stable crack propagation, and (3) Final fracture failure (True failure) or unstable crack propagation as shown in Figure 2.6 (Aglan and Figueroa, 1993, Matthews et al., 1993, and Shen and Carpenter, 2007). During the first phase, crack initiation, the damage resulting from repeated applications of stress/strain leads to the gradual loss of asphalt concrete mixtures integrity and stiffness. This loss starts with the initiation of micro-cracks which grow due to insufficient healing time or mechanism from a microscopic size to a critical size of about 7.5 mm (Little et al., 2001). Secondly, in the crack propagation phase, these micro-cracks grow and tend to form a coalescing which produce macro-cracks. With the continuity of cracks propagation, these macro-cracks gradually lead to the reduction of cross-sectional area and in turn results in materials weakness. This weakness finally completes the disintegration process and results in the complete fracture or final pavement failure. The required cycles in each phase are different and it is difficult to quantify because the specimen experiences different mechanism through the three phases (Shen and Carpenter, 2007).

The majority of the fatigue life is assumed to be consumed through the crack propagation stage, therefore, quantitative models have been proposed on the basis of this stage (Matthews et al., 1993, Aglan and Figueroa, 1993). In addition, Paris and Erdogan, 1963 related the length of crack, a, to the number of cycles of applied load, N, with the range of stress, σ, and materials constants, Ci as following:

$$\frac{d_a}{d_N} = f(\sigma, a, C_i) \qquad 2.6$$

Where: $d_a/d_N$: average crack speed.

Majidzadeh et al., 1972 stated that Paris law for crack growth is applicable to asphalt concrete mixtures supported on elastic foundation. Furthermore, the literature presented several forms of crack-propagation laws and the following

basic relation has been used as one of these forms (Tangella et al., 1990, Matthews et al., 1993):

$$\frac{d_a}{d_N} = A(K_1)^n \qquad 2.7$$

Where:

a = the crack length,

K1= the stress intensity factor [tension; stress × (length) $^{0.5}$]

N= the number of load applications, and

A and n =experimental coefficients.

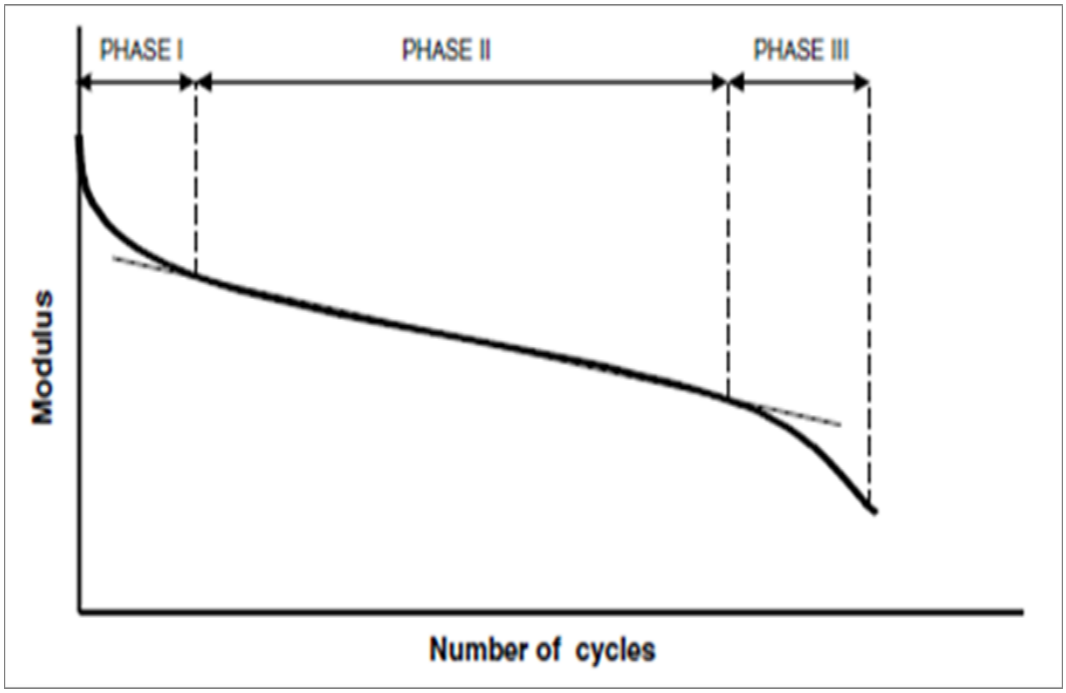



Figure 2.6: Modulus variation during a fatigue test. (Estimation of asphalt concrete fatigue curves – A damage theory approach).

This relation assumes that stable crack growth takes place between some initial crack length, $a_o$, and a critical length, $a_c$, which terminates the fatigue life and is determined by $K_{1C}$, the critical value of $K_1$. Many researchers described the fatigue behaviour models based on crack propagation stage. However, these models are empirical or semi empirical functions in terms of the stress-intensity factor K. Consequently, A and n in relation 2.6 are empirical constants, they could be constant for some conditions, but not related to material properties (Aglan and Figueroa, 1993).

### 2.2.3 Dissipated energy approach

The dissipated energy approach was developed by Van Dijk et al., 1972. It is defined as the loss of energy per loading cycle in any repeated or dynamic test (Van Dijk, 1975, Van Dijk and Visser, 1977, SHRP, 1995). This approach is not influenced by mode of loading, testing temperature, and binder and mix types. Therefore, it is considered as a promising technique to characterise the fatigue behaviour of asphalt materials. The dissipated energy per cycle, change in dissipated energy and cumulative dissipated energy all these parameters are used to evaluate the development and accumulation of fatigue damage (Van Dijk et al., 1972, Rowe, 1993 and 1996, Shen and Carpenter, 2007).

The rheological behaviour of viscoelastic materials is the base for this approach. When a material is experiencing an external loading, the energy being input into the material can be represented by calculating the area under the resulting stress – strain curve. For a non-pure elastic material, there is always an association between the energy dissipation with the process of loading and unloading because there is no overlap between their paths. This is called "hysteresis loop'' as shown in Figure 2.7 and the area inside of this hysteresis loop cycle represents the dissipated energy amount for one loading cycle (Shen and Carpenter, 2007).

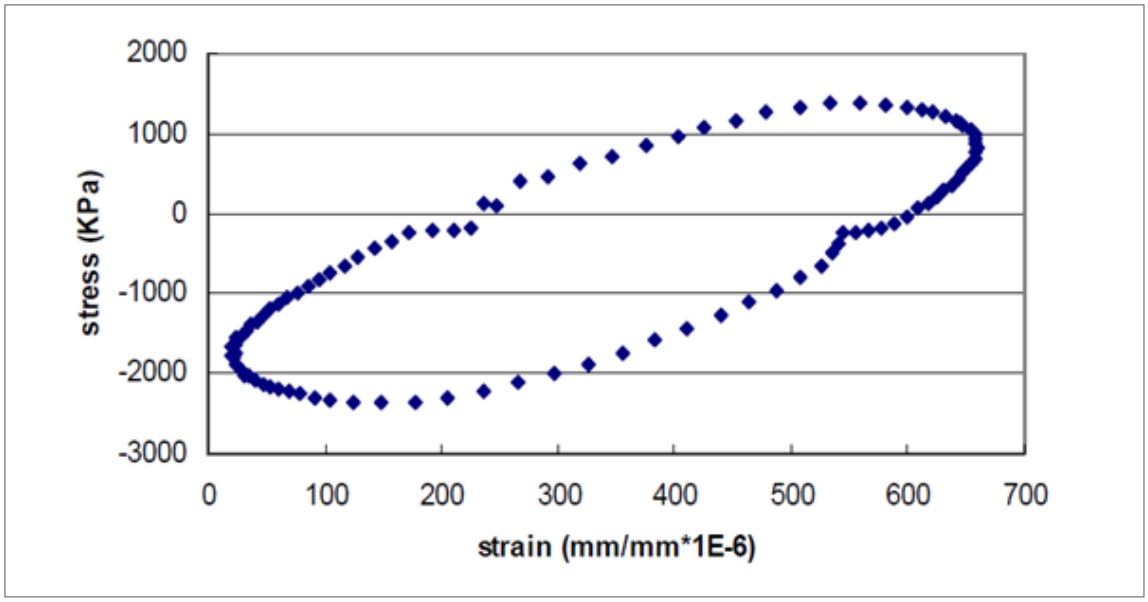



Figure 2.7: A stress-strain hysteresis loop (one loading cycle), controlled-strain testing (Shen and Carpenter, 2007).

Abojaradeh (2013) also referred to the importance of the dissipated energy approach as a good indicator of fatigue characterisation. Furthermore, this approach has greater significance than a simple strain indicator because it picks up both behaviours; the elastic and viscous. This approach indicates consistently to the level of deterioration in the specimen in terms of accumulated damage or remaining life. Therefore, it is considered as a promising tool for fatigue response. It also can be generally applied by using flexure fatigue tests with controlled strain or controlled stress conditions. At each loading cycle, the following parameters; the strain, stiffness and phase angle are measured by means of software. Furthermore, the following equation can be used to calculate the dissipated energy:

$$W_i = \pi \varepsilon_i^2 S_i Sin\emptyset_i \quad 2.8$$

Where

$W_i$= Dissipated energy at load cycle i;

$\varepsilon_i$ = Strain amplitude at load cycle i;

$S_i$ = Mix stiffness at load cycle i;

$\varphi_i$ = Phase shift between stress and strain at load cycle i.

Then, the dissipated energy accumulates over load cycle progress is:

$$W_n = \sum_i^{N_f} W_i \quad 2.9$$

Where:

$W_n$ is the cumulative dissipated energy over N cycles.

Then number of cycles to failure relates to the cumulative dissipated energy to failure is presented through the following unique relationship:

$$W_n = A(N_f)^z \quad 2.10$$

Where:

A and z are experimentally determined constants

### 2.3 Laboratory fatigue testing methods

Over the last several decades, different testing methods have been developed to characterise and simulate the fatigue behaviour of asphalt materials. The quality of fatigue life prediction of these tests depends on the accuracy of the

method to simulate the loading condition, support of test specimen, stress state, and environmental conditions. Furthermore, in addition to equipment availability and cost, selecting any of these methods will depend on specimen fabrication requirements, and simplicity and quickness of use. Figure 2.8 presents most of the available fatigue test methods. On the other hand, it is impossible to completely simulate the condition of in-service pavement by these testing methods. Conditions such as random rest periods, multi stress state compound loading, and specimen size and shape are generally not considered in these tests. Therefore, there is a difference in fatigue life predicted based on laboratory and field conditions and a shifting factor usually applied to consider laboratory to field performance. The magnitude of the shift factor is vary and depending upon many factors such as mix properties, environmental conditions, the traffic volume and composition, the thickness of the asphalt layer, fatigue failure criterion, and type of fatigue test. For instance, Harvey et al., 1997 reported that shifting factors values varies between 10 and 100.

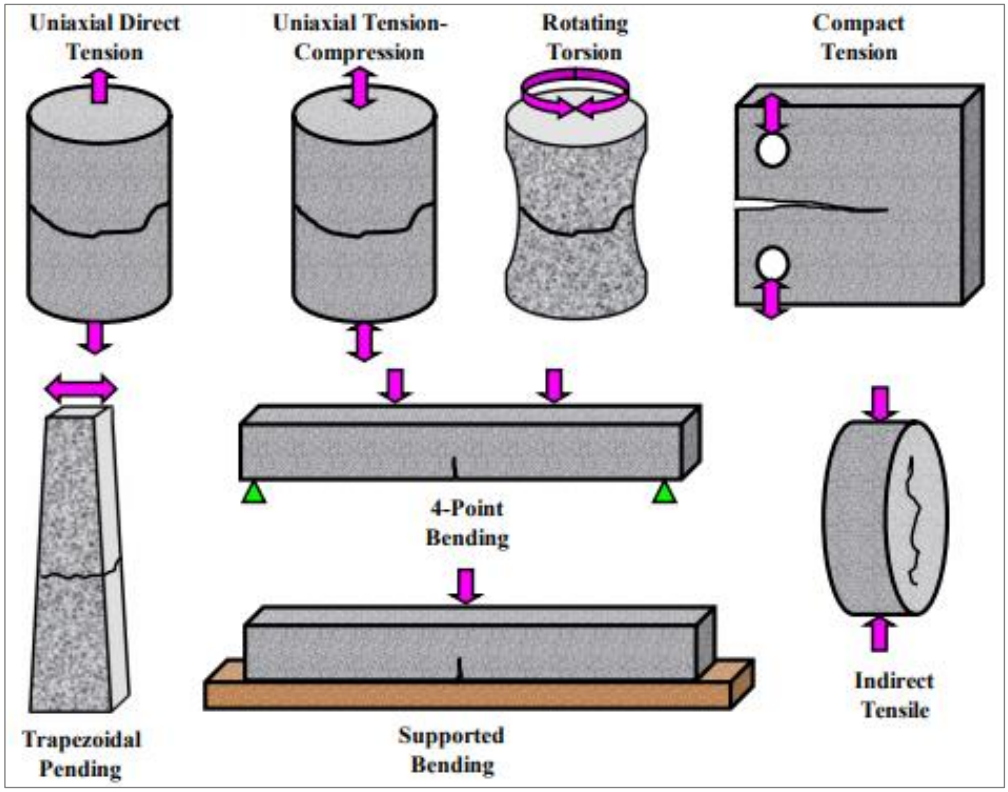



Figure 2.8: Commonly used fatigue test arrangements (Zeiada, 2012).

Following a summary of most popular fatigue test methods with the advantages, disadvantages and limitations as reported by Tangella et al., 1990:

### 2.3.1 Flexural fatigue tests

The flexural fatigue test has widely been used by various researchers to evaluate the fatigue performance of asphalt pavements (Witczak et al., 2001). It can be divided into the following:

**1. Simple flexure test** is commonly used for measuring the stiffness modulus and assessing the fatigue characteristics of asphaltic paving mixtures. It is well known and widespread in use. A number of' different types of flexural equipment have been developed to study the fatigue resistance of asphalt-concrete mixtures including:

- **Three and Four-point bending tests:** The centre-point loading equipment was used by Shell Laboratory at Amsterdam to test specimens in the controlled-deflection (strain) mode with dimensions of (30×40x230) mm. In four-point test, the dimension of the beam specimens can vary from one laboratory to another according to the followed standard. The AASHTO T321-2003 and SHRP M-009 require dimensions of 380±6 mm in length, 50±6 mm in height, and 63±6 mm in width without specifying a specific method for this preparation. Several compaction methods have been used to prepare slabs or beam specimens in the laboratory including rolling vibratory loading, miniature rolling wheel compaction, and full scale wheel compaction.

- **Cantilever beam rotating test**

At the University of Nottingham in the UK, Pell and Hanson, 1973 used a rotating cantilever machine to induce a bending stress of constant amplitude through a specimen fixed vertically on a rotating cantilever shaft. The load is applied at the top of the specimen. The test was generally carried out at a temperature of 10°C and a speed of 1000 rpm (16.7 Hz). Dynamic stiffness modulus was measured by applying a constant sinusoidal amplitude deformation. A controlled-strain torsional fatigue machine was also used by Pell to carry out a different way of this test where a specimen is clamped vertically on a shaft. The

bottom of the specimen is fixed to the bottom of the machine to induce a sinusoidal shear strain of constant amplitude into the specimen.

- **Trapezoidal cantilever beam test**

The trapezoidal cantilever beam test is widespread in Europe. Tests on trapezoidal specimens have been conducted by Van Dijk, 1975 and Bonnot, 1986. The larger dimension of the trapezoidal specimen (base) is fixed and the smaller end (top) is loaded by either a sinusoidal stress or strain. The dimensions of a specimen tested by Van Dijk had a base cross section of 55 mm by 20 mm and a top cross section of 20 mm by 20 mm with a height of 250 mm.

**2. Supported flexure test**

Supported flexure test was used to improve the simulation of stress state and mode of loading of in-service pavements. Many researchers have mainly used this test with two different specimen shapes; beam and circular slab. Majidzadeh et al., 1971 used a circular specimen supported on a rubber mat. A circular shaped repeated load applied to the centre of the slab resulting in a similar stress state to that occurring in the pavement structure. In addition, Barksdale, 1977 used asphalt concrete beam supported by a rubber mat of 4 inch in thickness. The beam loaded by a haversine load pulse of 0.06 second loading time and 45 cpm loading frequency (0.75 Hz).

### 2.3.2 Direct tension test

The Transport and Road Research Laboratory (TRRL) of the United Kingdom has conducted a series of uniaxial tensile tests in the controlled-stress mode using a 25 Hz loading frequency, 40 milliseconds loading time, and variable rest periods from 0 to 1 sec. It was found that fatigue life increases rapidly with an increase in the rest period up to 0.4 second while an insignificant increase in the fatigue life was observed beyond 0.4 second (Raithby and Ramshaw, 1972). Later on, direct tension tests in the controlled-strain mode have been conducted in the Netherlands (Kunst, 1989) at loading frequencies of 0.1 and 1Hz using haversine pulse. More recently, this test have been used in the US by Texas A &M and North Carolina State Universities to study and characterise the

phenomenon of micro-damage healing in asphalt binder and asphalt mixtures using dissipated energy, fracture micromechanics, and viscoelastic continuum damage approaches. One advantage of the direct tension test is the variety of test specimen which has either circular or rectangular cross section. It is also rapid test and not expensive. However, the main disadvantage of this test is that loading conditions do not necessarily simulate that in the field.

### 2.3.3 Tension/compression test

The tension/Compression fatigue test was developed at the Transport and Road Research Laboratory (TRRL) in the UK by means of in a servo-controlled electro-hydraulic machine (Raithby and Ramshaw, 1972). Axial tensile and compressive loading was applied to prism specimens of 75 mm square cross sections and 225 mm lengths at loading frequencies of 16.7 and 25 Hz. The influence of shape of wave form, rest periods, and the sequence of load application (tension/compression, compression/tension, tension only, and compression only) was considered.

The effect of load form was found to be not influential. However, a sinusoidal load pulse would seem to be a reasonable representation. It was also found that pure compressive cyclic loading had the largest fatigue life followed by tensile/compressive cyclic loading, tensile cyclic loading, and compressive/tensile cyclic loading. In addition, short rest periods between successive axle load applications have a significant effect on the fatigue life.

Despite the fact that this test simulates the loading pulse observed in practice, this test does not well represent real conditions of the field. It also requires more time and more specialised equipment. Therefore, it is more expensive.

### 2.3.4 Diametral test

The diametral fatigue test is an indirect tensile test (ITT) conducted by applying a repetitive compressive loading to a cylindrical specimen along the vertical diametral plane. A reasonable uniform tensile stress develop at the centre of the specimen perpendicular to the direction of the applied load and along the vertical diametral plane. Test specimens are usually 100 mm or 150 mm in diameter and 40-75 mm in high. A 12.5 mm wide loading strip is used to transmit the loading to the sides of the circular cylinder. A haversine/sine load

pulse can typically be applied. The most commonly used loading frequency is between 20 to 120 cycles per minute. The unique asset of this test is that applicability to characterise a wide range of asphalt mixture properties; resilient modulus, fatigue cracking, thermal cracking, and permanent deformation (Kennedy, 1977).

This test is simple, more representing to field condition due to a biaxial state of stress exists, and it can be performed to laboratory specimens and field cores. Disadvantages of this test method are that accumulation of permanent deformation and the absence of stress reversal. It is also considered significantly underestimated of fatigue life when the tensile stress is used as the damage indicator.

### 2.3.5 Triaxial test

To improve the simulation of the stress state of in situ, this test has been developed at the University of Nottingham (Pell and Cooper, 1975) and the University of California, Berkeley (Sousa, 1986). Pell and Cooper reported that a sinusoidal varying axial stress was applied to cylindrical specimen sealed off in a triaxial cell with a diameter of 100 mm and a height of 200 mm. In this kind of test, one concern arisen about the shear strains which need to be well controlled, otherwise the prediction of fatigue life could be significantly different from that of in service pavement.

Moreover, Sousa, 1986 developed equipment to apply repeated or constant shear strains by torsion together with radial tensile stress to hollow cylindrical specimens but to recent date only shear fatigue (torsion) tests have been conducted (Zeiada, 2012) . Thus, further development of this equipment to apply repeated radial tensile stresses can be conducted through the pulsating fluid within the hollow cylindrical specimens for better simulating of the real shear and vertical stresses.

One of advantages of the triaxial test is that simulating of the field loading condition in terms of compression is followed by tension and therefore the results can be used for mixture design. The results also can be used for structural design if field correlation factors are applied. On the other hand, this type of test is expensive because it requires specialized equipment. It is also time consuming.

### 2.3.6 Wheel-tracking test

The wheel-tracking test has been developed to study fatigue characteristics of asphalt pavements, to better simulate the influence of rolling wheel on asphalt pavements, and to better understanding of crack initiation and propagation. It can be conducted either in the laboratory or on large scale pavement sections. Van Dijk, 1975 has developed a laboratory loaded wheel with a pneumatic tire that moves back and forward over a fabricated slab of asphalt concrete mixtures. The wheel has a diameter of 25 cm with a width in the range of 5 to 7 cm and its path is 60 cm long. The slab is supported on a rubber mat. Strains at the bottom of the slab, and the detection of crack initiation and propagation can be measured. Three fatigue stages can be recognised; first, the development of hairline cracks, second, real cracks, and third, failure of the slab. Based on the analysis of test results, Van Dijk suggested that controlled strain test may be more appropriate to define asphalt pavement cracking than controlled stress test. The small dimensions of laboratory wheel-track tests and the slow speed of the rolling wheel are the main limitations in comparison with field conditions. In addition, the test is time consuming and does not measure a basic mixture property such as stiffness modulus. Moreover, for low stiffness mixtures, manifestation of rutting is serious and may affect fatigue predictions.

Well-known examples of full-scale testing facilities include the circular tracks have been built in the United Kingdom (TRRL), at Nantes in France, Denmark, in Australia (ARRB), New Zealand (Canterbury), the Federal Highway Administration's ALF (Accelerated Loading Facility), CALTRAN’s Heavy Vehicle Simulator in California, at Pullman, near the Washington State University campus. These tracks are often divided into sections, each one with a different pavement structure, and loads can be applied by several sets of dual truck tires. Full-scale testing facilities provide the opportunity to observe the effect of changes in the section of pavement structure on pavement performance. Fatigue in addition to other forms of pavement distresses can be investigated. One the other hand, a supplementary laboratory working in parallel is still required because fundamental mixture properties cannot be directly measured by these field track tests. In addition, high cost of initial investment and annual operation and maintenance costs are considered the main disadvantages.

## 2.4 Healing phenomenon in asphalt mixtures

Asphalt pavements are prone to cracking due to repetitive traffic loadings and severe environmental factors. Cracks are considered detrimental to pavements in different ways by adversely affecting their mechanical properties and durability. Cracking is possible access for water to enter the pavement structure and accelerate their deterioration. Cracks are also the main cause of different pavement distresses such as stripping in asphalt concrete layers and loss of subgrade support. Therefore, pavement damage caused by cracking needs for repair and rehabilitation which are usually costly. Consequently, there is a critical need to evaluate the properties and factors may enhance the cracking resistance of asphalt concrete pavement (Pamulapati et al., 2017).

Healing potential of asphaltic materials is one of these properties that has been reported by pavement engineers in the last few decades. However, its effect on the fatigue behaviour of asphalt mixtures is still far from clear understanding. Maggiore, 2014 indicated that Healing is one of the factors that significantly affect fatigue performance of asphalt materials. It is still a very complicated phenomena to evaluate. It might be attributed to availability of testing machines which are suitable to properly set up a rest period after loading cycle. Moreover, Carpenter and Shen, 2006 stated that healing was used to explain the observed differences between the predicted and actual fatigue performance.

Rest periods between successive traffic loadings is also identified as one of the important factors affecting healing potential of asphalt mixtures (Bonnaure et al., 1982). Despite it was reported that the understanding of healing potential is still in need of further investigation, it has been demonstrated in laboratory tests that the rest period between loading cycles is effective for extending the fatigue life of asphalt mixture specimens (Bonnaure et al., 1982). Mashaan et al., 2014 found that rest periods between successive loads allow for the strains and stresses to relax and this assists cracks in the bituminous specimens to heal as a result of the viscous flow behaviour of the asphalt binder.

In addition, the loading history and binder property are one of major factors affecting the healing in asphalt pavement. Kim and Little, 1990 identified the healing potential of asphalt materials by applying cyclic load tests with varying

rest periods on notched beam specimens. It was found that rest periods enhance the fatigue life of investigated mixtures through healing and relaxation.

Further factors affecting the healing asset is asphalt binder viscosity. It was demonstrated by SEM (Scanning Electron Microscopy) image analysis that the degree of healing was also significantly influenced by the viscosity of asphalt binder (Kim et al., 1991).

The temperature also affects the healing phenomenon. If the testing temperature increases during rest periods, a substantial recovery of modulus takes place. Fatigue damage in asphalt concrete at high temperatures (higher than 15$^{o}$C) is governed by thixotropic effect, which states under repeated loading asphalt binder changes from a gel to a sol structure. Thus, the healing at high temperatures is a process of changing from a sol to a gel structure of asphalt binder. On the other hand, at low temperatures (lower than 5$^{o}$C), structural damage in asphalt concreter is mainly associated with fatigue and fracture and the full recovery from the structural damage is not possible to occur through the rest periods. Therefore, the recovery of the structural damage caused by the repeated loading would only be partial (Verstraeten, 1991).

Francken and Clauwaert, 1987 reported that the strength recovery of asphalt concrete mixture is greater with softer asphalt binders and the rest periods have generally greater beneficial effect in the mixture of soft binder with higher binder content. In the same line. Bonnaure et al., 1982 reported that mixture recovery is greater with softer bitumen. On the other hand, Si et al., 2002 found that adding the hydrated lime to asphalt mixtures improved the healing potential of the mixtures. It was also found that stiffer mixtures have generally better healing performance and longer rest periods resulted in greater healing.

## 2.5 Factors affecting fatigue performance of asphalt paving mixtures

### 2.5.1 Rest period

The prediction of fatigue life of asphalt concrete mixture in laboratory fatigue tests is based on the application of a continuous loading condition in both stress and strain modes. However, the conditions of these tests do not simulate the prevailing loadings condition in practice. In practice, the pavement is loaded discontinuously and the passage of front and rear axles of one vehicle or successive vehicles is interrupted by rest period (Bonnaure et al., 1982, Mashaan et al., 2014). Under real traffic loads, a wide variation in the load applications commonly happens and results in different rest periods at different times during the day depending on the traffic volumes and roads types (Mashaan et al., 2014). Therefore, it is important to study the influence of rest periods on the fatigue response of asphalt concrete mixtures to replicate the real traffic loading patterns on asphalt pavement structure.

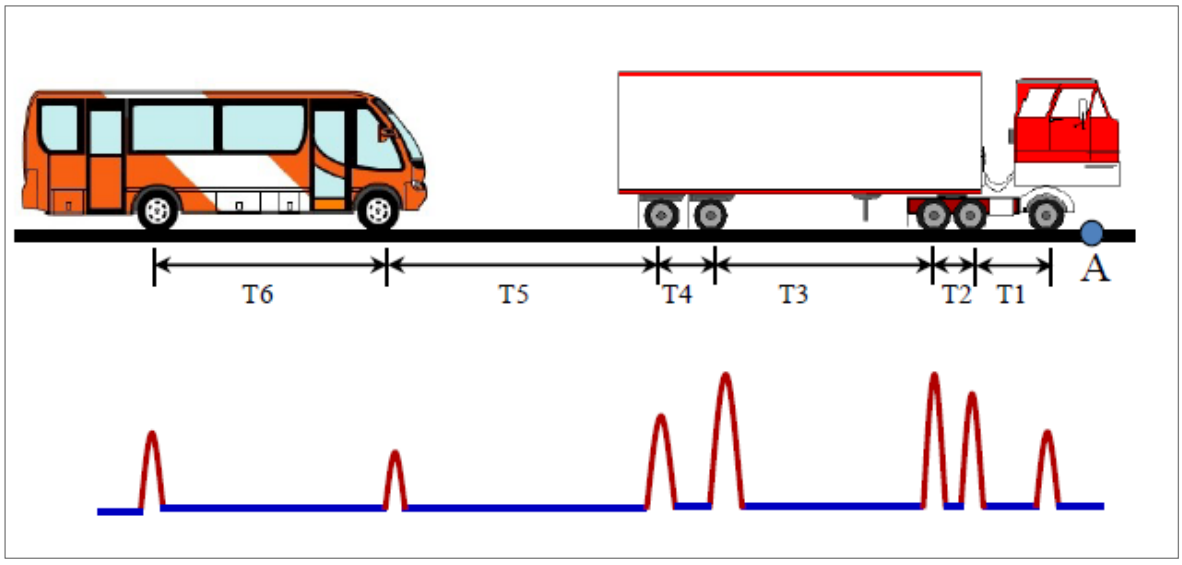



Figure 2.9: Rest times between vehicle's axles passing over the pavement (Zeiada, 2012).

Many researchers investigated the influence of rest period in laboratory fatigue tests and all of them found that fatigue lives of the evaluated bituminous mixes increased by incorporating rest periods in the loading conditions (Bonnaure et al., 1982, Bonnaure et al., 1980, Raithby and Sterling, 1972, Van Dijk and Visser, 1977). For instance, Castro and Sánchez, 2006 conducted flexural beam fatigue tests with and without rest periods. As a consequence, a constant rest

period of 1 second following every 0.1 second loading could increase the fatigue life of asphalt mixture up to 10 times, compared to tests without rest periods. Mashaan et al., 2014 also stated that an increase in the number of cycles to failure of 25 times resulted from the application of one-second rest period in comparison with the fatigue life under continuous sinusoidal loading without rest period. However, there is a limit for the effect of rest periods increase depends on test temperature where more than this limit the fatigue life will not be affected by an additional rest periods (Raithby and Sterling, 1972, Raithby and Sterling, 1970).

In general, laboratory fatigue testing programs attempt to introduce the rest period to consistent with the actual traffic loading patterns applied to asphalt pavement structure. A rest period can be defined as the time between successive applications of traffic wheel loads (Bonnaure et al., 1980, Raithby and Sterling, 1972, Van Dijk and Visser, 1977).

Bonnaure et al., 1982 stated that two different procedures can be used to introduce rest periods into fatigue testing as following:

- Discontinuous loading, which is applied in traditional fatigue tests by applying periods of continuous loading for a certain time followed by a rest period or storage period where the specimen is hold under the test conditions without loading.
- Intermittent Loading, by subjecting the specimens to discontinuous or intermittent loading and this can be done by applying rest period after each loading cycle.

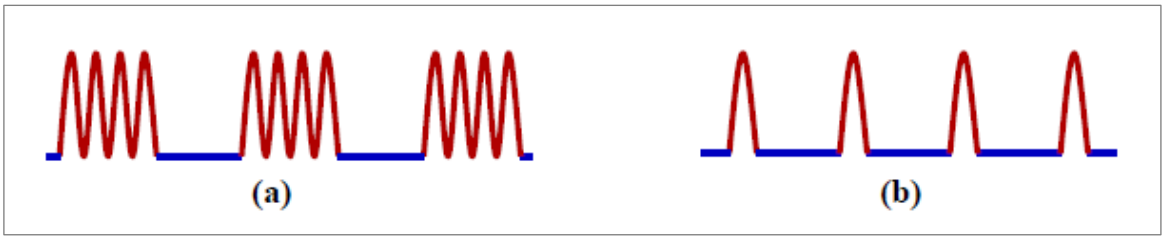



Figure 2.10: Fatigue tests (a) Discontinuous loading and (b) Intermittent loading (Zeiada, 2012).

Clearly, method two simulates the sequence of traffic pulses more than method one although both result in longer fatigue life as compared to that without rest periods regardless the loading conditions or sample geometry (Baburamani, 1999, Walubita et al., 2005). A number of studies have been carried out on this effect using these two ways as in the following sections:

### 2.5.1.1 Studies applied discontinuous loading (storage periods)

A significant effect of long storage periods on the fatigue response of a partly fatigued asphalt mix was observed by Bazin and Saunier, 1967. A two-point bending apparatus was used to test the specimens at 50Hz and 10˚C. Then the samples were tested under the same conditions after applying storage periods at the same temperature for different times (from a number of hours up to 100days). These new situations resulted in a new fatigue life $N_R$. The life ratio $N_i/N_C$ exhibited those storage periods had an advantageous effect by extending the fatigue life up to 100 percent.

Mc Elvaney and Pell, 1973 investigated the effect of rest periods on the fatigue life of a base course bituminous mix by using rotating bending fatigue apparatus in controlled stress condition. The results indicated that a rest period between successive loading cycles is beneficial depending on the level of accumulated damage during loading periods. Strain recovery occurred and rest periods increased the fatigue life when this damage does not exceed a certain level. According to the applied loading conditions of the study, they found that no evidence of at a certain limit of rest period beyond which no more benefits are acquired from rest period. However, studies stated the limits of such findings (Raithby and Sterling, 1970, Raithby and Sterling, 1972).

Verstraeten, 1976 used the dynamic two point bending tests in a constant stress condition at 54 Hz and two testing temperatures; -5˚C and 15˚C to evaluate the fatigue life of standard Belgian mix. The applied loading continued up to 80% of fatigue life or until cracking manifestation. Then storage periods from 3 hours until 21 hours were used at temperatures from -5˚C to 35˚C. He concluded that no specific value can be used to quantify the influence of both rest periods and temperature variations on the response of investigated mixes to fatigue

cracking, although Raithby and Sterling, 1970 stated that. On the other hand, the beneficial influence of rest periods appeared to be greater at higher temperatures than that at lower temperatures. The greater beneficial effects were acquired when the higher the temperature and the longer the storage periods were applied.

Doan, 1976 used the dynamic two point bending tests in a constant strain condition at 30Hz and 10˚C on to investigate the susceptibility of fatigue cracking of a typical French asphalt concrete wearing mixtures. He applied varying storage periods from 1 to 24 hours at temperatures of 10 and 20˚C. The tests results showed that both the applied temperature and the duration of the storage period have significant beneficial consequences by increasing the fatigue life of investigated mixtures. On the other hand, the benefit would be less when French binder course mixtures of lower bitumen content were tested.

Recently, Maggiore, 2014 applied a wide range of rest periods and loading times to beam specimens tested by the 4PB machine in constant strain test. It was found that loading time increase lead to reduce the number of cycles to failure. While this number increases if resting time increases.

#### 2.5.1.2 Studies applying intermittent loading

Raithby and Sterling, 1972 used a dynamic push-pull machine in a constant stress condition to investigate the effect of different wave forms with 25Hz frequency and various temperatures between 10 and 40˚C on the fatigue life of rolled asphalt base course mix. They found that short rest periods similar with those occurring in practice under traffic loading increased the fatigue life but this increase depends significantly on the test temperature. A maximum increase of fatigue life of about 25 times resulted when the specimens were tested at temperature of 10˚C and 25˚C. On the other hand, at temperature above 25˚C the beneficial influences of these short rest periods decreased.

Ugé et al., 1976 tested a typical French asphalt concrete mixtures in a constant stress condition by using a two point bending machine at 50 Hz and varying temperatures from 5 to 35˚C. They found an increase in the fatigue life of tested

mixtures with the application of rest period. The higher influence increased with increasing rest period duration and test temperature.

Van Dijk and Visser, 1977 used a three-point bending testing machine to study the fatigue response of rolled asphalt base course mixes in a constant strain condition with loading ratio (ratio of load cycles to rest period) ranging from 1/1 to 1/25 at 20˚C and 40 Hz. The result of fatigue tests showed an increase in the fatigue life of these mixtures as the rest periods increased. They suggested based on extrapolation that the life ratio ($N_i/N_C$) of about 10 would be acquired at an approximate loading ratio of 1/50.

Francken, 1979 used the two point bending tests in a constant stress condition at 55.6 Hz and 15˚C to investigate the fatigue life of standard Belgian mix. Based on the results he proposed the following empirical formula (restricted for the investigated mix) between the life ratio (Ni/Nc) and the loading ratio (nr/nc):

$$\frac{N_i}{N_C} = 1 + 2.8\,(\frac{n_r}{n_C})^{0.44} \qquad 2.11$$

Where:

nr= number of rest periods in cycles, and

nc= number of loading cycles.

Bonnaure et al., 1982 used the three point bending machine to investigate the fatigue life of Dutch asphaltic concrete incorporating intermittent loadings. He concluded that the fatigue life has been significantly influenced by rest periods and the maximum effect occurs around a rest period equals to 25 times the loading cycles. It was also found that the beneficial effect increased as the test temperature increased. In addition, they stated that the stress and strain levels had negligible effect on the beneficial effect of rest periods, although the constant stress approach resulted in more fatigue life than the constant strain condition.

In addition, Bonnaure et al., 1982 reported that no coherent quantitative picture occurs from the studies presented earlier because they focused on different mix types and test methods. Therefore, further experimental investigations are still required.

Robertus, 1993 tested multi-grade bitumen mix using three point-bending with sinusoidal loading at 40 Hz, 15˚C and loading ratio (the duration of rest period to that of loading) range between 5 and 10. He found that an increase in the fatigue life of Shell 70 penetration multi-grade bitumen mix from 3 to 10 time due to rest period incorporating. Hsu and Tseng, 1996 also tested the influence of rest period at various temperatures (15, 25, and 40)Cº and different asphalt contents (5.0%, 5.5% and 6.0%) on the fatigue resistance of hot asphalt mixtures using a series of third-point bending apparatus in constant stress mode. They introduced the rest period in terms of loading ratio (1, 4, and 8) which is defined as the ratio of the duration of rest period to that of loading. The results indicated that an increase in the number of repetitions to failure as the loading ratio increased. In addition, an increase of 0.5% in the bitumen content more than the optimum (5.5%) prolongs the fatigue life at the same loading ratio with low temperature. While at high temperature of 40˚C and loading ratio equals 1, the fatigue life was shorter due to the softening of asphalt concrete.

Recently, Maggiore, 2014 combined both types of loading; discontinuous and intermittent to carry out healing study on core specimens tested by the ITFT in constant strain method. It was found that healing ratio (the number of cycles of a fatigue test with rest period to the number of cycles of a fatigue test without rest period) decreases if loading time increases while it increases if resting time increases up to certain limit. Shorter rest periods and the accumulation of permanent deformation might not allow the specimen to recover and heal properly. It was also found that the optimum value of rest period equals 10,000 cycles loading but no significant improvement in the fatigue life was observed for higher rest periods.

### 2.5.2 Binder content

Asphalt binder content is one of the important factors affecting fatigue response of bituminous mixtures. Increasing the bitumen content increases the fatigue resistance of a mix (Mashaan et al., 2014). Monismith et al., 1970 found that the maximum fatigue life resulting by the flexure bending tests in constant stress occurred at an asphalt content that was associated with the highest stiffness modulus of the mixture manufactured with 60-70 penetration grade.

Pell and Cooper, 1975 displayed similar findings after conducting the rotating bending tests on the mixtures fabricated with 197 penetration grade asphalt. In addition, Adedimila and Kennedy, 1975 showed that the mixtures at optimum asphalt content from the Marshall design method exhibited the maximum fatigue life when using the indirect tensile test. It was also indicated that mixture design procedures should consider the fact that the optimum asphalt contents for maximum tensile strength, fatigue life, modulus of elasticity, and density are not necessarily the same. Thus, the mixture should be designed to produce the desired properties. Epps et al., 1969 presented controlled stress fatigue tests results indicating that the optimum asphalt content exists for best fatigue results. This asphalt content is dependent upon aggregate type and aggregate grading (Epps and Monismith, 1972). The optimum asphalt content for best fatigue performance appears to correspond to the optimum asphalt content required to provide maximum mixture stiffness and is in excess of that determined for mixtures based on mixtures stability requirements (Epps et al., 1969). Goddard et al., 1978 have shown that a one-percent reduction in bitumen content can reduce the fatigue life by 70%. Gibb, 1996 stated that for the longest fatigue life the volume of bitumen should be as high as possible, but limited according to permanent deformation requirements. Similarly, for the longest fatigue life, the volume of bitumen should be as high as possible, but this is limited according to permanent deformation requirements (Read and Collop, 1997). Harvey et al., 1995 found that for controlled-strain testing of a typical California asphalt concrete mix, an increase in asphalt content within the range tested (4.0, 4.5, 5.0, 5.5 and 6.0 percent, by weight of aggregate) results in an increase in laboratory fatigue life and a decrease in mix stiffness.

In summary, Read, 1996 stated that bitumen content affects the fatigue response in the following manner:

- The increase of the bitumen content, within a particular range, will increase the fatigue resistance of a mixture, and
- For a given mixture there is optimum bitumen content for fatigue and this is higher than that for the best resistance to permanent deformation.

### 2.5.3 Binder type and hardness

Stiffness and thermal susceptibility are the most important properties of bitumen for fatigue cracking resistance. These are normally expressed in terms of stiffness modulus, penetration, viscosity, softening point and penetration index (Whiteoak and Brown, 1990). The effect of asphalt type and hardness on fatigue characteristics of bituminous materials can be considered for by their effect on mix stiffness. Generally, in the controlled stress mode of loading, as the hardness of the bitumen is increased, thus the mixtures stiffness is increased resulting in a higher fatigue life at a particular stress level. The reverse will be true in the constant strain mode of loading. This has been verified experimentally for both cases: strain controlled by Epps and Monismith, 1972 and for stress controlled by Copper and Pell, 1974.

Brown et al. 1982 and Brown, 1988 recommended the use of hard bitumen (50pen) for thick bituminous base layers and a bitumen content of 4% in comparison to conventional base material which is made from 3.5% of 100pen bitumen. According to the analytical calculations this will give a considerable increase in fatigue life or allow a reduction in thickness, for a typical design situation, resulting in a considerable cost saving.

From the results of controlled strain tests on a range of mixtures, Kirk, 1967 has suggested that the fatigue strain at 1000000 applications of load is independent of asphalt hardness for penetration ranging from 50 to 200. In a more extensive testing program on mixtures containing asphalts with a range in penetration from various crude sources, Santucci and Schmidt, 1969 indicate that fatigue life in the controlled strain mode of testing is dependent upon asphalt hardness. This testing program also contained a series of tests conducted on artificially aged specimens. Their results indicate that the softer the asphalt the longer the fatigue life. In addition, Baaj et al., 2005 used the tension-compression test in constant strain and constant stress methods to study the effect of binder penetration as a part of binder characteristics effects on the fatigue damage rate of cylindrical specimens of different asphalt mixtures. It was concluded that mixtures produced with hard binders (16 pen)

show a lower damage rates than those made with intermediate (60 pen) and soft binders (84 pen).

### 2.5.4 Air voids content

Air voids related to binder content and binder viscosity have a significant effect on fatigue resistance. As the percentage of air voids in the pavement increases, either by design or lack of compaction, pavement fatigue life is drastically shortened. The influence of voids content, or compaction level, has been evaluated by many researchers and the results of which indicate that the lower the volume of air voids the higher the fatigue life (Judycki, 1991, Mashaan et al., 2014). Epps and Monismith, 1972 have also shown that the fatigue life of asphaltic concrete is reduced from 10 to 30 percent for each one percent increase over the normal content of air voids. The influence of air voids on controlled stress fatigue has been reported by Pell and Taylor, 1969. Results indicated that mixes containing high air void contents exhibit comparatively short fatigue lives. These data suggested that the structure of the voids (size, shape, and degree of interconnection) and their absolute volume might be significant. In the same perspective, it has been suggested that the voids properties are important; shape, degree of interconnection, and size. Even though no data has been found which quantify the effects (Epps and Monismith, 1972, Read, 1996). Similarly, Harvey et al., 1995 found that for controlled-strain testing, an increase in air void content results in a decrease in both; laboratory fatigue life mixtures stiffness. It was also found that air void content is more important than asphalt binder content relative to the design target values. For a typical California asphalt concrete mixture targeted at 5% binder content and 5% air voids will suffer a 30% reduction in fatigue life if the air void content exceeds its target by 1% but only a reduction of 12% if the asphalt content is less of its target by 1%.

### 2.5.5 Compaction efforts

Proper compaction is the most important factor for asphalt mixtures to have the same characteristics as that of in-service pavement. It is widely accepted that different laboratory compaction methods produce samples with different orientations and distributions of aggregates, and different distributions and

shapes of voids (Hartman et al., 2001). Air voids content is controlled by the compaction effort which is one of the most important variables affecting the fatigue resistance of bituminous mixtures (Harvey et al., 1994).

Rolling wheel compaction appears to be the most simulating because of its similarities with field compaction (in terms of compaction action and air void distribution). The roller compactor has also been found to produce specimens of greater fatigue strength compared to kneading and gyratory compaction (Sousa et al., 1993). Hartman et al., 2001 investigated the effect of different laboratory compaction procedures (roller, Marshall, vibrating hammer, and gyratory techniques) on the indirect tensile stiffness and fatigue properties of two standard Irish bituminous mixtures; 14 mm open graded sandy mix hot rolled asphalt (HRA) and a 20 mm continuous grading mix dense base coarse macadam (DBC). It was found that all fatigue lines for HRA mixtures seem to be very close to each other. This is also true, but to less extent, for the DBC mixtures except Marshall compacted specimens which show significantly lower fatigue strengths. For DBC, the Marshall compaction technique would probably produce specimens have significantly located in the low rank of indirect tensile fatigue strengths.

### 2.5.6 Environmental conditions

Environmental variables including temperature, moisture, and the alteration of material properties during the service life of asphalt pavements due to oxidative ageing are extremely important (Epps and Monismith, 1972). For instance, the temperature may significantly fluctuate creating a substantial change in the stiffness of asphalt binder and thus the stiffness and fatigue of asphalt aggregate mixtures (Epps and Monismith, 1972). The bituminous binder also exposures to atmospheric oxygen in the course of the long term of in-service pavements which results in more hardening (ageing) of the binder. This hardening will affect the modulus stiffness of asphalt mixtures and in turn their fatigue lives (Walubita et al., 2005). The following sections discuss the effect of environmental variables on the fatigue response of asphalt mixtures:

### 2.5.6.1 Moisture

The structural integrity of asphalt concrete can be deteriorated by water damage through either loss of cohesion in the bitumen or failure of the adhesive bond between the bitumen and aggregate (Kennedy, 1985, Airey and Choi, 2002). Epps and Monismith, 1972 indicated that no data are available on the effects of moisture on the fatigue response of asphalt concrete. It is possible that the absorption of moisture by mixtures may lead to a reduction in stiffness and a potential reduction in fatigue life, but this has not been conclusively demonstrated yet. More recently, Virgili et al., 2008 indicated that conventional techniques commonly used for asphalt testing do not take into consideration the combined action of environmental factors; temperature and water, and repeated loading which may affect adversely mix design performance. It was found that fatigue damage process of asphalt pavements can be considerably accelerated by environmental factors such as; moisture and temperature. However, the moisture influence being more detrimental than the temperature. Lu and Harvey, 2008 also found that moisture conditioning duration and moisture content have less effect on the extent of moisture induced damage in fatigue tests. It was also recommended that the typical 4PB fatigue test conducted at 20˚C, 10 Hz, and 200με can distinguish between mixes of different moisture sensitivities and rank them. In addition, Barra et al., 2012 observed also a conclusive reduction in the fatigue life of asphalt mixes due to water immersion and that effect can be more intense when including temperature influence leading to reduce the predicted design period. Moreover, Jaskula and Judycki, 2014 found a decrease in the fatigue life of open graded asphalt base course material by water and detrimental frost damage which could be critical to the service life of asphalt pavements. Finally, Teresa and Rodrigo, 2016 found that water in standard conditions has very little influence on fatigue damage.

With regard to healing perspective, Mehrara and Khodaii, 2015 carried out cyclic IDT (cyclic indirect strength tests) tests on asphalt mixture specimens exposed to moisture damage. It was found that moisture damage does not significantly affect the potential recovery of asphalt mixture. Further, Sol-Sánchez et al., 2015 applied a rest period at 5˚C for 60 days after moisture conditioning (specimens immersed in water at 40˚C) of the same period. It was found that

an important recovery of both mixtures properties; stiffness modulus and indirect tensile strength tested at 20˚C can be observed signifying that moisture damage in the mixture is a reversible process. In the same perspective, Apeagyei et al., 2014 found similar findings. However, Mannan et al., 2017 demonstrated that the healing potential of asphalt binder was significantly influenced by the moisture which reduced the healing rate of asphalt binder in the long-term.

### 2.5.6.2 Ageing

Ageing of bituminous binder is a phenomenon which can significantly affect paving materials durability under long-term performance. That generally takes place because the asphalt binder experiences a gradual hardening (ultimately perpetual hardening) due to two factors. The first factor is the oxidation process, which is a chemical reaction that happens when the oxygen in the air attacks the asphalt material resulting in more polar compounds of strong associations with each other. Volatilisation is the second factor affects the hardening of bitumen. It is evaporation of the lighter hydrocarbons, volatile or oily constituents, from the bituminous material to the air or from the aggregate or from both (Glover, et al., 2005). Additionally, Wu, 2009 stated that as the bitumen is hardening, the asphalt concrete mixture will turn into brittle (stiff) material and its ability to resist stresses and strains induced by traffic may significantly decrease. Deterioration of the pavement may result due to induced cracking. The adhesion between the bitumen and aggregate can also be weakened due to excessive hardening. This weakness can result in a loss of materials at the surface of pavement and increase the risk of fatigue cracking.

The effect of ageing on fatigue characterisation of asphalt mixtures has been investigated by many researchers. Vallerga et al., 1967 performed constant stress tests on asphalt mixtures made with un-aged and aged bituminous binders. The results indicated that mixtures with harder asphalt binders produced high stiffness moduli and in turn longer fatigue lives. However, the slopes of initial strains versus fatigue lives relationships were nearly identical for all mixtures. Jimenez and Gallaway, 1962 have presented a similar relationship between asphalt penetration and fatigue life. In addition, Harvey et

al., 1995 tentatively found that the applied long-term ageing of (0, 3, and 6 days) has a slight influence on the laboratory fatigue life of typical California asphalt mixtures using 3-PB test at 10 Hz, 19±1˚C and 150 and 300με. In addition, they indicated that ageing was influenced by air void content to a great extent. Further study by Harvey and Tsai, 1997 found that the influence of ageing on the predicted fatigue life was binder type dependant. However, there was no significant effect of LTOA on beam fatigue life. Nunn et al., 1997 surveyed a number of in-service truck roads and motorways in the UK and found no detrimental effect of age hardening in the lower asphaltic layers. In these pavement, age hardening was shown to reduce pavement deflection over time and reduce the risk of fatigue cracking. However, it is still essential that bitumen in the surface layer should remain ductile and does not harden significantly. Raad et al., 2001 carried out an investigation to study the influence of field ageing on the fatigue performance of two California mixes; conventional asphalt concrete dense graded (CAC-DG) and asphalt-rubber hot mix gap-graded (ARHM-GG). Laboratory fatigue tests were conducted in strain controlled mode using beam specimens cored from an old pavement section of 10 years in southern California. These tests were performed at 22C˚ and –2C˚ to determine both stiffness and fatigue results which were compared with previous available data for unaged materials. It was indicated that a reduction in the beam fatigue life of CAC-DG resulted due to field ageing for the testing conditions used in the study. This reduction was more significant for tests run at –2˚C than at 22˚C. The ageing of ARHM-GG had a negligible effect on the fatigue life at 22˚C while the reduction in the fatigue life of ARHM-GG at –2˚C was more severity but less significance than CAC-DG. Raad et al., 2001 also evaluated new pavement construction and overlaid pavement sections, the predicted fatigue life for ARHM-GG was longer than for CAC-DG, in both aged and unaged conditions. Ageing of the CAC-DG could be detrimental to pavement fatigue. In comparison, ageing of ARHM-GG showed better fatigue performance.

On the other hand, Walubita et al., 2005 indicated that ageing of asphalt concrete mixtures should be incorporated in the fatigue analysis and design due to the adverse influence on their healing properties and in turn fatigue resistance. Moreover, Walubita, 2006 concluded that HMA resistance to fatigue cracking and its ability to heal has been reduced due to binder oxidative ageing

and this resistance is both environmental condition and pavement structure dependent. Jung et al., 2007 investigated the binder oxidation effects on the fatigue response of hot-mix asphalt and found that the laboratory fatigue resistance measured in constant strain test decreases significantly due the binder oxidative hardening.

Sánchez et al., 2015 applied a rest period at 5˚C for 10 days after thermal ageing of 10 days at 80˚C to evaluate the potential recovery of aged mixtures by measuring the stiffness modulus and indirect tensile strength at 20˚C. The applied recovery method seems to be ineffective to heal the damage caused by thermal aging in cylindrical specimens asphalt mixtures. However, no indication of damage was highlighted by the measured stiffness modulus (increased after ageing) and the damage was only considered due to a decrease of less than 20% in the measured strength. Moreover, Sánchez et al., 2015 suggested further research to study the effect of these climate actions on mixtures resistance to fatigue cracking.

Finally, Teresa and Rodrigo, 2016 found a significant reduction in the fatigue cracking resistance of asphalt mixtures after ageing.

#### 2.5.6.3 Temperature

Temperature plays an important role in the viscoelastic behaviour of bituminous mixtures and the response of asphalt pavement layers subjected to external loadings (Hsu and Tseng, 1996). Pell and Taylor, 1969 have shown that the influence of temperature within limits can be explained in terms of specimen stiffness. As the temperature is reduced, the stiffness of an asphalt mixture is increased; thus for a specific stress the deformation (or strain) is less, resulting in longer fatigue life. Epps and Monismith, 1972 stated that in general, as the temperature is decreased, the fatigue life at a particular stress is increased.

Furthermore, constant stress diametral fatigue tests was conducted by Kim et al., 1991. A significant effect of temperature on the fatigue life was statistically demonstrated. Lower temperature results in the longer fatigue determined by using recoverable horizontal strain. While the reverse is true to that determined

by using maximum total horizontal train. However, Bonnaure et al., 1982 indicated that an increase in temperature could increase the beneficial effect on the fatigue life of asphalt concrete. Mandula and Olexa, 2017, found that the fatigue life of asphalt mixtures was positively influenced by increasing testing temperature to 27˚C. But this influence seems to be negative more than positive if the deterioration of complex modulus was examined. This deterioration was very rapid and there was only 10 % of the specimen life had complex modulus higher than 65 % of its initial value. Therefore, it was recommended to consider the reduction of stiffness modulus during the first phase of the sample life for a better design of asphalt pavement layers. Recently, de Mello et al., 2018 applied different methodologies to analyse the 4PB test results and it was found that temperature has an obvious influence on the fatigue performance. This effect need to be considered during the study of damage evolution of the in-service pavement.

## 2.6 Summary

Based on the review of literature of this study, the following arises either as research gaps or are still in need of further investigations:

- The combined effect of prevailing environmental conditions, such as ageing, moisture damage, and temperature fluctuation on fatigue resistance and healing susceptibility of asphalt mixtures have not been investigated enough in the literature and still in need of further research. It also needs to explore more about this combined influence on the resilient and complex dynamic moduli of asphalt mixtures.
- It was noticed that random or non-uniform rest periods between successive loadings have not been explored so far. It is required to study their effects on fatigue performance to simulate better the loading conditions of in-service pavement.
- Mixture parameters, such as air void contents, binder grades, and binder contents, should be considered in study the effect of environmental conditions on fatigue behaviour of asphalt materials for their relationship with different environmental factors.
- Combine the effect of both rest period types together in the same test; discontinuous loading and intermittent Loading has not been examined enough.
- The effect of different loading conditions, such as the type and shape of loading pulse with combined environmental factors needs to be considered in fatigue research.
- The influence of individual and combined long-term climatic conditions on fatigue characterisation requires extensive study.

# Chapter Three: Materials and Testing Methodology

## 3.1 Introduction

This chapter is divided into four main parts to describe briefly testing materials, fabrication of test specimens, testing methods and preparation of testing conditions that were utilised and applied to achieve the aim of this study.

## 3.2 Materials

### 3.2.1 Bitumen

In this research project, the experimental programme was carried out using three different unmodified penetration grade bitumens. It is well known that binder grades have a great influence on the ageing susceptibility of asphalt mixtures and in turn on their mechanical properties. Therefore a wide range of penetration grade bitumens include 10/20 Pen, 40/60 Pen and 100/150 Pen were selected. The physical properties are presented in Chapter Five.

### 3.2.2 Aggregate

Limestone aggregate from Tunstead quarry was used with the different asphalt binder grades in a continuously graded dense bitumen macadam (DBM) asphalt mixture. This used a maximum aggregate size of 14mm in accordance with the BS 4987-1:2005 Standard as shown in Figure 3.1.

Limestone was selected to use in manufacturing the asphalt mixtures due to its availability in England and common use in lower layers of pavement construction where the bottom-up fatigue cracking expected to occur. However, it is not used as aggregate in road surface courses because it typically has a low resistance to polishing (Dunford, 2013, Thom and Brown, 1987, BS 4987-1:2005). Limestone is also well known as hydrophobic substances and therefore has a good resistance to stripping (www.pavementinteractive.org).

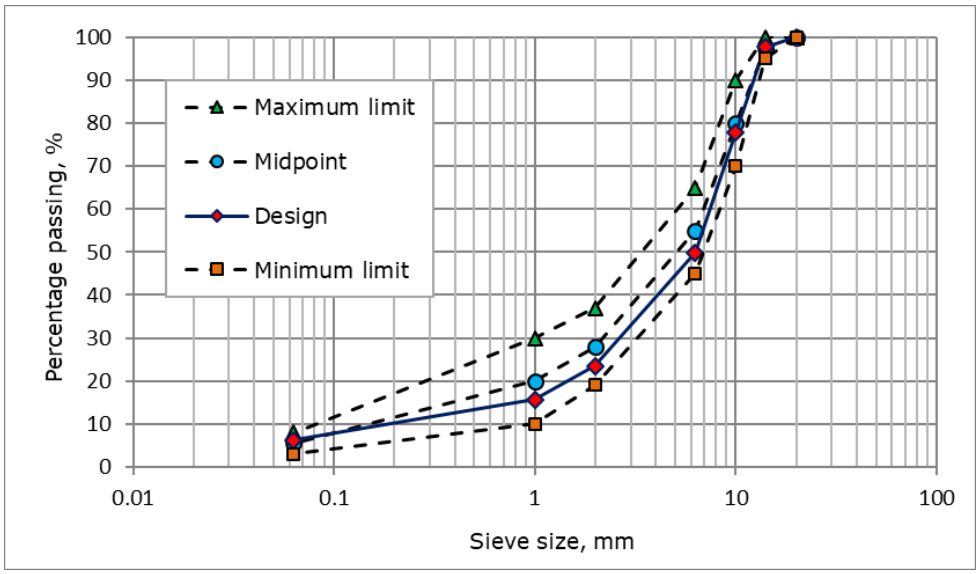



Figure 3.1: Gradation curve for 14mm DBM mixtures.

## 3.3 Fabrication of test specimens

### 3.3.1 Mixing and compaction

Laboratory mixing and compacting by roller compactor were carried out in accordance with BS EN 12697-35: 2004 and BS EN 12697-33: 2003 respectively. Once the aggregates, bitumen and filler are uniformly mixed and the temperature before compaction is within the specified range, a desired amount of hot mixture is poured into pre-heated square moulds to produce two types of slabs. First, 306 mm × 306 mm × 60mm for cylindrical cores and second 500 mm × 500 mm × 83mm for prismatic beams. Then the produced mixtures were compacted to the design slab thickness that achieves the target air void content. The rolling compactor was used in this study for its similarities with field compaction (i.e., compaction action and air void distribution). It was found that the roller compactor produces specimens of greater fatigue strength compared to kneading and gyratory compaction (Sousa et al., 1993, Hartman et al., 2001). More details were discussed earlier in Chapter two.

### 3.3.2 Cutting and trimming of test specimens

After the compaction of asphalt mixtures, the manufactured slabs have been left to cool and then extracted from the moulds for cutting and trimming stage. Figure 3.2 shows the procedures of mixing, compaction, cutting and trimming of asphalt concrete specimens. According to the requirements of each testing

machine the produced slabs were cored or sawed in different shapes to prepare the required test specimen shapes. For the Indirect Tensile Stiffness Modulus (ITSM) test and Indirect Tensile Fatigue Test (ITFT), five cylindrical specimens (cores) were cored and trimmed from each slab of (306 mm × 306 mm × 60mm) as shown in Figure 3.3. The required dimensions of these core specimens are 100 mm in diameter and 40 mm thickness. These two tests were used in this work because they are widely utilised in the United Kingdom for measuring the stiffness modulus and fatigue cracking resistance of cylindrical specimens cored from asphalt roads or manufactured in the laboratory. More details are shown in Chapters Four and Seven.

In addition, prismatic beam specimens were sawed and trimmed by sawing machine as shown in Figures 3.4 from the slab of (500 mm × 500 mm × 83 mm) to be used in the Four Point Bending Test (4-PBT). This test was used in this study as an example of tension compression flexural fatigue testing methods which is different from the ITFT. Because of the testing equipment complexity and long testing times, the flexural fatigue test is primarily a research test and is not a traditional test in the standards mix design or quality assurance testing in the United Kingdom.

The target dimensions of these prismatic beam specimens are 360 mm × 50 mm × 60 mm. After trimming the produced specimens, they were placed on absorbent papers and allowed to dry out at room temperature. Subsequently, the dry specimens should be labelled to be used in testing the required characteristics.

### 3.3.3 Volumetric properties

The dimensions of each specimen are measured and the specimens are then tested for bulk density as detailed in BS EN 12697-6: 2003. The bulk densities are used together with the maximum theoretical densities, which were determined on loose mix samples by the volumetric procedure BS EN 12697-5: 2009, to calculate the actual percentage of air voids of each test specimen according to BS EN 12697-8: 2003. The specimens were classified into different groups of air voids content as shown in the following chapters.

### 3.3.4 Storage

To prevent distortion of the cored and sawed specimens, they were stored in a dry atmosphere at 5˚C. Specimens were only removed from this controlled environment to be conditioned and tested at the required testing temperature and conditions.



Figure 3.2: Mixing, compacting, and sawing or coring for prismatic beam or core specimens.

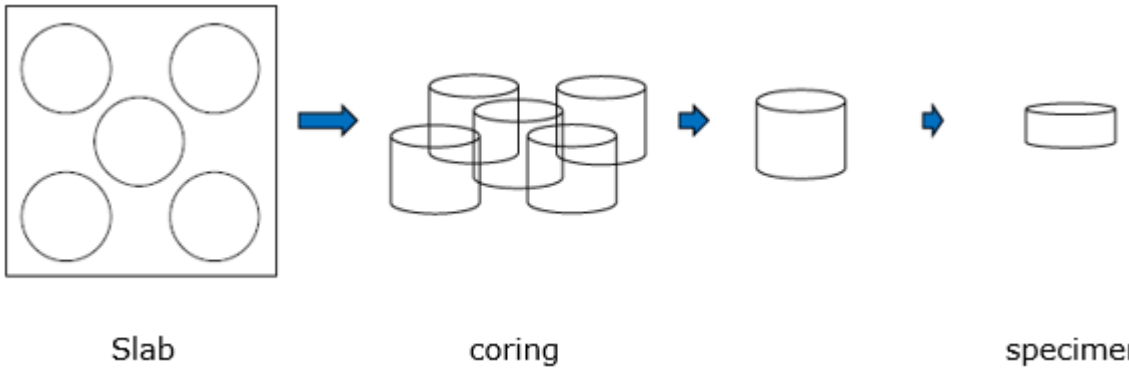



Figure 3.3: Coring and trimming procedure for ITSM and ITFT tests.

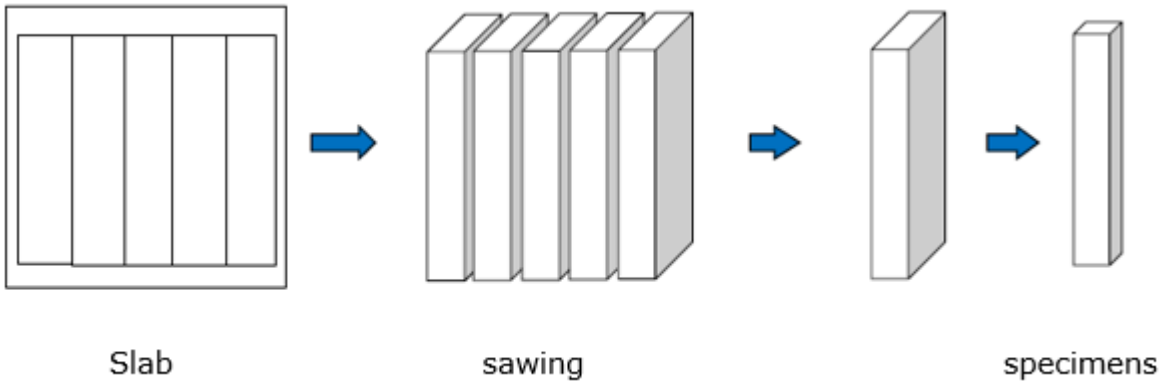



Figure 3.4: Sawing and trimming procedure for 4PB tests.

### 3.4 Preparation of testing conditions

In this study, the asphalt mixtures can be categorized according to the applied conditions into the following:

1- Control (reference) asphalt mixtures (no conditions were applied to these mixtures),
2- Immersed control asphalt mixtures in water (Moisture conditioning was applied to control mixtures in accordance with two different methods),
3- Short Term Oven Ageing (STOA) mixtures (STOA was applied to the control loose mixtures at 135(±3)˚C for 4h±5 minutes before compaction),
4- Long Term Oven Ageing (LTOA) mixtures (after STOA, LTOA was applied to compacted asphalt mixtures at 85(±2)˚C for 120(±0.25) hours), and
5- Long Term Oven Ageing (LTOA) mixtures immersed in water (after LTOA, moisture conditioning was applied to LTOA mixtures in accordance with two different methods).

The following sections explain the preparation of these testing conditions. The conditions of ageing and moisture sensitivity methods were applied to asphalt mixtures to simulate the field conditions as stated by the more traditional standards used in the UK (BS EN 12697-12:2008) or the quality assurance testing (British Board of Agrément (BBA) - Appendix A.2).

### 3.4.1 Ageing conditions

Ageing of asphalt mixtures was considered in this study as one of the main variables that affects the stiffness of asphalt mixtures and in turn fatigue resistance. Both ageing types were applied to the same mixture as following:

### 3.4.2 Short-term oven ageing (STOA)

Short Term Oven Ageing (STOA) of asphalt binders was typically applied to loose asphalt mixtures to simulates the effects of manufacture, transport and laying of hot mix asphalt (HMA). In this study, STOA was applied to the loose mixtures at 135(±3) ˚C for 4h±5 minutes before compaction according to AASHTO P-2002 as shown in Figure 3.5. This type of ageing simulates the hardening of the bitumen in the mixture preceding to in service period. In particular, mixtures production at hot mix plants, hauling and compaction stages. After that the loose mixtures were compacted using a roller compacter. In order to evaluate the effect of STOA on the progress of stiffness modulus from the virgin condition to LTOA circumstances, ITSM of short-term aged specimens was measured before moving the compacted specimens to the Long-Term Oven Ageing (LTOA) stage.




Figure 3.5: Short Term Oven Ageing (STOA) of loose mixture at 135˚C.

### 3.4.3 Long-term oven ageing (LTOA)

This conditioning can be carried out in accordance with AASHTO P-2002. The ageing simulates the hardening of the bitumen in the mixture subsequent to construction (in service). The practice should result in ageing representative of 5 to 10 years in service for dense-graded mixtures. The prepared specimens (cores or beams) were collected and supported in the wire mesh baskets or steel cages shown in Figures 3.6 and 3.7. Stainless steel ties can also be used with these cages to avoid specimens' distortion. Then the testing samples were placed on a rack in the forced-draft oven at a temperature of 85(±2) ˚C for 120(±0.25) hours. The specimens were left to cool after LTOA. After that they were collected once more to measure the stiffness modulus and fatigue characteristics. Figures 3.8 and 3.9 present the procedures of applying the LTOA to core specimens and prismatic beam specimens respectively.



Figure 3.6: Cages for core specimens.

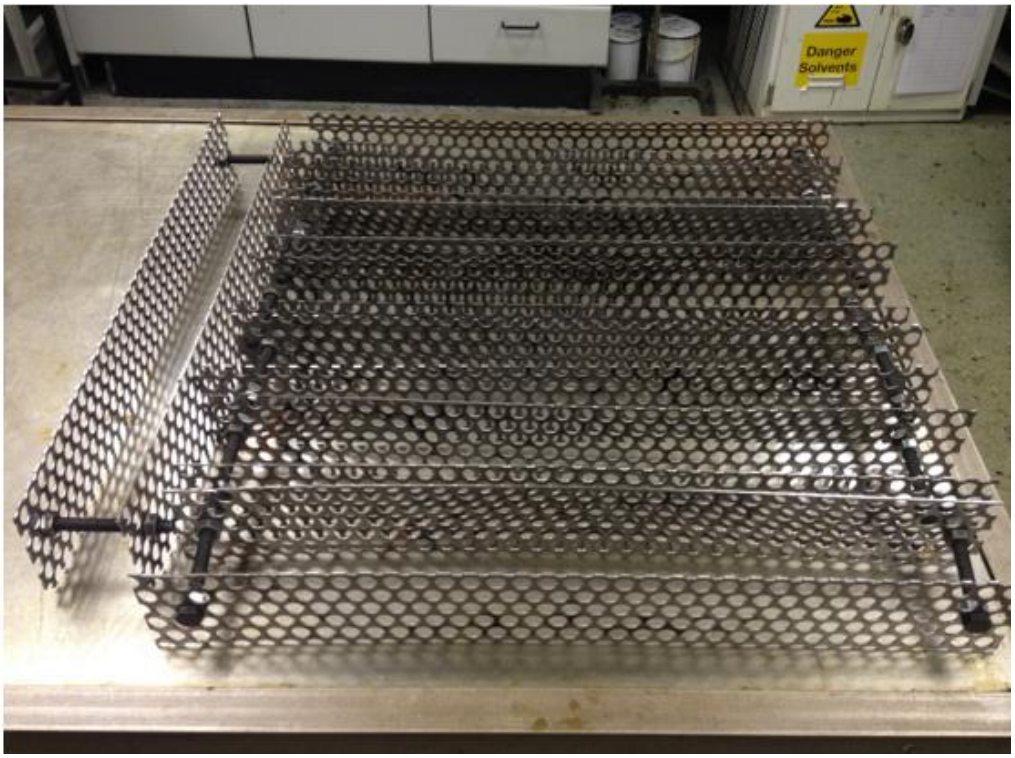



Figure 3.7: Cages for prismatic beam specimens.



Figure 3.8: LTOA for compacted core specimens at 85˚C for 120 hours.

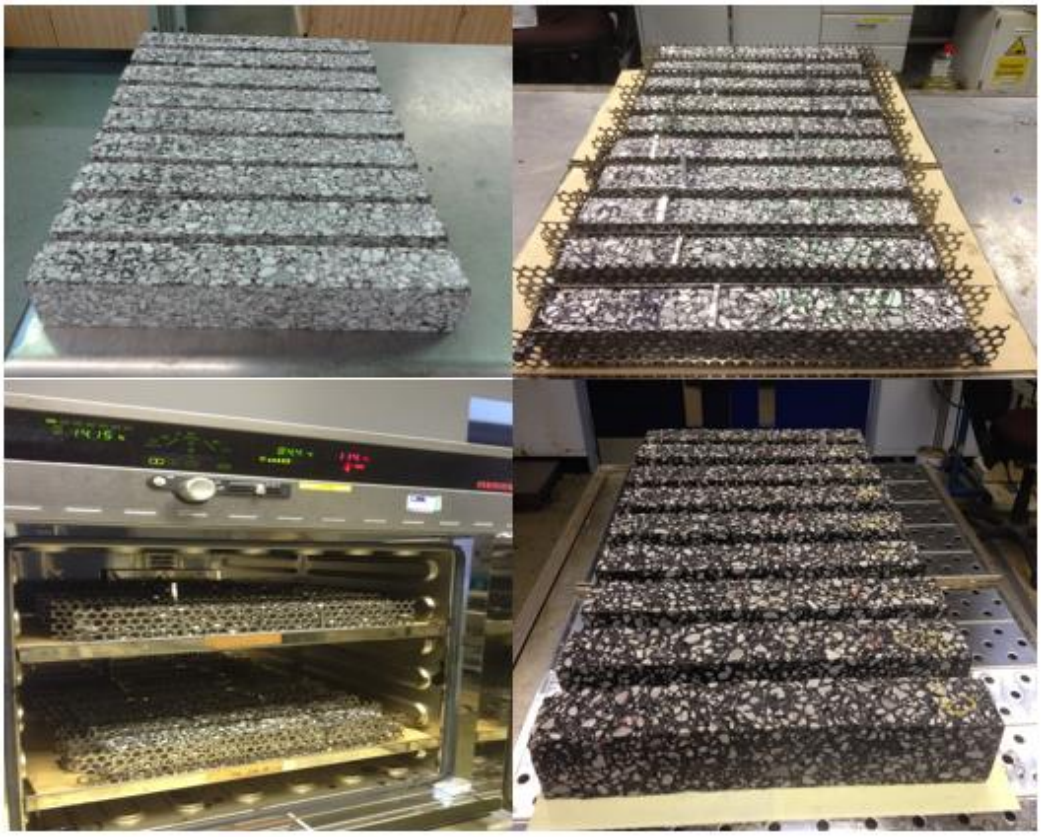


Figure 3.9: LTOA for compacted beam specimens at 85˚C for 120 hours.

### 3.4.4 Moisture conditioning

Moisture conditioning was considered in this study as one of the main variables that affects the stiffness of asphalt mixtures and in turn fatigue resistance. The effect of moisture was evaluated for two specimen sets; the control asphalt mixtures (un-aged) and LTOA asphalt mixtures. In this study, British Board of Agrément (BBA) - Appendix A.2: 2008 (BBA) protocol was applied to the specimen cores and BS EN 12697-12:2008 was applied to both cylindrical cores and prismatic beams.

#### 3.4.4.1 British Board of Agrément (BBA)

This protocol was applied to cylindrical core specimens in accordance with British Board of Agrément (BBA) - Appendix A.2: 2008 as follows:

1. Determine the unconditioned stiffness characteristics of the specimen in accordance with BS EN 12697-26:2012 for ITSM,
2. Place the specimens in the vacuum desiccator shown in Figure 3.10, cover it with distilled water at 20(±1) ˚C, seal the apparatus, and apply a partial vacuum of 510(±25) mm Hg or 680(±33) mbar for 30(±1) minute. Remove the specimen from the vacuum desiccator,
3. Place it in a hot water bath at 60(±1) ˚C for 6(±1) hours. The samples may be supported by a wire mesh baskets if necessary to minimize distortion.
4. Remove the specimen from the hot water bath and immediately place it in a cold water bath at 5(±1) ˚C for 16(±1) hours.
5. Remove the specimen from the cold water bath and immediately place it in a water bath at 20(±0.5) ˚C (or at the specified testing temperature) for at least 2 hours.
6. Determine the conditioned stiffness/fatigue characteristics of the specimen in accordance with BS EN 12697-26:2012 for ITSM and BS EN 12697-24:2012 for ITFT.

#### 3.4.4.2 BS EN 12697-12:2008

BS EN method was carried out as following:

1. Place the wet subset of specimens on the perforated shelf in the vacuum container shown in Figure 3.10 and then fill it with distilled water at (20 ± 5)˚C to a level at least 20 mm above the upper surface of the test specimens,

2. Apply a vacuum to obtain an absolute (residual) pressure of (6.7 ± 0.3) kPa within (10 ± 1) min. Decrease the pressure slowly to avoid expansion damage of the specimens,
3. Maintain the vacuum for (30 ± 5) min. Then let the atmospheric pressure slowly into the vacuum container,
4. Leave the specimens submerged in water for another (30 ± 5) min,
5. Calculate the volume of the specimens in accordance with one of the methods in EN 12697-6:2003. Reject any specimen which has increased by more than 2 % in volume,
6. Place the wet subset of specimens in a water bath at (40 ± 1) ˚C for a period of 68 h to 72 h.

A different vacuum desiccator was manufactured and used for prismatic beam specimens as displayed in Figure 3.11. Caution should be considered during the vacuuming of beam specimens to avoid distortion.

Finally, Table 3.1 shows a summary of the applied testing conditions in this work.




Figure 3.10: Applied vacuum to core specimens.



Figure 3.11: Applied vacuum to prismatic beam specimens.

Table 3.1: Testing conditions.

<table>
<tr><th colspan="2">Mixtures exposed to testing conditions</th></tr>
<tr><td colspan="2">Control mixture, dry condition (No specific conditions were applied)</td></tr>
<tr><td rowspan="2">Control mixture, immersed in water according to:</td><td>BBA method (vacuum the compacted mixture at (68 ± 3.3) kPa for (30 ± 1) minutes and immersed in water at 60˚C for 6 hrs then at 5˚C for 16 hrs).</td></tr>
<tr><td>BS EN method (vacuum the compacted mixture at (6.7 ± 0.3) kPa for (30 ± 5) minutes and immersed in water at 40˚C for 72 hours).</td></tr>
<tr><td colspan="2">STOA mixture, dry condition (loose mixtures exposed to 135˚C for 4 hours)</td></tr>
<tr><td colspan="2">LTOA mixture, dry condition (after STOA for 4 hrs at 135˚C the compacted mixture exposed to 85˚C for 120 hours).</td></tr>
<tr><td rowspan="2">LTOA mixture, (after STOA for 4 hrs at 135˚C the compacted mixture exposed to 85˚C for 120 hrs) then immersed in water according to:</td><td>BBA method (vacuum the compacted mixture at (68 ± 3.3) kPa for (30 ± 1) minutes and immersed in water at 60˚C for 6 hrs then at 5˚C for 16 hrs).</td></tr>
<tr><td>BS EN method (vacuum the compacted mixture at (6.7 ± 0.3) kPa for (30 ± 5) minutes and immersed in water at 40˚C for 72 hours).</td></tr>
</table>

## 3.5 Testing methods

A wide range of test methods were carried out in this work. These tests can be divided into main and supplementary tests.

### 3.5.1 Main tests

These tests were performed on asphalt mixtures that were exposed to different testing conditions to find their resilient stiffness modulus, complex dynamic modulus, fatigue cracking resistance, and healing characteristics. Some indices were calculated from the results of these testing methods to assess the individual and combined effect of ageing and moisture damage. These tests include the following:

1. Indirect Tensile Stiffness Modulus Test (ITSM), BS EN 12697-26:2012
2. Complex Modulus Test, BS EN 12697-26:2012
3. Indirect Tensile Fatigue Test (ITFT), BS EN 12697-24:2012
4. Four Point Bending Test (4PBT), BS EN 12697-24:2012
5. Healing Test using Four Point Bending machine and Nottingham Asphalt Tester (NAT).

### 3.5.2 Supplementary tests

The Supplementary tests were performed on the neat and recovered asphalt binders from mixtures exposed to different testing conditions to find their rheological and physical properties; shear complex modulus, penetration grade and softening point. The purpose for conducting these supplemental tests was to find any evidence that can benefit the understanding of some surprising results. These tests are:

1. Penetration test, BS EN2000-49:2007 Standard,
2. Ring and Ball Softening Point test, BS EN 2000-58:2015 Standard,
3. Dynamic Shear Rheometer (DSR), AASHTO T 315-12.

More details about the main and supplementary tests will be presented in following chapters with discussion of each test results. Finally, a flow chart is presented in Figure 3.12 to show a summary of the testing methodology of this work.

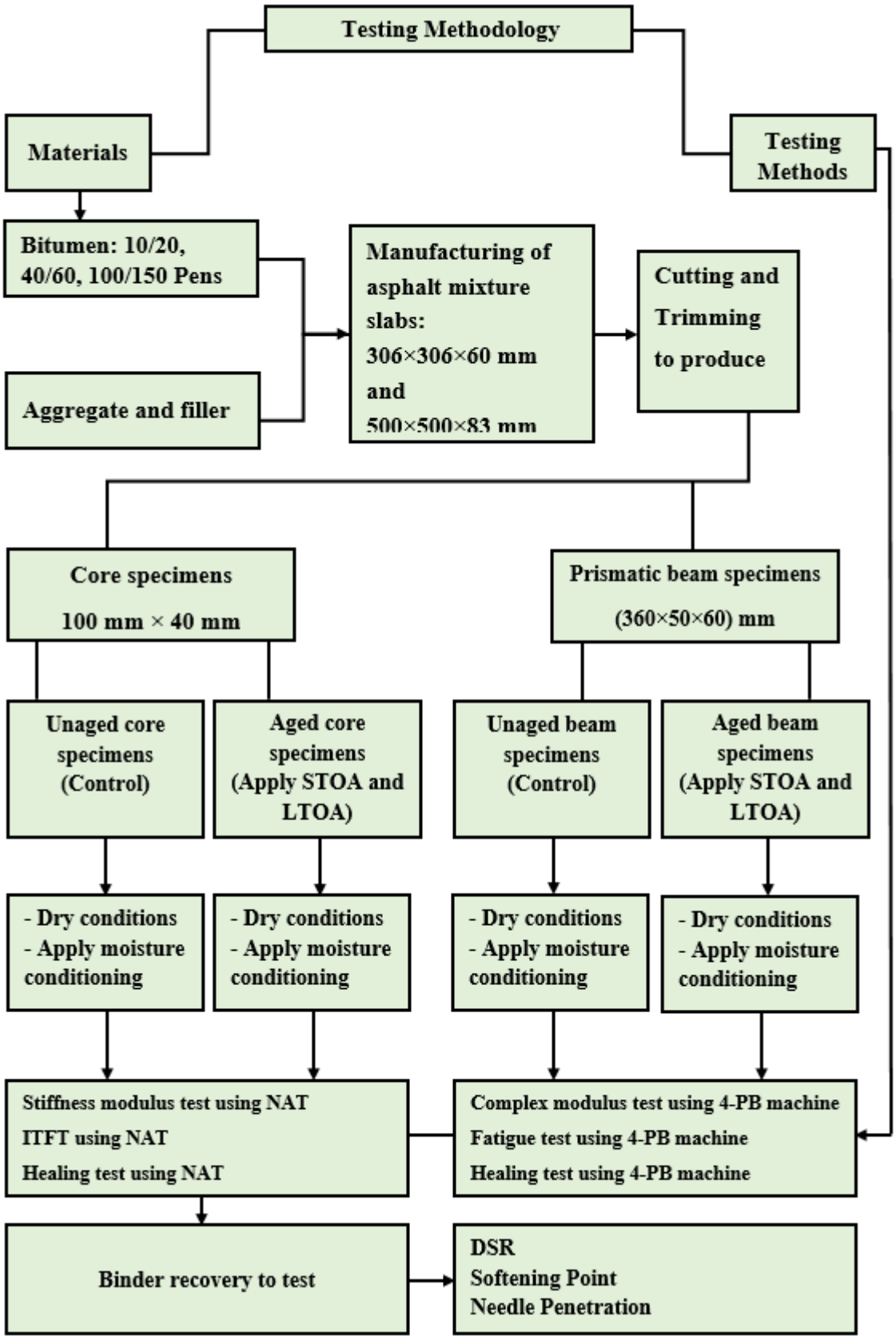



Figure 3.12: Flow chart of testing methodology.

# Chapter Four: Evaluation of Environmental Effects on Stiffness Modulus of Asphalt Mixtures

## 4.1 Introduction

The stiffness modulus of bituminous materials is an important parameter of their capacity to resist traffic loads and weather conditions. It is also important for the evaluation of fatigue performance of these materials which is the main theme of this study. Therefore, the assessment of stiffness modulus of asphalt-aggregate mixtures is essential for a proper design period of the in-service pavement structure. Previously, extensive studies have investigated the influence of different factors; different material constituents, testing conditions and testing methods to quantify the stiffness modulus of asphalt concrete mixtures (Schmidt and Graf, 1972, Pell and Cooper, 1975, Deacon et al., 1994 Di Benedetto and Roche, 1998, Airey and Choi, 2002. Zaumanis et al., 2017).

The primary environmental factors affecting bituminous paving mixtures durability are bituminous binder hardening and moisture damage. Age hardening of the bituminous binder is manifested as an increase in its stiffness modulus or viscosity. Oxidative ageing of asphalt binder and asphalt mixtures is one of the important factors contributing to serious pavement distresses such as fatigue and thermal cracking (Chen and Huang, 2000, Woo et al., 2008). The ageing can be grouped into two categories; first, Short-term ageing represents hardening of asphalt binder during mixtures production at hot mixing plants, hauling and lay-down operations. Secondly, long-term ageing represents in-situ asphalt binder hardening. Over time, both short and long-term ageing result in a gradual increase in the stiffness of hot mix asphalt (Houston et al., 2007).

Another phenomenon, moisture damage is generally identified as a loss of adhesion (stripping or adhesive failure) between the bitumen and aggregate interface and/or loss of cohesion (cohesive failure) in the asphalt mixture. Loss of cohesion results in a strength and stiffness reduction of asphalt mixtures and thus reduces the pavement structure capacity to resist traffic loads and the resulting stresses/strains. Loss of bond between the bitumen binder and aggregate results in a further reduction of pavement support. Therefore, both

moisture damage mechanisms can lead to serious distresses of asphalt pavement such as cracking and rutting and in turn the complete deterioration of pavement structure (Airey and Choi, 2002, Zaumanis et al., 2017).

Accordingly, the stiffness of asphalt mixtures is supposed to be decreased by the effect of moisture damage and increased due to ageing of asphalt binder. Therefore, a new perspective is seriously required to understand the combined influence of these environmental conditions on the stiffness modulus of flexible pavement structures to ensure a proper design period of the in-service pavement structure.

## 4.2 Plan of Chapter Four

This chapter discusses and analyses the individual and combined effect of environmental factors on the stiffness modulus of asphalt mixtures. Specifically, it examines the susceptibility of paving mixtures manufactured with different binder grades; 10/20 Pen, 40/60 Pen and 100/150 Pen to the effect of different environmental factors. These factors; temperatures, ageing and moisture damage were carefully selected to investigate their influences individually and simultaneously as environmental variables.

This chapter also involves the measurements of different stiffness indices obtained from performing the Indirect Tensile Stiffness Modulus (ITSM) test (BS EN 12697-26:2012). Two indices: Ageing Index (AI) and Index of Retained Stiffness Modulus (IRSM) were used to assess the effect of temperatures, moisture damage and ageing on the stiffness modulus of asphalt mixtures which is defined as the ratio of repeated stress to reversible strain (Olard et al., 2006).

Fourier transform infrared spectroscopy (FTIR) was also used as a technique to describe the chemical changes in the recovered bitumen. It was limited to characterise the ageing behaviour of two binders 40/60 Pen and 100/150 Pen.

## 4.3 Testing methods

### 4.3.1 Indirect Tensile Stiffness Modulus Test (ITSM)

Test methods; indirect tensile strength test, stiffness modulus test, and dynamic modulus test are recommended to evaluate the effects of ageing on asphalt mixtures. More tests on recovered asphalt binders will also be important such as chemical fractionation, micro viscosity and ductility tests (Bell, 1989). The ITSM is the most common test for stiffness measurement of bituminous mixtures in the UK. Brown, 1995 reported lots of advantages from carrying out this test. It is suitable for cylindrical specimens manufactured in the laboratory or cored from the field, typically either 100 or 150 mm in diameter. Another advantage of this test is that the test specimen does not need to be long, ITSM of 30 to 80mm specimen thickness can be measured. This is suitable for specimens cored from asphalt pavements. In addition, it can be quickly carried out compared to other methods of stiffness measurement of asphalt mixtures. It was also reported by Brown, 1995 that up to 100 specimens can be tested in a working day. It offers a suitable means of applying tensile stress under compressive loading. Moreover, he stated that the load to be applied to the test specimen is lower than that required, for example in a direct compression testing method. Finally, one of the most important advantages of this test is measuring the modulus of the same samples before and after any specific conditions and evaluating its evolution.

In this study, ITSM was selected to measure the stiffness modulus of 14mm DBM manufactured with three binder grades in different conditions. These conditions include ageing the samples of different binder grades and submerging them in water to compare their stiffness with that of virgin and dry conditions. This results in assessing the Ageing Index (AI) and Index of Retained Stiffness Modulus (IRSM) of manufactured specimens.

#### 4.3.1.1 Test description

The non-destructive stiffness modulus test, ITSM, was carried out for measuring the stiffness modulus of 14mm DBM in accordance to the BS EN 12697-26: 2012. In this test, a compressive load pulse is applied by means of a load actuator along the vertical diameter of a cylindrical specimen. The resultant

(indirect tensile) peak transient deformation is measured along the horizontal diameter using linear variable displacement transducers (LVDTs), whereas the vertical load is measured using a load cell as shown in Figure 4.1.
The following test parameters were applied in this test:
(a) Test temperature: 10˚C and 20˚C
(b) Poisson's ratio: 0.35
(c) Loading rise-time: 124 ms
(d) Peak transient horizontal deformation: 5 μm.
The captured signals from the transducers were used to calculate the stiffness modulus as a function of vertical load, horizontal deformation, specimen dimensions and an assumed Poisson's ratio for the tested material. The following relationship was applied to calculate stiffness modulus $S_m$ (in MPa):

$$S_m = \frac{F}{z.h}(\upsilon + 0.27) \qquad 4.1$$

Where F is the peak value of the applied vertical load (N), z is the peak horizontal diametric deformation resulting from the applied load (mm), h is the mean thickness of the test specimen (mm), and υ is Poisson's ratio for the bituminous mixture at the test temperature.

During the ITSM test, ten conditioning pulses are followed by five test pulses, which are used to determine an average stiffness modulus. The test is then repeated after rotating the specimen through 90° and the average stiffness from the two tests is recorded as the indirect stiffness modulus of the asphalt mixture specimen.

According to the followed standard BS EN 12697-26: 2012, if the mean value of the stiffness modulus from this test shall be within +10 % or −20 % of the mean value recorded for the first test (first axis), the mean for the two tests (two axis) shall be calculated and recorded as the stiffness modulus of the tested specimen.

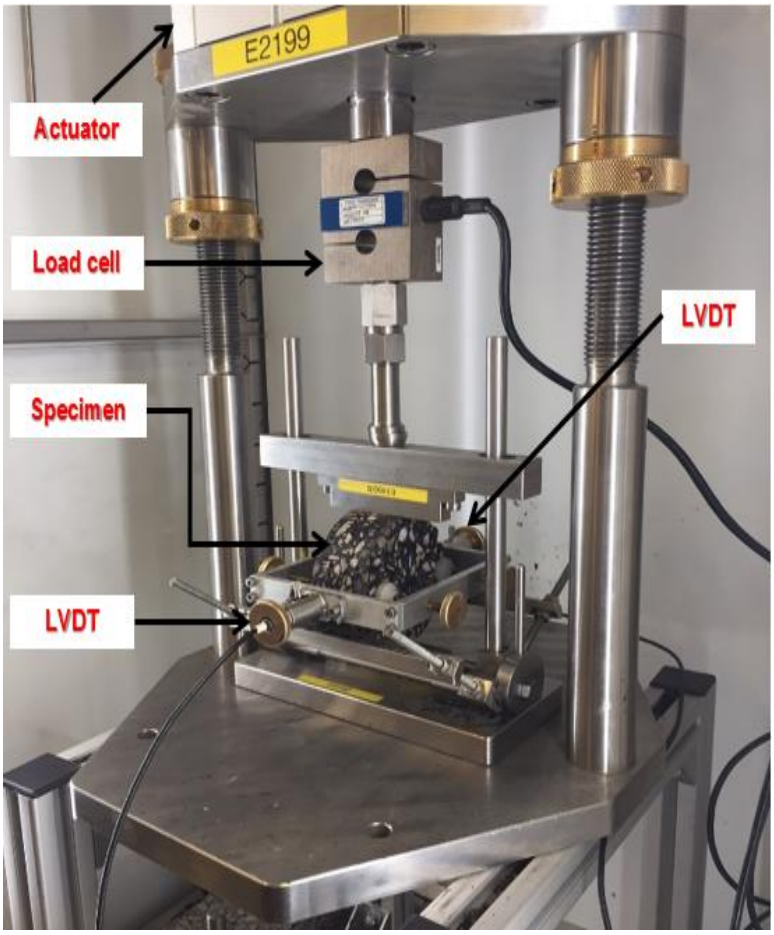



Figure 4.1: Indirect Tensile Stiffness Modulus Test (ITSM).

### 4.3.2 Fourier Transform Infrared Spectroscopy (FTIR)

Fourier transform infrared (FTIR) spectroscopy is one of the techniques that describe the chemical changes in the bitumen due to ageing. It is sensitive and easy to apply to bituminous materials (Lamontagne, 2001, Ouyang et al., 2006, Mouillet et al., 2008, Wu, 2009, Yang et al., 2014, Marsac et al., 2014; Alfaqawi, 2018). The concept of this test involves the excitation of investigated materials with Infra-Red light to quantify the various kinds of molecular bonds by characterising the absorption bands in the infra-red light spectrums. The major functional groups formed through the process of oxidative ageing are Carbonyl groups characterised by C=O and Sulfoxide groups characterised by S=O. Many researchers have demonstrated that the formation of carbonyl changes the physical properties of asphalt binders and therefore it can be used as an index to quantify the evolution of chemical changes may occur in these binders as a result of ageing (Lamontagne, 2001, Ouyang et al., 2006, Wu, 2009,

Mikhailenko et al., 2016). Figure 4.2 shows an example of FTIR absorbance spectrum for an aged binder sample (Hofko et al., 2018).

In this study, a Bruker Tensor 27 infrared machine (FTIR spectrometer) was used to measure the oxygenated functions or ageing indices (Carbonyl C=O and Sulfoxide S=O) of the neat and recovered bitumen before and after applying ageing and moisture conditions to different asphalt mixtures. The used spectra were the average of 32 scans (per sample) with a 4 $cm^{-1}$ resolution and a band range of 4000 to 400 $cm^{-1}$. The FTIR crystal was cleaned with ethanol before each test to place approximately 0.5 g of the bitumen as a solid (neat or recovered) at ambient temperature on the crystal. The scan was conducted and the average of the 32 scans was recorded (Lamontagne, 2001, Alfaqawi, 2018).

Lamontagne, 2001 introduced a spectrometric index calculation method by calculating the structural and functional indices from measuring the area below the absorbance spectrum around a peak as following:

$$\text{Carbonyl index} = \frac{A_{1700}}{\sum A} \quad 4.2$$

$$\text{Sulfoxide index} = \frac{A_{1030}}{\sum A} \quad 4.3$$

$\Sigma A = A_{1700}+A_{1600}+A_{1460}+A_{1376}+A_{1030}+A_{864}+A_{814}+A_{743}+ A_{724}+A_{(2953, 2923, 2862)}$.

It was found that the increase in carbonyl index was correlated to other ageing indices which calculated from the physical and rheological properties of the bitumen such as softening point, viscosity, and complex modulus while the sulfoxide Ageing Index was less correlated (Lu and Isacsson, 2002, Lu et al., 2008, Abdullah et al., 2013, Yut and Zofka, 2014, Alfaqawi, 2018).

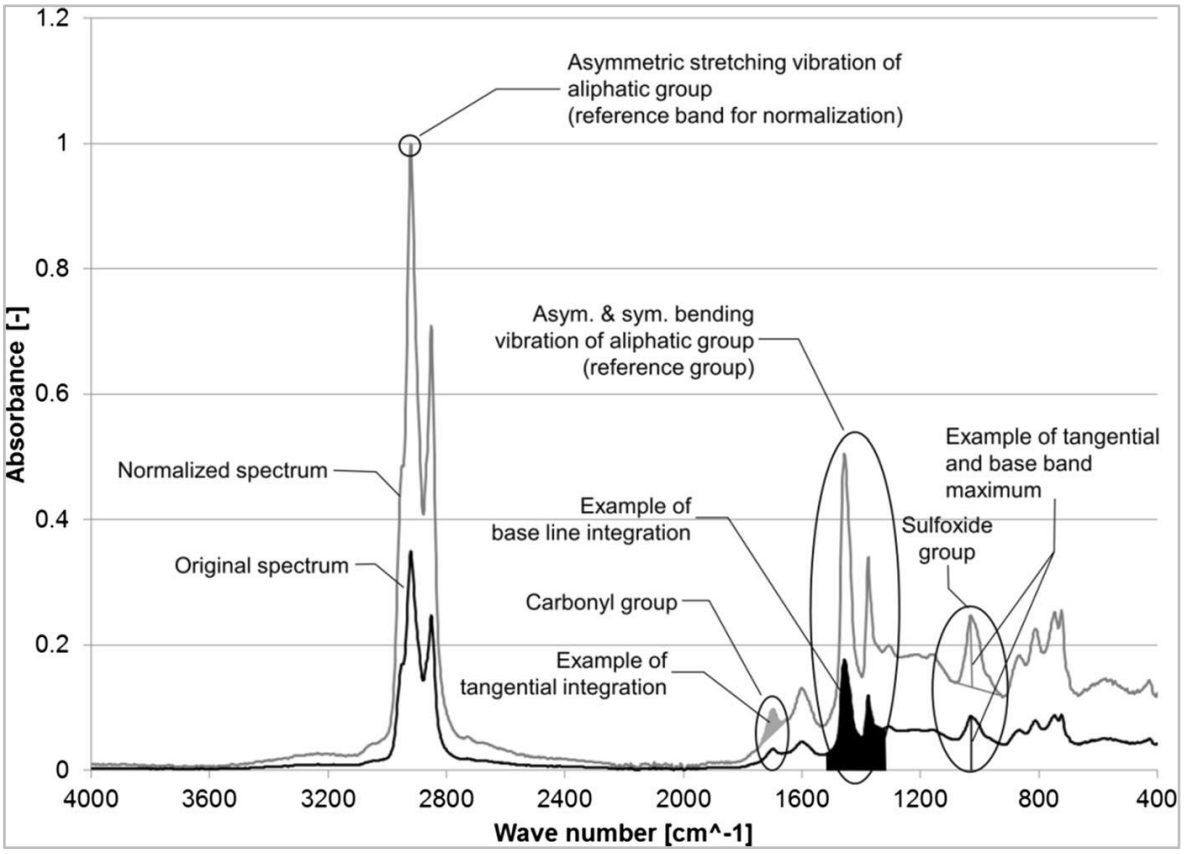



Figure 4.2: Example of FTIR absorbance spectrum for an aged binder sample (Hofko et al., 2018).

### 4.4. Investigated variables

The environmental factors effect can be expressed in terms of two indices. Firstly, Ageing Index (AI) and secondly, Index of Retained Stiffness Modulus (IRSM). In the first part, the stiffness modulus was measured using the Indirect Tensile Stiffness Modulus (ITSM), to evaluate the effect of testing temperatures, air voids content, binder grades and binder contents on the Ageing Index of bituminous materials. To achieve this objective, two sets of 14mm DBM (Dense Bitumen Macadam) cylindrical test specimens were manufactured with the variables shown in Table 4.1. ITSM was measured for the first set which was without any ageing conditions and categorized as control mixtures ($ITSM_{control}$). The second set involves two ageing phases applied to the same specimen; short-term oven ageing (STOA) and long-term oven ageing (LTOA). In details, ITSM was measured for the second group of specimens at two stages; after compaction, coring, and trimming of STOA loose mixtures ($ITSM_{STOA}$), then after applying the LTOA condition to the same compacted specimens ($ITSM_{LTOA}$) which

experienced STOA. This results in assessing the Ageing Index of the same specimen to be more reliable as following:

$$Ageing\ Index\ (AI) = ITSM_{LTOA}/ITSM_{STOA} \qquad 4.4$$

The conditioning of STOA was applied to loose mixtures at 135(±3)˚C for 4h±5 minutes and LTOA was applied to compacted specimens at 85(±2)˚C for 120(±0.25) hours. More details were explained earlier in Chapter Three.

The investigated variables include three binder bitumen penetration grades; 100/150, 10/20, and 40/60 at 5% binder content (BC) of each. A further binder content of 6% was applied to 40/60 Pen to examine the effect of binder content on ageing. In addition, specimens of 40/60 Pen and 5% BC manufactured with different air voids content were collected and sorted out into groups of (2, 4, 6, 8, 10, and 12%) to study air voids influence on Ageing Index. DBM mixtures of 10/20 and 100/150 Pens are classified into three air voids content groups; (4, 8, and 12%). Moreover, only two sets of specimens of air voids content; 8% and 12% from DBM of 40/60 Pen and 6% BC were tested for ITSM. Finally, all prepared 14mm DBM with these variables were tested at 10˚C and 20˚C to evaluate testing temperatures effect on Ageing Index. Table 4.1 presents a summary of these variables and a comparison between their influences takes place in this study as following:

Table 4.1: Summary of investigated variables.

| **Variables** | **Binder grades** | | | |
|---|---|---|---|---|
| | **40/60** | **100/150** | **10/20** | **40/60** |
| **Binder content, %** | 5.0 | 5.0 | 5.0 | 6.0 |
| **Air voids content, %** | 2.0, 4.0, 6.0, 8.0, 10.0, 12.0 | 4.0, 8.0, 12.0 | 4.0, 8.0, 12.0 | 8.0, 12.0 |
| **Testing temperatures, ˚C** | 10<br>20 | 10<br>20 | 10<br>20 | 10<br>20 |

## 4.5 ITSM results

### 4.5.1 Effect of air voids content and testing temperature on ageing

To evaluate the relationship between air voids content and Ageing Index (AI) from one perspective and between testing temperatures and Ageing Index from other perspective, 14mm DBM specimens manufactured with the three specified binder grades were collected and sorted according to the specified air voids content and tested at 10˚C and 20˚C for ITSM. First, for 14mm DBM manufactured with 40/60 Pen and 5% BC, a comparison between ITSM of control, STOA, and LTOA mixtures is presented in Figure 4.3 at two different testing temperatures, 10˚C and 20˚C and at different air voids content (2, 4, 6, 8, 10, and 12%). Table 4.2 shows the errors of the average values of all ITSM results presented in Figure 4.3. It can be observed that ITSM increased due to applying STOA and LTOA to asphalt mixture specimens. It also increased due to the decrease of testing temperature from 20 to 10˚C regardless of mixtures were control (unaged) or aged (STOA or LTOA). On the other hand, it decreased as the air voids content increased.

The increase of ITSM due to ageing (STOA and LTOA) might be attributed to an increase in the content of two components of the asphalt binder; sulfoxide and carbonyl. This increase causes a transformation of lightweight small molecules to large contributing to increase the quantity of large molecules. Consequently, higher molecular weight molecules results in the stiffness increase of the binder and in turn of the asphalt mixture (Lu and Isacsson 2002, Liu et al., 2013, Aguiar-Moya et al. 2017).

The FTIR test was conducted on 40/60 Pen and on the recovered binder from mixtures manufactured with the same binder and exposed to LTOA. It can be seen from the absorbance graph presented in Figure 4.4 the increase in both components sulfoxide (S=O) and carbonyl (C=O) at wave numbers; 1030 and 1700 respectively.

Moreover, the increase of ITSM at the different air voids content due to the decrease of testing temperature can be attributed to the binder consistency. Anderson et al., 1994 stated that the magnitude and rate of the physical

hardening increases with decreasing temperature. In addition, Airey, 1997 stated that at low temperature, bitumen behaves as a glass-like elastic solid. Therefore, it seems that reducing the temperature from 20 to 10˚C motivated the bituminous binder to behave towards the zone of glassy solid rather than behaves as fluid (at intermediate temperature) or viscous fluid (at high temperature). This transition of the behaviour towards a glassy solid region increased the stiffness of bituminous material and in turn the stiffness of investigated mixtures at 10˚C.

The effect of air voids content on ITSM is also presented in Figure 4.3. Whether the mixture was control or exposed to STOA or LTOA, it was obviously found that the increase of air voids content from 2% to 12% resulted in the decrease of ITSM. The reason of this decrease can be explained in terms of the role of air voids increase in reducing the cross section area of the material which can be used to distribute the applied loading (Steiner et al., 2016). The results of this parameter are in agreement with Kennedy et al., 1984 and Harvey et al., 1995.

Error bars are graphical representations that give a general idea of how precise a measurement is, or conversely, how far from the reported value the true (error free) value might be. They often represent one standard deviation of uncertainty, one standard error, or a particular confidence interval (e.g., a 95% interval). These quantities are not the same and so the measure selected should be stated explicitly in the graph or supporting text (Cumming, 2007). In this work, error bars were used to show the variability of data on graphs to indicate the error or uncertainty in the ITSM measurements. Table 4.2 shows the values of error bars which were calculated based on the standard deviation as shown below. All values were less than the 10% of the measured ITSM which is considered within the tolerance of this test (BS EN 12697-26: 2012).

$$SE = \frac{SD}{\sqrt{N}} \quad 4.5$$

Where:

*SE:* Standard error, and

*SD: S*tandard deviation, calculated as following:

$$SD = \sqrt{\frac{\sum(X-M)^2}{N-1}} \quad 4.6$$

Where:

*X*: the observed value (ITSM) of the sample,

M: the mean value of these observations (Mean value of five replicates of the same conditions and parameters tested for ITSM),

*N*: Number of observations in the sample (Five replicates of the same conditions and parameters tested for ITSM).

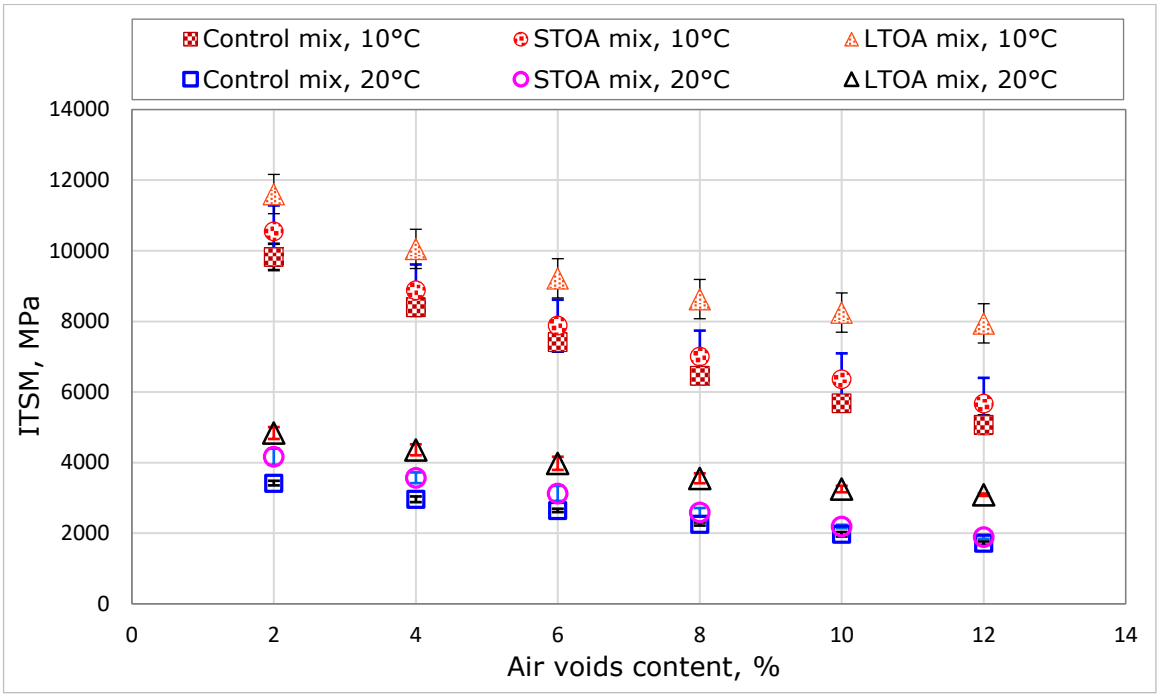



Figure 4.3: Effect testing temperature and air voids content on ITSM of 14mm DBM manufactured with 40/60 Pen and 5% binder content.

Table 4.2: Error bars of the average values of ITSM results (Five samples were tested to find the average) presented in Figure 4.3.

| **Condition** / **Air voids Content, %** | LTOA 10˚C | STOA 10˚C | Control 10˚C | LTOA 20˚C | STOA 20˚C | Control 20˚C |
|---|---|---|---|---|---|---|
| 2 | 721 | 181 | 373 | 169 | 229 | 65 |
| 4 | 861 | 337 | 105 | 156 | 152 | 81 |
| 6 | 332 | 276 | 268 | 187 | 213 | 48 |
| 8 | 251 | 155 | 78 | 141 | 120 | 44 |
| 10 | 287 | 350 | 190 | 92 | 49 | 64 |
| 12 | 304 | 242 | 263 | 34 | 55 | 48 |

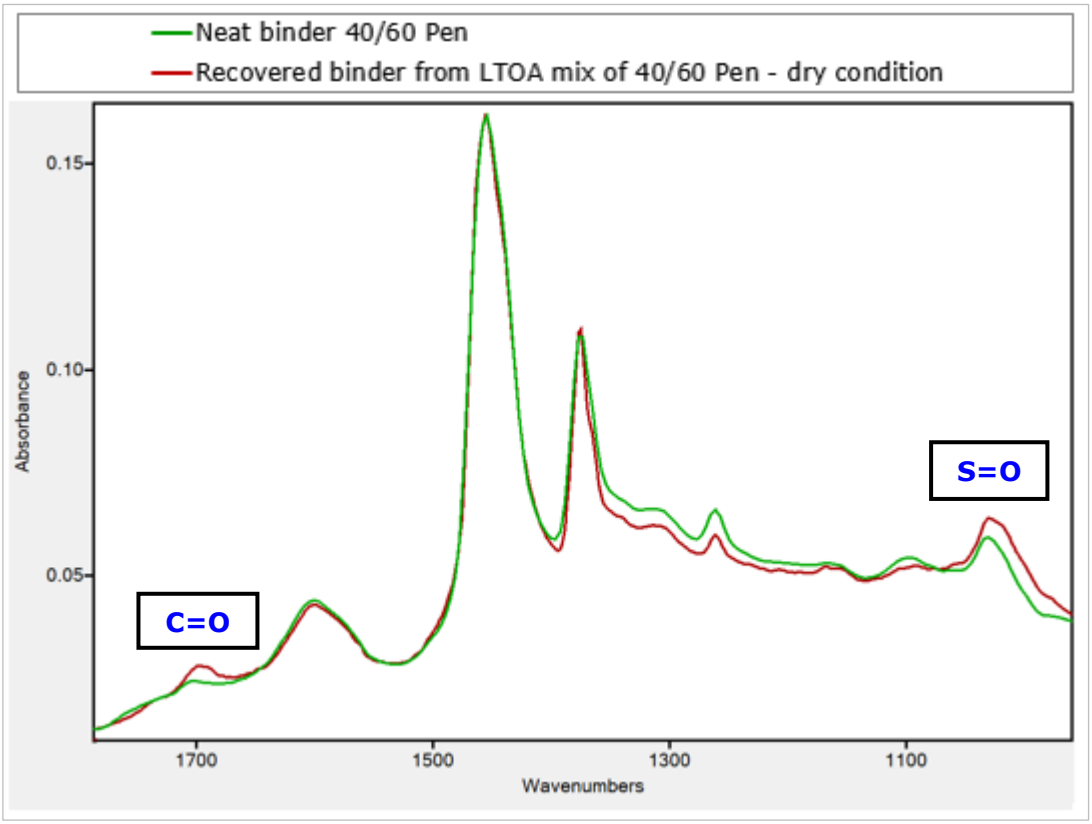



Figure 4.4: FTIR absorbance graph.

Furthermore, Figure 4.5 shows the Ageing Index at these testing temperatures and air voids content. In general, it can be observed that the higher the air void content the higher the Ageing Index. This means increased air voids allows more access for oxidation and in turn more ageing of bituminous material.

It can also be observed that the resulting Ageing Index (calculated according to Equation 4.4) at 20˚C is greater than at 10˚C for the different air voids content. The reason might be attributed to the temperature susceptibility (A change in consistency with temperature) of asphalt mixtures. In general, decreasing the testing temperature from 20 to 10˚C is a hardening factor contributing to an increase in the stiffness modulus of asphalt mixtures. If the mixture is originally highly temperature susceptible (undergo a significant change in consistency) such as mixtures exposed to LTOA condition, there will be less potential to acquire more stiffness when the testing temperature decreases from 20 to 10˚C. This might be due to the role of the bitumen binder which experienced a hardening during the LTOA condition of asphalt mixtures showing a shifting towards the region of glassy solid before testing them at 10˚C. On the other

hand, the mixture exposed to STOA is originally less temperature susceptible and therefore may be more susceptible for being stiffer at 10˚C. This means the rate and magnitude of hardening of the short-term aged mixture (STOA) at 10˚C was generally higher than the rate of hardening of the same mixture being stiffer due to applying LTOA process. This resulted in reducing the magnitude of Ageing Index at 10˚C ($AI = ITSM_{LTOA}/ITSM_{STOA}$). While a difference in the rate and magnitude of hardening at 20˚C between the STOA and LTOA conditions of the same specimen might be not significant or less than at 10˚C contributing to higher Ageing Index at 20˚C than at 10˚C.

Figure 4.5 also shows that the difference between these ageing indices produced at 10 and 20˚C increases as the air voids content increase. It seems that the increase of air voids content might be more influential at 20˚C than at 10˚C. Simply, the reason of this difference might be related to the effect of air voids content discussed earlier. The increase of air voids content contributed to more access for oxidation and therefore more ageing of bituminous material. The influence of this ageing may be more obvious at 20˚C than at 10˚C for the reason of temperature susceptibility explained earlier. Additional effect should not be disregarded is the decreased modulus of asphalt mixtures as the air voids content increase. This may affect unequally their susceptibility for being stiffer at 10 and 20˚C in short and long-term ageing conditions and complicates the explanation of this issue.

Therefore, it may be complicated to explain precisely the reason of this difference by the means of AI resulting from the measurements of ITSM only. AI might be considered as a simple Ageing Index while ageing causes a significant change in the rheology of the asphalt binder and requires testing the time-temperature dependency rheological properties such as the complex modulus, $|E^*|$.

Second, the same trends of ITSM and AI were found for 14mm DBM mixtures manufactured with 10/20 and 100/150 Pens, 5% BC, and different air voids content (4, 8, and 12%). The results will be presented in the following section to avoid repetitions.

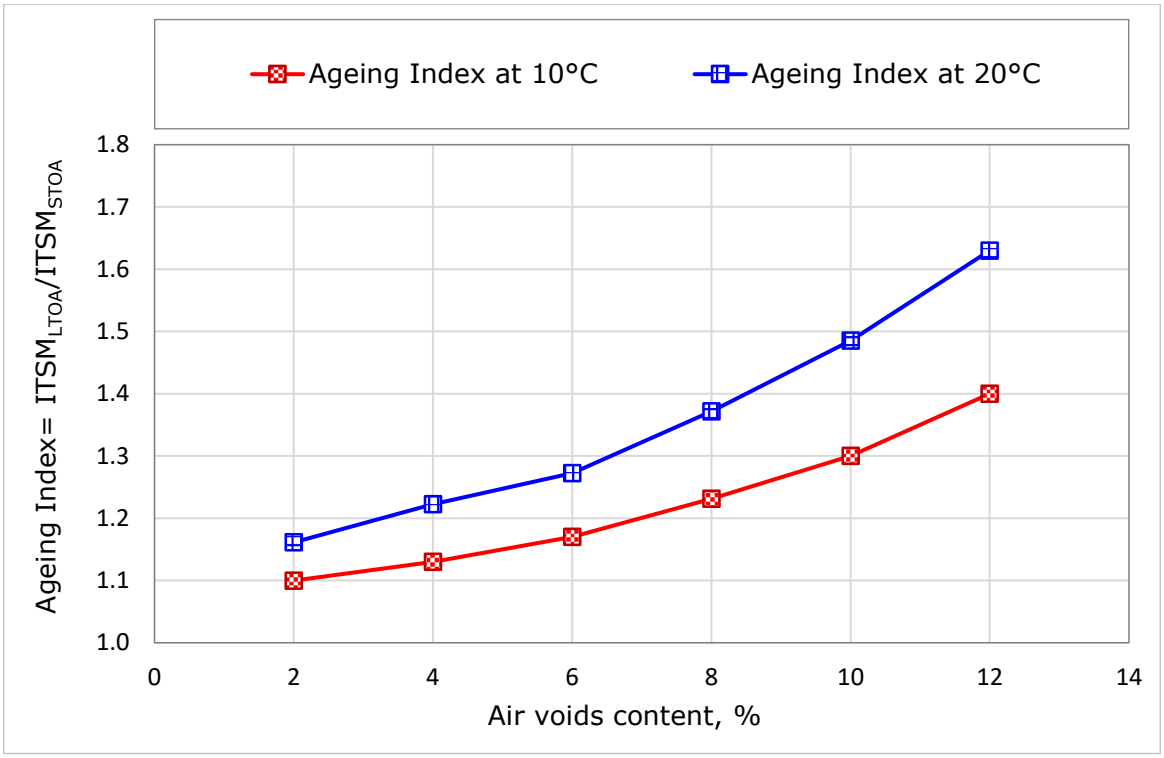



Figure 4.5: Effect of testing temperature and air voids content on the Ageing Index of 14mm DBM manufactured with 40/60 Pen and 5% binder content.

### 4.5.2 Effect of binder grades on ageing

The overall comparisons between the influence of three binder grades; 100/150, 40/60, and 10/20 on the ITSM and Ageing Index are shown in Figures 4.6, 4.7, and 4.8. Table 4.3 shows the errors of the average values of all ITSM results presented in Figures 4.6 and 4.7. This influence was evaluated at 5% BC, three air voids content; (4, 8, 12%), and at two testing temperatures; 10˚C and 20˚C. It was found that the Ageing Index is also reliant on binder grades. Figures 4.6 and 4.7 show that the mixture of hard binder, 10/20 Pen have the highest ITSM at 10 and 20˚C respectively followed by the mixture of 40/60 pen regardless of the mixture was unaged (control) or aged (STOA or LTOA).

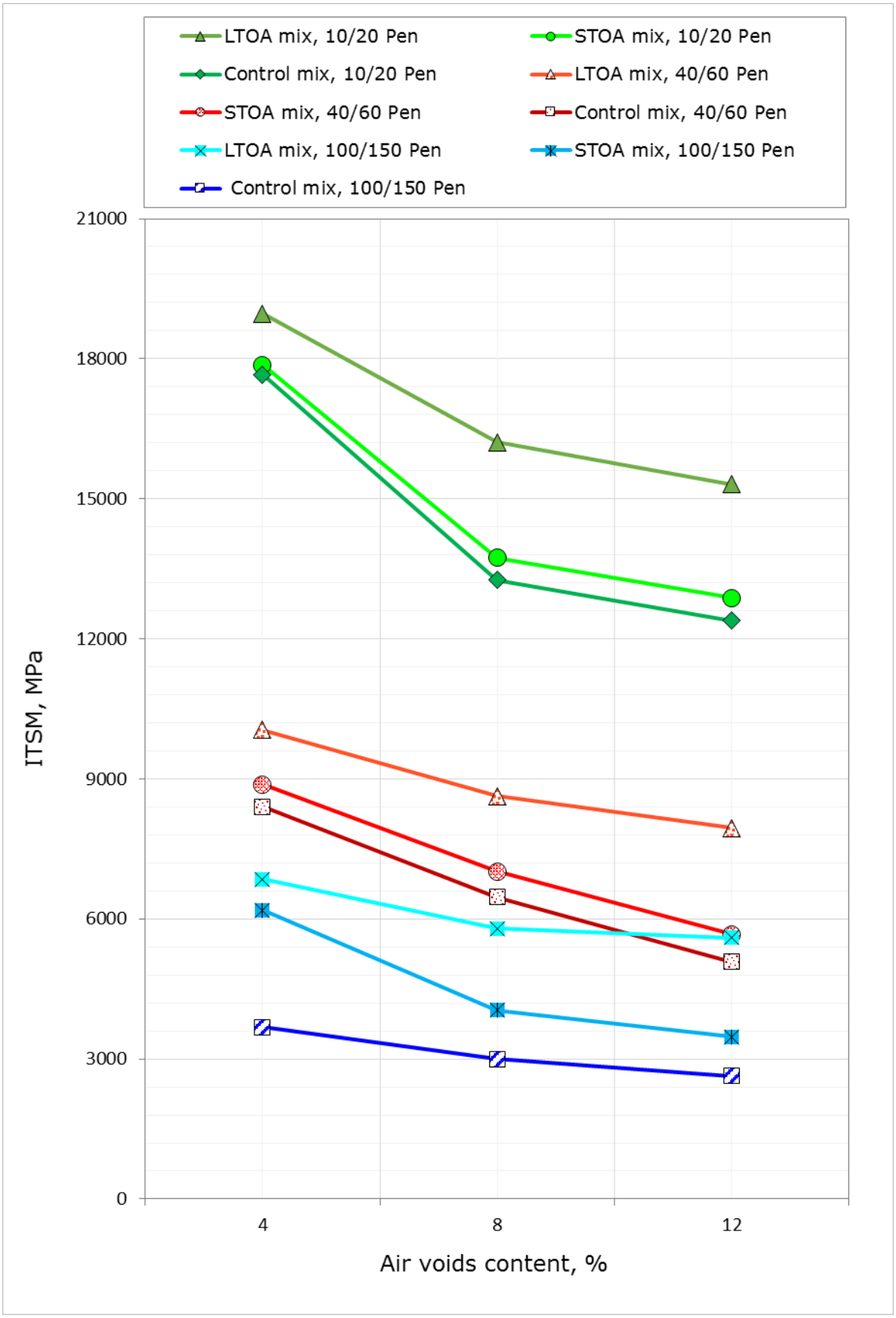



Figure 4.6: Effect of binder grades on ITSM of 14mm DBM at 10˚C and different air voids content.

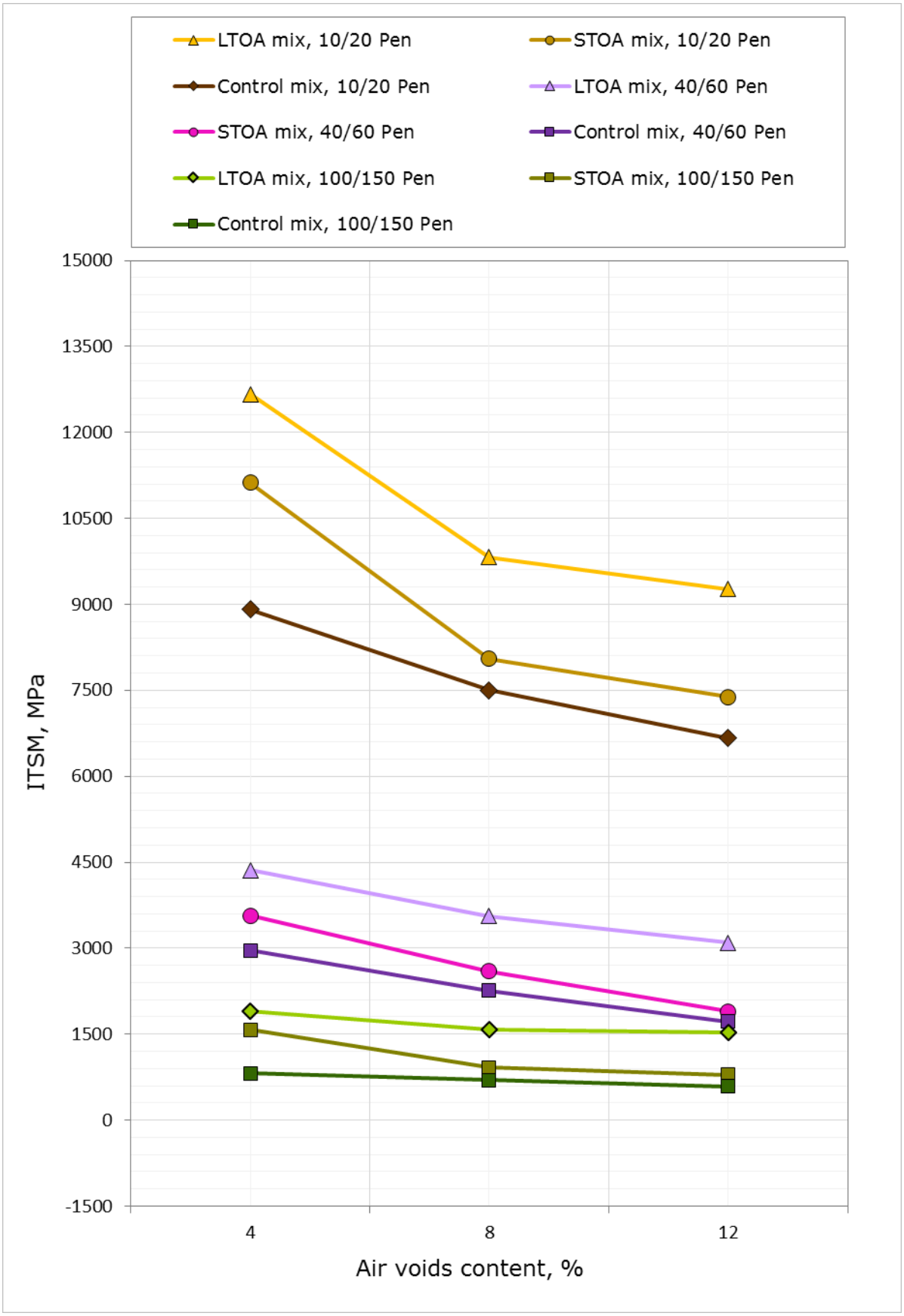



Figure 4.7: Effect of binder grades on ITSM of 14mm DBM at 20˚C and different air voids content.

Table 4.3: Errors of the average values of ITSM results presented in Figures 4.5 and 4.6.

| **Condition** | | LTOA 10˚C | STOA 10˚C | Control 10˚C | LTOA 20˚C | STOA 20˚C | Control 20˚C |
|---|---|---|---|---|---|---|---|
| **Binder grade** | **Air voids Content, %** | | | | | | |
| 10/20 | 4 | 426 | 141 | 255 | 205 | 138 | 173 |
| | 8 | 614 | 328 | 269 | 285 | 316 | 79 |
| | 12 | 335 | 190 | 322 | 200 | 85 | 157 |
| 100/150 | 4 | 179 | 165 | 89 | 61 | 95 | 48 |
| | 8 | 329 | 136 | 188 | 85 | 37 | 58 |
| | 12 | 120 | 54 | 212 | 28 | 20 | 35 |

Moreover, Figure 4.8 presents the Ageing Index calculated according to Equation 4.4 ($ITSM_{LTOA}/ITSM_{STOA}$) of asphalts mixtures manufactured using three binder grades; 100/150, 40/60, and 10/20. This index was calculated using equation 4.4 ($AI=ITSM_{LTOA}/ITSM_{STOA}$) after measuring the ITSM at 10 and 20˚C of these asphalt mixtures exposed to STOA and LTOA. This figure indicates that as a general rule, the softer the asphalt mixture the higher the Ageing Index. The reason might be attributed to the content of the responsible components for ageing in each of these binder grades which consequently affects their potential for ageing. In this perspective, the FTIR test was conducted on two binders; 40/60 and 100/150 Pens (The researcher couldn't perform FTIR on 10/20 pen for the time limitation of the study) and on the recovered binder from mixtures manufactured with the same two binders and exposed to LTOA. It can be seen from the absorbance graph presented in Figure 4.9 the increase in both components sulfoxide and carbonyl at wave numbers 1030 and 1700 respectively. Additionally, Figure 4.10 presents the increment of carbonyl component (C=O) of both binders due to applying the LTOA. Obviously, the carbonyl increment of the binder recovered from the aged mixture of 100/150 Pen is higher than the increment of other binder and therefore may explain the highest Ageing Index of this binder presented in Figure 4.8.

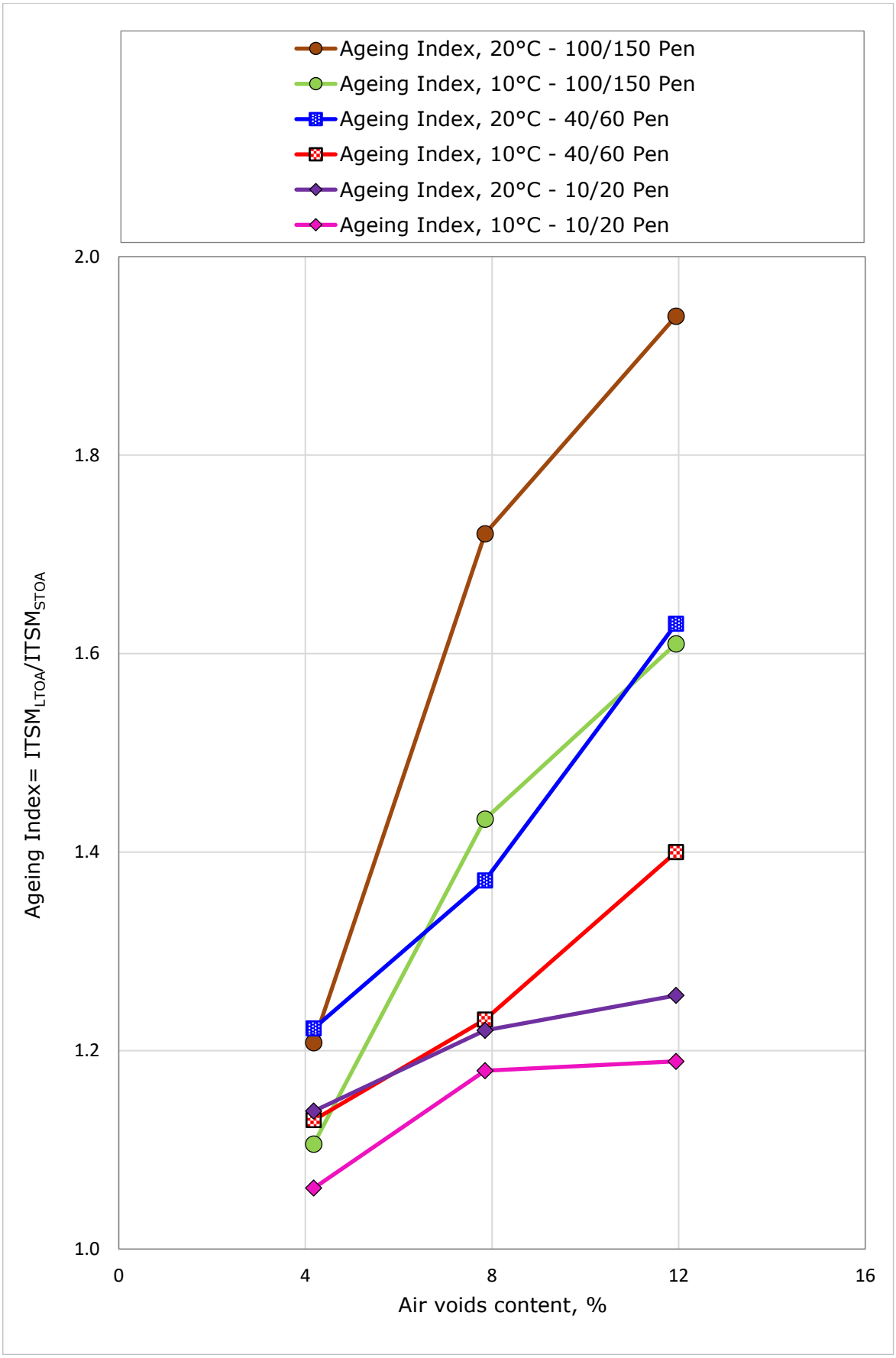
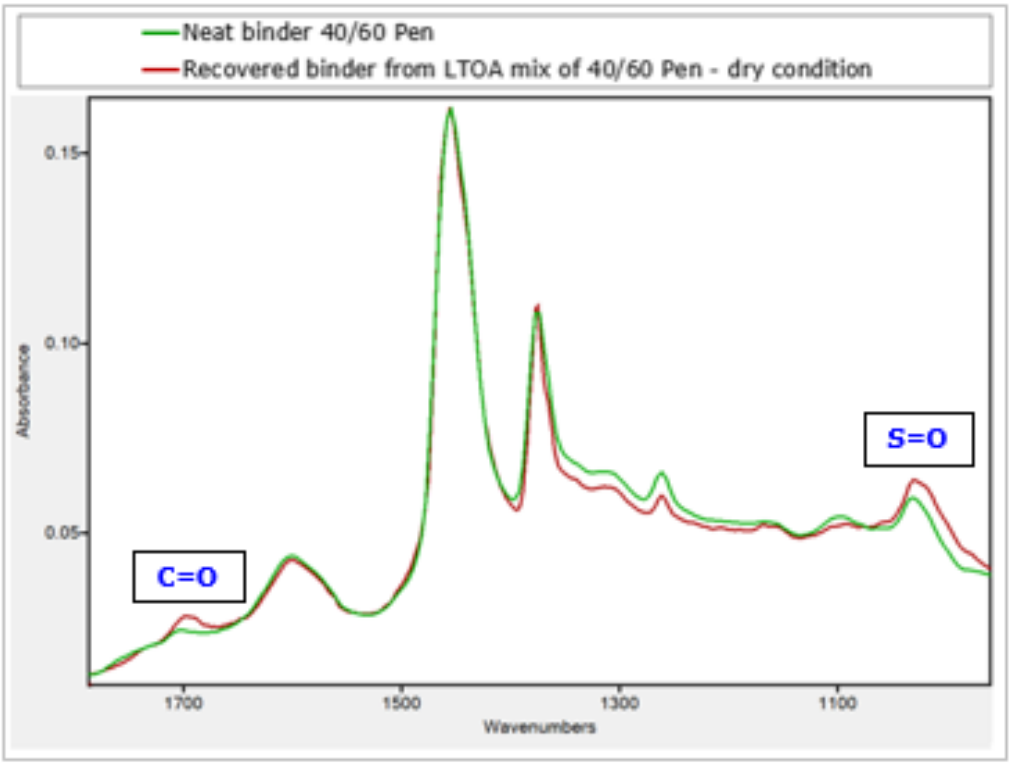
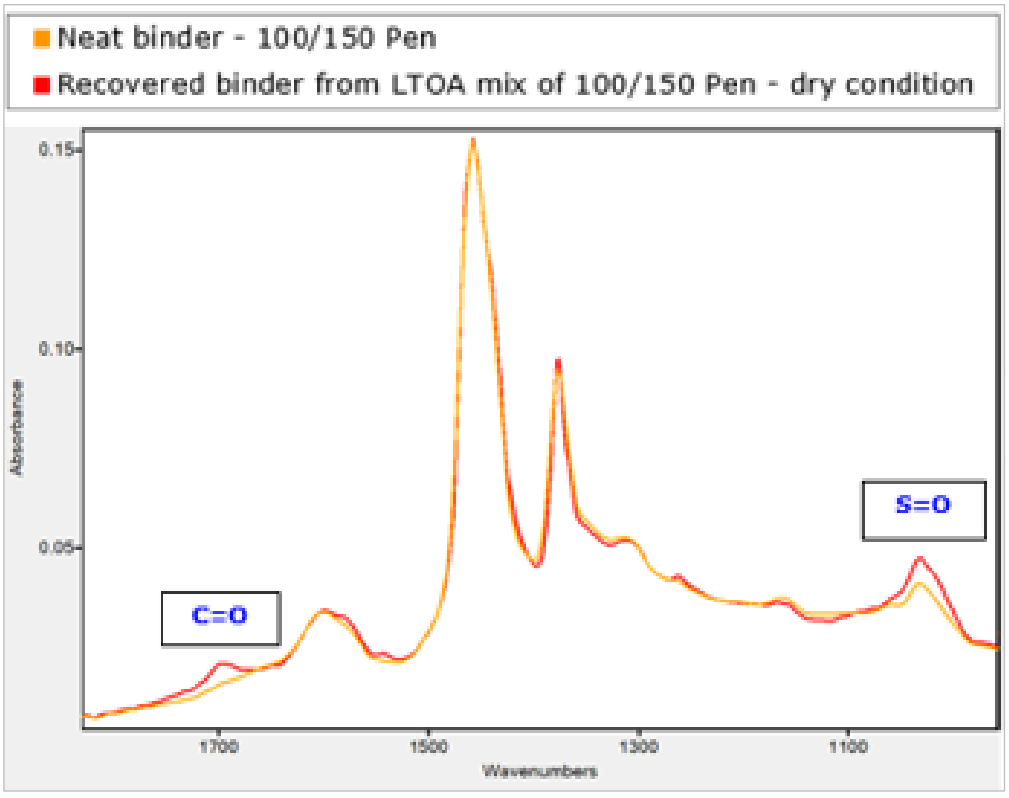



Figure 4.8: Effect of binder grades on the Ageing Index (ITSM$_{LTOA}$/ITSM$_{STOA}$) of 14mm DBM at different testing temperatures and air voids content.




A: 40/60 Pen (neat and aged binders).




B: 100/150 Pen (neat and aged binders).

Figure 4.9: FTIR absorbance graph shows the effect of binder grades on ageing in terms of sulfoxide (S=O) and carbonyl (C=O) components at wave numbers; 1030 and 1700 respectively.

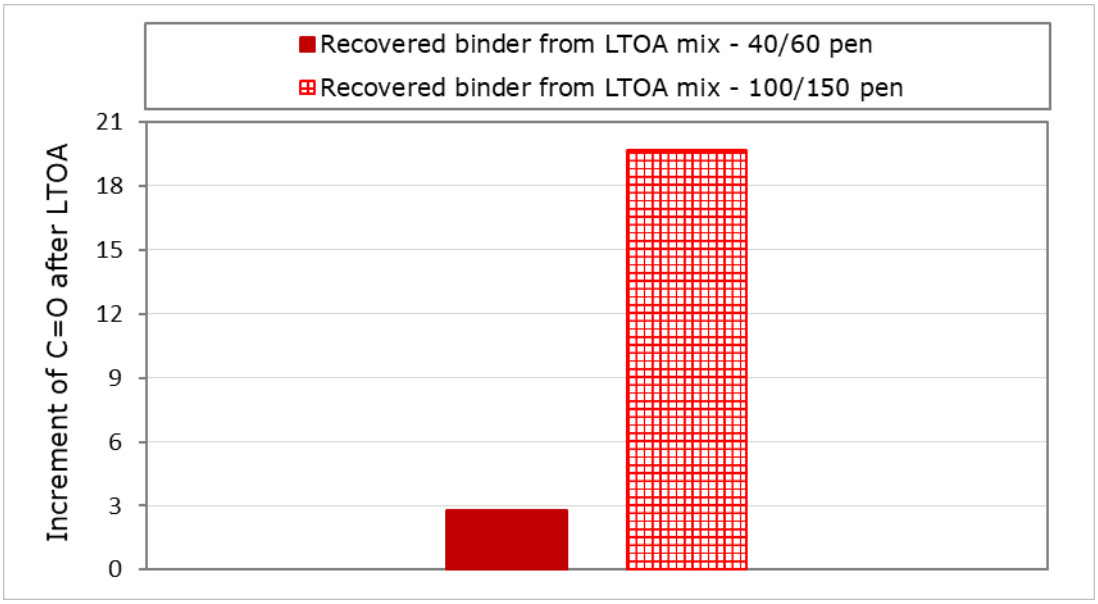



Figure 4.10: Effect of binder grades on the increment of carbonyl component.

### 4.5.3 Effect of binder contents on ageing

Moreover, the comparisons between the two binder contents effect; 5% and 6% for the 40/60 Pen are exhibited in Figures 4.11 to 4.13. This effect was tested at two air voids content; (8 and 12%), and at two testing temperatures; 10˚C and 20˚C. Figure 4.13 displays that the Ageing Index decreased due to increase of binder content to 6%. A possible explanation for this may be related to the bitumen film thickness. The greater the thickness of the bitumen coating on the aggregate surface the longer the required time for the whole bitumen film thickness to become hardened and vice versa (Kumar and Goetz, 1976). However, the collected results of this variable were not sufficient to judge on its effect due to time limitations of this work.

In addition, these general findings shown in the previous figures are summarised in Table 4.4. This table also presents the calculated Ageing Index for all investigated parameters at all conditions; $ITSM_{STOA}/ITSM_{Control}$, $ITSM_{LTOA}/ITSM_{STOA}$, $ITSM_{LTOA}/ITSM_{Control}$.

In summary, the most important findings to emerge from the discussion of this part are the obvious influences of air voids content, temperature, and binder grades on the Ageing Index.

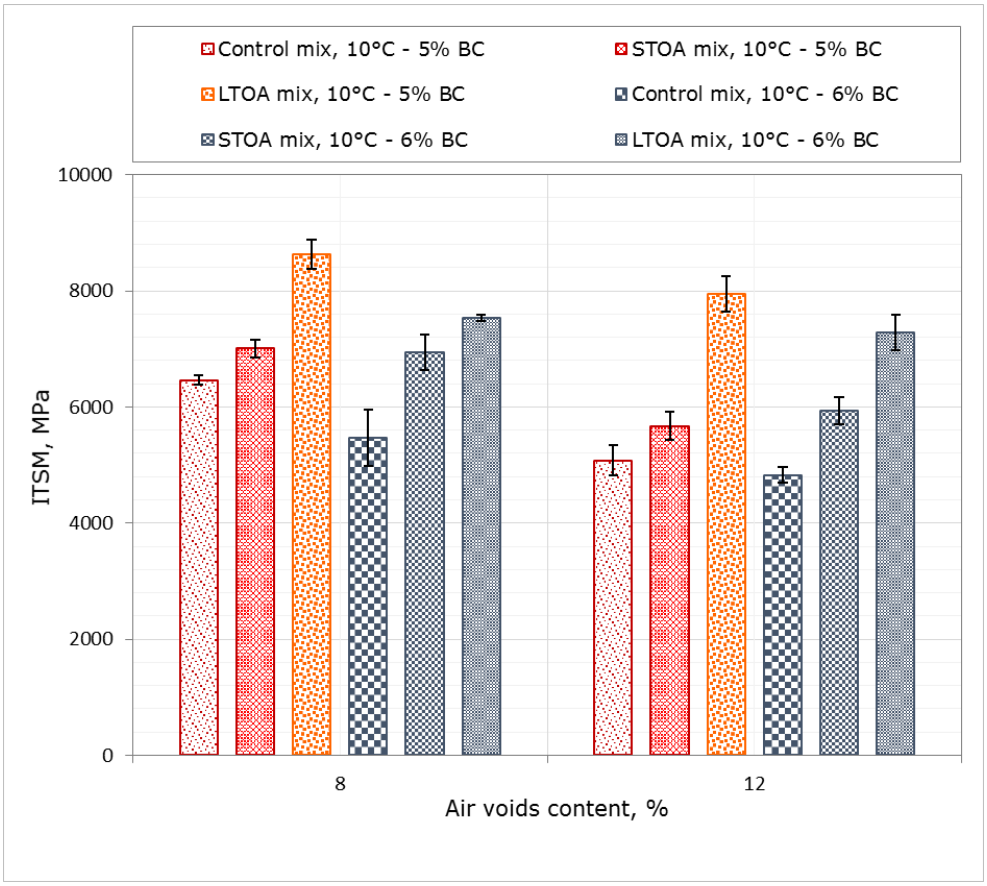



Figure 4.11: Effect of binder contents on ITSM of 14mm DBM at 10˚C.

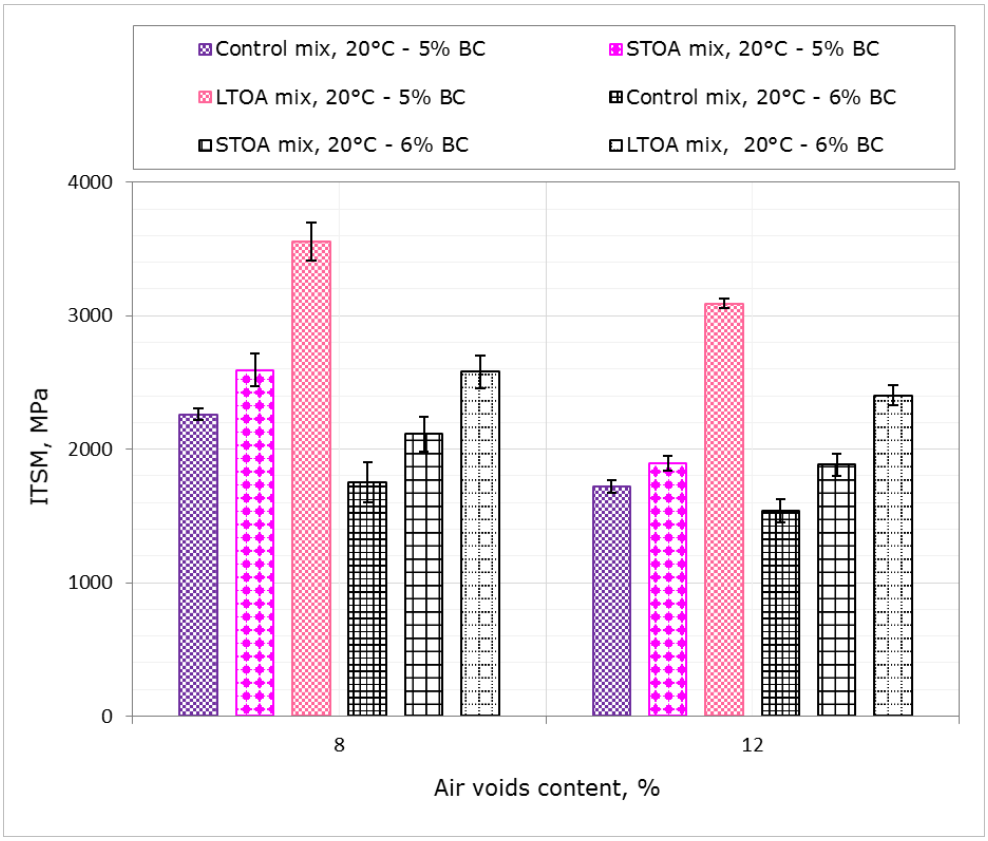



Figure 4.12: Effect of binder contents on ITSM of 14mm DBM at 20˚C.

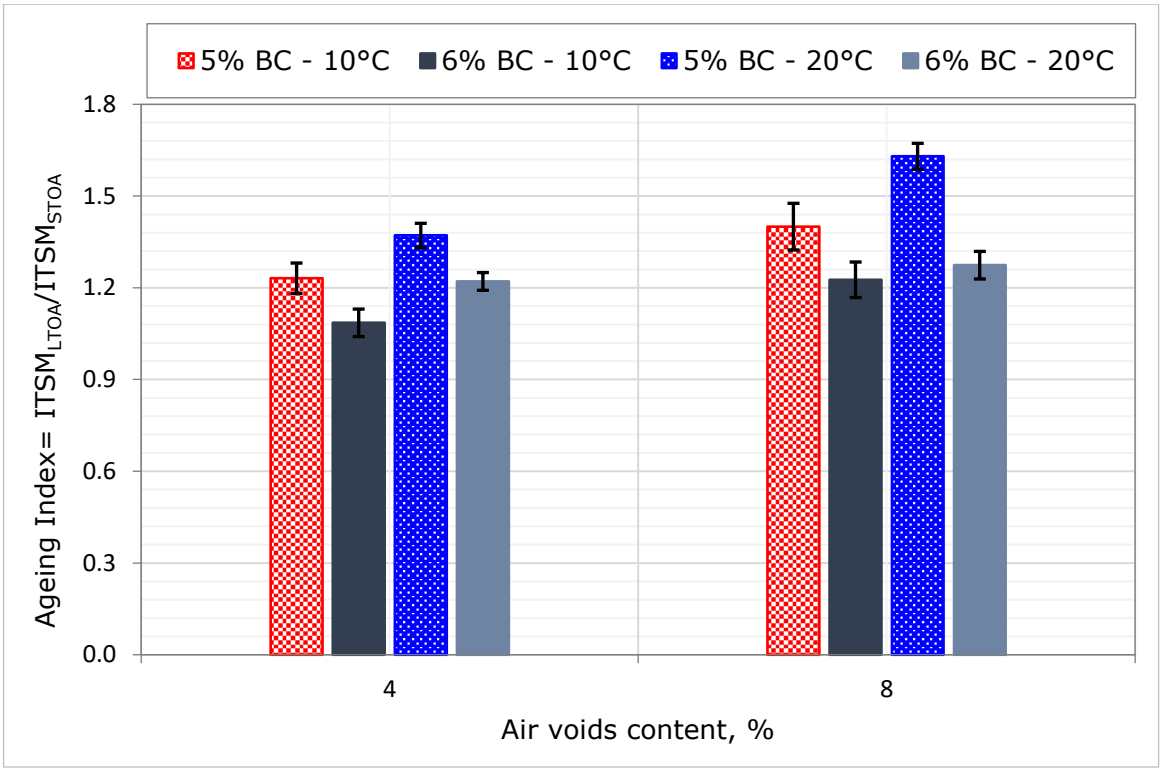



Figure 4.13: Effect of binder contents on the Ageing Index of 14mm DBM at different testing temperatures and air voids content.

Table 4.4: Ageing Index for all tested parameters and conditions.

| Binder grades | Ageing Index | ITSM$_{STOA}$/ITSM$_{Control}$ | | *ITSM$_{LTOA}$/ITSM$_{STOA}$ | | ITSM$_{LTOA}$/ITSM$_{Control}$ | |
|---|---|---|---|---|---|---|---|
| | Air voids, % | T, ˚C | | T, ˚C | | T, ˚C | |
| | | 10 | 20 | 10 | 20 | 10 | 20 |
| 100/150 5% BC | 4.0 | *1.68* | *1.93* | 1.11 | 1.21 | 1.86 | 2.34 |
| | 8.0 | 1.35 | 1.32 | 1.43 | 1.72 | 1.93 | 2.27 |
| | 12.0 | 1.32 | 1.34 | 1.61 | 1.94 | 2.13 | 2.15 |
| 10/20 5% BC | 4.0 | 1.01 | *1.25* | 1.06 | 1.14 | 1.07 | 1.42 |
| | 8.0 | 1.07 | 1.07 | 1.18 | 1.22 | 1.22 | 1.31 |
| | 12.0 | 1.04 | 1.11 | 1.19 | 1.26 | 1.27 | 1.40 |
| 40/60 5% BC | 4.0 | 1.06 | 1.21 | 1.13 | 1.22 | 1.20 | 1.47 |
| | 8.0 | 1.08 | 1.15 | 1.23 | 1.37 | 1.34 | 1.57 |
| | 12.0 | 1.12 | 1.10 | 1.40 | 1.63 | 1.56 | 1.66 |
| 40/60 6% BC | 4.0 | - | - | - | - | - | - |
| | 8.0 | 1.27 | 1.20 | 1.09 | 1.22 | 1.38 | 1.47 |
| | 12.0 | 1.23 | 1.23 | 1.23 | 1.27 | 1.51 | 1.56 |

*ITSM was measured after STOA and LTOA for the same specimen.

### 4.6 Individual and combined effects of moisture and ageing

Stiffness modulus plays an important role in determining the performance of asphalt mixtures (Kim et al., 1986). It was found that a non-destructive stiffness modulus test can be more effective for moisture susceptibility investigation of asphalt treated mixes than conventional tests. However, any changes in these mixtures were not evidenced by obvious stripping or debonding (Schmidt and Graf, 1972). In this part, the stiffness modulus was measured using the Indirect Tensile Stiffness Modulus (ITSM) test, to evaluate the individual influence of water and its combined effect with ageing at different testing temperatures, air voids content, binder grades and binder contents. It was carried out to calculate the Index of Retained Stiffness Modulus (IRSM) by measuring the ITSM of the same specimen before and after moisture conditioning. To achieve this objective, two main sets of 14mm DBM cylindrical test specimens were manufactured using each one of the specified variables (see Table 4.5) and divided into two groups; unconditioned (dry) and conditioned (soaked). The first main set was without any ageing conditions which is branded as control mixtures. The second main one involves LTOA of compacted specimens subjected to STOA before compaction (loose mixture). ITSM was measured for both control and LTOA specimens before and after water immersion. This results in assessing the Index of Retained Stiffness Modulus (IRSM) of the same specimen as following:

$$IRSM = ITSM_{conditioned}/ITSM_{unconditioned} \qquad 4.7$$

Two different methods were applied for the determination of water sensitivity; the first one was carried out according to the British Board of Agrément (BBA) - Appendix A.2: 2008 and the second one was in accordance with BS EN 12697-12:2008. The two methods produced two different saturation of levels. From applying BBA Protocol, the saturation level was approximately (25-30%), although the samples were manufactured with high air voids content. On the other hand, it was approximately (50-60%) from applying BS EN Method. This variance is due to the different applied vacuum pressure during both conditioning as mentioned earlier in Chapter 3. The main reason for the vacuum is to allow the water penetration into the specimen and shorten the time required for the specimen to achieve the desired saturation level. Table 4.5

presents a summary of investigated variables (Five replicates were used for measuring the ITSM of each condition or variable).

Table 4.5: Summary of investigated mixture variables and conditions.

| **Mixtures exposed to specific conditions** | | **T, ˚C** | **Mixture of 5% binder content and binder grade:** | | |
|---|---|---|---|---|---|
| | | | 40/60* | 100/150 | 10/20 |
| Control mixture, dry condition | | 0<br>10<br>20<br>30 | ✓ | ✓ | ✓ |
| Control mixture, immersed in water according to: | BBA method (vacuum the compacted mixture at (68 ± 3.3) kPa for (30 ± 1) minutes and immersed in water at 60˚C for 6 hrs then at 5˚C for 16 hrs before ITSM test). | 10<br>20 | ✓ | ✓ | ✓ |
| | BS EN method (vacuum the compacted mixture at (6.7 ± 0.3) kPa for (30 ± 5) minutes and immersed in water at 40˚C for 72 hours before ITSM test). | 0<br>10<br>20<br>30 | | | |
| LTOA mixture, dry condition (after STOA for 4 hrs at 135˚C the compacted mixture subjected to 85˚C for 120 hours before ITSM test). | | 0<br>10<br>20<br>30 | ✓ | ✓ | ✓ |
| LTOA mixture, (after STOA for 4 hrs at 135˚C the compacted mixture subjected to 85˚C for 120 hrs) then immersed in water according to: | BBA method (vacuum the compacted mixture at (68 ± 3.3) kPa for (30 ± 1) minutes and immersed in water at 60˚C for 6 hrs then at 5˚C for 16 hrs before ITSM test). | 10<br>20 | ✓ | ✓ | ✓ |
| | BS EN method (vacuum the compacted mixture at (6.7 ± 0.3) kPa for (30 ± 5) minutes and immersed in water at 40˚C for 72 hours before ITSM test). | 0<br>10<br>20<br>30 | | | |

***** 6% binder content was investigated using BBA only.

## 4.7 Index of Retained Stiffness Modulus (IRSM) results

### 4.7.1 Effect of testing temperatures on IRSM

To assess the effect of testing temperatures on $IRSM_{control(unaged)}$ and $IRSM_{LTOA(aged)}$, 14mm DBM specimens were manufactured utilising the three investigated binder grades and divided into two groups according to the specified air voids content collections of 8%, and 12%. The $ITSM_{unconditioned}$ of control (unaged) and aged (LTOA) specimens was measured at four testing temperatures 0˚C, 10˚C, 20˚C, and 30˚C in dry conditions. Then the BS EN method was applied to these specimens and $ITSM_{conditioned}$ was measured at the same temperatures. The same procedure was repeated to other specimens set utilising BBA protocol at only 10˚C and 20˚C. Then, IRSM was calculated and the results are presented in Figures 4.14 and 4.15.

In general, the ratio of the acceptance criterion (strength/stiffness) such as the Tensile Strength Ratio (TSR) for moisture induced damage resistance of asphalt mixtures should be at least 80%. However, some agencies use 70% as criterion (Anderson, 2002, Apeagyei et al., 2006, Buss et al., 2016). The main surprising finding of Figures 4.14 and 4.15 is that most of the IRSM results of investigated mixtures are greater than 100% and the rest are greater than the minimum acceptance criterion of 80%. According to these limitations and findings, the asphalt limestone aggregate mixtures manufactured with 40/60 Pen and evaluated by different water sensitivity methods at different testing temperatures have no significant moisture damage issue. Even if this damage was applied after LTOA. Moreover, the effect of testing temperatures on $IRSM_{BSEN}$ (see Figure 4.14) was not unexplained and not constant. In some occasions, IRSM decreased with the increase of testing temperature and vice versa in other occasions. However, the effect of increasing the temperature from 10 to 20˚C on the $IRSM_{BBA}$ (see Figure 4.15) was more obvious which in general, increased slightly except in the case of 12% air voids control mixtures increased more than 30%. These unexplained increases in the IRSM and the strange behaviour of most conditioned control and aged mixtures with the increase of testing temperature might be attributed to possible ageing that may take place during the period of moisture conditioning (40˚C for 72 hours in BS EN method and 60˚C for 6 hours in BBA protocol). It was also found that the moisture

condition together with oxygen and heat results in stiffer and more brittle binder behaviour. Therefore, moisture has a remarkable role in the long-term aging of the bitumen binder and causes damaging effect on the durability of asphalt pavements (Ma et al., 2011). Some literatures showed similar increases in the stiffness or strength due to moisture exposure conditions, although different materials and determination methods of moisture induced damage were used in these literature (Apeagyei et al., 2006 and 2014, Xibo et al., 2007, Buss et al., 2016, Lopez and Miro, 2016).

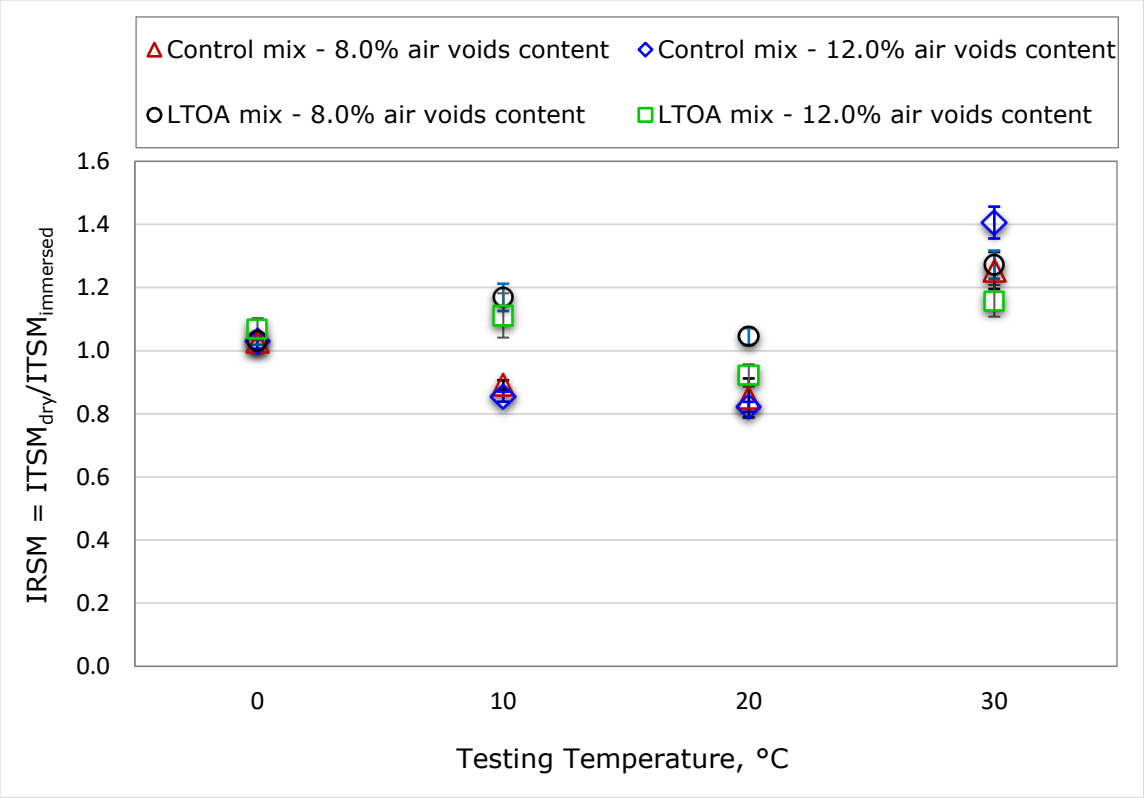



Figure 4.14: IRSM of 14mm DBM with 40/60 Pen using BS EN method.

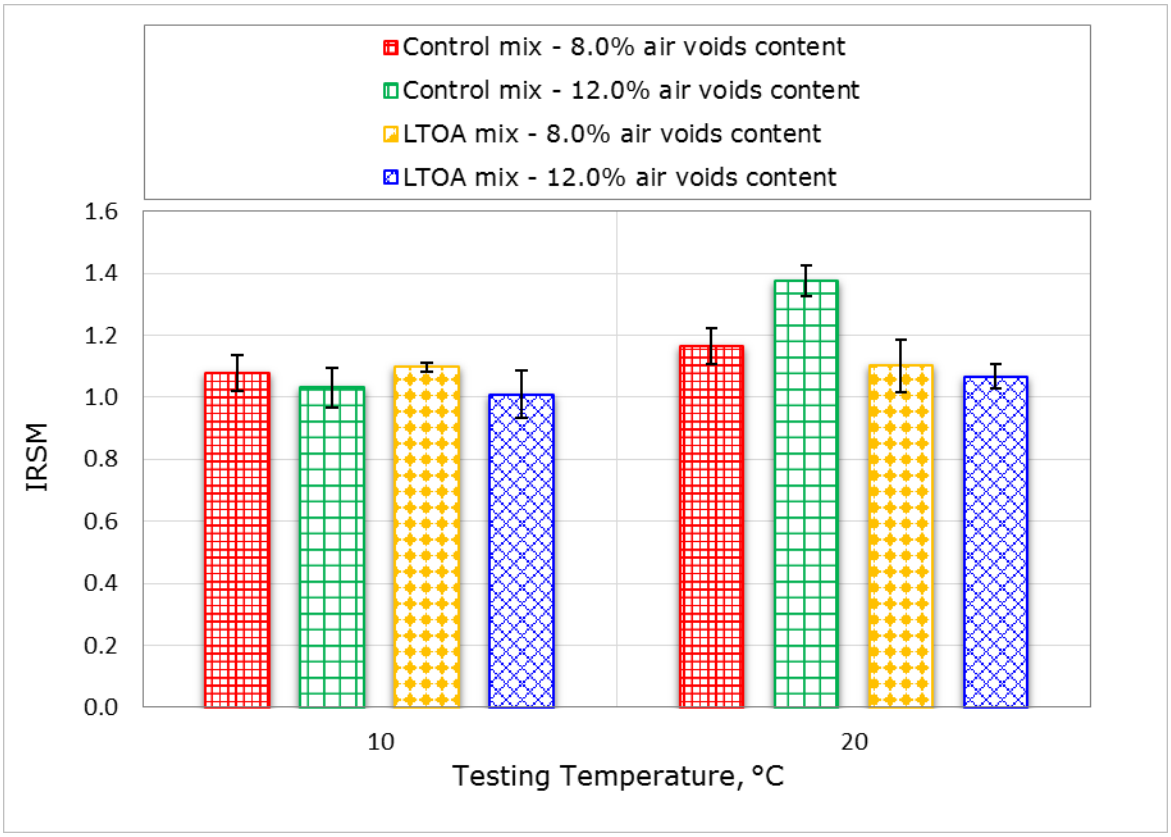



Figure 4.15: IRSM of 14mm DBM with 40/60 Pen using BBA method.

### 4.7.2 Effect of binder grades on IRSM

Asphalt mixtures of three binder grades; 10/20, 40/60, and 100/150 Pens were used to investigate the effect of binder grades on the IRSM of control and aged mixtures conditioned (soaked) in accordance with BS EN and BBA moisture sensitivity methods. The results are presented in Figures 4.16 to 4.19.

According to the acceptance criterion stated earlier and the findings of this investigated variable, the asphalt limestone aggregate mixtures manufactured with different binder grades have no significant moisture damage issue. IRSM values are greater than 0.80 as shown in Figures 4.16 to 4.19 and therefore no indication of moisture damage was observed for the different control (unaged) and aged (LTOA) asphalt mixture specimens. However, these mixtures were also manufactured with high air voids content (8 and 12%) to provide more access to water and tested at different testing temperatures. It is also obviously shown that IRSM values are still greater than 0.80 regardless of whether the moisture conditioning was conducted using the BS EN or BBA methods.

For the control mixtures evaluated by BS EN method, there is an increase of (22-40%) in IRSM with the increase of testing temperature from (0-30˚C). In addition, using the BBA protocols have showed similar increase for mixtures manufactured with 40/60 Pen and 100/150 Pen at 12% air voids content when the testing temperature increased from 10˚C to 20˚C. No increase was observed in the IRSM of 10/20 Pen mixtures. On the other hand, it was noticed some unexplained decrease in IRSM with temperature increase, in particular at 10˚C and 20˚C. In general, it seems to be no obvious pattern relating the moisture sensitivity of these binder grades and testing temperatures. However, Barra et al., 2012 found that the moisture damage was more intense with an increase in testing temperatures which contributed to the removal of the bitumen binder film from the aggregate particles. It also appears that no ranking of moisture sensitivity can be concluded for the mixtures of the different binder penetration grades.

Furthermore, the combined effect of moisture and ageing has generally shown a decrease in the $IRSM_{BSEN}$ at 30˚C and in the $IRSM_{BBA}$ at 20˚C (only of 40/60 Pen and 100/150 Pen mixture) compared to IRSM of control mixtures. However, there is some unexplained increases in $IRSM_{BSEN}$ of some conditioned aged mixtures at 0 and 10˚C. It was found from the results of field study of 92 different asphalt mix designs in eight American states that aging does not significantly affect the TSR (Solaimanian et al., 1993). However, other studies demonstrated that laboratory aging reduced moisture damage resistance (Al-Swailmi et al., 1993, Poulikakos et al., 2014). Das et al., 2015 suggested that the bitumen source and its aging conditions may be reason for such contradicting findings.

In general, the control and LTOA mixtures of 40/60 Pen exhibited the most resistance to moisture damage. In particular, at 30 and 20˚C when BS EN and BBA methods were applied respectively. However, mixtures with other binder grades showed the better resistance in some occasions.

In summary, first, no moisture damage issue was arisen from the effect of binder grades even when this damage was applied after ageing. Similarly, Bagampadde et al., 2006 found that the investigated penetration grade; 50/70

and 70/100 Pens did not influence moisture sensitivity of asphalt mixtures. However, it has been in general accepted that neat binder with higher viscosity creates a stronger adhesion with aggregate particles compared to neat binder with lower viscosity (Brown et al., 2009). The higher viscosity may indicate higher concentrations of asphaltene or large polar molecules which can create greater adhesion tension (Brown et al., 2009).

Second, two different issues were observed. Firstly, the increase of IRSM to more than 100% which might be related to possible ageing takes place during the moisture conditioning period. This possible ageing might contribute to an increase in the ITSM of conditioned mixtures and in turn an increase in the IRSM of these mixtures. Secondly, the variation of IRSM findings with the different variables. It is difficult to precisely explain the variation of these results due to the wide range of investigated variables; temperature, air voids content, mixture conditions (unaged or aged), and methods of moisture induced damage that were combined with the influence of bitumen binder grades.

There are other important factors that should not be disregarded such as the effect of aggregate type, testing method, the time and temperature of moisture conditioning. The type of aggregate which is limestone in this study may play an important role in these findings. Limestone is generally classified as hydrophobic (water-hating) substances and therefore has a good resistance to stripping (http://www.pavementinteractive.org/aggregate/). Preston, 1991 found that an increase in the elastic stiffness of limestone aggregate mixtures after moisture conditioning. It was indicated that limestone offers very good cohesive properties with bitumen, as this type of aggregate is not observed for stripping failures. This is also might suggest that this type of aggregate used in this study is not susceptible to fatigue distress through moisture related mechanisms in this research.

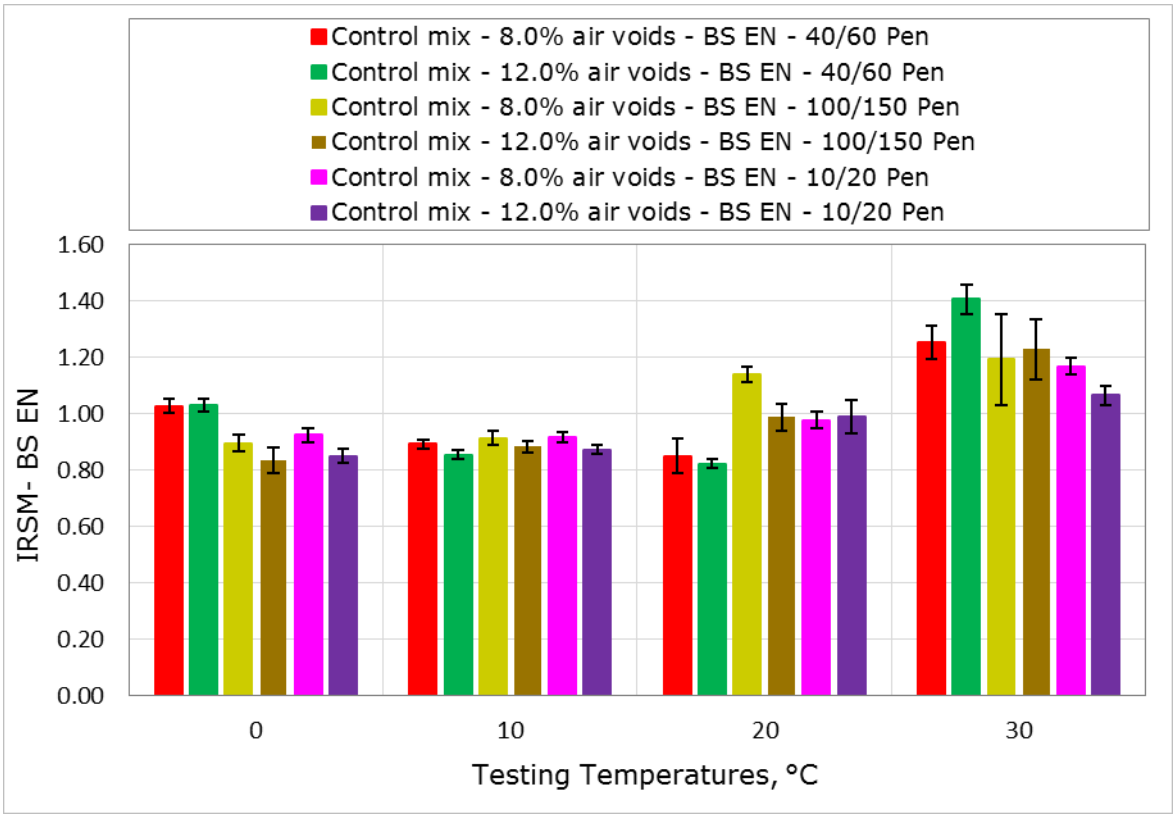



Figure 4.16: IRSM of control 14mm DBM with different binder grades (Individual effect of moisture damage).

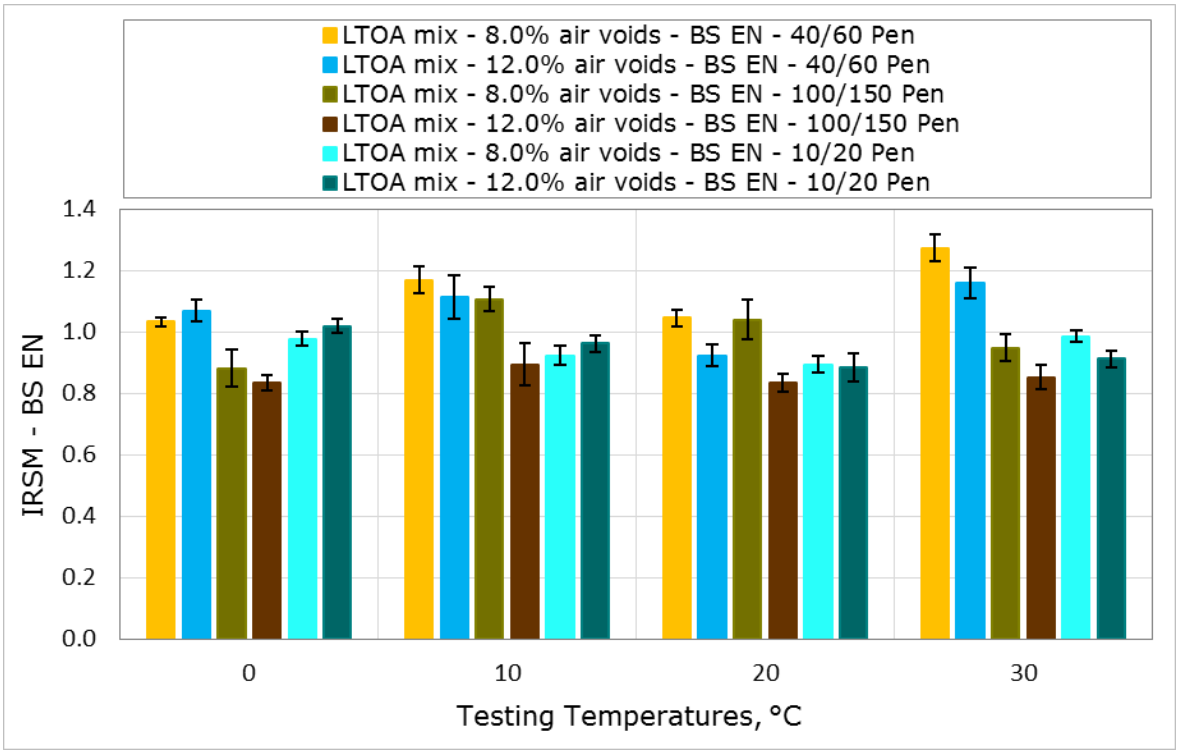



Figure 4.17: IRSM of LTOA 14mm DBM with different binder grades (combined effect of moisture and ageing).

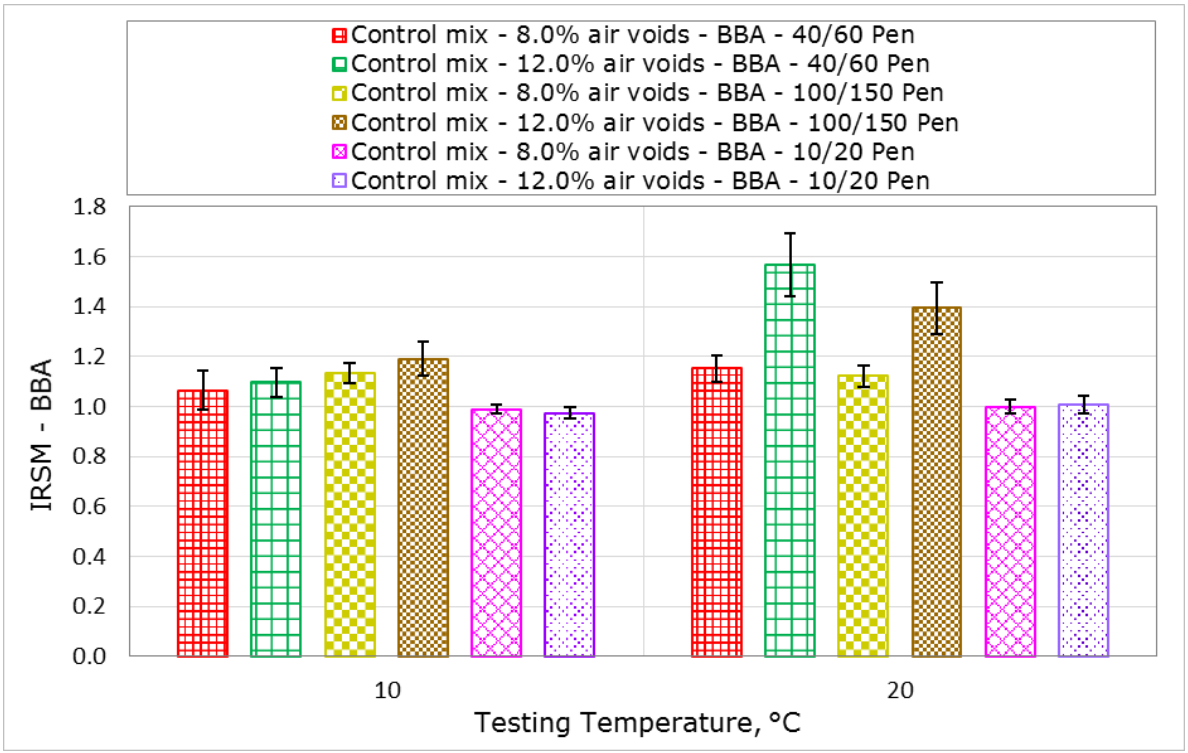



Figure 4.18: IRSM 14mm DBM with different binder grades (Individual effect of moisture damage).

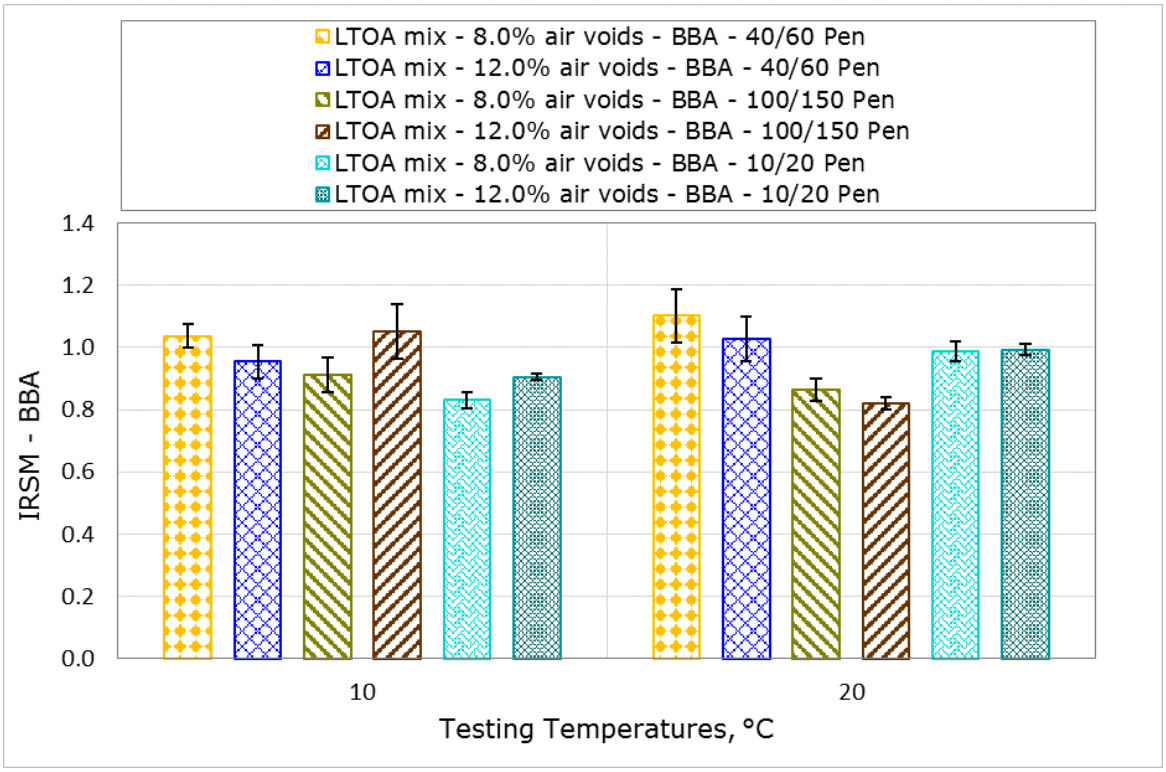



Figure 4.19: IRSM of LTOA 14mm DBM with different binder grades (combined effect of moisture and ageing).

The FTIR test was conducted on two binders; 40/60 and 100/150 Pens (The researcher couldn't perform FTIR on 10/20 pen for the time limitation of the study) and on the recovered binder from mixtures manufactured with the same two binders and exposed to moisture damage and/or LTOA. It can be seen from the absorbance graph presented in Figures 4.20 and 4.21 that increase in both components carbonyl at wave numbers 1700. Figures 4.22 and 4.23 presents the increment of the content of carbonyl component (C=O) of both binders due to applying moisture damage and/or LTOA. Obviously, there is more increase in the carbonyl component of the binders recovered from mixtures exposed to ageing and/or moisture damage. This may enhance the purposed ageing during the moisture conditioning.

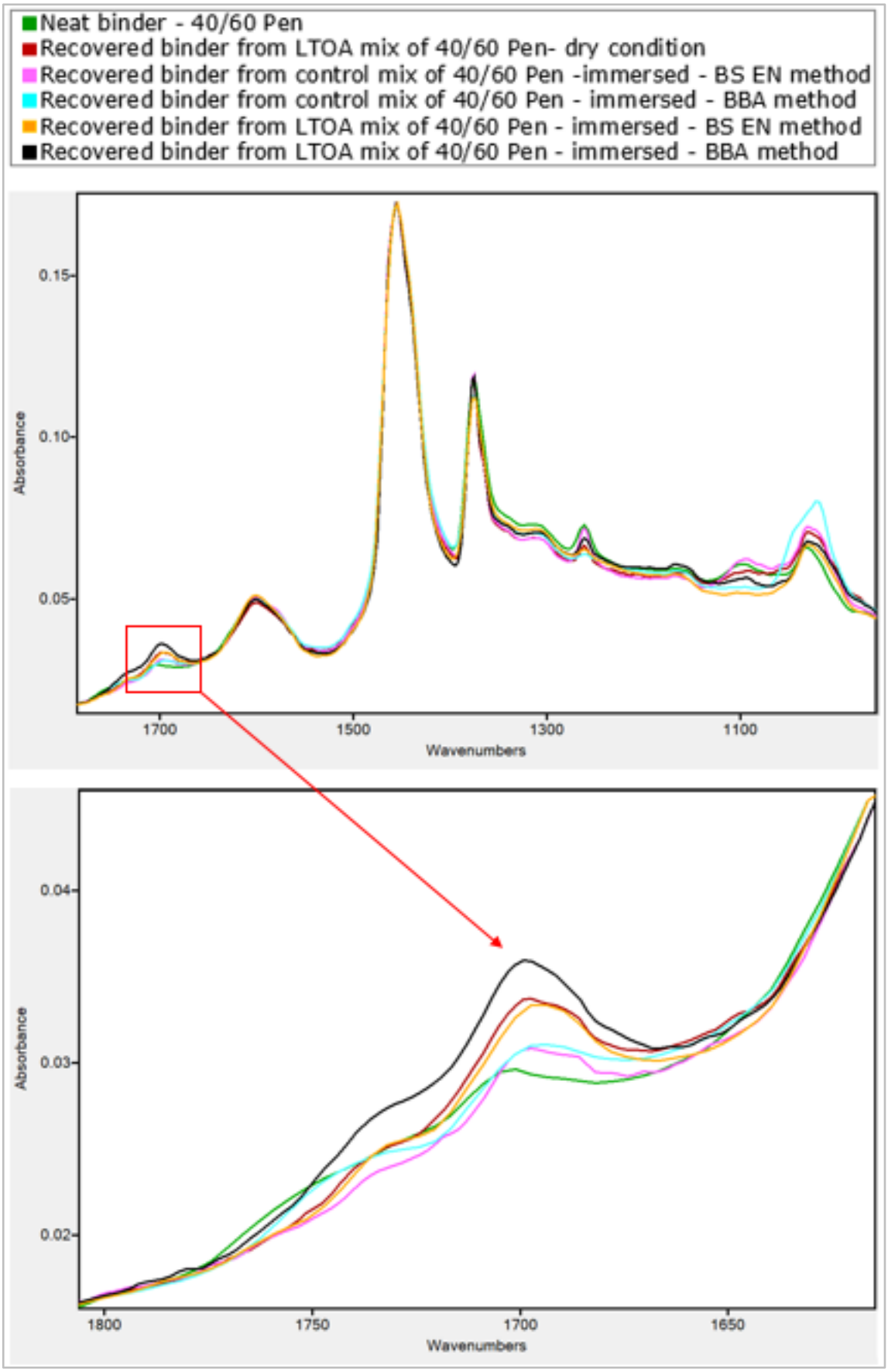



Figure 4.20: FTIR absorbance graph of asphalt binders recovered from mixtures of 40/60 Pen exposed to ageing and/or moisture damage.

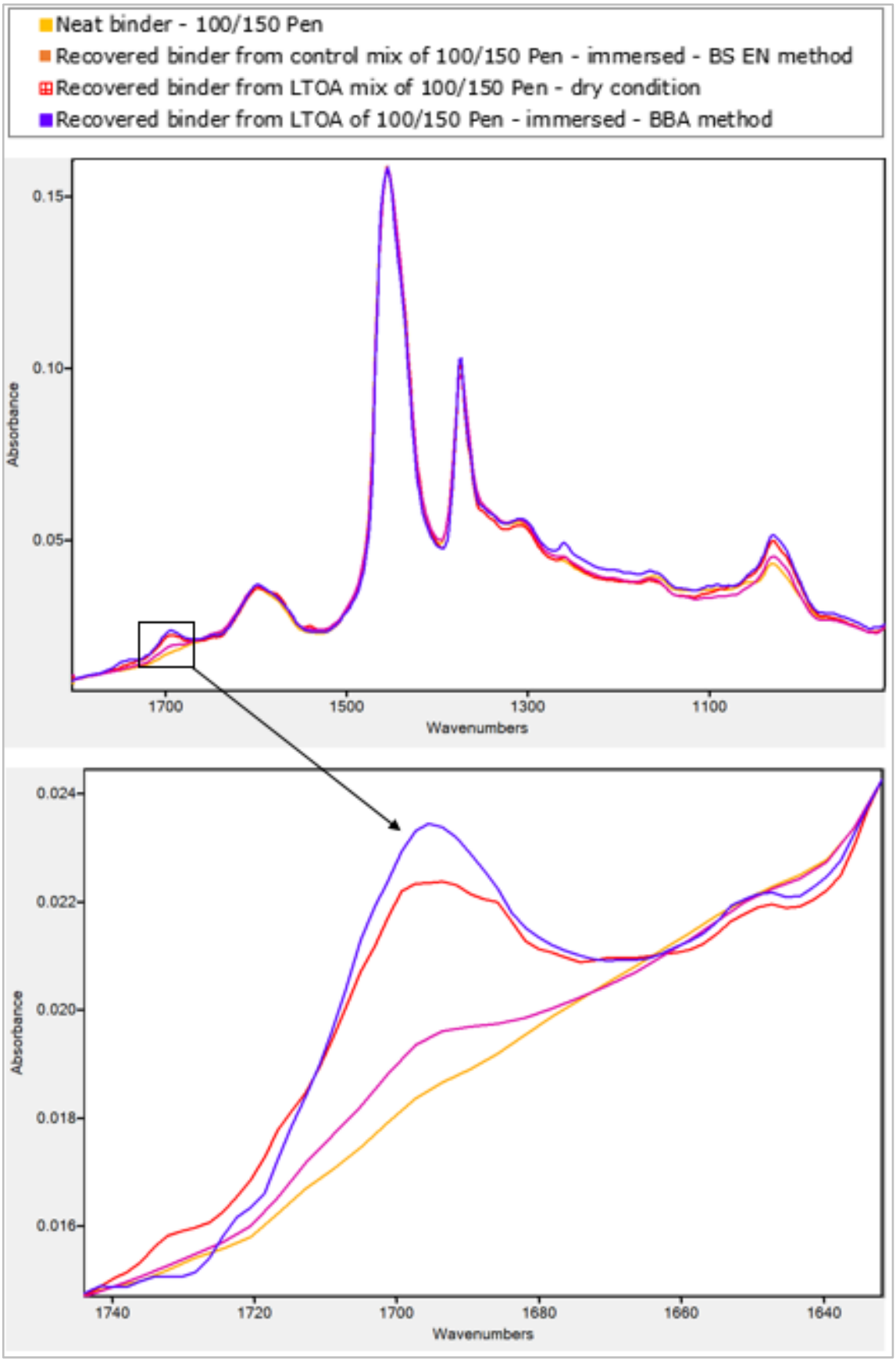



Figure 4.21: FTIR absorbance graph of asphalt binders recovered from mixtures of 100/150 Pen exposed to ageing and/or moisture damage.

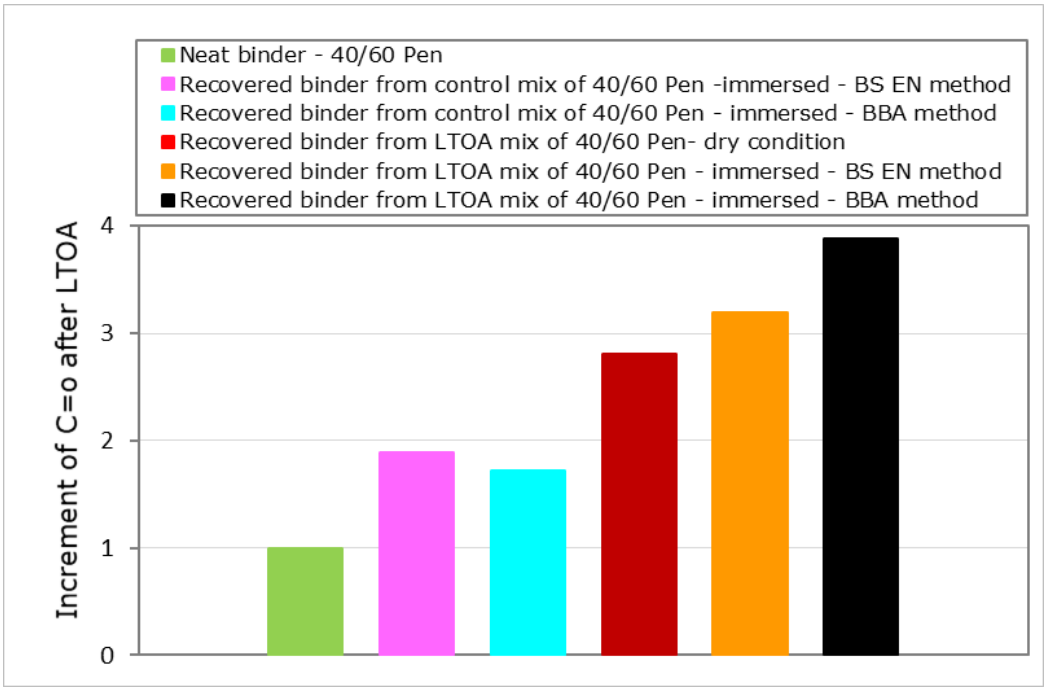



Figure 4.22: Effect of ageing and/or moisture damage on the increment of carbonyl component of asphalt binders recovered from mixtures of 40/60 Pen.

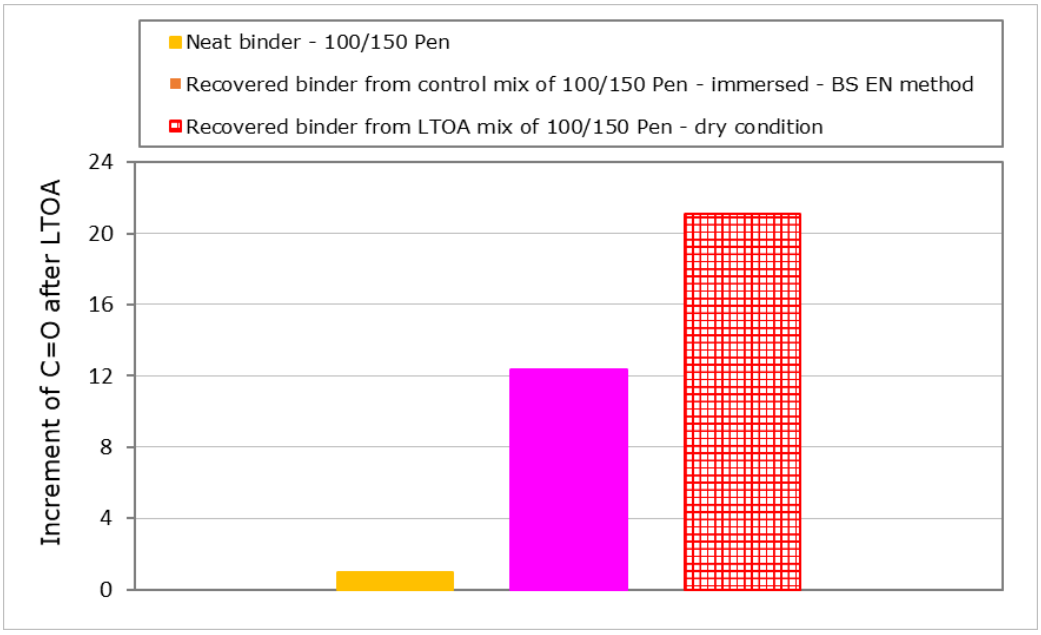



Figure 4.23: Effect of ageing and moisture damage on the increment of carbonyl component of asphalt binders recovered from mixtures of 100/150 Pen.

### 4.7.3 Effect of binder contents on IRSM

A small study using BBA method was performed to examine the effect of binder content (BC) on IRSM. 14mm DBM specimens were manufactured utilising only 40/60 Pen with 5% and 6% binder contents. The collected specimens were divided into two groups of 8%, and 12% air voids content. The specimens were tested for $ITSM_{unconditioned}$ at two testing temperatures 10˚C, and 20˚C in dry conditions. Then the BBA method was applied to these specimens and $ITSM_{conditioned}$ was measured at the same temperatures in wet conditions. The same procedure was repeated to other specimens set after applying LTOA. Figure 4.24 displays IRSM of both control and LTOA 14mm DBM mixtures. It also compares between the individual effect of moisture and the combined effect of moisture and ageing. In general, the IRSM of asphalt mixtures of 5% BC was slightly higher than IRSM of those of 6% BC when evaluated at two different air voids content 8% and 12%. Similarly, Airey et al., 2008 found that decreasing the air voids content from approximately 10–4% or increasing the bitumen content from 4% to 5% have a negligible effect on the retained stiffness values for both the acidic and basic DBM mixtures when tested in the Saturation Ageing Tensile Stiffness (SATS) test. Maupin and Diefenderfer, 2006 also found that higher binder content causes only a negligible increase in TSR.

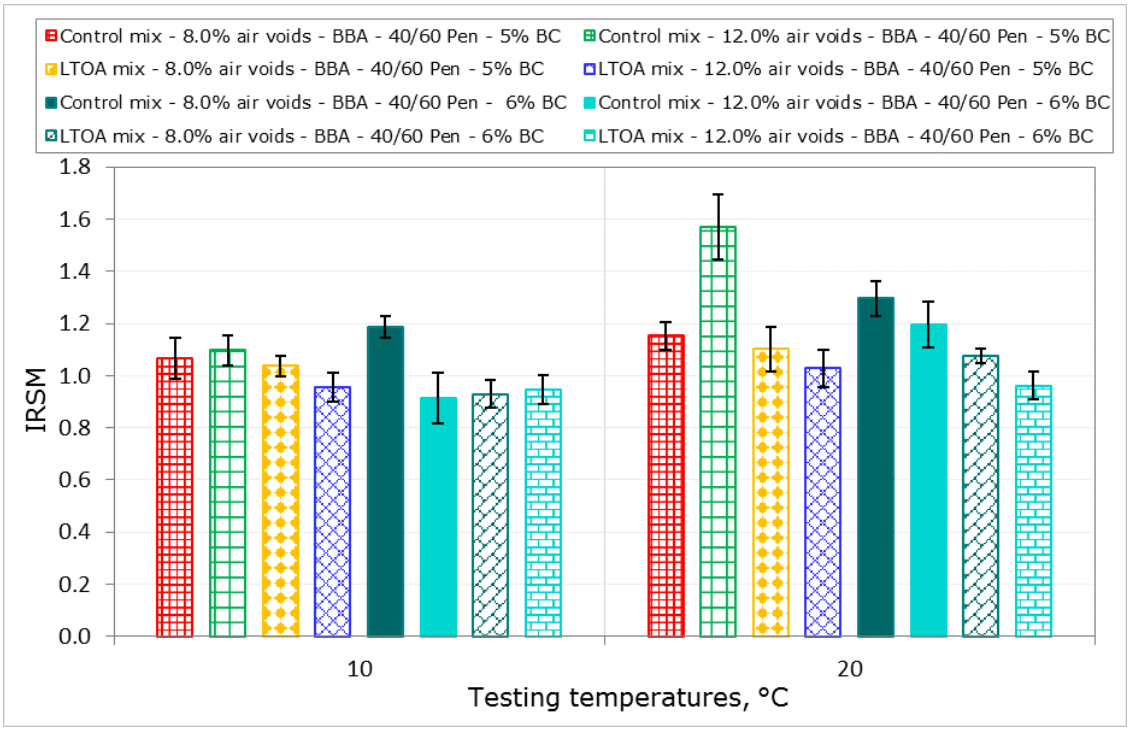



Figure 4.24: IRSM of 14mm DBM with different binder contents.

Finally, a summary of IRSM findings has been prepared for the investigated parameters and presented in Table 4.6. It compares between the different methods of moisture induced damage, the individual effect of moisture and the combined effect of moisture and ageing, the effects of binder grades and content, air voids content, and testing temperatures.

Table 4.6: Summary of IRSM results (index used to evalute the effect of moisture damage).

| Parameters | | $IRSM = ITSM_{conditioned}/ITSM_{unconditioned}$ | | | | | | | | | | | | | | | |
|---|---|---|---|---|---|---|---|---|---|---|---|---|---|---|---|---|---|
| Mix condition | | Control Mix | | | | | | | | LTOA Mix | | | | | | | |
| Binder grades and content | | 10/20 Pen 5% BC | | 100/150 Pen 5% BC | | 40/60 Pen 5% BC | | 40/60 Pen 6% BC | | 10/20 Pen 5% BC | | 100/150 Pen 5% BC | | 40/60 Pen 5% BC | | 40/60 Pen 6% BC | |
| Testing Method | Air voids % | 8 | 12 | 8 | 12 | 8 | 12 | 8 | 12 | 8 | 12 | 8 | 12 | 8 | 12 | 8 | 12 |
| | T, °C | | | | | | | | | | | | | | | | |
| BBA | 10 | 0.99 | 0.98 | 1.13 | 1.19 | 1.07 | 1.10 | 1.19 | 0.91 | 0.83 | 0.91 | 0.91 | 1.05 | 1.04 | 0.96 | 0.93 | 0.95 |
| | 20 | 1.00 | 1.01 | 1.12 | 1.39 | 1.15 | 1.57 | 1.30 | 1.20 | 0.99 | 0.99 | 0.86 | 0.82 | 1.10 | 1.03 | 1.08 | 0.96 |
| BS EN | 0 | 0.93 | 0.85 | 0.89 | 0.83 | 1.03 | 1.03 | - | - | 0.98 | 1.07 | 0.88 | 0.83 | 1.03 | 1.07 | - | - |
| | 10 | 0.92 | 0.87 | 0.91 | 0.88 | 0.89 | 0.85 | - | - | 0.92 | 0.96 | 1.11 | 0.89 | 1.17 | 1.11 | - | - |
| | 20 | 0.98 | 0.99 | 1.14 | 0.99 | 0.85 | 0.82 | - | - | 0.89 | 0.89 | 1.04 | 0.83 | 1.05 | 0.92 | - | - |
| | 30 | 1.17 | 1.07 | 1.19 | 1.23 | 1.25 | 1.41 | - | - | 0.99 | 0.91 | 0.95 | 0.85 | 1.27 | 1.16 | - | - |

## 4.8 Summary

This study set out to find the individual and combined effects of ageing and moisture damage on the stiffness modulus of asphalt mixtures. To achieve the purpose of this part, different mixtures, different testing parameters and conditions, and different methods of moisture sensitivity determination were used in this work. AI and IRSM were used as indicators of these effects. Accordingly, the following points can be summarised:

1. The current study has found that ITSM of asphalt mixtures has increased due to applying both phases of ageing; STOA and LTOA. LTOA has expectedly caused more increase in ITSM than STOA at all evaluated conditions and variables. Lowering the testing temperature from 20 to 10°C has also increased ITSM.

2. Air voids content has a great influence on ageing and therefore Ageing Index seems to be air voids content dependent. In general, the higher the air voids content, the higher the Ageing Index. This means air voids increase allows more access for oxidation and in turn more ageing of bituminous material.

3. One of the interesting finding is the effect of testing temperature on the Ageing Index of asphalt mixtures manufactured with different binder grades. It was found that the Ageing Index at 20˚C is greater than at 10˚C. The reason might be attributed to the temperature susceptibility of asphalt mixtures. The mixtures exposed to LTOA condition are less potential to acquire more stiffness when the testing temperature decreases from 20 to 10˚C while the mixture exposed to STOA is originally less temperature susceptible and therefore should be more susceptible for being stiffer at 10˚C. This resulted in reducing the magnitude of Ageing Index at 10˚C (AI= $ITSM_{LTOA}/ITSM_{STOA}$).

4. It was found that Ageing Index is reliant on binder grades. In general, the softer the binder the higher the Ageing Index and vice versa. The reason seems to be related to the content of the responsible components for ageing such as sulfoxide and carbonyl in each of these binder grades and their increment after ageing. The neat softer binder has a smaller amount of these components and therefore has more potential ageing due to the increase of these component after ageing compared to the neat harder binder which already has more.

5. AI has decreased due to the increase of binder content to 6%. A possible explanation for that may be related to the bitumen film thickness. The greater the thickness of the bitumen coating on the aggregate surface the longer the required time for the whole bitumen film thickness to become hardened and vice versa. However, the collected results of this variable were not sufficient to judge on its effect due to time limitations of this work.

6. The assessment of Ageing Index based on the measured ITSM might be considered as a simple Ageing Index. Measuring the ITSM over a wide range of loading frequency is not possible by using the NAT (Nottingham Asphalt Tester) and therefore deriving the Master curve is not possible. The investigation of Ageing Index by a more advanced test such as the complex modulus test, $|E^*|$

should be considered. The $|E^*|$ test typically provides the opportunity to generate a Master curve. This curve will provide the opportunity to look at the change in $|E^*|$ values due to applying oxidative ageing to different bituminous mixtures where ageing affects the viscous component of these mixtures. This curve specifically contributes to understanding the mixture behaviour at low frequencies (equivalent to high-temperature response where the viscous component of bituminous mixture dominates) and at high frequencies (equivalent to low-temperature response where the elastic component of bituminous mixture dominates).

7. IRSM values were greater than 80% in all circumstances of this study. Therefore, no significant moisture damage issues have arisen from using different water sensitivity testing methods to evaluate the asphalt limestone aggregate mixtures manufactured with different variables. Even if this damage was applied after LTOA to these mixtures.

8. The effect of moisture conditioning at different testing temperatures was unexpected. In general, there is a slight to significant increase due to testing temperature increase. On the other hand it was noticed some decrease in IRSM with temperature increase. These increases in the IRSM might be caused by possible ageing may take place during the period of moisture conditioning. In general, no obvious trend was found, although it was expected that the moisture influence will be more detrimental with the increase of testing temperatures.

9. In general, the control and LTOA mixtures of 40/60 Pen and 5% BC exhibited the most resistance to moisture damage. In particular, at 30 and 20˚C when BS EN and BBA methods were carried out respectively. But this increase with testing temperatures shifted to be more scattered when the moisture conditioning was applied to LTOA mixes.

10. The increase of ITSM of conditioned mixtures and in turn the increase of IRSM may be attributed to possible ageing that may take place during the course of moisture conditioning (40˚C in the course of BS EN method and 60˚C in the course of BBA protocol).

11. Testing the recovered binders may be a beneficial tool to find rational explanations of these findings. These results therefore need to be interpreted with caution.

12. It is purposed that there are two important opposite roles of moisture contradicting each other and affecting the results of this study. The first one reduces the stiffness due to the loss of cohesion/adhesion of asphalt mixtures. The second one increases the stiffness due to the supposed possible ageing.

13. There are other important factors that should not be disregarded such as the effect of aggregate type, testing method, the time and temperature of moisture conditioning. The type of aggregate which is limestone in this study may play an important role in these findings. Limestone is generally classified as hydrophobic (water-hating) substances and therefore has a good resistance to stripping. Therefore, it would be sensible to test more aggregate types, different conditioning temperatures and longer conditioning time.

# Chapter Five: Evaluation of Physical and Rheological Properties of Neat and Recovered Binders

## 5.1 Introduction

Rheological properties of bituminous materials can change due to loading time and different conditions; temperature fluctuations and exposure to oxidation while in-service pavements. Consequently, studying these properties of the asphalt binder before and after the applied conditions in Chapter Four may explain some of the findings presented earlier in Chapter Four.

Therefore, this chapter set out to evaluate the rheological and physical properties of binders recovered from different asphalt mixtures exposed to moisture conditioning and/or ageing. It also aims to compare the resulting properties with that of neat binders to understand more the effect of applied environmental conditions.

To find a rational explanation for the findings presented earlier in Chapter 4, it was decided to carry out the following supplementary tests; Dynamic Shear Rheometer (AASHTO T 315-12), Softening Point (BS 2000-58:2015) and Needle Penetration (BS 2000-49:2007). These tests were applied to neat and recovered binders to obtain the shear complex modulus ($G^*$), phase angle (δ), softening point and penetration of these binders.

## 5.2 Bitumen recovery method

In this work, the fractionating column method was used in accordance with BS EN 12697-4:2015 for extracting the bitumen from the different asphalt mixtures as following:

### 5.2.1 Extraction of the bitumen and removal of insoluble matter

In this recovery test, the following steps should be applied to extract sufficient bitumen for performing a binder test such as DSR. Place a sufficient amount of the bituminous mixture in a suitable container and add about 1500 ml of dichloromethane (or other suitable solvent) to remove the bitumen from the aggregate and add sufficient silica gel to absorb any water present in the sample. Stir the contents of the container until the mineral aggregate is clear

and all of the soluble bitumen has dissolved. Allow the bitumen solution to stand for about 10 min, pour out the bitumen solution through a 63 μm sieve to remove the larger particles of aggregate and then free from other insoluble material. This can be achieved by separation by centrifuging as following: Remove insoluble matter from the bitumen solution by centrifuging at an acceleration of at least 15000 $m/s^2$ for (20 ± 5) min in a sample tube centrifuge. After removal of the aggregate, the bitumen solution was concentrated by atmospheric distillation in a fractionating column. The last traces of solvent were removed from the concentrate by distillation at a temperature of 100˚C above the expected softening point or 175˚C, whichever is the higher, with the pressure reduced from atmospheric pressure 100 kPa to 20 kPa with the aid of a stream of carbon dioxide gas.

Finally, prepare samples of bitumen for testing in accordance with EN 12594.

Branthaver et al., 1993 indicated that the binder recovery technique through solvent extraction is a process that can have a significant effect on the properties of the recovered binder. The used standard in this work, BS EN 12697-4:2015, stated that the use of the hot extraction methods may harden the binder and hence affect the results from subsequent tests. However, this hardening is usually regarded as approximately balancing the softening resulting from any remaining solvent. With regard to the phenomenon that some recovered binders were softer than the neat binder, Jiantao, 2009 concluded that the adsorption of some bitumen fractions is irrecoverable using this recovery techniques. However, there is another possible reason that could cause this result. Some chemical compositions from the solvent used in binder recovery might remain in the binder and could decrease the bitumen stiffness. The standard also indicates that to avoid the possibility of significant hardening of this method complete the total procedure (extraction and recovery) within 24 h.

Consequently, Amma et al., 2018 recommended that users should have caution when compare the results of a specific test of recovered asphalt binder to that derived for neat asphalt binders.

## 5.3 Rheological properties

### 5.3.1 Dynamic Shear Rheometer (DSR)

Dynamic Shear Rheometer (DSR) shown in Figure 5.1 is applicable to asphalt binders having a value of dynamic shear modulus in the range from 100 Pa to 10 MPa. This is typically obtained at a loading frequency of 10rad/sec (1.59 Hz) over a wide range of temperatures between 6 and 88˚C (AASHTO T 315-12). DSR can be carried out at a wide range of temperatures and loading times for the determination of Dynamic Mechanical Analysis (DMA) of bitumen (Petersen et al., 1994).

This test method is commonly conducted using an oscillatory (sinusoidal) loading form in the strain-controlled mode within the region of linear viscoelastic response to determine the dynamic shear modulus and phase angle of asphalt binder. In this method, the phase angle, δ, is the phase or lag difference between the sinusoidal stress and strain, can be measured to give an indication of the viscoelastic state of materials. In addition, the shear complex modulus can be measured by applying a sinusoidal strain to the asphalt binder specimen and reporting the resulting monitored stress as a function of frequency. The determination and analysis of DMA in this method is more common than the stress controlled method in which a specimen is tested in a sinusoidal stress to measure the resulting strain response (Airey, 1997). The configuration of DSR test is presented in Figure 5.2.




Figure 5.1: CVO - ADS Rheometer (AASHTO T-315).

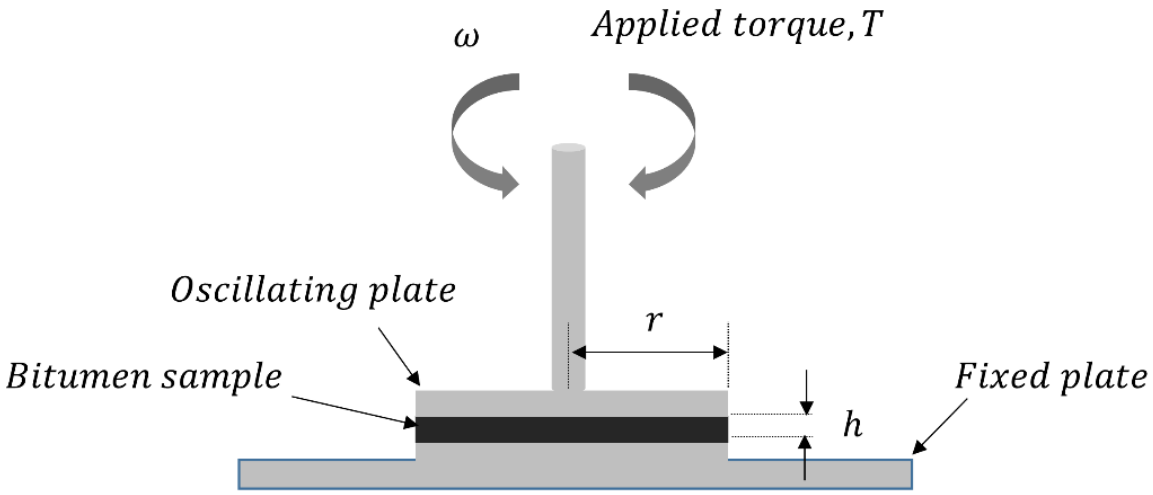



Figure 5.2: The DSR testing configuration (Subhy, 2017).

The monitored stress or strain are calculated based on the measured torque and angular rotation as follows:

$$\sigma = \frac{2\tau}{\pi r^3} \qquad 5.1$$

Where:

$\sigma$ = maximum shear stress (N/ mm2)

$\tau$ = torque (N.m)

r = radius of the parallel disks (mm)

$$\gamma = \frac{\theta r}{h} \qquad 5.2$$

Where:

$\boldsymbol{\gamma}$= shear strain

$\theta$ = deflection angle (radians)

h= gap between parallel plates (mm)

In addition, the complex shear modulus, $G^*$, can be calculated from the following:

$$G^* = \frac{\sigma_{max}}{\gamma_{max}} \qquad 5.3$$

Obviously, from Equations 5.1 and 5.2, the geometric properties of the oscillating plate, i.e. the gap between the upper and the lower parallel plates and radius of the parallel plates substantially affect the magnitudes of the shear stress and strain. Therefore, different sizes of parallel plate should be selected in the DSR testing according to the expected stiffness of tested materials to be in the same line of device's compliance. In general, for reliable measurements of viscoelastic properties of the tested bitumen, the plates of larger radius are typically used at higher testing temperatures while that of smaller radius are typically used at lower testing temperatures. Anderson et al., 1994 have used two different specimen geometries in the DSR testing to measure a wide range of bitumen stiffness; an 8-mm diameter parallel plate geometry for a range of temperatures from approximately 5 to 35˚C and 25-mm diameter plates configuration at temperatures above 35˚C.

In this work, the dynamic mechanical analysis (DMA) of the neat and recovered binders was undertaken by means of CVO-ADS Rheometer (AASHTO T 315) shown previously in Figure 5.1. Two test specimens of 2mm thick by 8mm in diameter and 1mm thick by 25mm in diameter are individually sandwiched between two parallel metal plates as shown in Figure 5.3. One of these two plates is oscillated with respect to the other at the applied loading frequencies from 0.1Hz to 10Hz and a wide range of testing temperatures; from 0˚C to 30˚C and from 25˚C to 70˚C for plates of 8mm and 25mm in diameter respectively.

The amplitude strain of 1% was found to be within the linear range of viscoelastic response of neat and recovered binders. It was determined according to the 95% SHRP definition using strain sweep test. This procedure was applied to neat and recovered binders from asphalt mixtures of 40/60 Pen and 100/150 Pen at different conditions. The details are shown in Table 5.1. The complex shear moduli and phase angles were measured at the selected loading times and at each testing temperature to produce the Master curve. The samples were tested with two replicates.

### 5.3.2 Master curve for complex shear modulus and Phase angle

The viscoelastic measurements of bituminous materials, i.e. shear complex modulus ($G^*$) and phase angle (δ) tested at different temperatures and loading times can be shifted to represent the viscoelastic behaviour at a reference temperature over a wide range of loading times. The principle is known as the Time-Temperature Superposition Principle (TTSP) or reduced variables method. The shifting to a reference temperature can be carried out by multiplying the loading times by a shift factor to produce a continuous curve which is known as a Master Curve (Anderson, et al. 1991, Airey 1997).

In this work, the main aim of the master curve is to inspect the effect of moisture conditioning procedures on the used asphalt binder. A master curve is developed using WLF equation (Williams, Landel and Ferry equation) for a selected reference temperature of 20˚C. This equation has been widely used to describe the relationship between the shift factor $\alpha T$ and temperatures. The master curve provides an evaluation of temperatures influence on viscoelastic properties of the tested material at the defined range of loading frequencies. It was prepared by shifting all other curves horizontally without changing the shape to correspond with the reference curve and forming a unique smooth master curve. For more details, Airey, 1997 described the manual shifting process in order to combine the different curves into a unique continuous one.

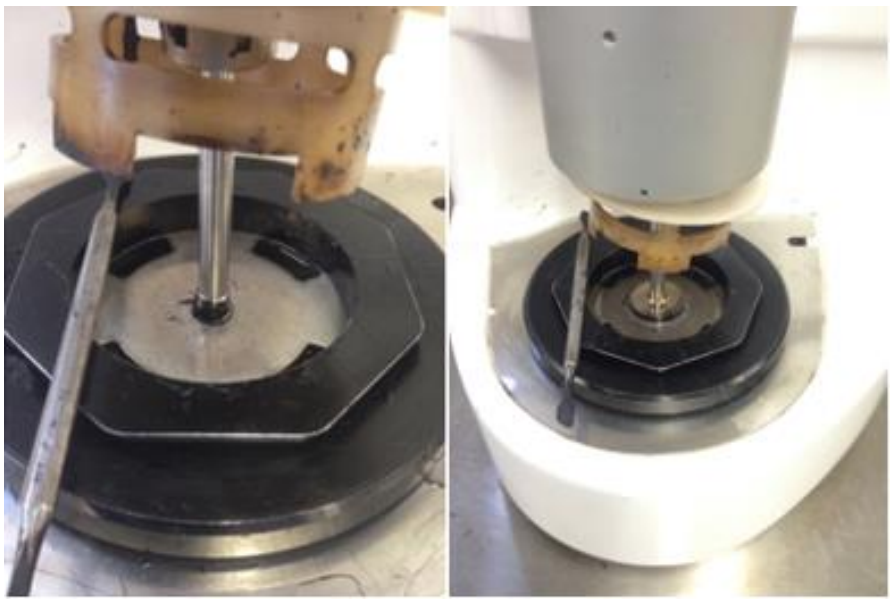


Figure 5.3: Dynamic Shear Rheometer (DSR) apparatus and specimens set up.

Table 5.1: Details of recovered binders for DSR test.

| Binder status | | The neat or initial binder Pen used in mixtures manufacturing | |
|---|---|---|---|
| | | 40/60 | 100/150 |
| Neat binder (Not recovered) | | ✓ | ✓ |
| Recovered from | Control mix exposed to moisture sensitivity – BS EN method BS EN method (vacuum the compacted mixture at 6.7 ± 0.3 kPa for 30 ± 5 minutes and immersed in water at 40˚C for 72 hours before ITSM test). | ✓ | ✓ |
| | Control mix exposed to moisture sensitivity – BBA method (vacuum the compacted mixture at 68 ± 3.3 kPa for 30 ± 1 minutes and immersed in water at 60˚C for 6 hrs then at 5˚C for 16 hrs before ITSM test). | ✓ | - |
| | LTOA mix - dry condition | ✓ | ✓ |
| | LTOA mix exposed to moisture sensitivity – BS EN method BS EN method (vacuum the compacted mixture at 6.7 ± 0.3 kPa for 30 ± 5 minutes and immersed in water at 40˚C for 72 hours before ITSM test). | ✓ | - |
| | LTOA mix exposed to moisture sensitivity – BBA method (vacuum the compacted mixture at 68 ± 3.3 kPa for 30 ± 1 minutes and immersed in water at 60˚C for 6 hrs then at 5˚C for 16 hrs before ITSM test). | ✓ | ✓ |

### 5.3.3 Dynamic Mechanical Analysis (DMA)

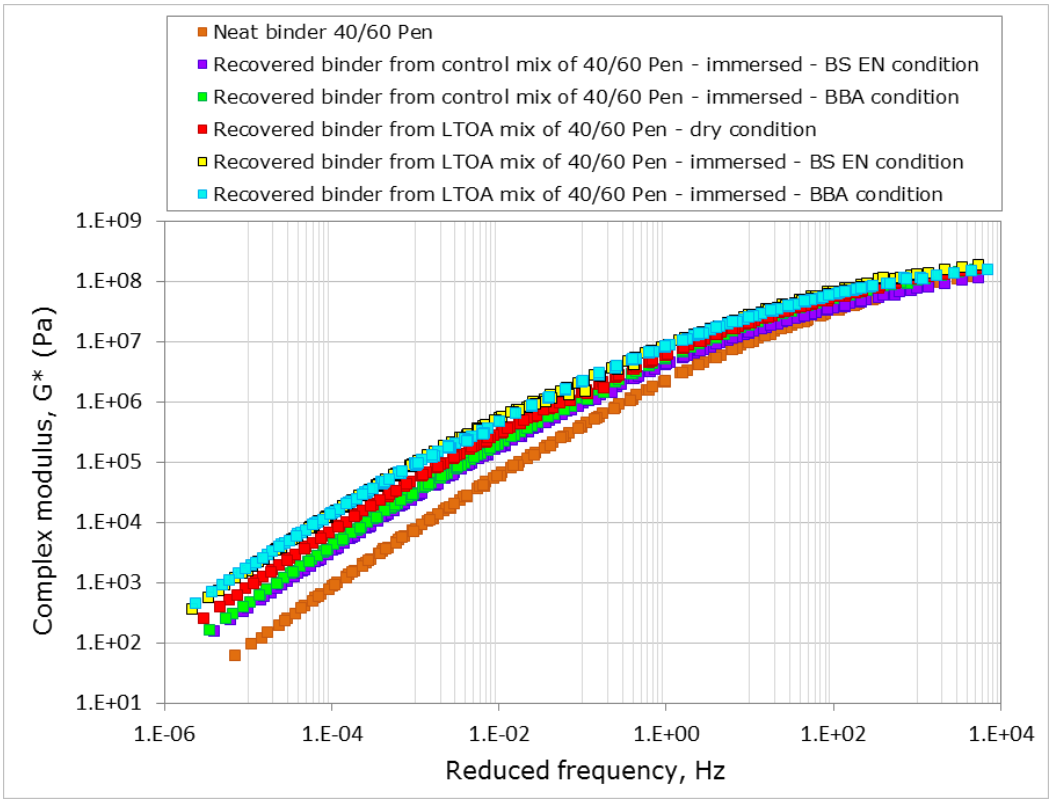
It is important to evaluate the rheology and viscoelastic properties of the neat and recovered binders from mixtures subjected to different ageing and water immersion conditions under different loading times and temperatures. This evaluation has been achieved by means of DMA to define the stress-strain-time-temperature response of the binders.

Master curves of complex modulus at a reference temperature of 20˚C were produced for these binders using the Time-Temperature Superposition Principle

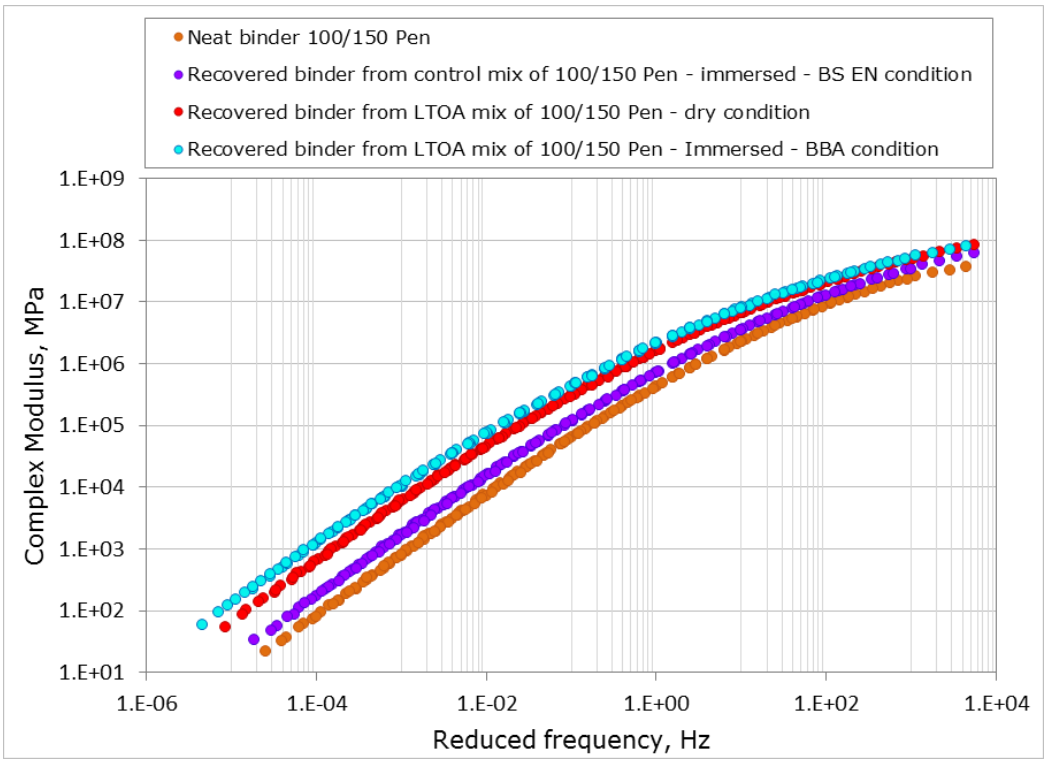
(TTSP) and William, Landel and Ferry (WLF) equation. Figure 5.4 shows the Master curves for the neat and recovered binders from mixtures manufactured with 40/60 Pen and 100/150 Pen respectively. It is obvious from this figure that the both applied moisture sensitivity methods (BBA and BS EN) have influenced the final properties of the recovered binder. The master curves of the recovered binders from conditioned control mixtures shows that both moisture sensitivity methods has resulted in a significant increase in the complex modulus, in particular, at low frequencies (equivalent to high-temperature response). However, this increase is less and it relatively seems constant in the case of 100/150 Pen and all related recovered binders. This increase in the complex modulus of recovered binders may explain that increase of the ITSM that happened after exposing the asphalt mixtures to moisture conditioning as shown previously in Chapter Four.

This increased stiffness can be attributed to possible ageing that may take place during these procedures of moisture conditioning. Before testing, these mixtures have been exposed to 40˚C for 72 hours in the BS EN method and 60˚C for 6 hours followed by 5˚C for 16 hours in the BBA method. However, this increase was less when these mixtures stiffened earlier due to applying the STOA and LTOA before moisture conditioning.

Additionally, the phase angle master curves presented in Figure 5.5 shows a general decrease in the phase angle due to the effect of ageing or both moisture sensitivity methods. However, this decrease was less when these mixtures stiffened earlier due to applying the STOA and LTOA before moisture conditioning methods. In general, this decrease of phase angle refers to an increase in the elastic behaviour which generally take place due to ageing (Airey, 1997). That decrease of phase angle may enhance the assumption that ageing might take place during the procedure of both moisture sensitivity methods.

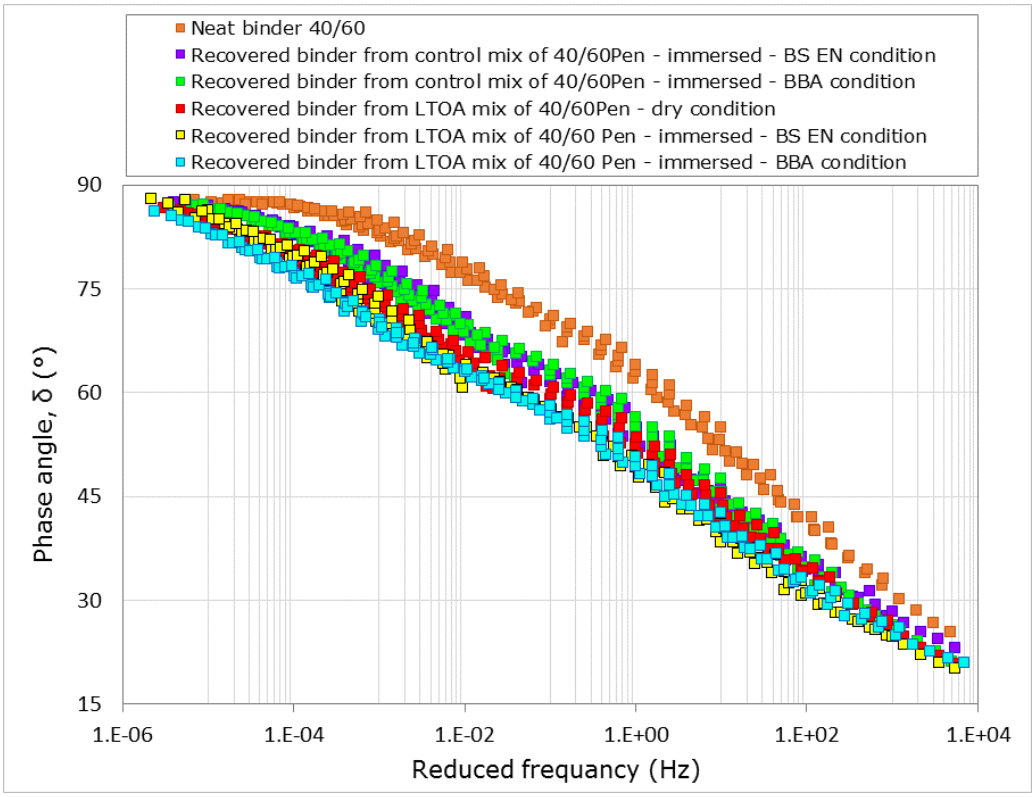



A: $G^*$ for neat and recovered binders from mixtures of 40/60 Pen.

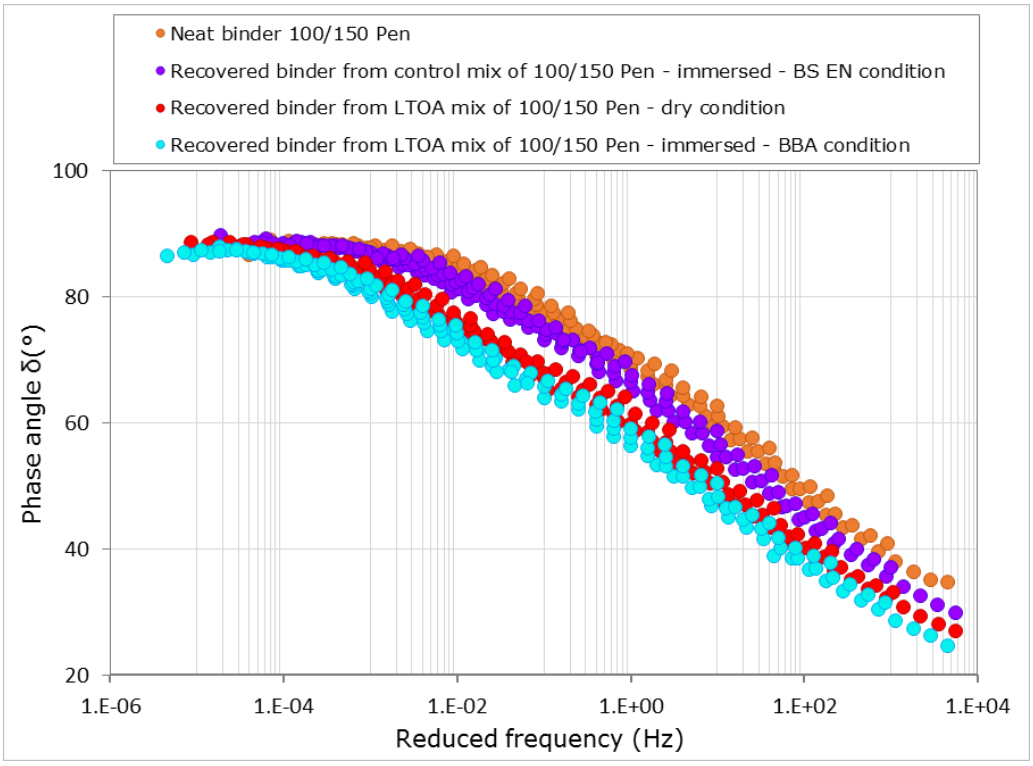



B: $G^*$ for neat and recovered binders from mixtures of 100/150 Pen.

Figure 5.4: Master curves for the shear complex modulus ($G^*$) at 20˚C reference temperature (RT) - effect of ageing and moisture conditions.




A: δ for neat and recovered binders from mixtures of 40/60 Pen.




B: δ for neat and recovered binders from mixtures of 100/150 Pen.

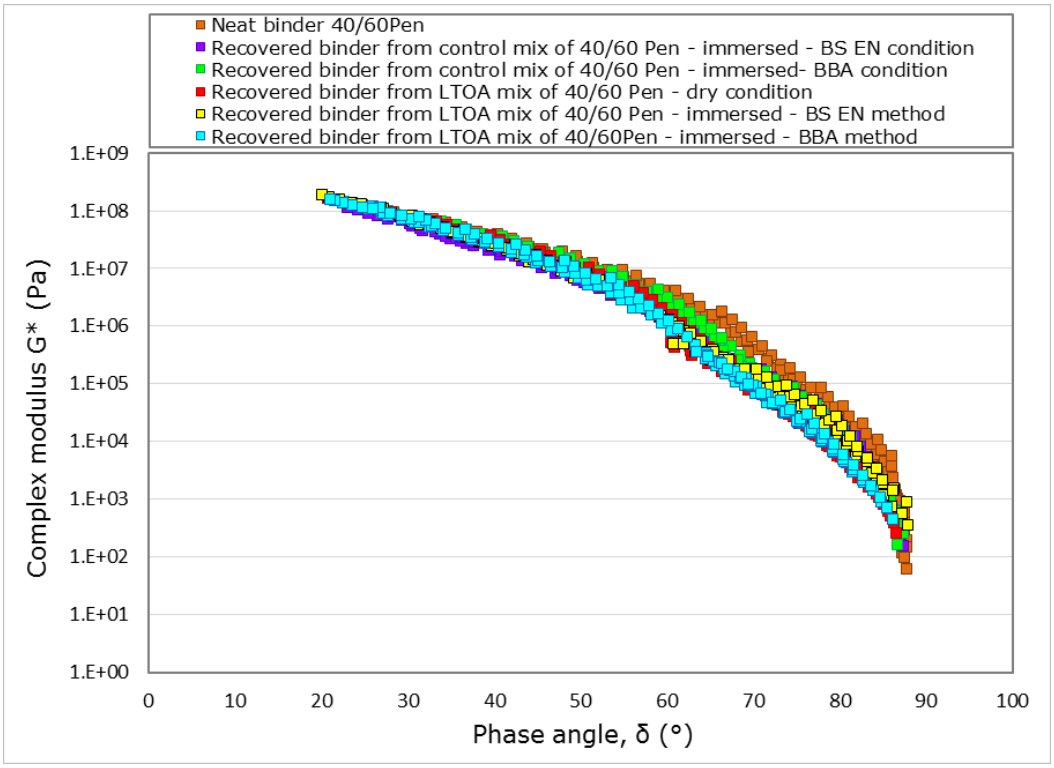
Figure 5.5: Master curves for phase angles (δ) at 20˚C reference temperature (RT) - effect of ageing and moisture conditions.

The black diagrams can be used to show the relation between the stiffness and viscoelastic behaviour of bituminous materials without applying any shift factors to the raw data as required for master curves (Airey, 2002).

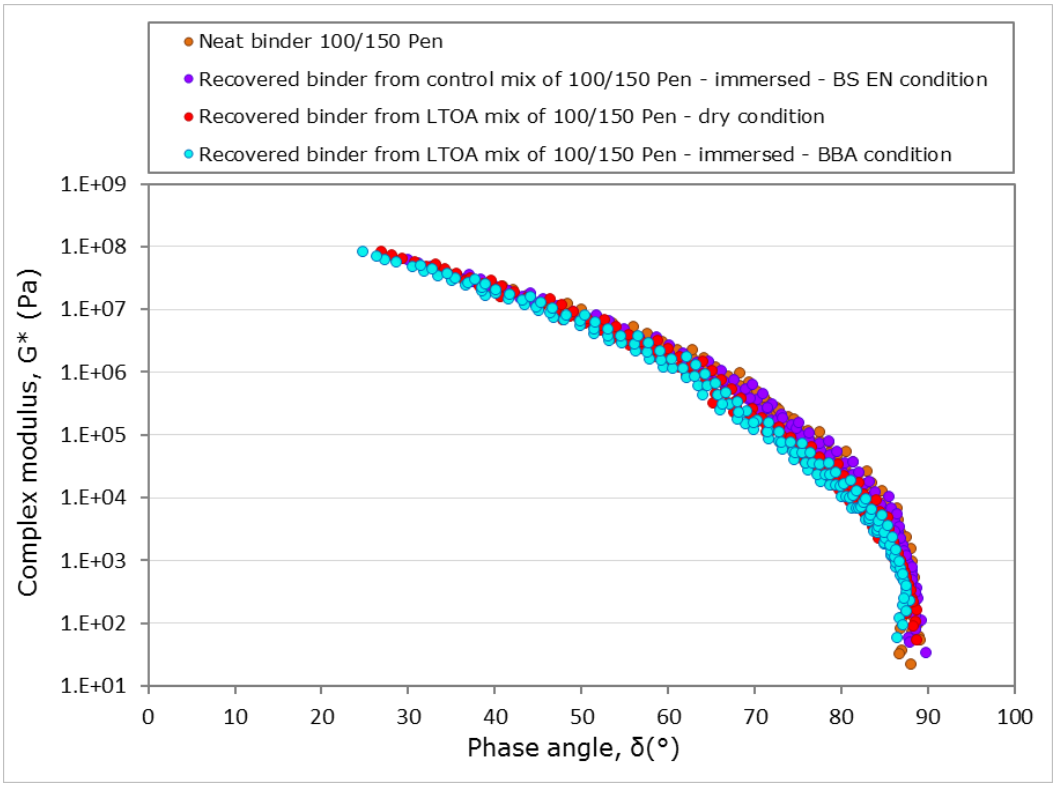
Figure 5.6 shows that diagram for the neat and different recovered binders. After ageing/moisture, there is an obvious continuous shift of the curves towards lower phase angles. However, it seems less obvious for the 100/150 pen and all related recovered binders. This shifting have resulted from the action of two factors; the increase of complex modulus, indicating the hardening of the bitumen and the decrease of phase angle, indicating an increase in the elastic behaviour of bitumen.

Airey, 1997 found that the shifting of Black diagram curves towards lower phase angle values with more 'solid-like' properties and a great percentages of elastic (brittle) behaviour is due to the action of these two factors. In addition, Lu and Isacsson, 2002 found that the mechanical properties of aged bitumens become more solid-like as a result of the chemical changes, which is indicated by increased complex modulus and decreased phase angle. Hofko et al., 2017 also found that ageing seems to induce a significant reduction in the phase angle after long-term ageing with the PAV.

In general, the increase of complex modulus and the decrease of phase angle shown by Black diagram curves may enhance the assumption of ageing manifestation during the procedure of moisture submersion.




A: Black diagram for neat and recovered binders from mixtures of 40/60 Pen.




B: Black diagram for neat and recovered binders from mixtures of 100/150 Pen.

Figure 5.6: Black diagram curves - effect of ageing and moisture conditions.

### 5.3.4 Shear Complex Modulus Index (SCMI)

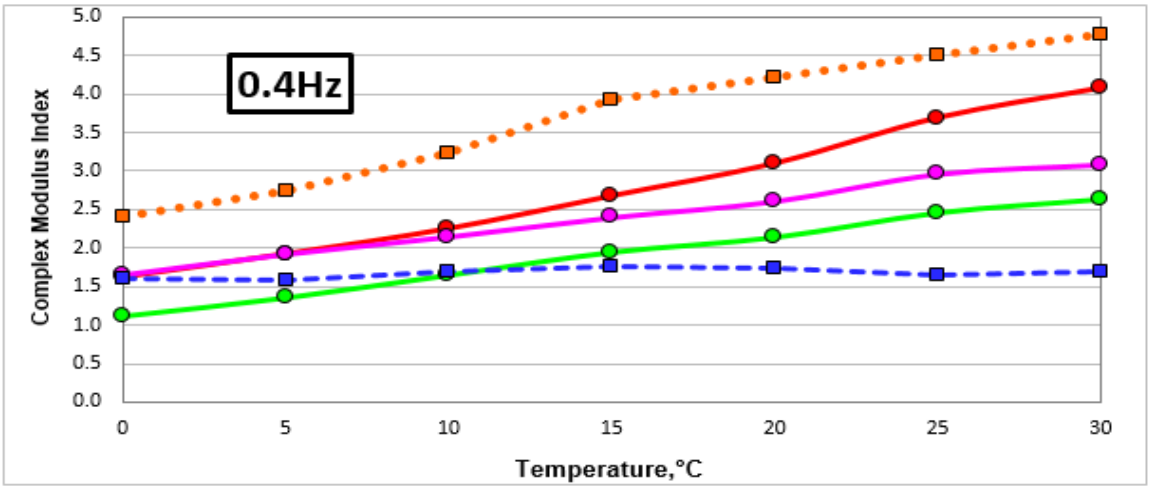
A shear complex modulus index (SCMI) was calculated to compare between the effects of ageing and/or moisture conditions applied in this work as following:

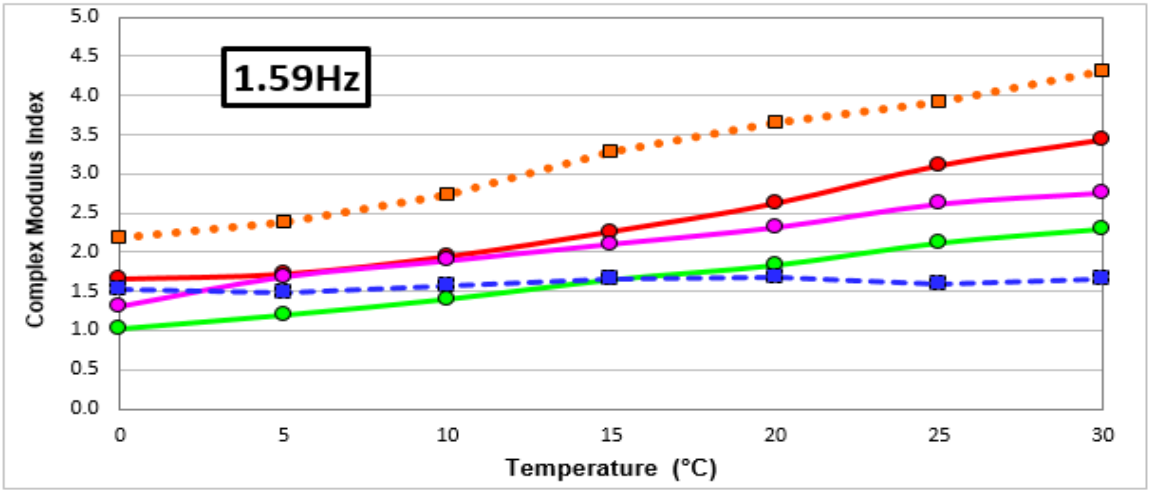
$$SCMI = Complex\ modulus_{recovered\ binder} / Complex\ modulus_{neat\ binder} \quad 5.4$$

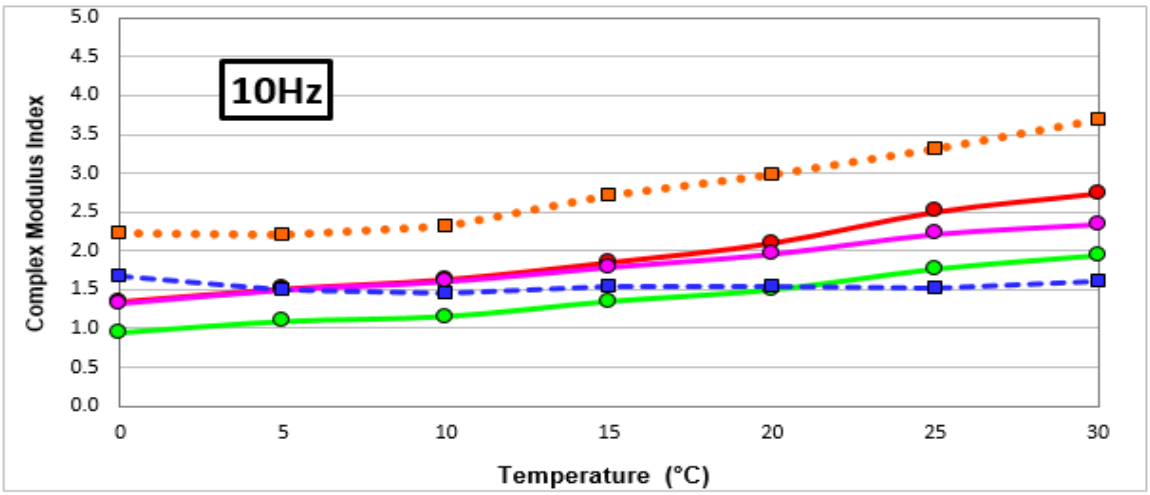
Figure 5.7 presents the resulting indices at different temperatures (0˚C-30˚C) and frequencies 0.4, 1.59 and 10 Hz from the 8-mm diameter parallel plate geometry. Although the SCMI due to LTOA of recovered binder from 100/150 Pen mixtures is substantially greater than that from 40/60 Pen mixtures, the SCMI due to moisture submersion is less pronounced. It is also relatively constant about 1.5 and not significantly influenced by testing temperature or loading times. On the other hand, all other indices are clearly reliant on testing temperatures and less on frequencies. It is difficult to understand that relative constant behaviour of the recovered binder from 100/150 Pen mixtures after moisture conditioning. It may be part of the complicated ageing and moisture damage behaviours.

Additionally, the recovered binder from mixtures exposed to BBA protocol have showed more increase in the complex modulus than BS EN one. However, these mixtures have been exposed to 60˚C for 6 hours followed by 5˚C for 16 hours compared to 40˚C for 72 hours in the BS EN method. It may reflect the importance of temperature and resulting degree of saturation (relatively 30% from BBA and 60% from BS EN) more than time of conditioning. The highest degree of saturation seems to produce the lowest the value of SCMI.

Moreover, samples of isochrones plot for complex modulus and phase angle at 10Hz and different conditions are presented in Figure 5.8. Obviously, for control mixtures, the modulus has increased and the phase angles has decreased after moisture submersion. Similar behaviour was observed when aged mixtures of 40/60 and 100/150 Pens were immersed in water in accordance with BBA method. These isochrones plot may also refer to an ageing taking place during the moisture conditioning itself.



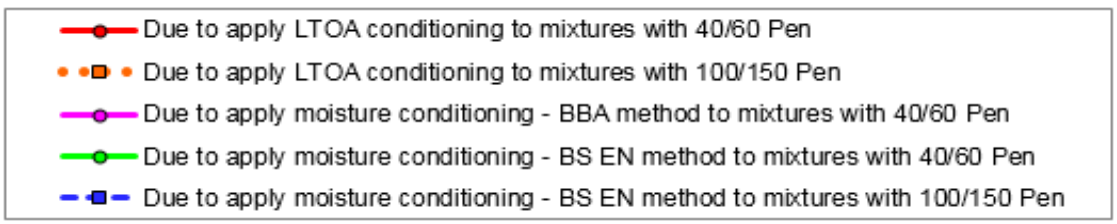
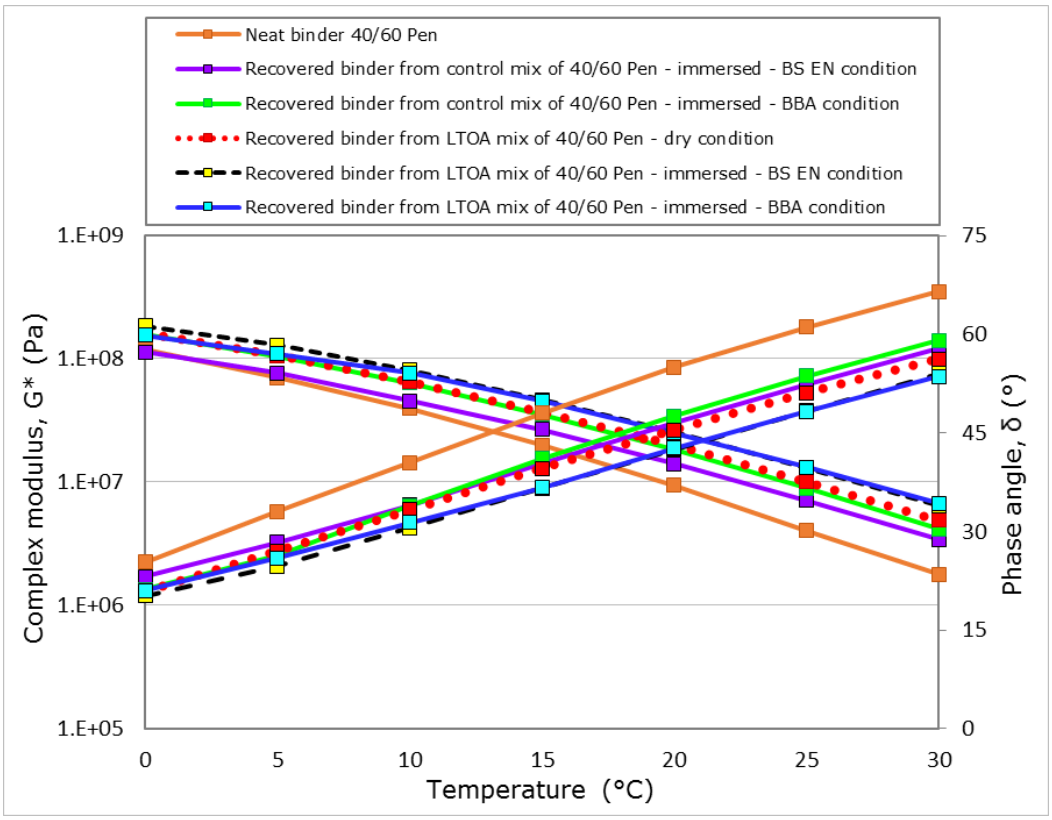
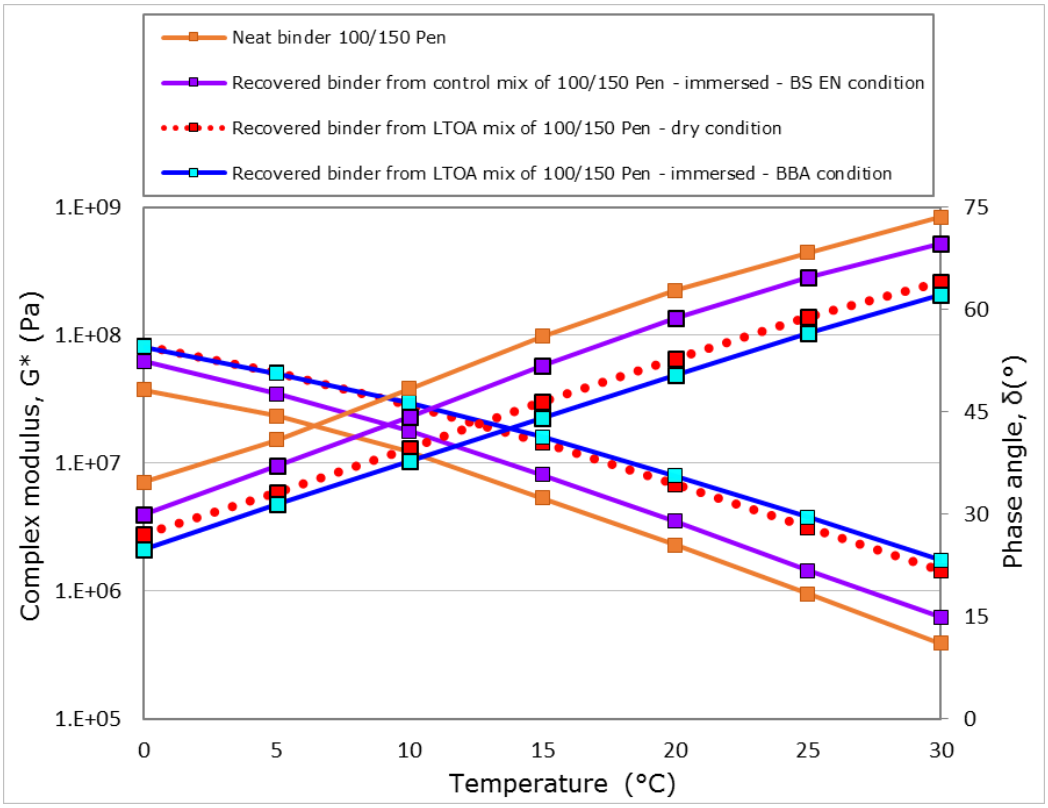




Figure 5.7: Shear complex modulus index (SCMI) at 20˚C of recovered binders from mixtures manufactured with 40/60 Pen and 100/150 Pen and exposed to ageing and moisture conditions.




A: Isochrones plot for neat and recovered binders from mixtures of 40/60 Pen.




B: Isochrones plot for neat and recovered binders from mixtures of 100/150 Pen.

Figure 5.8: Effect of ageing and moisture conditions on isochrones plot at 10Hz.

Finally, samples of WLF fitting of the shift factors aT are also presented in Figure 5.9 for the Master curve production.

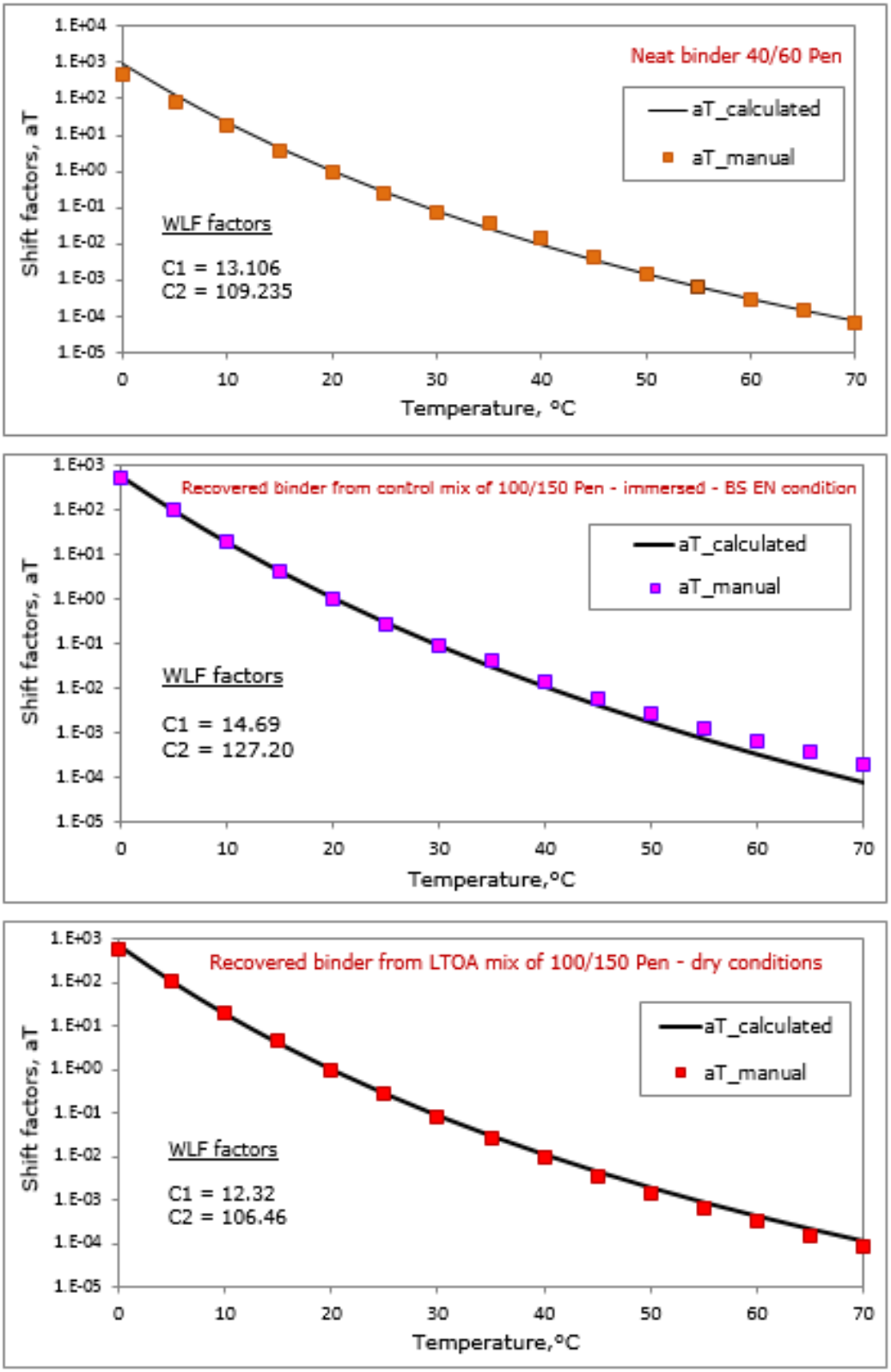



Figure 5.9: Samples of WLF fitting of the shift factors aT for the production of master curves.

## 5.4 Physical properties

The Penetration test and Ring and Ball Softening Point test were carried out for the neat binders; 10/20 Pen, 40/60 Pen, and 100/150 Pen. They also were carried out for the recovered binders from asphalt mixtures that were manufactured with these neat binders and exposed to ageing and/or moisture conditioning.

### 5.4.1 Penetration test

The penetration grade of the neat and recovered binders was determined using Needle Penetration Test in accordance with BS 2000-49:2007 Standard. The penetration is a measure of the bitumen consistency which is defined as the distance in tenths of millimetre (decimillimetre) that a standard needle is vertically allowed to penetrate into a bitumen sample under a specific load and loading time, and fixed testing temperature of 25˚C. Therefore, the softer the bitumen the greater the penetration and vice versa (Read and Whiteoak, 2003).

The Ageing Index was calculated from the penetration test results using Equation 5.5. Table 5.2 shows the results of penetration test and calculated Ageing Index.

$$Ageing\ Index\ (AI) = \frac{P_{neat\ binder}}{P_{recovered\ binder}} \quad 5.5$$

Where:

$P_{neat\ binder}$: Penetration grade as measured on the neat bitumen,

$P_{recovered\ binder}$: Penetration grade as measured on the recovered bitumen after the mixtures has been exposed to ageing and/or moisture.

### 5.4.2 Ring and Ball Softening Point test

The softening point of the neat and recovered binders was determined using Ring and Ball Softening Point test in accordance with BS 2000-58:2015 Standard. This test is an empirical test used to measure the equiviscous temperature at which the bitumen consistency is between solid and liquid. Regardless of the grade of the bitumen, the consistency will be the same for different grade bitumens at their respective softening point temperatures.

The softening point increment was calculated in accordance with Equation 5.6 as an indicator to measure the degree of actual and possible ageing.

$$\Delta S = S.P_{recovered\ binder} - S.P_{neat\ binder} \quad 5.6$$

Where:

ΔS: The softening point increment,

$S.P_{neat\ binder}$: The softening point as measured on the neat bitumen,

$S.P_{recovered\ binder}$: The softening point as measured on the recovered bitumen after the mixtures has been exposed to ageing and/or moisture.

The results of softening point test and calculated softening point increment are shown in Tables 5.3.

The analysis of penetration value at 25˚C and softening point temperature have shown a difference after ageing and/or moisture exposure. In general, the results of AI calculated from penetration test and softening point increment presented in Tables 5.2 and 5.3 refer to possible ageing may take place during the moisture conditioning of asphalt mixtures.

Table 5.2: Needle penetration test results and Ageing Index (AI).

| Binder status | | Needle penetration test results @25˚C, dmm (Pen) and calculated Ageing Index, ($AI=P_{neat\ binder}/P_{recovered\ binder}$). | | | | | |
|---|---|---|---|---|---|---|---|
| | | Binder 40/60 | | Binder 100/150 | | Binder 10/20 | |
| | | Pen | AI | Pen | AI | Pen | AI |
| Neat binder (Not recovered) | | 44 | 1.0 | 110 | 1.0 | 11 | 1.0 |
| Recovered from | Control mix exposed to moisture sensitivity – BS EN method | 29 | 1.52 | 75 | 1.47 | 10 | 1.1 |
| | Control mix exposed to moisture sensitivity – BBA method | 30 | 1.47 | - | - | - | - |
| | LTOA mix - dry condition | 26 | 1.69 | 50 | 2.20 | 7.0 | 1.57 |
| | LTOA mix exposed to moisture sensitivity – BS EN method | 21 | 2.10 | - | - | - | - |
| | LTOA mix exposed to moisture sensitivity – BBA method | 22 | 2.02 | 45 | 2.44 | 7.0 | 1.57 |

Table 5.3: Ring and Ball Softening Point temperatures and the Softening Point Increment (ΔS).

| Binder status | | Ring and Ball Softening Point, ˚C and the softening point increment, ($\Delta S = S.P_{recovered\ binder} - S.P_{neat\ binder}$) | | | | | |
|---|---|---|---|---|---|---|---|
| | | Binder 40/60 | | Binder 100/150 | | Binder 10/20 | |
| | | T, ˚C | ΔS | T, ˚C | ΔS | T, ˚C | ΔS |
| Neat binder (Not recovered) | | 50.9 | 0.0 | 43.2 | 0.0 | 74.4 | 0.0 |
| Recovered from | Control mix exposed to moisture sensitivity – BS EN method | 57.1 | 6.2 | 45.8 | 2.6 | 86.0 | 11.6 |
| | Control mix exposed to moisture sensitivity – BBA method | 56.2 | 5.3 | - | - | - | - |
| | LTOA mix - dry condition | 59.9 | 9.0 | 50.8 | 7.6 | 93.4 | 19.0 |
| | LTOA mix exposed to moisture sensitivity – BS EN method | 59.8 | 8.9 | - | - | - | - |
| | LTOA mix exposed to moisture sensitivity – BBA method | 61.3 | 10.4 | 52.4 | 9.2 | 95.0 | 20.6 |

## 5.5 Summary

In summary all supplementary tests in this work; DSR, penetration and softening point were carried out to find rational reasons for observed results in Chapter Four. Consequently, it can be summarised the following:

1. The investigated rheological and physical properties; complex shear modulus, phase angle, penetration grades, and Ring and Ball Softening Point temperatures have indicated that ageing of bitumen is possible to take place during moisture conditioning methods; BBA and BS EN.

2. It also should indicate that some of this ageing might be related to the STOA which is expected to happen during the production of asphalt mixtures; heating, mixing and compaction.

3. The main reason of this possible ageing may be related to the high temperatures, 60˚C and 40˚C that are applied during BBA and BS EN methods respectively.

4. Black diagram curves have showed more elastic (brittle) behaviour of binders recovered from mixtures exposed to moisture conditions which may enhance ageing manifestation during moisture conditioning.

5. SCMI due to LTOA of binder recovered from 100/150 Pen mixtures is substantially greater than SCMI of binder recovered from 40/60 Pen mixtures.

6. SCMI of the binder recovered from 100/150 Pen mixtures exposed to BS EN water sensitivity method is less pronounced. It is relatively constant about 1.5 and not significantly influenced by testing temperature or loading frequencies. On the other hand, all other indices are clearly reliant on testing temperatures and less on frequencies. It is difficult to understand that relative constant behaviour and it might be part of the complicated ageing and moisture damage behaviours.

7. SCMI of binder recovered from 40/60 Pen mixtures exposed to the conditions of BBA method is greater than SCMI of that exposed to the conditions of BS EN method. That may reflect the important difference of moisture conditioning temperature, resulting saturation level and time of moisture conditioning.

8. The behaviour of the investigated bitumens can be generally described after the actual ageing (STOA and LTOA) and supposed ageing due to moisture conditioning as more elastic, less viscous, stiffer rheological properties.

9. Finally, it is recommended that these results need to be considered with caution due to the disadvantages of binder recovery procedure stated earlier.

# Chapter Six: Evaluation of Environmental Effects on Dynamic Modulus of Asphalt Mixtures

## 6.1 Introduction

Understanding the individual and combined effect of moisture and ageing in combination with repeated loading is important. It can be efficient in assessing the influence of moisture damage and ageing on fatigue cracking. It can also be beneficial in selecting an appropriate blending of paving materials to resist these types of distresses.

Water damage in asphalt pavement generally occurs when the repeated traffic loading is applied at different temperatures to saturated pavement, inducing water movement or transitory pressure in the void structure of asphalt pavement (Kim and Coree, 2005). At the same time, the pavement will be exposed to another important factor, oxidation. Hence, if the asphalt binder ages and stiffens excessively due to oxidation, the asphalt mixture will be more susceptible to thermal and fatigue cracking. Therefore, various simulations are needed to consider these combinations of asphalt pavement conditions to produce simulative, rigorous, realistic, and practical laboratory testing protocols. One of these tests is the complex modulus $|E^*|$ test which measures a fundamental property of asphalt mixtures. It is defined as the relationship of stress strain amplitude as function of temperature and loading frequency (Zaumanis et al., 2017). This type of testing can consider the substantial relationship between the measurement of dynamic modulus and time of loading and temperature variations. Therefore, it was decided in this chapter to evaluate the combination of load frequency and testing temperature with the individual and combined influences of moisture and ageing to measure the complex modulus. This part was carried out by the 4PB machine in accordance with BS EN 12697-26: 2012.

One of the rare investigation to study the effect of moisture damage by the dynamic modulus test was carried out by Nadkarni et al., 2009. This test was used to determine the ratio of retained stiffness, identified as $|E^*|$ Stiffness Ratio (ESR). The results indicated that no statistically significant difference between the values of measured ESR and TSR (Tensile Strength Ratio) was found for the

same mixture. Consequently, it was recommended to potentially use ESR instead of TSR test to assess moisture induced damage of in situ asphalt mixtures. Further recommendation was to expand the testing programme and database for future works and analyses.

## 6.2 Complex Modulus Test |E*|

The complex modulus |E*| is widely used to characterise and define the stress strain relationship under a continuous sinusoidal loading of viscoelastic materials such as hot mix asphalt. The results of this test can be used directly in the Mechanistic-Empirical Pavement Design Guide (MEPDG) and are also considered a powerful representation of the expected performance of in-situ asphalt mixtures. However, further research is still needed to study how moisture can affect the complex modulus results (Williams, and Breakah, 2010). Therefore, the main objective of this part is to evaluate the usefulness of the complex modulus tests in the evaluation of moisture and/or ageing effects. It is also useful to produce a dynamic modulus master curve to represent the viscoelastic behaviour at a reference temperature over a wide range of loading times. The complex modulus can be calculated as the ratio of the peak stress to the peak strain. This term is called the norm of the complex modulus and can be expressed as following:

$$|E^*| = \frac{\sigma_t}{\varepsilon_t} \quad 6.1$$

Where:

|E*|= complex modulus

$\sigma_t$= Maximum tensile stress (Pa), $\sigma_t = (0.357P)/(bh^2)$ 6.2

P= load applied by actuator, in Newton,

b= average specimen width, in meters, and

h= average specimen height, in meters.

$\varepsilon_t$ = Maximum tensile strain, $\varepsilon_t = (12\delta h)/(3L^2 - 4a^2)$ 6.3

δ= maximum deflection at the centre of beam, in meters,

a= space between inside clamps, 0.357/3 m, (0.119m), and

L= length of beam between outside clamps, 0.357m

Furthermore, the lag between the load and deformation shown in Figure 6.1 can be expressed as a phase angle and calculated at each cycle as following:

$$\emptyset = 360fs \qquad 6.4$$

Where:
$\emptyset$= Phase angle (°),
$f$= load frequency in Hz, and
$s$= time lag between $P_{max}$ and $\delta_{max}$, in seconds.

The phase angle is a further related to the complex modulus as follows:
For a pure elastic material, the phase lag, Ø=0°, while for a pure viscous material, Ø=90°. The typical range of Ø for most asphalt mixtures varies from 0° to 60° (Rowe et al., 2009).

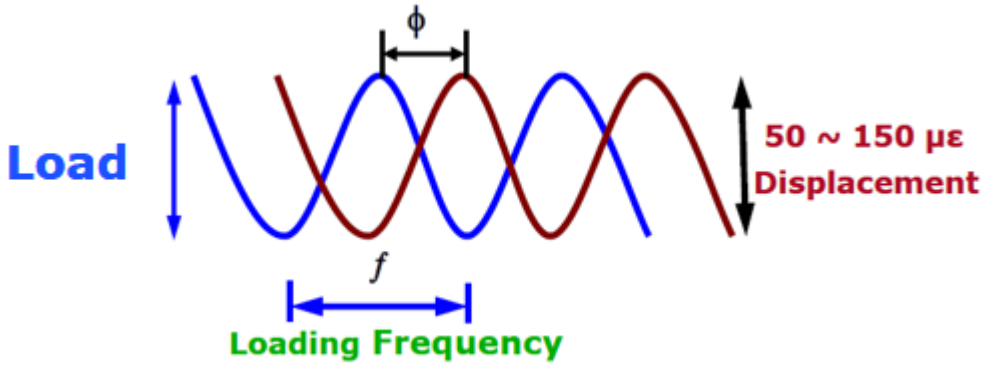



Figure 6.1: Typical sinusoidal wave during the complex modulus test.

The modulus is a complex quantity, of which the real part represents the elastic stiffness (storage modulus) and the imaginary part (loss modulus) characterises the internal damping of the materials. The storage modulus is called the elastic component of the complex modulus and it reflects the amount of energy which can be stored and released elastically. Whereas the loss modulus is identified as the viscous component or the imaginary part of the complex modulus (Airey, 1997). Accordingly, the absolute value of the complex modulus which is commonly referred to as the dynamic modulus can be calculated as following:

$$|E^*| = [E_1^2 + E_2^2]^{1/2} \qquad 6.5$$

Where:

$E_1$ = Storage modulus = $|E^*|$ cos Ø and

$E_2$ = Loss modulus = $|E^*|$ sin Ø

Figure 6.2 exhibits a representation of the complex modulus.

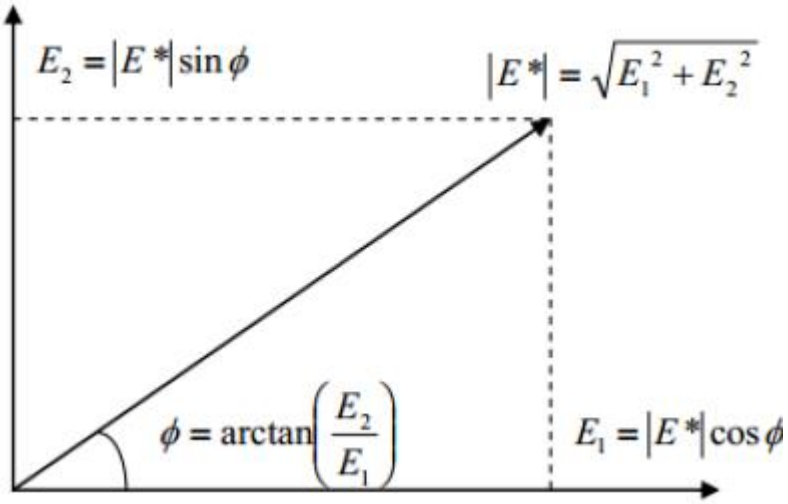



Figure 6.2: Representation of complex modulus (Airey, 1997).

The determination of $|E^*|$ and developing the representative master curve for the complex modulus/phase angle according to BS EN 12697-26: 2012 requires testing of three specimens of each asphalt mixture at 50με over a wide range of testing temperatures and loading frequencies. From each specimen, the $|E^*|$ should be measured at 10 loading frequencies and at 4 temperatures and the difference between them shall be at least 10˚C. In addition, it can be carried out in accordance with AASHTO TP 62, the measurement of $|E^*|$ requires testing at least two asphalt mixture specimens at six loading frequencies (0.1, 0.5, 1, 5, 10, 25 Hz) and five temperatures (-10, 4.4, 21.1, 37.8, 54.4 ˚C). However, Bonaquist and Christensen, 2005 and Bennert and Williams, 2009 have already recommended eliminating high and low temperatures to improve the precision of AASHTO TP 62.

In this work, $|E^*|$ testing being used to evaluate the performance of different asphalt mixtures subjected to different conditions by the four point bending machine. A test profile was written by the researcher due to the unavailability of specific software to perform that directly in the 4PB machine. A test profile sample is presented in Appendix A-1. A spectrum of loading frequencies (1, 2, 5, 8, 10, 15, 20, 25, 30, 40, 50, 60 Hz) and 6 different testing temperatures

(-10, 0, 5, 10, 20, 30 ˚C) were applied to test specimens at 50 με. In this study, two replicates were used to measure the complex (dynamic) modulus and the average was considered. At each loading frequency, a representative number of loading cycles shall be applied in order to measure the $|E^*|$ precisely. For higher frequencies 100 load repetitions can be applied while at lower frequencies 50 loading cycles are enough (BS EN 12697-26: 2012). In this test, it was decided to eliminate 50 and 60 Hz because the phase angle became unstable at higher frequency and lower temperature. The reason may be attributed to the testing machine which is not stiff enough at higher frequency and lower temperature compared to the stiffness of the tested specimen and therefore it was unstable. This consequence is consistent with that observed by Maggiore, 2014.

The principal concepts of the four point bending test (4PBT) with the key are shown in Figure 6.3 and Table 6.1 respectively. The prismatic beam specimens were fabricated as explained in Chapter Three using two binder grades; 40/60 and 100/150. Table 6.2 presents the applied conditions to manufactured mixtures. Damage check tests for each mixture were carried out at -10˚C to examine any possible damage which might take place during the dynamic modulus series tests. A sample is presented in Figure 6.4 between the $|E^*|$ at commencement of $|E^*|$ series tests and $|E^*|$ at the end. It seems from this figure that there is slight difference in $|E^*|$ which might be considered not significant and within the test limitations.

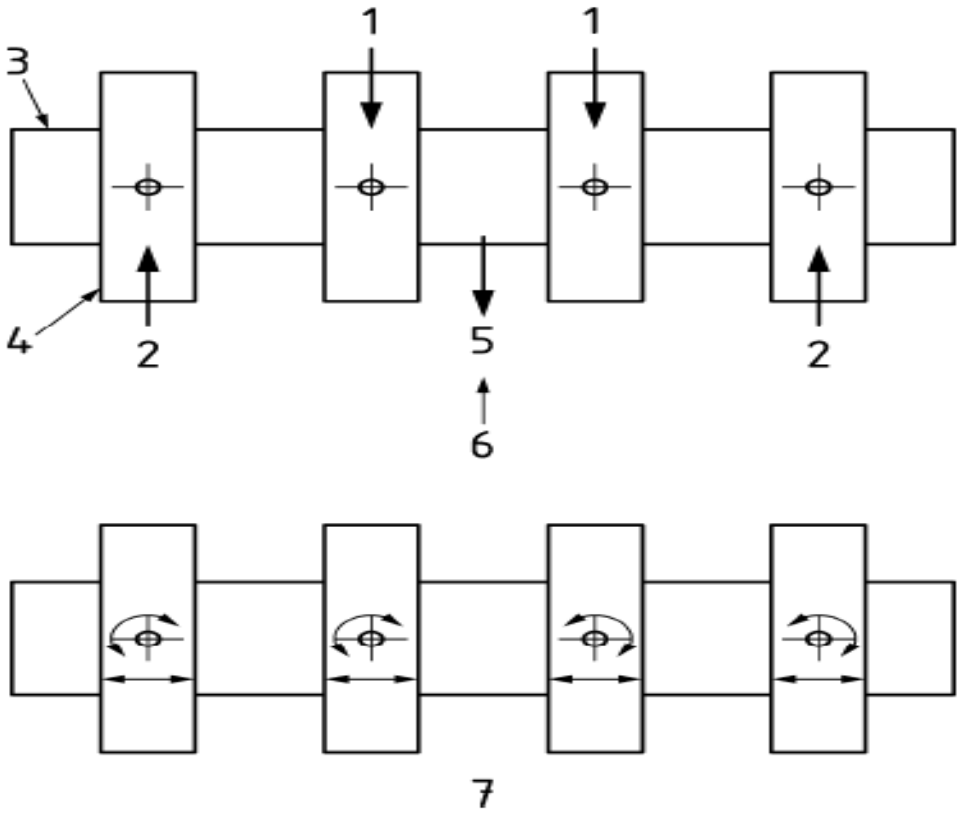



Figure 6.3: Basic principles of 4- point bending (BS EN 12697-26: 2012).

Table 6.1: Key of basic principles of 4- point bending shown in Figure 5.3.

| | |
|---|---|
| 1 | Applied load |
| 2 | Reaction |
| 3 | Specimen |
| 4 | Specimen clamp |
| 5 | Deflection |
| 6 | Return to original position |
| 7 | Free translation and rotation |

Table 6.2: Summary of investigated mixture conditions for complex modulus tests.

| **Mixtures exposed to specific conditions** | **Mixture manufactured with binder grade** | |
|---|---|---|
| | **40/60** | **100/150** |
| Control mixture, dry prismatic beams | √ | √ |
| Control mixture, immersed prismatic beams in water according to BS EN method as detailed in Table 4.5. | √ | √ |
| LTOA mixture, dry prismatic beams (before compaction, the loose mixture subjected to 135˚C for 4 hours then, the compacted mixture subjected to 85˚C for 120 hours). | √ | √ |
| LTOA mixture, immersed prismatic beams (the loose mixture subjected to 135˚C for 4 hours then the compacted mixture subjected to 85˚C for 120 hours) in water according to BS EN method as detailed in Table 4.5. | √ | √ |

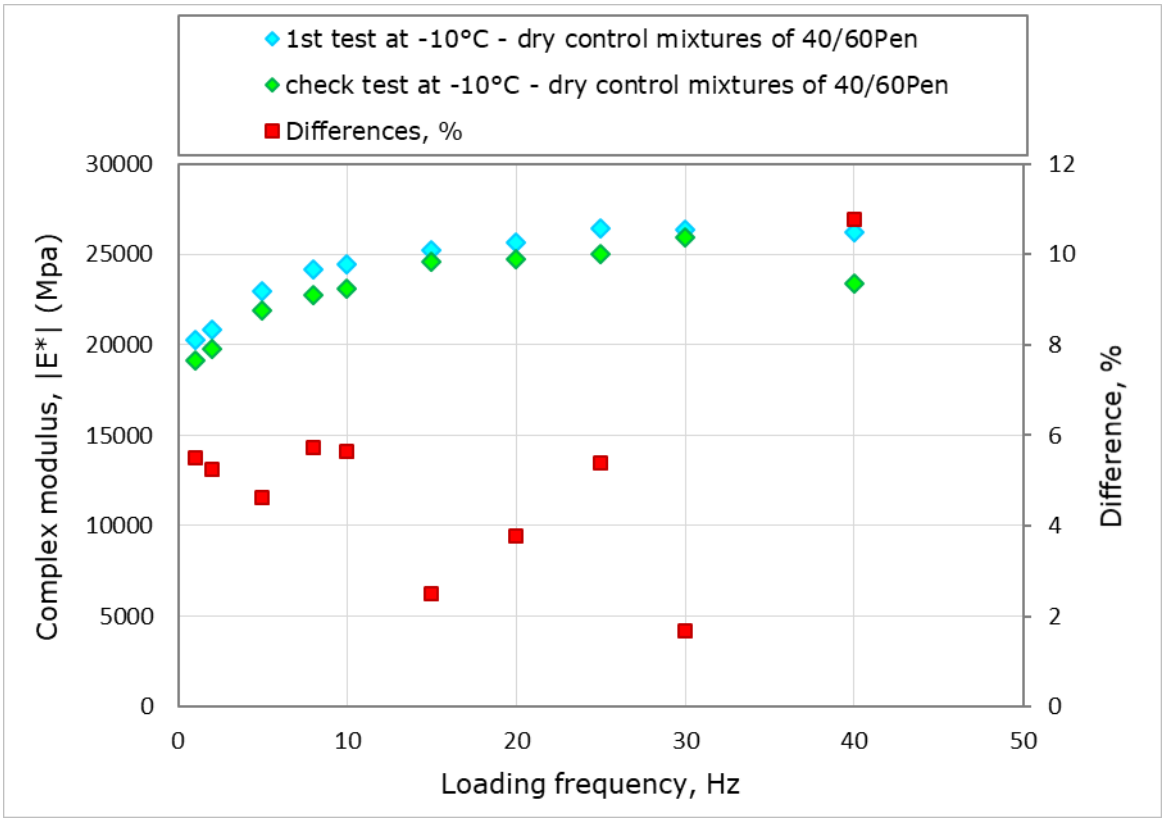



Figure 6.4: Check test of the damage during the dynamic modulus.

### 6.3 Master curve for the complex modulus |E*| and Phase angles δ (°)

The construction of the complex modulus, |E*| master curve for asphalt mixtures is considered one of the important key inputs required for mechanistic-empirical pavement design and evaluation. There are several reasons for this importance; first, it provides the ability to forecast |E*| at temperatures and/or frequencies that would be not possible to determine in the laboratory due to equipment limitations or time constraints. Second, |E*| master curve can be used to model pavements across wide range of possible pavement climatic and loading conditions. Third, it is useful to compare between different mixtures performance in terms of fatigue cracking and rutting resistance (Apeagyei and Diefenderfer, 2011).

A master curve for |E*| and δ are constructed in this study using WLF equation (Williams, Landel and Ferry equation) for a selected reference temperature of 20°C. The same procedures were previously explained in Chapter 5. It can be also constructed in accordance with AASHTO PP 62, 2009 (Apeagyei and Diefenderfer, 2011).

### 6.4 Discussion of complex modulus |E*| and Phase angles δ (°) results

Performing the dynamic modulus test and constructing the master curve provide the opportunity to examine the behaviour of asphalt mixtures subjected to ageing and/or moisture over a wide range of temperatures and loading frequencies. It can also provide more simulation and understanding of the influence of different factor combinations on these mixtures at the same time. All the dynamic modulus test results of the fabricated prismatic beam specimens are presented in Figures 6.5 to 6.12. These figures show the constructed master curves for |E*|, $|E^*|_{index}$, master curves for δ, black diagrams, E1-E2 relationship, and isochronal plots respectively. $|E^*|_{index}$ was calculated as an indicator for ageing and/or moisture damage as following:

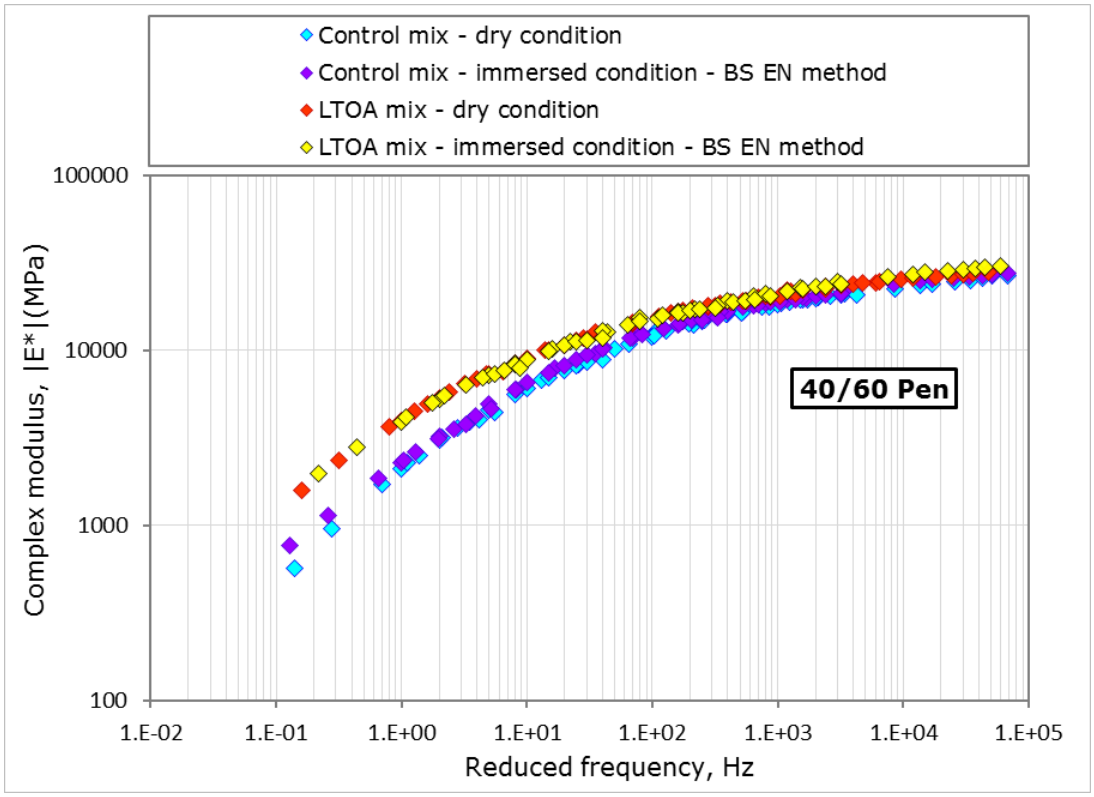
$$|E^*|_{\text{index}} = \frac{|\text{E}^*| \text{ of conditioning mixture}}{|\text{E}^*| \text{ of unconditioning mixture}} \qquad 6.6$$

Some points can be highlighted from these figures. First, it can be observed from Figures 6.5 and 6.6 that there is some general convergence at high

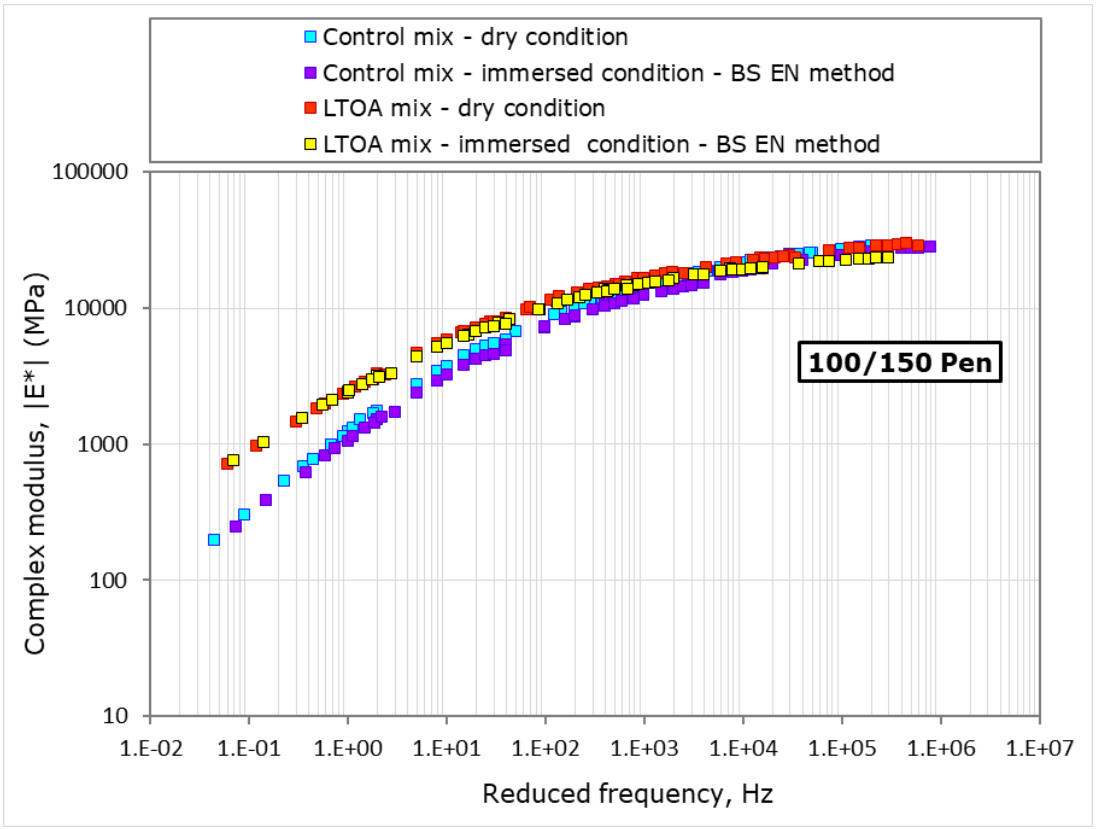
frequencies (equivalent to low-temperature response) at different conditions. Second, it is also obvious that $|E^*|$ magnitudes have expectedly increased due to LTOA. Additionally, the phase angle master curves presented in Figure 6.6 shows a general decrease in the phase angle due to the effect of ageing even when this ageing is combined with moisture. Where the elastic behaviour of these aged/immersed mixtures will be more dominate. On the other hand, the phase angle behaviour of control mixtures was more variable due to water exposure over the wide range of testing temperatures and loading frequencies. Third, no moisture damage issue arises from these results even when the aged mixtures were exposed to moisture conditioning. However, it seems more serious for 100/150 Pen mixtures as shown in Figure 6.5 where the master curve has dropped over a wide range of temperatures (see the yellow and purple lines).

In general, the $|E^*|_{index}$ is more than 80% for 40/60 pen mixtures and more than 70% in the case of 100/150 Pen mixtures as shown in Figures 6.7 and 6.8 respectively (see the purple lines of 100/150Pen). It can also be observed from the same figures that there is a slight increase in $|E^*|$ of control mixtures exposed to moisture conditioning. The reason of $|E^*|$ increase may be attributed to possible ageing during the moisture conditioning itself. These results are relatively similar to ITSM results as shown earlier in Figures 4.18 to 4.23.

In addition, Figure 6.7 indicates that $|E^*|_{index}$ of aged mixtures have experienced a slight to considerable decrease when these mixtures are exposed to moisture and tested at 0, 10 and 20˚C (see the red and brown lines). On the other hand, there is an increase at -10 and 30˚C. A similar behaviour can be noticed from Figure 6.8 except that increase has occurred at 30˚C only. The other finding which can also be spotted from Figure 6.7 is a decrease of $|E^*|_{index}$ of immersed aged mixtures to less than that of immersed control mixtures at most temperatures. That might be explained by the important role of testing the effect of moisture/ageing over a wide range of temperatures and loading frequencies. It may also show the influence of ageing when combines with moisture (see the yellow and purple points).

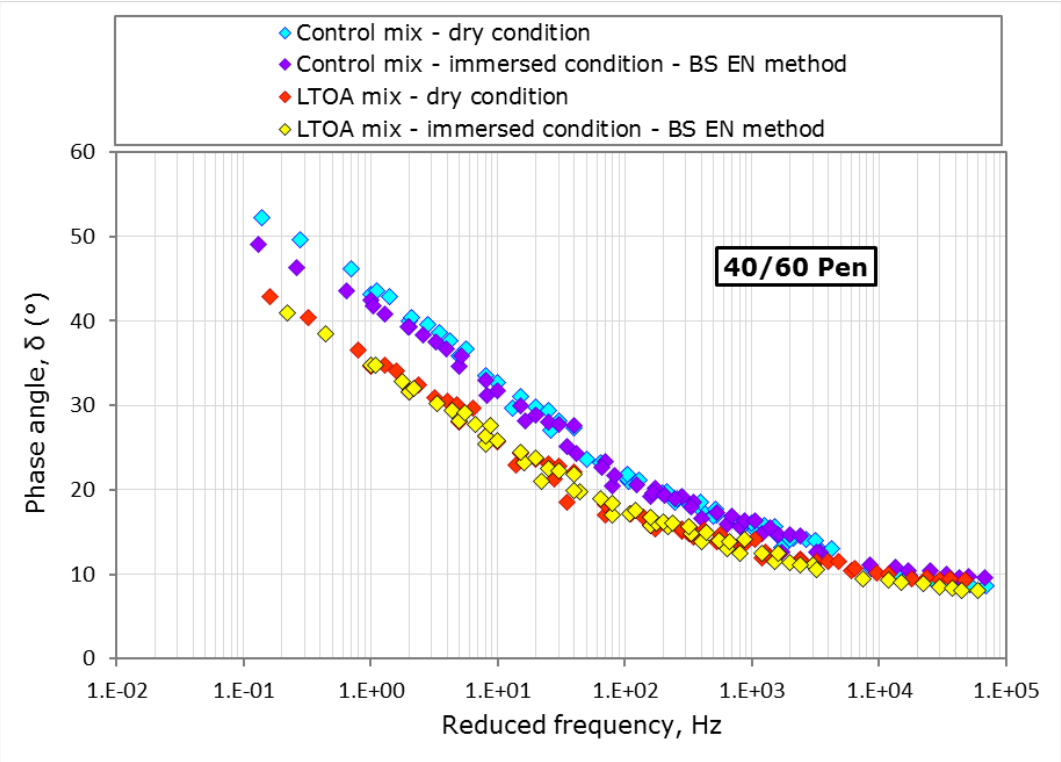



A: $|E^*|$ for mixtures manufactured with 40/60 Pen.

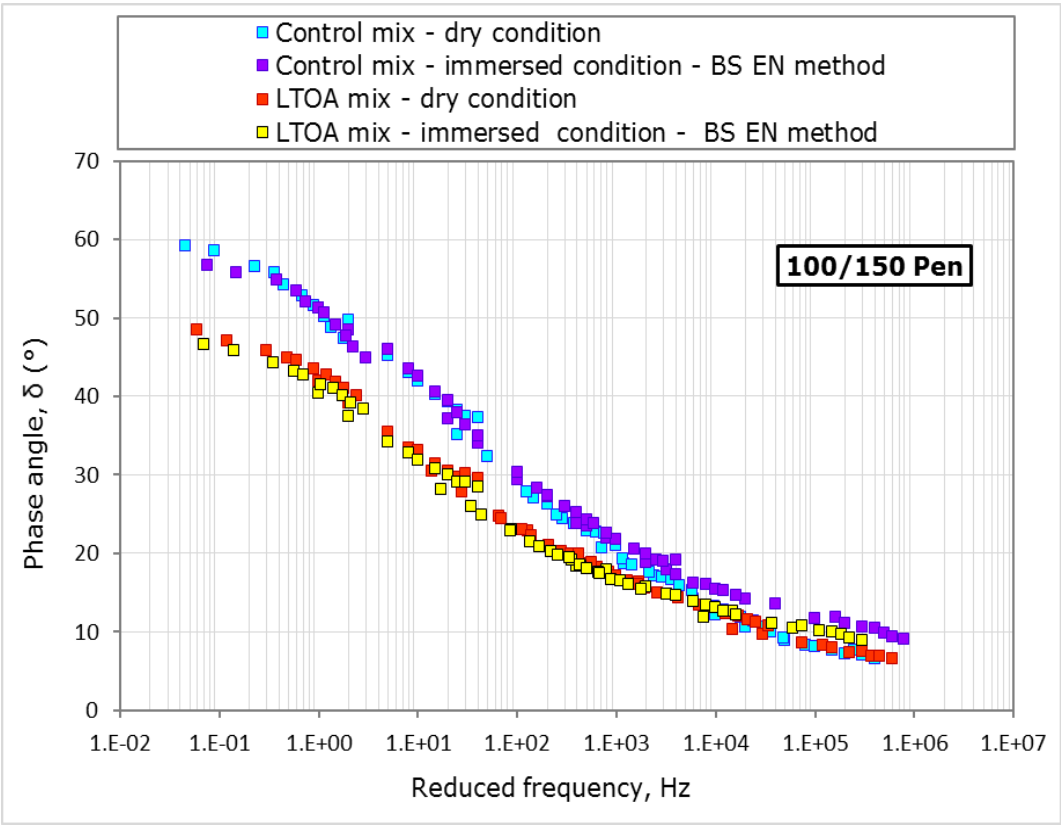



B: $|E^*|$ for mixtures manufactured with 100/150 Pen.

Figure 6.5: Master curves for $|E^*|$ at 20˚C reference temperature (RT) - effect of ageing and moisture conditions.

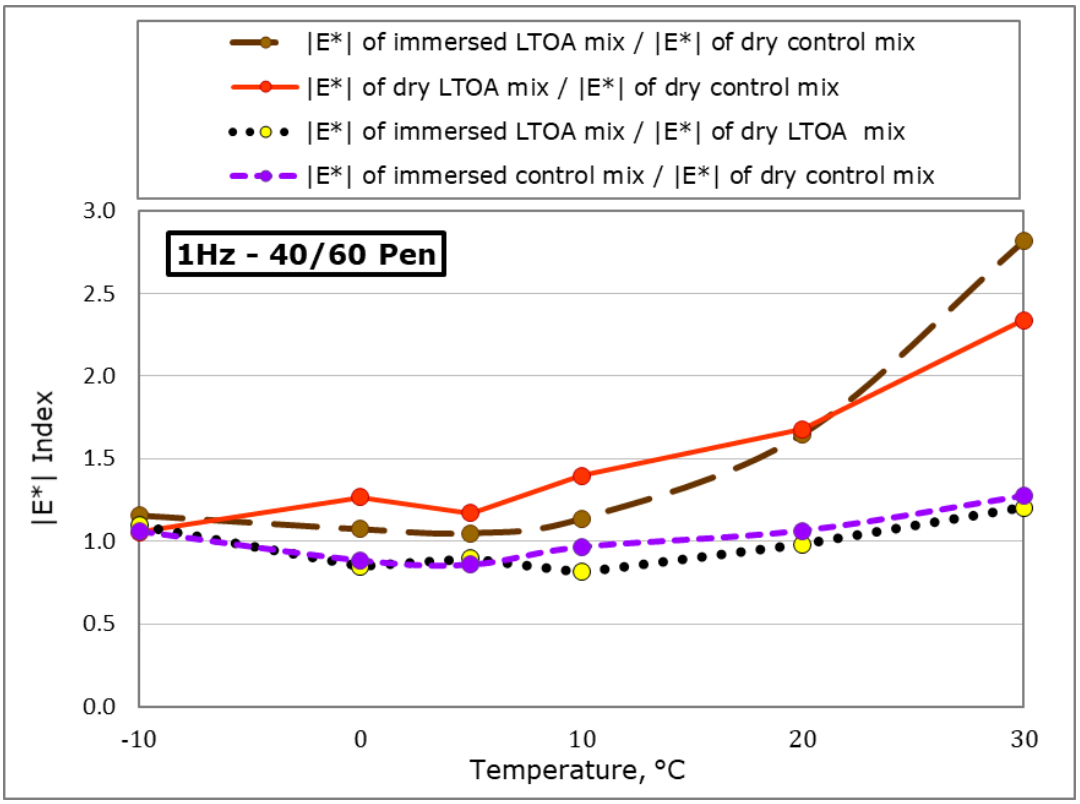



A: *δ* for mixtures manufactured with 40/60 Pen.

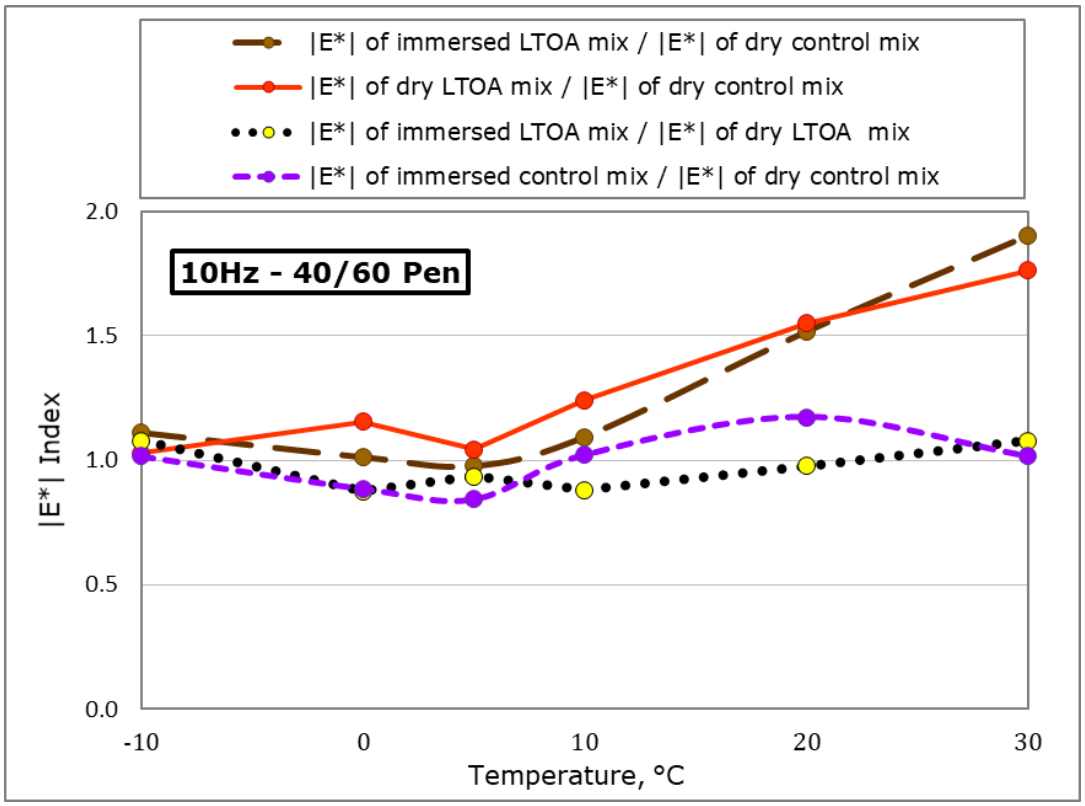



B: *δ* for mixtures manufactured with 100/150 Pen.

Figure 6.6: Master curves for δ at reference temperature 20˚C (RT) - effect of ageing and moisture conditions.

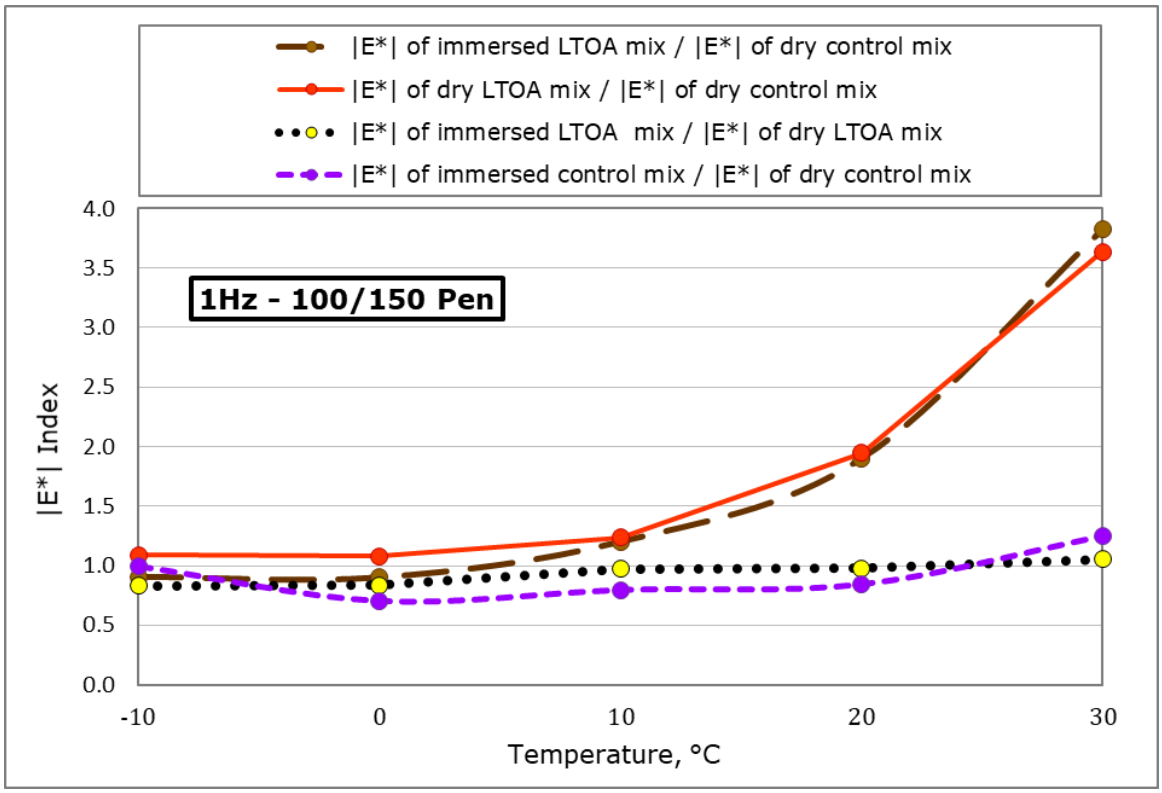



A: at 1Hz.

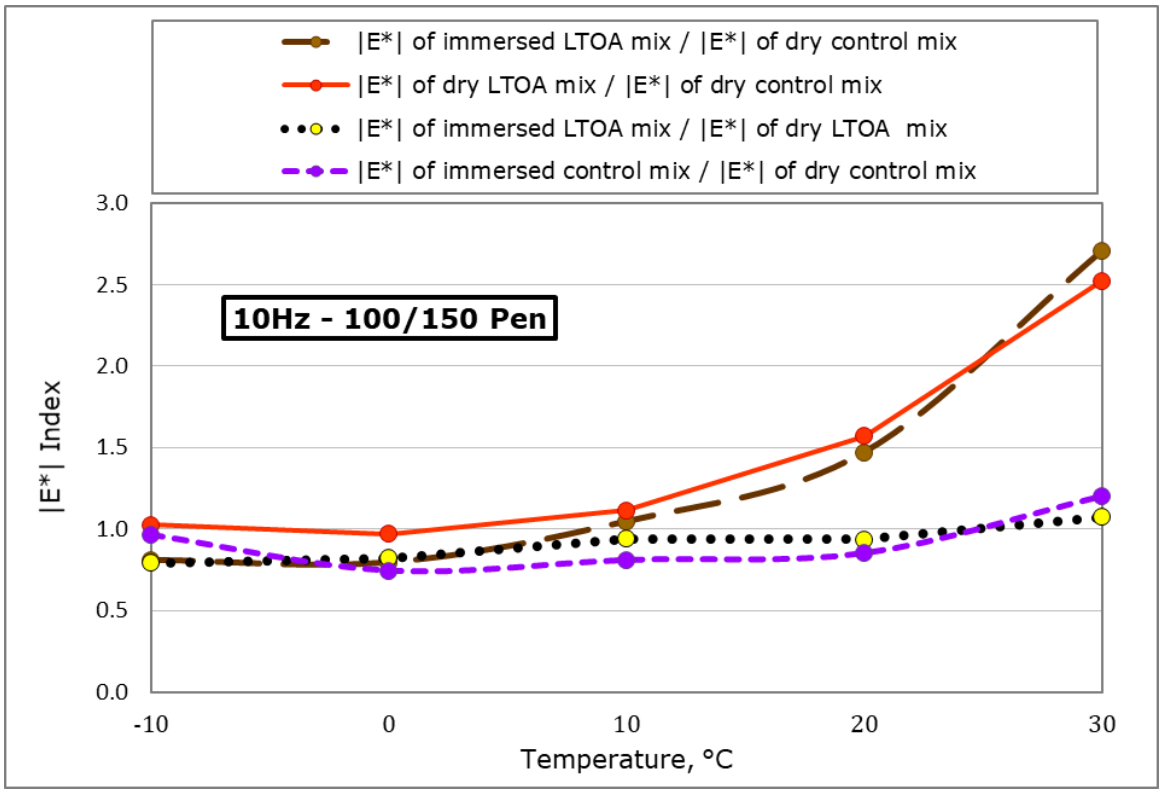



B: at 10Hz.

Figure 6.7: $|E^*|_{index}$ of mixtures manufactured with 40/60 Pen - effect of ageing and moisture conditions.




A: at 1Hz.




B: at 10Hz.

Figure 6.8: |E*| index of mixtures manufactured with 100/150 Pen - effect of ageing and moisture conditions.

In addition, the black diagram can be beneficial in investigating the relation between the complex modulus and viscoelastic behaviour of bituminous materials. It can be used without applying shift factors to the raw data as required for the master curve (Airey, 2002).

Figure 6.9 shows the black diagram of investigated asphalt mixtures at different conditions. The Black diagram curves have obviously showed some convergence (at low temperatures) between the four applied conditions. Then follows a shifting in these curves towards lower phase angle values (at higher temperatures) when moisture conditioning and/or ageing were applied to these mixtures. In general, this shifting has resulted from the increase of complex modulus, indicating more hardening and the decrease of phase angle, indicating more elastic (brittle) behaviour of asphalt mixtures.

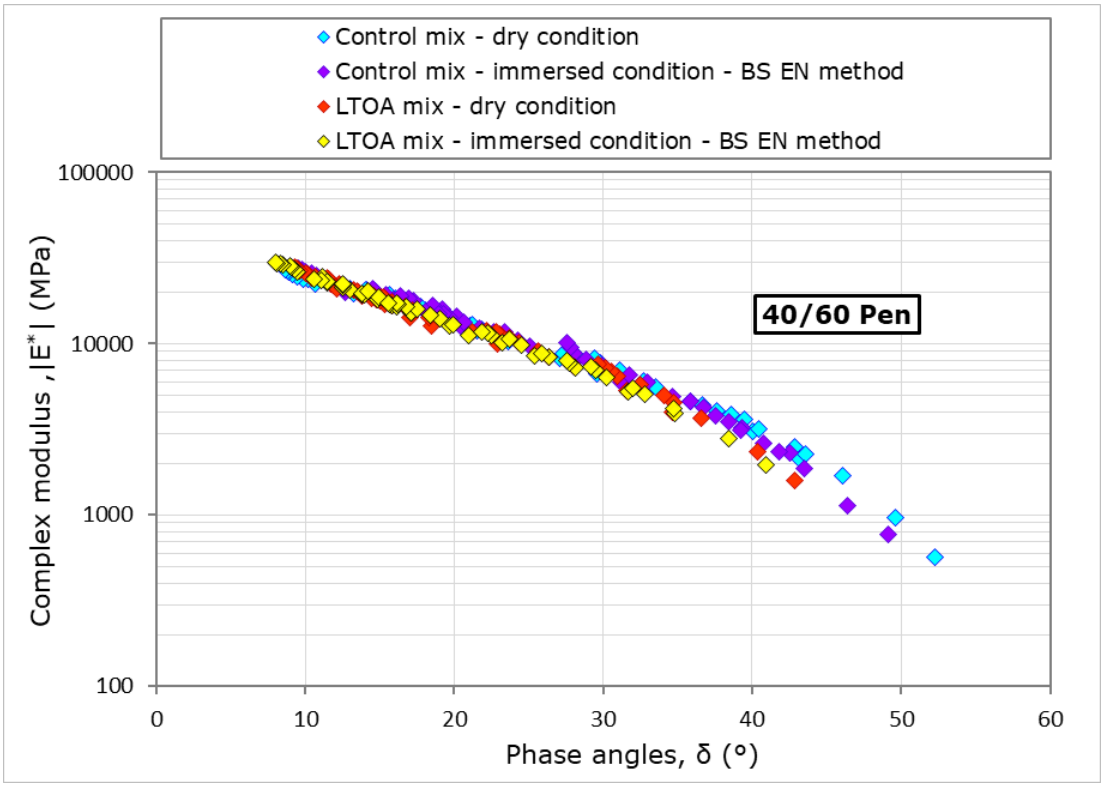
The Cole-Cole diagram was developed to give an indication of the viscoelastic balance without using testing temperatures and/or loading frequencies as one of the axes. At a particular testing temperature and loading frequency, as the materials having a larger increase in storage modulus than loss modulus, the viscoelastic balance of the material becomes more elastic and less viscous (Airey, 1997).

The Cole-Cole diagram is shown in Figure 6.10 for the evaluated mixtures at different circumstances. Two stages can be highlighted from this figure. Firstly, at low temperature, there is a relative difference between all four Cole-Cole diagrams of different conditions. The asphalt mixture at this stage have a larger increase in storage modulus than loss modulus as it stiffens more due the actual ageing and/or the possible ageing during moisture conditioning. Therefore, the Cole-Cole diagrams have shifted towards the lower right-hand corner. That means shifting towards more elastic (brittle) and stiffer rheological behaviour. This explanation can be true at a specific temperature and loading frequency.

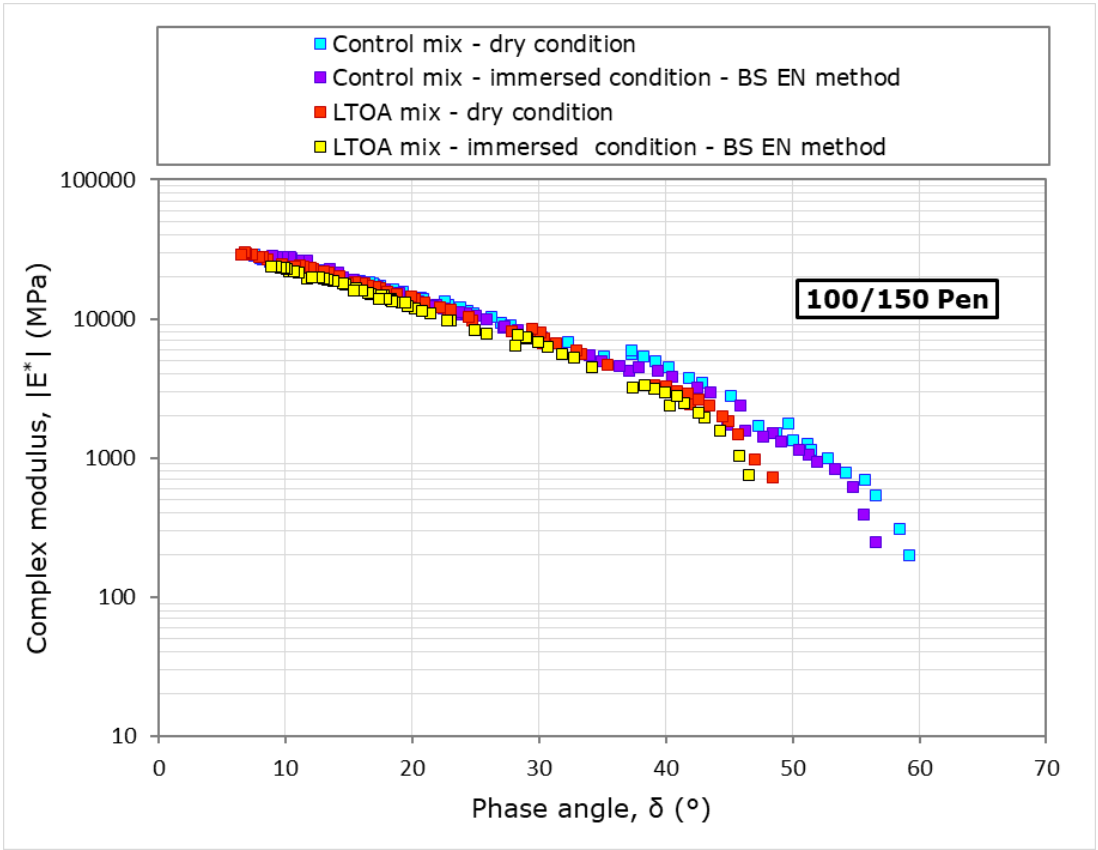
In addition, the second stage can be noticed at the higher temperature where the viscoelastic behaviour is more predominate. This stage can be distinguished by a noticeable convergence and it was found that asphalt mixture have a larger increase in loss modulus than storage modulus. However, this was slightly more

obvious for control mixtures. Once more, this explanation can be true at a specific temperature and loading frequency.

Finally, samples of isochronal plots for complex modulus and phase angle at different conditions are presented in Figures 6.11 and 6.12.

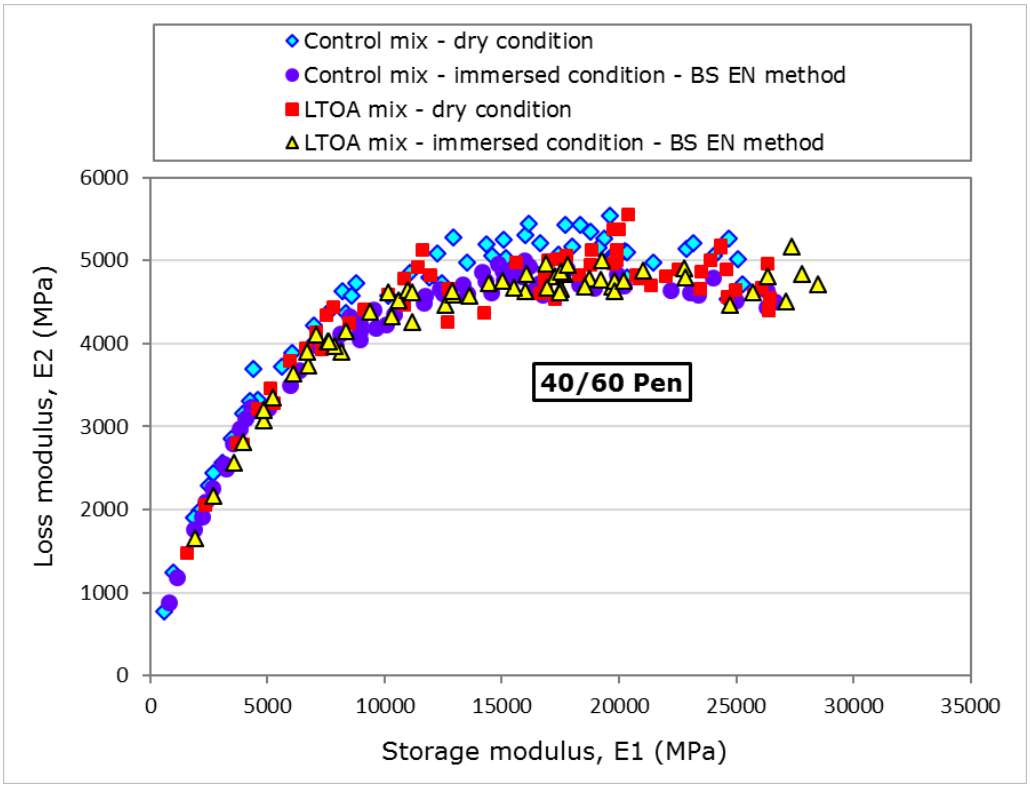



A: Black diagram for mixtures manufactured with 40/60 Pen.

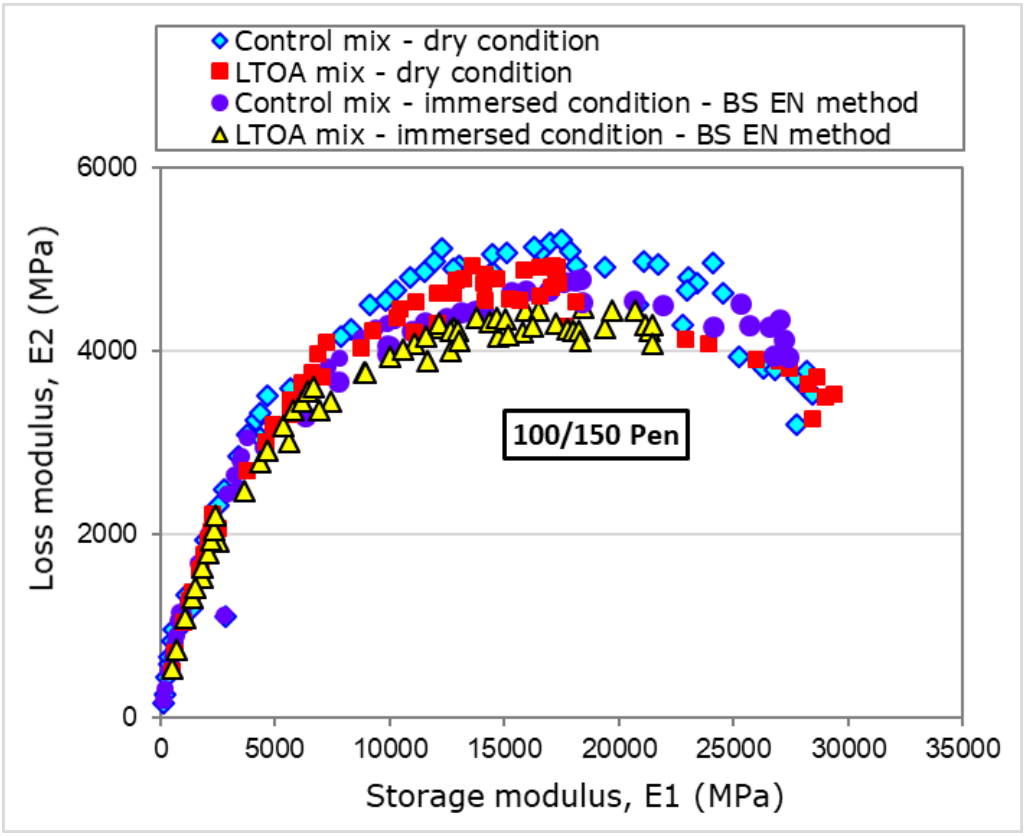



B: Black diagram for mixtures manufactured with 100/150 Pen.

Figure 6.9: Black diagrams at 20˚C reference temperature (RT) - effect of ageing and moisture conditions.

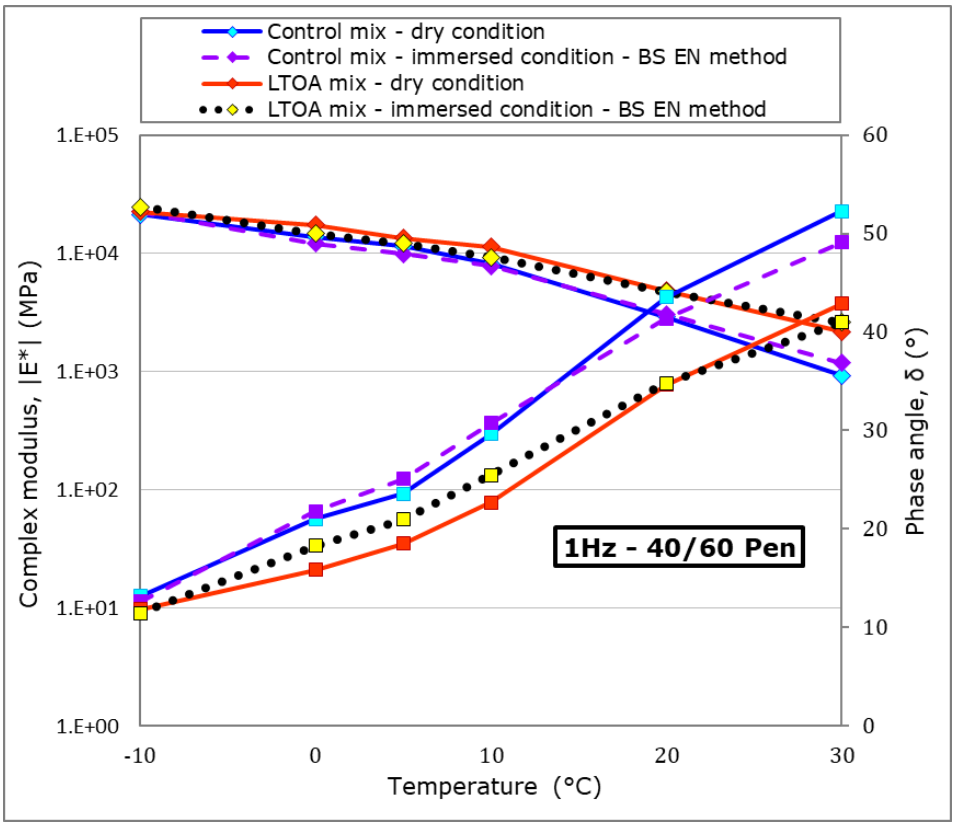



A: Cole – Cole diagram for mixtures manufactured with 40/60 Pen.

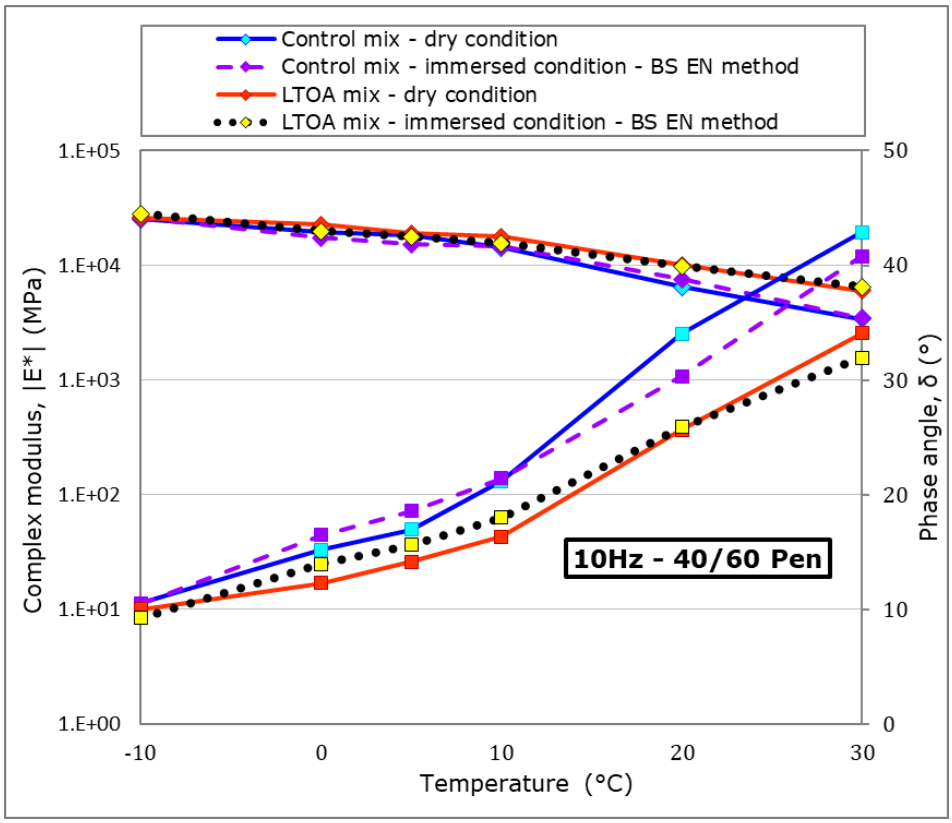



B: Cole – Cole diagram for mixtures manufactured with 100/150 Pen.

Figure 6.10: Cole – Cole diagram - effect of ageing and moisture conditions.

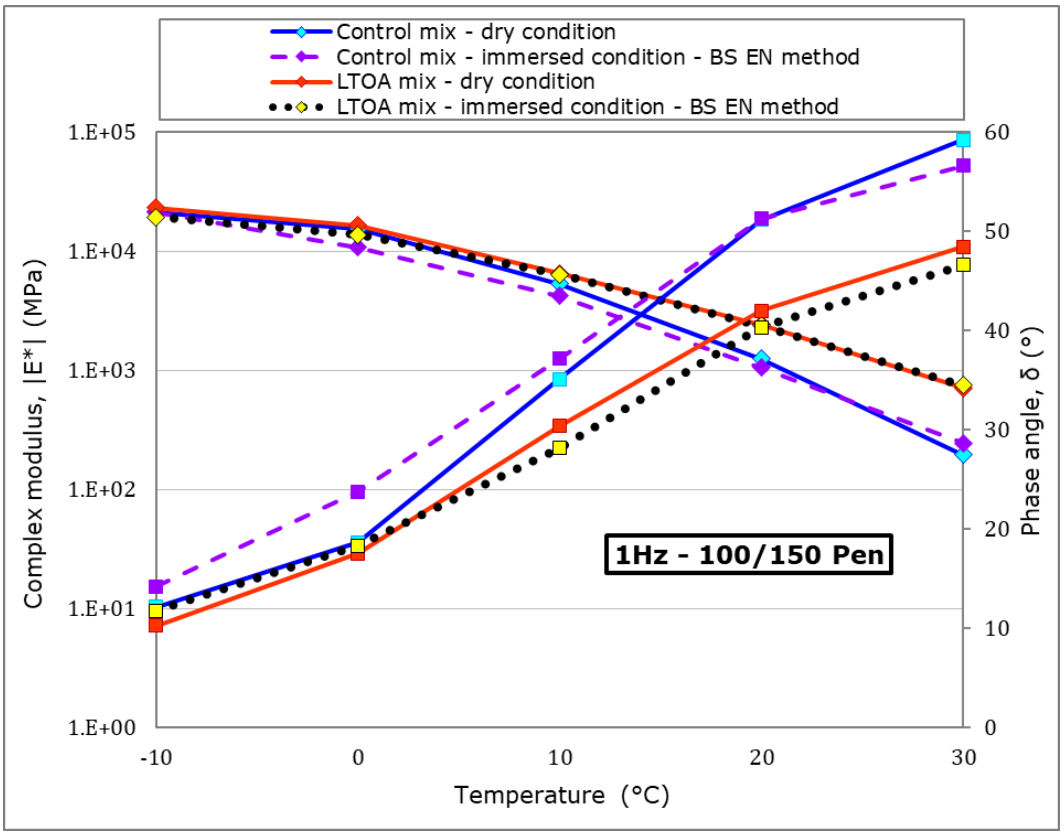



A: at 1Hz.

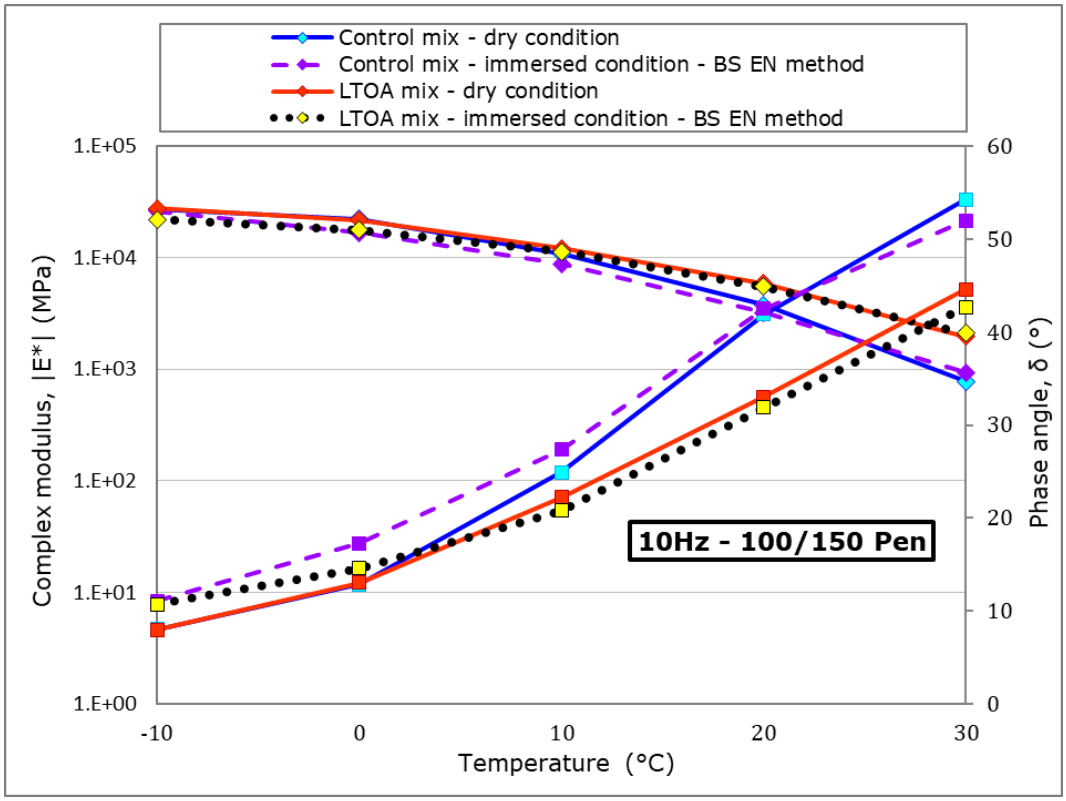



B: at 10Hz.

Figure 6.11: Isochrones plot for mixtures manufactured with 40/60 Pen - effect of ageing and moisture conditions.




A: at 1Hz.




B: at 10Hz.

Figure 6.12: Isochrones plot for mixtures manufactured with 100/150 Pen - effect of ageing and moisture conditions.

## 6.5 Summary

This part was carried out by the 4PB machine to measure the complex modulus of asphalt mixtures exposed to ageing and/or moisture conditioning. The following points can be summarised.

1. The complex modulus and phase angle have been measured for different asphalt mixtures of 40/60 and 100/150 Pens exposed to different conditions; ageing and/or moisture. Representative Master curves were also developed for the complex modulus and phase angle to investigate the individual and combined influences of ageing and moisture damage on rheological properties of asphalt mixtures.

2. $|E^*|$ values have expectedly increased due to LTOA. However, there was obvious convergence at high frequencies (equivalent to low-temperature response) at the investigated conditions.

3. No moisture damage issue arises from $|E^*|_{index}$ results even when the aged mixtures exposed to the moisture conditioning. However, it seems more serious for 100/150 Pen mixtures. In general, $|E^*|_{index}$ was greater than the minimum criteria.

4. A slight to considerable increase in $|E^*|$ of control mixtures exposed to the moisture conditioning can be surprisingly observed. The reason of this increase may be attributed to possible ageing during the moisture conditioning itself. These results are relatively in the same line with that of ITSM.

5. Two different stages can be highlighted from the Cole-Cole diagram at a specific temperature and loading frequency. Firstly, at low temperature, the asphalt mixture have a larger increase in storage modulus than loss modulus as it stiffens more due to the actual ageing and/or the possible ageing during moisture conditioning. The second stage can be noticed at the higher temperature where asphalt mixtures have a larger increase in loss modulus than storage modulus. However, this was slightly more obvious for control mixtures.

# Chapter Seven: Evaluation of Environmental Factor Effects on Fatigue Performance of Asphalt Mixtures using the Modified ITFT

## 7.1 Introduction

The fatigue characteristics of bituminous mixtures under repeated load can be carried out using the traditional Indirect Tensile Fatigue Test (ITFT) in a constant stress mode. It is widely utilised in the United Kingdom since it was developed at the University of Nottingham using the Nottingham Asphalt Tester (NAT) (Read, 1996). It is simple to conduct and suitable to characterise the stiffness and fatigue properties of cylindrical specimens cored from asphalt roads or manufactured in the laboratory. However, the accumulation of permanent deformation is considered the main disadvantage of this testing arrangement. This permanent deformation tends to hide the real fatigue damage and therefore the ITFT cannot directly assess the behaviour of fatigue damage, particularly when the viscoelastic behaviour is more prevailing at high temperatures (Read, 1996, Hartman et al., 2001, Cocurullo et al., 2008).

In general, no permanent deformation is involved in pure fatigue tests such as four-point and two-point bending beam tests which are characterised by a sinusoidal loading waveform about the zero-stress point. Consequently, the ITFT in constant strain mode was developed by Cocurullo at the Nottingham Transportation Engineering Centre (NTEC) using the NAT (Papadimitriou et al., 2011). The robustness of this test was assessed by Maggiore, 2014 at NTEC using the NAT to compare its fatigue results with that of pure fatigue tests. It is developed to apply repeated deformation amplitude with a haversine signal to the vertical diameter plane of the tested cylindrical specimen. It was basically developed on resilient deformation in accordance with BS EN 12697-24: 2012 to not include the permanent deformation (Maggiore, 2014).

In this work, the modified ITFT was used to evaluate the fatigue performance of asphalt mixtures exposed to individual and combined environmental conditions; moisture damage and ageing. Different parameters were also investigated to achieve this aim; testing temperature, air voids content, binder grades and binder contents. LTOA with two different methods for moisture

induced damage were also applied to the specimens as explained earlier in Chapter Three.

### 7.2 Calculation of maximum tensile strain ($\varepsilon_0$)

ITFT is typically undertaken in controlled stress mode where a repeated compressive load with a haversine signal is applied to the vertical diameter plane of the tested cylindrical specimen. This loading arrangement results in repeated tensile stress cycles perpendicular to the direction of the applied load. Under these repeated loads the specimen will fail by splitting along the vertical plane. The maximum tensile stress ($\sigma_{max}$) at the centre of the specimen can be calculated from the following equation:

$$\sigma_{max} = \frac{2P}{\pi \times t \times D} \qquad 7.1$$

Where:

- P is the vertical applied load (in Newtons),
- t is the specimen's thickness of the test specimen (in mm),
- D is the specimen's diameter of the test specimen (in mm),

The resulting maximum tensile strain ($\varepsilon_0$) can be calculated in accordance with Equation 7.2 (Read, 1996). This method requires to measure the stiffness modulus of each specimen using ITSM test in controlled stress method at the same stress level that will be applied to the same specimen in the ITFT.

$$\varepsilon_0 = \frac{\sigma_{max} \times (1 + 3\nu)}{S_m} \times 1000 \qquad 7.2$$

Where

- $S_m$ is the indirect stiffness modulus at the applied $\sigma_{max}$ (MPa), and
- $\nu$ = Poisson's ratio.

In addition, it can be measured according to BS EN 12697-24: 2004 and BS EN 12697-24:2012 (ITFT in constant load method). In accordance with EN 12697-24:2004, Equation 7.1 is used to calculate the maximum tensile stress ($\sigma_{max}$ in MPa) at the centre of the tested specimen. The horizontal deformation (in mm)

can be directly measured by LVDTs during the fatigue test and therefore the initial strain ($\varepsilon_0$ in με) can be calculated according to the following equations:

$$\varepsilon_0 = \frac{2\Delta H}{D} \times \frac{1 + 3\nu}{4 + \pi \times \nu - \pi} \quad 7.3$$

If $\nu$ =0.35, then

$$\varepsilon_0 = 2.1 \times \frac{\Delta H}{D} \quad 7.4$$

Where:

- ΔH is the horizontal deformation (in mm), and
- D is the specimen's diameter of the test specimen (in mm),

In this standard, the initial strain value is calculated from finding the difference between the averages of maximum strains of 5 load cycles; 98$^{th}$ to 102$^{nd}$ cycle and minimum strains of 5 load cycles; 60$^{th}$ to 64$^{th}$ (see Figure 7.1). The strain amplitude (με) is defined as the distance between the segment that links between the maximum strain magnitudes of two consecutive cycles and the segment that links between the minimum strain magnitudes of two consecutive cycles as shown in Figure 7.2 in accordance with EN 12697-26:2004).

The same Equations 7.1 and Equation 7.4 can also be used to determine the maximum tensile stress and resilient strain ($\sigma_{max}$ in MPa) and ($\varepsilon_0$, in με) at the centre of the tested specimen according to the new standard EN 12697-24:2012. However, this standard introduces the resilient (or recoverable) strain value ($\varepsilon_0$, in με) as the total horizontal strain ($\varepsilon_T$, in με) at the 100$^{th}$ load cycles, minus the plastic (permanent) strain ($\varepsilon_p$, in με) as presented in Figure 7.3.

ITFT was developed to be applicable in controlled strain method based on the definition of initial strain in EN 12697-24:2012 (Maggiore, 2014).

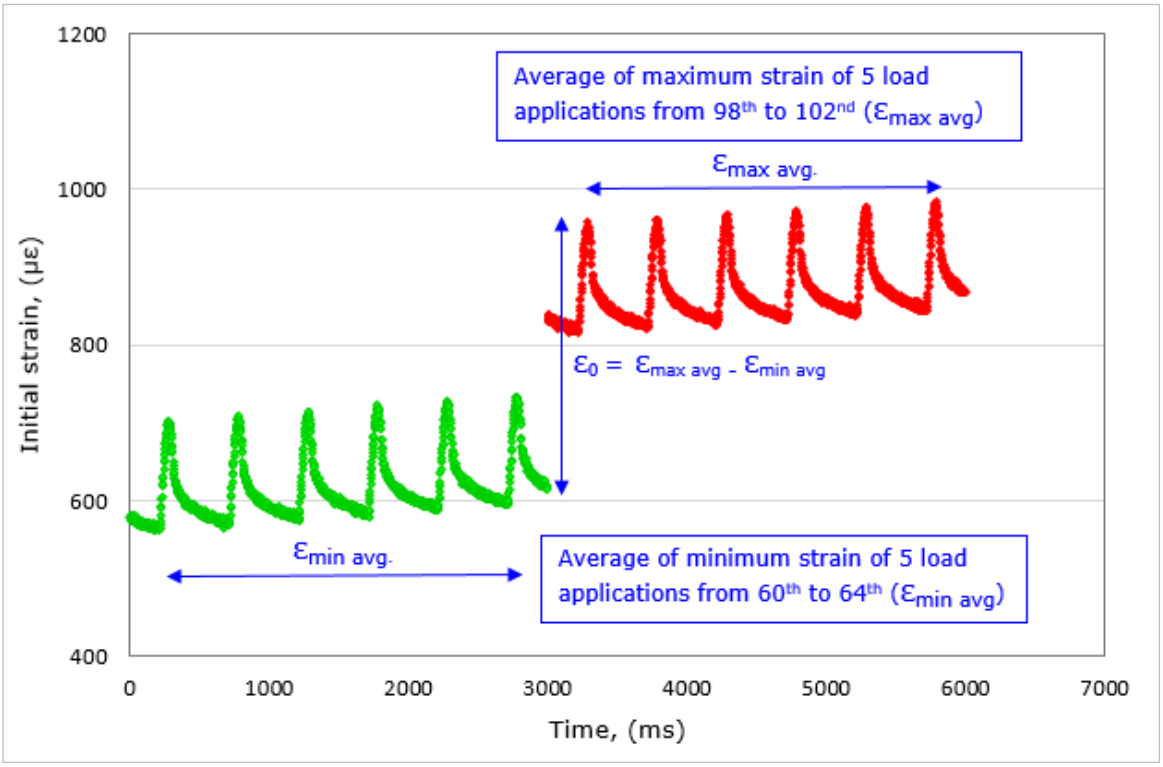



Figure 7.1: Initial strain calculation using ITFT EN 12697-24:2004.

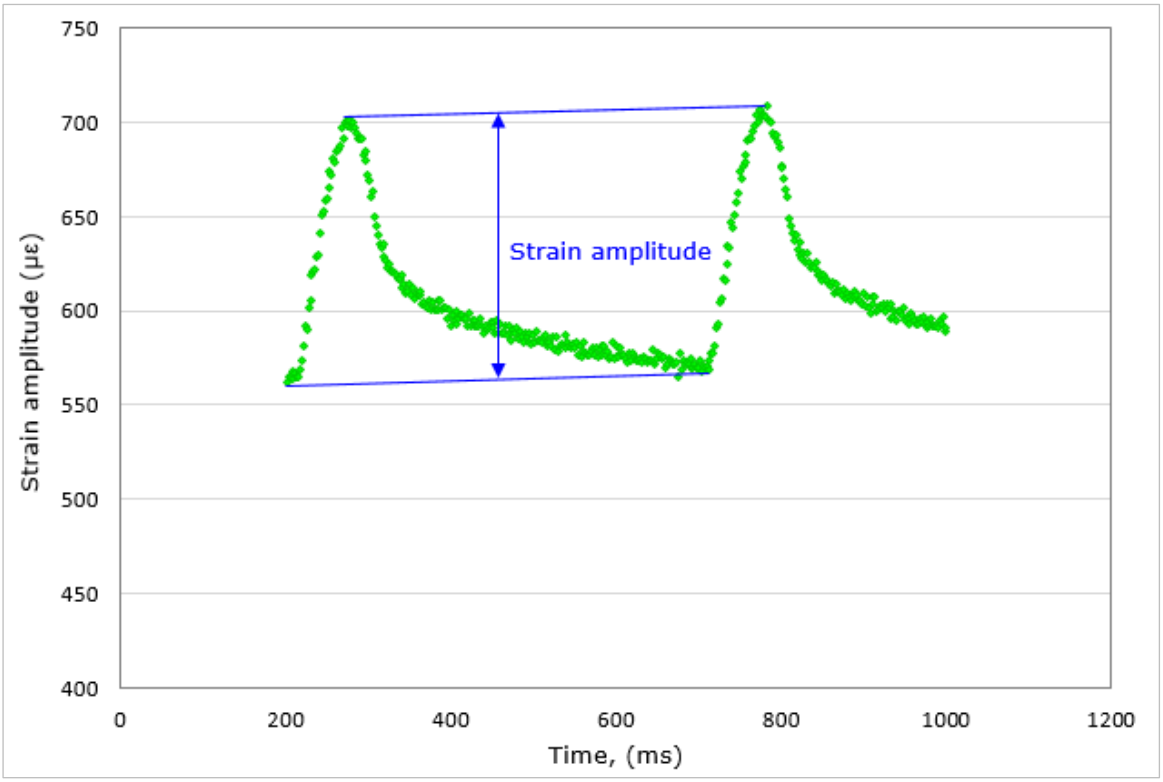



Figure 7.2: Calculation of strain amplitude according to EN 12697-26:2004.

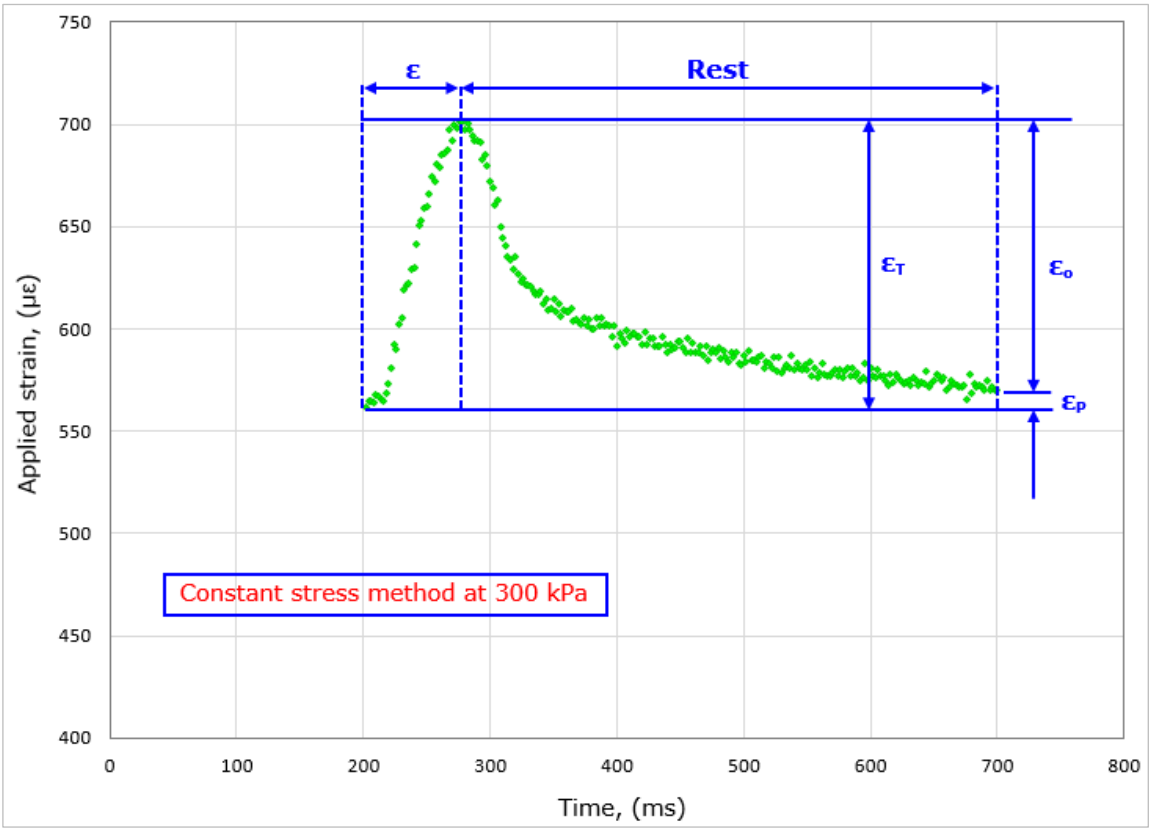



Figure 7.3: Initial strain (Resilient) calculation based on EN 12697-24:2012 – constant stress method.

### 7.3 ITFT in controlled strain method

In this test, the same preparations of the constant stress method in accordance with EN 12697-24:2012 will exactly be followed. The specimen preparation involves gluing two deformation strips using a position rig on the opposite sides of the horizontal diameter plane of the specimen as shown in Figure 7.4. These two deformation strips have a concave surface to hold two LVDTs located horizontally to capture the variation in the horizontal diameter by measuring the variation of the distance between the two glued deformation strips. Generally, the test stops when the LVDTs reach 90% of their range which is 2mm (90% is the end of their range to avoid LVDT's damage) as it was designed. At this point, readjustment will be required to resume the test once more. This point could be considered one of the disadvantages of this new arrangement. This is because a number of readjustments might be required, in particular for soft mixtures. It also requires from the operator to be in the laboratory during the test to do that readjustment, particularly at early stage of the test to avoid any possible stiffness recovery.

This fatigue test was modified in accordance with BS EN 12697-24: 2012 to be carry out by applying a constant strain, the constant parameter of the test, using NAT machine as shown in Figure 7.4. Typically, the single pulse of 0.5 sec haversine loading waveform consists of a loading time of 0.1 second followed by a 0.4 second rest period as shown in Figure 7.5.

The failure criteria in this test is usually specified by the user in terms of the initial stiffness reduction percentage, although the test may run out earlier if 10 mm vertical deformation occurs. It was generally determined in terms of 50% reduction of the initial stiffness which is typically measured between cycles $50^{th}$ and $60^{th}$ as shown in Figure 7.6. Different percentages of initial stiffness decrease up to 90% can also be used. For more details, a testing protocol was presented by Maggiore, 2014.

Whole fracture along the specimen's vertical diameter will not occur at failure as in the case of controlled stress mode. Failure is typically characterised by an apparent crack located along the vertical plane of the specimen and with a localised deformation at the edge of the two loading strips as shown in Figure 7.7.

Figures 7.8 and 7.9 show also picked up cracks along the vertical plane at 50% of initial stiffness modulus ($N_{f50}$) for different asphalt mixture specimens.




Figure 7.4: Set up of LVDTs in ITFT controlled strain method.

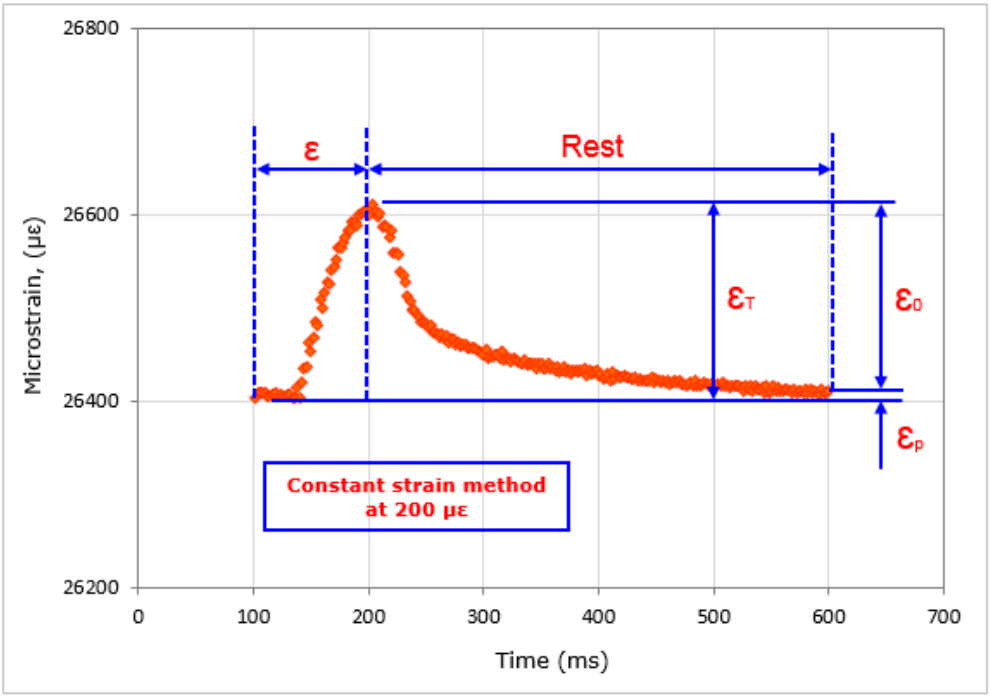



Figure 7.5: A single pulse of ITFT in constant strain method.

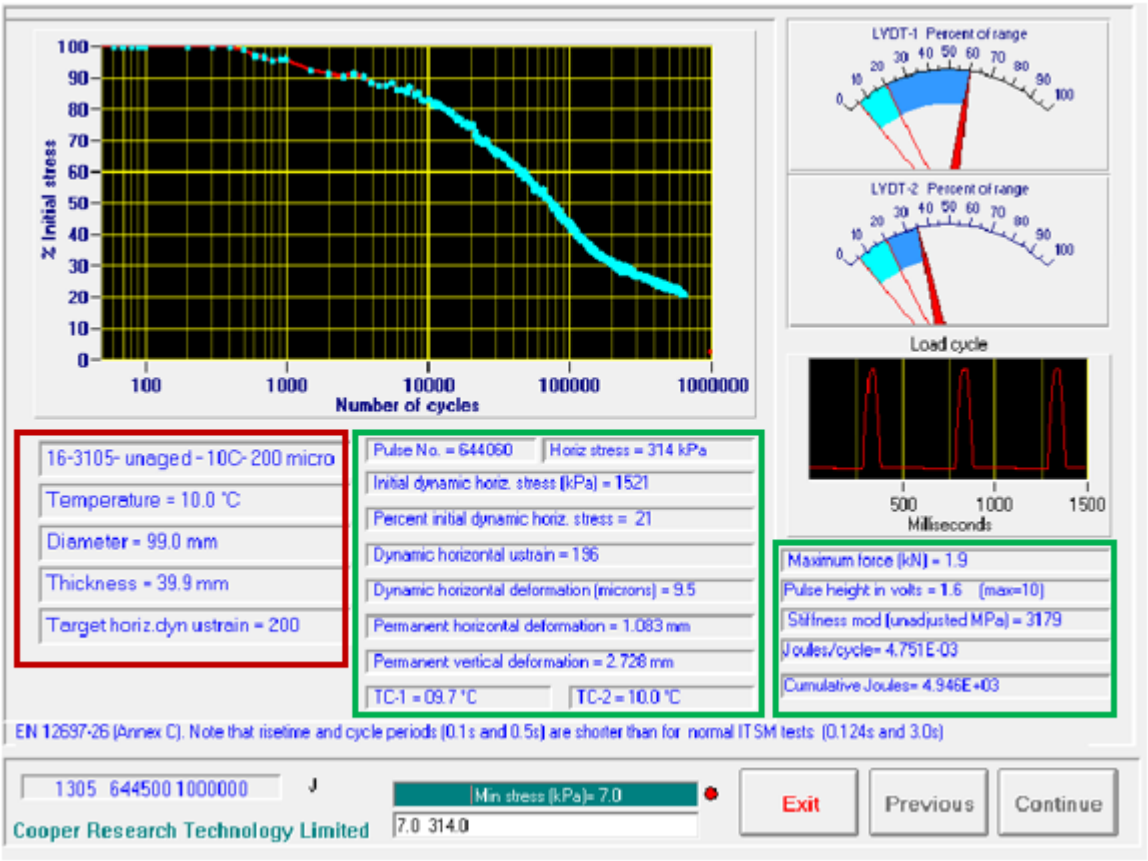



Figure 7.6: Inputs (red box) and outputs (green boxes) of modified ITFT software.

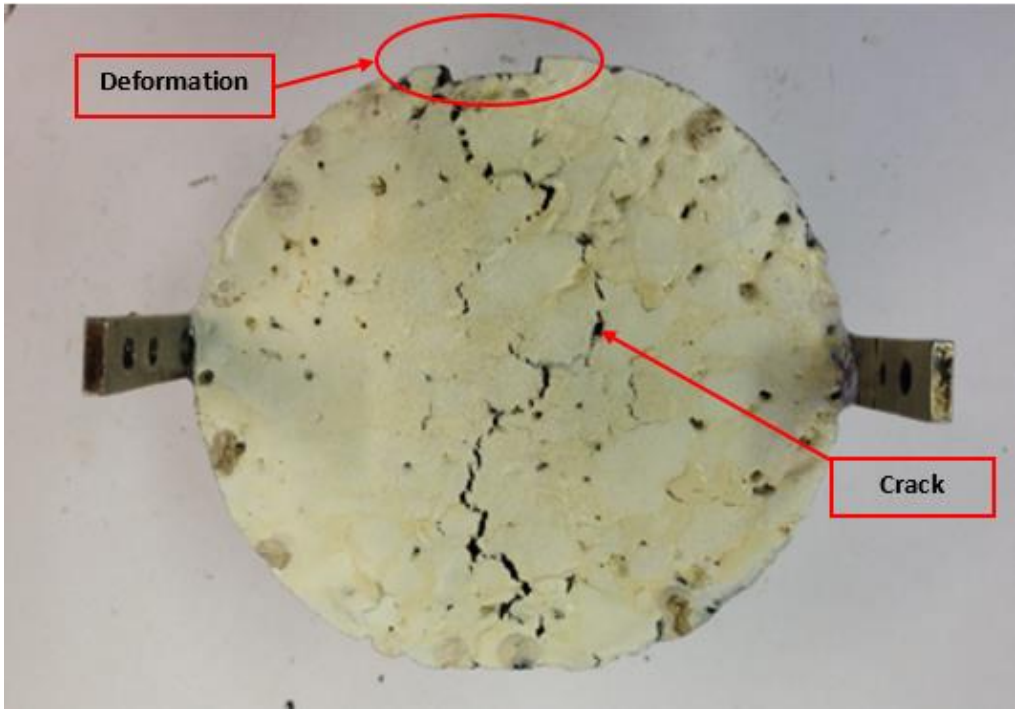
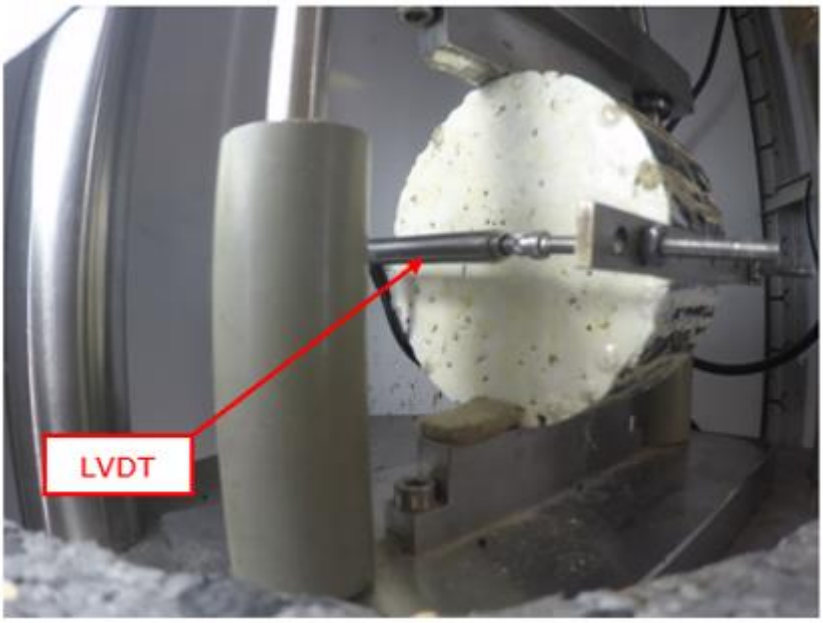
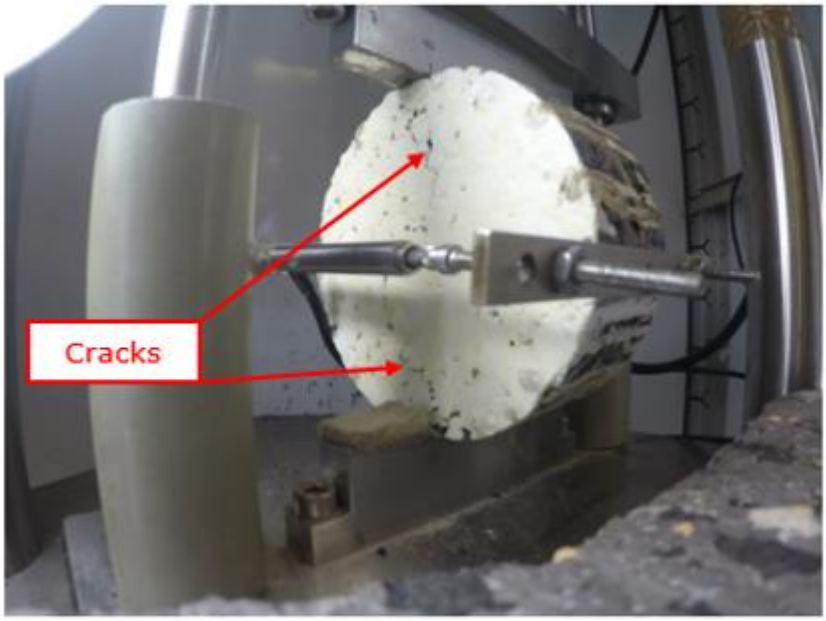



Figure 7.7: Failure in strain control mode (at 40% of initial stiffness).

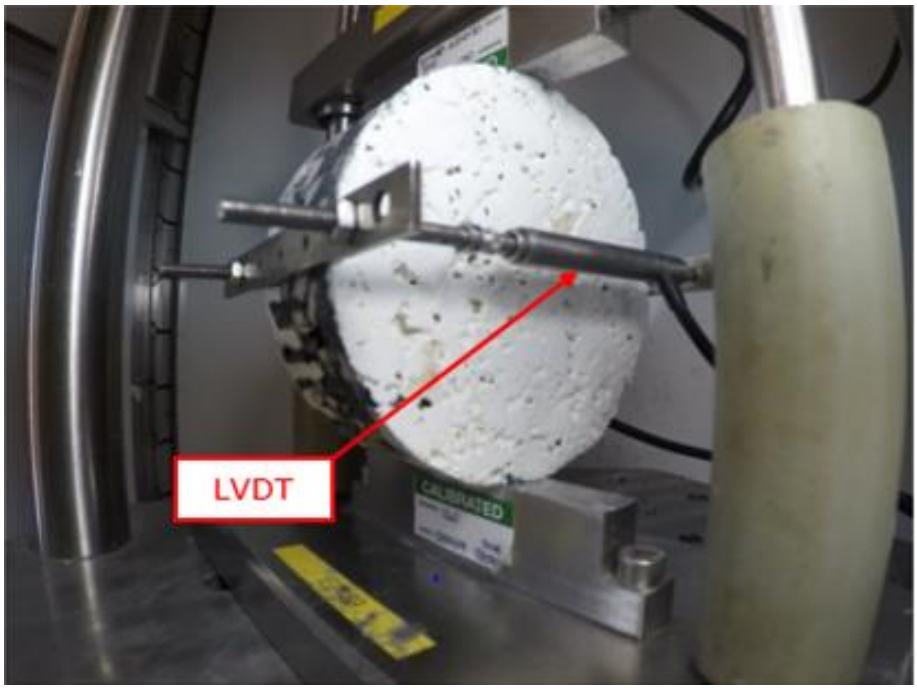



A: No cracks at 100% of initial stiffness modulus (6927 MPa) measured at the cycle 50$^{th}$.

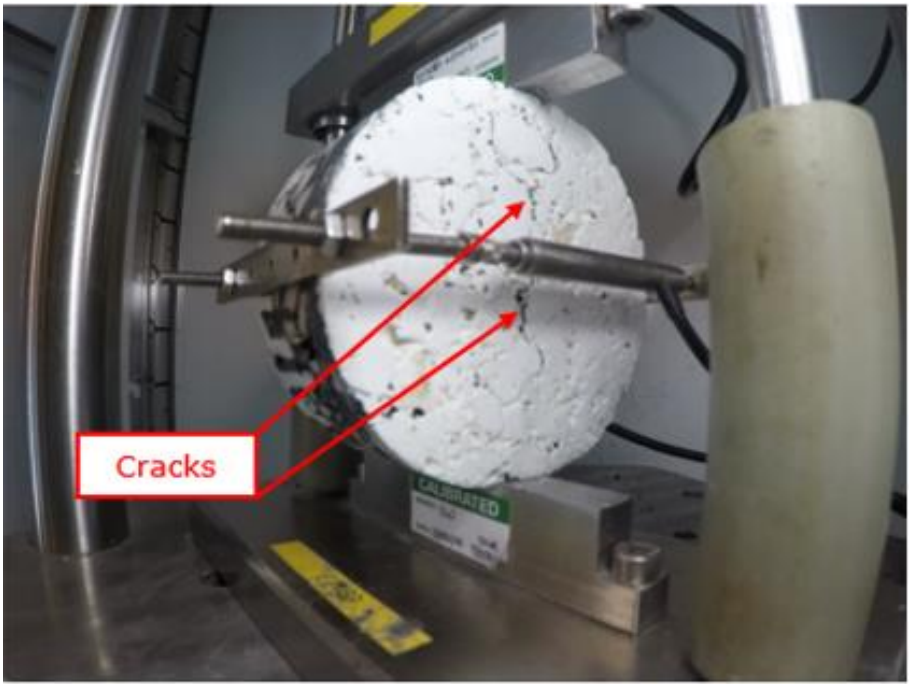



B: Cracks at 50% of initial stiffness modulus (3460 MPa) measured after 10500 cycles.

Figure 7.8: Cracks at 50% of initial stiffness of wet asphalt mixture specimen of 10/20 Pen and 6.3% air voids content.




A: No cracks at 100% of initial stiffness modulus (1645 MPa) measured at the cycle 50$^{th}$.




B: Cracks at 50% of initial stiffness modulus (835 MPa) measured after 7500 cycles.

Figure 7.9: Cracks at 50% of initial stiffness along the vertical plane of dry asphalt mixture specimen of 40/60 Pen and 12.7% air voids content.

Finally, Figure 7.10 displays a comparison beween different fatigue lines based on the different difinitions of intial strain in EN 12697-24: 2004 and 2012

(controlled stress method, 200-600 kPa were applied) and that based on the modified ITFT (controlled strain method, 120-400 με were applied). These ranges were selected to reduce the length of time needed for fatigue tests to a manageable level. It clearly shows a significant difference between the two lines of controlled stress method due to the different definition of initial strain as explained earlier. It is also observed that the fatigue life by the new test is closer to EN 12697-24:2012 definition than EN 12697-24:2004. That may enhance the precision of EN 12697-24: 2012 definition of initial strain (resilient strain). Subhy, 2017 indicated that using EN 12697-24: 2004 standard in fatigue analysis can be biased and misleading due to the inclusion of permanent horizontal deformation in the initial strain calculation. On the other hand, EN 12697-24:2012 standard provides unbiased and more reliable comparison between the fatigue characteristics of different asphalt mixtures. It does not include the effect of permanent deformation by considering the resilient strain.

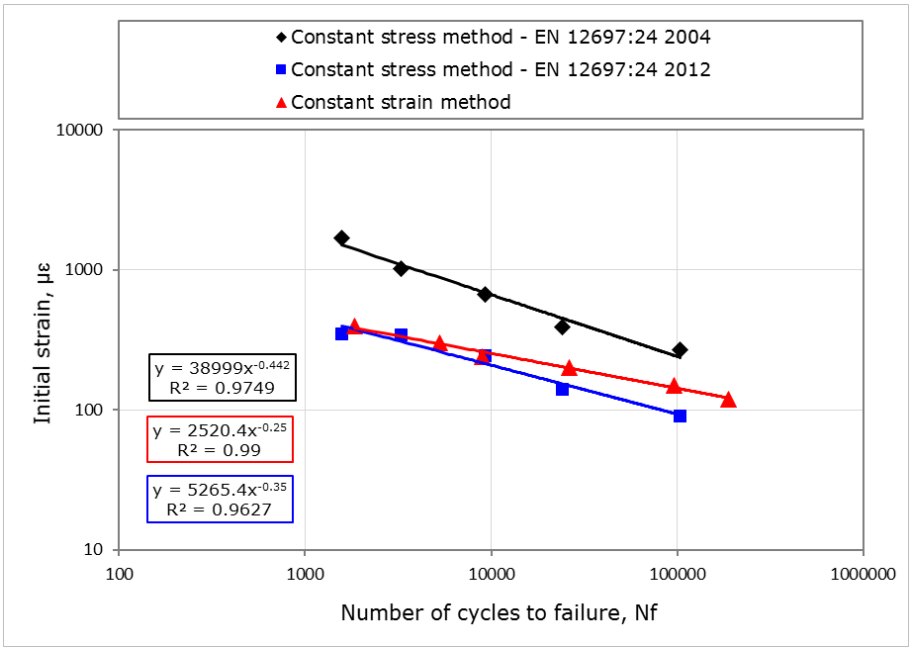



Figure 7.10: Fatigue life from constant stress and strain methods using ITFT.

### 7.4 Investigated mixture parameters and testing conditions

ITFT was applied to different asphalt mixtures that had been exposed to different conditions as shown in Table 7.1. In addition to the main variables in this table, air voids content and testing temperature effects were also investigated.

Table 7.1: Summary of the main investigated parameters (One specimen was used at each strain level to find the number of cycles to failure).

| **Mixtures exposed to specific conditions** | | **Mixture of 5% binder content and binder grade:** | | |
|---|---|---|---|---|
| | | **40/60*** | **100/150** | **10/20** |
| Control mixture, dry condition | | ✓ | ✓ | ✓ |
| Control mixture, immersed in water according to: | BBA method (vacuum the compacted mixture at (68 ± 3.3) kPa for (30 ± 1) minutes and immersed in water at 60˚C for 6 hrs then at 5°C for 16 hrs). | ✓ | ✓ | ✓ |
| | BS EN method (vacuum the compacted mixture at (6.7 ± 0.3) kPa for (30 ± 5) minutes and immersed in water at 40˚C for 72 hours). | | | |
| LTOA mixture, dry condition (after STOA for 4 hrs at 135˚C the compacted mixture exposed to 85˚C for 120 hours). | | ✓ | ✓ | ✓ |
| LTOA mixture, (after STOA for 4 hrs at 135°C the compacted mixture exposed to 85˚C for 120 hrs) then immersed in water according to: | BBA method (vacuum the compacted mixture at (68 ± 3.3) kPa for (30 ± 1) minutes and immersed in water at 60˚C for 6 hrs then at 5°C for 16 hrs). | ✓ | ✓ | ✓ |
| | BS EN method (vacuum the compacted mixture at (6.7 ± 0.3) kPa for (30 ± 5) minutes and immersed in water at 40˚C for 72 hours). | | | |

*6% binder content was investigated using BBA method only.

## 7.5 Possible fatigue analysis methods for ITFT

### 7.5.1 The phenomenological approach ($N_{f50}$)

The phenomenological approach (50% reduction of initial stiffness modulus) is a simple and traditional fatigue analysis which can be used for ITFT to find the number of cycles to failure. However, ITFT software provides the opportunity to increase the failure criterion up to 90% (max) reduction of initial stiffness modulus. Although the initial stiffness modulus is typically measured at cycle 50$^{th}$, it may need more cycles to pick up the initial stress based on testing conditions and investigated materials. In this work, this conventional approach was mainly used to find the number of cycles to failure. Additionally, the following sections examine the possibility of using a different approach to quantify the resulting fatigue damage from using the new arrangement of ITFT.

### 7.5.2 Hysteresis loop distortion

Alkhateeb and Shenoy, 2004 found a distinctive fatigue failure criterion in terms of the change in hysteresis loops shape. This approach observes the distortion of hysteresis loops shape through the progress of the applied fatigue test. Alkhateeb and Shenoy's criterion is presented in Figure 7.11 to show the distortion of hysteresis loops shape through the Four Point Bending Test (4PBT).

In this study, dissipated energy is traditionally the hysteresis loop when stress pulse (raw data) is plotted against strain pulse (raw data) as shown in Figure 7.12. In bending tests, stress (sinusoidal waveform) is typically plotted against strain (sinusoidal waveform) and its shape is elliptical. In the ITFT, these loops look like half of elliptical because the strain (or stress) is characterised by a haversine waveform due to the rest time after loading as shown earlier in Figure 7.3. Consequently, dissipated energy can be calculated as a half of a typical elliptical hysteresis loop shown in Figure 7.13 as following:

$$DE_1 = \frac{(\sigma_{1+}\ \sigma_2).(\varepsilon_{1-}\ \varepsilon_{2)}}{2} \qquad 7.5$$

$$DE = \sum_{i=1}^{N} DE_i \qquad 7.6$$

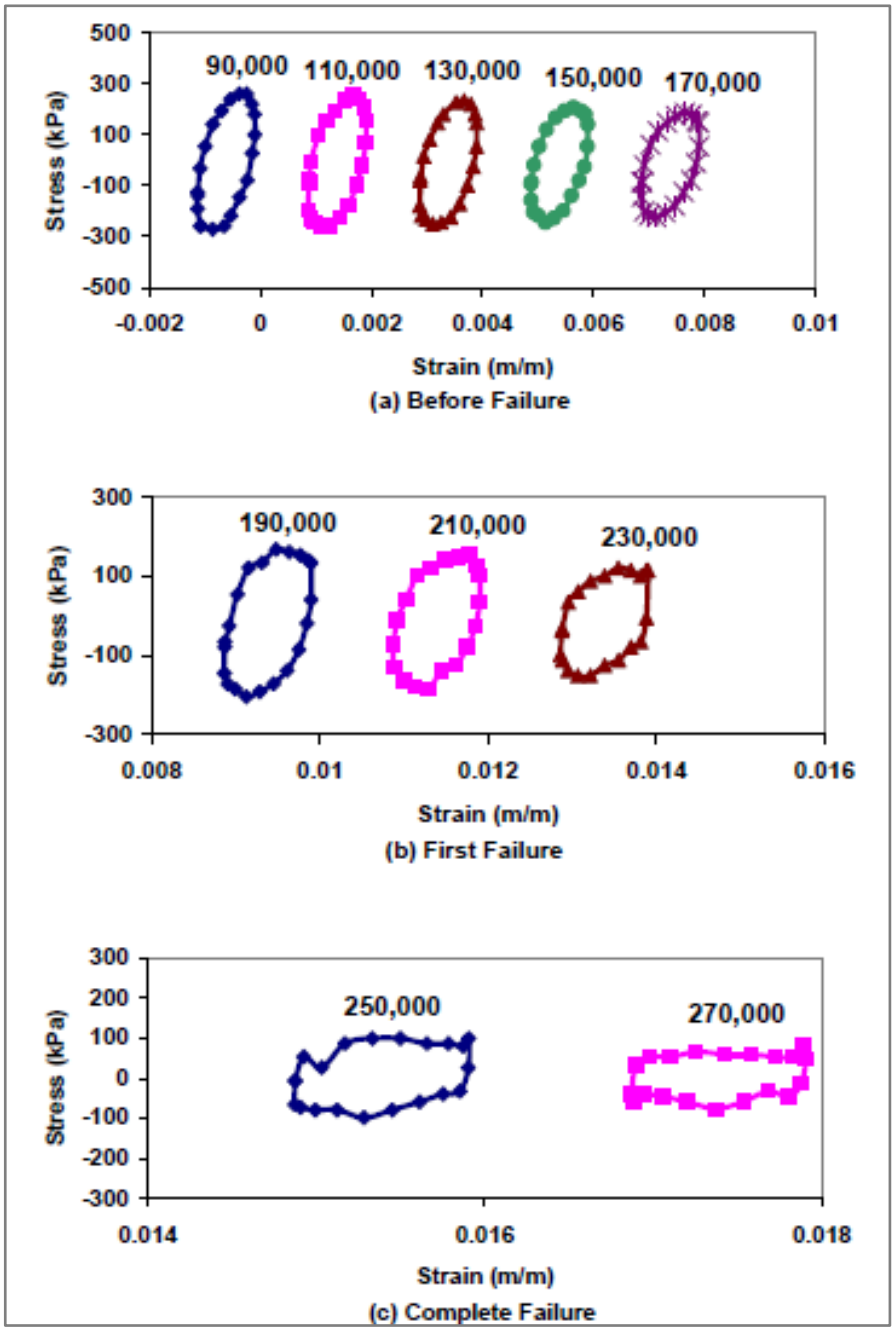



Figure 7.11: Stress-Strain Hysteresis Loop through the Progress of Fatigue Failure (Alkhateeb and Shenoy, 2004).

Figures 7.14 to 7.16 show samples of the real hysteresis loop resulting from applying the constant strain ITFT at 200 με to different asphalt mixtures exposed to different conditions. It can be observed that as the material have stiffened more due to ageing the loop have shifted left. It can also be seen that loops have shifted right or left due to applying the two methods of moisture sensitivity. Consequently, this could possibly refer to some ageing that has occurred during the two procedures of moisture conditioning. However, the hysteresis loops of

mixtures manufactured with 10/20 Pen have less shifting under the test conditions. Furthermore, these applied conditions seem to have more influence on the shape of hysteresis loops in the case of 100/150 Pen mixtures.

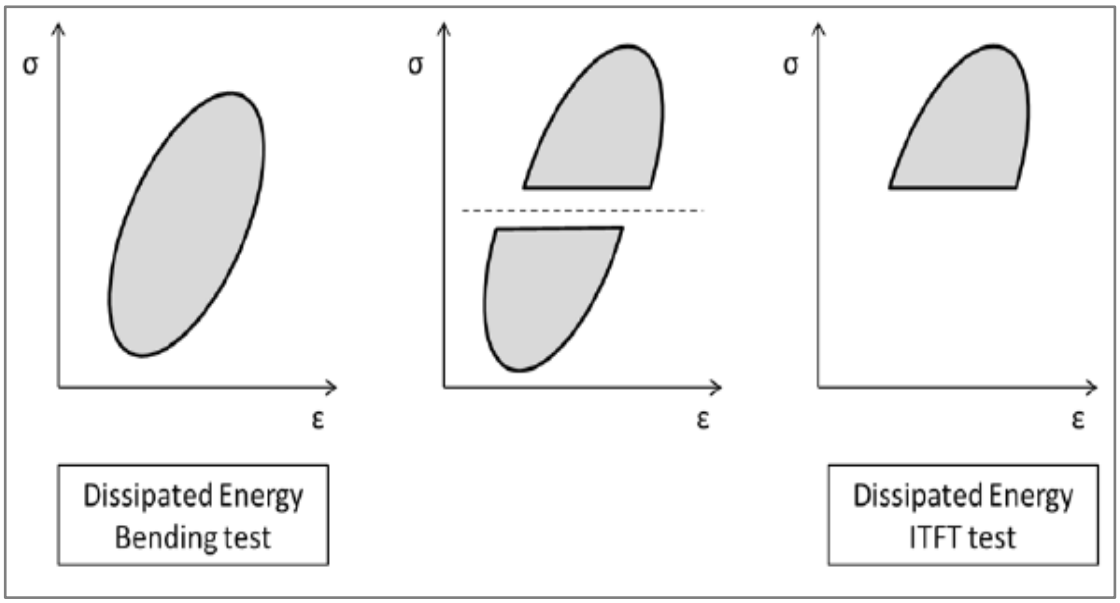



Figure 7.12: Dissipated energy for a bending test and the ITFT (Maggiore, 2014).

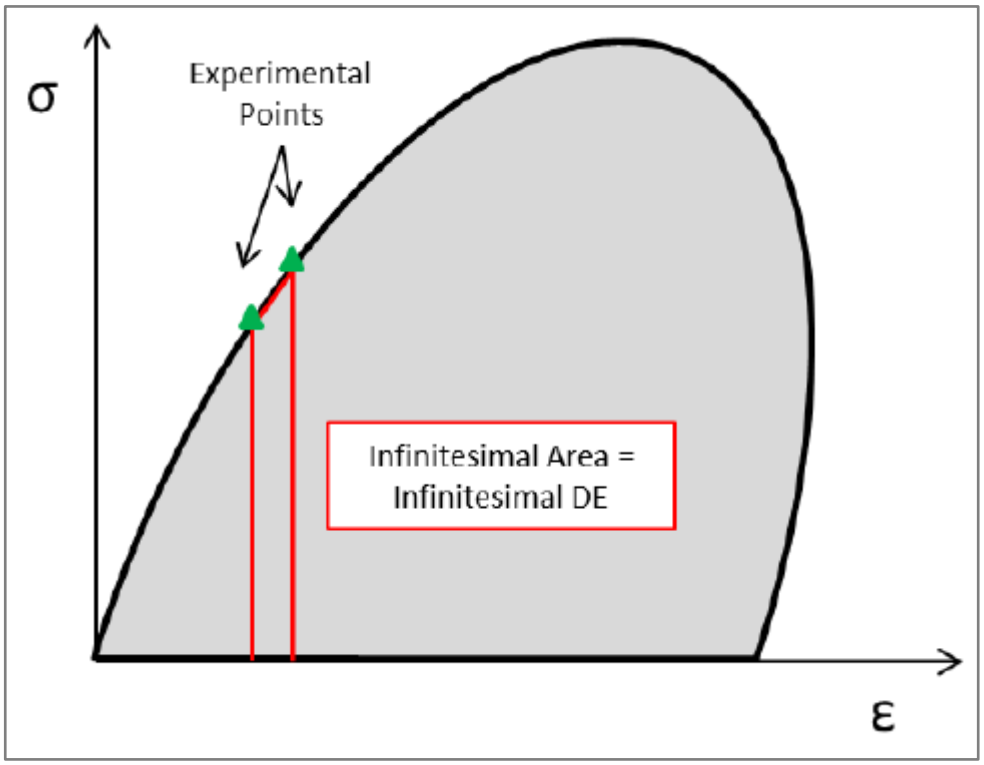



Figure 7.13: Calculation of Dissipated Energy (Maggiore, 2014).

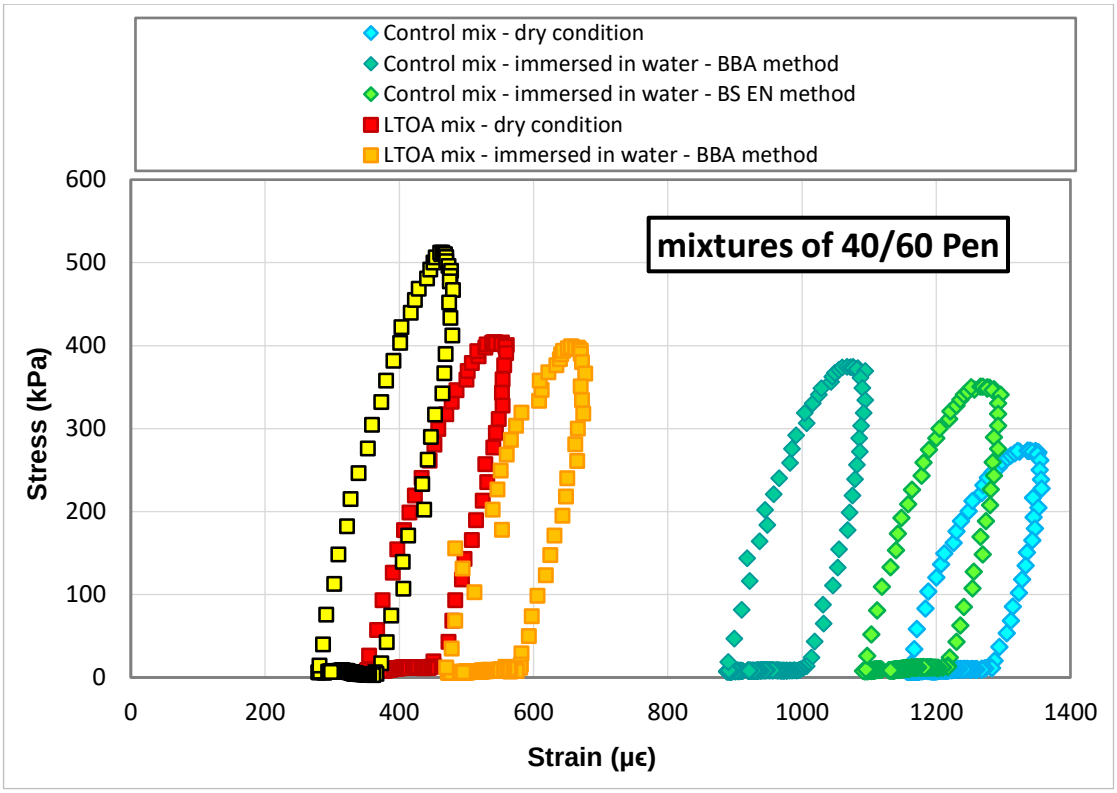



Figure 7.14: Sample of hysteresis loop for a single pulse in ITFT at cycle 50$^{th}$ – asphalt mixture specimen of 40/60 Pen.

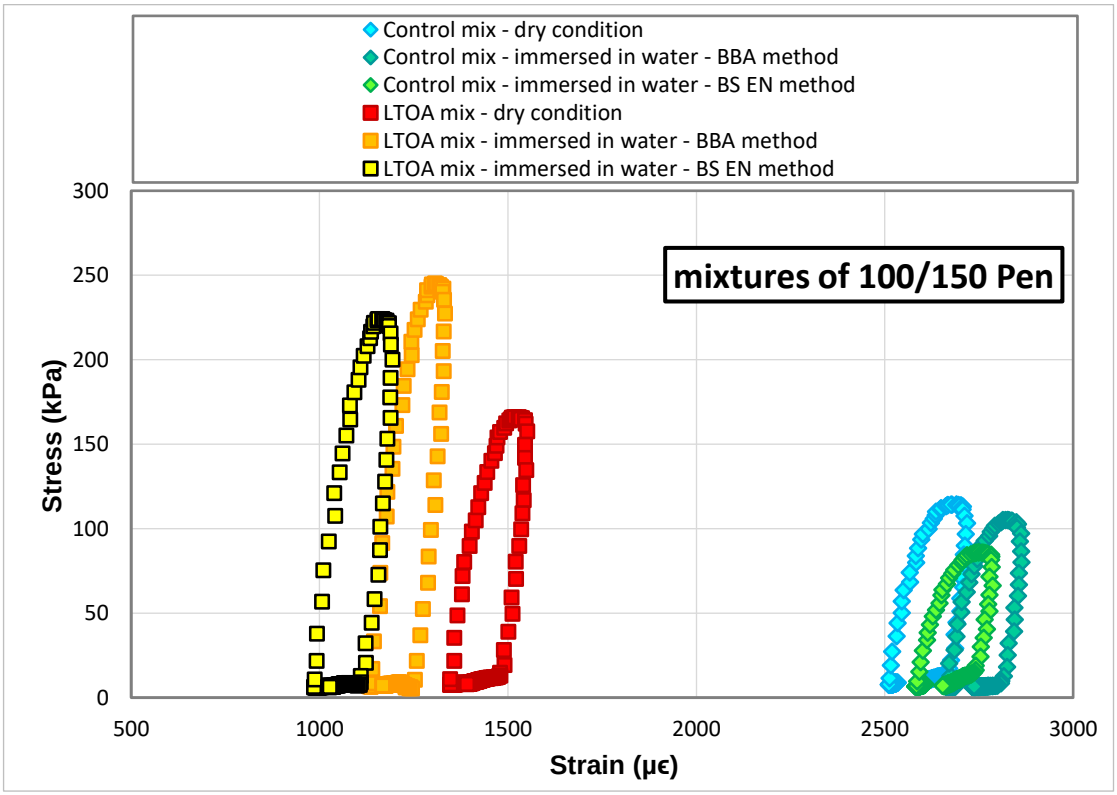



Figure 7. 15: Sample of hysteresis loop for a single pulse in ITFT at cycle 50$^{th}$ – asphalt mixture specimen of 100/150 Pen.

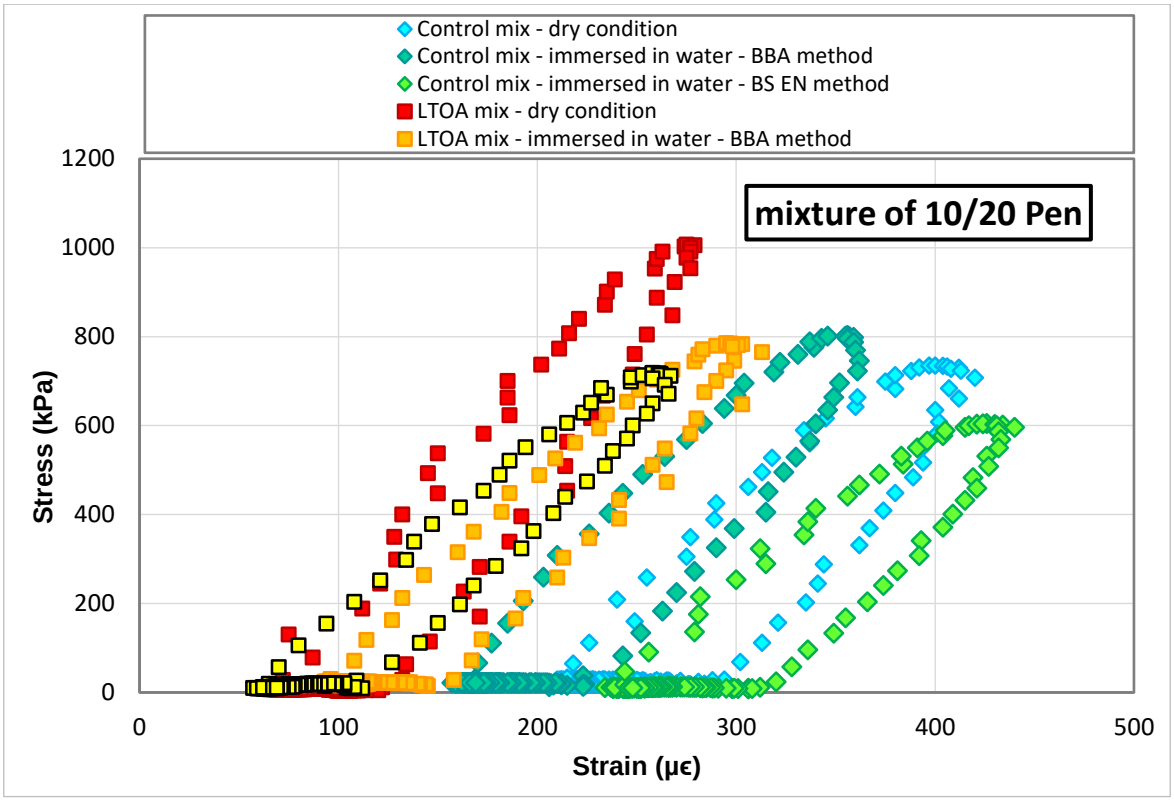


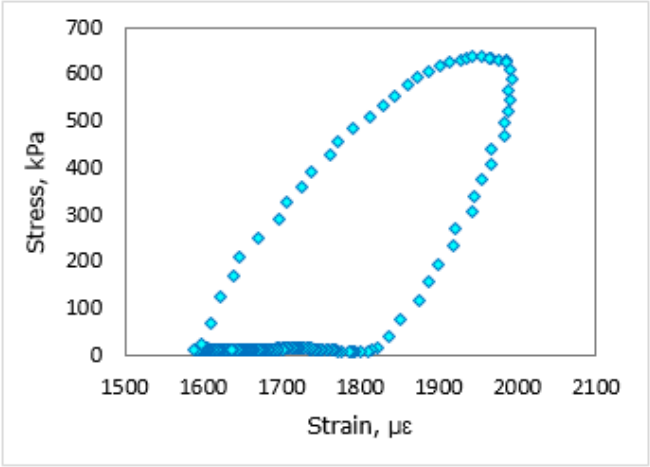

Figure 7.16: Sample of hysteresis loop for a single pulse in ITFT at cycle 50$^{th}$ – asphalt mixture specimen of 10/20 Pen.

Figure 7.17 presents a sample of hysteresis loops progress of asphalt mixture specimen tested at 400 με and at 20˚C. The progress was examined by the hysteresis loop index (HLI) calculated at the cycles 50, 2500, and 6500 where the initial stress reductions are 0% and approximately 50 and 80 % respectively. Equation 7.7 was used to calculate the HLI. The area under the hysteresis loop (trapezoidal area shown in Figure 7.13) was determined at cycle 50$^{th}$ (reference point), 100$^{th}$, and then each 500 cycles until the end of the test (the total number of load repetitions was 6650) as shown in Appendix A-1.

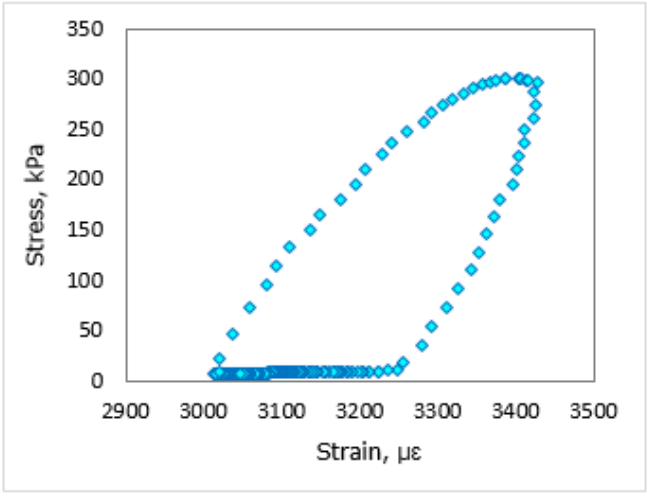
$$HLI = \frac{area\ of\ the\ loop\ at\ \ cycle\ i}{area\ of\ the\ loop\ at\ \ cycle\ 50^{th}} \times 100 \qquad 7.7$$

No significant distortion in the shape of these loops can be observed at the end of ITFT as shown in Figure 7.17 compared to that was observed by Alkhateeb and Shenoy, 2004 in Figure 7.11 shown earlier (More details are presented in Appendix A-1). Therefore it seems not possible to use the resulting hysteresis loops from ITFT in the same line with Alkhateeb and Shenoy's criterion. It might be due to using different testing method (4-PB) at high strain level (1000 με) in

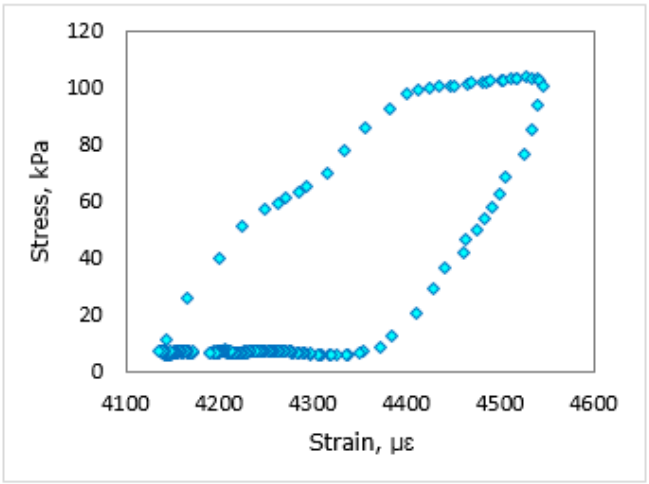
that test. The rest period of ITFT pulse is also a possible reason to retain the hysteresis loop shape from any significant distortion through the ITFT in this study.




At cycle 50th, HLI=100%




At cycle 2500th, HLI=52.3%




At cycle 6500th, HLI=20.2%

Figure 7.17: Sample of hysteresis loops progress of ITFT at 400 με and 20˚C.

It was also found that the area of these loops decreased (due to the decrease of initial stress) as the number of loading cycles increased. Figure 7.18 shows the relationship between the reduction of initial stiffness and HLI progress. HLI progress seems compatible to the reduction of initial stiffness which is rational because both are depending on the initial stress variation of the tested specimen. That may enhance the reliability of ITFT in constant strain mode.

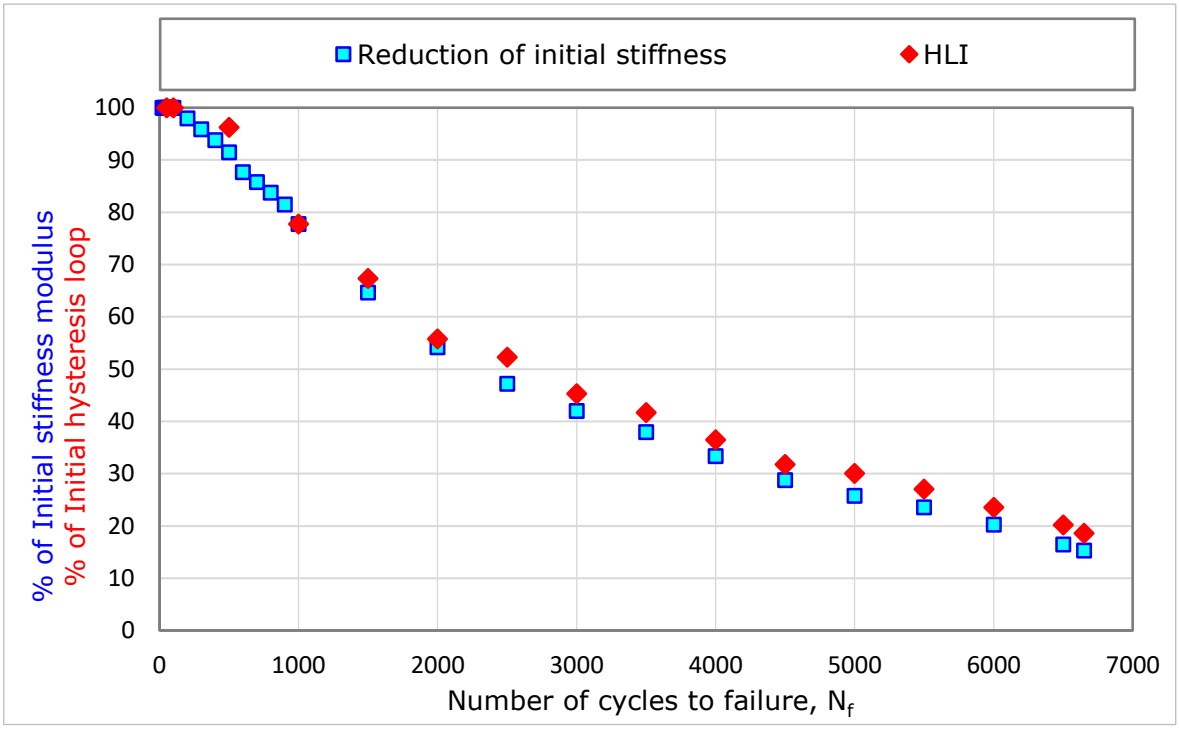



Figure 7.18: The reduction of initial stiffness and HLI progress.

### 7.5.3 Rowe and ASU methods

Besides the traditional method of 50% reduction of initial stiffness, the software of modified ITFT can provide the opportunity to use different fatigue failure criteria; Rowe's method (Rowe, 1996), and ASU (Arizona State University) method (Abojaradeh, 2013, Abojaradeh et al., 2007, Soliman et al., 2012).

Firstly, for controlled strain test data, Rowe defined $N_1$ as the point at which the slope of the energy ratio versus number of cycles deviates from a straight line as shown in Figure 7.19. Rowe indicated that the evidence for crack initiation at this point ($N_1$) was visually confirmed by observations and by earlier work at Nottingham (McCarthy, 1960) where similar reductions in stiffness modulus occurred prior to the observed crack propagation. Figures 7.19 and 7.20 show $N_1$ (crack initiation) for asphalt mixture specimens of 40/60 Pen and 100/150

Pen respectively tested at 400 με and 20˚C. Rowe stated that the definition of $N_1$ in constant strain tests is very much harder compared to constant stress tests (peak value).

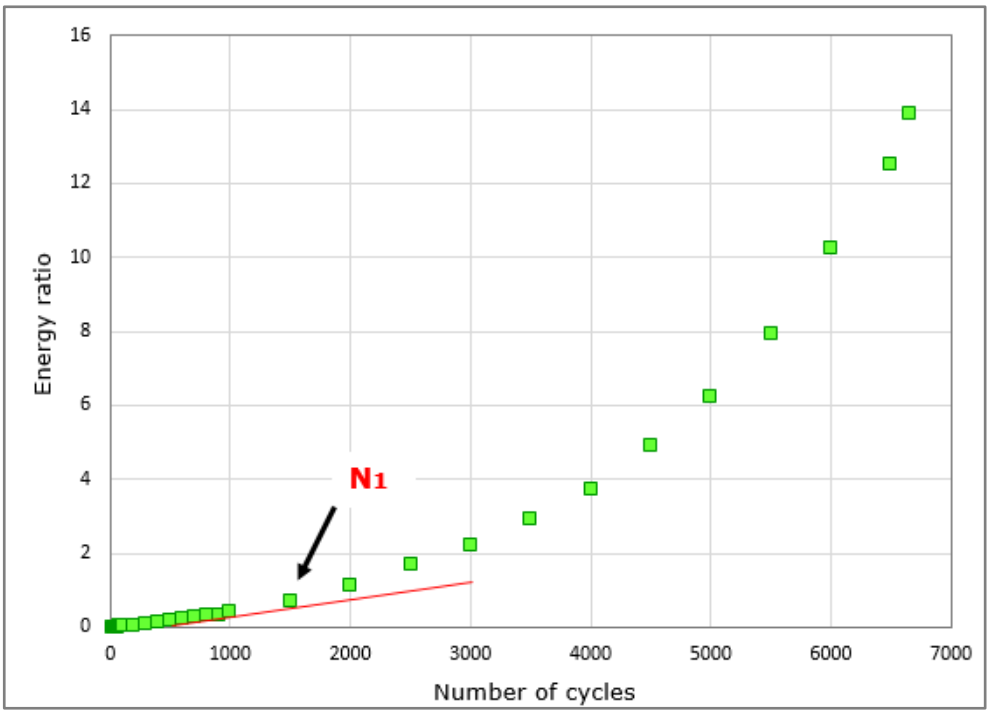



Figure 7.19: Fatigue analysis method for ITFT of 40/60 Pen asphalt mixture.

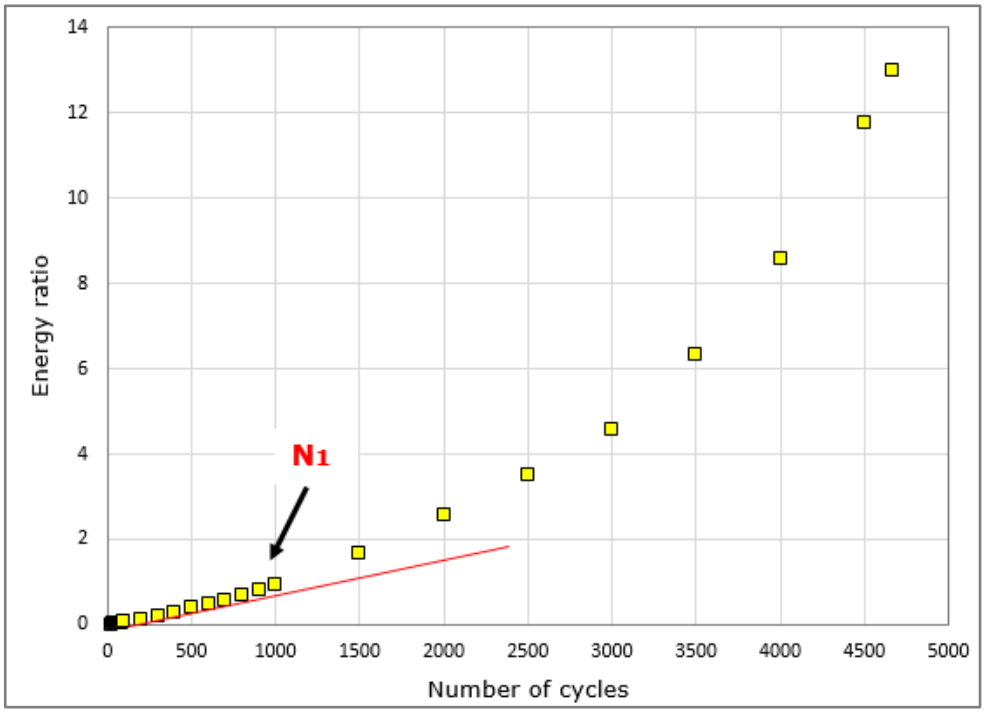



Figure 7.20: Fatigue analysis method for ITFT of 100/150 Pen asphalt mixture.

Secondly, the ASU method was developed by normalising the stiffness ratio failure criteria ($SR=N_i \times S_i$). The normalizing can be done by dividing this ratio by the initial stiffness $S_0$ to be in the form ($SR=N_i * S_i / S_0$). Where SR= the stiffness ratio, $N_i$ = load cycle, $S_i$= the stiffness at cycle i, and $S_0$ = the initial stiffness measured at the cycle $50^{th}$. This method is independent of test modes. It defines the failure as the total number of load applications at the peak value of the curve for either constant stress or constant strain methods as shown in Figures 7.21 and 7.22. These figures show the difference in the resulting number of cycles to failure at 400 με and 20˚C for asphalt mixture specimens of 40/60 Pen and 100/150 Pen respectively. From the traditional analysis method $N_f$ is 2300 cycles while it is 4000 cycles when ASU was applied as shown in Figure 7.21. For 14mm DBM specimen of 100/150 Pen, the cycles numbers are 1800 and 3000 respectively. The traditional approach clearly shows less number of cycles to failure than the ASU method.

However, using non-traditional approach should be taken carefully. First, it requires to increase the failure criteria of initial stiffness mentioned earlier up to 10% (maximum allowable limit) instead of 50% to reach the inflection point. That needs more testing time which might be considered time consuming. This is especially important for the ITFT constant strain method as it can only apply two pulses per second. However, this is still faster than the traditional ITFT. Second, the vertical deformation may possibly reach 10mm earlier than reaching the specified failure criteria. If this happens the data might not be enough to perform the ASU analysis method. In particular, this generally occurs in this study with asphalt mixtures of soft binder (100/150 Pen).

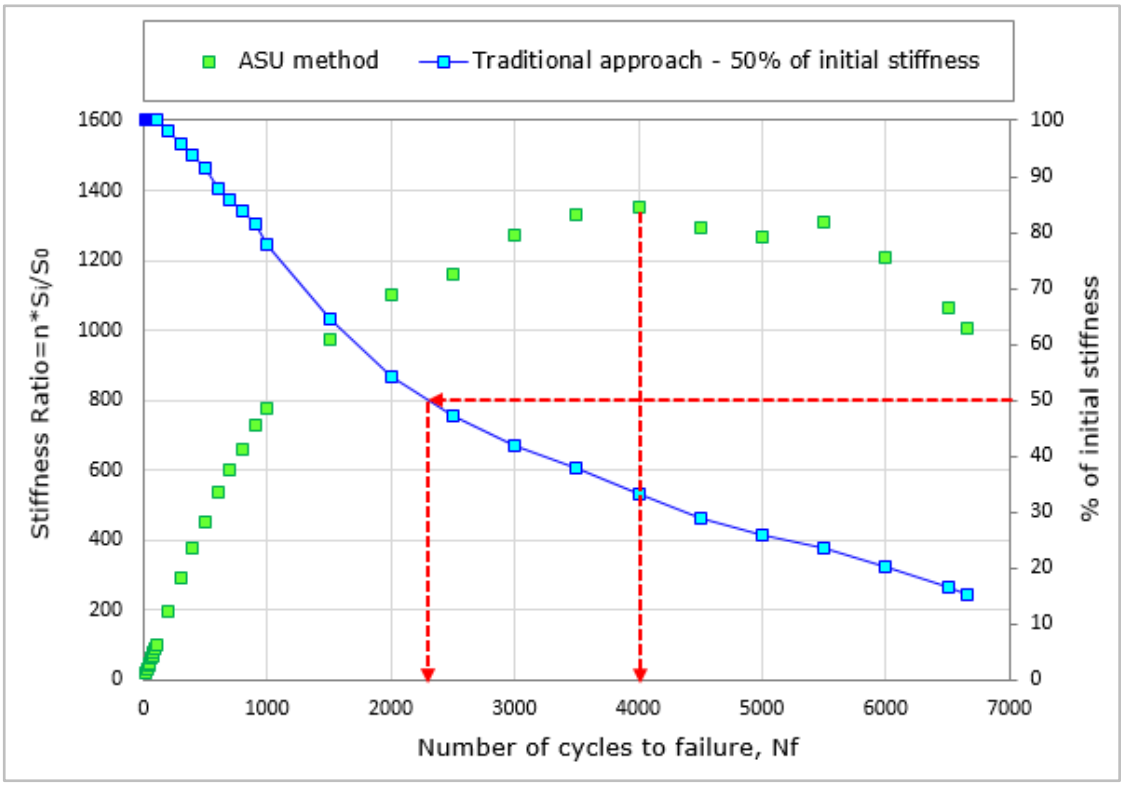



Figure 7.21: Fatigue analysis methods for ITFT of 40/60 Pen asphalt mixture.

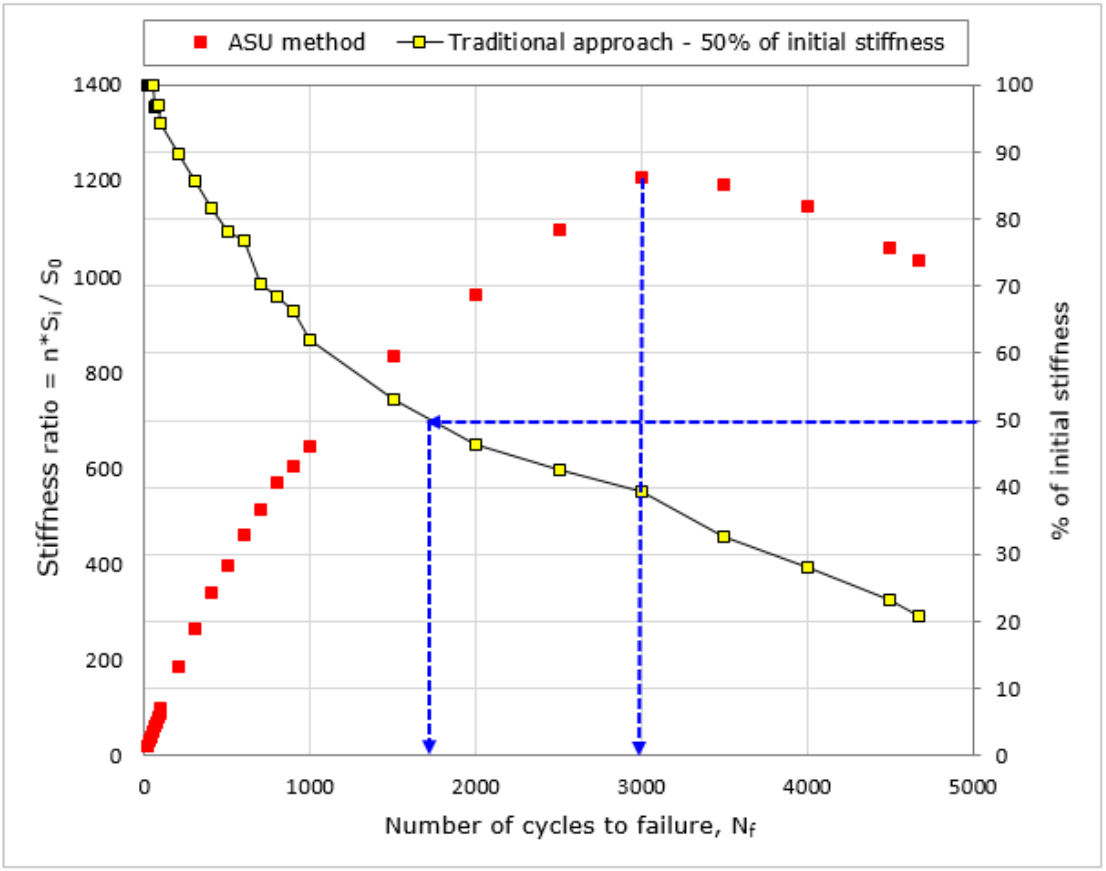



Figure 7.22: Fatigue analysis methods for ITFT of 100/150 Pen asphalt mixture.

Additionally, another specimen of hard binder (10/20) was tested by ITFT at 200 με and 20˚C. The test has carried on up to 80% reduction of initial stiffness as shown in Figure 7.23. Although no peak being clearly seen in this curve, two points at which a change in the direction of curvature occurs can be observed. The first one may refer to possible formation of microcracks and the second one may refer to possible formation of macro cracks. The traditional approach of failure assessment ($N_{f50}$) specifies the cycle 68000$^{th}$ as the failure point where 50% reduction of initial stiffness occurred at this point. On the other hand, it is not simple to precisely specify the failure point by using the ASU method. It can be estimated at the cycle 90000$^{th}$. However, the failure point could have occurred earlier according to Rowe's definition ($N_1$). That makes the failure point assessment in terms of the inflection point not practical for some circumstances.

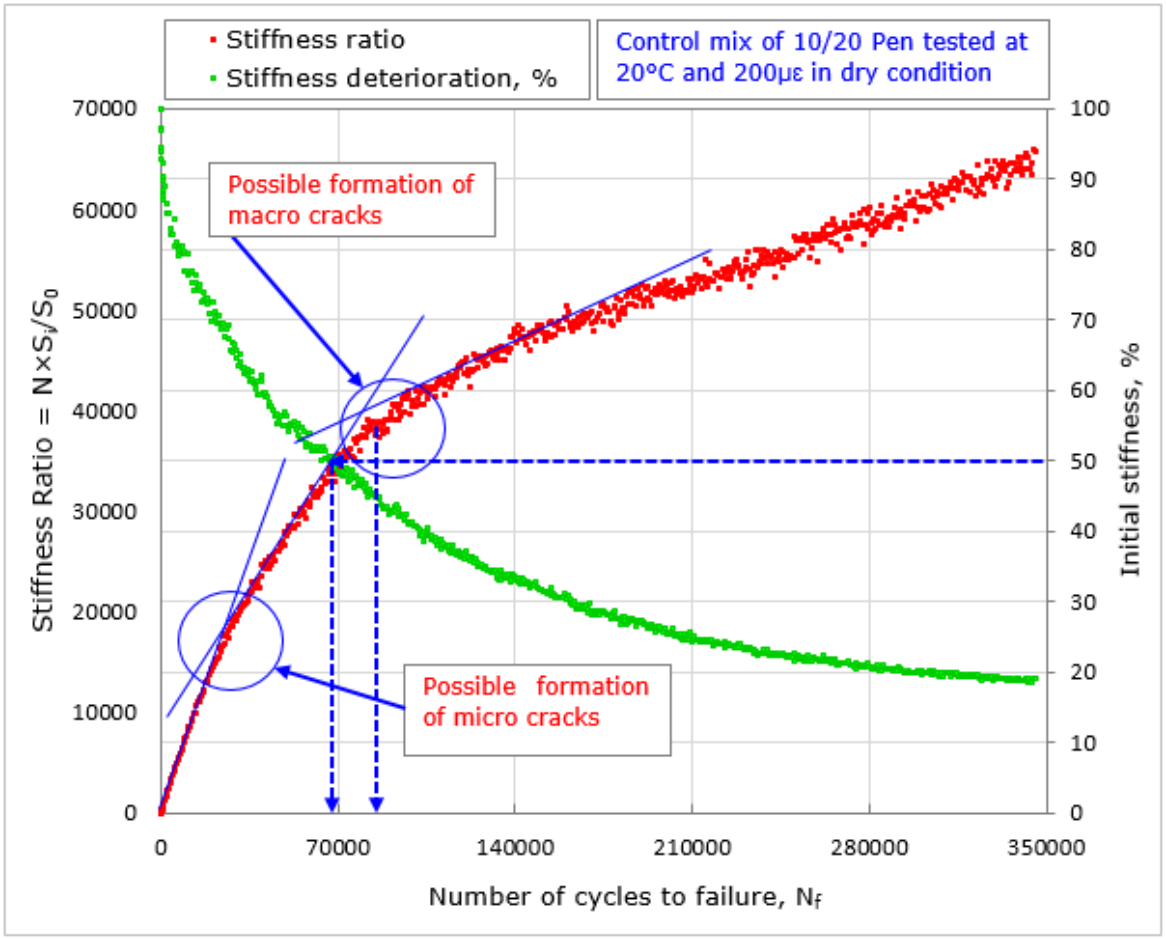



Figure 7.23: Fatigue analysis methods for ITFT of 10/20 Pen asphalt mixture.

Finally, Maggiore, 2014 has applied different fatigue analyses; Dissipated Energy Ratio by Pronk, Ratio of Dissipated Energy Change (RDEC) by Shen and Rowe's method. It was found that Pronk's method generates fatigue life smaller than the traditional approach, although the fatigue lines were almost coincident. In addition, the generated fatigue life by Rowe's method was greater and that by RDEC was slightly greater than the traditional one.

### 7.5.4 X-ray Computer Tomography (CT)

X-ray Computer Tomography (CT) has been simply used to examine the possibility of using this technique with ITFT in constant strain method for fatigue damage investigation. Image analysis grading of the aggregate (ImageJ) was used to analyse the X-ray images of the compacted 14mm DBM specimen of 40/60 pen. These images were taken at four stages; before ITFT at 100% of initial stiffness, ITFT at 80 % of initial stiffness, ITFT at 70% of initial stiffness, ITFT at 40% of initial stiffness as shown in Figure 7.24. No significant change in air voids content and distribution was observed after testing the specimen up to 20% reduction of initial stiffness as shown in Figures 7.25 and 7.26. It was also observed from the scanning of the asphalt mixture specimen tested in ITFT that the volume of air void content has non-uniformly increased throughout the specimen (see Figure 7.25).

Based on damage mechanics theory (Dietmar et al., 2006), the damage of material occurs due to nucleation, growth and coalescence of micro voids. It supposes that the growth of internal voids/cavities causes new micro defects. Damage can be quantified by a scalar parameter D of values between 0 (undamaged) and 1 (fully damaged). D can be calculated based on initial stiffness reduction as following:

$$D = 1 - \frac{E_i}{E_0} \qquad 7.8$$

Where:

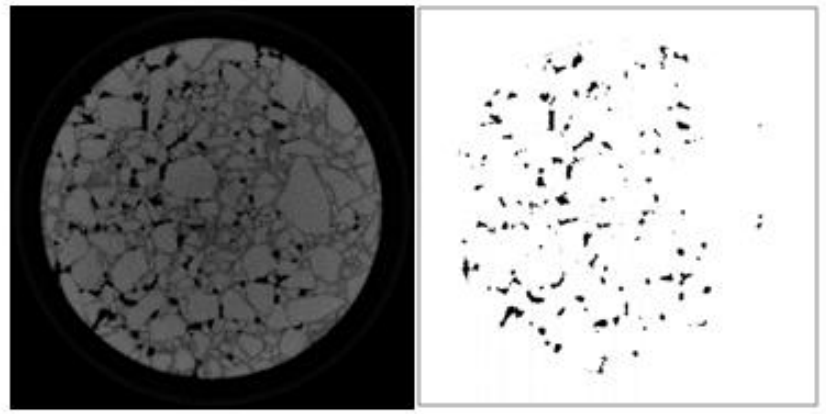
D: Damage parameter,

$E_0$: Initial stiffness modulus measured at cycle $50^{th}$, and

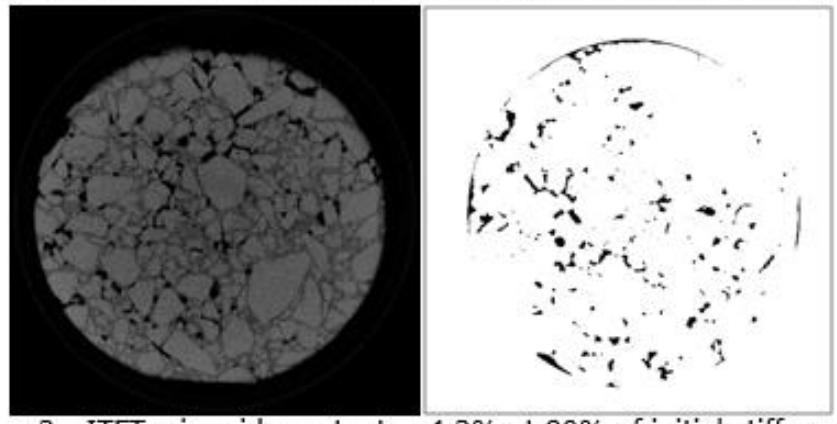
$E_i$: Stiffness modulus measured at cycle i.

Similarly, damage parameter D was calculated from X-ray image analysis by

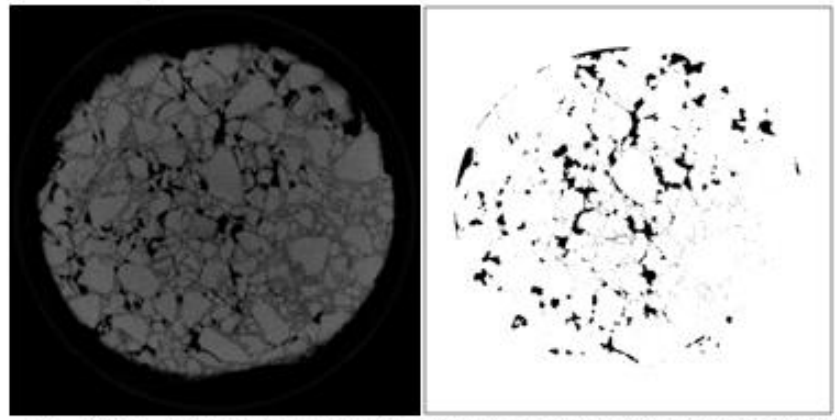
assuming that it is proportional to air void content increase where the initial air void content corresponds to D=0 and the air void content at failure corresponds to D=1 (Khan and Collop, 2010). The ratio of stiffness modulus $E_i/E_0$ was measured from ITFT and plotted against the damage parameter D from both methods in Figure 7.27. It can be noticed that the damage parameter resulting from the increase of air voids is greater than the damage parameter resulting from the reduction of stiffness modulus.



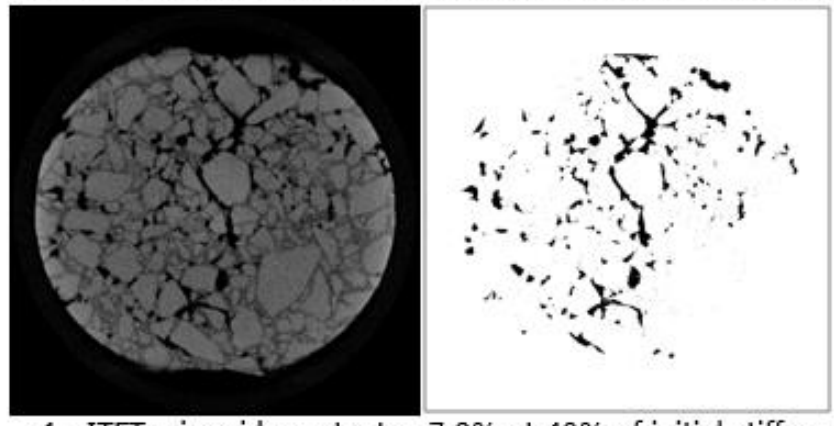
1- Before ITFT, air voids content = 4.2% at 100% of initial stiffness.



2- ITFT, air voids content = 4.2% at 80% of initial stiffness.



3- ITFT, air voids content = 6.7% at 70% of initial stiffness.



4- ITFT, air voids content = 7.9% at 40% of initial stiffness.

Figure 7. 24: Original X-ray images (left) and Binary images of air voids (right).

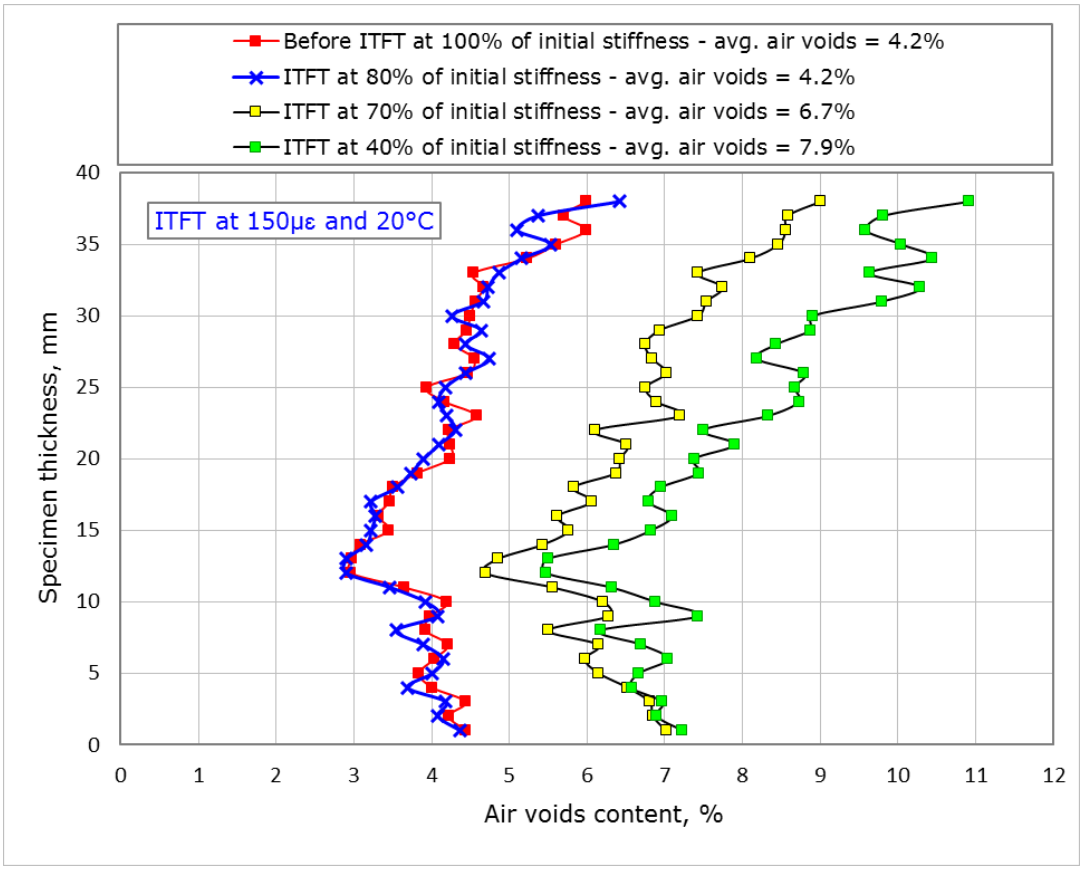



Figure 7.25: Air voids variation along the height of asphalt mixture specimen.

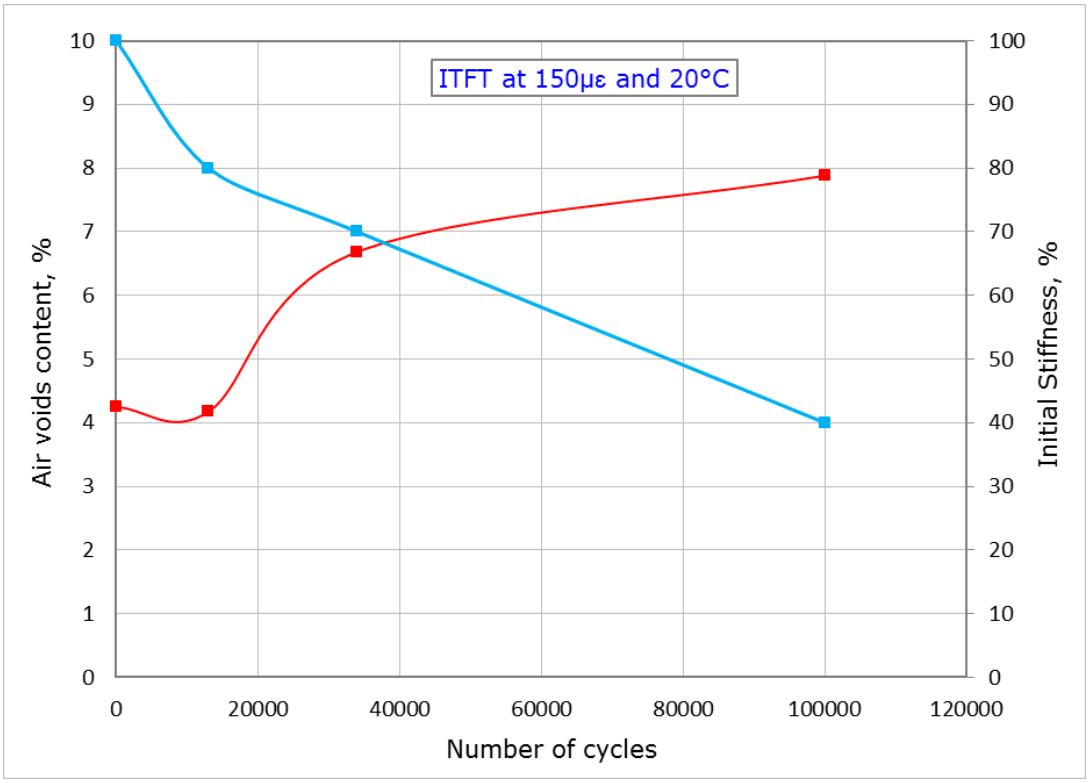



Figure 7.26: Variation of stiffness modulus and air voids content in ITFT.

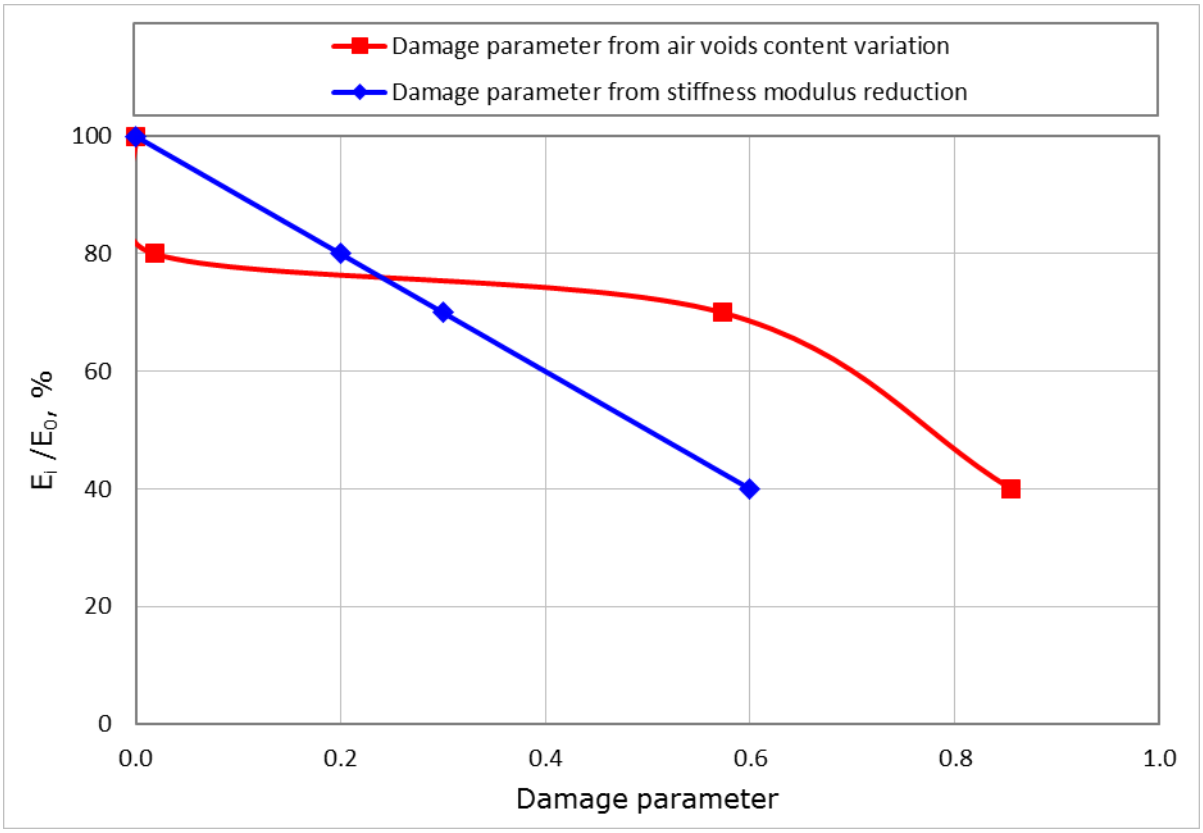



Figure 7.27: Stiffness ratio vs. damage parameter from X-ray CT and ITFT.

Based on these findings of different fatigue failure criteria and X-ray Computer Tomography (CT), it was decided to use the phenomenological approach ($N_{f50}$) to specify the number of cycles to failure for fatigue tests carried out by ITFT in constant strain method. This approach was mainly selected for its simplicity, practicality and suitability for the new arrangement of ITFT. It was also chosen due to time limitations of the study. In addition, the ASU method was used to analyse ITFT data of 40/60 Pen asphalt mixtures tested at different conditions.

### 7.6 Results of ITFT in constant strain method

In this work, an extensive study was performed to understand the performance of ITFT. Fatigue tests were carried out at different strain levels 120 – 400 με, different air voids content, two testing temperatures, and different testing conditions. The main parameters and conditions are previously presented in Table 7.1 and investigated by ITFT in constant strain method.

### 7.6.1 Effect of air voids

Figures 7.28 to 7.33 show the effect of air voids content on the characterisation of fatigue life of different asphalt mixtures. Figures 7.28 and 7.29 show this effect at three air voids content 4%, 8%, 12% at 10˚C and 20˚C for control asphalt mixtures of 40/60 Pen. The 20˚C is the standard testing temperature of fatigue tests according to BS EN 12697-24:2012 while the 10˚C was also applied to specimens for comparison. No significant effect of air voids content can be generally observed from these figures. Figure 7.30 present this effect at the same air voids content for LTOA asphalt mixtures of 40/60 Pen. It can be noticed that fatigue characterisation of aged mixtures with 12% air voids content shows some shifting compared to mixtures of 4% and 8%. It might be due to the effect of ageing which is influenced by air voids content as shown previously in Chapter Four. Figures 7.31 and 7.32 display the influence of air voids content; 8% and 12 % at 20°C for two different binder grades; 10/20, and 100/150 respectively. The fatigue lines are relatively compatible when 10/20 Pen was used (Figure 7.31). However, there is a rational difference between these line in the case of using 100/150 Pen. From testing observations, asphalt mixtures of 100/150 Pen were more susceptible to the setting of the new ITFT arrangement in terms of their susceptibility to the resulting permanent horizontal and vertical deformations. Similar results and reasons were observed when 40/60 Pen was used at 6% content as shown in Figure 7.33.

Ghuzlan and Carpenter, 2003 stated that no statistical difference between the fatigue coefficients ($K_1$ and $K_2$) were found because of the influence of two air voids content; 4 and 7 % on the number of loading cycles to failure of prismatic beam specimens. They also suggested to carry out the same study by ITFT.

The analysis of variance, ANOVA, was used in this study to compare two or more different regression lines and test if differences between the slopes of generated fatigue lines ($N_{f50}$) are significant or no. Usually a null hypothesis ($H_0$: $\mu_1=\mu_2=\mu_3=\mu_n$) states no statistical significant difference between the slopes of these lines and an alternative hypothesis ($H_A$: $\mu_1\neq\mu_2\neq\mu_3\neq\mu_n$) states there is a statistical significant difference between them are set up. Where $\mu$ is a fatigue regression line generated from ITFT results. If the probability is less than the

level of significance, usually α=5% (or if $F \geq F_{Critical}$) then $H_0$ is rejected and the alternative hypothesis, $H_A$ is true. That means the slopes are not all equal. The ANOVA test results are presented in Table 7.2. It was found that all p-values are greater than 0.05 and therefore $H_0$ is accepted. That means the differences between the slopes of the lines in each of the next figures (7.28–7.33) mentioned in Table 7.2 are not statistically significant. In addition, some p-values are approaching 1.0 which might indicate that fatigue lines are completely compatible and there is no effect of air voids content on the fatigue life as determined by ITFT. However, some p-values decreased when other testing parameters and conditions (ageing and moisture conditioning) were investigated. Similar results of tests of significance were found when immersed asphalt mixtures of 8 and 12% air voids content were tested for fatigue by ITFT (Results are not presented in Table 7.2). In summary, ITFT in controlled strain mode is not susceptible to the change in air voids content. However, air voids content might slightly have more effect if it is combined with the influence of other mixture variables and testing conditions. This is not crucial and may require more investigation.

Table 7.2: Results of test of significance (ANOVA test – single factor method) for the effect of air voids content on fatigue performance of asphalt mixtures.

| **Binder grades** | **Condition** | **T, ˚C** | **Figure Number** | **F** | **P-value** | **$F_{Critical}$** |
|---|---|---|---|---|---|---|
| 40/60 Pen | Control mix - dry | 10 | 7.28 | 0.004 | 0.996 | 3.555 |
| 40/60 Pen | Control mix - dry | 20 | 7.28 | 0.158 | 0.855 | 3.592 |
| 40/60 Pen | Aged mix - dry | 20 | 7.30 | 0.418 | 0.665 | 3.592 |
| 10/20 Pen | Control mix - dry | 20 | 7.31 | 0.002 | 0.965 | 5.318 |
| 100/150 Pen | Control mix - dry | 20 | 7.32 | 0.399 | 0.545 | 5.318 |
| 40/60 Pen (6% binder content) | Control mix - dry | 20 | 7.33 | 0.422 | 0.534 | 5.318 |

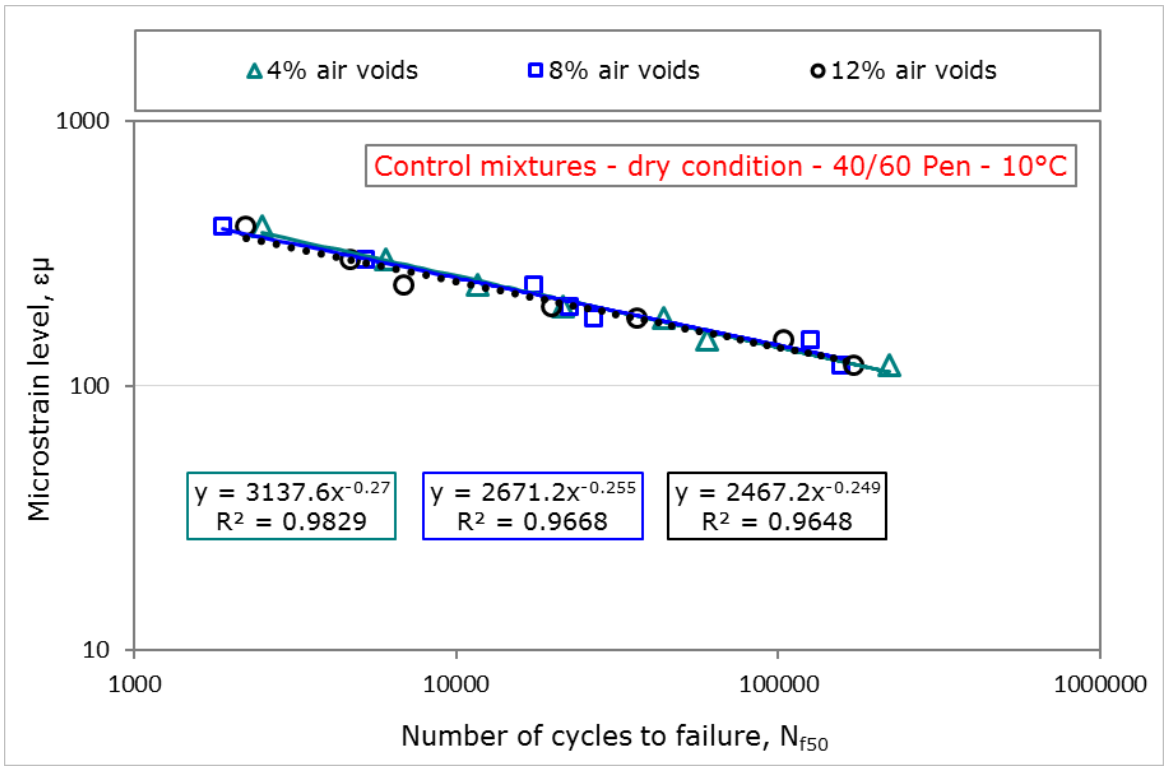



Figure 7.28: Effect of air voids content on fatigue characterisation at 10˚C.

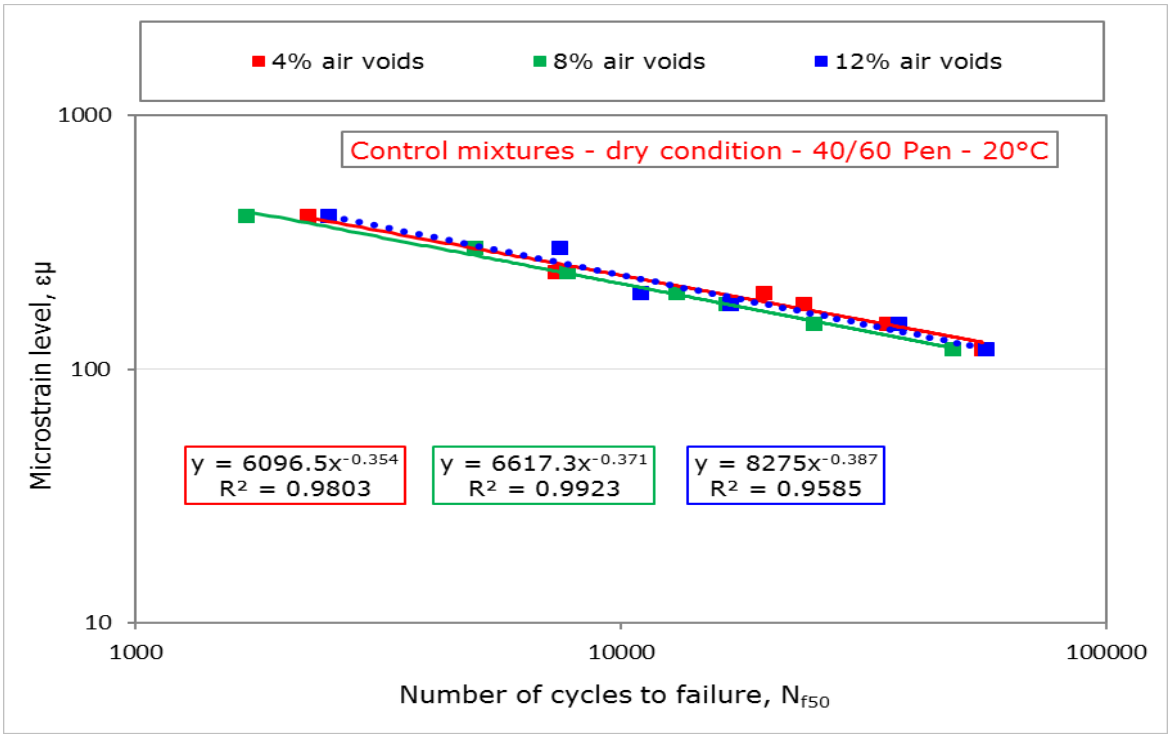



Figure 7.29: Effect of air voids content on fatigue characterisation at 20˚C.

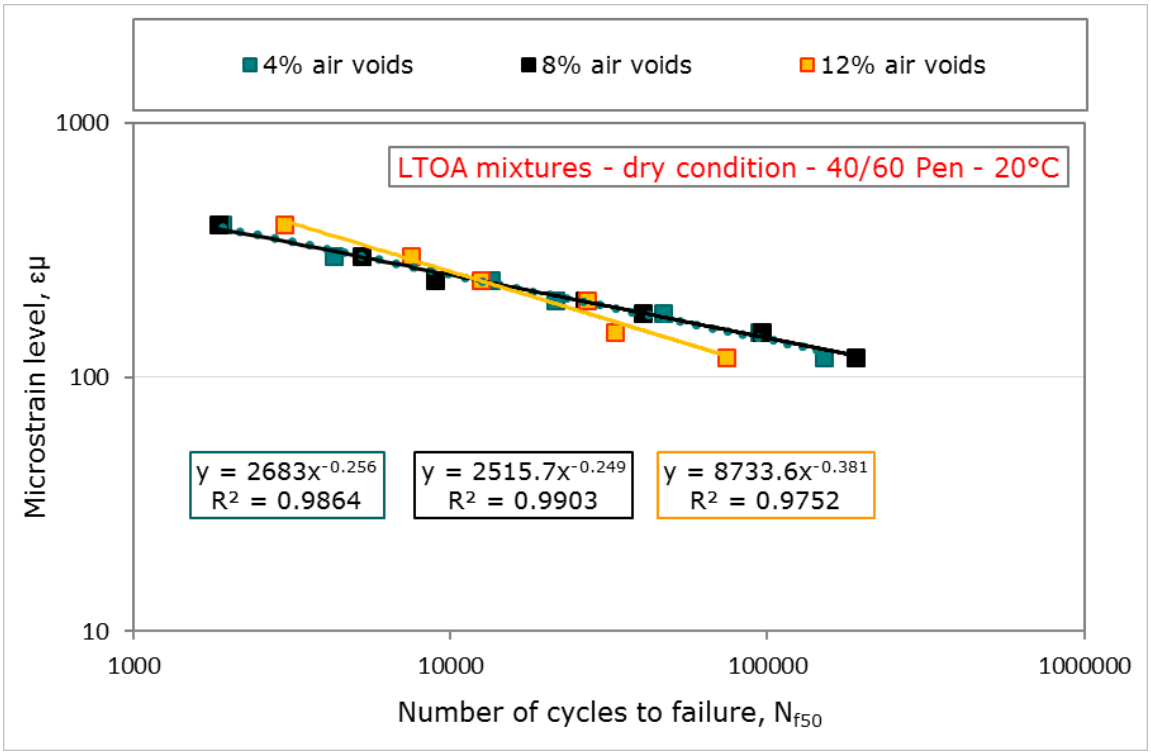



Figure 7.30: Effect of air voids content on fatigue characterisation at 20˚C.

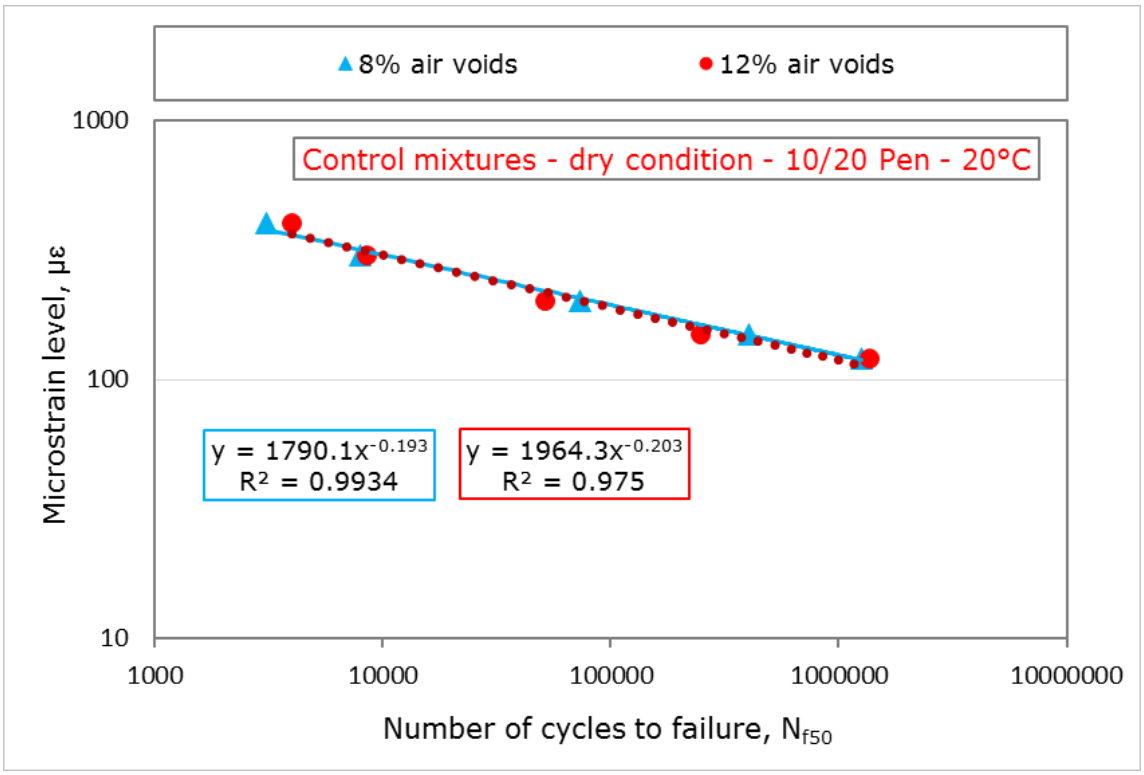



Figure 7.31: Effect of air voids content on fatigue characterisation at 20˚C.

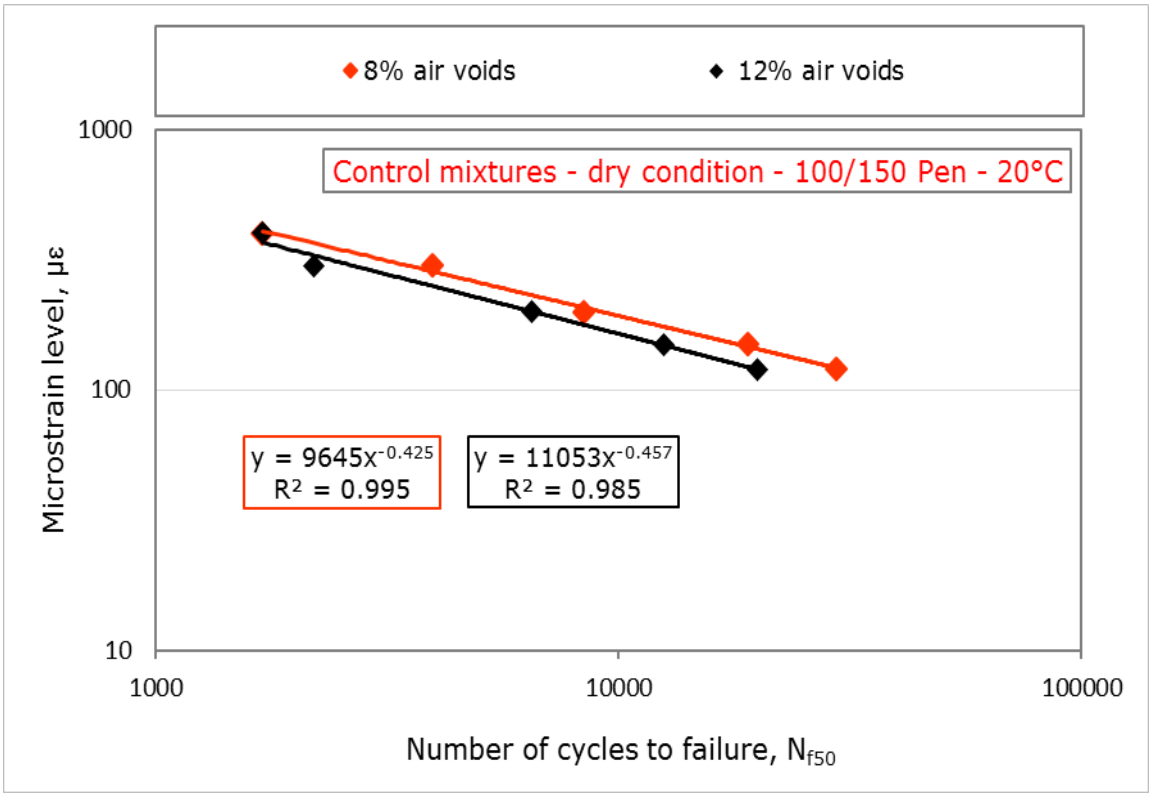



Figure 7.32: Effect of air voids content on fatigue characterisation at 20˚C.

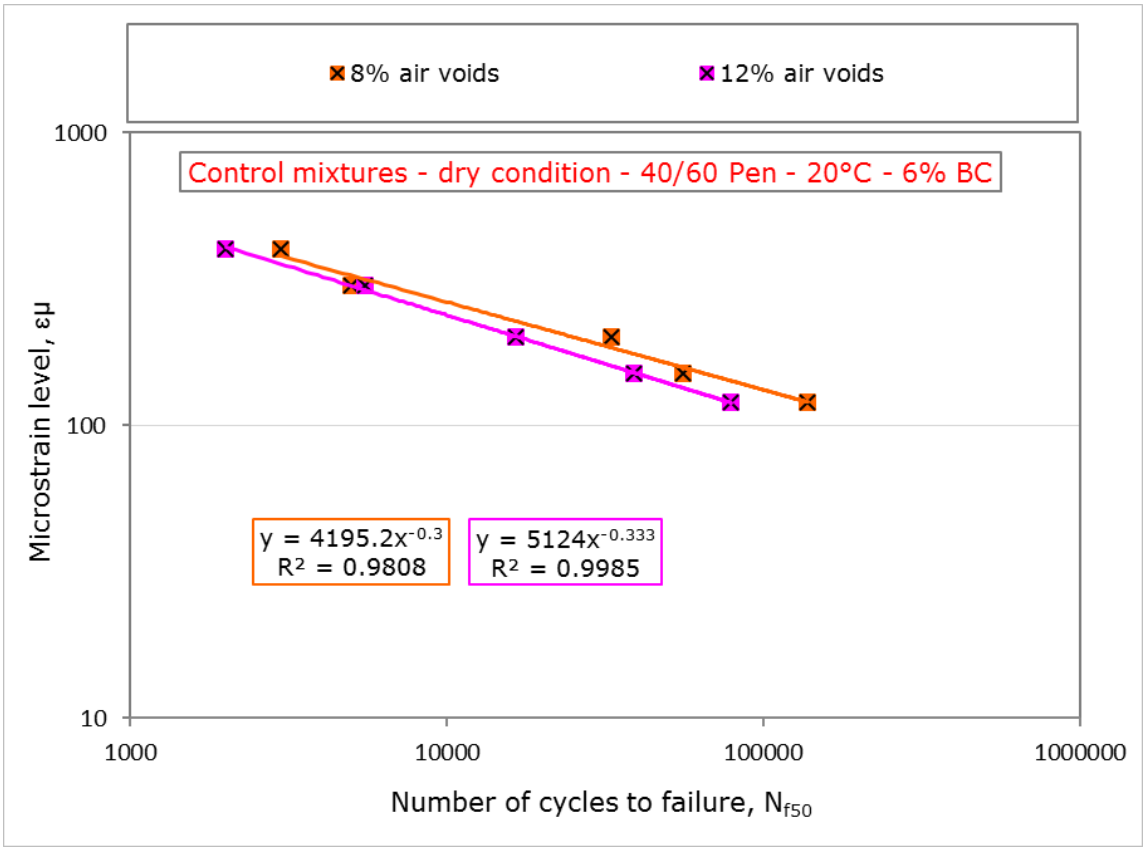



Figure 7.33: Effect of air voids content on fatigue characterisation at 20˚C.

### 7.6.2 Effect of testing temperatures

In addition, two testing temperatures were applied to investigate their effect at three air voids content (4, 8, and 12%) on fatigue characterisation of dry and wet control and LTOA mixtures of 40/60 Pen as shown in Figures 7.34 to 7.39. It was observed an increase in the fatigue life (with shifting at 12% air voids content) of asphalt mixtures when these mixtures stiffen due to the decrease of testing temperature conditioning from 20˚C to 10˚C. However, there is some convergence at 300 and 400 με which could be attributed to the rapid deterioration of stiffness at these levels regardless of other testing parameters. This increase of fatigue life is still pronounced and is more obvious when the investigated mixtures stiffened more due to ageing as shown in Figure 7.37 or when exposed to moisture conditions as seen in Figure 7.38 and 7.39. The reason of this increase may be attributed to the role of reducing the testing temperature from 20 to 10˚C in motivating the elastic properties of the bitumen to dominate rather than viscoelastic or viscous properties. This might increase the ability of asphalt mixtures to recover their original shape and release of stress during the 0.4-second rest period following the load application of ITFT and therefore might generally result in a longer fatigue life.

As determined by ANOVA test and shown in Table 7.3, no statistical significant difference was found between the slopes of all fatigue lines presented in Figures 7.34 to 7.39 for the effect of temperatures (each figure was taken individually).

Table 7.3: Results of test of significance (ANOVA test – single factor method) for the effect of testing temperature on fatigue performance of asphalt mixtures.

| **Parameters** | **Condition** | **Air voids, %** | **Figure Number** | **F** | **P-value** | **$F_{Critical}$** |
|---|---|---|---|---|---|---|
| Effect of testing temperature | Control mix - dry | 4 | 7.34 | 1.073 | 0.321 | 4.747 |
| | Control mix - dry | 8 | 7.35 | 1.936 | 0.189 | 4.747 |
| | Control mix - dry | 12 | 7.36 | 0.978 | 0.344 | 4.844 |
| | LTOA mix – dry | 8 | 7.37 | 1.051 | 0.325 | 4.747 |
| | Control mix – immersed - BBA | 8 | 7.38 | 1.457 | 0.262 | 5.318 |
| | LTOA mix – immersed - BBA | 8 | 7.39 | 1.479 | 0.259 | 5.318 |

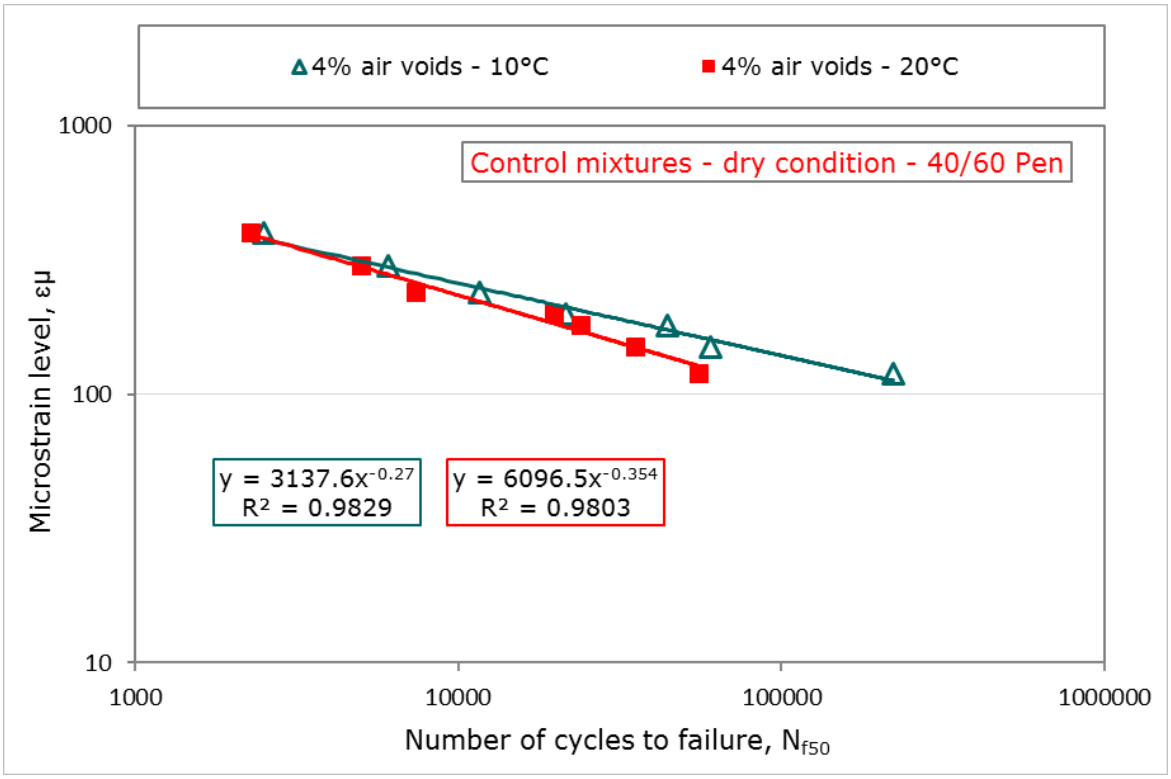



Figure 7.34: Effect of testing temperature on fatigue characterisation at 4% air voids content.

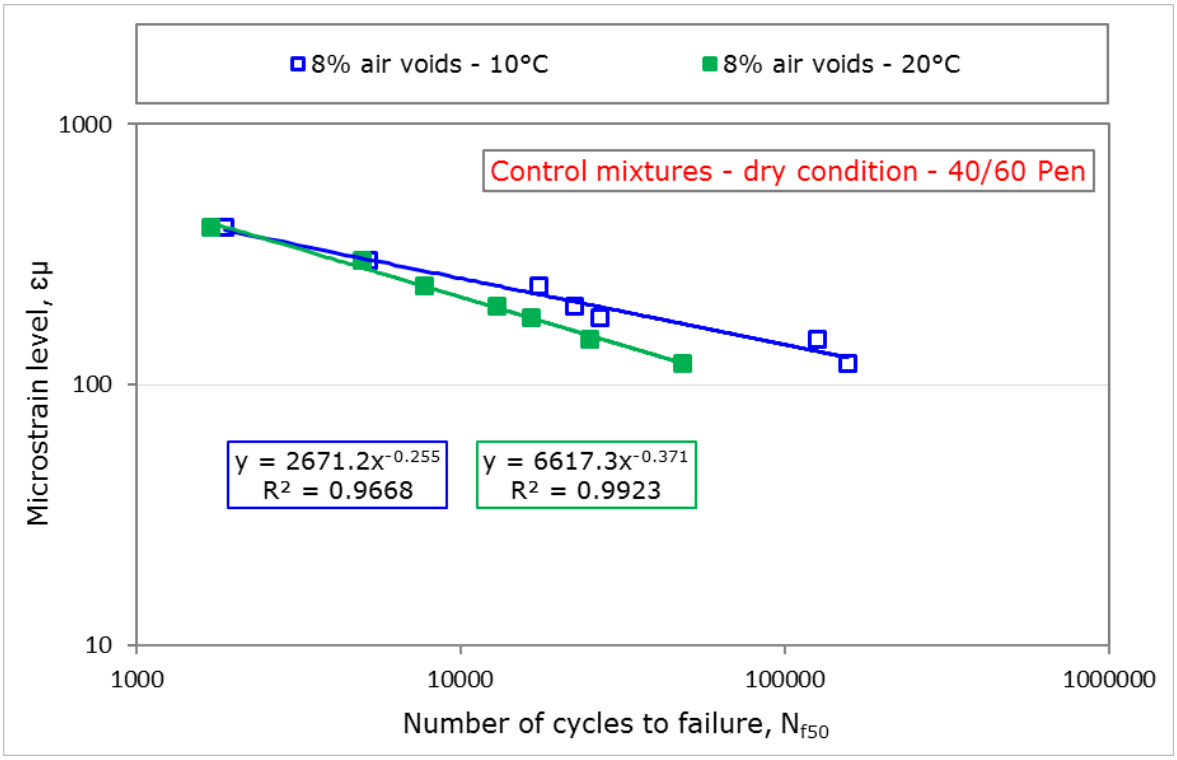



Figure 7.35: Effect of testing temperature on fatigue characterisation at 8% air voids content.

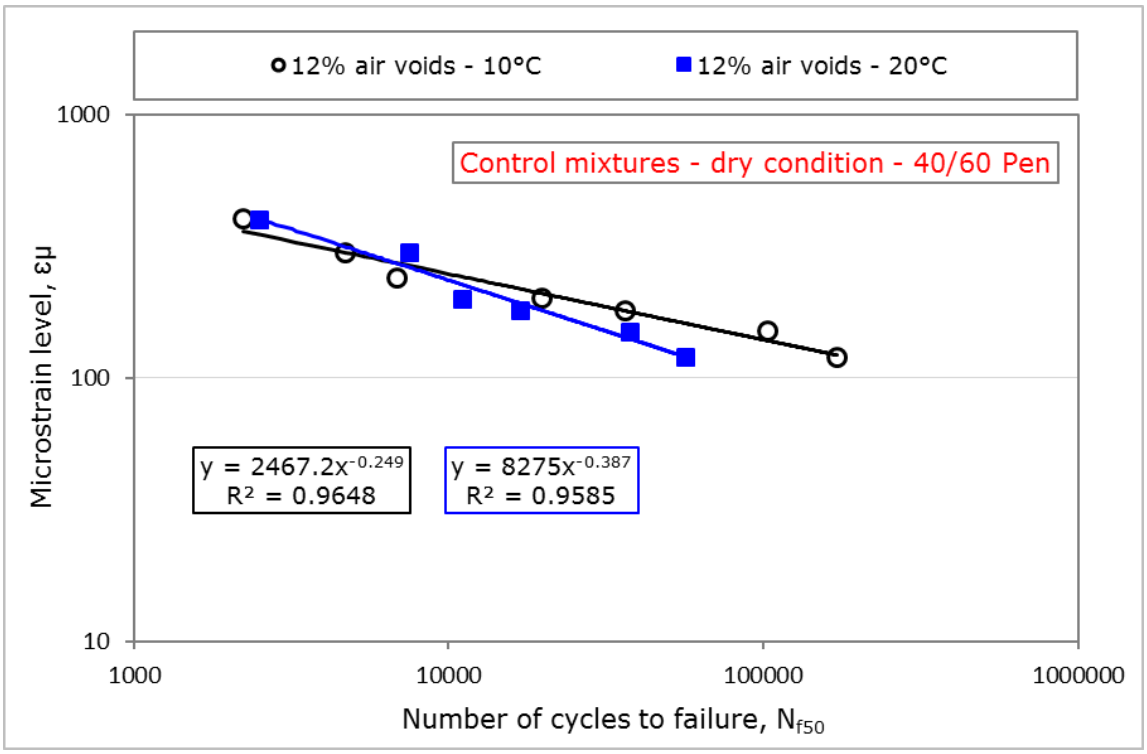



Figure 7.36: Effect of testing temperature on fatigue characterisation at 12% air voids content.

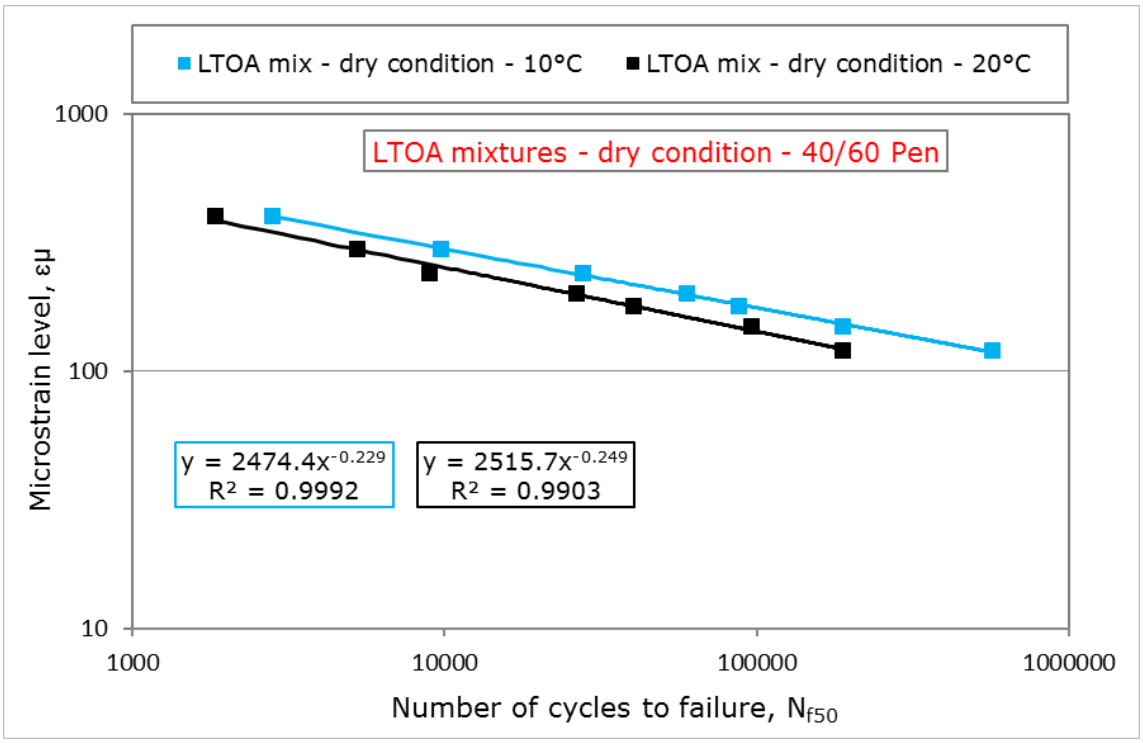



Figure 7.37: Effect of testing temperature on fatigue characterisation of LTOA dry mixtures.

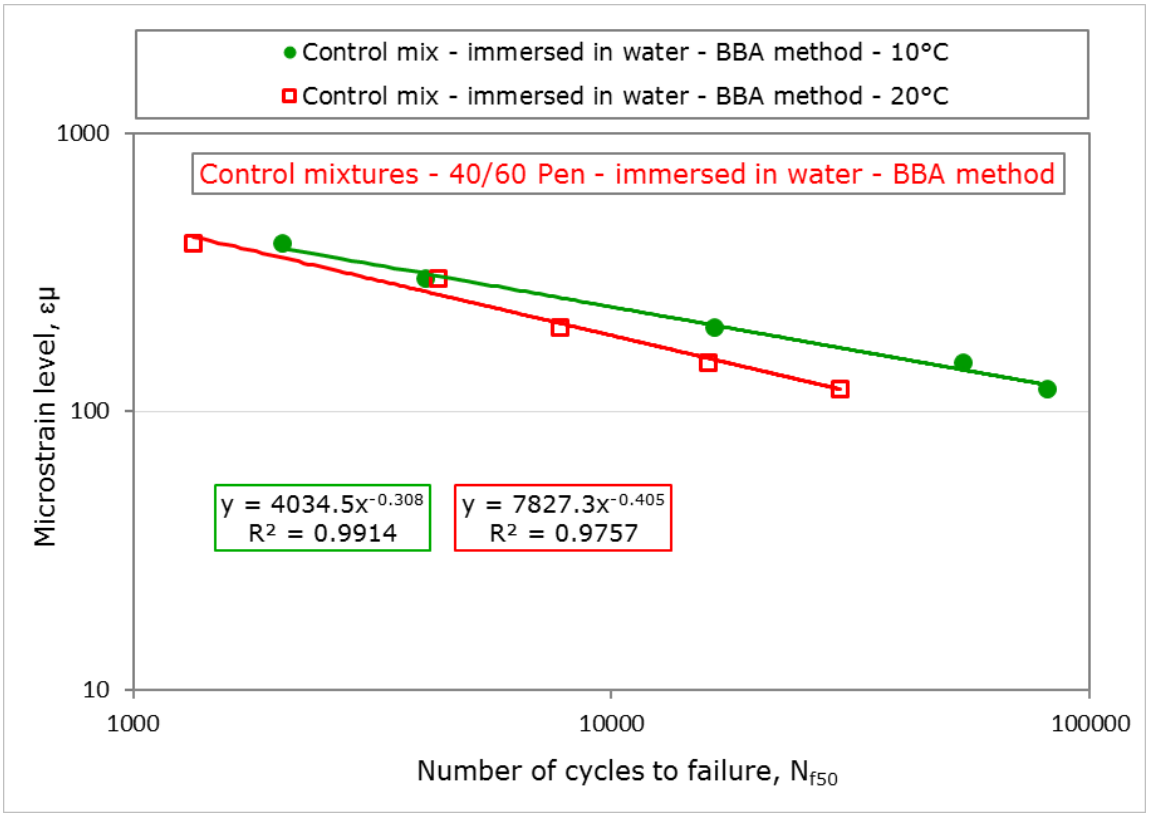



Figure 7.38: Effect of testing temperature on fatigue characterisation of control wet mixtures.

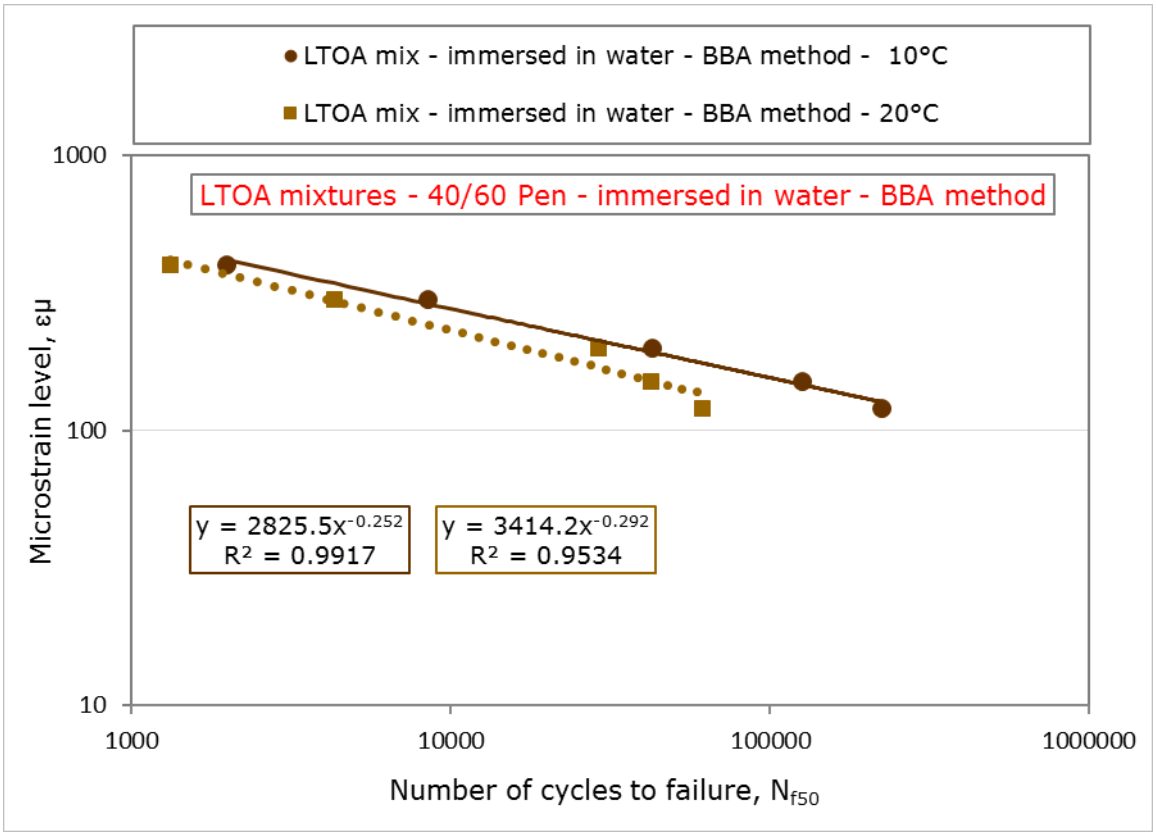



Figure 7.39: Effect of testing temperature on fatigue characterisation of LTOA wet mixtures.

### 7.6.3 Effect of binder grades

The effect of binder grades on fatigue characterisation of asphalt mixtures is shown in Figures 7.40 to 7.45. It was carried out at different testing circumstances and two air voids content using three different binder grades; 10/20 Pen, 40/60 Pen, and 100/150 Pen. It is obviously shown in these figures that mixtures of 10/20 have the best fatigue performance regardless of whether the mixture is control or aged and the condition is dry or wet. However, there is still some convergence between fatigue lines of these binder grades at high strain levels; 300με and 400με. Similarly, Artamendi and McHale, 2015 found that the fatigue resistance determined using the four-point bending under controlled strain method showed a longer fatigue life of the mixtures manufactured with the harder grade bitumen (15/25) compared to the softer ones (30/45 and 40/60). Furthermore, mixtures of 40/60 Pen have generally the second ranking at different circumstances while that of 100/150 shows a poor fatigue performance. This good fatigue performance of the stiff mixtures may be explained in terms of their behaviour to be more elastic (brittle) than the soft mixtures. This will increase the recovery of horizontal deformation during the 0.4-second rest period following the load application of ITFT and therefore this might generally increase their fatigue life.

It was also observed that the hard mixtures of 10/20 Pen had high resistance to permanent vertical deformations. Read, 1996, and Maggiore, 2014 stated that this deformation under loading strip might affect the loading transfer and hide the real fatigue performance and therefore it is considered one of the drawbacks of this fatigue test arrangement. A reduction in this deformation was observed by using a hard binder (10/20 Pen) or by reducing the testing temperature from 20 to 10˚C. This reduction might make certain that the failure in ITFT is tension not shear or compressive.

As determined by ANOVA test and shown in Table 7.4, no statistical significant difference was found between the slopes of all fatigue lines presented in Figures 7.40 to 7.45 for the effect of binder grades (each figure was taken individually).

Table 7.4: Results of test of significance (ANOVA test – single factor method) for the effect of binder grades on fatigue performance of asphalt mixtures.

| **Parameters** | **Condition** | **Figure Number** | **F** | **P-value** | **$F_{Critical}$** |
|---|---|---|---|---|---|
| Effect of binder grades | Control mix – dry | 7.40 | 1.364 | 0.272 | 2.621 |
| | Control mix - immersed BS EN | 7.41 | 1.080 | 0.396 | 2.621 |
| | Control mix – immersed BBA | 7.42 | 1.987 | 0.135 | 2.866 |
| | LTOA mix – dry | 7.43 | 1.459 | 0.240 | 2.621 |
| | LTOA mix – immersed BS EN | 7.44 | 2.082 | 0.103 | 2.621 |
| | LTOA mix – immersed BBA | 7.45 | 1.541 | 0.229 | 2.866 |

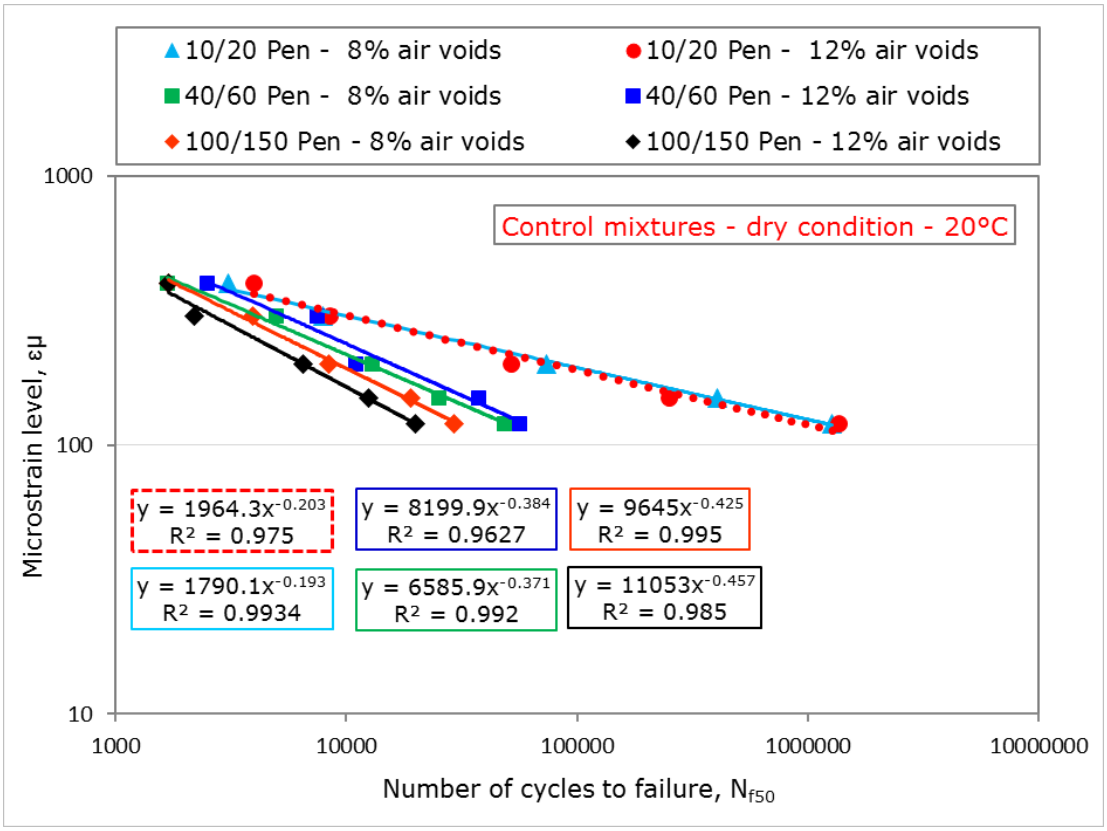



Figure 7.40: Effect of binder grades on fatigue characterisation in dry conditions.

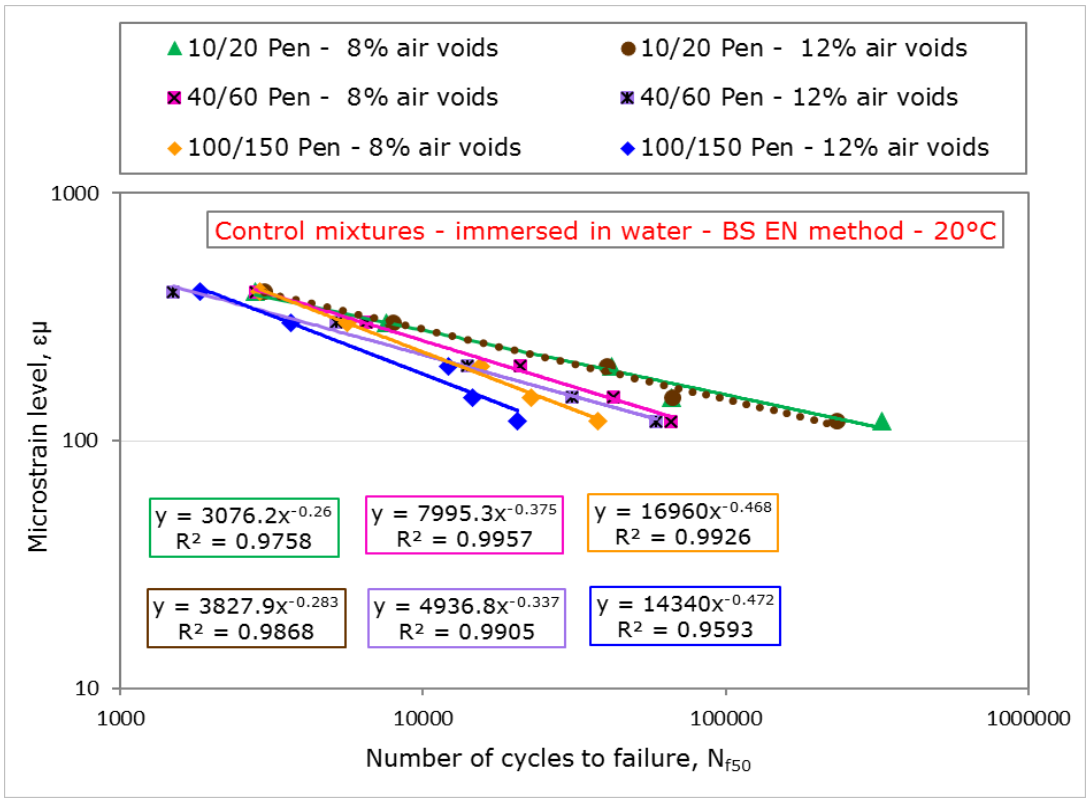



Figure 7.41: Effect of binder grades on fatigue characterisation in wet conditions.

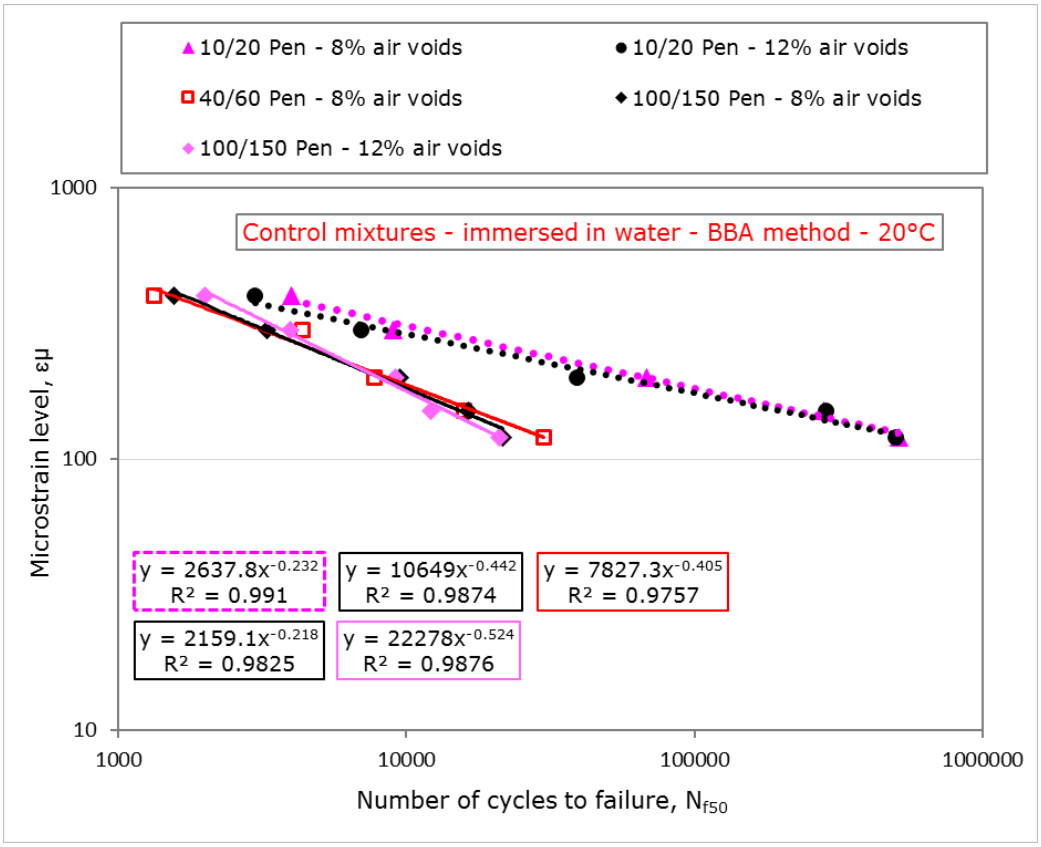



Figure 7.42: Effect of binder grades on fatigue characterisation in wet conditions.

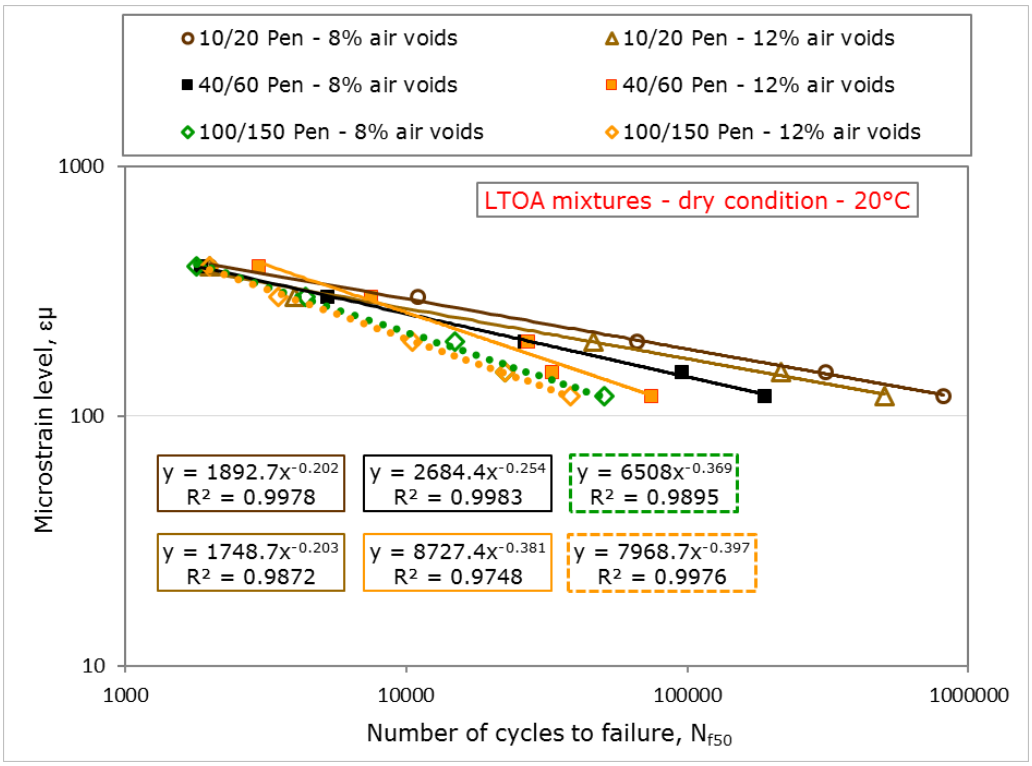



Figure 7.43: Effect of binder grades on fatigue characterisation in dry conditions.

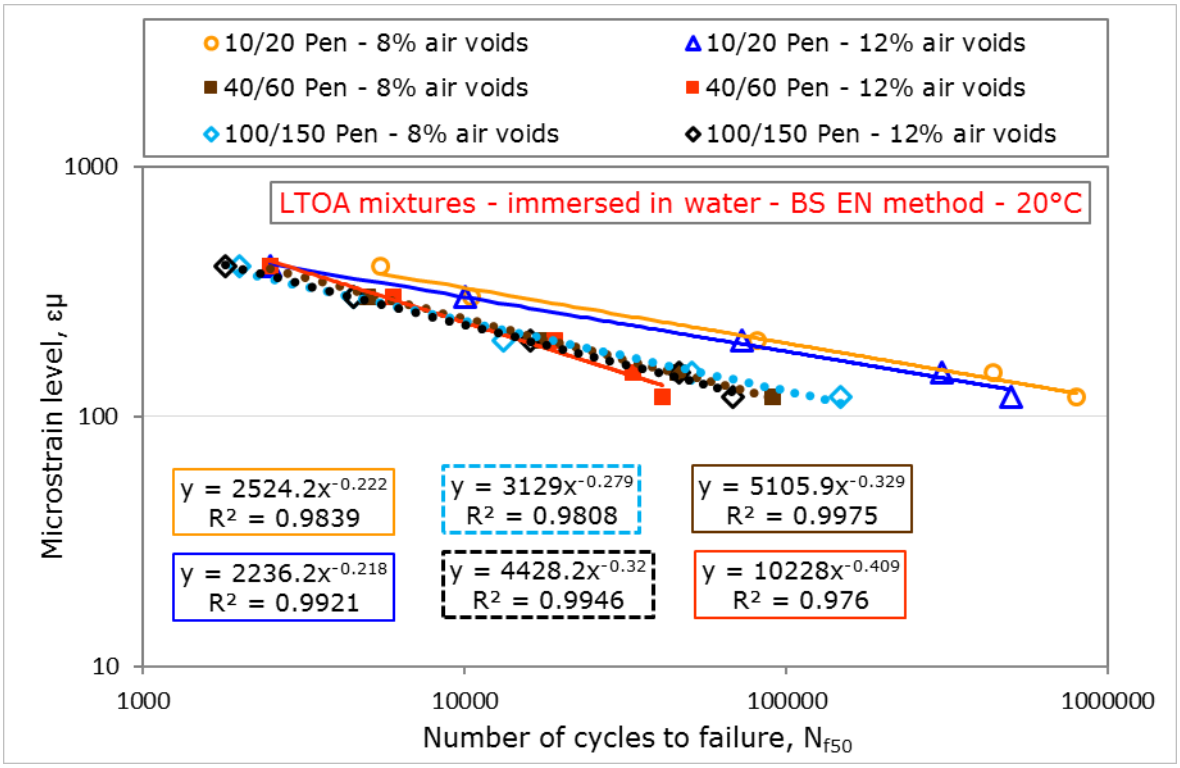



Figure 7.44: Effect of binder grades on fatigue characterisation of LTOA mixtures in wet conditions - BS EN method.

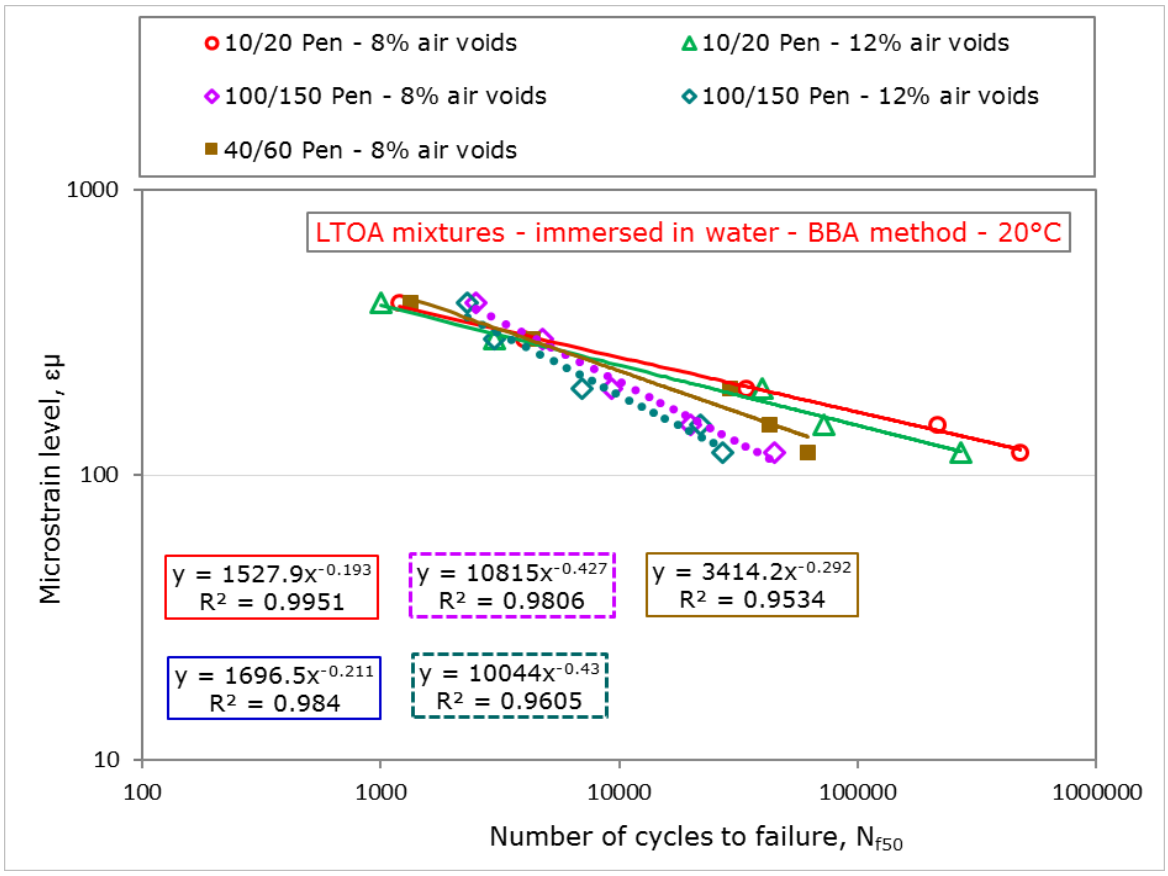



Figure 7.45: Effect of binder grades on fatigue characterisation in wet conditions - BBA method.

### 7.6.4 Effect of binder content

Two binder contents 5 and 6% were used with 40/60 Pen at two air voids content and different testing conditions. ITFT results are presented in Figures 7.46 to 7.49. Obviously, using 6% BC improves the fatigue cracking resistance of investigated mixtures. However, there is some overlapping particularly due to LTOA which caused some bleeding which may affect these results as shown in Figure 7.48.

As determined by the ANOVA test, no statistical significant difference was found between the slopes of all fatigue lines presented in Figures 7.46 to 7.49 (each figure was taken individually).

The reason of this non-significant results of these parameters (testing temperatures, binder grades and binder content) might attributed to the convergence between $N_{f50}$ at some strain levels (300 and 400 με). However, it seems not rational in some circumstances. This might suggest to test these results in a more advanced statistical analysis.

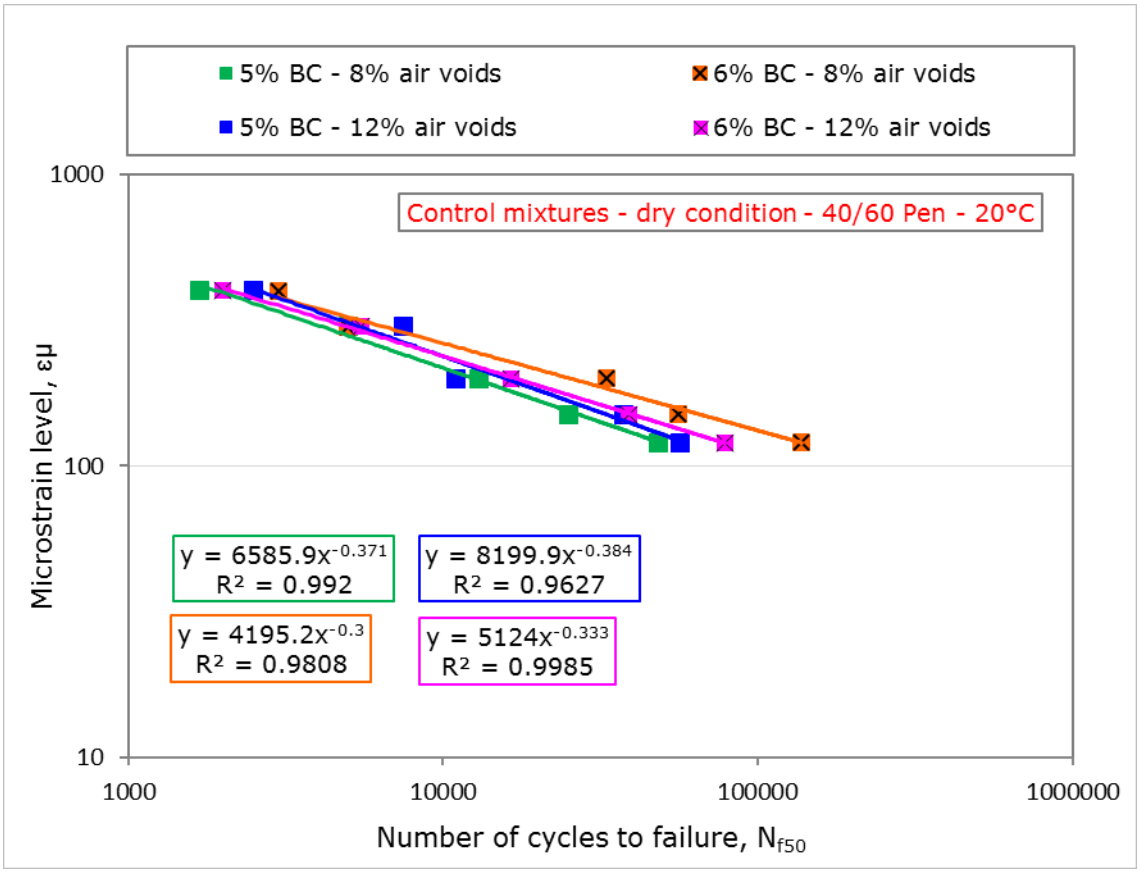



Figure 7.46: Effect of binder contents on fatigue characterisation in dry condition.

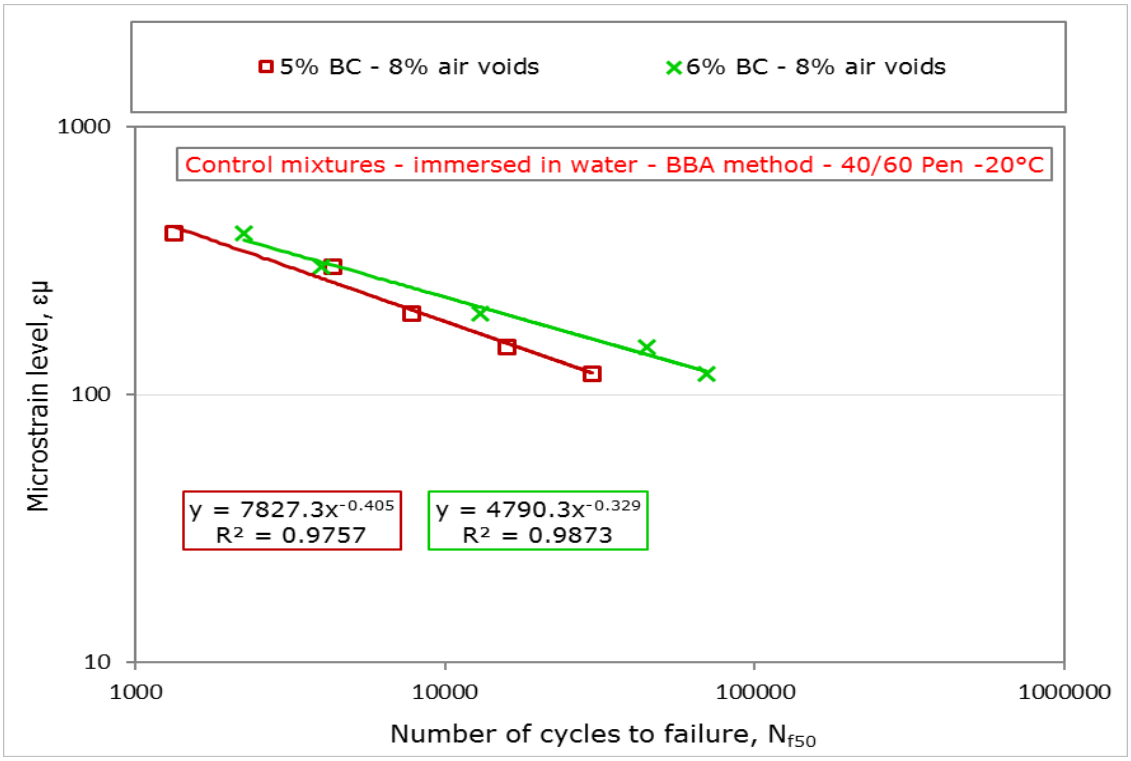



Figure 7.47: Effect of binder contents on fatigue characterisation in wet conditions.

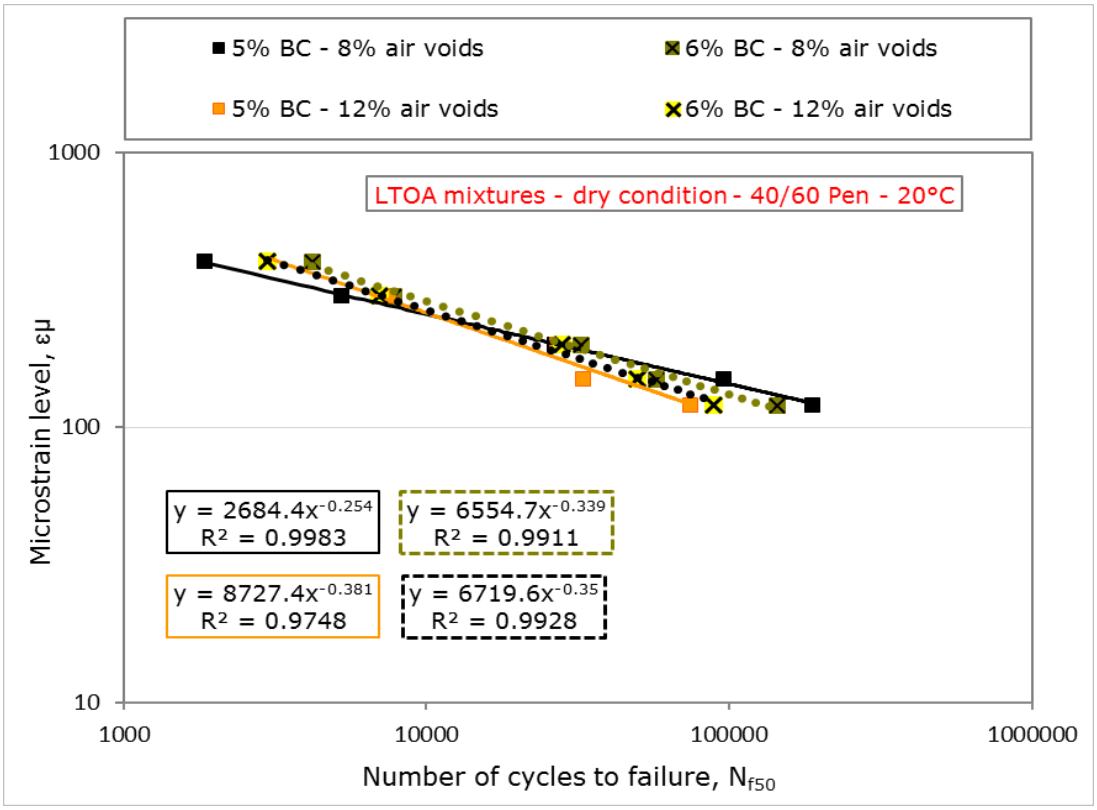



Figure 7.48: Effect of binder contents on fatigue characterisation in dry condition.

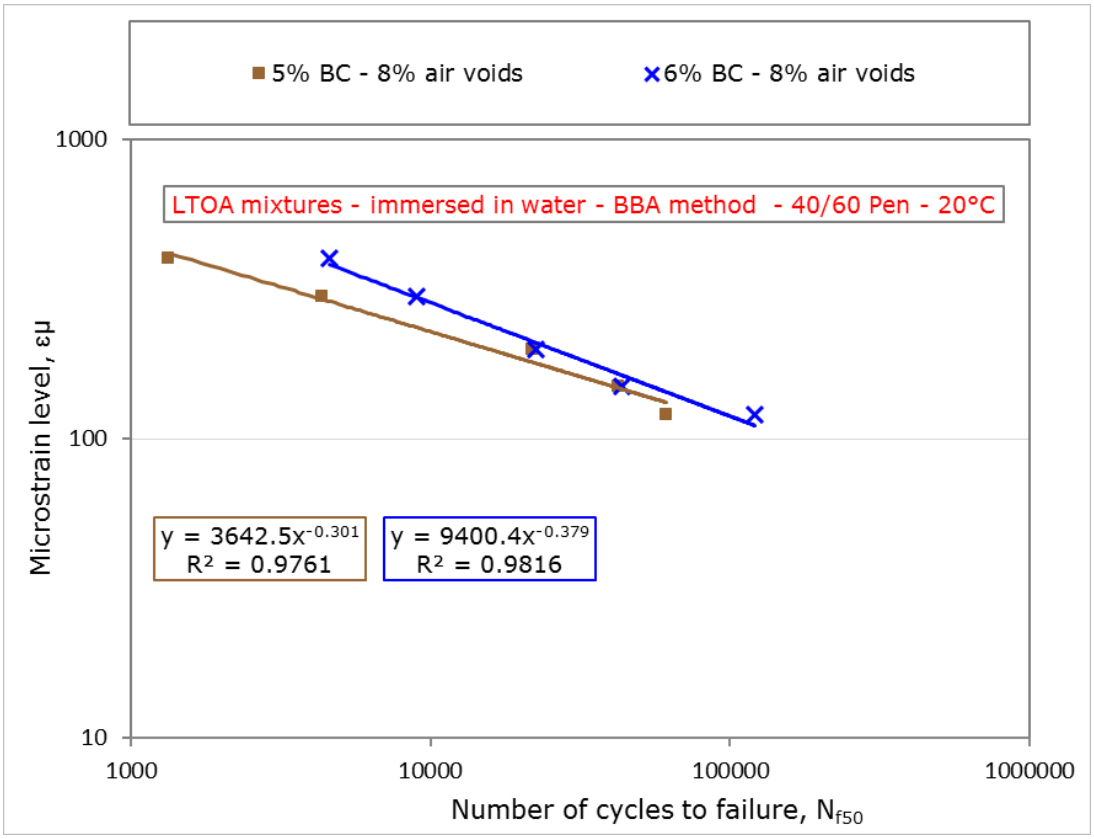



Figure 7.49: Effect of binder contents on fatigue characterisation in wet conditions.

## 7.7 Effect of individual and combined environmental factors effect

Studying the effect of environmental factors under load repetitions is important and necessary to evaluate the fatigue performance of asphalt mixtures. This combination provides more simulation of the real conditions that affect asphalt pavement structures. Virgili et al., 2008 indicated that conventional techniques commonly used for asphalt testing do not take into consideration the combined action of environmental factors; temperature and water, and repeated loading which may adversely affect mix design performance. They found that fatigue damage process of asphalt pavements can be considerably accelerated by environmental factors such as moisture and temperature.

In this study, ITFT was applied to asphalt mixtures exposed to different conditions as shown in Table 7.1 at different strain levels; 120, 150, 200, 300, and 400 με. In addition to use ITFT to evaluate some important factors; air voids content and testing temperatures which may affect the fatigue performance of asphalt mixtures, ITFT was generally carried out to study the effect of moisture damage, ageing, and the combined effect of moisture damage and ageing on this performance.

Two different methods were applied to consider the effect of moisture damage; BBA and BS EN as explained earlier in Chapter Three. The fatigue life of asphalt mixtures was determined in terms of 50% reduction of initial stiffness ($N_{f50}$). Figure 7.50 presents the fatigue characterisation at 10˚C of asphalt mixtures exposed to different conditions. The presented fatigue lines indicate a decrease in the number of cycles to failure of control mixtures due to the influence of moisture conditioning and an increase in the same number due to LTOA. Even when LTOA was combined with moisture the fatigue cracking resistance is still better than control mixture performance. However, the differences between these lines seem to disappear at high strain levels. Rahman, 2004 found that fatigue lives determined by ITFT under controlled stress method for highly compacted and short-term aged control mixture are slightly improved following moisture conditioning.

Moreover, Figures 7.51 and 7.52 show the same characterisation at 20˚C. It was observed from these Figures, a significant increase in the fatigue life of 14mm DBM mixtures at low to moderate strain levels; 120, 150 and 200 με when these mixtures stiffen due to LTOA. This increase occurred at all testing

conditions. The reasons may be attributed to firstly, the increased stiffness after applying LTOA, and secondly, to the decrease of permanent deformation. Both might refer to the shifting of materials towards the elastic behaviour and showing more recovery.

It was also noticed from these figures that fatigue life of control mixture decreases due to moisture effects by BBA method which is only applied at 8% air voids. On the other hand, applying the moisture damage to control mixture by BS EN method shows unexpected increase (at 8% air voids) in $N_{f50}$ as observed Figure 7.51. This increase is either due to the possible ageing during the moisture conditioning procedure or it may be considered as unexplained behavior of moisture damage and fatigue. In addition, at 12% air voids content, the effect of water (BS EN method) on fatigue damage of control mixture was fluctuated over the different applied microstrains.

The effect of water on aged mixtures at 20˚C is also shown in Figures 7.51 and 7.52. In general, there is some decrease in $N_{f50}$ of aged mixtures when these mixtures were exposed to moisture submersion by both methods as shown in Figure 7.51 (compared to dry aged). However, the combined influence of ageing and moisture at 8% air voids (BS EN method) shows more resistance to fatigue cracking than control mixtures. Whereas the same combination influence is relatively compatible with that of control mixture at 12% air voids as shown in Figure 7.52.

It was also shown in Figure 7.53 that both vertical and horizontal deformations of tested mixtures decrease as they stiffen due to LTOA or due to temperature conditioning at 10˚C. On the other hand, less stiffness mixtures; control mixtures tested at 20˚C deforms more. Therefore, it is important to make certain that failure is tensile and not shear or compressive failures by minimising the effect of permanent deformation. Decreasing the testing temperature may play an important role in minimising this deformation.

In general, there is an observable convergence between fatigue lines at 300 and 400 με, in particular at 20˚C. Figure 7.54 shows how the stiffness modulus deteriorates sharply at 300 με which may explain that overlapping of $N_{f50}$ at these levels.

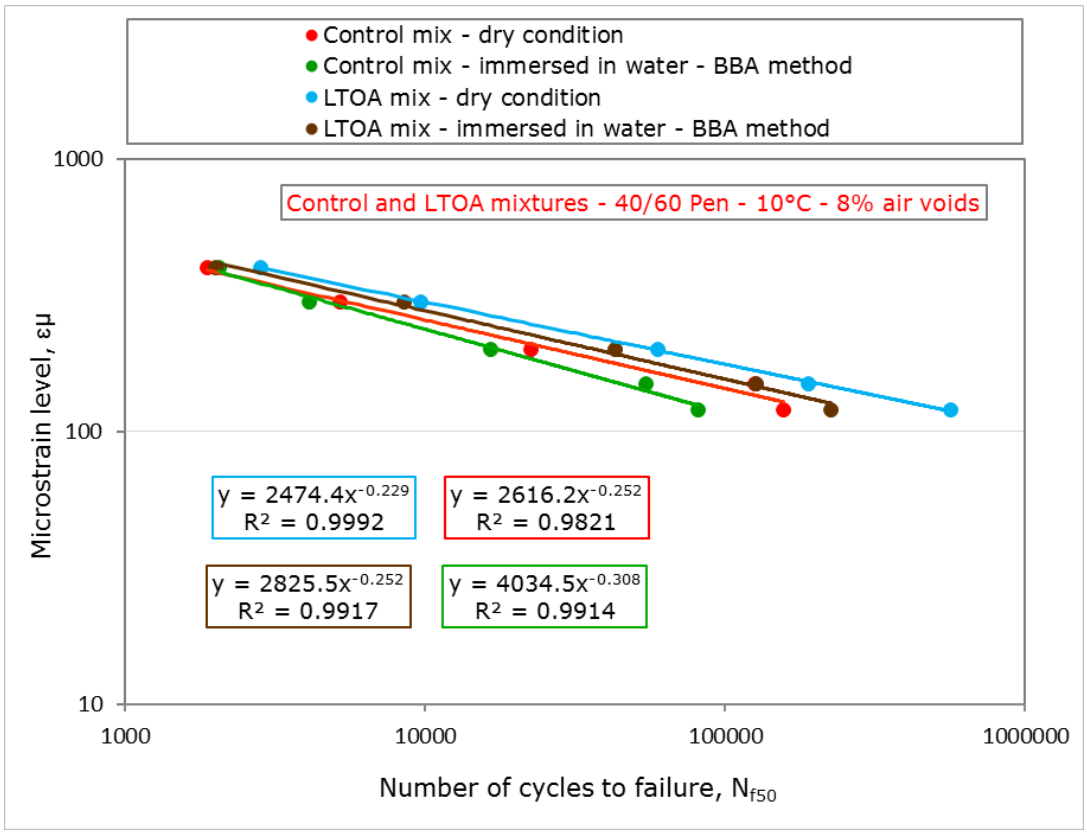



Figure 7.50: Effect of environmental factors on fatigue characterisation at 10˚C.

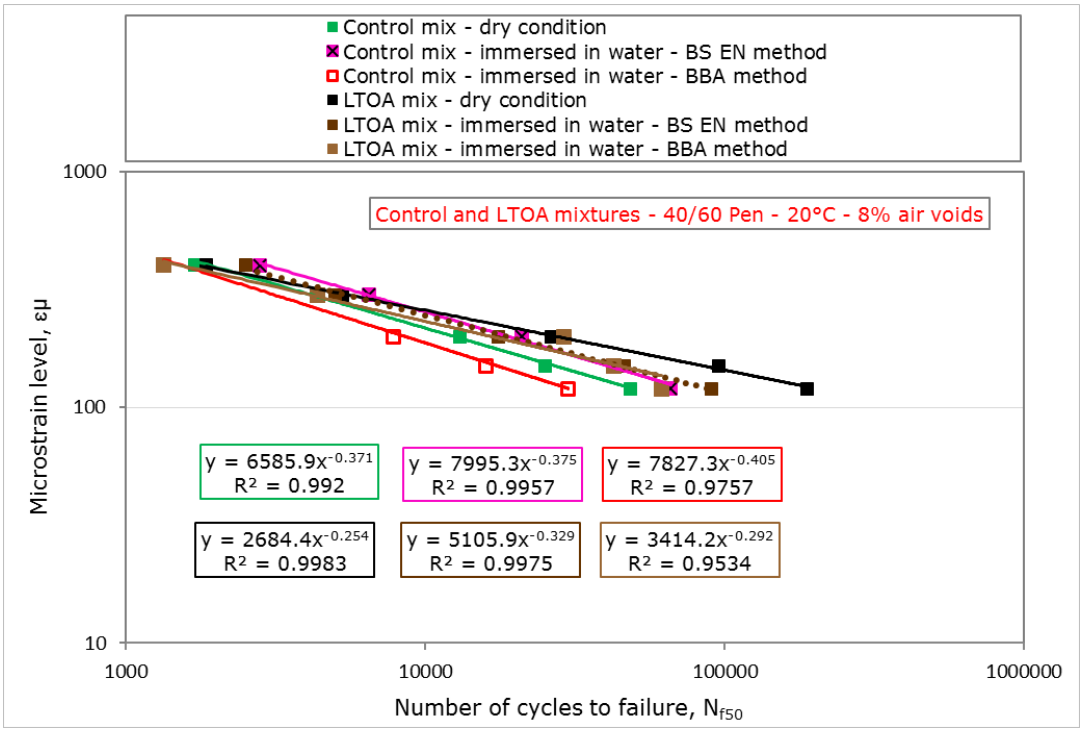



Figure 7.51: Effect of environmental factors on fatigue characterisation at 20˚C.

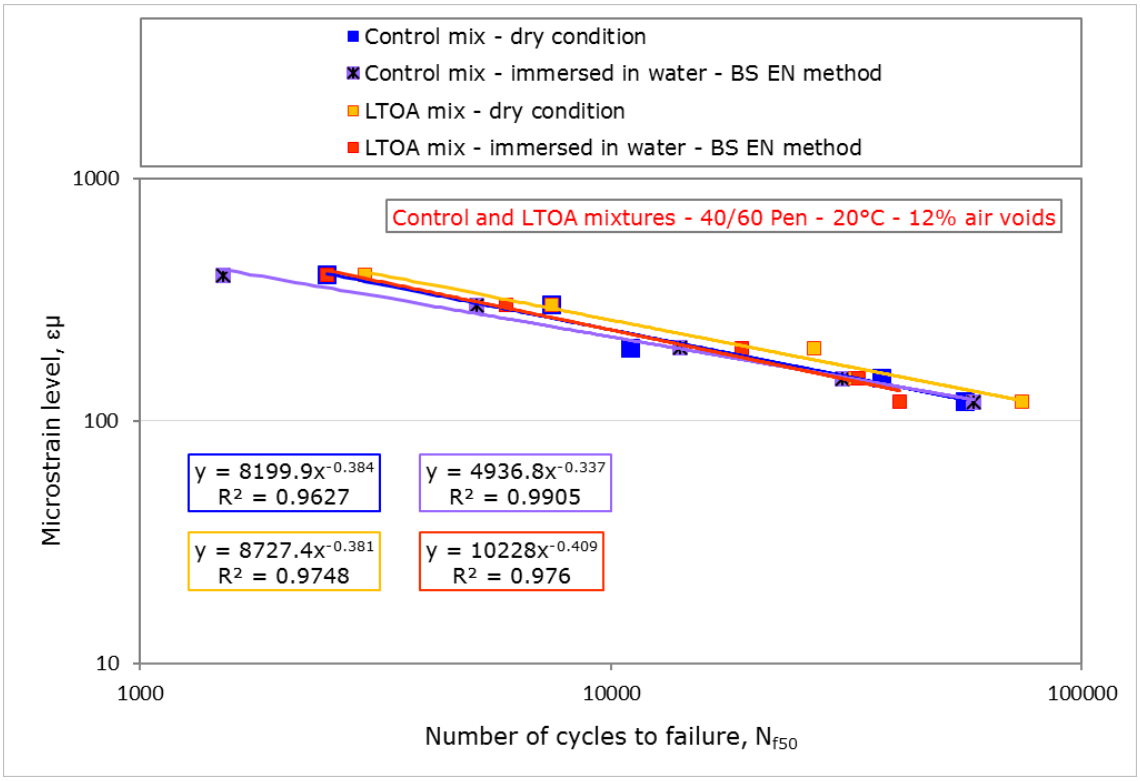



Figure 7. 52: Effect of environmental factors on fatigue characterisation at 20˚C.

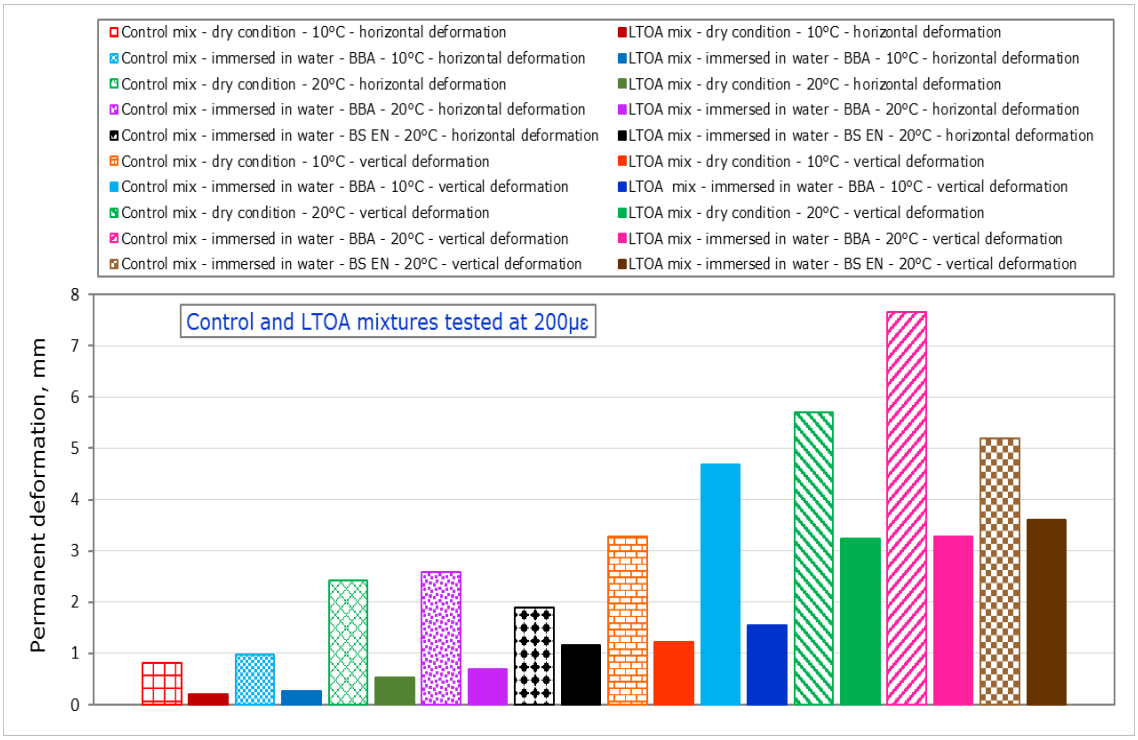



Figure 7. 53: Horizontal and vertical deformations of 40/60 Pen asphalt mixtures at different conditions.

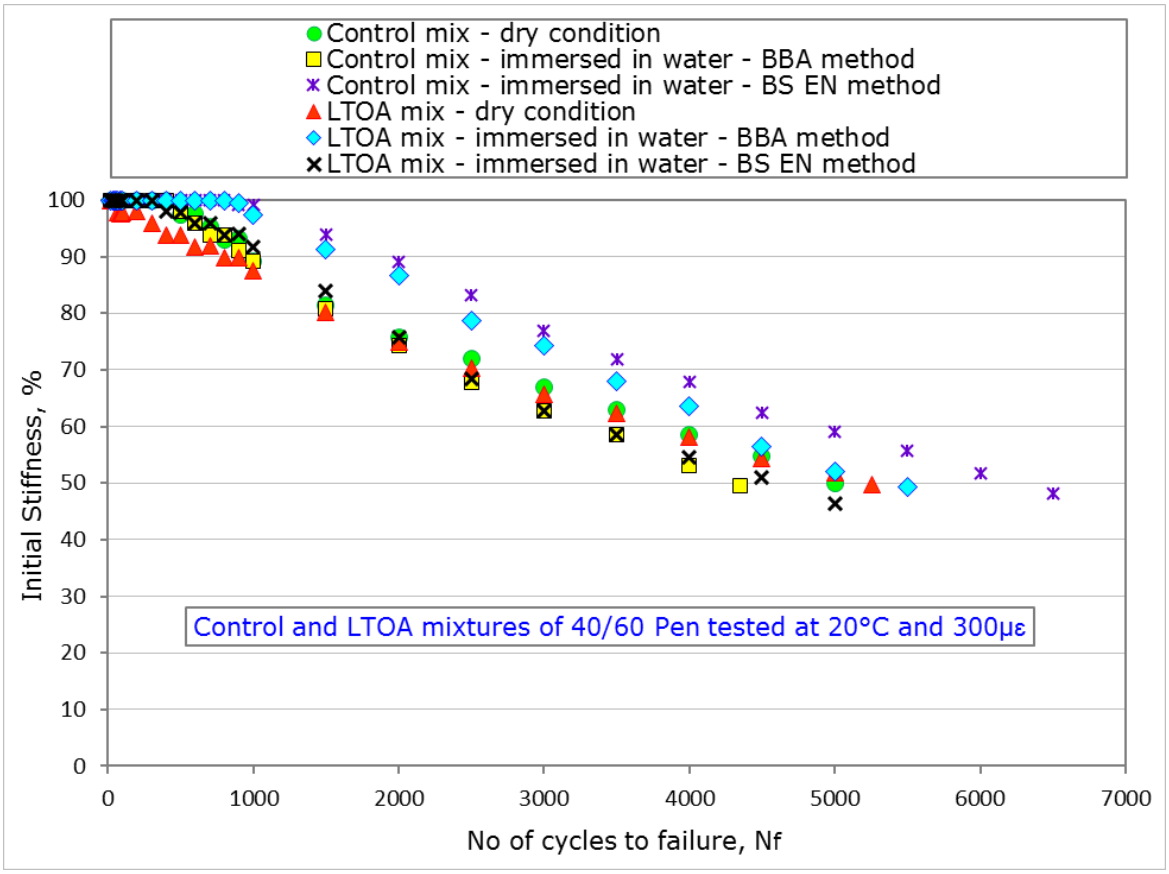



Figure 7.54: Effect of environmental factors on stiffness deterioration of 40/60 Pen asphalt mixtures.

In addition, stiffness deterioration is presented in Figure 7.55 to find the number of cycles to failure ($N_{f50}$) and compare it with that number resulting from the ASU method. This method was only performed for mixtures of 40/60 Pen at the specified testing conditions shown in Figure 7.56. The results of comparison are displayed in Table 7.5. Obviously, the ASU method showed the greater number of cycles to failure.

This table shows fatigue life (number of cycles to failure) of individual specimens. This is because the ASU method requires more time due to setting a different failure criteria (up to 90% reduction in the initial stress versus 50% in the traditional circumstance). Therefore a one-way analysis of variance (ANOVA) was used to test whether there are any statistically significant differences between the means of the traditional fatigue analysis ($N_{f50}$) and the Arizona State University method (ASU). Specifically, it tests the null hypothesis: $H_0$: $\mu_{Nf50}=\mu_{ASU}$ (No statistically significant difference between the mean of $N_{f50}$

and ASU methodologies) and an alternative hypothesis, $H_A$: $\mu_{Nf50} \neq \mu_{ASU}$ (There is a statistical significant difference between them).

Where:

$\mu$ = group mean.

If the resulting p-value is greater than 0.05 then there will be no statistically significant differences between the means of groups and vice versa.

The results of p-value, F and $F_{Critical}$ as determined by one-way ANOVA test conducted using Excel software 2016 are presented in Table 7.5. The results of p-values are less than 0.05 (approaching zero) and therefore there are statistically significant differences between the means of both groups ($H_A$ is accepted).

Table 7.5: Number of cycles to failure of 40/60 Pen mixtures exposed to different testing conditions using $N_{f50}$ and the ASU methods with ANOVA test results.

| **Mixture conditions** | **ASU** | **$N_{f50}$** | **P-value** | **ANOVA Test** | |
|---|---|---|---|---|---|
| | | | | **F** | **$F_{Critical}$** |
| Control mixture, dry condition | 24000 | 13000 | 1.21309E-22 | 142.553 | 3.914 |
| Control mixture, immersed in water – BS EN method | 23000 | 21000 | 7.09323E-24 | 150.696 | 3.910 |
| Control mixture, immersed in water – BBA method | 11000 | 8000 | 1.34056E-10 | 54.792 | 3.963 |
| LTOA mixture, dry condition | 56000 | 27000 | 6.11789E-89 | 776.715 | 3.870 |
| LTOA mixture, immersed in water – BS EN method | 26500 | 19000 | 1.61468E-30 | 206.870 | 3.900 |
| LTOA mixture, immersed in water – BBA method | 61500 | 29000 | 2.165E-108 | 975.256 | 3.865 |

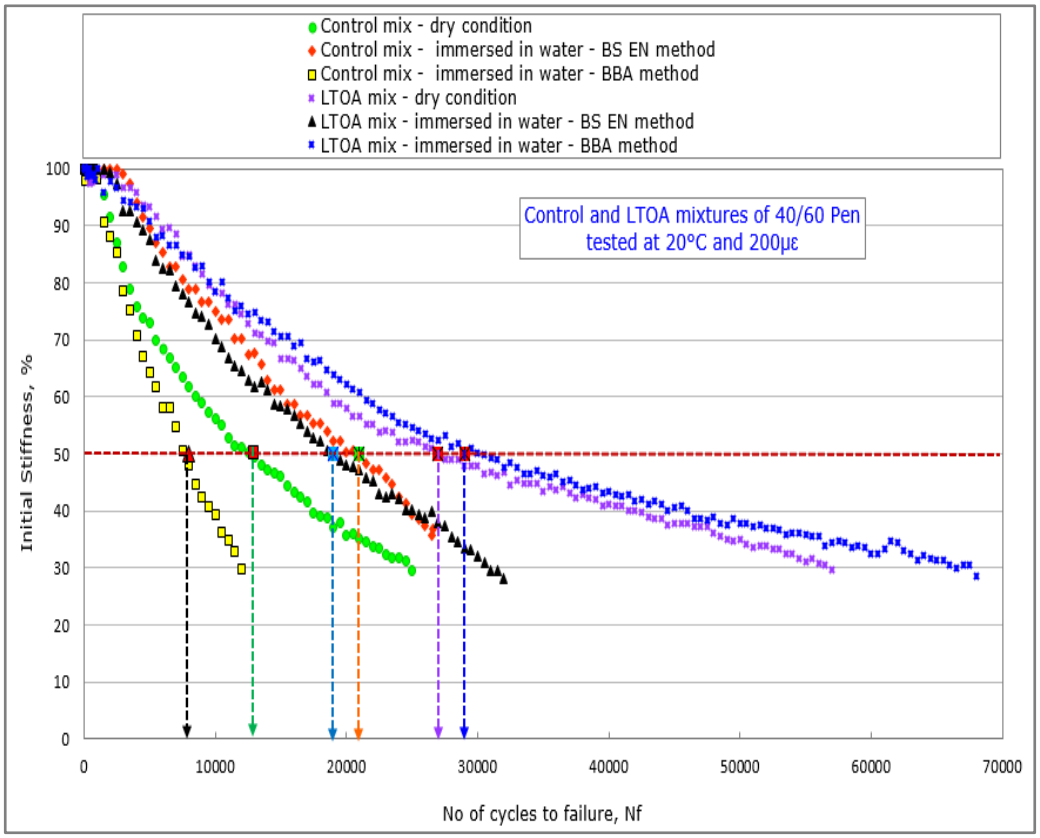



Figure 7. 55: Number of cycles to failure by traditional approach Nf50.

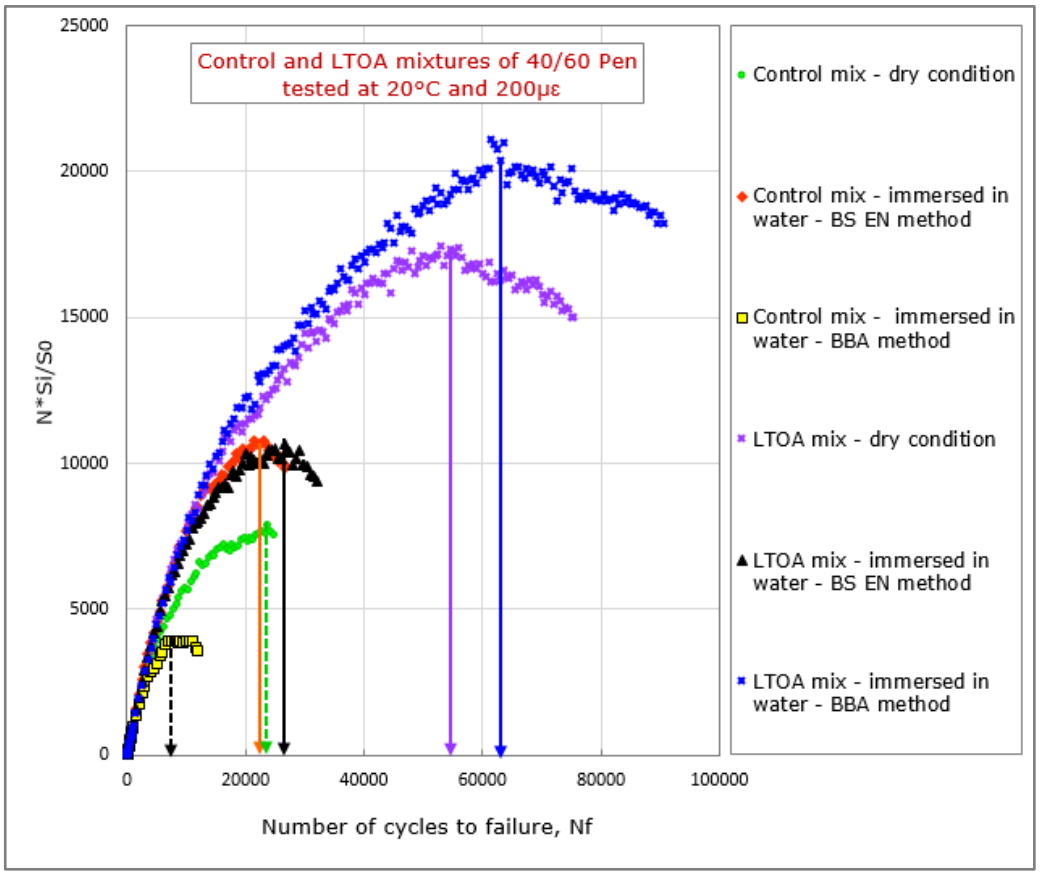



Figure 7. 56: Number of cycles to failure by the ASU method.

Similarly, Figures 7.57 to 7.60 display the effect of individual and combined environmental factors for mixtures of 10/20 Pen and 100/150 Pen binders respectively. It can be noticed that these factors have a clear influence on fatigue characterisation of 10/20 Pen mixtures. Obviously, all fatigue lines resulting from the applied conditions have relatively shifted down compared to that of control mixture. Generally, 10/20 Pen asphalt binder is considered less susceptible to ageing and can be categorized as a non-susceptible to moisture damage as shown in Chapter Four. However, the results indicated that DBM mixtures of 10/20 Pen were more susceptible to fatigue cracking when they subjected to ageing and moisture conditions. It may be attributed to the role of hard binder grade more than the effect of other testing parameters and conditions. This hard binder might show brittle behaviour after ageing when tested for fatigue using the ITFT.

Furthermore, the results are more complicated for asphalt mixtures of the soft binder 100/150. As shown in Figures 7.59 and 7.60 the number of cycles to failure has surprisingly increased due to LTOA. It is also unexpectedly increased more due to the exposure of control and aged mixtures to moisture submersion using BS EN method. It is observed by inspecting the generated fatigue lines that moisture susceptibility by BBA method was more aggressive than BS EN.

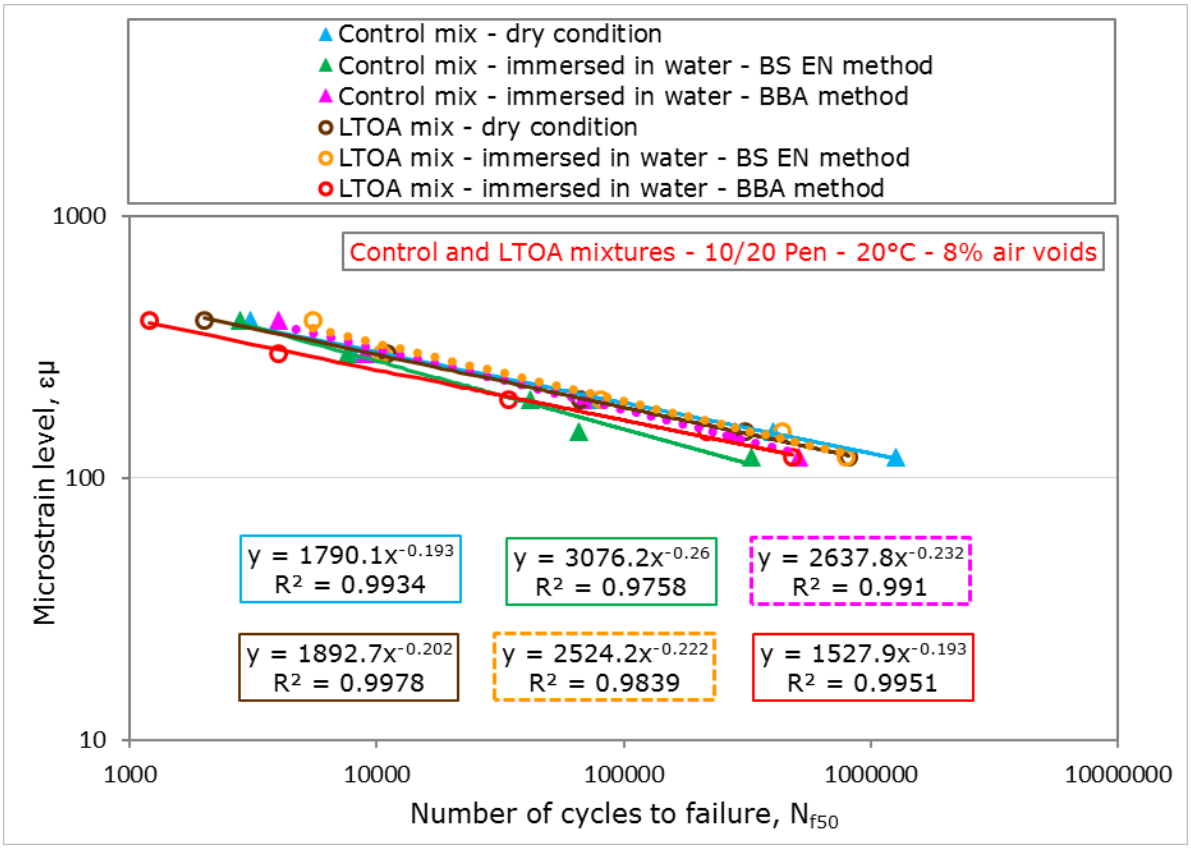



Figure 7. 57: Effect of environmental factors on fatigue characterisation at 20˚C.

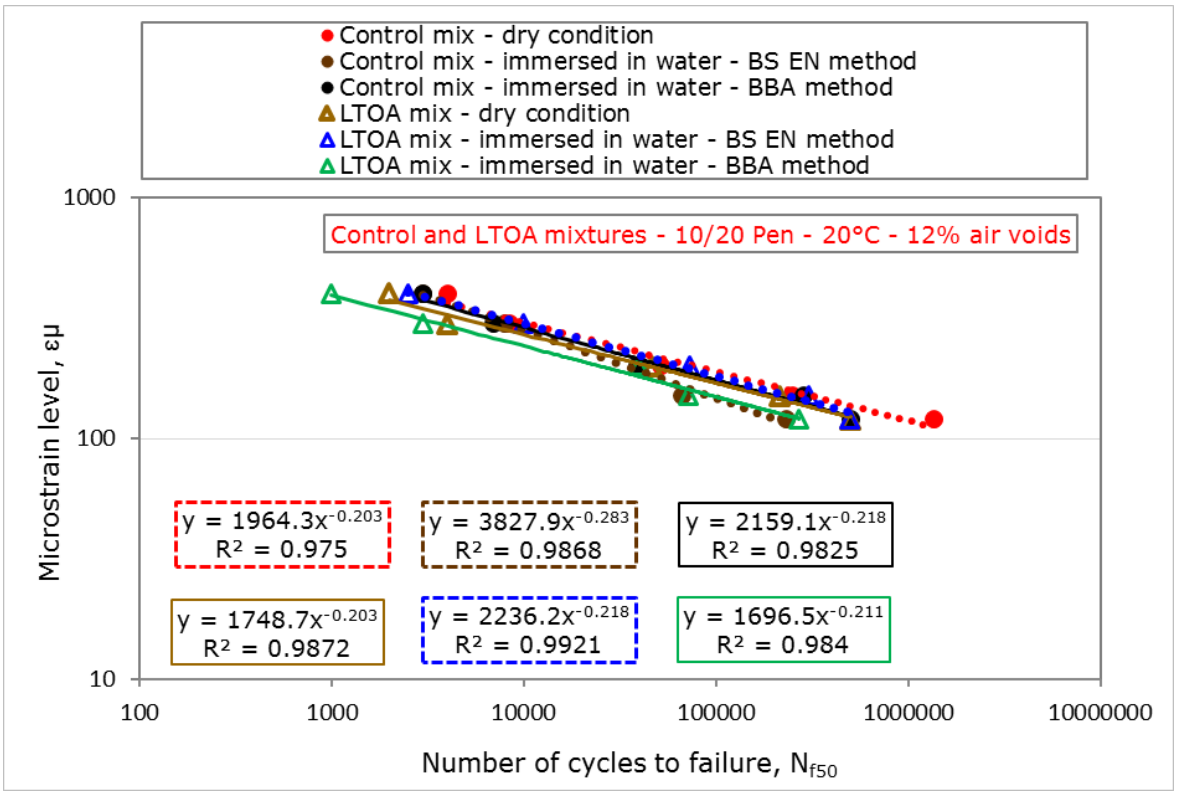



Figure 7. 58: Effect of environmental factors on fatigue characterisation at 20˚C.

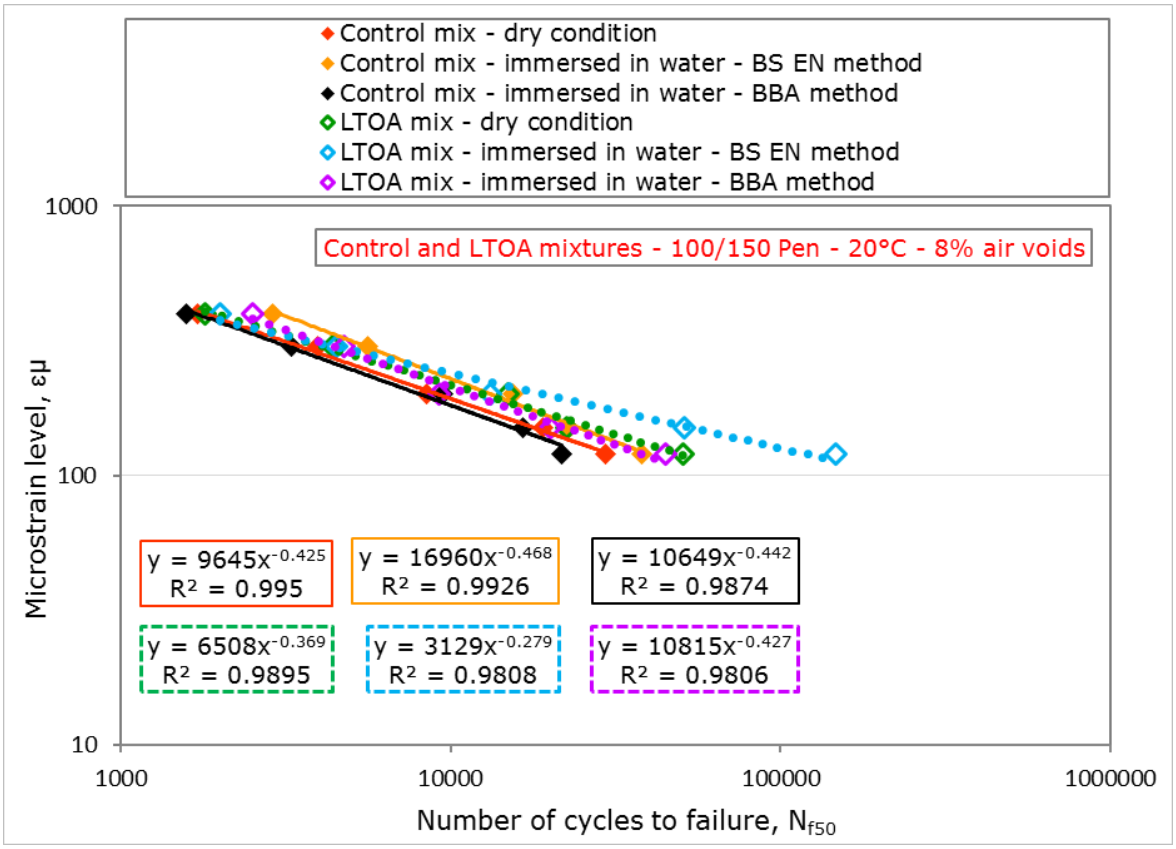



Figure 7.59: Effect of environmental factors on fatigue characterisation at 20˚C.

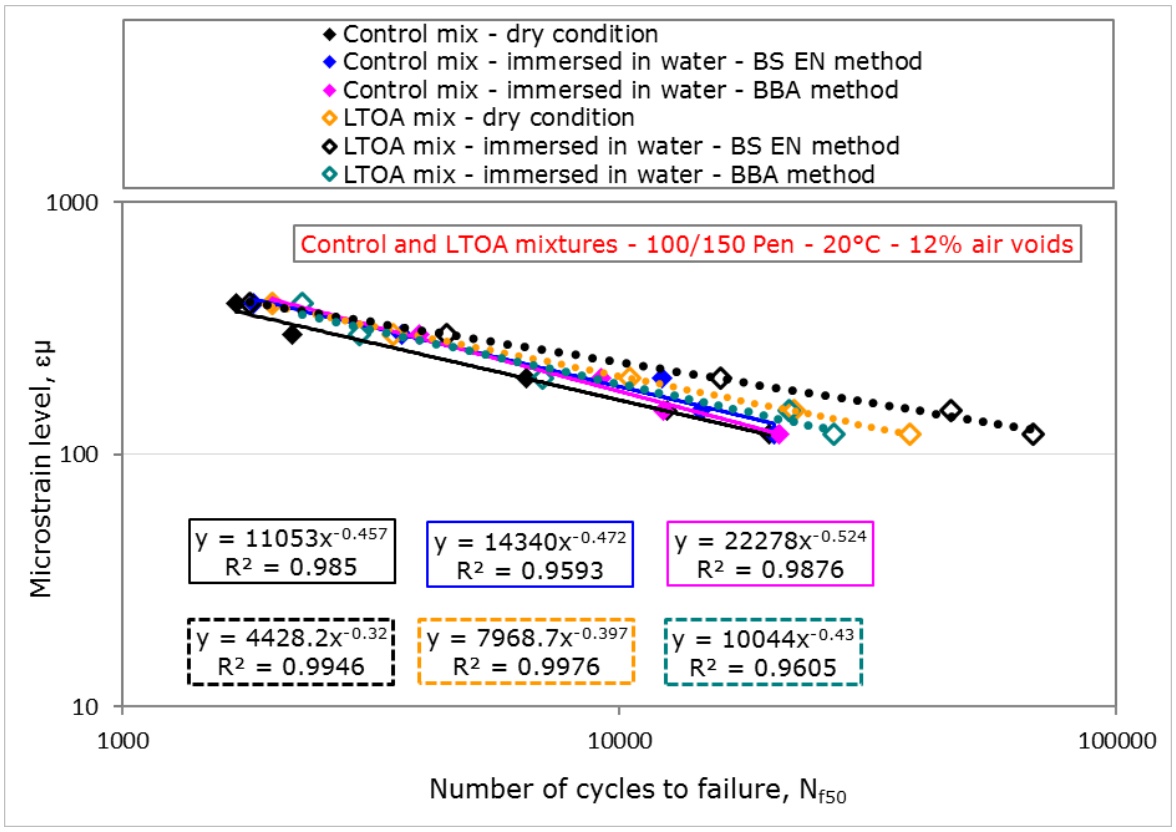



Figure 7.60: Effect of environmental factors on fatigue characterisation at 20˚C.

Finally, Figures 7.61 and 7.62 show the effect of individual and combined environmental factors on fatigue cracking resistance of 14mm DBM of 6% BC. Noticeably, fatigue lines of aged mixtures have shifted up with some convergence at the low applied strain level even when LTOA influence was combined with that of water. On the other hand, fatigue lines of control mixtures has shifted down due to the effect of moisture conditioning using BBA method.

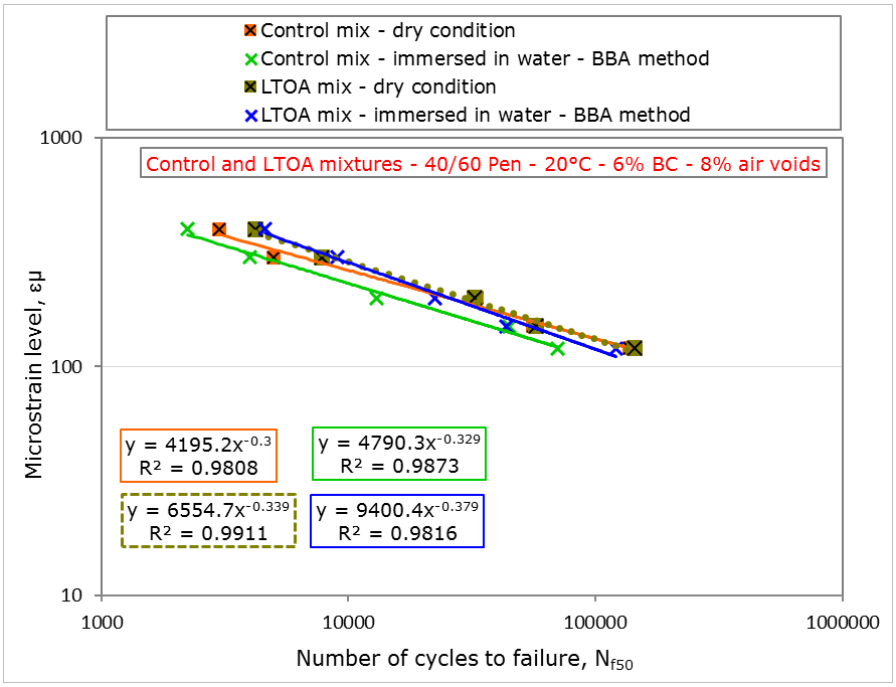



Figure 7.61: Effect of environmental factors on fatigue characterisation at 20˚C.

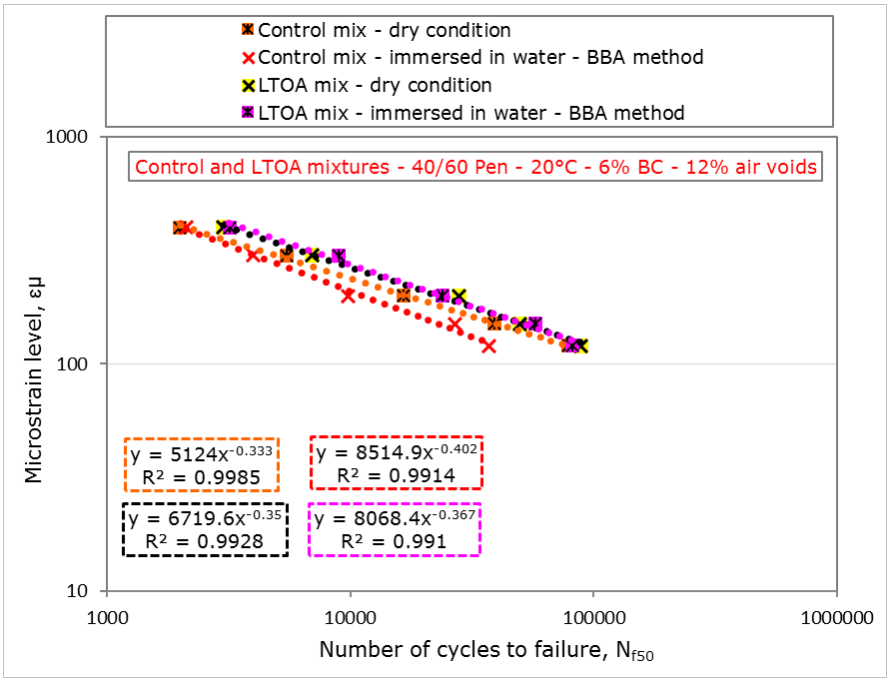



Figure 7.62: Effect of environmental factors on fatigue characterisation at 20˚C.

In summary, the fatigue relationships for different asphalt mixtures and the fatigue parameters of these mixtures are presented in Tables 7.6 and 7.7 respectively. A specific value of strain called ($\varepsilon 10^6$) can be determined using WÖHLER or S-N curve (fatigue line) when the strain amplitude is used for the presentation as shown in Figure 7.63. This value of strain is very commonly considered to characterise the fatigue resistance of bituminous mixtures (Corté and Goux, 1996, De La Roche, 1996, Di Benedetto et al., 1998, Airey, 2004). It refers to the value of the strain level that results in the fatigue life of 1,000,000 cycles.

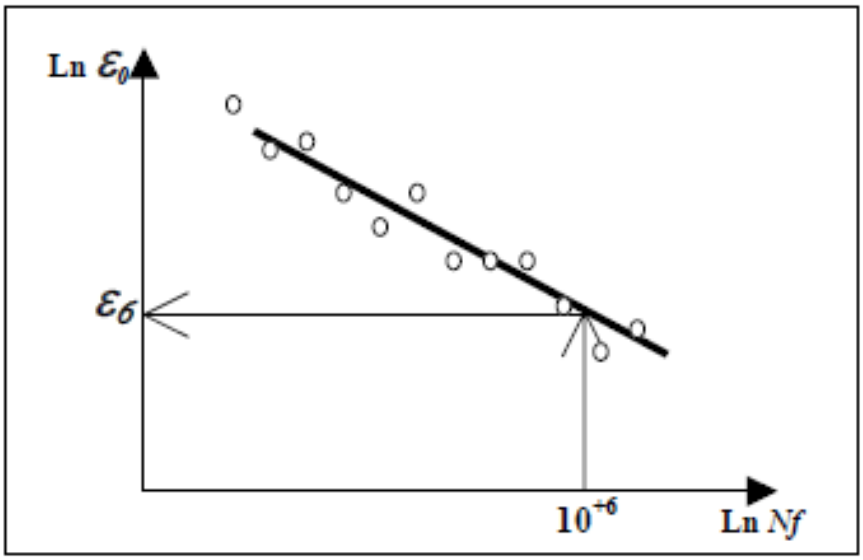



Figure 7.63: Determination of $\varepsilon 10^6$ from WÖHLER (or S-N) curve.

It can be observed from the ranking in Table 7.7 that nine of the first ten ranks are occupied by 10/20 Pen asphalt mixtures regardless of their testing conditions. The tenth one is occupied by 40/60 Pen asphalt mixtures (aged and tested at 10˚C). On the other hand, nine of the last ten ranks are occupied by 100/150 Pen asphalt mixtures of different conditions. The tenth one is occupied by 40/60 Pen asphalt mixtures (Control mixture immersed in water by applying BBA method and tested at 20˚C). That has confirmed the superior fatigue performance of 10/20 Pen mixtures exposed to different conditions, however, the dry control mixtures of different air voids occupy the first two ranks. It has also confirmed the poor fatigue performance of soft binder asphalt mixtures (100/150 Pen). These findings resulting from carrying out ITFT in constant strain method enhance the previous explanation of the superior fatigue performance

of the stiffer mixtures. However, it seems that 10/20 Pen asphalt mixture was more elastic (brittle) due to LTOA and that may explain the slight reduction in the fatigue life of these mixtures after ageing (brittle behaviour). That may show an indication that ageing could affect the fatigue performance when the penetration grade drops to 10 or less due to ageing. Otherwise it may improve fatigue cracking resistance as shown with ITFT results of 40/60 pen and 100/150 Pen mixtures.

In general, it can be concluded that the stiffer the asphalt mixture, the better the fatigue performance. However, this may not necessary hide the influence of some important factors affecting the fatigue damage such as binder content increase. Despite the increase from 5% to 6% binder, which has reduced the asphalt mixture stiffness, this has resulted in a relatively improved the fatigue cracking resistance as presented in Table 7.7.

Table 7.6: Fatigue relationships for asphalt mixtures exposed to different testing conditions.

| Condition of asphalt mixtures | Binder grade | T, °C | Air voids % | Fatigue functions | $R^2$ |
|---|---|---|---|---|---|
| Control - dry | 40/60 With 5% Binder content | 10 | 4 | $N_f=6.14*10^{12}\varepsilon^{-3.64}$ | 0.983 |
| | | | 8 | $N_f=1.44*10^{13}\varepsilon^{-3.80}$ | 0.967 |
| | | | 12 | $N_f=1.86*10^{13}\varepsilon^{-3.87}$ | 0.965 |
| Control- immersed in water – BBA method | | | 8 | $N_f=4.56*10^{11}\varepsilon^{-3.22}$ | 0.991 |
| LTOA - dry | | | 8 | $N_f=6.14*10^{14}\varepsilon^{-4.36}$ | 0.999 |
| LTOA - immersed in water – BBA method | | | 8 | $N_f=4.25*10^{13}\varepsilon^{-3.94}$ | 0.992 |
| Control - dry | 40/60 With 5% Binder content | 20 | 4 | $N_f=3.68*10^{10}\varepsilon^{-2.77}$ | 0.980 |
| | | | 8 | $N_f=1.78*10^{10}\varepsilon^{-2.67}$ | 0.992 |
| | | | 12 | $N_f=7.64*10^{9}\varepsilon^{-2.48}$ | 0.958 |
| Control- immersed in water – BBA method | | | 8 | $N_f=2.96*10^{9}\varepsilon^{-2.41}$ | 0.976 |
| Control- immersed in water – BS EN method | | | 8 | $N_f=2.46*10^{10}\varepsilon^{-2.66}$ | 0.996 |
| | | | 12 | $N_f=8.10*10^{10}\varepsilon^{-2.94}$ | 0.991 |
| LTOA - dry | | | 4 | $N_f=1.85*10^{13}\varepsilon^{-3.85}$ | 0.986 |
| | | | 8 | $N_f=3.58*10^{13}\varepsilon^{-3.97}$ | 0.990 |
| | | | 12 | $N_f=1.54*10^{10}\varepsilon^{-2.56}$ | 0.975 |
| LTOA - immersed in water – BBA method | | | 8 | $N_f=5.28*10^{11}\varepsilon^{-3.26}$ | 0.953 |
| LTOA - immersed in water – BS EN method | | | 8 | $N_f=1.73*10^{11}\varepsilon^{-3.03}$ | 0.998 |
| | | | 12 | $N_f=4.76*10^{9}\varepsilon^{-2.39}$ | 0.976 |
| Control - dry | 10/20 | 20 | 8 | $N_f=6*10^{16}\varepsilon^{-5.143}$ | 0.993 |
| | | | 12 | $N_f=8*10^{15}\varepsilon^{-4.799}$ | 0.975 |
| Control- immersed in water – BBA method | | | 8 | $N_f=4*10^{14}\varepsilon^{-4.266}$ | 0.991 |
| | | | 12 | $N_f=1*10^{15}\varepsilon^{-4.501}$ | 0.983 |
| Control- immersed in water – BS EN method | | | 8 | $N_f=2*10^{13}\varepsilon^{-3.747}$ | 0.976 |
| | | | 12 | $N_f=4*10^{12}\varepsilon^{-3.486}$ | 0.987 |
| LTOA - dry | | | 8 | $N_f=2*10^{16}\varepsilon^{-4.951}$ | 0.998 |
| | | | 12 | $N_f=7*10^{15}\varepsilon^{-4.874}$ | 0.987 |
| LTOA - immersed in water – BBA method | | | 8 | $N_f=3*10^{16}\varepsilon^{-5.162}$ | 0.995 |
| | | | 12 | $N_f=1*10^{15}\varepsilon^{-4.658}$ | 0.984 |
| LTOA - immersed in water – BS EN method | | | 8 | $N_f=1*10^{15}\varepsilon^{-4.432}$ | 0.984 |
| | | | 12 | $N_f=2*10^{15}\varepsilon^{-4.549}$ | 0.992 |
| Control - dry | 100/150 | 20 | 8 | $N_f=2*10^{9}\varepsilon^{-2.342}$ | 0.995 |
| | | | 12 | $N_f=6*10^{8}\varepsilon^{-2.156}$ | 0.985 |
| Control- immersed in water – BBA method | | | 8 | $N_f=1*10^{9}\varepsilon^{-2.235}$ | 0.987 |
| | | | 12 | $N_f=2*10^{8}\varepsilon^{-1.884}$ | 0.988 |
| Control- immersed in water – BS EN method | | | 8 | $N_f=1*10^{9}\varepsilon^{-2.122}$ | 0.993 |
| | | | 12 | $N_f=4*10^{8}\varepsilon^{-2.034}$ | 0.959 |
| LTOA - dry | | | 8 | $N_f=2*10^{10}\varepsilon^{-2.68}$ | 0.990 |
| | | | 12 | $N_f=6*10^{9}\varepsilon^{-2.51}$ | 0.998 |
| LTOA - immersed in water – BBA method | | | 8 | $N_f=2*10^{9}\varepsilon^{-2.297}$ | 0.981 |
| | | | 12 | $N_f=1*10^{9}\varepsilon^{-2.232}$ | 0.961 |
| LTOA - immersed in water – BS EN method | | | 8 | $N_f=6*10^{9}\varepsilon^{-2.51}$ | 0.998 |
| | | | 12 | $N_f=2*10^{11}\varepsilon^{-3.108}$ | 0.995 |
| Control - dry | 40/60 With 6% Binder content | 20 | 8 | $N_f=8*10^{11}\varepsilon^{-3.267}$ | 0.981 |
| | | | 12 | $N_f=1*10^{11}\varepsilon^{-2.997}$ | 0.999 |
| Control- immersed in water – BBA method | | | 8 | $N_f=1*10^{11}\varepsilon^{-3.001}$ | 0.987 |
| | | | 12 | $N_f=5*10^{9}\varepsilon^{-2.464}$ | 0.991 |
| LTOA - dry | | | 8 | $N_f=2*10^{11}\varepsilon^{-2.921}$ | 0.991 |
| | | | 12 | $N_f=8*10^{10}\varepsilon^{-2.834}$ | 0.993 |
| LTOA - immersed in water – BBA method | | | 8 | $N_f=2*10^{10}\varepsilon^{-2.587}$ | 0.982 |
| | | | 12 | $N_f=4*10^{10}\varepsilon^{-2.699}$ | 0.991 |

Table 7.7: Fatigue parameters of asphalt mixture exposed to different testing conditions.

| Condition of asphalt mixtures | Binder grade | T, °C | Air voids % | $N_f^{100\ \mu\varepsilon}$ | $\varepsilon 10^6$ (με) | Ranking in terms of $\varepsilon 10^6$ |
|---|---|---|---|---|---|---|
| Control - dry | 40/60 with 5% Binder content | 10 | 4 | 322232 | 75 | 19 |
| | | | 8 | 361712 | 78.8 | 16 |
| | | | 12 | 338464 | 79.1 | 15 |
| Control- immersed in water – BBA | | | 8 | 165564 | 57 | 24 |
| LTOA - dry | | | 8 | 1169953 | 105 | 10 |
| LTOA - immersed in water – BBA | | | 8 | 560259 | 87 | 12 |
| Control - dry | 40/60 with 5% Binder content | 20 | 4 | 106132 | 46 | 33 |
| | | | 8 | 81362 | 39.3 | 38 |
| | | | 12 | 83771 | 39.4 | 37 |
| Control- immersed in water – BBA | | | 8 | 44801 | 29.1 | 43 |
| Control- immersed in water – BS EN method | | | 8 | 117743 | 45 | 34 |
| | | | 12 | 106779 | 47 | 32 |
| LTOA - dry | | | 4 | 369124 | 78 | 17 |
| | | | 8 | 411039 | 81 | 14 |
| | | | 12 | 116821 | 45 | 35 |
| LTOA - immersed in water – BBA | | | 8 | 159453 | 60 | 23 |
| LTOA - immersed in water – BS EN method | | | 8 | 150677 | 54 | 25 |
| | | | 12 | 78996 | 36 | 39 |
| Control - dry | 10/20 | 20 | 8 | 3105641 | 124 | 1 |
| | | | 12 | 2018785 | 119 | 2 |
| Control- immersed in water – BBA method | | | 8 | 1175060 | 107 | 6 |
| | | | 12 | 995405 | 106 | 9 |
| Control- immersed in water – BS EN method | | | 8 | 641254 | 85 | 13 |
| | | | 12 | 426638 | 77 | 18 |
| LTOA - dry | | | 8 | 2506282 | 116 | 4 |
| | | | 12 | 1250541 | 106 | 8 |
| LTOA - immersed in water – BBA method | | | 8 | 1422726 | 106 | 7 |
| | | | 12 | 483059 | 92 | 11 |
| LTOA - immersed in water – BS EN method | | | 8 | 1367729 | 118 | 3 |
| | | | 12 | 1595989 | 110 | 5 |
| Control - dry | 100/150 | 20 | 8 | 41403 | 19 | 49 |
| | | | 12 | 29252 | 20 | 48 |
| Control- immersed in water – BBA method | | | 8 | 33884 | 24 | 46 |
| | | | 12 | 34122 | 16 | 50 |
| Control- immersed in water – BS EN method | | | 8 | 57016 | 26 | 44 |
| | | | 12 | 34203 | 21 | 47 |
| LTOA - dry | | | 8 | 87303 | 40 | 36 |
| | | | 12 | 57300 | 33 | 41 |
| LTOA - immersed in water – BBA method | | | 8 | 50937 | 30 | 42 |
| | | | 12 | 34356 | 26 | 45 |
| LTOA - immersed in water – BS EN method | | | 8 | 57300 | 66 | 21 |
| | | | 12 | 121627 | 53 | 27 |
| Control - dry | 40/60 with 6% Binder content | 20 | 8 | 233932 | 66 | 20 |
| | | | 12 | 101391 | 51 | 29 |
| Control- immersed in water – BBA method | | | 8 | 99541 | 51 | 30 |
| | | | 12 | 59016 | 33 | 40 |
| LTOA - dry | | | 8 | 287760 | 61 | 22 |
| | | | 12 | 171826 | 53 | 26 |
| LTOA - immersed in water – BBA method | | | 8 | 133977 | 50 | 31 |
| | | | 12 | 159978 | 51 | 28 |

## 7.8 Statistical Model

A statistical model was generated to predict the number of cycles to failure ($N_f$) using the modified ITFT results of testing conditions presented in Table 7.6. To generate this model the following steps were followed:

First, measure the correlation of testing parameters shown in Table 7.6 with the number of cycles to failure. These parameters include the applied strain which is the main dominator of fatigue models as indicated earlier in Chapter Two. In addition, the stiffness modulus was used as a representative value of testing conditions such as moisture conditioning and ageing. It also can reflect the effect of different binder grades and contents used in this study. The stiffness modulus was measured during the modified ITFT at the cycle $50^{th}$. The effect of air voids content and testing temperatures were also suggested to be included within the parameters of this model for their relationship with ageing and moisture damage. However, the effect of testing temperature might be included in the effect of stiffness modulus (Monismith et al., 1985).

Pearson coefficient and Spearman coefficient were used to measure this correlation using Minitab software version 17.2.1. In statistics, the Pearson correlation coefficient is a measure of the linear correlation between two variables X and Y. It is widely used in sciences. Spearman rank-order correlation (also called Spearman's rho) was also used because it evaluates the monotonic functions between two continuous or ordinal variables. In a monotonic relationship, the variables tend to change together, but not necessarily at a constant rate. Each correlation coefficient has a value between +1 and -1, where +1 is total positive correlation, 0 is no correlation, and -1 is total negative correlation. A value of +1 indicates that a linear/monotonic equation describes the relationship between X and Y perfectly, with all data points lying on a line/ monotone functions for which Y increases as X increases. A value of -1 suggests that all data points lie on a line/ monotone functions for which Y decreases as X increases. A value of 0 recommends that there is no linear/ monotone functions correlation between the variables (Lehman et al., 2013). Figure 7.64 shows examples of scatter diagrams with different values of correlation coefficient.

The row data of each parameter was plotted versus $N_f$ as shown in Figures 7.65 to 7.68. Spearman and Pearson coefficients were calculated using Minitab software version 17.2.1 and the results are presented in Table 7.8. The values of both coefficients are approximately similar. When the data are roughly elliptically distributed as shown in Figure 7.67 and 7.68 or there are no prominent outliers, the Spearman correlation and Pearson correlation give similar values. Based on this analysis, it was decided to neglect the effect of air voids content and testing temperatures because the correlation coefficients are approaching zero.

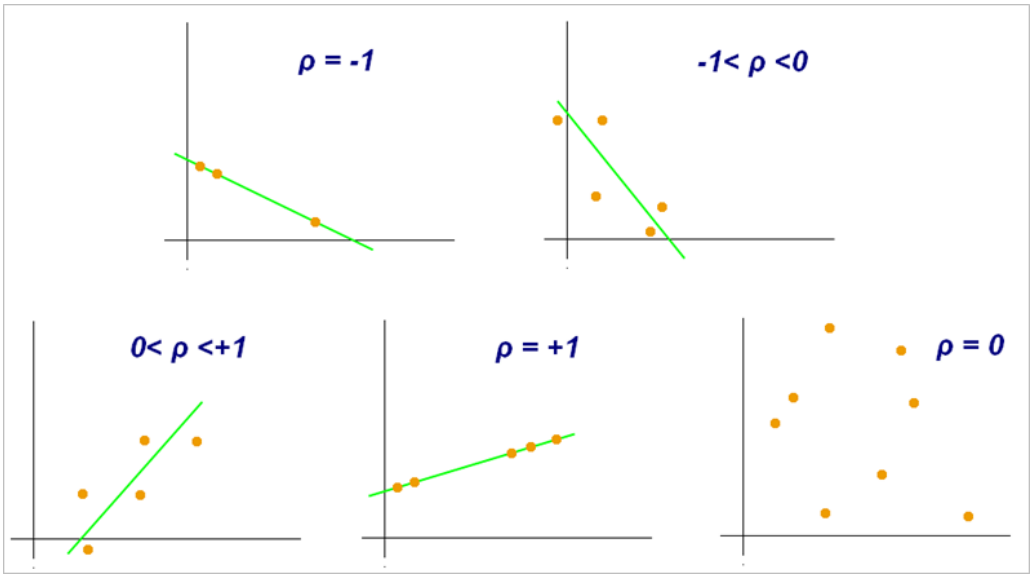



Figure 7.64: Examples of scatter diagrams with different values of correlation coefficient (ρ).

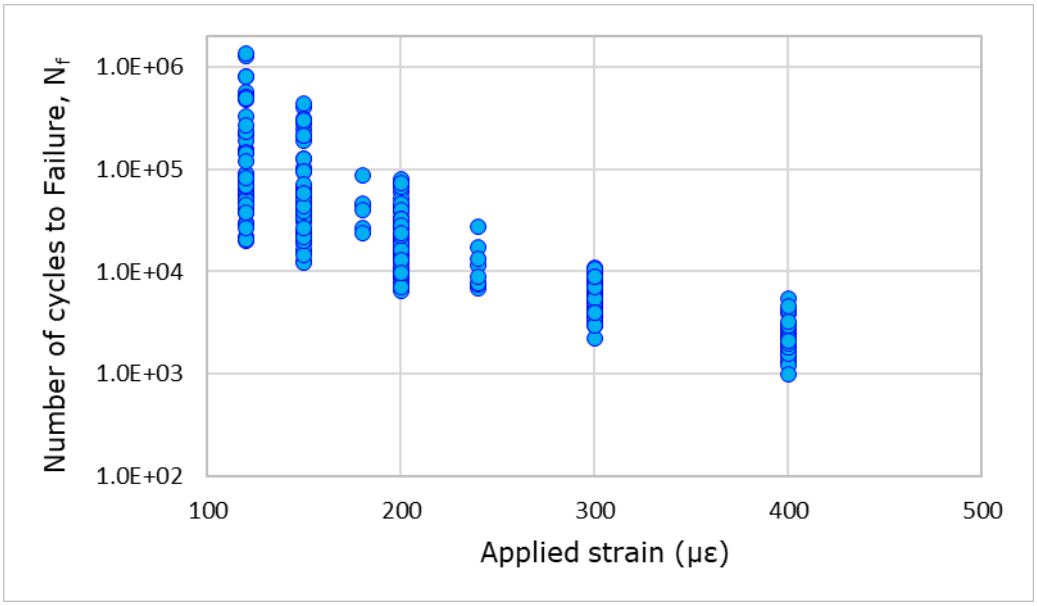



Figure 7.65: Number of cycles to failure ($N_f$) versus applied strain.

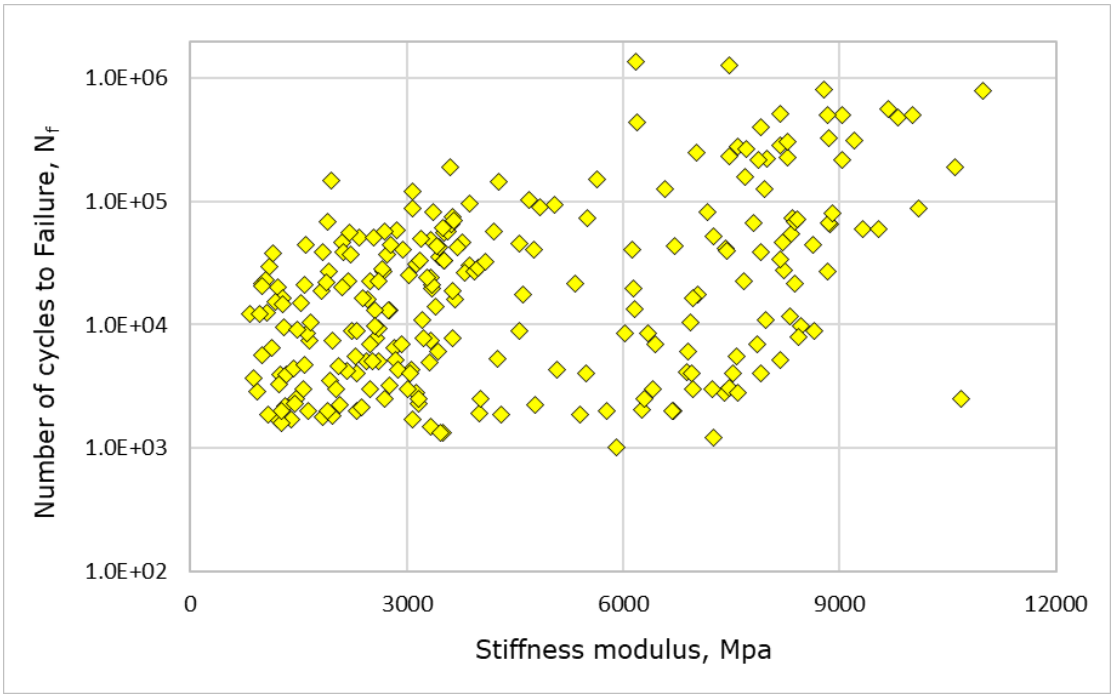



Figure 7.66: Number of cycles to failure ($N_f$) versus stiffness modulus.

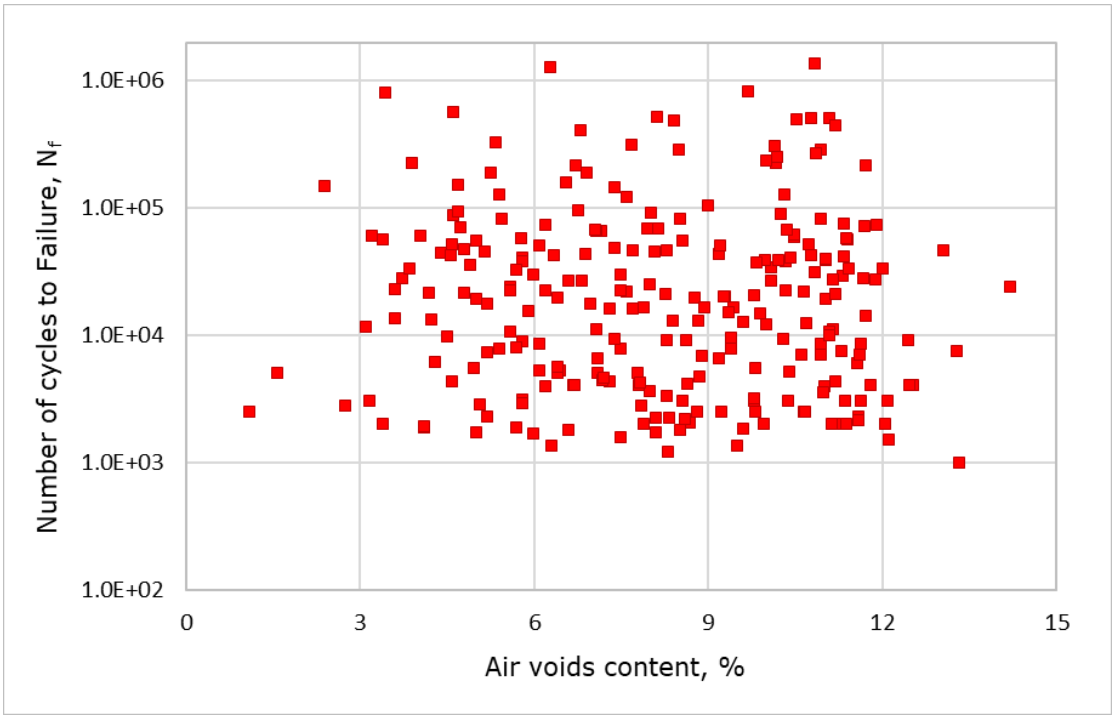



Figure7.67: Number of cycles to failure ($N_f$) versus air voids content.

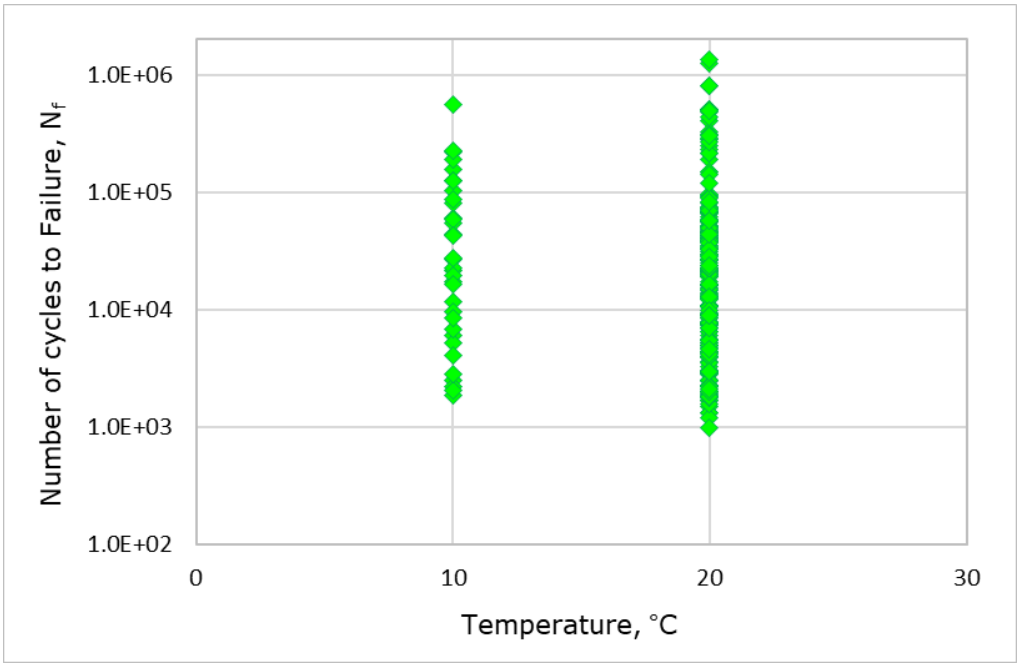



Figure 7.68: Number of cycles to failure ($N_f$) versus testing temperatures.

Spearman and Pearson coefficients were calculated using Minitab software version 17.2.1 and the results are presented in Table 7.8. The values of both coefficients are approximately similar. When the data are roughly elliptically distributed as shown in Figure 7.67 and 7.68 or there are no prominent outliers, the Spearman correlation and Pearson correlation give similar values.

Table 7.9 also presents how the $R^2$ values change if the suggested model includes different parameters in each time. Obviously, no change can be noticed if the temperatures and air voids are not taken into consideration. On the other hand, the stiffness modulus might have more influence on the predicted number of cycles to failure, $N_f$ in terms of the change of $R^2$ values.

Based on this analysis, it was decided to neglect the effect of air voids content and testing temperatures because the correlation coefficients are approaching zero.

Table 7.8: Spearman and Pearson correlation coefficients.

| **Independent parameters** | **Correlation coefficients** | | **Effect of independent parameter** |
|---|---|---|---|
| | **Spearman** | **Pearson** | |
| Strain vs $N_f$ | -0.895 | -0.868 | Negative correlation |
| Stiffness vs $N_f$ | 0.411 | 0.431 | Positive correlation |
| Air voids content vs $N_f$ | -0.054 | -0.038 | Very weak negative correlation (negligible) |
| Temperature vs $N_f$ | -0.073 | -0.065 | Very weak negative correlation (negligible) |

Table 7.9: Effect of using different parameters on the change of $R^2$.

| **Included independent parameters in the Model** | **Suggested functions to find the number of cycles to failure ($N_f$) using Minitab 17.2.1** | **$R^2$** |
|---|---|---|
| Strain (με), Stiffness modulus (MPa), Air voids content (%), Testing temperature (°C) | $N_f = 9.706\ (\varepsilon)^{-0.329}\ (S)^{0.094} (AV)^{-0.0069}\ (T)^{0.0585}$ | 0.895 |
| Strain (με), Stiffness modulus (MPa), Air voids content (%), | $N_f = 12.265\ (\varepsilon)^{-0.331}\ (S)^{0.0851}\ (AV)^{0.0014}$ | 0.889 |
| Strain (με), Stiffness modulus (MPa), | $N_f = 12.319\ (\varepsilon)\text{-}0.331\ (S)^{0.085}$ | 0.889 |
| Strain (με), | $N_f = 26.01\ (\varepsilon)^{-0.331}$ | 0.771 |

Third, the statistical model was generated using Minitab software version 17.2.1 after neglecting the effect of air voids content and testing temperatures. Equation 7.9 shows the suggested statistical model.

$$N_f = 12.32\ (\varepsilon)^{-0.331}\ (S)^{0.085} \qquad 7.9$$

Where:

$N_f$: Number of cycles to failure,

ε: Tensile strain measured in με,

E: Stiffness modulus of asphalt mixtures measured in MPa.

Figure 7.69 shows a linear relationship between the predicted and observed $N_f$ values with high coefficient of determination (R-squared) value (89%). R-squared is a statistical measure of how close the data are to the fitted regression line. It also explains the percentage of the response variable variation (variation/total variation) that is explained by a model (Devore, 2012). Therefore this coefficient may indicate that the model explains 89% of the variability of the response data around its mean. The rest (11%) of unexplained variability could be attribute to the fact that fatigue testing might induce variability in the results at the same conditions and therefore it is classified as a scattered test. It also could be related to the wide range of testing conditions shown in Table 7.6 that were applied to asphalt mixture specimens and resulted in a wide range of $N_f$ values.

Finally, Chi-square goodness of fit test was used to find out how the observed value of fatigue tests are significantly different from the expected value. In Chi-square goodness of fit test, the term goodness of fit is used to compare the observed sample distribution with the expected probability distribution. Chi-square goodness of fit test determines how well a theoretical distribution (such as normal, binomial, Chi-square or Poisson) fits the empirical distribution (Devore, 2012). The formula for the Chi-square statistic used in the Chi-square test is:

$$X^2 = \sum \frac{(O-E)^2}{E} \qquad 7.10$$

Where:

$X^2$= Chi-square goodness of fit test,

O= observed value,

E= expected value.

The calculations was carried out manually and presented in Appendix A-2. Minitab software version 17.2.1 was also used for the same purpose and shows the same result.

Hypothesis testing in Chi-square goodness of fit test is the same as in other tests, such as t-test, ANOVA, etc. The calculated value of Chi-square goodness of fit test is compared with the table value. If the calculated value of Chi-square goodness of fit test is greater than the table value, the null hypothesis ($H_0$) will be rejected and it can be concluded that there is a significant difference between the observed and the expected values. That means the alternative hypothesis ($H_A$) should be accepted. If the calculated value of Chi-square goodness of fit test is less than the table value, the null hypothesis ($H_0$) will be accepted and it can be concluded that there is no significant difference between the observed and expected value.

A Chi-square test also gives a p-value where the p-value indicates if the test results are significant or not. The smaller the p-value (typically ≤ 0.05), the greater the statistical incompatibility of the data with the null hypothesis. A large p-value (> 0.05) indicates weak evidence against the null hypothesis and therefore it is not possible to reject the null hypothesis. (Wasserstein and Lazar, 2016).

To find the table value, the following steps need to follow:

1. State the hypothesis, use null hypothesis ($H_0$) which states there is no significant difference between the observed and expected values,
2. Calculate the expected values,
3. Use the observed and expected values to calculate the Chi-square value,
4. Establish the significance level (usually 95%, α = 5%) and the number of degrees of freedom (DF). DF equals the number of observations minus 1, DF = 254 (255-1),
5. Compare the Chi-square statistic with the critical value from the table,
6. Make a decision about the hypothesis.

Table 7.10 shows the results of calculated and table Chi-square values at α=0.05. Since the calculated value of Chi-square (3.2) is less than the table value (292.2) and the p-value (0.999) is greater than 0.05, the null hypothesis ($H_0$) is accepted and there is no significant difference between the observed and expected values. The p-value can also indicate that the data are compatible with the generated statistical model under the level of significant of 99%.

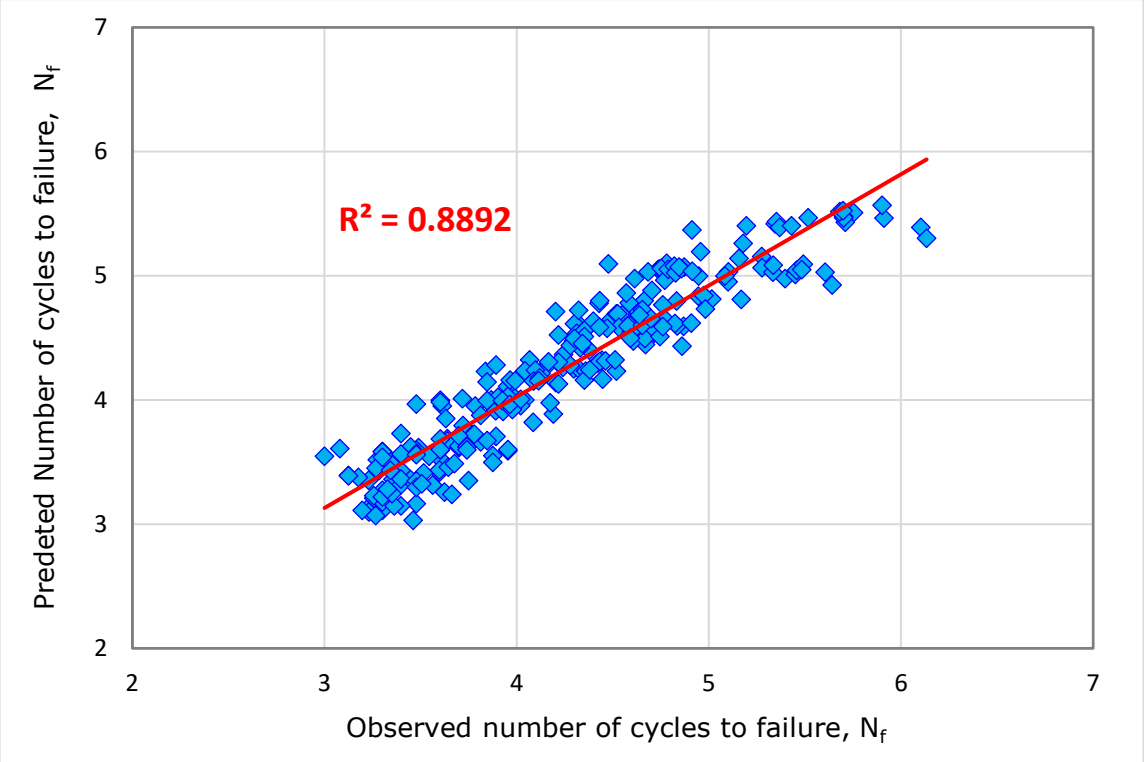



Figure 7.69: The predicted and observed number of cycles to failure ($N_f$).

Table 7.10: Chi-square goodness of fit test results.

| Calculated Chi-square value | Degree of freedom | Chi-square critical value (table value) | p-value | Decision |
|---|---|---|---|---|
| 3.2 | 254 | 292.2 | 0.999 | Accept the null hypothesis ($H_0$) and conclude that there is no significant difference between the observed and expected values. |

## 7.9 Summary

ITFT in constant strain method was used to study the fatigue performance of different asphalt mixtures exposed to individual and combined environmental factors; moisture damage and ageing. Based on ITFT findings, the following summary can be drawn for this chapter:

- There was obvious convergence at 300 and 400 με apart from testing conditions and parameters. It could be attributed to the rapid deterioration of

stiffness at these strain levels. The used limestone aggregate (from Tunstead quarry) could be not hard enough to resist these high strain levels.

- The results of ITFT in constant strain method show a general behaviour, the stiffer the asphalt mixture the better the fatigue performance. This behaviour occurred when the asphalt mixtures stiffen more due to using hard binder or applying ageing or reducing the testing temperature from 20 to 10˚C.
- ITFT in constant strain mode is not susceptible to the change in air voids content unless the air voids are combined with other testing parameters. However, this is not crucial and may require more investigation.
- The effect of testing temperature on ITFT results was significant compared to that of air voids content. It was observed an increase in the fatigue life of asphalt mixtures when these mixtures stiffen due to the decrease of testing temperature from 20 to 10˚C.
- Asphalt mixtures of the harder binder 10/20 Pen have clearly and surprisingly superior fatigue performance regardless of whether the mixture is control or aged and the condition is dry or wet. Furthermore, mixtures of 40/60 Pen have generally the second ranking while that of 100/150 show a poor fatigue performance.
- It was observed a significant increase in the fatigue life of 40/60 Pen and 100/150 Pen asphalt mixtures when these mixtures stiffen due to LTOA. On the other hand, LTOA has slightly adverse effect on the fatigue life of 10/20 Pen asphalt mixtures. Despite 10/20 Pen asphalt binder being considered less susceptible to ageing, it may show more brittle behaviour when it stiffened more due to LTOA and tested for fatigue using the ITFT. Therefore it had slightly less fatigue life than unaged 10/20 Pen mixtures.
- No obvious trend from investigating the individual effect of moisture conditioning on the fatigue performance was found. Even when this effect was combined with LTOA. In some occasions, moisture conditioning by BBA protocol reduced the resistance to fatigue cracking while BS EN method improved it. There were obvious fluctuations that could be attributed to two conflicting roles of water and moisture conditioning. One increases the stiffness and the second decreases the stiffness. The type of used aggregate which may play an important role in these results should also not be ignored.
- The poor and superior fatigue performance of tested mixtures may be explained in terms of the asphalt binder behaviour. Using the hard bitumen

(10/20 Pen), ageing the investigated asphalt mixtures and reducing the testing temperature from 20 to 10˚C may motivate the elastic properties of the bitumen to dominate rather than viscoelastic or viscous properties. This might increase the ability of asphalt mixtures to recover their original shape and release of stress during the 0.4-second rest period following the load application of ITFT and therefore might generally result in a longer fatigue life.

- The fatigue cracking resistance of asphalt mixtures improved with the increase of binder content from 5 to 6%.
- Due to the disadvantage of permanent deformation of ITFT, it is important to make certain that failure is tensile and not shear or compressive failures by for example decreasing the testing temperature to minimise the vertical permanent deformation.
- It was possible to use the ASU to analyse the data of ITFT. However, the resulting number of cycles to failure from this method was greater than the traditional approach $N_{f50}$.
- X-ray Computer Tomography (CT) seems to be an applicable tool with ITFT in constant strain method. However, minimising the effect of vertical deformation is important for more reliability.
- A statistical model was generated to predict the number of cycles to failure (fatigue failure). The applied strain levels to different asphalt mixtures exposed to ageing or/and moisture conditioning and the resulting initial stiffness modulus measured at the cycle $50^{th}$ in the modified ITFT were used to generate this model. However, the robustness of this this model requires an assessment.
- More cycles and more methods of moisture damage might be important for more investigation of their influence on fatigue damage.
- It may also be important to study the temperature effect of water immersion to examine if it may cause any possible ageing during the period of this immersion.
- Investigation of the effect of more types of aggregate on moisture damage and in turn on fatigue damage is required for more understanding of this issue.
- Finally, one important issue arises from these findings, the importance of using other fatigue testing method to evaluate the investigated parameters and conditions.

# Chapter Eight: Evaluation of Environmental Factor Effects on Fatigue Performance of Asphalt Mixtures using the Four-Point Bending Test

## 8.1 Introduction

The study of fatigue cracking is important for enhancing the durability of asphalt pavement structure. In the last few decades, extensive progress has been achieved in understanding the fatigue phenomenon of bituminous materials, although some unanswered questions are still in need of further investigation. The majority of studies do not consider the combined influence of environmental factors on fatigue damage. For instance, the asphalt binder stiffens excessively due to oxidation or reduction in temperature but at the same time the stiffness modulus of asphalt mixtures is supposed to be decreased by the effect of moisture damage. It is well known that stiffness increase makes asphalt mixtures more brittle and susceptible to fatigue cracking. But limited data is available to explain the effect of stiffness decrease due to moisture damage on fatigue cracking.

The multi factors influence arises due to the significant change in weather conditions and traffic loadings. Therefore, it is important to assess the combined effect of variables which may affect the properties of asphalt pavement materials such as ageing, temperature, moisture under repeated loadings. In this work, the question arises as to what extent the stiffness increase due to ageing or temperature decrease and the stiffness reduction because of moisture damage can affect the fatigue damage.

A number of different loading arrangement fatigue tests are commonly in use today include two, three and four-point bending tests in additional to those conducted in direct tension-compression mode (Rowe et al.,2012). Moreover, fatigue testing can also be carried out in indirect tension mode (Read, 1996). Figure 8.1 presents samples of fatigue test arrangements.

Several studies have been carried out at The University of Nottingham using different fatigue testing methods (Pell and Cooper, 1975, Read, 1996, Rowe, 1996, Thom, 2006, Oliveira, 2006, Cocurullo et al., 2008, Maggiore, 2014).

In this study, the Four Point Bending (4PB) testing machine shown in Figure 8.2 was used to investigate the effect of ageing and/or moisture conditioning on fatigue damage of asphalt mixtures. It was also used to examine the effect of other parameters; air voids content, testing temperature, and binder grades.

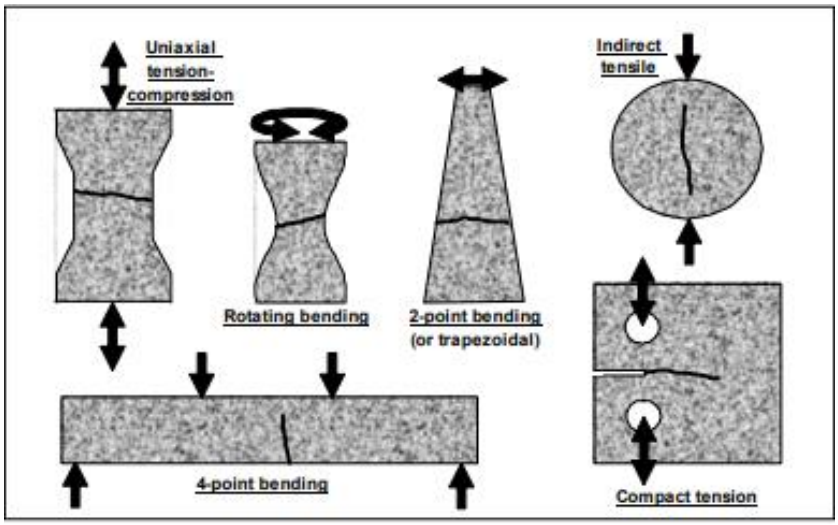



Figure 8.1: Commonly used fatigue test arrangements (Thom, 2006).

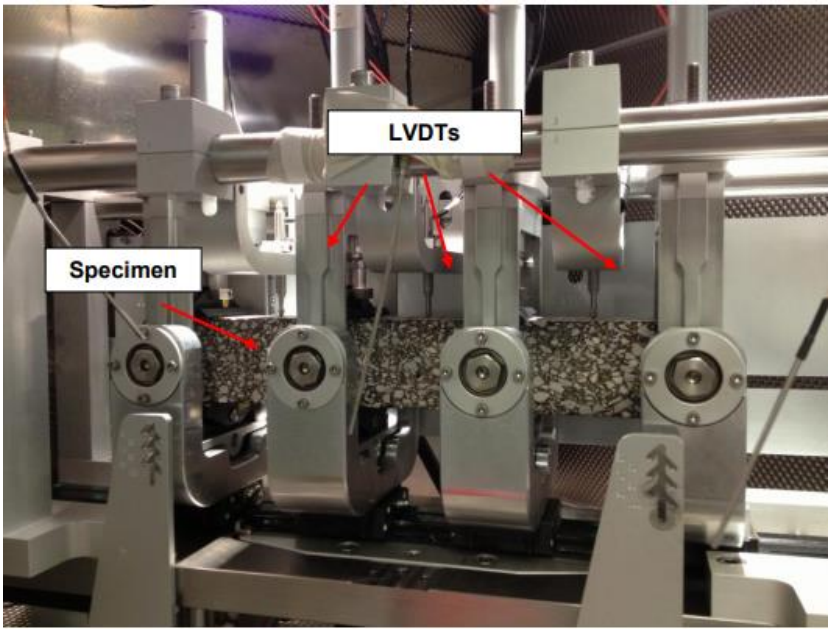



Figure 8.2: 4-PB equipment at the University of Nottingham (Maggiore, 2014).

## 8.2 Four-point bending (4-PB) test

The prismatic beam specimens required for 4PB fatigue tests were sawn and trimmed from the manufactured asphalt mixture slabs of (500 × 500 × 83 mm) to the desired dimensions shown in Table 8.1. These dimensions are in accordance with BS EN 12697-24:2012. The prismatic beam specimens of two different binder grades; 40/60 and 100/150 pens and of two air voids content 6 and 12% were classified into different sets based on their conditions. Table 8.2 presents the applied environmental conditions to the investigated asphalt mixtures.

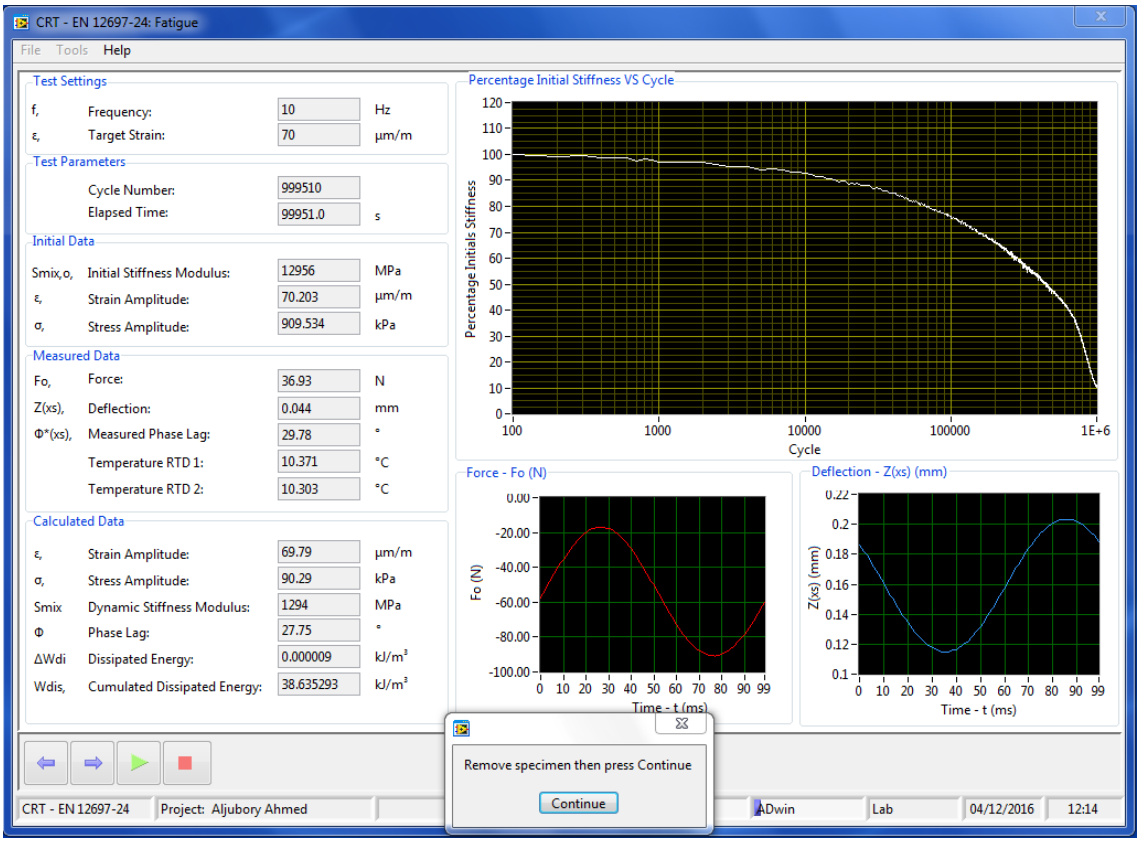
Table 8.1: Dimensions of prismatic beam specimens, BS EN 12697 24:2012.

| *Dimensions of the specimens* | *mm* |
|---|---|
| L | 380 |
| W | 50 |
| H | 60 |

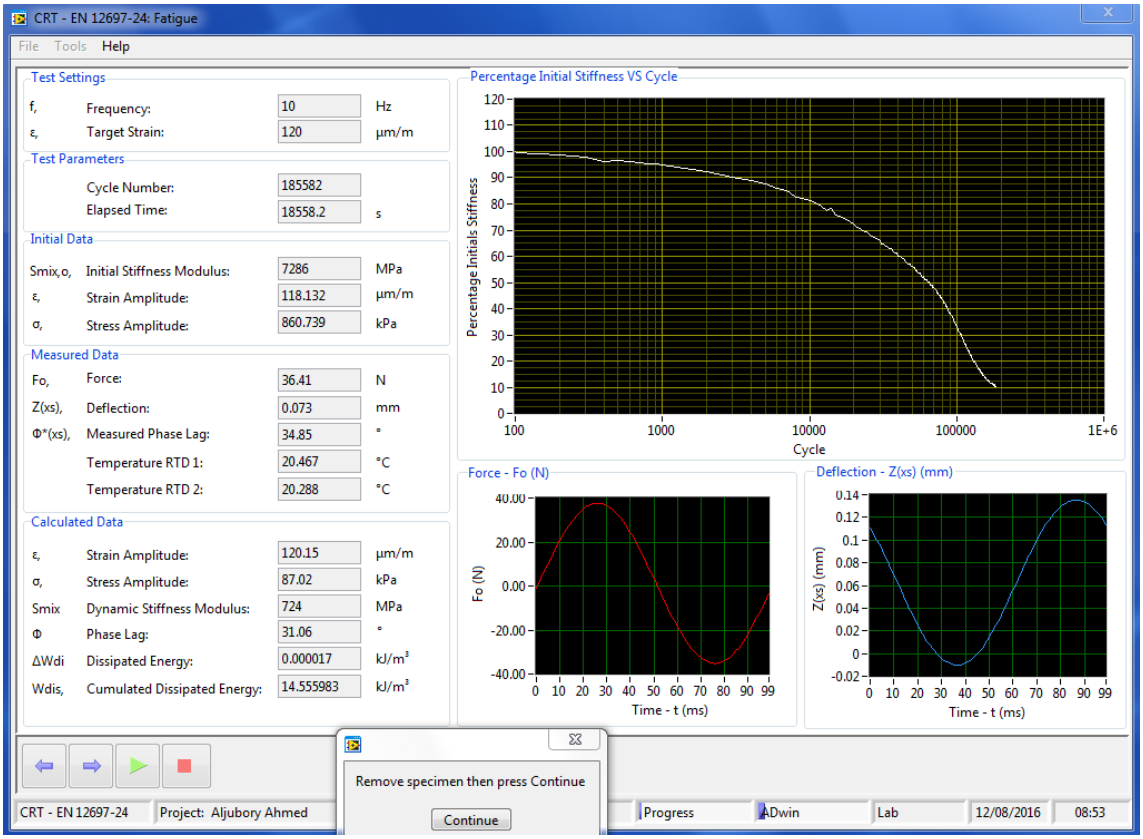
Table 8.2: Summary of investigated mixture conditions for fatigue test by 4PB (Two replicates were used to find the number of cycles to failure).

| **Mixtures exposed to specific conditions** | **14mm DBM manufactured with binder grades** | |
|---|---|---|
| | **40/60** | **100/150** |
| Control mixture, dry prismatic beams | ✓ | ✓ |
| Control mixture, immersed prismatic beams in water according to BS EN method as detailed in Table 4.5. | ✓ | ✓ |
| LTOA mixture, dry prismatic beams (before compaction, the loose mixture subjected to 135°C for 4 hours then, the compacted mixture subjected to 85°C for 120 hours). | ✓ | ✓ |
| LTOA mixture, immersed prismatic beams (the loose mixture subjected to 135°C for 4 hours then the compacted mixture subjected to 85°C for 120 hours) in water according to BS EN method as detailed in Table 4.5. | ✓ | ✓ |

Fatigue tests were carried out in controlled strain method for the different 14mm DBM asphalt mixtures at 10 and 20°C and at 10 Hz. 10 Hz is the most commonly used loading frequency for simulating repetitive traffic loading (ASTM D7460, 2010). This frequency simulates in-service pavement stress pulses corresponding to vehicle speeds in the range of 24 to 48 km/h range. It is sufficiently large enough to conduct rapid testing that represents the load pulses generated by rapid moving traffic (Deacon et al. 1994). In addition, the applied strain levels were in the range of 70 to 300 με. Two selective samples of typical fatigue tests carried out at 70 με, 10°C, and 10 Hz (See Figure 8.3.a) and at 120 με, 20°C, and 10 Hz (See Figure 8.3.b) by the 4PB machine is presented in Figure 8.3. This figure shows the inputs and outputs of the software and stiffness deterioration during the whole test.




a




b

Figure 8.3: Samples of typical fatigue tests using the 4PB machine.

### 8.3 Assessment of fatigue failure point

The fatigue data resulting from the 4PB testing method was analysed firstly in accordance with the phenomenological approach, $Nf_{50}$, which conventionally assumes that the failure point occurs at the 50% of initial stiffness (Deacon et al., 1994). Secondly, the Normalised Modulus × Cycles (ASTM D7460-10) offers an alternative definition of the failure point. Fatigue assessment according to ASTM D7460-10 was based upon dissipated energy concepts (Rowe et al., 2012). In ASTM D7460-10 the failure Point, $N_f$ (Number of cycles to failure) occurs at the peak value of Normalised Modulus × Cycles (See Figure 8.4) when plotted versus Number of Cycles. The parameter S.n (stiffness multiplied by number of load cycles) peaks at the point where the dissipated energy per loading cycle starts to change significantly. This point signifies coalescences of micro cracks to form a sharp crack which then propagates more rapidly through the prismatic beam specimen. This method also does not rely upon a curve fitting to find the failure point compared to AASHTO T321. However, it can do it by the 6-order polynomial fitting to remove any spikes (Rowe et al., 2012).

The Normalised Modulus × Cycles can be calculated according to ASTM D7460-10 as shown in equation 8.1.

$$NM = (Si \times Ni)/(So \times No) \quad 8.1$$

Where:

NM = normalised modulus × cycles,

$S_i$ = flexural beam stiffness at cycle i (MPa),

$N_i$ = cycle i,

$S_o$ = initial flexural beam stiffness (MPa), estimated at approximately 50 cycles, and

$N_o$ = actual cycle number where initial flexural beam stiffness is estimated, 100 cycles in this work.

Moreover, a comparison between the applied fatigue failure approaches is presented in Figure 8.5 showing the difference in number of cycles to failure. Obviously, ASTM D7460 has produced the greatest number.

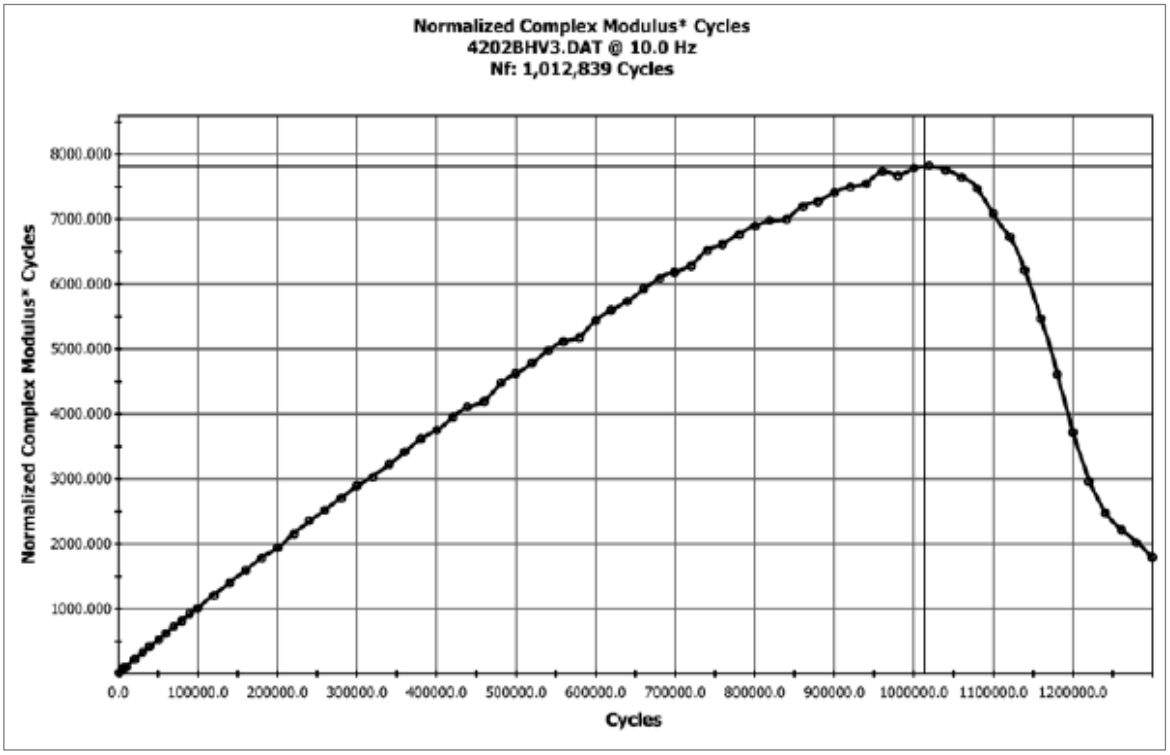



Figure 8.4: Normalised complex modulus × cycles versus loading cycles (ASTM D7460-10).

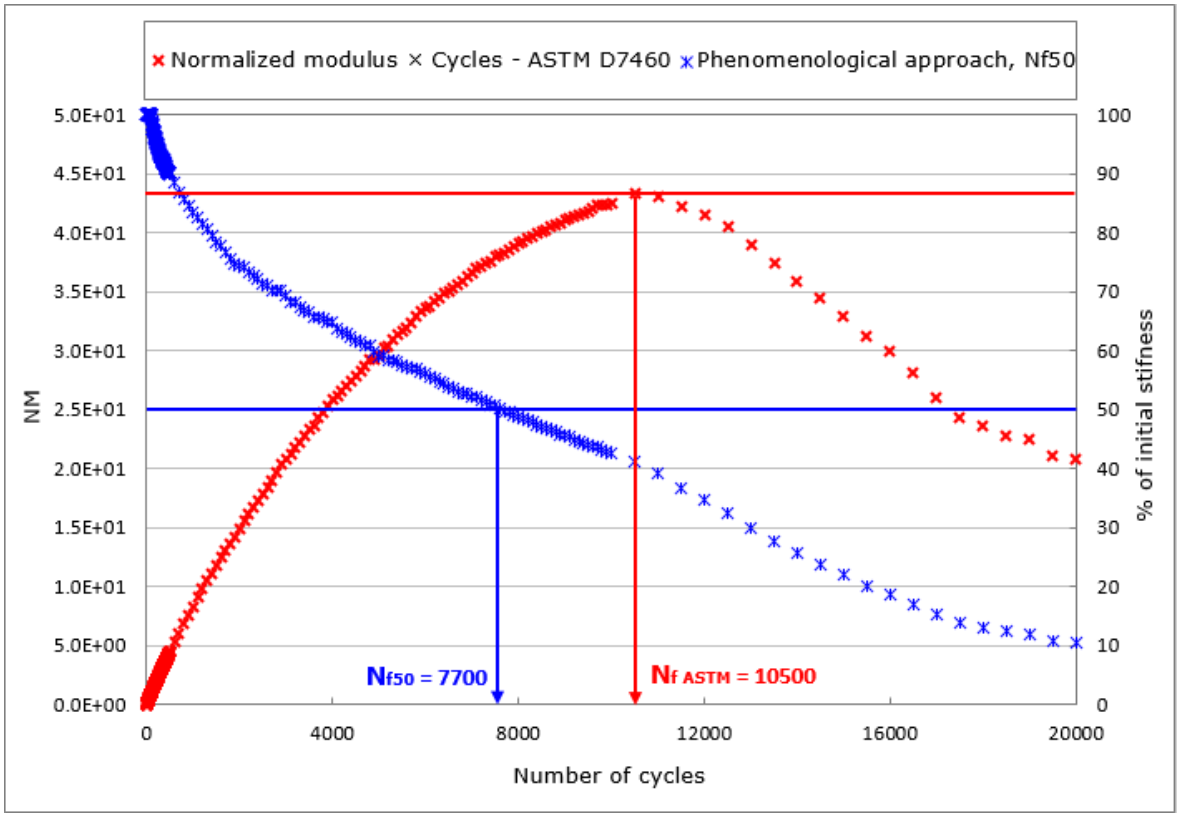



Figure 8.5: A comparison of phenomenological approach, Nf50 and Normalised complex modulus × cycles versus loading cycles.

## 8.4 Test results

Different parameters have been investigated in this work to understand their influence on the number of cycles to failure. The phenomenological approach, $Nf_{50}$, was mainly considered to find the failure point.

### 8.4.1 Effect of air voids content

The fabricated asphalt mixtures of 40/60 pen with 6% and 12% air voids content were tested at 10 and 20°C by the 4PB method to investigate the influence of air voids content on fatigue performance. Figures 8.6 and 8.7 show the resulting fatigue lines from applying a spectrum of strain levels (70 to 300 με) to these mixtures.

It can be observed from Figures 8.6 and 8.7 that air voids content has less effect at high micro-strain at both testing temperature 10 and 20°C. Despite the observed convergence between the two lines, the lower air voids content mixtures produced the higher number of cycles to failure, in particular, at low micro-strain levels. The increase of micro-strain levels caused more convergence between the failure points and more compatibility between both fatigue lines. It might be better to assess the air voids content influence at a specific strain level rather than over a wide range of applied strains. The high applied strain such as 300 με and the low one such as 70 με are not practical at assessing this influence. In addition, the resulting fatigue characterisation of this variable seems partially similar to that found earlier by the ITFT in Chapter 7, although data collected by the 4PB test is not significant to assess this variable.

Harvey and Tsai, 1996 indicated that the simulations of air void contents effect on the fatigue life of several overlays using the models resulting from laboratory-controlled strain flexural beam testing showed an increase in the predicted pavement fatigue life of lower air void contents. In addition, Pell and Taylor, 1969 found that air voids have a detrimental influence upon fatigue resistance. An increase in air voids content being associated with a decrease in fatigue cracking resistance when evaluated under stress controlled condition. Moreover, the same pattern as for controlled stress tests was found by Santucci

and Schmidt, 1969. Results of controlled strain tests indicated that air voids content reduction led to longer fatigue lives.

Finally, it was decided to use the 12% air voids content mixtures to evaluate the applied environmental conditions to provide more access to water saturation and oxidation and in turn more moisture damage and ageing.

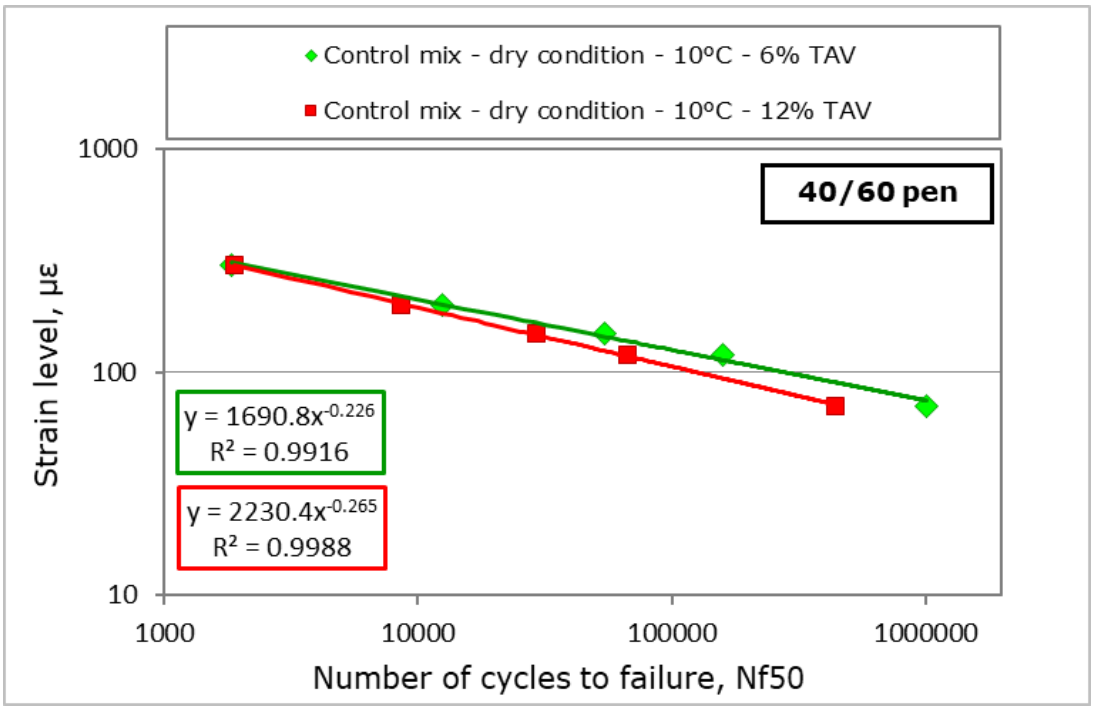



Figure 8.6: Effect of air voids content on fatigue life at 10°C – dry condition.

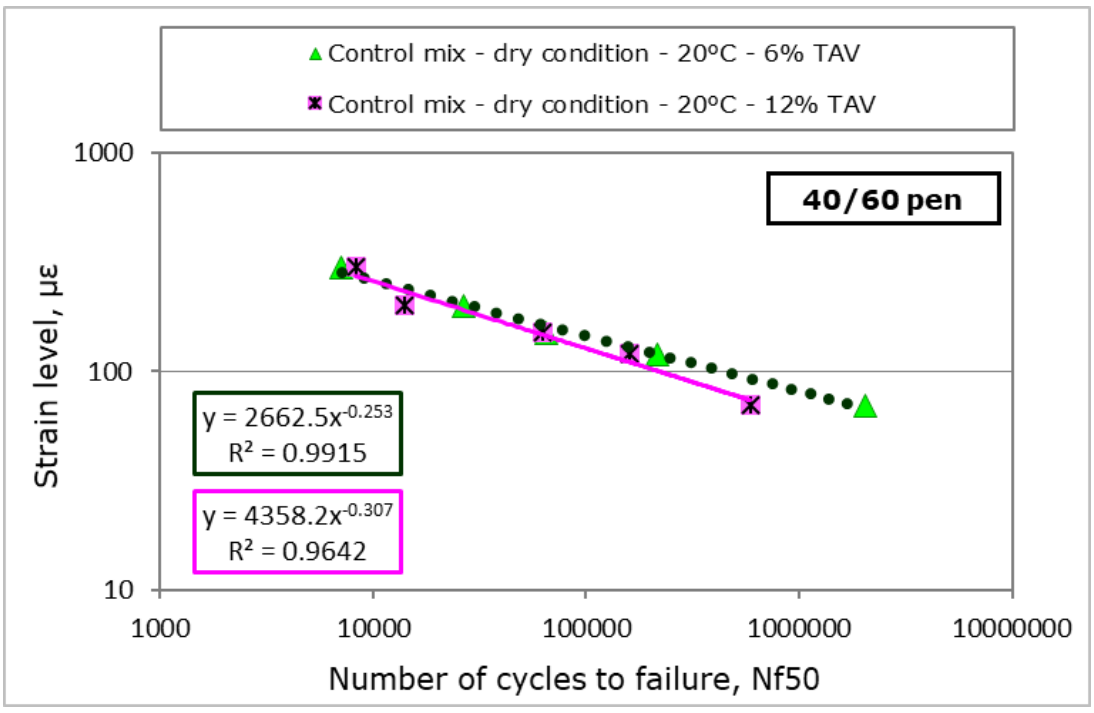



Figure 8.7: Effect of air voids content on fatigue life at 20°C – dry condition.

### 8.4.2 Effect of testing temperature

The fabricated asphalt mixtures of 40/60 pen with 6% (control mixtures only) and 12% air voids content were tested at 10 and 20°C by the 4PB method to investigate the influence of testing temperature on fatigue performance. Figures 8.8 to 8.12 show the resulting fatigue lines from applying a spectrum of strain levels to control mixtures; dry and conditioned (wet) and to aged (LTOA) mixtures; dry and wet.

In general, it can be observed from these figures that decreasing the testing temperature from 20 to 10°C caused an increase in the number of cycles to failure regardless of the mixture condition and air voids content. However, observable convergence between the two lines at 70 and 120 με was noticed. As expected, the decrease of testing temperature has increased the stiffness modulus of asphalt mixtures and in turn reduced the fatigue life. However, the resulting fatigue characterisation of this variable seems inconsistent with that was found earlier by the ITFT in Chapter 7.

In general, Monismith, 1970 indicated that the decrease of testing temperature results in stiffness increase and consecutively in fatigue life increase in controlled stress tests and in fatigue life decrease in controlled strain tests. At a specific stress level, Jimenez and Gallaway, 1962 generally found that the fatigue life increased when the temperature decreased. Pell and Taylor, 1969 have stated that the specimen stiffness can be used to explain within limits the effect of temperature. For a specific stress, as the temperature is decreased, the stiffness of an asphalt mixture specimen is increased resulting in less deformation and in turn in longer fatigue life. A series of test results conducted by Pell and Taylor, 1969 for a temperature range from 0 to 30°C have shown that the slope of the strain-fatigue life relationship increased as the temperature increased. This change in slope can be attributed to the non-linear behaviour of asphalt mixtures with stress resulting from the increased testing temperature. Pell, 1962, illustrated the influence of temperature on controlled strain fatigue tests. In general, with an increase in temperature, the fatigue life at a particular strain level is increased. This may be due in part to the slower rate of crack propagation at the higher temperatures.

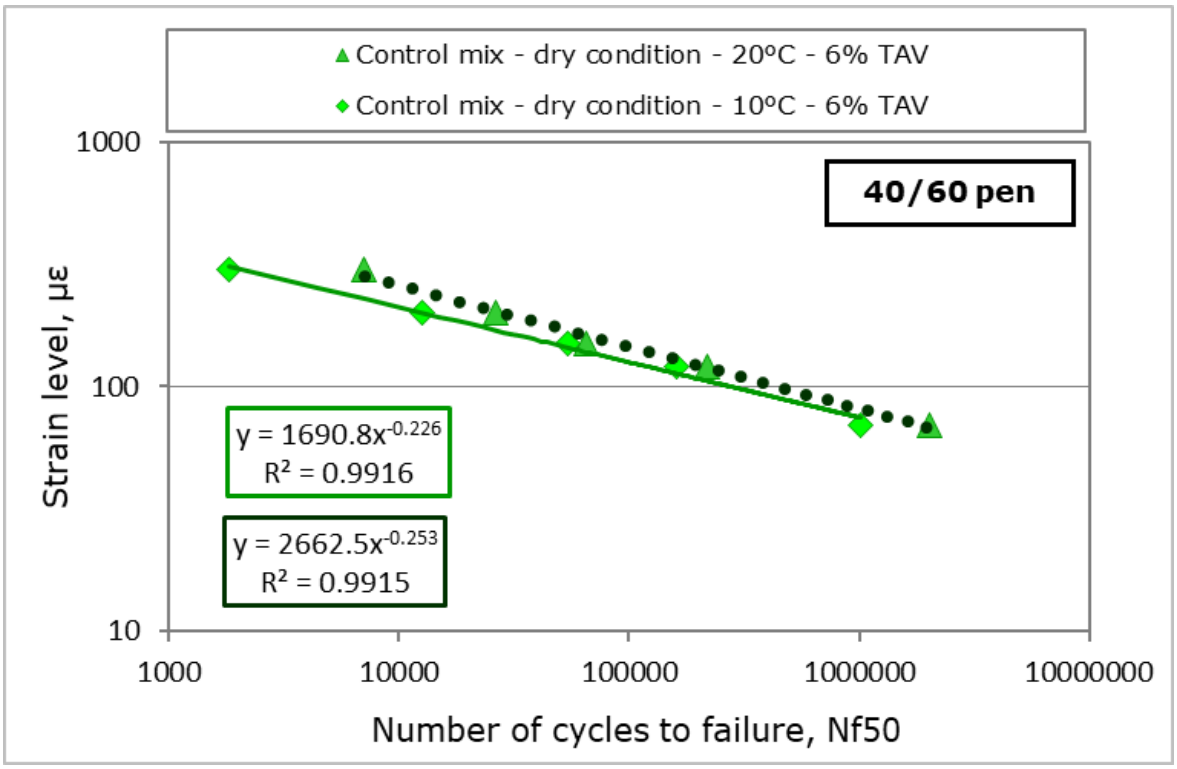



Figure 8.8: Effect testing temperature on fatigue life of dry control mixtures (6% air voids content).

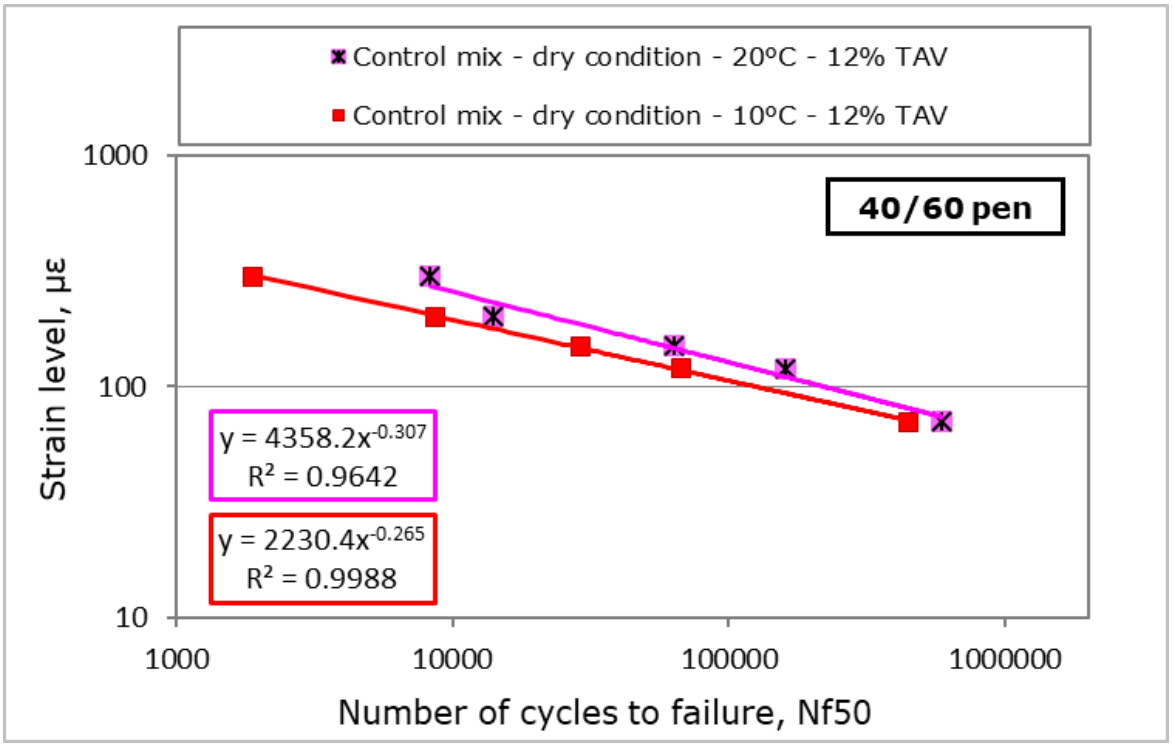



Figure 8.9: Effect of testing temperature on fatigue life of dry control mixtures (12% air voids content).

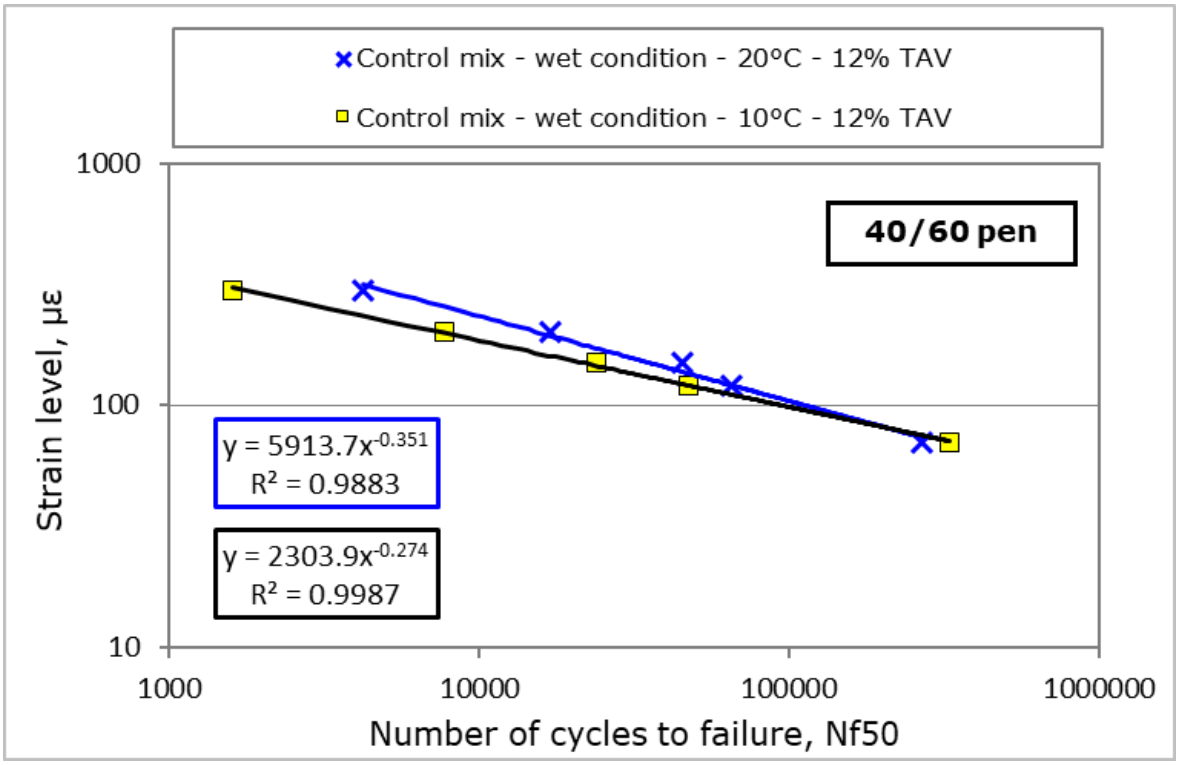



Figure 8.10: Effect of testing temperature on fatigue life of immersed control mixtures (12% air voids content).

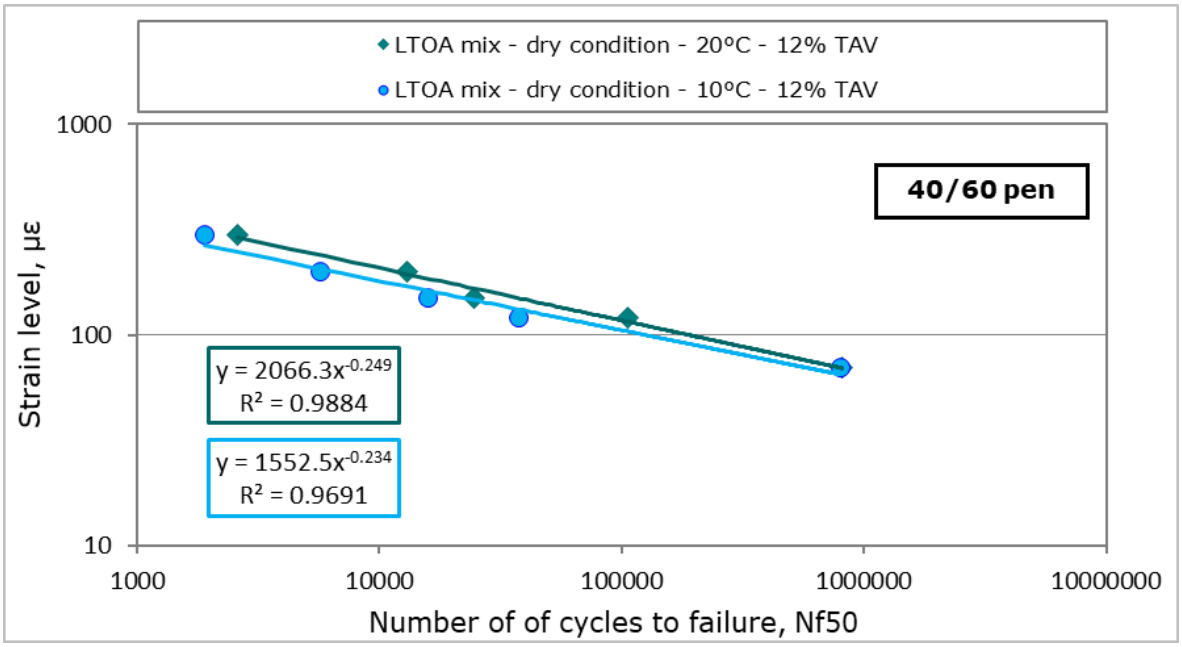



Figure 8.11: Effect of testing temperature on fatigue life of dry aged mixtures (12% air voids content).

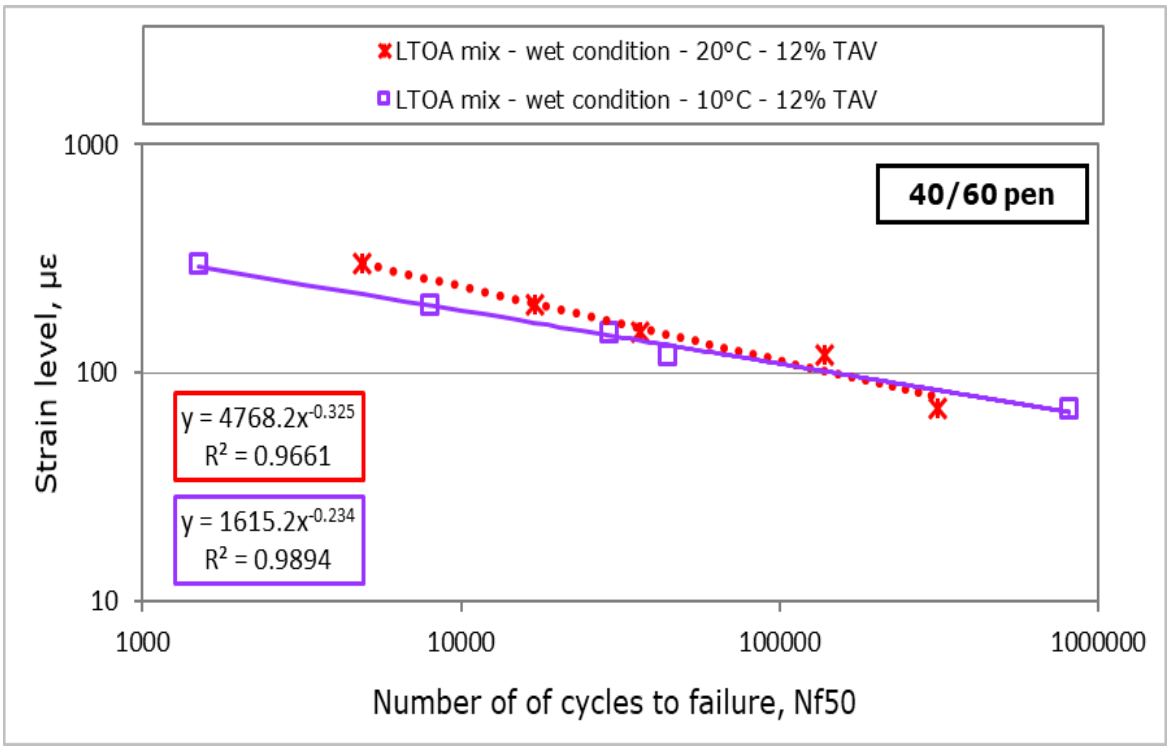



Figure 8.12: Effect of testing temperature on fatigue life of wet aged mixtures (12% air voids content).

### 8.4.3 Effect of moisture conditioning

The fabricated asphalt mixtures have been exposed to moisture conditions displayed in Table 8.2 and tested by the 4PB method in strain control method. Figure 8.13 and 8.14 show the fatigue performance ($N_{f50}$) of dry control asphalt mixtures and that exposed to moisture conditioning and tested at 10 and 20°C respectively. It seems obviously that moisture conditioning has less effect at 10 than at 20°C.

In addition, Figure 8.15 shows the fatigue analysis in terms of ASTM D 7460 method. The graph shows the overlapping between the two fatigue lines. However, a change in the slope of fatigue line due to the effect of moisture was observed.

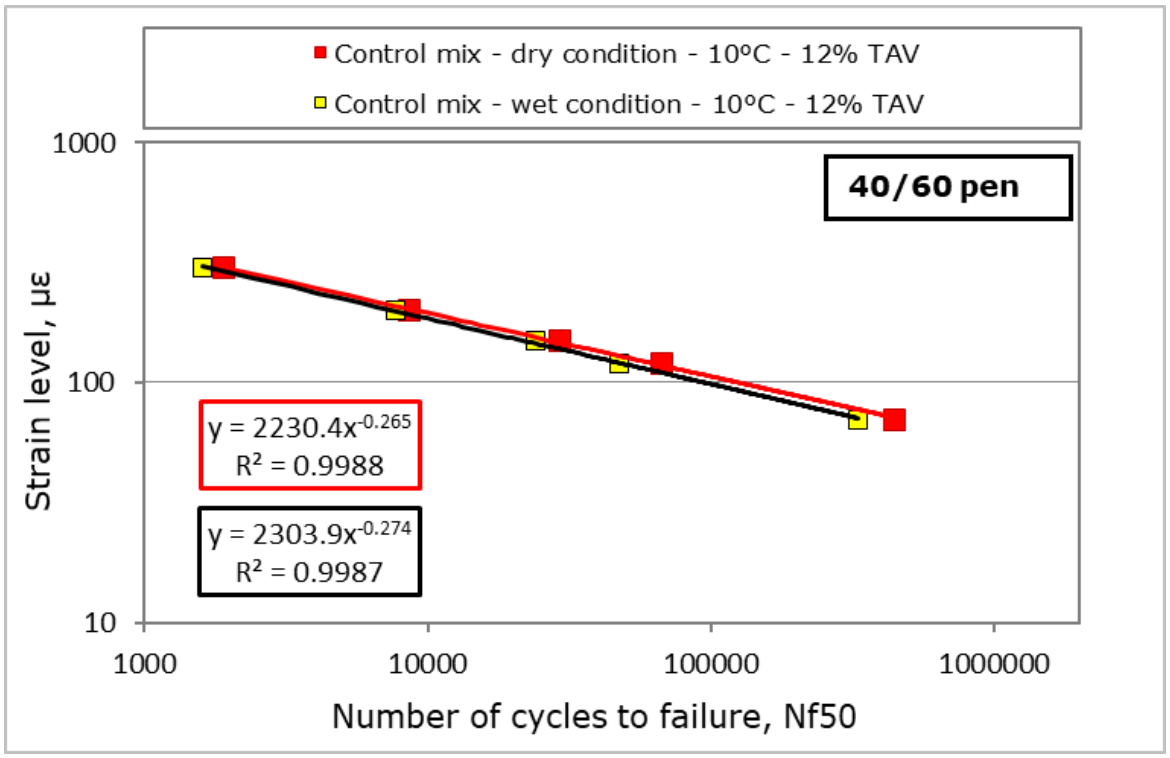



Figure 8.13: Moisture conditioning effect on fatigue life of control mixture at 10°C.

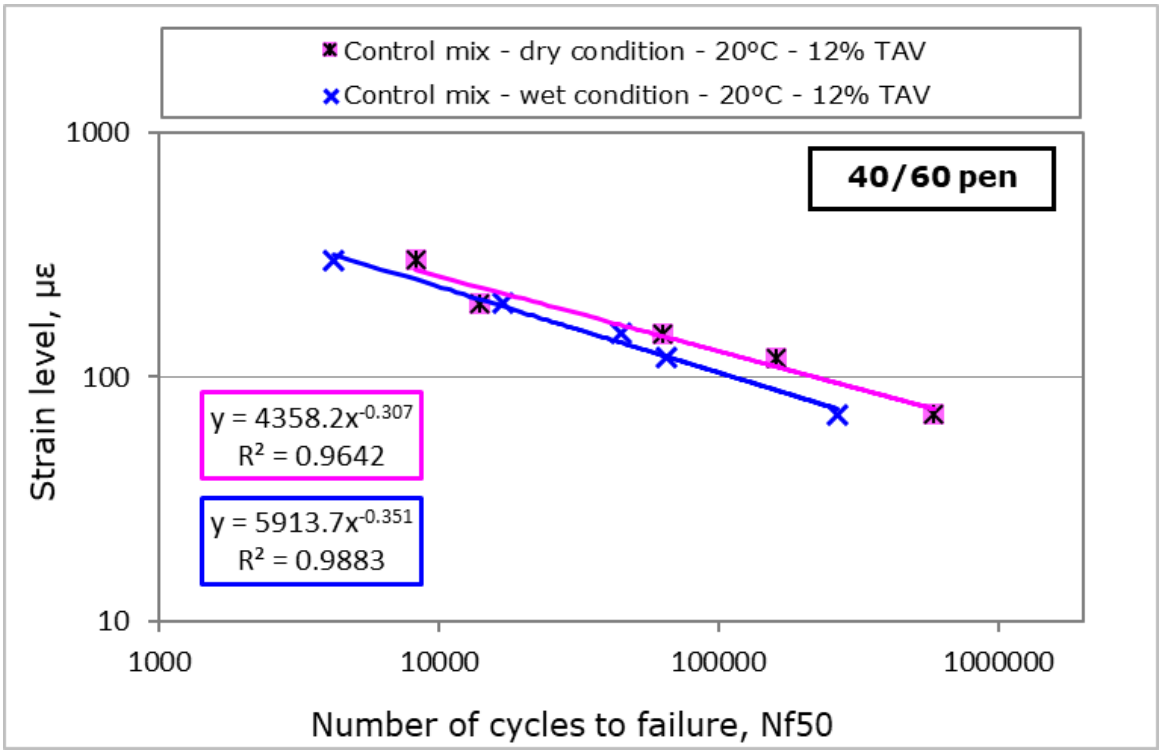



Figure 8.14: Moisture conditioning effect on fatigue life of control mixture at 20°C.

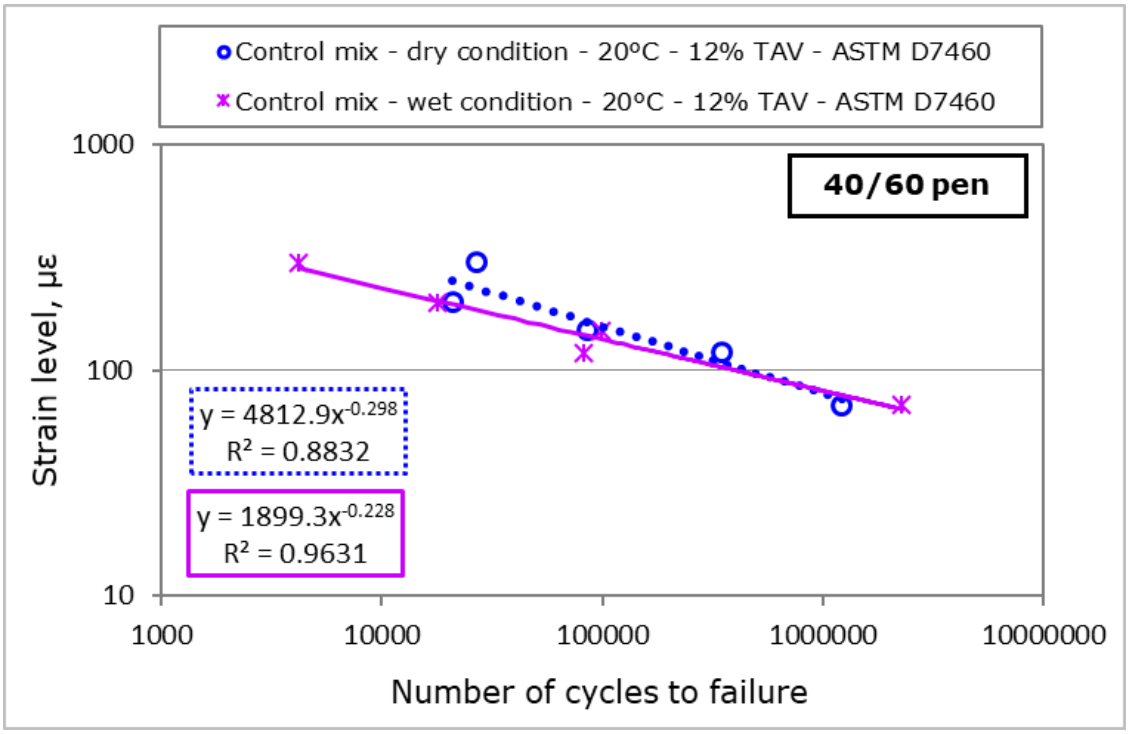



Figure 8.15: Moisture conditioning effect on fatigue life of control mixture at 20°C – ASTM D 7460.

Similarly, the fabricated asphalt mixtures have been exposed to ageing conditions displayed in Table 8.2 and tested by the 4PB method in strain control mode for moisture conditioning effect. Figures 8.16 and 8.17 show the fatigue performance ($N_{f50}$) of dry aged asphalt mixtures and that exposed to moisture conditioning and tested at 10 and 20°C respectively. It seems that the fatigue life of aged mixtures has generally improved at 10 and 20°C when asphalt mixtures were exposed to moisture conditioning. In particular, it was observed that moisture conditioning caused some increase in $N_{f50}$ of aged mixtures in the range of 120 to 200 με at 10°C and in the range of 120 to 300 με at 20°C.

Additionally, Figure 8.18 shows the fatigue life resulting from applying ASTM D 7460 analysis. The figure shows a similar fatigue characterisation of aged mixtures to that by the traditional analysis ($N_{f50}$) when exposed to moisture conditions. However, the change in the slope of fatigue line was more obvious due to moisture exposure.

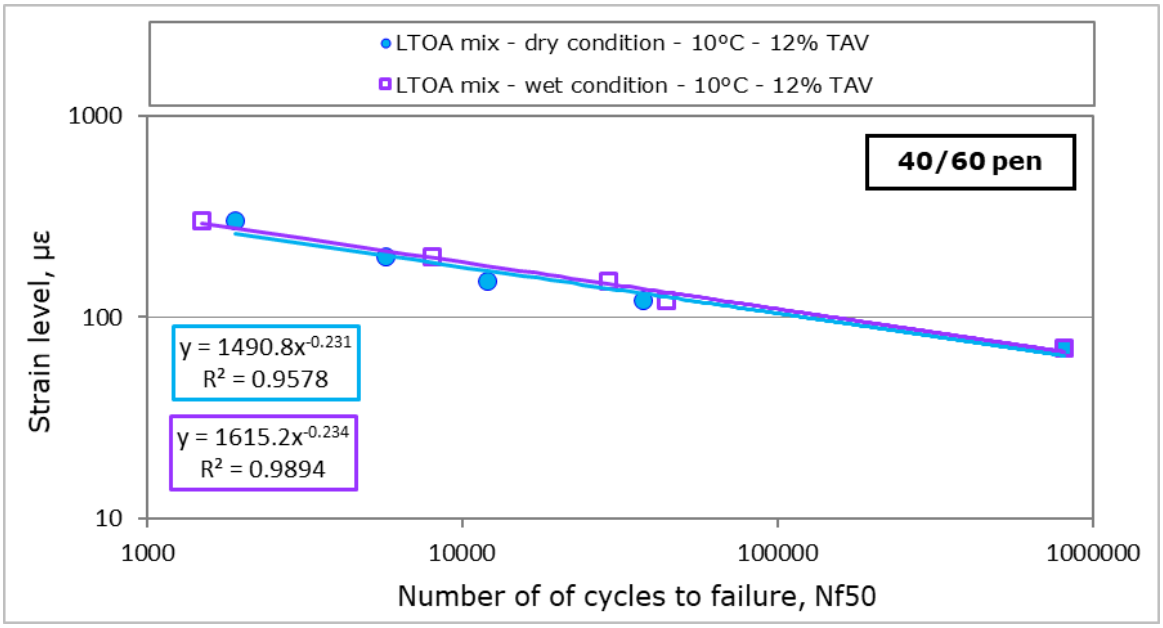



Figure 8.16: Moisture conditioning effect on fatigue life of aged mixtures at 10°C.

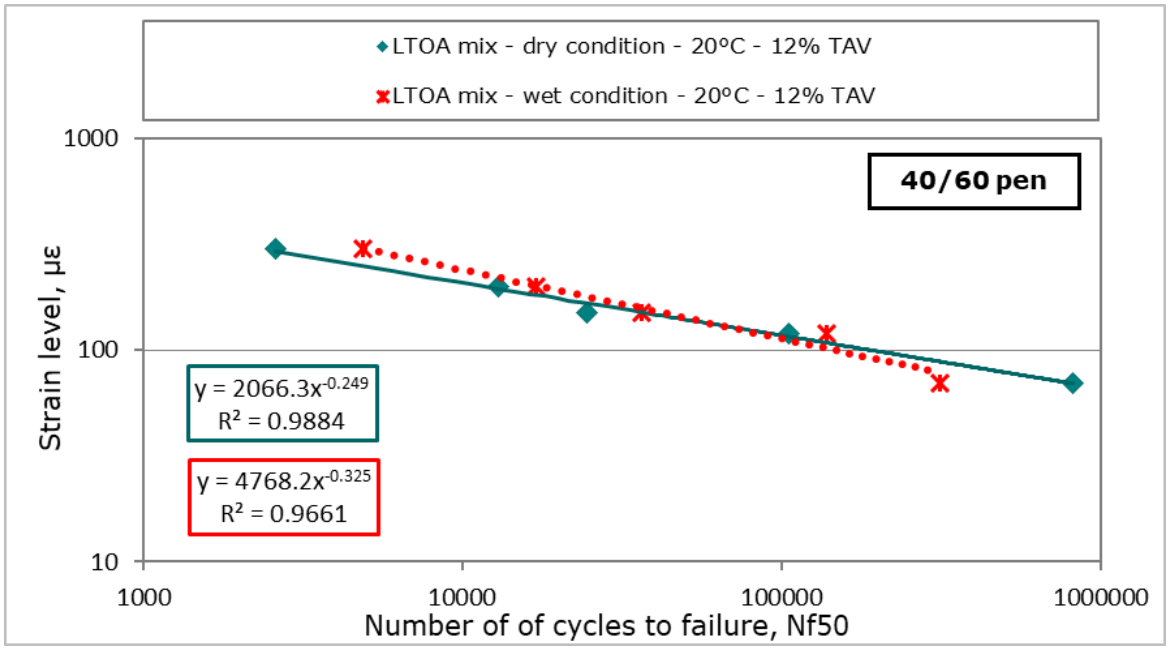



Figure 8.17: Moisture conditioning effect on fatigue life of aged mixtures at 20°C.

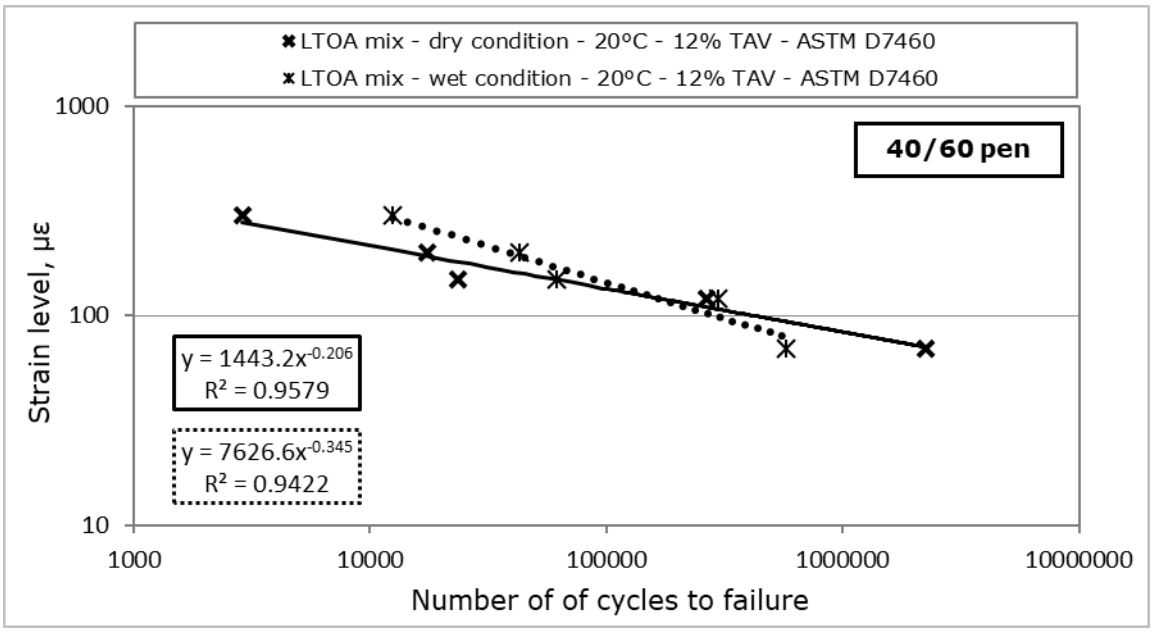



Figure 8.18: Moisture conditioning effect on fatigue life of aged mixtures at 20°C.

### 8.4.4 Effect of ageing

The fabricated asphalt mixtures have been exposed to ageing conditions displayed in Table 8.2 and tested by the 4PB method in strain control mode of loading. Figures 8.19 and 8.20 show the fatigue performance ($N_{f50}$) of dry control asphalt mixtures and that exposed to ageing and tested at 10 and 20°C respectively. It seems obvious that ageing has less effect at 10 than at 20°C. The two lines are more compatible at 10 than at 20°C. The reason could be attributed to the minimal difference between the temperature susceptibilities of aged and unaged mixtures at 10°C. In general, there is some fatigue life decrease due to ageing except the 70 με at 10 and 20°C, and 300 με at 10°C.

The fatigue analysis in terms of ASTM D method is also displayed in Figure 8.21 showing a similar fatigue behaviour to that in Figure 8.19. There is decrease with some overlapping due to ageing.

Epps and Monismith, 1972 indicated that the effect of asphalt hardness on fatigue behaviour can significantly be considered due to its effect on asphalt mixture stiffness. In general, at a specific stress level in the controlled stress test as the asphalt hardness is increased, the stiffness of asphalt mixture is

increased. Therefore, a large increase in the number of cycles to fracture may be expected. On the other hand, the reverse will be expected in the controlled strain method of loading. Moreover, Kirk, 1967 has suggested from the controlled strain test results on a range of asphalt mixtures, that the constant strain fatigue at 1 000 000 load applications is independent of asphalt hardness for 50 to 200 asphalt penetration grades. In a more extensive study on aged asphalt mixtures with a range in binder penetrations from different crude sources, Santucci and Schmidt, 1969 found that fatigue life in the controlled strain tests is dependent upon asphalt hardness where the softer the asphalt binder the longer the fatigue life.

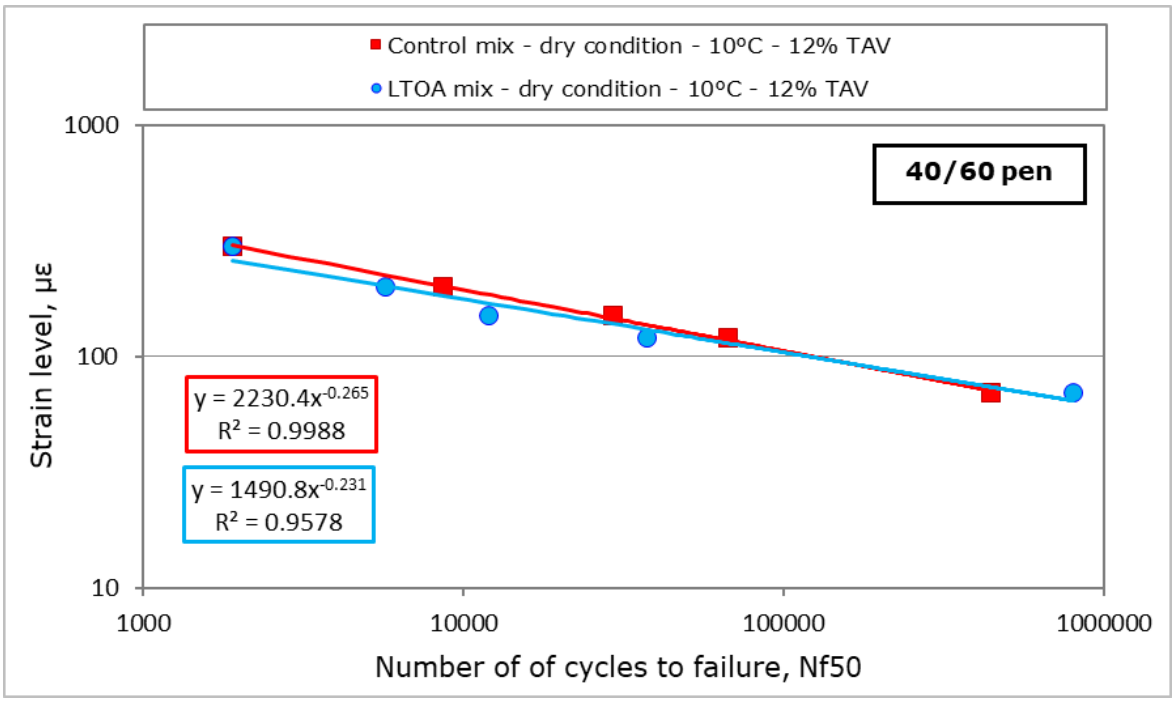



Figure 8.19: Ageing (LTOA) effect on fatigue life at 10°C.

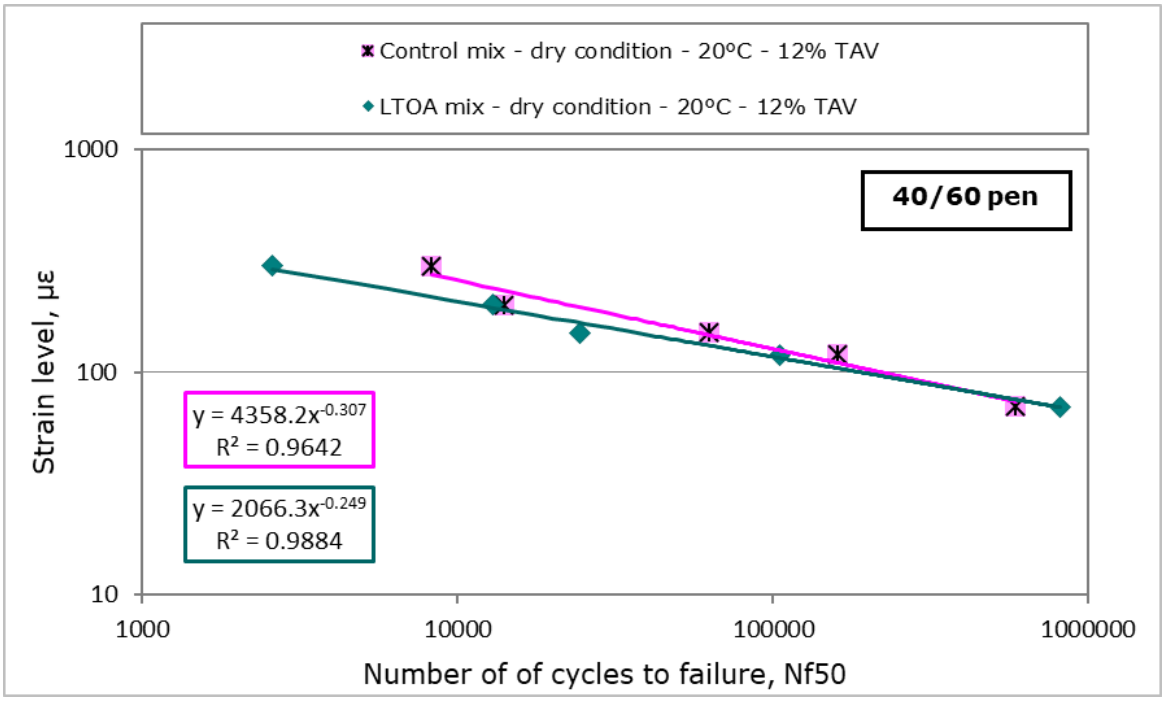



Figure 8.20: Ageing (LTOA) effect on fatigue life at 20°C.

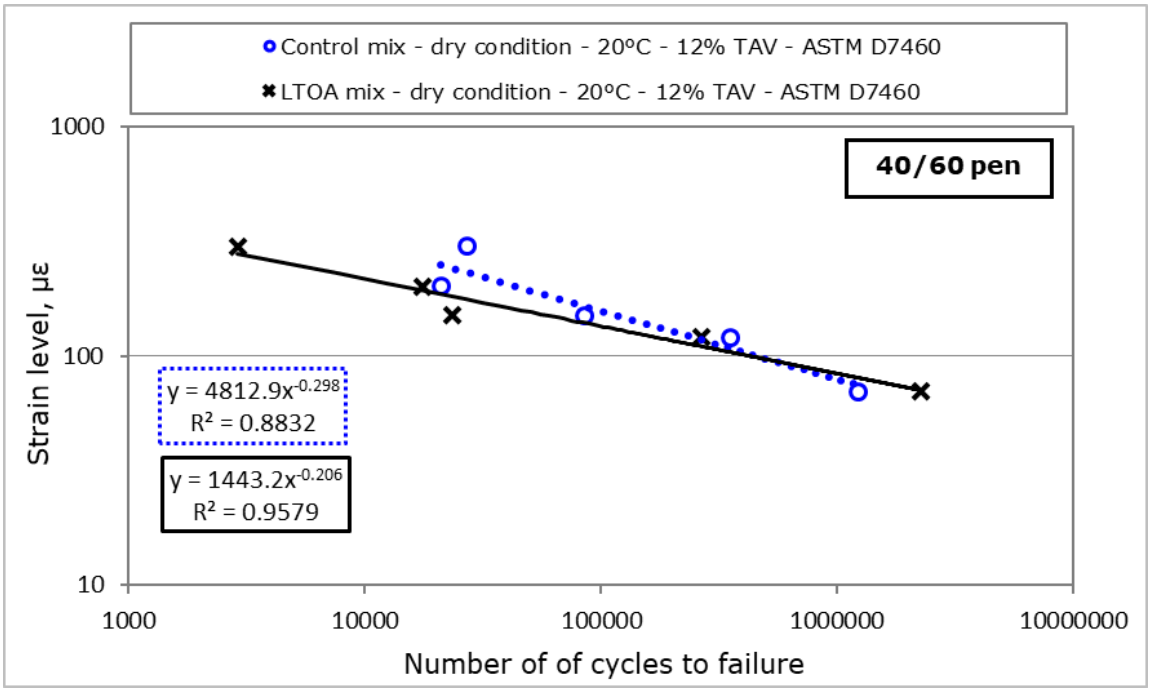



Figure 8.21: Ageing (LTOA) effect on fatigue life at 20°C – ASTM D 7460.

### 8.4.5 Combined effect of ageing and moisture conditioning

The fabricated asphalt mixtures have been exposed to moisture and ageing conditions displayed in Table 8.2 and tested by the 4-PB machine in controlled strain method. Figures 8.22 and 8.23 show the fatigue performance ($N_{f50}$) under this combination at 10 and 20°C compared to that of dry control mixtures. In general, it was observed that the fatigue life of aged mixtures has generally improved at 10 and 20°C when asphalt mixtures exposed to moisture conditioning. In particular, moisture conditioning caused an increase in $N_{f50}$ of aged mixtures in the range of 120 to 200 με at 10°C and in the range of 120 to 300 με at 20°C compared to $N_{f50}$ of dry aged mixtures. The reason of this increased $N_{f50}$ might be attributed to the increased flexibility of aged specimens due to moisture. However, no significant change was highlighted in the Ageing Index when dry aged mixtures were exposed to moisture as shown in Table 8.3 which is in the same line with results presented earlier in Chapter 6. Lu and Harvey, 2008 found that the moisture conditioning increased the fatigue life of stiffer specimens treated with hydrated lime instead of decreasing even for the specimens that have been preconditioned at 60°C.

Furthermore, Figure 8.24 displays the fatigue life resulting from applying the ASTM D 7460 analysis. Noticeably, there is a change in the slope of fatigue line of immersed aged mixtures in comparison to that of dry aged mixture shown in Figure 8.21. It was also found that this analysis showed a similar increase in $N_{f50}$ of immersed aged mixtures compared to that of dry aged mixtures.

Table 8.3: Ageing Index.

| **Temperature** | **Dry Ageing Index** (Stiffness of dry aged mix/ Stiffness of dry control mix) | **Wet Ageing Index** (Stiffness of wet aged mix/ Stiffness of dry control mix) |
|---|---|---|
| 10 | 1.317 | 1.319 |
| 20 | 1.751 | 1.771 |

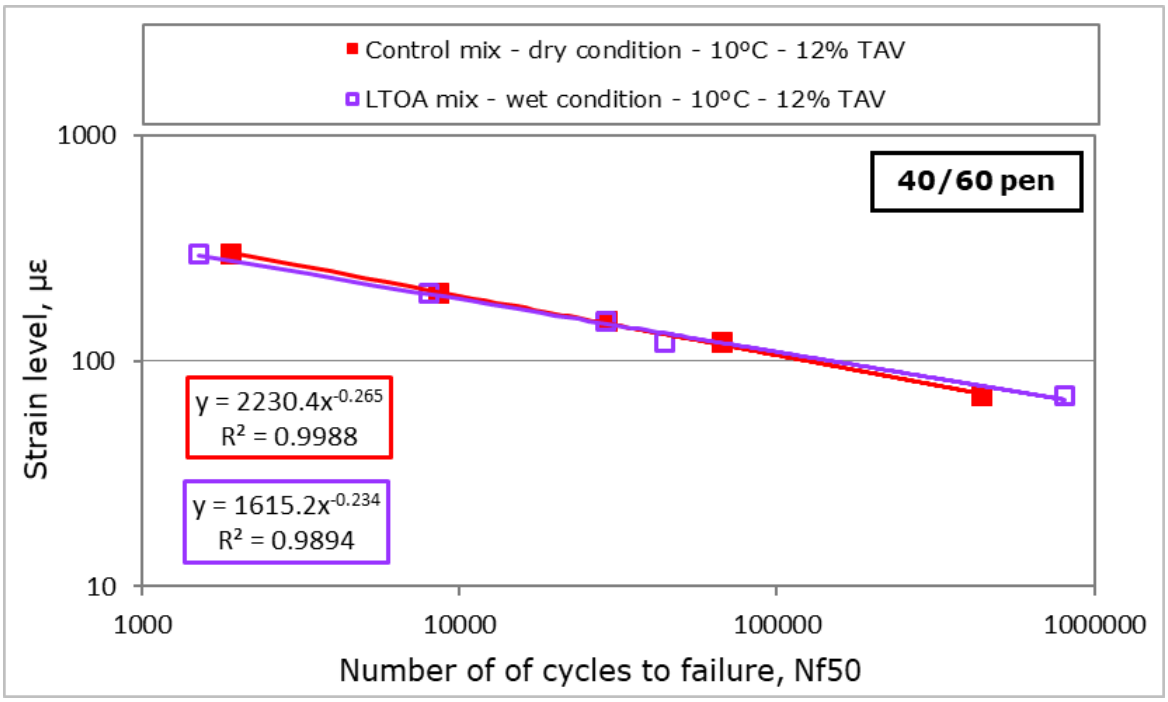



Figure 8.22: Combined effect of moisture and ageing on fatigue life at 10°C.

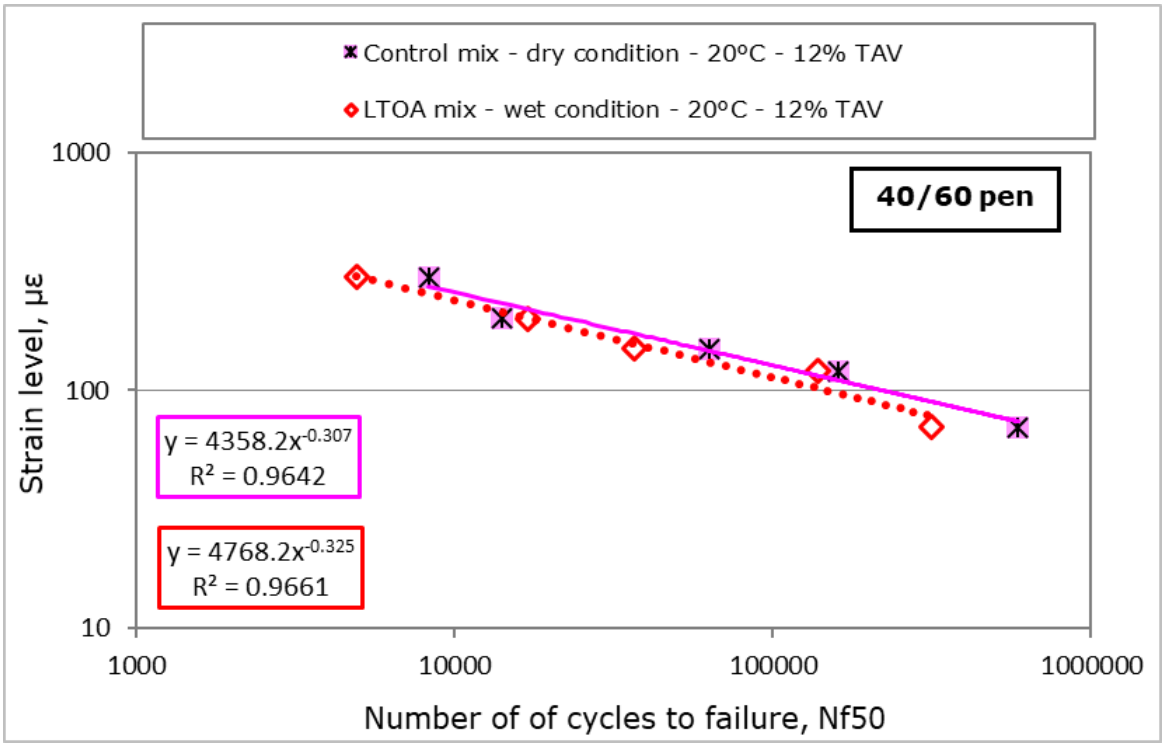



Figure 8.23: Combined effect of moisture and ageing on fatigue life at 20°C.

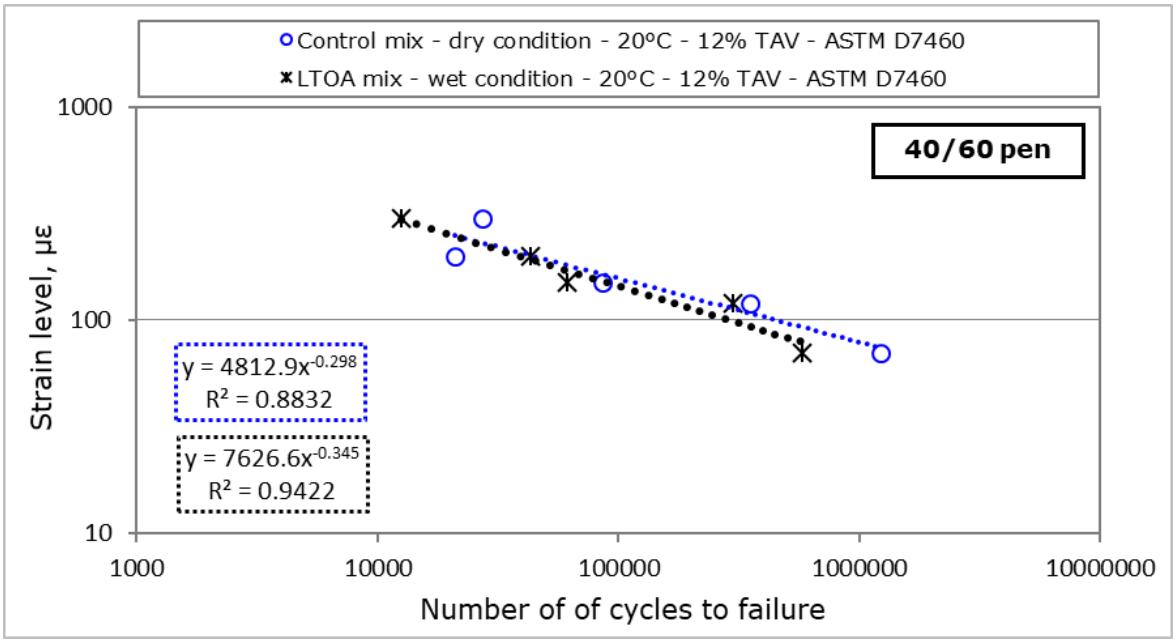



Figure 8.24: Combined effect of moisture and ageing on fatigue life at 20°C – ASTM D 7460.

## 8.5 Effect of fatigue analysis methods

As mentioned earlier, two fatigue analysis methods are used in this chapter. Firstly, the traditional phenomenological approach ($N_{f50}$) which is more extensively used. Secondly, limited use in accordance with ASTM D 7460. The analysis was conducted as shown earlier in Figure 8.5. Samples for both analysis methods is presented in Figure 8.25. Table 8.4 shows a comparison between the numbers of cycles to failure resulting from both methods. Asphalt mixtures exposed to conditions presented in Table 8.2 includes two binder penetrations; 40/60 pen (main binder) and 100/150 pen (limited use). Two testing temperatures were applied to specimens. A range of strain levels, 70-300 με were also applied to 40/60 pen mixtures at 20°C and only 200 με was applied to other mixtures as shown in Table 8.4. It can be observed that differences between the two methods where ASTM D 7460 has predominantly produced more number of cycles to failure than the traditional method $N_{f50}$. However, these differences become less at high strain levels.

The main reasons for the differences in the number of cycles to failure shown in Table 8.4 can be attributed to two points. First, the different concept of the two methods where the traditional method $N_{f50}$ does not try to find the location at

which the crack is initiated as in ASTM D 7460. The second reason which might be more important, is sensitivity to the initial stiffness of the specimen. In the phenomenological method, the failure point is directly defined as the point at which 50% of the measured initial stiffness occurs and therefore it is sensitive to the initial stiffness modulus. On the other hand, ASTM method uses the normalised stiffness modulus which is effectively defined as the stiffness ratio of the modulus ($S_i$) at any cycle ($N_i$) to that measured initially ($S_0$). In spite of the normalised stiffness modulus being used in ASTM D 7460 method, the definition of the peak point will be identical irrespective of whether the normalised or the actual stiffness modulus is used. Accordingly, this method is not sensitive to the initial modulus (Rowe et al., 2012).

The peak in the dissipated energy ratio approach appears to be the best method to define where micro-cracks have propagated and merged to form a macro-cracks among different procedures trying to define the same location in a specimen (Ajideh et al., 2010). The main advantage of the ASTM D 7460 method developed upon the peak in the dissipated strain energy approach is that failure point can be defined by a simple and reproducible parameter. This parameter could be notated as S.n (stiffness multiplied by number of load cycles) peak at the point where a significant change in the dissipated energy per loading cycle occurs. In this method the peak is basically defined as the data point which produces the maximum value with no smoothing applied to the data. However, an alternate method of defining the peak, the 6-order polynomial fitting, can also be applied for some smoothing of the data and possibly for a better definition of the maximum value by removing any spikes (Rowe, 1993, 1996, Rowe et al., 2012).

Finally, it was also found that the concept of ASTM D 7460 is compatible with ASU method ($SR=N_i*S_i/S_0$) as explained earlier in Chapter 7 because both methods were developed based on Rowe's failure definition (Rowe, 1993, Rowe, 1996).

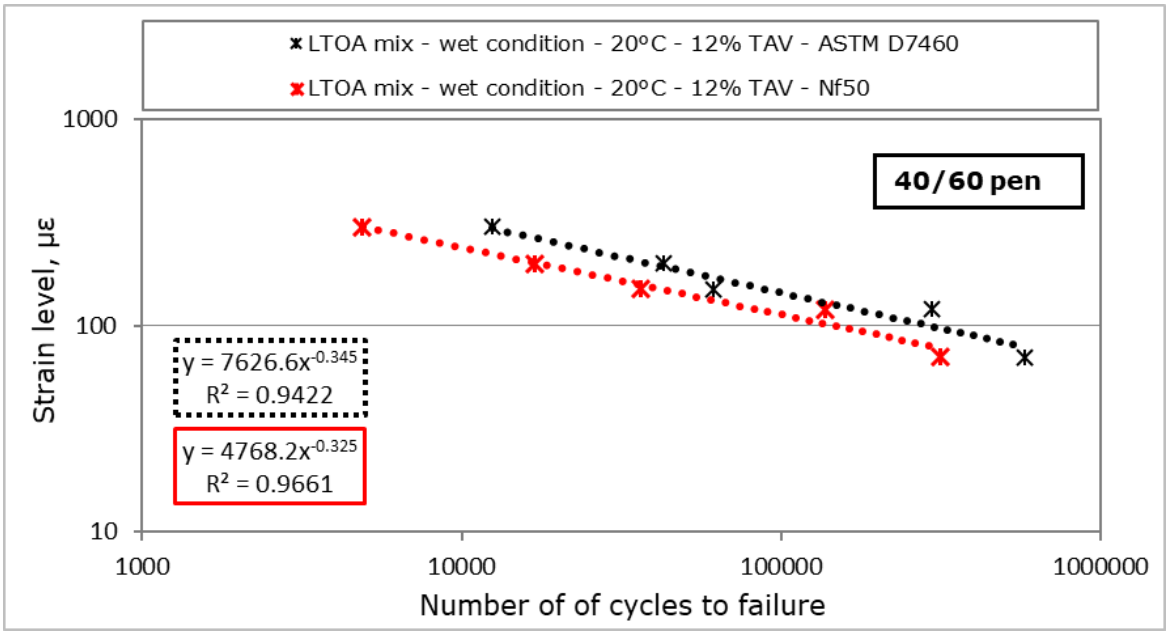



Figure 8.25: A comparison of phenomenological (Nf50) and ASTM D 7460 fatigue analysis methods.

Table 8.4: A comparison of phenomenological ($N_{f50}$) and ASTM D 7460 fatigue analysis methods.

| Mixture condition | | | Control dry | | Control wet | | LTOA dry | | LTOA wet | |
|---|---|---|---|---|---|---|---|---|---|---|
| Used Pen | T, °C | με | $N_{f50}$ | ASTM D 7460 | $N_{f50}$ | ASTM D 7460 | $N_{f50}$ | ASTM D 7460 | $N_{f50}$ | ASTM D 7460 |
| 40/60 | 20 | 70 | 588500 | 1221000 | 266500 | 2286000 | 816500 | 2242000 | 314500 | 576500 |
| | | 120 | 161000 | 351500 | 65000 | 83000 | 105500 | 265500 | 138000 | 297500 |
| | | 150 | 63000 | 85500 | 45000 | 99000 | 24500 | 23500 | 36500 | 61500 |
| | | 200 | 14000 | 21000 | 17000 | 18000 | 13000 | 17500 | 17000 | 43000 |
| | | 300 | 8300 | 27000 | 4200 | 4200 | 2600 | 2900 | 4900 | 12500 |
| 40/60 | 10 | 200 | 8600 | 9300 | 7700 | 10500 | 5700 | 29000 | 8000 | 20500 |
| 100/150 | 20 | 200 | 25000 | 61000 | 53000 | 163000 | 13000 | 16500 | 29000 | 28000 |
| 100/150 | 10 | 200 | 17500 | 37500 | 13000 | 12500 | 19000 | 51000 | NA | NA |

## 8.6 Effect of binder penetration grades

From the comparison between asphalt mixtures of 40/60 and 100/150 pens at 200 με and 10 and 20°C shown in Table 8.6, the soft binder mixtures of 100/150 pen produced the greater number of cycles to failure in most circumstances. The reason might be attributed to the relationship between the stiffness and hardness of asphalt mixtures as explained earlier. However, caution should be taken with soft asphalt mixtures to avoid digging problem of the clamps inside the tested specimen where the confining force must be considered. Therefore testing these mixtures at 10 or 15°C is recommended more than at 20°C.

## 8.7 Effect of fatigue testing method

One of the aims from developing the ITFT in strain controlled method was to directly compare the results of ITFT with that of other tests such as flexural testing methods (Maggiore, 2014). In this work, a comparison takes place between two different fatigue testing methods; 4PB and ITFT. Both methods were applied in controlled strain mode of loading to asphalt mixtures manufactured with 40/60 pen and exposed to the same testing conditions presented in Table 8.2. A spectrum of 70-300 με were applied to prismatic beams and 120-400 με were applied to cylindrical cores specimens. The traditional method was used to find the number of cycles to failure, $N_{f50}$. Figures 8.26 to 8.29 display this comparison at 20°C for different testing conditions.

Despite the fatigue characterisation of immersed control mixtures showing a relative compatible result between the fatigue lines of both methods, other circumstances have resulted in different slopes of fatigue lines. At the same applied strain; 120 150, 200, and 300 με, the 4PB method has generally produced the greatest number of cycles to failure as shown in Figures 8.26 and 8.27 for dry and wet control mixtures. On the other hand, ITFT has produced the greatest value at some failure points of other circumstances (dry and wet aged mixtures) as shown in Figures 8.28 and 8.29.

The dissimilarities between fatigue results of ITFT and 4PB methods can be attributed to the differences in the specimens shape, size, type of testing method; indirect tensile (ITFT) and flexural (4PB), the 0.4 second rest period in ITFT versus no rest period included in 4PB test, pulse type; haversine in ITFT

versus sinusoidal in 4PB. However, the ANOVA test indicates that no statistical difference between the slopes of fatigue lines of both methods was found.

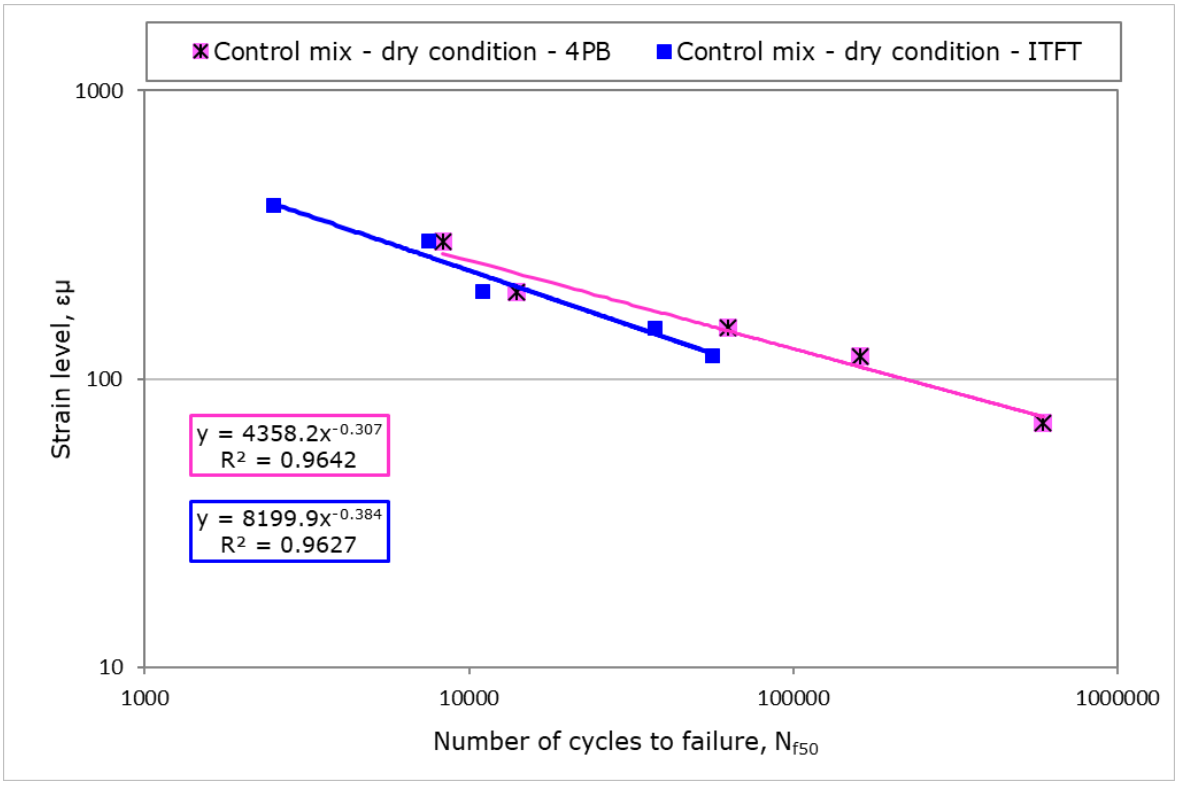



Figure 8.26: A comparison between 4PB and ITFT for dry control mixtures.

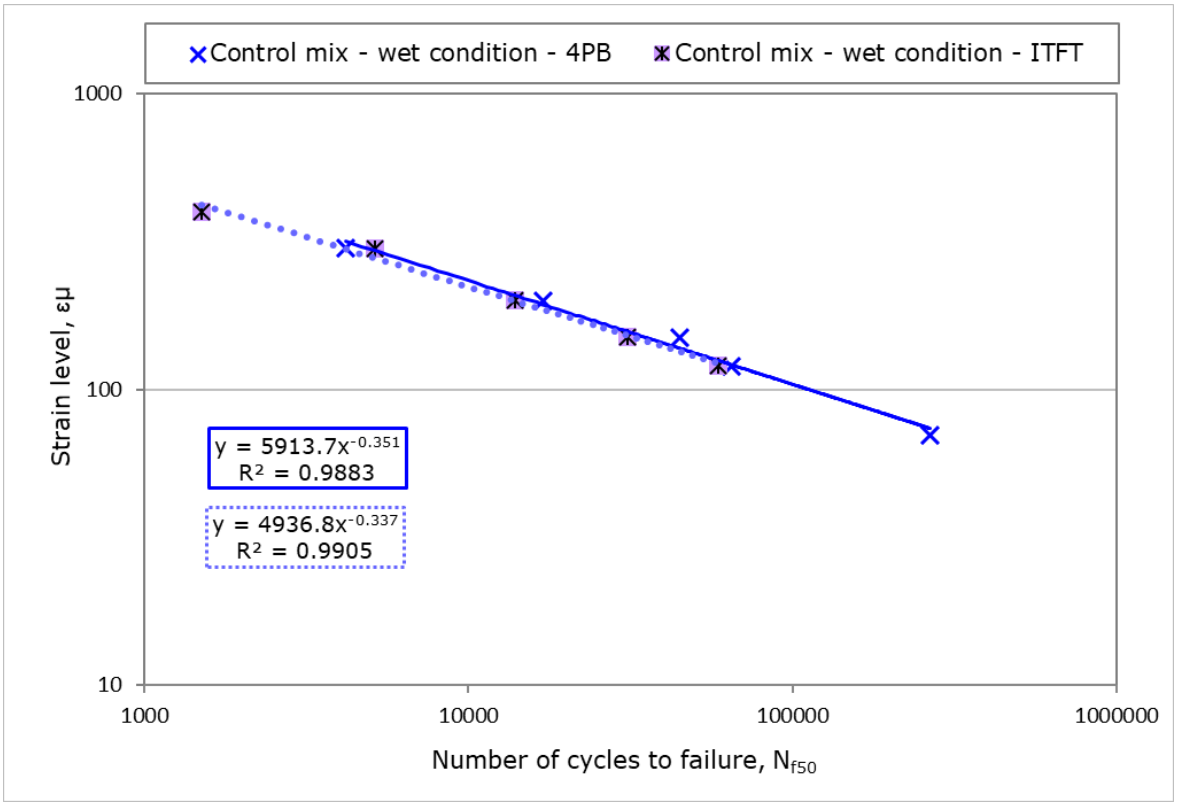



Figure 8.27: A comparison between 4PB and ITFT for wet control mixtures.

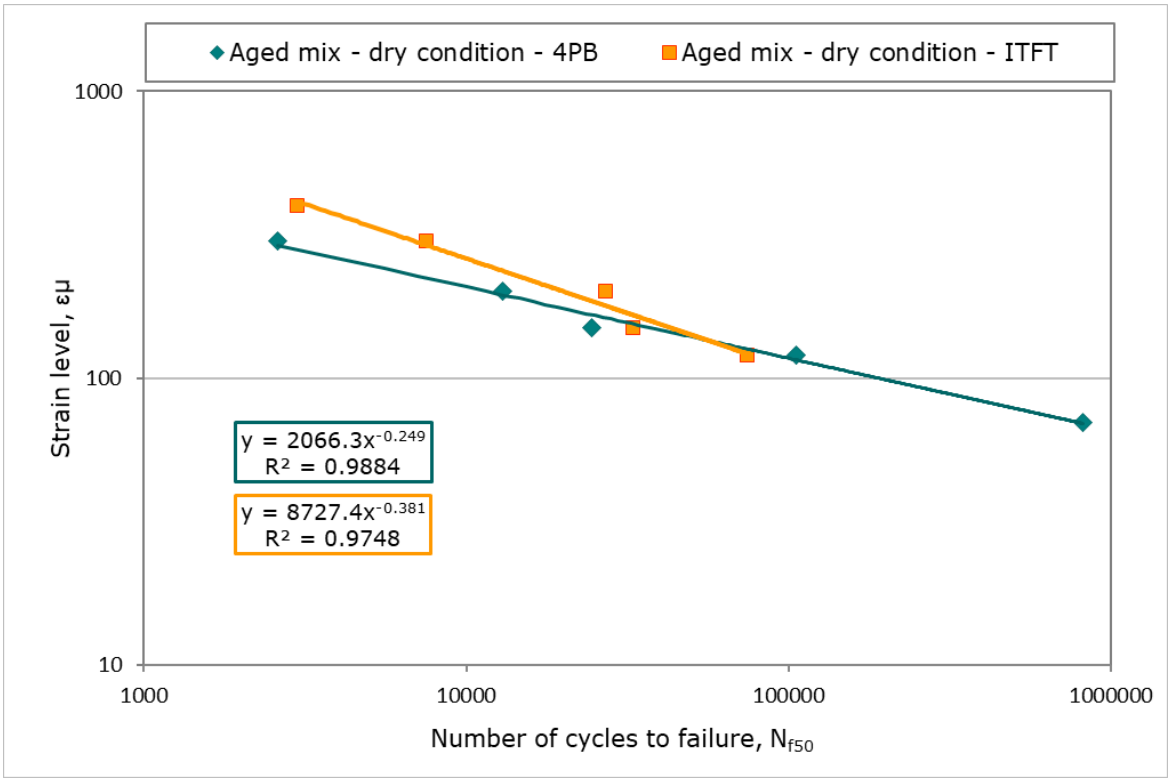



Figure 8.28: A comparison between 4PB and ITFT for dry aged mixtures.

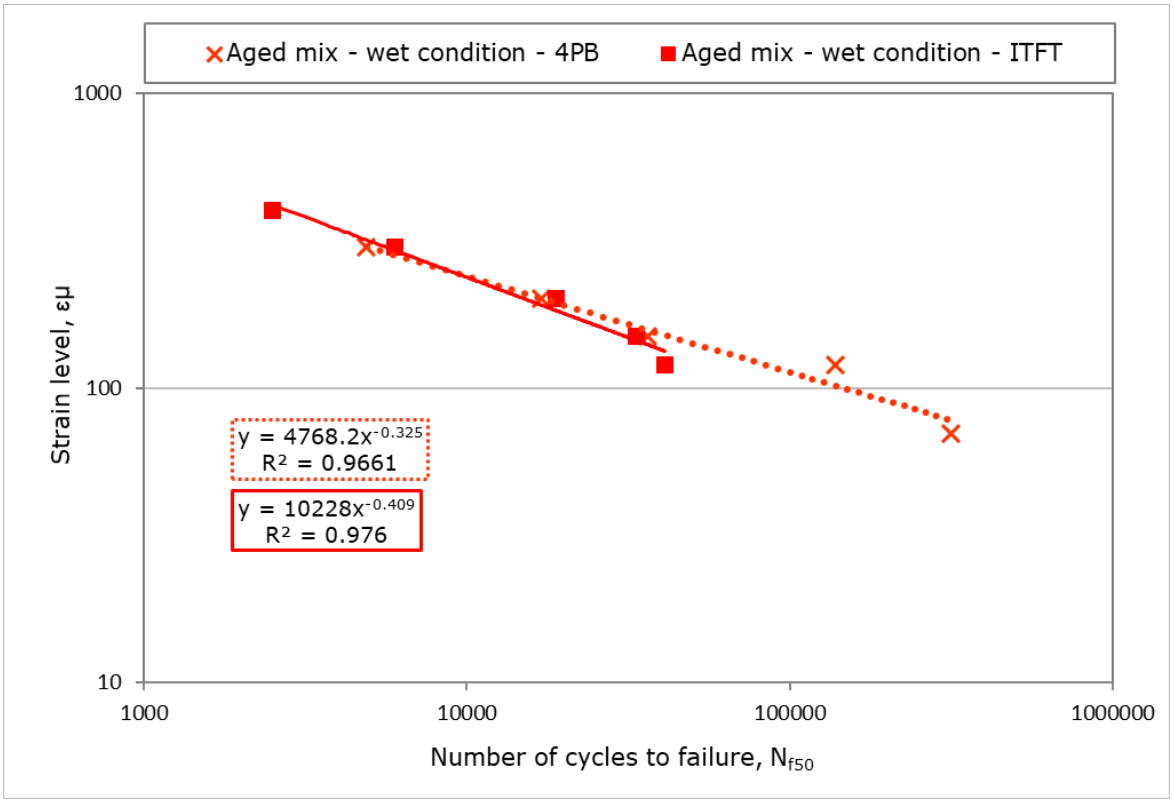



Figure 8.29: A comparison between 4PB and ITFT for wet aged mixtures.

## 8.8 Summary

In this work, an attempt was made to answer an important question, to what extent the combination of stiffness increase due to ageing or due to temperature decrease and the stiffness reduction because of moisture damage can affect the fatigue damage. Different testing parameters and conditions and two fatigue analysis methods were investigated. The following perspectives can be summarised:

1. Despite the observed convergence between the fatigue lines of 6 and 12% air voids content, the lower air voids content mixtures produced the more number of cycles to failure irrespective of the testing temperature, in particular, at low micro-strain levels. In addition, the resulting fatigue characterisation of this variable seems partially similar to that found by the ITFT in Chapter 7.

2. In general, it was found that decreasing the testing temperature from 20 to 10°C causes an increase in the number of cycles to failure regardless of air voids content and the mixture condition if it is control or aged or wet. However, observable convergence between the two lines at 70 and 120 με was noticed. As expected, the decrease of testing temperature have increased the stiffness modulus of asphalt mixtures and in turn reduced the fatigue life. In addition, an obvious change in the slope of fatigue line at 10°C of wet mixtures (control and aged) was highlighted regardless of the slight convergence between the fatigue lines. However, the resulting fatigue characterisation of this variable seems inconsistent with that found by the ITFT in Chapter 7.

3. It was found that moisture conditioning has reduced the fatigue life of control asphalt mixtures but it has less effect at 10 than at 20°C.

4. In general, there is also some fatigue life decrease due to ageing (LTOA). However, it has less effect at 10 than at 20°C. The two fatigue lines are more compatible at 10 than at 20°C.

5. The fatigue life of aged mixtures has generally improved at 10 and 20°C when asphalt mixtures exposed to moisture conditioning. In particular, it was observed that moisture conditioning caused some increase in $N_{f50}$ of aged

mixtures in the range of 120 to 200 με at 10°C and in the range of 120 to 300 με at 20°C.

6. In general, ASTM D 7460-10 has predominantly produced more number of cycles to failure than the traditional method $N_{f50}$. However, these differences become less at high strain levels. The main reasons can be attributed to first, the different concept of the two methods where the traditional method ($N_{f50}$) does not try to find the location at which the crack is initiated. While ASTM D 7460 was based upon the peak in the dissipated strain energy approach. The second reason is the sensitivity to the initial stiffness of the specimen. The failure point of phenomenological method is directly defined in terms of 50% reduction of the initial stiffness and therefore it is sensitive to the initial stiffness modulus. On the other hand, ASTM method is not sensitive to the initial modulus because the actual stiffness modulus is used to define the failure (peak) point.

7. Investigating the effect of binder penetration grades on the fatigue cracking resistance at 200 με and at 10 and 20°C have generally shown that the softer the asphalt binder the longer the fatigue life. However, this finding was not supported in some circumstances (ageing).

8. Despite the fatigue characterisation of wet control mixtures showing a relative compatibility between the fatigue lines of 4PB and ITFT methods, other circumstances have resulted in different slopes of fatigue lines. At the same applied strain; 120, 150, 200, and 300 με, the 4PB method has generally produced the greatest number of cycles to failure for dry and wet control mixtures. On the other hand, ITFT has produced the greatest value at some failure points of other circumstances; dry and wet aged mixtures.

# Chapter Nine: Evaluation of Environmental Factor Effects on Healing Susceptibility of Asphalt Mixtures using the 4-PB Test and ITFT

## 9.1 Introduction

To ensure a proper design period of in-service pavement, it is important to understand the spontaneous behaviour of asphalt mixtures during rest periods between successive applications of traffic loading. This behaviour is termed recovery potential or self-healing potential of asphalt mixtures.

The healing susceptibility of asphalt mixtures is an important property for the development of sustainable asphalt pavements. Recently, lots of research has demonstrated this asset of bituminous materials (Ayar et al., 2015). Rest periods, ageing, temperatures, air voids, and binder grades are the most important factors that can affect this property (Mehrara and Khodaii, 2015).

Some previous studies at The University of Nottingham investigated the effect of rest period on the response of asphalt mixtures to the compound-loading conditions using a rotating bending fatigue machine (Mc Elvaney and Pell, 1973). They referred to the importance of rest periods between repeated loading cycles. They also indicated that these rest periods will be beneficial if the damage incurred between them does not exceed a certain level. Moreover, Oliveira et al., 2009 carried out four-point bending fatigue tests with rest periods between loading cycles to establish a shift factor for grouted macadams. Maggiore, 2014 also indicated that the number of cycles to failure increases if resting time period increases.

More previous studies were carried out in different places to study the effect of rest period in combination with other factors on the healing potential of asphalt mixtures (Bonnaure et al., 1982, Hsu and Tseng, 1996, Carpenter and Shen, 2006, Castro and Sanchez, 2006, Mamlouk et al., 2012, Souliman et al., 2013).

Finally, Mehrara and Khodaii, 2015 carried out cyclic IDT tests at different testing temperatures on dry and moisture conditioned asphalt mixture specimens exposed also to ageing to investigate the potential damage recovery of these mixtures using different rest periods. It was found from NDCSE

(normalized dissipated creep strain energy) analysis that rest time is the most influential parameter followed by ageing and then testing temperatures (Mehrara and Khodaii, 2015).

## 9.2 Healing tests

No standard procedure for testing the influence of rest periods was presented in the literature. However, Mamlouk et al., 2012 presented a typical curve of stiffness ratio versus application of loading cycles for tests with and without rest period as shown in Figure 9.1.

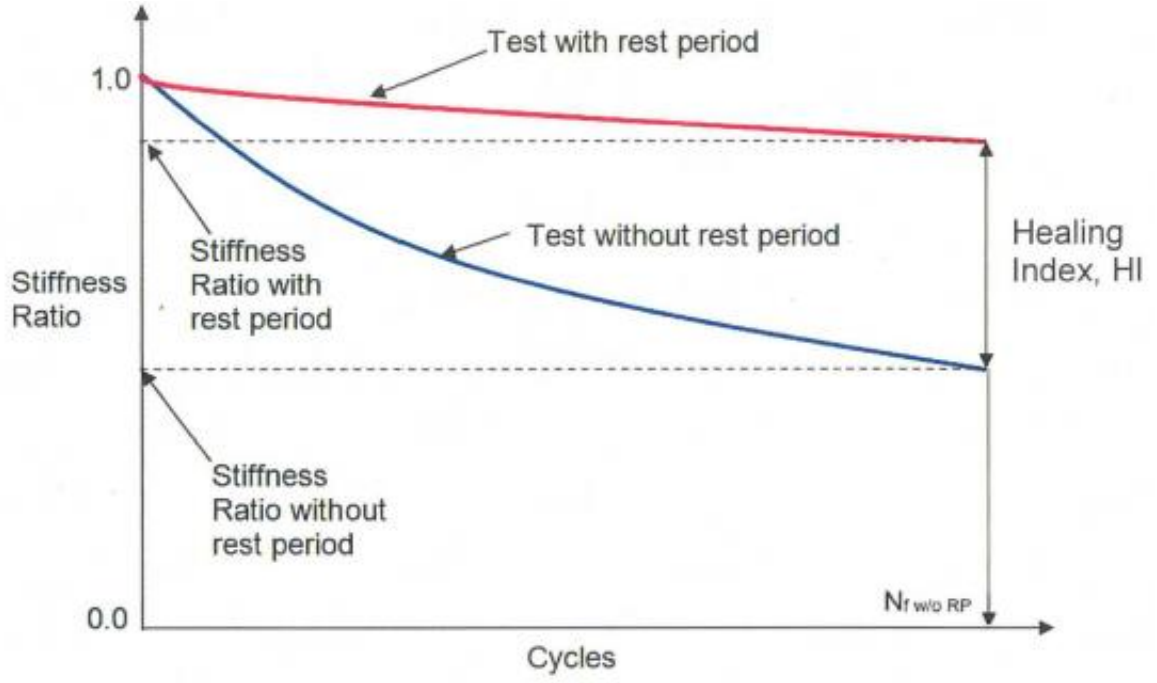



Figure 9.1: A typical curve of stiffness ratio versus application of loading cycles for tests with and without rest period (Mamlouk et al., 2012).

In addition, Mamlouk et al., 2012 indicated that it is very important to use a sinusoidal controlled deflection such as the AASHTO T-321 test to make a fair comparison and obtain accurate results from carrying out tests with and without rest periods. Zeiada et al., 2018 also concluded that rest period seems to have a remarkable increase in the fatigue life resulting from the intermittent sinusoidal fatigue tests. However, less rest period effect was also observed for haversine fatigue tests.

This work aims to study the effect of rest periods in combination with other important environmental factors, ageing and/or moisture damage. The 4PB and NAT machines have been used to carry out the sinusoidal flexural tests and haversine modified ITFT. Both were carried out in controlled strain mode.

## 9.3 Healing tests using the 4-PB machine

Specific four point bending fatigue tests with rest periods between loading applications were carried out by writing a detailed profile (See Appendix A-2). Then the results were compared with that of traditional (without rest periods) four point bending fatigue tests. Two different binder grades were used in asphalt mixtures; 40/60 pen and 100/150 pen. The applied environmental conditions to these mixtures are presented in Table 9.1. Healing tests were undertaken at 10 Hz, 10˚C and 200με. Table 9.2 shows a summary of loading time and rest time combinations chosen for healing tests by 4PB.

After some trials, it was concluded that it is not practical to apply short loading times or a small number of loading cycles to the investigated mixtures when using the 4PB machine. As shown in Figure 9.2, there is an obvious scatter in the measurement of stiffness modulus during loading cycles. It is well known that the testing machine needs a specific number of cycles for a proper measurement of the initial stiffness modulus depending on loading frequency. For instance, the 4PB and 2PB machines requires 100 loading cycles to measure the stiffness modulus at 10 Hz. As a result, it was decided to increase the applied number of loading cycles to 100 or more.

Two healing indicators were used to evaluate the effect of different parameters. First, Healing Ratio (HR) was calculated from Equation 9.1 at two different stages; at 50% of initial stiffness (failure criterion) and at end of the test (18000 loading cycles equals to 30 minutes of loading time). However, some tests endured more than 18000 cycles to reach the designated failure criterion ($N_{f50}$). Conventionally, fatigue failure is defined as the point when the stiffness modulus has decreased to 50% of its initial value (SHRP-A-404, 1994).

In addition, Healing Index (HI) was calculated from Equation 9.2 at 50% of initial stiffness (failure criterion).

$$HR = SR_{w/RP} - SR_{w/o\ RP} \quad 9.1$$

Where,

$SR_{w/RP}$= Stiffness ratio with rest period,

$SR_{w/o\ RP}$= Stiffness ratio without rest period.

$$HI = Nf_{w/RP} / Nf_{w/o\ RP} \quad 9.2$$

Where,

$Nf_{w/RP}$= Number of cycles at 50% of initial stiffness with rest period,

$Nf_{w/o\ RP}$= Number of cycles at 50% of initial stiffness ratio without rest period.

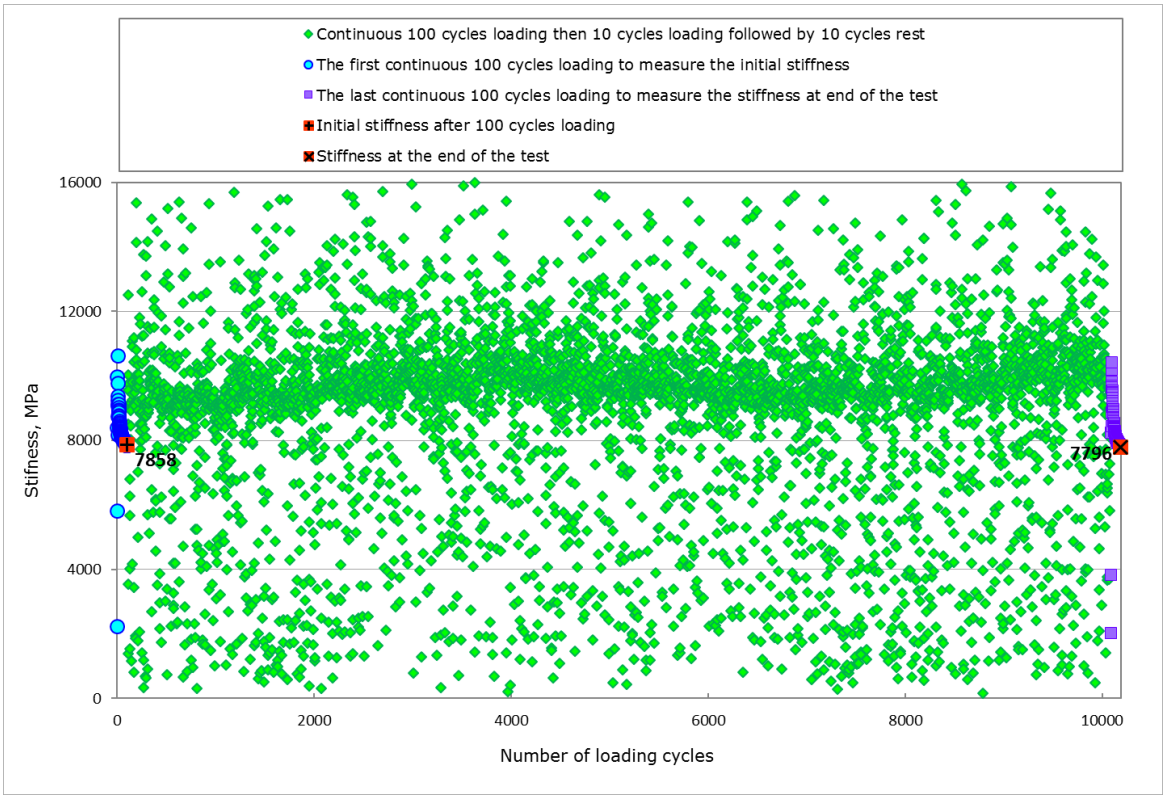



Figure 9.2: Effect of short loading time on initial stiffness modulus.

Table 9.1: Summary of investigated mixture conditions for healing test by 4PB (One or two replicates were used to find HR and HI).

| **Mixtures exposed to specific conditions** | **Mixture manufactured with binder grade** | |
|---|---|---|
| | **40/60** | **100/150** |
| Control mixture, dry prismatic beams | ✓ | ✓ |
| Control mixture, immersed prismatic beams in water according to BS EN method as detailed in Table 4.5. | ✓ | ✓ |
| LTOA mixture, dry prismatic beams (before compaction, the loose mixture subjected to 135°C for 4 hours then, the compacted mixture subjected to 85°C for 120 hours). | ✓ | - |
| LTOA mixture, immersed prismatic beams (the loose mixture subjected to 135°C for 4 hours then the compacted mixture subjected to 85°C for 120 hours) in water according to BS EN method as detailed in Table 4.5. | ✓ | - |

Table 9.2: Summary of loading time and rest time combinations chosen for healing tests using the 4-PB machine.

| Test Configurations | Loading ratio= No of loading cycles ÷ No of rest period cycles | | No of loading cycles | Loading time, seconds | No of rest period cycles | Rest time, seconds | Mixture manufactured with binder grade | |
|---|---|---|---|---|---|---|---|---|
| | | | | | | | 40/60 | 100/150 |
| **A** | Traditional test without rest period (continuous loading) | | | | | | ✓ | ✓ |
| **B** | 1 | | 100 | 10 | 100 | 10 | ✓ | ✓ |
| **C** | 1 | | 600 | 60 | 600 | 60 | ✓ | ✓ |
| **D** | 0.1 | | 600 | 60 | 6000 | 600 | ✓ | - |
| **E** | 0.033 | | 600 | 60 | 18000 | 3600 | ✓ | - |
| **F** | Non uniform | 1.0 | 600 | 60 | 600 | 60 | ✓ | - |
| | | 0.1 | | | 6000 | 600 | | |
| | | 0.033 | | | 18000 | 3600 | | |
| **G** | 1 | | 6000 | 600 | 6000 | 600 | ✓ | - |

### 9.3.1 Results of healing tests using the 4-PB machine

#### 9.3.1.1 Effect of air voids content

The influence of air voids was only investigated for control mixtures of 40/60 pen at two air voids contents of 6 and 12%. Figures 9.3 to 9.5 show samples of the air voids content effect on stiffness ratios with and without rest periods resulting from applying the loading conditions of tests A versus B, C, and D respectively.

Table 9.3 displays the results of HR and HI from carrying out test A versus tests B, C, D, E, F, and G respectively.

Various points can be highlighted from these figures and table. First, from Figure 9.3 and Table 9.3, the lower air voids mixture showed a slight increase in HR and HI at $N_{f50}$. While the higher air voids mixture had the highest HR after 18000 loading cycles. Second, from carrying out test A versus C, D, E, F, and G, there is generally obvious increase in the stiffness ratio of the 12% air voids mixture due to inclusion of different rest periods as shown in Table 9.3.

For the 6% air voids mixture, only test B was beneficial and significantly showed HR increase. Tests C, D, and F showed an unexpected damage with rest periods inclusion. Although the same damage was not obvious in test E, no significant HR increase was observed from applying the rest period. This damage might be attributed to the number of loading cycles (600 continuous loading cycles) at 10 Hz, 10°C and 200με. These testing conditions might hide the role of rest periods to be not beneficial because the resulting damage between them does exceed a certain level which prevents the recovery of 6% air voids mixtures during rest periods. Only test B compound loading conditions (100 cycles loading by 100 cycles rest) was beneficial in the case of 6% air voids content. That may reflect the importance of the applied loading time not only the rest time on the healing or recovery potential of bituminous material. As mentioned earlier, Mc Elvaney and Pell, 1973 indicated that rest periods benefit is reliant on damage incurred between rest periods. The damage should not exceed a certain level.

In summary, the damage recovery of 12% air voids mixtures was better than 6% air voids mixtures recovery. Meijide et al., 2016 reported that the maximum healing index reached by asphalt mixture was all the time better for higher air voids content mixtures than for dense asphalt. The reason for this is that more aggregates particles have broken during cracks evolution in dense asphalt mixtures. Cracks in aggregate particles can be filled by asphalt binder showing a partial healing not fully recovered.

In addition, unexpected negative values of healing indices at different stages of healing tests was highlighted in Figures 9.4, 9.5 and Table 9.3. A different section will discuss and present the possible reasons of this issue.

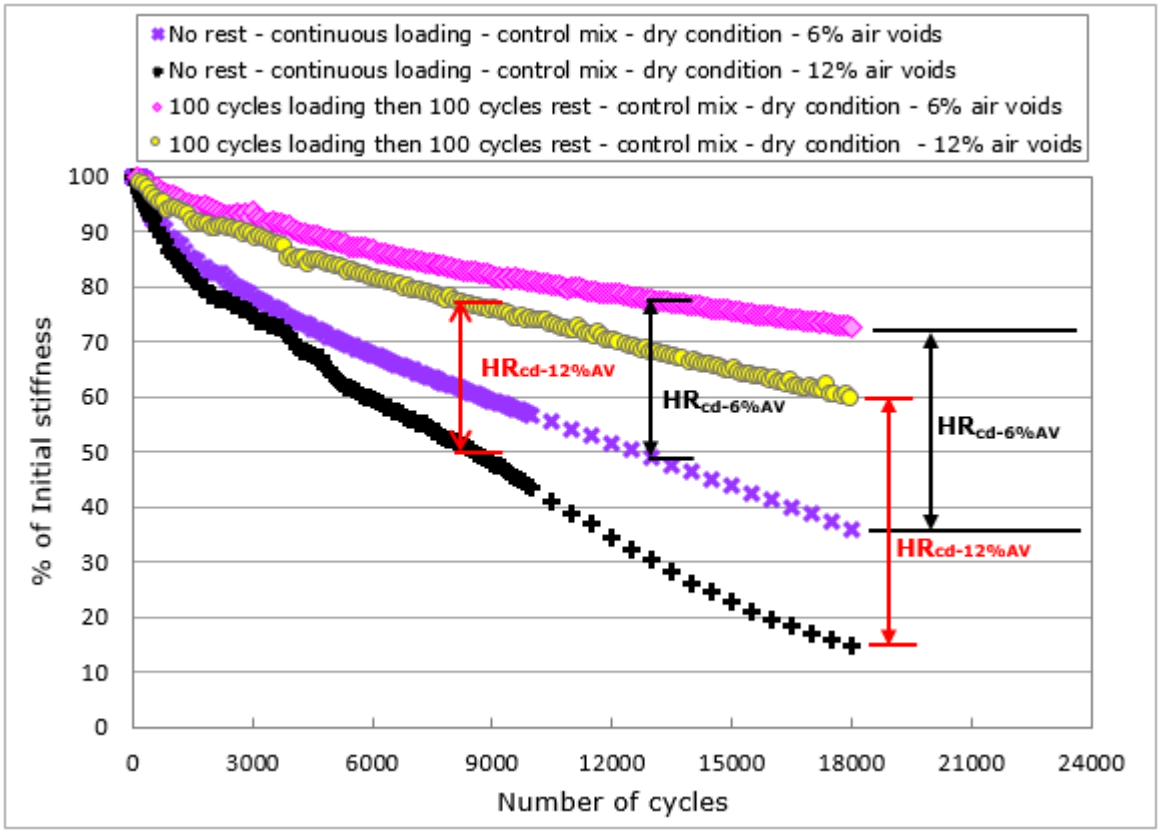



Figure 9.3: Test A versus test B of different air voids content mixtures.

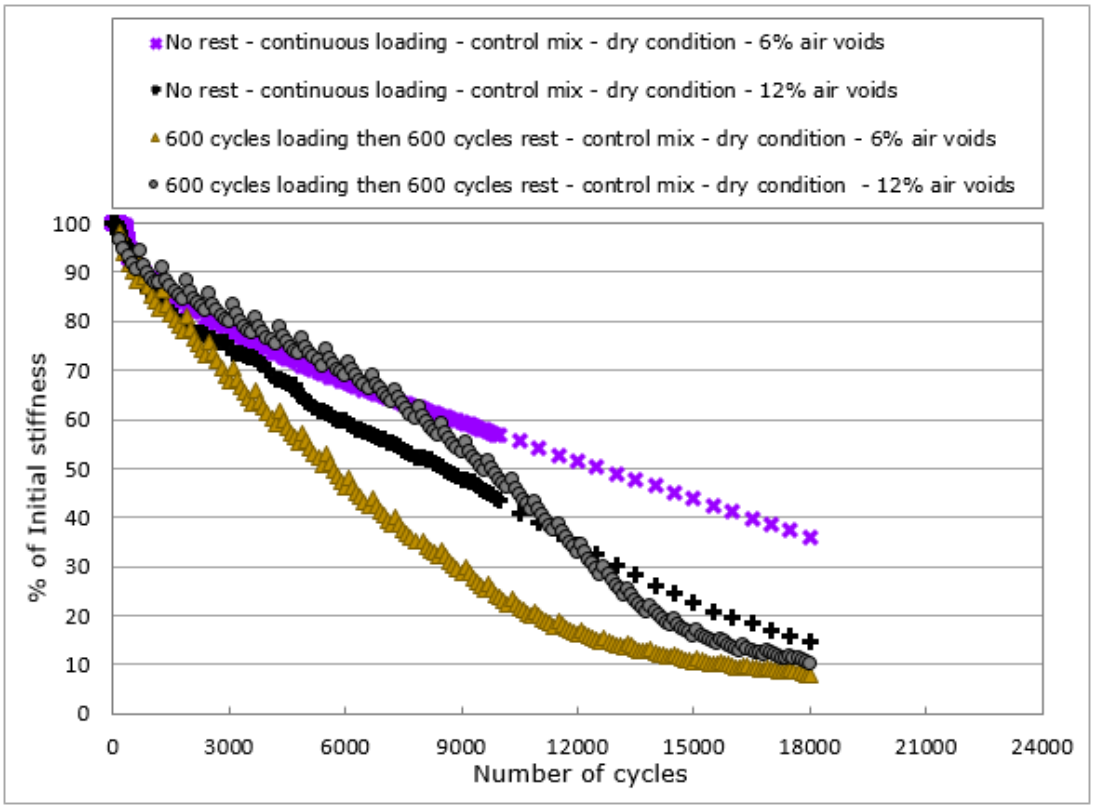



Figure 9.4: Test A versus test C of different air voids content mixtures.

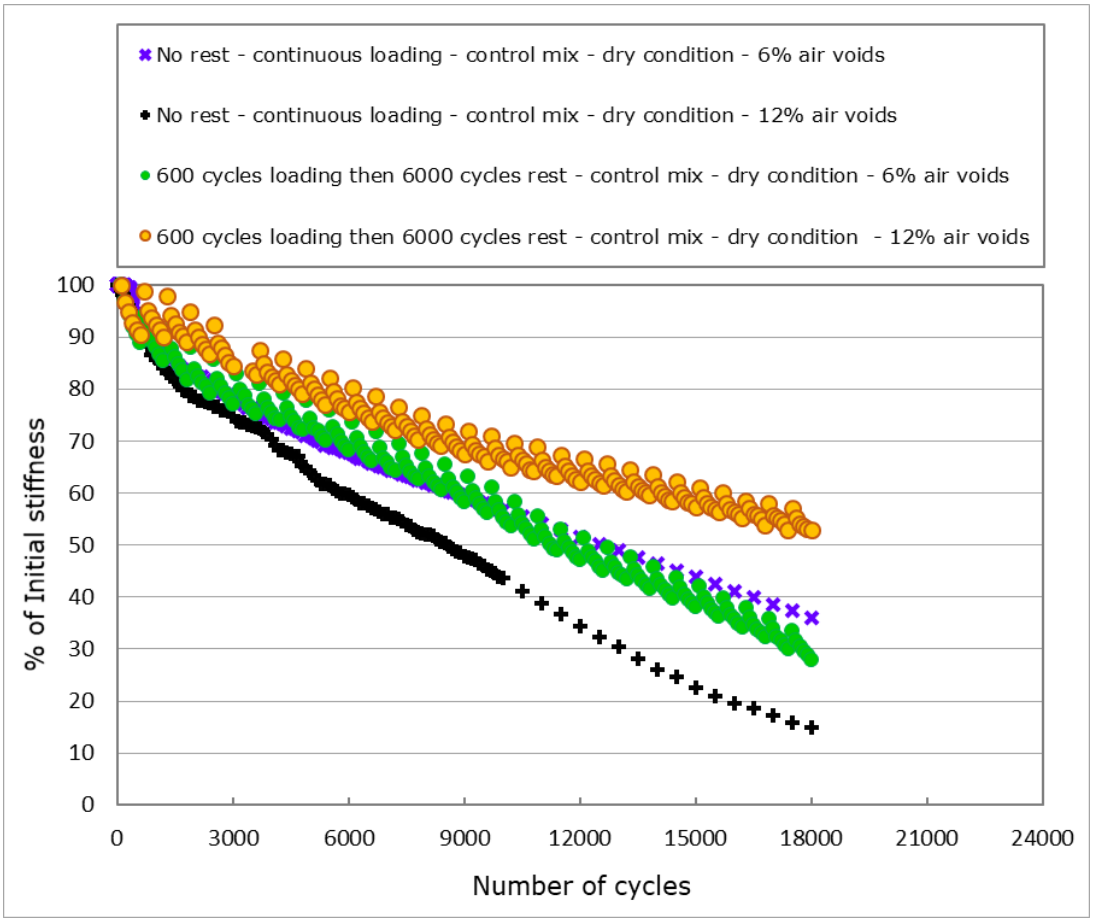



Figure 9.5: Test A versus test D of different air voids content mixtures.

Table 9.3: Effect of air voids on HR and HI results.

| **Compound-loading conditions** | **Air voids content** | |
|---|---|---|
| | **6%** | **12%** |
| **Test A** | **Reference test** | **Reference test** |
| **Test B** | | |
| HR at 50% of initial stiffness ($N_{f50}$), % | +27.7 | +26.4 |
| HR at 18000 loading cycles (30 minutes), % | +36.7 | +44.8 |
| HI at 50% of initial stiffness ($N_{f50}$) | 2.91 | 2.63 |
| **Test C** | | |
| HR at 50% of initial stiffness ($N_{f50}$), % | -19.0 | +7.7 |
| HR at 18000 loading cycles (30 minutes), % | -28.0 | -4.45 |
| HI at 50% of initial stiffness ($N_{f50}$) | 0.44 | 1.12 |
| **Test D** | | |
| HR at 50% of initial stiffness ($N_{f50}$), % | -4.34 | +21.2 |
| HR at 18000 loading cycles (30 minutes), % | -8.0 | +42.9 |
| HI at 50% of initial stiffness ($N_{f50}$) | 0.87 | 2.37 |
| **Test E** | | |
| HR at 50% of initial stiffness ($N_{f50}$), % | +0.012 | +13.0 |
| HR at 18000 loading cycles (30 minutes), % | +0.200 | +25.6 |
| HI at 50% of initial stiffness ($N_{f50}$) | 0.969 | 1.38 |
| **Test F** | | |
| HR at 50% of initial stiffness ($N_{f50}$), % | -25.1 | +8.7 |
| HR at 18000 loading cycles (30 minutes), % | -28.0 | +1.6 |
| HI at 50% of initial stiffness ($N_{f50}$) | 0.723 | 1.12 |
| **Test G** | | |
| HR at 50% of initial stiffness ($N_{f50}$), % | NA | +7.4 |
| HR at 18000 loading cycles (30 minutes), % | NA | +18.0 |
| HI at 50% of initial stiffness ($N_{f50}$) | NA | 1.28 |

### 9.3.1.2 Effect of loading and rest period times

The loading ratios can be defined as the number of loading cycles (time) divided by the number of rest period cycles (time). It is important to examine both loading time and rest period time because of their influences on damage. It was decided to select control mixtures exposed to moisture conditioning to show the influence of loading and rest period times. The reason for that is the rational behaviour of these mixtures under different loading and rest period times as shown in Figure 9.6.

HR of different compound-loading conditions was calculated at 50% of initial stiffness and at end of 18000 loading cycles (30 minutes) test. HI of the same compound-loading conditions was also calculated at 50% of initial stiffness only. HR and HI values are presented in Table 9.4. It can be seen that the best HR and HI values has resulted from carrying out tests B versus A. According to all indices shown in Table 9.4, rank 1 was occupied by the compound-loading conditions of test B. The stiffness ratio has increased by 39.1 at 50% of initial stiffness and 61% at the end of 18000 loading cycles test. It has also the highest HI. It is believed that the role of short loading time (10 seconds) is more predominate than rest time role (10 seconds) where the resulting damage allows specimens to considerably heal during rest periods. Therefore, it is not clear to observe the increase (leap up) of stiffness ratio after each rest period as shown in other curves (See the blue curve versus others).

On the other hand, test G configuration caused more damage during 6000 cycles loading (10 minutes) and therefore the initial stiffness curve occupied rank six as shown in Figure 9.6 (See the green curve versus others). This configuration resulted in the lowest values of HR and HI at 50% of initial stiffness compared to other configurations as shown in Table 9.4. However, test F rapidly caused a considerable incomprehensible decrease of initial stiffness after the 50% drop as shown in Figure 9.5 (see the purple curve). As a result, HR of test F at end of 18000 cycles loading was less than HR of test G. It was also observed that a similar decrease due to applying the compound-loading conditions of test F to other mixtures exposed to different conditions as shown in Table 9.5.

In general, Figure 9.6 refers to a reasonable order of stiffness ratio curves; B, then E, F, D, C, and G compared to the traditional reference fatigue test, A. However, there is some convergence between D and E. The four tests; E, F, D, and C have the same number of loading cycles (600) but different rest periods (30 minutes, random or non-uniform rest, 10 minutes, 1 minutes) respectively. In addition, Table 9.4 demonstrates a similar order except test F which occupied the ranking of test E in accordance with HR at 50% of initial stiffness but with more reasonable order in terms of HI; test B, then E, D, F, C and G. While test C is still occupied rank 5 due to the effect of shortest rest period (600 cycles or 1 minute) showing less damage recovery.

It is also important to refer to the change in ranking after 18000 cycles of loading. However, test B (100 cycles of loading by 100 cycles of rest) is still in rank 1 with an increase of HR of 22% compared to that at 50% drop of initial stiffness (61% - 39%). In addition, at end of 18000 cycles of loading, HR of test E was greater than HR of tests C, D, F and G. Consequently, it can be concluded that ranking the compound–loading tests based on HR may be variable through the whole test and the interval of rest periods may be less effective when the resulting damage increases. Therefore, it is not necessary that HR at 50% of initial stiffness will be equal to HR at end of the test. Except test F, HR values at end of tests are greater than HR at 50% of initial stiffness as shown in Table 9.4, which reflects the importance of rest periods in fatigue tests regardless how long they are.

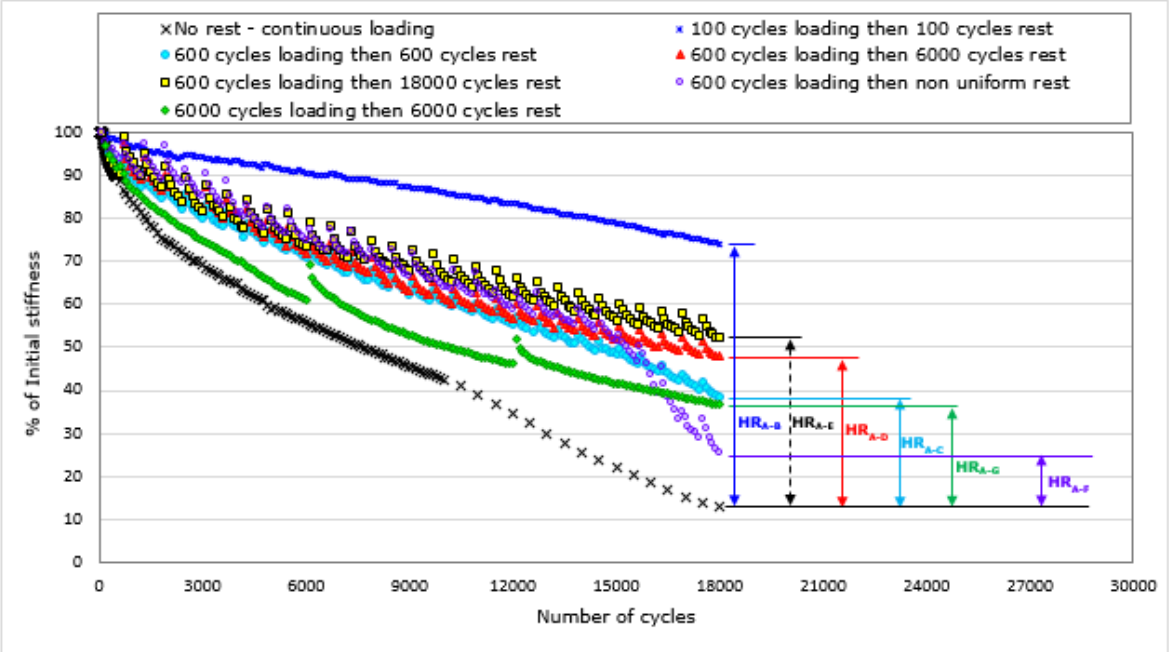



Figure 9.6: Effect of different loading and rest period times on healing ratio of control asphalt mixtures exposed to moisture conditioning.

Table 9.4: Ranking of compound-loading test conditions of different loading and rest period times based on HR and HI.

| **Test** | **HR at 50% of initial stiffness** | **Ranking of tests** | **HR at end of the test (18000 loading cycles)** | **Ranking of tests** | **Difference** $HR_{end} - HR_{50\%}$ | **HI at 50% of initial stiffness** | **Ranking of tests** |
|---|---|---|---|---|---|---|---|
| A | Reference test | 7 | Reference test | 7 | - | Reference test | 7 |
| B | 39.0 | 1 | 61.0 | 1 | 22.0 | 4.8 | 1 |
| C | 15.7 | 5 | 25.3 | 4 | 9.6 | 1.86 | 5 |
| D | 17.9 | 4 | 35.0 | 3 | 17.1 | 2.17 | 3 |
| E | 20.6 | 3 | 39.1 | 2 | 18.5 | 2.56 | 2 |
| F | 21.4 | 2 | 12.3 | 6 | -9.1 | 2.0 | 4 |
| G | 7.3 | 6 | 23.6 | 5 | 16.3 | 1.32 | 6 |

#### 9.3.1.3 Individual and combined effect of ageing and moisture

The individual and combined effects of ageing and moisture on the healing of asphalt mixtures were investigated using the 4PB machine. A summary of investigated mixture conditions of healing tests was presented in Table 9.1. Due to time limitations of this study and machine availability, it was not possible to study the individual influence of ageing and its combined effect with moisture on the healing asset of 100/150 asphalt mixtures. Table 9.5 presents the results of individual and combined effects of ageing and moisture on investigated mixtures using the 4PB machine.

Figure 9.7 indicates that no healing issue arises from performing test B configuration for all circumstances. The moisture-conditioned mixtures showed the best healing performance (see the blue curves). As explained previously the applied number of loading cycles (100 cycles or 10 seconds) has less destructive effect and permits the successive 10 seconds rest period to cause a high partial recovery. In addition, HR and HI of moisture-conditioned mixtures are better than HR and HI of most other tested mixtures as shown in Table 9.5 even when other test configurations, except for test D, were applied. HR and HI of tests; B to G presented in Table 9.5 show that moisture conditioning of control mixtures has less effect on the potential of damage recovery than ageing and ageing combined with moisture. Some improvement in this potential of moisture-conditioned mixtures was also noticed when compared to that of unconditioned control mixtures. Similarly, Mehrara and Khodaii, 2015 found that moisture conditioning does not significantly affect the potential of damage recovery of tested specimens by cyclic IDT tests.

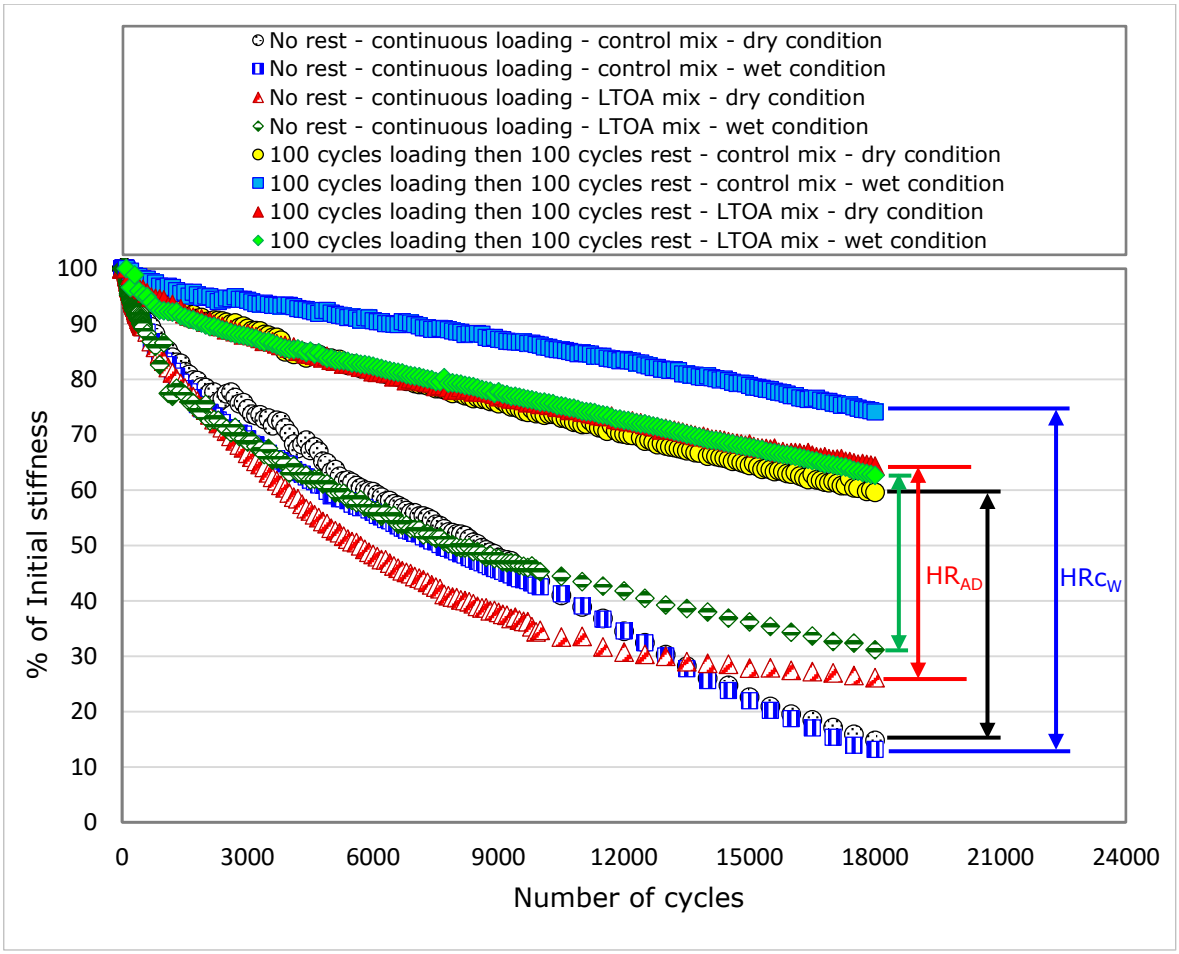



Figure 9.7: Effect of moisture conditioning and/or ageing on fatigue damage recovery using tests B versus A configurations.

Table 9.5: A summary of healing test results.

| Applied Conditions to mixtures | | Compound-loading test conditions | | | | | | | | | | | | | | | | | | |
|---|---|---|---|---|---|---|---|---|---|---|---|---|---|---|---|---|---|---|---|---|
| | | A | B | | | C | | | D | | | E | | | F | | | G | | |
| | | | HR at 50% | HR at end | HI at 50% | HR at 50% | HR at end | HI at 50% | HR at 50% | HR at end | HI at 50% | HR at 50% | HR at end | HI at 50% | HR at 50% | HR at end | HI at 50% | HR at 50% | HR at end | HI at 50% |
| 40/60 pen | Control - No condition | Reference Test | 26.4 | 44.8 | 2.63 | 7.7 | -4.45 | 1.12 | 21.2 | 42.9 | 2.37 | 13.0 | 25.6 | 1.38 | 8.7 | 1.6 | 1.12 | 7.4 | 18.0 | 1.28 |
| | Control - Moisture damage | | 39.0 | 61.0 | 4.80 | 15.7 | 25.3 | 1.86 | 17.9 | 35.0 | 2.17 | 20.6 | 39.1 | 2.56 | 21.4 | 12.3 | 2.0 | 7.3 | 23.6 | 1.32 |
| | Ageing - Dry condition | | 32.2 | 38.2 | 4.47 | 2.8 | -14.8 | 1.05 | 22.3 | 10.2 | 2.53 | 22.6 | 6.2 | 2.51 | -18.4 | -17.2 | 0.4 | -10.2 | -9.9 | 0.74 |
| | Ageing + Moisture damage | | 29.3 | 31.6 | 3.20 | 7.2 | 7.5 | 1.4 | 8.6 | -2.4 | 1.2 | -4.2 | -21.8 | 0.9 | -31.5 | -22.4 | 0.33 | -6.1 | -8.2 | 0.84 |
| 100/150 pen | Control - No condition | | 15.3 | 12.6* | 1.64 | 14.4 | 11.2* | 1.65 | NA | NA | NA | NA | NA | NA | NA | NA | NA | NA | NA | NA |
| | Control - Moisture damage | | 32.1 | 59.4* | 3.5 | -40.3 | -8.0* | 0.4 | NA | NA | NA | NA | NA | NA | NA | NA | NA | NA | NA | NA |
| | Ageing - Dry condition | | NA | NA | NA | NA | NA | NA | NA | NA | NA | NA | NA | NA | NA | NA | NA | NA | NA | NA |
| | Ageing + Moisture damage | | NA | NA | NA | NA | NA | NA | NA | NA | NA | NA | NA | NA | NA | NA | NA | NA | NA | NA |

* HR has been calculated at 24000 cycles (100/150 pen mixtures) not at 18000 cycles (40/60 pen mixtures).

In this work, for the chosen conditions; 10 Hz, 10˚C and 200με of fatigue test without rest period, the index of moisture damage resistance (IRSM= Initial Stiffness $_{\text{of moisture conditioned}}$/ Initial Stiffness $_{\text{of unconditioned}}$) was calculated. IRSM was greater than 80% for all conditions and therefore no significant indication of moisture damage. The main damage was therefore assumed to have resulted from the performed fatigue test. The initial stiffness curves of unconditioned and moisture conditioned mixtures were very similar and the difference between them at the end of 18000 cycles of loading was only 2% (See Figure 9.8). If the moisture damage does not significantly affect asphalt mixtures, the researcher believes that moisture conditioning may play an unexplained beneficial role.

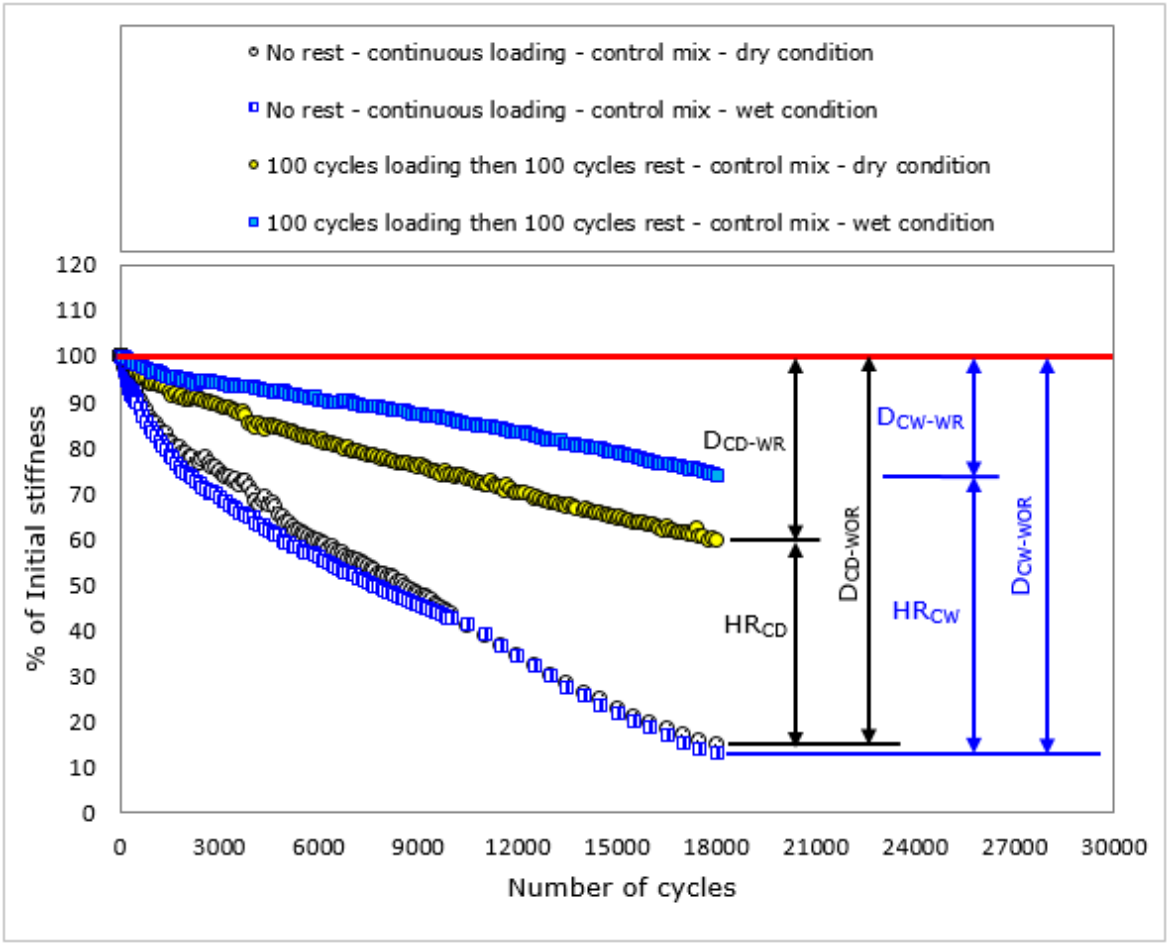



Figure 9.8: Effect of moisture conditioning on fatigue damage recovery using tests B versus A configurations.

Furthermore, tests C to F of 600 loading cycles and different rest periods and test G of 6000 by 6000 loading cycles and unloading caused more damaging than test B regardless of the applied conditions and mixture types (See Table 9.5).

These compound-loading test configurations have resulted in negative values of HR and HI (similar results presented in Figures 9.4 and 9.5, and Table 9.3). These negative indices are completely opposite to the main assumption of healing which assumes that rest periods heal the resulting damage in asphalt mixture specimens and increase their fatigue life. It is complicated to explain the reasons of these negative indices, in particular, for 40/60 pen mixtures exposed to combined effect of ageing and moisture conditioning (See Figure 9.9). It was also observed for 100/150 pen mixtures exposed to moisture conditioning and experiencing test C loading conditions. The successive applied one-minute loading time (600 cycles) of tests C-F or 10 minutes (6000 cycles) of test G with the chosen test conditions 10 Hz, 10˚C and 200με can cause considerable damage even if they are followed by rest periods. Mamlouk et al., 2012 found similar results and identified them as a ''negative healing'' without explaining the reasons (See Figure 9.10).

These negative values of healing indices can be attributed to two possible reasons. The first possible interpretation of these negative indices is the shape of the stiffness modulus curve such as the curve of test configuration F (See the black curve in Figure 9.9) which shows an unexplained substantial decrease (25%) in stiffness modulus might change the traditional shape of the modulus curve. Secondly, during each fatigue test, there are three different phases appearing successively as shown in Figure 9.11. The first stage is characterised by a rapid decrease in stiffness modulus of the tested specimen due to repetitive loadings. Then this modulus continuously decreases with the increase of loading cycles until it reaches an asymptote where the variation of stiffness versus loading cycles is approximately zero. However, this modulus decrease cannot be the result of fatigue damage. Heating and thixotropy probably play roles that are more important during this stage (Di Benedeto, et al., 2004, Soltani and Anderson, 2005, Di Benedeto, et al., 2011). Therefore, because of the repetition of this loading condition up to 60 times (30 loading and 30 rest), it is believed

that only stage I will occur showing more stiffness modulus decrease with every round (loading and unloading). No asymptotes resulted from this reduction of modulus and therefore no transition to the second stage II occurred. During phase II the fatigue damage will be more predominate and the effect of thermal heating and thixotropy is minor. These negative healing indices results may reflect the importance of selecting appropriate loading and testing conditions in the laboratory.

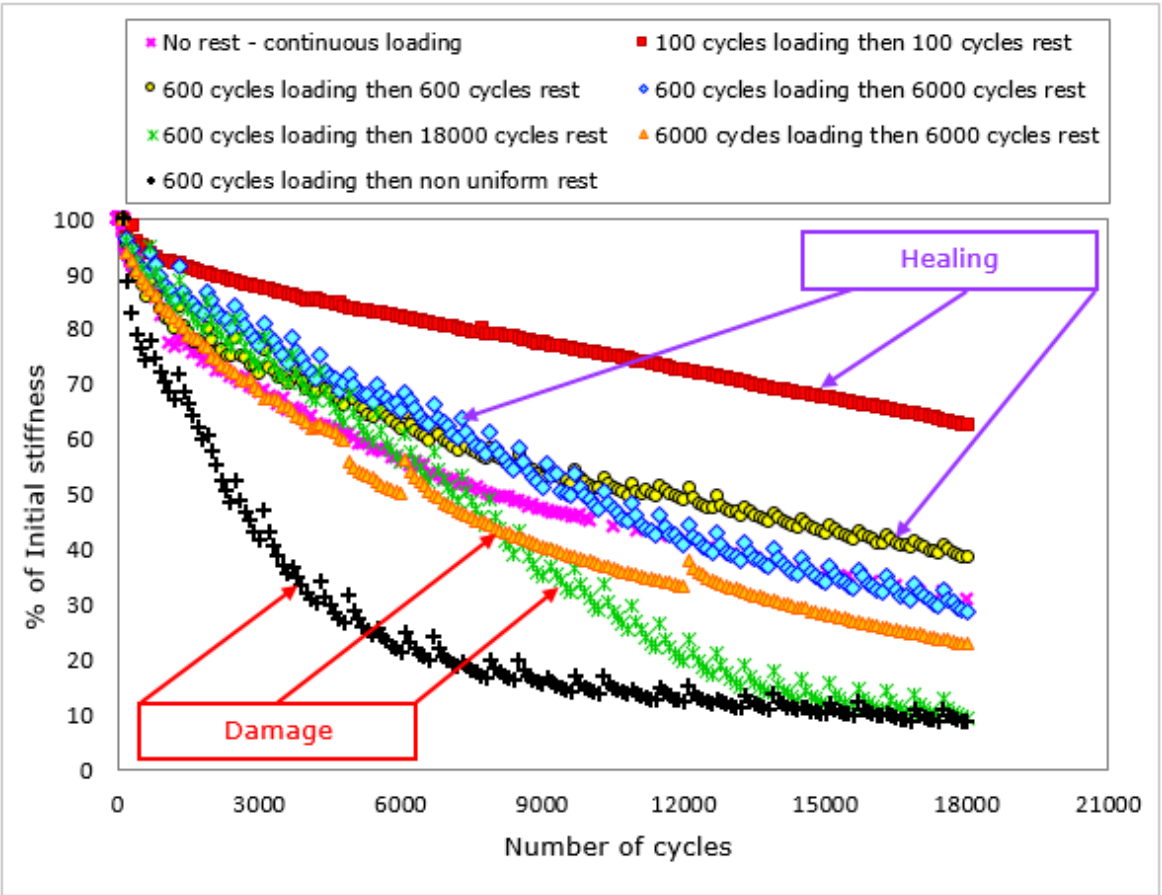



Figure 9.9: Samples of healing tests for combined conditions (aged and moisture conditioned asphalt mixtures).

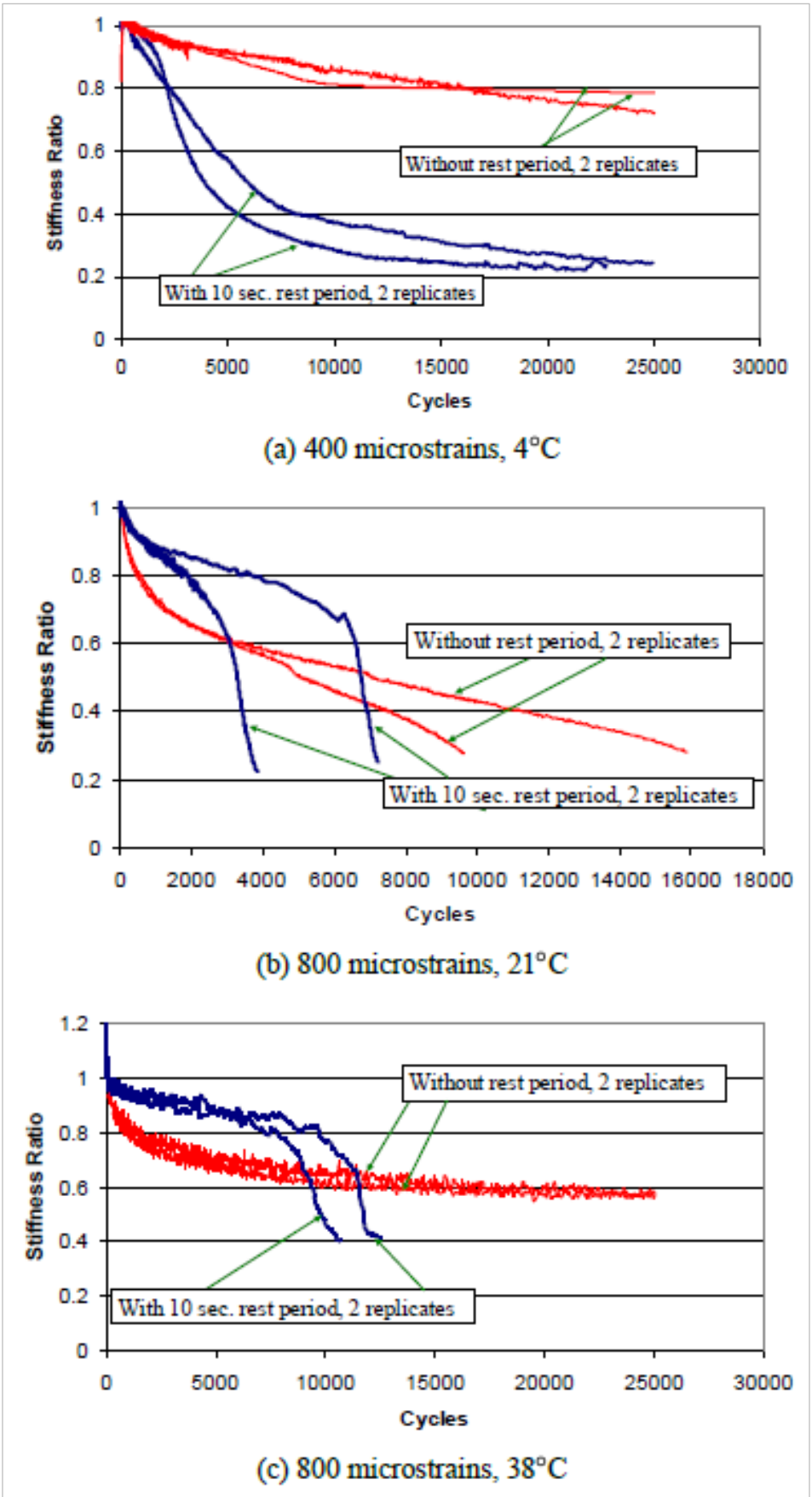



Figure 9.10: Examples of beam fatigue test results using haversine deflection-control with and without rest periods (Mamlouk et al., 2012).

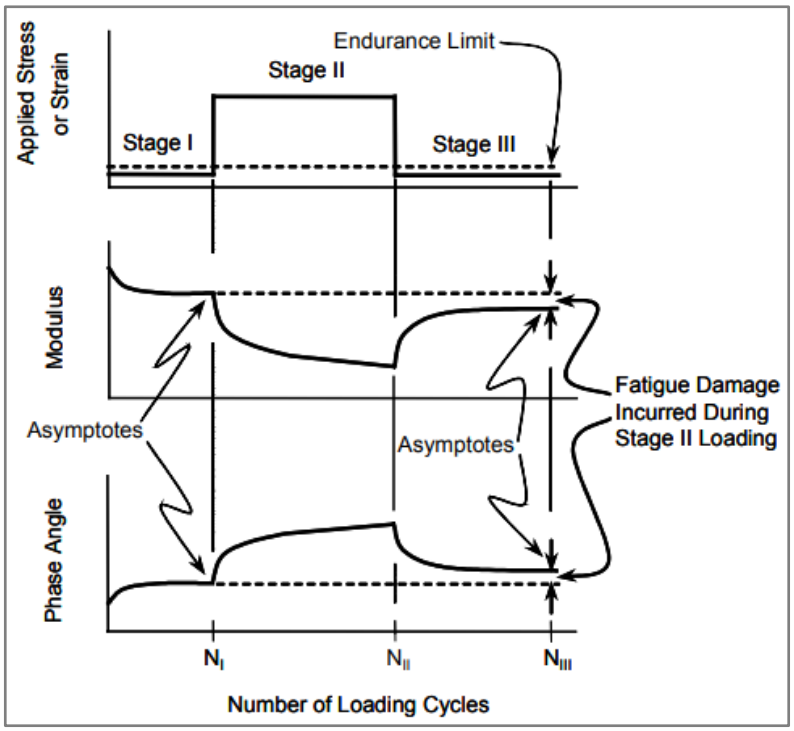



Figure 9.11: Schematic of loading in stages; I, II, III of fatigue test (Soltani and Anderson, 2005).

### 9.4 Healing tests using the modified ITFT

In general, the standard pulse of the ITFT consists from 0.1 second loading followed by 0.4-second rest as shown in Chapter 7. The software of this test cannot provide the opportunity to change the 0.4-second rest period. Therefore, it is not possible to study the effect of rest periods in the same traditional way by changing the rest period every time. However, the author unsuccessfully attempted to change the resting time of this ITFT arrangement by means of Universal Software.

Maggiore 2014 investigated the healing property of asphalt mixtures by keeping the standard pulse of ITFT and carrying out additional intermittent healing tests using nine combinations of loading and unloading times as shown in Table 9.6. Maggiore, 2014 concluded that the healing of asphalt mixtures resulting from ITFT data is less pronounced if compared with that from 4PB. However, the resulting fatigue life values of ITFT tests with nonstandard rest period (shown in Table 9.6) were longer than fatigue life values of standard pulses. It was also found that the 10000 cycles loading followed by 10000 cycles rest produced the optimum fatigue life.

Table 9.6: Loading times and rest times (Maggiore, 2014).

| Number of pulses | |
|---|---|
| Loading time | Rest time |
| 5,000 | 1,000 |
| | 5,000 |
| | 10,000 |
| | 15,000 |
| 10,000 | 5,000 |
| | 10,000 |
| 15,000 | 5,000 |
| | 10,000 |
| | 15,000 |

In this work, the researcher believes that using intermittent ITFT healing tests is not always practical. It was found from different attempts that using intermittent settings could affect the accuracy of initial stiffness measurements because it requires the ITFT software after the specified number of loading cycles to be stopped and resumed again after the specified rest time. That means the software will measure a new initial stiffness modulus which will be occasionally less than that at the end of the previous test, which is not true. This issue be more serious at 20°C and at high micro-strain values because the disadvantage of permanent deformation accumulation. Consequently, the modified ITFT was used to study the healing by applying a non-uniform or random rest periods between standard pulses to keep the ITFT software running until the end based on the same initial stiffness modulus. The different conditions that were applied in these tests are presented in Table 9.7. Healing test was carried out at 10°C to minimize the effect of permanent deformation and at 200 με in controlled strain mode. Generally, the test stops when the LVDTs reach 90% of their range (the end of their range to avoid LVDT's damage). At this point, readjustment will be required to resume the test. As shown in Figure 9.12, a 20% of the LVDTs range (i.e. setting back by 70% of the range) was chosen to randomly control the number of loading cycles. The test will run until one or both of the LVDT's reach 90%.

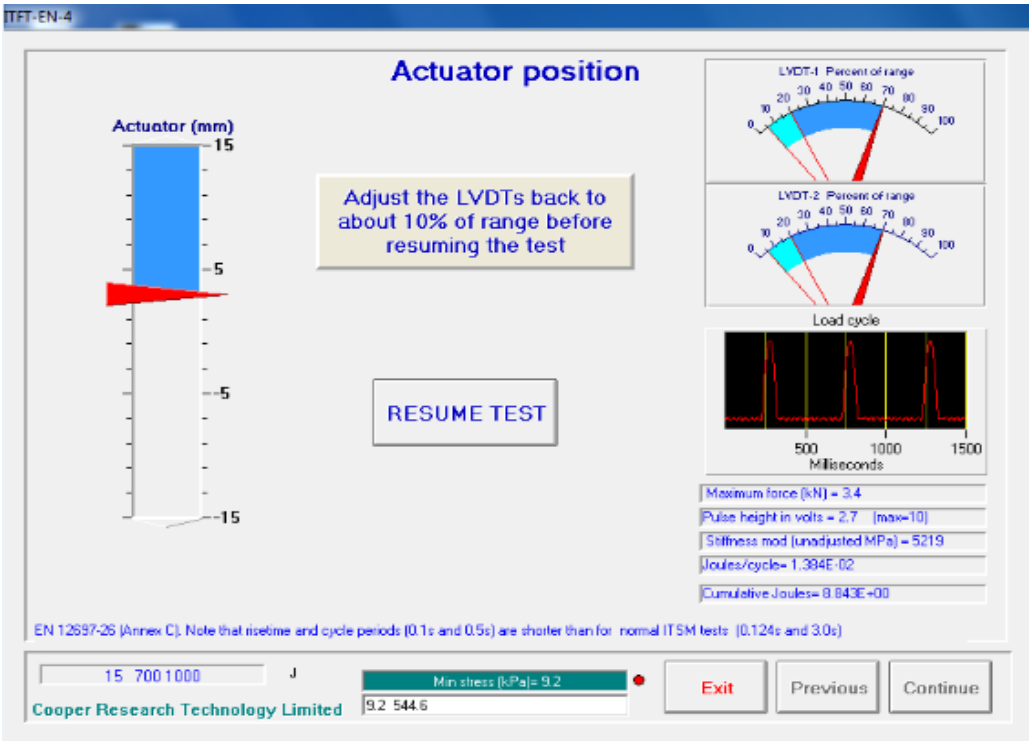



Figure 9.12: LVDT's setting in the healing test.

### 9.4.1 Results of healing tests using the modified ITFT

A comparison takes place between the traditional setting of ITFT and random procedure to observe the stiffness deterioration and recovery as shown in Figures 9.13 and 9.14. Table 9.7 presents the HR and HI indices at 50% of initial stiffness and at end of the test as calculated in accordance with equations 9.1 and 9.2. Table 9.8 shows the resulting number of loading cycles and the selected random rest period from this setting. The applied healing test included six stages for each condition. The moisture induced damage was applied to asphalt mixtures of 10% air voids only in accordance to BBA method as detailed in Chapter 3. Moreover, STOA and LTOA conditions were applied to the mixtures of 10% air voids content in accordance with AASHTO procedure as explained in Chapter 3.

Figures 9.13 and 9.14 display the stiffness deterioration and recovery of 40/60 pen mixtures exposed to specific conditions. One interesting finding from these figures and Table 9.7 is that an increase in the number of cycles to failure due to the applied non-uniform rest period regardless of mixture circumstances.

At end of the test, both dry and wet control mixtures have relatively the same HR, although the wet mixture showed the highest HI and HR at 50% of initial stiffness. In addition, $HR_{at\ end}$ and $HI_{at\ 50\%}$ of dry aged mixture were more than $HR_{at\ end}$ and $HI_{at\ 50\%}$ of other circumstances. However, it produced more number of cycles. On the other hand, the $HR_{at\ 50\%}$ of combined effects of moisture and ageing showed more stiffness recovery. The general reasons seem to be the same as discussed earlier in Chapter 7, the stiffer the mixture (or less deformed) the more the number of cycles to failure.

In addition, the stiffness recovered 10-15% of the initial value in the dry conditions of control and aged mixtures due to a long rest period of 16 hours at 40°C (See stage 5 in Table 9.7). This may reflect the important role of temperature in the healing of asphalt materials.

Despite there being some stiffness recovery, this complicated phenomenon is still not obvious in this test as in the 4PB test. That may be attributed to the main disadvantages of ITFT; the absence of stress reversal and the accumulation of vertical permanent deformation, although it was carried out at 10°C. It can also be concluded that the Healing Ratio (HR) may be different during the whole test and might occasionally not be compatible with the Healing Index (HI).

Table 9.7: HR and HI indices of healing test by ITFT.

| Mixture Conditions | HR at 50% of initial stiffness | HR at end of the test | HI at 50% of initial stiffness |
|---|---|---|---|
| Unaged - dry condition | 12.1 | 9.9* | 1.50 |
| Unaged - wet condition (BBA method) | 15.4 | 10.2* | 1.66 |
| Aged - dry condition | 14.7 | 21** | 1.86 |
| Aged - wet condition (BBA method) | 18.3 | 2.9** | 1.50 |

*After end of the test at 32000 cycles. **After 94000 cycles.

Table 9.8: Random number of loading cycles and random number of rest period cycles as resulted from the test.

| **Mixture Conditions** | **Test stage** | **random loading cycles** | **Applied random rest period after random loading cycles** |
|---|---|---|---|
| Unaged dry condition | 1 | 1943 | Random rest period = 1*loading cycles = 1943 |
| | 2 | 2690 | Random rest period = 3*loading cycles = 8070 |
| | 3 | 3090 | Random rest period = 5*loading cycles = 15450 |
| | 4 | 2940 | Random rest period = 6*loading cycles = 17640 |
| | 5 | 3220 | Storing the sample after stage 5 for 16 ± 2hrs at 40°C then for 4hrs at testing temperature 10°C. |
| | 6 | 18117 | The test was stopped at 32000 cycles, vertical deformation = 8.780mm and horizontal deformation =3.555mm. |
| Unaged wet condition (BBA method) | 1 | 2253 | Random rest period = 1*loading cycles = 2253 |
| | 2 | 2340 | Random rest period = 3*loading cycles = 7020 |
| | 3 | 2170 | Random rest period = 5*loading cycles = 10850 |
| | 4 | 2070 | Random rest period = 6*loading cycles = 12420 |
| | 5 | 2160 | Storing the sample after stage 5 for 16 ± 2hrs at 40°C then for 4hrs at testing temperature 10°C. |
| | 6 | 21007 | The test was stopped at 32000 cycles, vertical deformation = 9.005mm and horizontal deformation =3.804mm. |
| LTOA dry condition | 1 | 4743 | Random rest period = 1*loading cycles = 4743 |
| | 2 | 14320 | Random rest period = 3*loading cycles = 42960 |
| | 3 | 16260 | Random rest period = 5*loading cycles = 81300 |
| | 4 | 16490 | Random rest period = 6*loading cycles = 98940 |
| | 5 | 14160 | Storing the sample after stage 5 for 16 ± 2hrs at 40°C then for 4hrs at testing temperature 10°C. |
| | 6 | 84027 | The test was stopped at 150000 cycles, vertical deformation =7.594mm and horizontal deformation = 3.408mm. |
| LTOA wet condition (BBA method) | 1 | 5993 | Random rest period = 1*loading cycles = 5993 |
| | 2 | 5630 | Random rest period = 3*loading cycles = 16890 |
| | 3 | 6390 | Random rest period = 5*loading cycles = 31950 |
| | 4 | 7050 | Random rest period = 6*loading cycles = 42300 |
| | 5 | 7220 | Storing the sample after stage 5 for 16 ± 2hrs at 40°C then for 4hrs at testing temperature 10°C. |
| | 6 | 117717 | The test was stopped at 150000 cycles, vertical deformation =8.279mm and horizontal deformation = 4.730mm. |

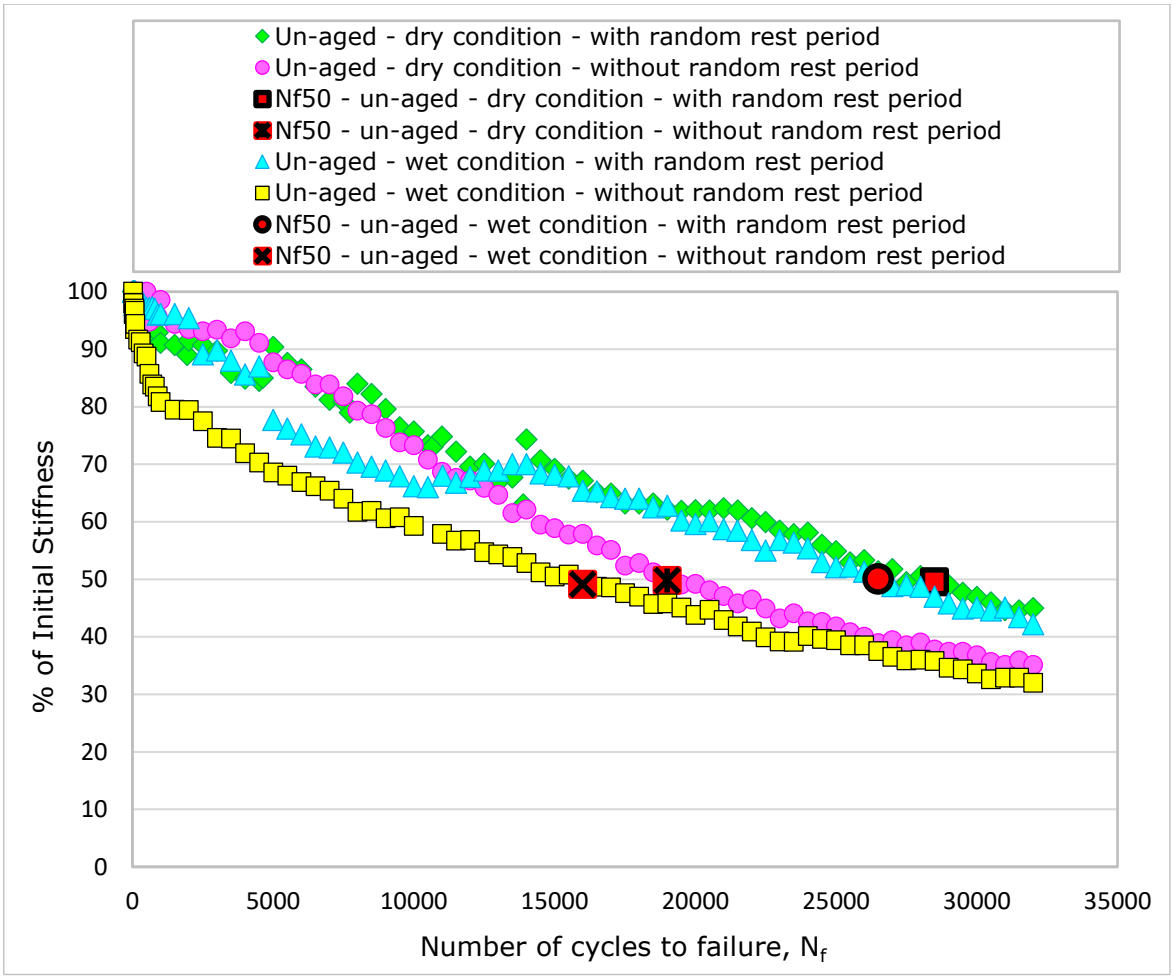



Figure 9.13: Effect of random rest periods on stiffness degradations of unaged mixtures.

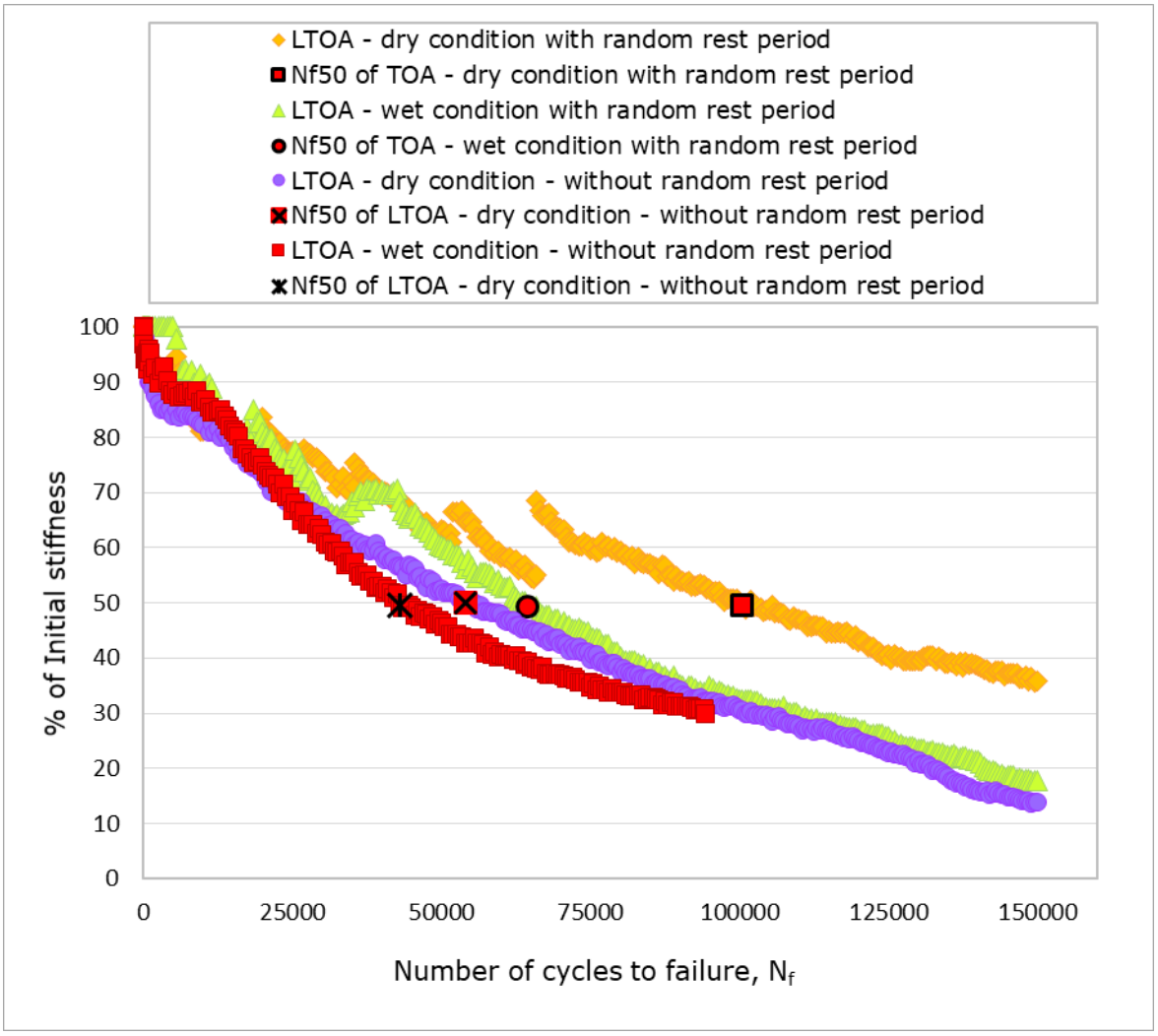



Figure 9.14: Effect of random rest periods on stiffness degradations of LTOA mixtures.

## 9.5 Summary

In this chapter, an attempt was set out to find the effect of air voids content, and time of loading and rest period length in combination with the individual and combined effects of ageing and/or moisture damage. Based on the collected results, the following points can be summarised:

1. In terms of the 4PB healing test, it was not possible to apply short loading at 10Hz of less than 100 cycles due to the accuracy of stiffness measurements.

2. Healing tests of 100 cycles loading by 100 cycles rest showed the best healing indices and performance at all circumstances. It may indicate that the incurred damage plays an important role in introducing the role of the rest period to heal the resulting damage. This configuration of compound loading has less destructive effect and allows the successive 10 seconds rest periods to cause a high partial recovery. Increasing the number of loading cycles excessively might be not beneficial for healing study.

3. Air voids content may significantly affect the healing of asphalt mixtures. The 12% air voids mixtures showed better healing performance than 6% air voids mixtures. More investigation is important to evaluate more contents of air voids and to take into account the effect of air voids shape and size.

4. In general, HR and HI of moisture-conditioned mixtures were better than HR and HI of most other tested mixtures. Consequently, moisture conditioning of control mixtures has less effect on the potential of damage recovery than ageing and ageing combined with moisture.

5. Negative healing indices have been unexpectedly arisen from healing tests performed by the 4PB machine at different conditions and compound loadings. In particular, for aged mixtures when exposed to moisture conditioning.

6. Healing Ratio (HR) may be different during the whole test based on the resulting damage and rest periods. It also might occasionally not be compatible with the Healing Index (HI).

7. In terms of modified ITFT healing test, one interesting finding is the increase in the number of cycles to failure due to the applied non-uniform rest periods regardless of mixture circumstances. In all circumstances, asphalt mixtures showed a considerable increase in $N_{f50}$; 50% (dry control), 66% (wet control), 86% (dry aged), and 50% (wet aged).

8. The surprising findings by ITFT healing study may be attributed to the same concept discussed earlier in Chapter 7, the stiffer mixture (or less deformed) produced the higher number of cycles to failure.

9. It is important to minimize the effect of permanent deformation for healing studies using the ITFT. It may require finding an optimum temperature, although using 10°C seems to be rational. Selecting a proper microstrain level is significantly important to avoid rapid damage.

10. Healing study by ITFT was based on the standard pulse of 0.1 second loading followed by 0.4-second rest. To improve the future explorations of fatigue and healing by ITFT in strain-controlled method, it could be interesting to change the loading time and resting time. Beeson, 2012 have already used the Universal Software to change the rest time for ITFT in stress control mode of loading.

11. It is necessary to evaluate the effect of combined environmental factors on healing phenomenon, using other tests such as controlled-strain tension-compression (Push-Pull) uniaxial fatigue test. Investigation of different analysis methods is also important.

12. Applying non-uniform rest period or random rest period to 4PB fatigue tests is a new challenge. It needs more investigation to be more realistic and identical to that of in-service asphalt pavements.

# Chapter Ten: Summary of Ageing and Moisture Damage Indices

## 10.1 Introduction

This chapter discusses all the conditions investigated in this research using the different stiffness modulus testing methods conducted to find the required indices. These indices were calculated using the following general equation to assess the individual and combined effects of ageing and moisture conditioning.

$$\text{Index} = \frac{\text{stiffness modulus of conditioned mixture}}{\text{stiffness modulus of unconditioned mixture}} \qquad 10.1$$

Readers are referred to earlier chapters for background on abbreviations and rationale behind the testing that has generated the results summarised in this chapter.

## 10.2 Effect of ageing

### 10.2.1 ITSM results

From conducting the ITSM test, the ageing indices derived from short and long-term oven ageing are presented in Table 10.1 to show the effect of ageing using different testing temperatures, binder grades and content and air voids content.

The most important findings to emerge from the discussion of this part are the obvious influences of air voids content on the Ageing Index ($ITSM_{LTOA}/ITSM_{STOA}$) when the ITSM of the same specimen was measured after applying the STOA to a loose mixture and the LTOA to a compacted specimen. The effect of this variable on the Ageing Index was shown previously in Figures 4.5 and 4.8. The increase of air voids provides more access for oxidation and in turn more ageing of bituminous material.

It was also observed that the Ageing Index ($ITSM_{LTOA}/ITSM_{STOA}$) calculated using the same specimen is more reliable than the Ageing Indices ($ITSM_{STOA}/ITSM_{Control}$ or $ITSM_{LTOA}/ITSM_{Control}$) calculated using different specimens. Using the same specimen makes certain that other variables such as the distribution of aggregate particles and air voids will not affect the measurements of ITSM.

Table 10.1: Summary of Ageing Index (AI) results using the ITSM (The average of five replications was used to measure the ITSM).

| Binder grades and content | Air voids, % | Ageing Index= | | | | | |
|---|---|---|---|---|---|---|---|
| | | $ITSM_{STOA}/ITSM_{Control}$ | | $ITSM_{LTOA}/ITSM_{STOA}$ | | $ITSM_{LTOA}/ITSM_{Control}$ | |
| | | Testing temperatures, ˚C | | Testing temperatures, ˚C | | Testing temperatures, ˚C | |
| | | 10 | 20 | 10 | 20 | 10 | 20 |
| **100/150 5% BC** | 4.0 | *1.68* | *1.93* | 1.11 | 1.21 | 1.86 | 2.34 |
| | 8.0 | 1.35 | 1.32 | 1.43 | 1.72 | 1.93 | 2.27 |
| | 12.0 | 1.32 | 1.34 | 1.61 | 1.94 | 2.13 | 2.15 |
| **10/20 5% BC** | 4.0 | 1.01 | *1.25* | 1.06 | 1.14 | 1.07 | 1.42 |
| | 8.0 | 1.07 | 1.07 | 1.18 | 1.22 | 1.22 | 1.31 |
| | 12.0 | 1.04 | 1.11 | 1.19 | 1.26 | 1.27 | 1.40 |
| **40/60 5% BC** | 4.0 | 1.06 | 1.21 | 1.13 | 1.22 | 1.20 | 1.47 |
| | 8.0 | 1.08 | 1.15 | 1.23 | 1.37 | 1.34 | 1.57 |
| | 12.0 | 1.12 | 1.10 | 1.40 | 1.63 | 1.56 | 1.66 |
| **40/60 6% BC** | 4.0 | - | - | - | - | - | - |
| | 8.0 | 1.27 | 1.20 | 1.09 | 1.22 | 1.38 | 1.47 |
| | 12.0 | 1.23 | 1.23 | 1.23 | 1.27 | 1.51 | 1.56 |

### 10.2.2 $|E^*|$ results

Table 10.2 shows the effect of ageing using the 4-PB machine to measure the dynamic complex modulus, $|E^*|$ at different testing temperatures and frequencies. All mixtures were manufactured at 12% air voids content only. The $|E^*|_{A\text{-index}}$ was used to assess the effect of ageing. This table also presents the calculated ageing indices for all investigated parameters at all conditions, $|E^*|_{STOA}/|E^*|_{Control}$, $|E^*|_{LTOA}/|E^*|_{STOA}$, and $|E^*|_{LTOA}/|E^*|_{Control}$.

The most important findings to emerge from the discussion of these results are the obvious influence of testing temperature on the Ageing Index (AI). In particular, when $|E^*|$ of the same specimen was measured after applying the STOA to a loose mixture and the LTOA to a compacted specimen to find the Ageing Index. It was obviously observed that $|E^*|_{A\text{-index}}$ increased with the

increase of testing temperatures. The effect of ageing at the lowest temperature -10 and 0˚C was not obvious. The convergence at high frequencies (equivalent to low-temperature response) between the different mixtures tested at different conditions was shown in the produced Master curves in Chapter Six (See Figures 6.5 and 6.6). The reason might be attributed to the fact that a shifting towards more elastic (brittle) behaviour of these mixtures might occur due to ageing. Therefore, this shifting might reduce the sensitivity of aged mixtures for being stiffer at these temperatures. These results are in the same line with that observed in the ITSM. However, two testing temperatures only, 10 and 20˚C were applied to measure the ITSM of different asphalt mixture specimens. It was also highlighted that loading frequencies have obviously less effect than temperatures on the Ageing Index.

Some of $|E^*|_{index}$ results were less than 1.0 which might indicate some cohesion failure during the LTOA procedure. Kim et al., 1986 and Von et al., 1988 found similar results. However, the behaviour of bituminous materials at the high frequencies (equivalent to low-temperature response) might be considered the reason as explained earlier.

Table 10.2: Summary of Ageing Index ($|E^*|_{A\text{-index}}$) results using $|E^*|$ test (The average of two replications was used to measure $|E^*|$).

| Binder grades | Frequency, Hz | Ageing Index, AI = $\frac{|E^*| \text{ of STOA mixture}}{|E^*| \text{ of control mixture}}$ | | | | | *Ageing Index, AI = $\frac{|E^*| \text{ of LTOA mixture}}{|E^*| \text{ of STOA mixture}}$ | | | | | Ageing Index, AI = $\frac{|E^*| \text{ of LTOA mixture}}{|E^*| \text{ of control mixture}}$ | | | | |
|---|---|---|---|---|---|---|---|---|---|---|---|---|---|---|---|---|
| | | Testing temperatures, °C | | | | | Testing temperatures, °C | | | | | Testing temperatures, °C | | | | |
| | | -10 | 0 | 10 | 20 | 30 | -10 | 0 | 10 | 20 | 30 | -10 | 0 | 10 | 20 | 30 |
| 40/60 | 1 | 0.92 | 0.95 | 1.11 | 1.17 | 1.22 | 1.15 | 1.34 | 1.26 | 1.44 | 1.91 | 1.06 | 1.27 | 1.40 | 1.68 | 2.34 |
| | 10 | 0.93 | 0.93 | 1.06 | 1.21 | 1.03 | 1.11 | 1.24 | 1.17 | 1.29 | 1.70 | 1.03 | 1.15 | 1.24 | 1.55 | 1.76 |
| | 25 | 0.93 | 0.92 | 1.05 | 1.16 | 1.01 | 1.09 | 1.20 | 1.15 | 1.25 | 1.59 | 1.02 | 1.11 | 1.21 | 1.45 | 1.61 |
| 100/150 | 1 | 1.21 | 1.15 | 1.08 | 1.07 | 1.43 | 0.90 | 0.94 | 1.14 | 1.83 | 2.54 | 1.09 | 1.08 | 1.23 | 1.95 | 3.64 |
| | 10 | 1.14 | 1.03 | 0.99 | 0.97 | 1.28 | 0.90 | 0.94 | 1.12 | 1.62 | 1.96 | 1.02 | 0.97 | 1.11 | 1.57 | 2.52 |
| | 25 | 1.12 | 1.03 | 0.99 | 0.94 | 1.15 | 0.92 | 0.93 | 1.10 | 1.54 | 1.88 | 1.03 | 0.96 | 1.09 | 1.45 | 2.16 |

*$|E^*|$ was measured for the same specimen after applying STOA and then LTOA.

## 10.3 Effect of Moisture

### 10.3.1 ITSM results

From conducting the ITSM, the IRSM (Index of Retained Stiffness Modulus) is presented in Table 10.3 to show the effect of moisture conditioning using different testing temperatures, air voids content, and two different moisture sensitivity methods. This index was calculated using Equation 10.1 after measuring the ITSM for both conditions; dry and immersed in water (wet) of all investigated parameters. This was done by measuring the ITSM of the specimen in dry condition then measuring the ITSM after submerging the same specimen in water to find more reliable indices. The submersion in water was applied to the investigated specimen according to BBA and BS EN methods. A set of five specimens was prepared for each method to find the IRSM of each parameter.

The most important findings to emerge from the results of this part that all IRSM values were greater than 80% (the criterion selected in Section 4.7.1) in all circumstances of this study. Therefore no significant moisture damage issues have arisen from using different water sensitivity testing methods to evaluate the different asphalt limestone aggregate mixtures, even if this damage was applied after LTOA to these mixtures. The role of limestone as an anti-stripping aggregate should not be ignored in these results.

Moreover, the increase of ITSM of conditioned mixtures (wet) and in turn the increase of IRSM was observed. It might be attributed to possible ageing that may take place during the course of moisture conditioning (40˚C in the course of BS EN method and 60˚C in the course of BBA protocol). The results of rheological and physical properties of neat and recovered binders shown in Chapter Five may support this assumption (possible ageing during moisture conditioning). However, caution should be considered in interpreting these results due to the disadvantages described in Section 5.2 of the used bitumen recovery method.

### 10.3.2 $|E^*|$ results

From conducting the dynamic complex modulus test, the $|E^*|_{MD\text{-}index}$ (index to assess the moisture damage using the complex modulus test, $|E^*|$) is presented in Table 10.4 to show the effect of moisture conditioning using different binder grades, testing temperatures and loading frequencies. This index was calculated using the general Equation 10.1. This was done by measuring $|E^*|$ of the specimen in dry condition then measuring $|E^*|$ after submersion the same specimen in water to find more reliable indices. The submersion in water was applied to the investigated specimen according to BS EN method. A set of two prismatic beam specimens of 12% air voids content was prepared to find the $|E^*|_{MD\text{-}index}$ of each parameter.

The results of $|E^*|_{MD\text{-}index}$ indicate that no moisture damage issue arises from applying the moisture conditioning, even when this conditioning was applied to asphalt mixture specimens after long-term oven ageing. In general, $|E^*|_{MD\text{-}index}$ was greater than the minimum criterion of 80% (the criterion selected in Section 4.7.1). However, some $|E^*|_{MD\text{-}index}$ values of 100/150 Pen mixtures were less than 80% but still greater than 70% (recommended by many authorities).

In addition, a slight to considerable increase in $|E^*|_{MD\text{-}index}$ of control and aged mixtures exposed to the moisture conditioning can be observed. The reason of this increase may be attributed to possible ageing during the moisture conditioning itself. Finally, these results are relatively in agreement with that of ITSM.

Table 10.3: Summary of IRSM results using ITSM (The average of five replications was used to measure the ITSM).

| Mixture type | | | IRSM= $ITSM_{dry}/ITSM_{wet}$ | | | | | | | | | | | |
|---|---|---|---|---|---|---|---|---|---|---|---|---|---|---|
| | | | Control Mix | | | | | | LTOA Mix | | | | | |
| Binder grades | | | 10/20 | | 100/150 | | 40/60 | | 10/20 | | 100/150 | | 40/60 | |
| Methods | Air voids, % | | 8 | 12 | 8 | 12 | 8 | 12 | 8 | 12 | 8 | 12 | 8 | 12 |
| BBA | Testing temperatures, °C | 10 | 0.99 | 0.98 | 1.13 | 1.19 | 1.07 | 1.10 | 0.83 | 0.91 | 0.91 | 1.05 | 1.04 | 0.96 |
| | | 20 | 1.00 | 1.01 | 1.12 | 1.39 | 1.15 | 1.57 | 0.99 | 0.99 | 0.86 | 0.82 | 1.10 | 1.03 |
| BS EN | | 0 | 0.93 | 0.85 | 0.89 | 0.83 | 1.03 | 1.03 | 0.98 | 1.07 | 0.88 | 0.83 | 1.03 | 1.07 |
| | | 10 | 0.92 | 0.87 | 0.91 | 0.88 | 0.89 | 0.85 | 0.92 | 0.96 | 1.11 | 0.89 | 1.17 | 1.11 |
| | | 20 | 0.98 | 0.99 | 1.14 | 0.99 | 0.85 | 0.82 | 0.89 | 0.89 | 1.04 | 0.83 | 1.05 | 0.92 |
| | | 30 | 1.17 | 1.07 | 1.19 | 1.23 | 1.25 | 1.41 | 0.99 | 0.91 | 0.95 | 0.85 | 1.27 | 1.16 |

Table 10.4: Summary of $|E^*|_{MD\text{-}index}$ results using $|E^*|$ test (The average of two replications was used to measure $|E^*|$).

| Binder grades | Frequency Hz | Moisture Damage Index = $\|E^*\|_{MD-Index} = \frac{\|E^*\| \text{ of wet control mixture}}{\|E^*\| \text{ of dry control mixture}}$ | | | | | Moisture Damage Index = $\|E^*\|_{MD-Index} = \frac{\|E^*\| \text{ of wet aged mixture}}{\|E^*\| \text{ of dry aged mixture}}$ | | | | |
|---|---|---|---|---|---|---|---|---|---|---|---|
| | | Testing temperatures, °C | | | | | Testing temperatures, °C | | | | |
| | | -10 | 0 | 10 | 20 | 30 | -10 | 0 | 10 | 20 | 30 |
| 40/60 | 1 | 1.06 | 0.88 | 0.96 | 1.06 | 1.27 | 1.09 | 0.85 | 0.81 | 0.98 | 1.21 |
| | 10 | 1.02 | 0.89 | 1.02 | 1.17 | 1.02 | 1.08 | 0.88 | 0.88 | 0.98 | 1.08 |
| | 25 | 1.01 | 0.88 | 1.05 | 1.11 | 0.98 | 1.06 | 0.90 | 0.90 | 0.98 | 1.06 |
| 100/150 | 1 | 0.99 | 0.70 | 0.80 | 0.84 | 1.25 | 0.83 | 0.84 | 0.97 | 0.98 | 1.05 |
| | 10 | 0.97 | 0.75 | 0.81 | 0.85 | 1.20 | 0.79 | 0.82 | 0.94 | 0.94 | 1.07 |
| | 25 | 0.97 | 0.76 | 0.83 | 0.85 | 1.07 | 0.79 | 0.82 | 0.95 | 0.93 | 1.03 |

## 10.4 Combined effect of ageing and moisture conditioning

### 10.4.1 ITSM results

To assess the combined effects of ageing and moisture conditioning, Table 10.5 shows a combined index that represents both effects of ageing and moisture. This index symbolized as AI + IRSM was calculated as following:

$$AI + IRSM = \frac{ITSM\ \ of\ \ conditioned\ mixture\ \ (aged\ and\ immersed\ in\ water)}{ITSM\ \ of\ \ unconditioned\ mixture\ (dry\ control\ mixture)} \quad 10.2$$

The results presented in Table 10.5 indicates that AI+IRSM values increased as the testing temperature increased. Some values of this combined index were significantly increased at high temperatures (20 and 30˚C). The reason might be attributed to the asphalt mixtures' behaviour at low temperature as explained in the next section which shows similar results. This may reflect the role of actual ageing (STOA + LTOA) if the supposed ageing from the moisture conditioning procedure is not considered (See Chapter Five). Table 10.5 also highlights that no moisture damage arises from the investigated materials and conditions used in this study. However, it is well known that ageing may reduce the adhesion bond between the aggregate and bitumen.

### 10.4.2 |E*| results

To assess the combined effects of ageing and moisture conditioning, Table 10.6 shows a combined index that represents both effects of ageing and moisture. This index symbolized as $|E^*|_{A+MD\ index}$ was calculated as following:

$$|E^*|_{A+MD\ Index} = \frac{|E^*|\ of\ \ conditioned\ mixture\ \ (aged\ and\ immersed\ in\ water)}{|E^*|\ of\ \ unconditioned\ mixture\ (dry\ control\ mixture)} \quad 10.3$$

The results presented in Table 10.6 indicates that $|E^*|_{A+MD\ index}$ values increased as the testing temperature increased regardless of the applied frequencies. Most values are greater than 1.0 which may reflect the role of actual ageing (STOA + LTOA) if the supposed ageing from the moisture conditioning procedure is not

considered. On the other hand, all values of $|E^*|_{A+MD\ index}$ of less than 1.0 occurred at -10 and 0˚C. That means the ageing effect was more obvious at high temperatures (20 and 30˚C) than at low temperatures (-10 and 0˚C). This might be attributed to the fact that an increase in the stiffness modulus and in turn in elastic behaviour can be observed due to ageing. Therefore when the stiffer asphalt mixtures (aged) were tested at lower temperatures (when the elastic component of bituminous materials already dominates), the effect of ageing was not clearly manifested showing low indices. On the other hand, the same aged mixtures tested at higher temperatures showed higher indices because ageing affects the viscous component which dominates at high temperatures.

In summary, the performance in terms of $|E^*|_{A+MD}$ (using the 4-PB machine) are generally in agreement with that of AI+IRSM (using the NAT). Both indices indicate that no moisture damage was observed even after ageing. However, the differences in their values can be attributed to differences in the applied procedure and specimen size and shape. The $|E^*|$ test was conducted without applying rest period between the loading cycles compared to the ITSM test. A different number of cycles are applied to measure the modulus in each. In addition, a wide range of frequencies are applied in $|E^*|$ test versus a specific one in the ITSM. ITSM is classified as a quick and easy test to conduct while $|E^*|$ is more complicated.

Finally, Table 10.7 shows a comparison between the individual effect of ageing and the combined effect of ageing and moisture. The results of $|E^*|_{A\text{-}index}$ are very similar to that of $|E^*|_{A+MD\ index}$ at 20 and 30˚C which might indicate that the ageing effect was predominating more than the influence of moisture conditioning. The type of aggregate (limestone) may contribute to the findings.

Table 10.5: Summary of AI + IRSM results using ITSM (The average of five replications was used to measure the ITSM).

| Binder grades | Combined effect of ageing and moisture conditioning using ITSM $AI + IRSM = \frac{ITSM\ of\ wet\ LTOA\ mixture}{ITSM\ of\ dry\ control\ mixture}$ | | | | | | |
|---|---|---|---|---|---|---|---|
| | Moisture sensitivity method | BS EN method | | | | BBA method | |
| | Air voids, % | Testing temperatures, °C | | | | Testing temperatures, °C | |
| | | 0 | 10 | 20 | 30 | 10 | 20 |
| 40/60 | 8 | 0.96 | 0.99 | 1.02 | 2.04 | 1.35 | 1.18 |
| | 12 | 0.95 | 0.94 | 0.98 | 1.89 | 1.49 | 1.81 |
| 100/150 | 8 | 1.28 | 2.12 | 2.65 | 2.37 | 1.47 | 2.38 |
| | 12 | 1.06 | 1.62 | 2.25 | 2.07 | 2.14 | 2.48 |
| 10/20 | 8 | 0.98 | 0.99 | 1.27 | 2.13 | 0.92 | 1.20 |
| | 12 | 0.88 | 0.97 | 1.23 | 1.91 | 1.00 | 1.08 |

Table 10.6: Summary of AI + IRSM results using |E*| test (The average of two replications was used to measure |E*|).

**Combined effect of ageing and moisture conditioning:**

$$|E^*|_{A+MD\ Index} = \frac{|E^*|\ of\ \ wet\ LTOA\ mixture}{|E^*|\ of\ dry\ control\ mixture}$$

| Binder grades | Frequency, Hz | Testing temperatures, °C | | | | |
|---|---|---|---|---|---|---|
| | | -10 | 0 | 10 | 20 | 30 |
| 40/60 | 1 | 1.16 | 1.07 | 1.14 | 1.65 | 2.81 |
| | 10 | 1.11 | 1.01 | 1.09 | 1.51 | 1.90 |
| | 25 | 1.08 | 0.99 | 1.09 | 1.43 | 1.71 |
| 100/150 | 1 | 0.91 | 0.90 | 1.20 | 1.90 | 3.83 |
| | 10 | 0.81 | 0.80 | 1.05 | 1.47 | 2.71 |
| | 25 | 0.81 | 0.78 | 1.03 | 1.35 | 2.23 |

Table 10.7: Comparison between the individual effect of ageing and the combined effect of ageing and moisture.

| Binder grades | Frequency | Combined effect of ageing and moisture conditioning: $\lvert E^* \rvert_{A+MD\ Index} = \frac{\lvert E^* \rvert\ of\ wet\ LTOA\ mixture}{\lvert E^* \rvert\ of\ dry\ control\ mixture}$ | | | | | Ageing Index, AI = $\lvert E^* \rvert_{A-Index} = \frac{\lvert E^* \rvert\ of\ LTOA\ mixture}{\lvert E^* \rvert\ of\ control\ mixture}$ | | | | |
|---|---|---|---|---|---|---|---|---|---|---|---|
| | | Testing temperatures, °C | | | | | Testing temperatures, °C | | | | |
| | | -10 | 0 | 10 | 20 | 30 | -10 | 0 | 10 | 20 | 30 |
| 40/60 | 1 | 1.16 | 1.07 | 1.14 | 1.65 | 2.81 | 1.06 | 1.27 | 1.40 | 1.68 | 2.34 |
| | 10 | 1.11 | 1.01 | 1.09 | 1.51 | 1.90 | 1.03 | 1.15 | 1.24 | 1.55 | 1.76 |
| | 25 | 1.08 | 0.99 | 1.09 | 1.43 | 1.71 | 1.02 | 1.11 | 1.21 | 1.45 | 1.61 |
| 100/150 | 1 | 0.91 | 0.90 | 1.20 | 1.90 | 3.83 | 1.09 | 1.08 | 1.23 | 1.95 | 3.64 |
| | 10 | 0.81 | 0.80 | 1.05 | 1.47 | 2.71 | 1.02 | 0.97 | 1.11 | 1.57 | 2.52 |
| | 25 | 0.81 | 0.78 | 1.03 | 1.35 | 2.23 | 1.03 | 0.96 | 1.09 | 1.45 | 2.16 |

# Chapter Eleven: Conclusions and Recommendations for Future Works

## 11.1 Summary

This research commenced with the writing of a literature review about the fatigue performance and healing phenomenon of asphalt pavements. Although this review highlighted the main testing methods and approaches that characterise the fatigue behaviour of asphalt mixtures, attention was paid to the main factors affecting this behaviour. The main findings from the literature review spotted two gaps which are not covered enough in previous studies and that are still in need of further investigation or have never been investigated. The lack of existing information is related to the combination of environmental factors that affect fatigue damage simultaneously. The other research gap which is considered a new challenge is inserting random or non-uniform rest periods between the repeated loadings to simulate traffic loading wander. This new challenge is still difficult to simulate in the current laboratory fatigue testing methods. However, attempts were conducted in this study. Consequently, this study aims to develop an understanding of the way in which the moisture damage and/or ageing affect the fatigue and healing performance of the asphalt mixture.

To achieve this aims, an extensive laboratory testing programme was designed and conducted using the Nottingham Asphalt Tester (NAT) and Four Point Bending (4PB) machines. These machines have been utilised to carry out the stiffness modulus test, dynamic (complex) modulus test, ITFT, 4PB fatigue test, and non-standard healing tests.

A supplementary testing programme was also performed by the Dynamic Shear Rheometer (DSR), Ring and Ball Softening Point apparatus and Needle Penetration tester to find the rheological and physical properties of neat and recovered binder. Different mixture variables were used in the manufacturing of asphalt mixtures. Different testing parameters include; testing conditions and testing methods were applied to the manufactured asphalt mixture specimens. Different indices have been used to evaluate the effect of ageing and moisture damage on the resilient and complex moduli of asphalt mixtures. Different fatigue analysis methods were also undertaken to define the failure criteria and to determine the number of cycles to failure.

## 11.2 Conclusions

According to the findings of this study, the main conclusions that can be drawn as following:

### 11.2.1 Effect of moisture conditioning and ageing on stiffness moduli

This part was carried out using the NAT and 4-PB machine to measure the indirect tensile stiffness modulus (ITSM) and dynamic modulus, $|E^*|$ of asphalt mixtures exposed to oxidative ageing and/or moisture conditions. Based on the findings, the following points can be summarised:

1. Based on the calculated Ageing Index from ITSM tests conducted at 10 and 20°C, the current study found that air voids content has a great influence on ageing and therefore Ageing Index seems to be air voids content dependent. In general, the higher the air voids content, the higher the Ageing Index. The increase of air voids allows more access for oxidation and in turn more ageing of bituminous material. However, if an assessment of ageing is required, the results of this study reveal that this is best done at a higher, rather than a lower, temperature to be sure of obtaining a reliable assessment of ageing.

2. The index of retained stiffness modulus (IRSM) and the index of dynamic modulus, $|E^*|_{MD\text{-}index}$ were greater than the minimum criteria (80%) used in all circumstances of this study. However, some $|E^*|_{MD\text{-}index}$ values of 100/150 Pen mixtures were less than 80% but still greater than 70% (recommended by many authorities). Therefore no significant moisture damage issues have arisen, even if the moisture conditioning was applied after ageing to asphalt mixtures. The limestone aggregate may play a significant role in these results as a hydrophobic (water-hating) material.

3. Indices to measure the combined effect of ageing and moisture damage $|E^*|_{A+MD}$ (using 4-PB machine) and AI+IRSM (using NAT) were generated. These indices indicated that the influence of ageing in increasing the stiffness modulus of a specimen was predominating more than the influence of moisture conditioning in reducing the modulus of the same specimen. The type of aggregate (limestone) may contribute to this findings.

### 11.2.2 Effect of moisture conditioning and ageing on fatigue failure

ITFT and 4-PB tests in constant strain method were used to study the fatigue failure of different asphalt mixtures exposed to individual and combined effects of moisture damage and ageing. The following points can be concluded:

1. A general behaviour emerged from ITFT results. The results indicated the stiffer the asphalt mixture, the better the fatigue performance. This stiffening may motivate the elastic properties of the bitumen to dominate rather than viscoelastic or viscous properties. This might increase the ability of asphalt mixtures recovery and release of stress during the 0.4-second rest period following the load application of ITFT. On the other hand, a slight reduction in the fatigue life of asphalt mixtures as determined by 4-PB tests was observed due to the applied ageing.

2. The applied moisture conditioning caused a slight reduction in the fatigue life of asphalt mixtures as determined by 4-PB tests. However, the fatigue life of aged mixtures has generally improved at 10 and 20°C when asphalt mixtures are exposed to moisture conditioning. The increased flexibility of aged specimens due to moisture might contribute to this finding.

3. It was possible to use the ASU method to analyse the data of ITFT. It was found that the resulting number of cycles to failure from this method was significantly greater than the traditional approach, $N_{f50}$. In addition, ASTM D 7460-10 was used for analysing the 4-PB fatigue results. It has predominantly produced more number of cycles to failure than the traditional method, $N_{f50}$. The main reasons can be attributed to the different concept of both methods.

4. A statistical model was generated using the data of modified ITFT in constant strain method to predict the number of cycles to failure (fatigue failure) of asphalt mixtures exposed to ageing or/and moisture conditioning. The initial stiffness modulus measured by the software of modified ITFT was used in this model. However, the robustness of this this model requires an assessment.

5. A statistical test of significance (ANOVA) was used to test whether the slopes of the different fatigue lines are the same or no. The p-values indicated that no

statistical significant difference was found between the lines derived for specimens subjected to different assessment methods and environmental conditions. However, the results presented in Table 7.7 for $N_f^{100\ \mu\varepsilon}$ might be more rational and interpretable. Table 7.7 reveals that the stiffer mixtures have generally improved the fatigue cracking resistance. For example, using the hard mix of 10/20 Pen can resist a strain of 124 με resulting from $10^6$ load repetitions versus only 19 με when the 100/150 Pen mix was used at the same conditions. Therefore, the ANOVA test might be not suitable to statistically test these regression lines of fatigue and a different statistical test is required.

### 11.2.3 Effect of moisture conditioning and ageing on healing potential

In this section, an attempt was made to find the effect of air voids content, time of loading and different resting time in combination with the effects of ageing and/or moisture damage on the potential of damage recovery. Based on the collected results, the following can be summarised:

1. Optimising a reasonable number of loading cycles is important in inducing the amount of recoverable and irrecoverable damages within a reasonable timescale and in turn assessing properly the role of rest periods. Misleading might result from using too few number of loading cycles (for example 100 cycles) because most fatigue testing methods (in constant strain method) require between 50-100 cycles to measure the initial stiffness modulus properly based on the applied loading frequencies.

2. The moisture conditioning of control mixtures has less effect on the potential of damage recovery than ageing and ageing combined with moisture damage as shown earlier in Table 9.5. The reason is still not clear and in need of further research but it could be related to the role of water in making the asphalt mixture more flexible and in turn increasing the damage recovery during the applied rest periods.

## 11.3 Further work

There are many areas to develop this study in the future. The following section outlines the key perspectives which are in need of further investigation.

### 11.3.1 In terms of mixtures variables

1. It is important to investigate the combined effect of ageing and moisture damages on fatigue and healing performance of asphalt mixtures using different types of aggregate.

2. Study the effect of air voids shape and size and their distribution might be important for more investigation and understanding of their influence with moisture damage and ageing on fatigue and healing performance of asphalt mixtures.

### 11.3.2 In terms of testing conditions

1. Evaluating the effect of different moisture conditioning temperatures and times is important to optimize the best conditions that simulate the real pavement conditions. It will also be beneficial to examine the effect of time and temperature of moisture conditioning to make sure if the ageing is a possible result of this conditioning or not.

2. More cycles and more methods of moisture damage and ageing might be important for more investigation of their influence on fatigue damage.

### 11.3.3 In terms of rest periods

1. Applying short uniform or non-uniform rest periods (random) to 4PB fatigue tests is a new challenge. It needs more investigation to be more realistic and identical to that of in-service asphalt pavement.

2. ITFT was based on the standard pulse of 0.1 second loading followed by 0.4-second rest. To improve the future exploration of fatigue and healing by ITFT in strain-controlled method, it could be interesting to change these loading and resting times and investigate this with the influence of environmental factors.

### 11.3.4 In terms of testing methods

1. To evaluate more the effect of combined environmental factors on fatigue damage, using other homogeneous tests such as controlled-strain tension-compression (Push-Pull) uniaxial fatigue test is necessary.
2. Using the saturation ageing tensile stiffness (SATS) procedure to simulate the combined effect of moisture damage and oxidative ageing may provide the opportunity to investigate this combination effect on fatigue characterisation by means of ITFT. However, the productivity of this protocol should be considered and it will be preferred to investigate this at limited and appropriate strain levels.

### 11.3.5 In terms of analysis methods

More approaches of dissipated energy methods need to be undertaken in detail for the investigation of the combined effect of moisture damage and oxidative ageing on fatigue performance by means of 4PB test. Applying the Arizona State University (ASU) to analyse ITFT results can also be expanded. However, it requires increasing the failure criteria in terms of an initial stress for longer running of ITFT. This running of the ITFT will help to find the peak of the curve of normalised stiffness modulus versus the number of cycles. Similarly, applying ASTM D 7460-10 method to ITFT results might be interesting with increasing the failure criteria to more than 50% (traditional). This increase is important to find the peak (failure point) of the curve which may occur after a reduction of more than 50% of the initial stress. Minimising the vertical permanent deformation should be considered for proper application of these fatigue analysis methods.

## 11.4 Implications for future practice

### 11.4.1 Implications for laboratory practice

The main aim in this study was to explore the individual and combined effects of environmental factors on fatigue and healing performance of bituminous concrete mixtures. The moisture damage and oxidative ageing are the main detrimental environmental factors affecting the performance of asphalt pavement in the long-term. Therefore it was decided to emphasize their effects in this research. A considerable testing programme was carried out to achieve this aim and the main findings of stiffness modulus and fatigue and healing tests were reported and discussed. Some of these findings might have important implications for future practice. However, the implication of findings of research into the 'real world', regardless of discipline, has been shown to be one of the greatest hurdles associated with innovative developments (Preston, 1991).

First, the major practical contribution of the present research is that it provides much needed experimental data on time-dependent primary environmental factors affecting the stiffness modulus and fatigue performance of bituminous paving mixtures. However, the method of assessment of fatigue performance showed a different results and seems to have a great influence. The importance of using a unique way to determine the fatigue cracking resistance may arise from these findings as implications for future practice.

In some occasions, it was found that an increase in the stiffness and complex moduli of asphalt mixtures investigated in this study after moisture conditioning and even after applying ageing to these conditioned mixtures. Therefore the second implication of these findings suggests that optimising the proper temperature and time of moisture conditioning by the standard procedures might be necessary to avoid any possible ageing that might occur during these procedures. However, the role of using limestone aggregate should be taken into account.

Third, these findings have important implications to develop the application of non-uniform rest periods. However, this requires a promising software such as that provided by the 4PB machine at the University of Nottingham.

The dynamic modulus $|E^*|$ of asphalt mixtures is considered one of the major material characteristics for pavement design and analysis. Therefore, a further implication is that it is important to keep testing the effects of environmental factors on the durability of bituminous concrete mixtures using this technique. It might be used as a standard test for evaluating the moisture damage over a wide range of temperatures and loading frequencies.

Finally, the traditional procedure of ageing and moisture induced damage followed by this study is time consuming and therefore development of a practical and productive alternative apparatus is still in need to combine these conditions simultaneously for different types of asphalt mixtures.

### 11.4.2 Implications regarding in-site behaviour

Pavements suffer the combined effects of age hardening and moisture damage and it is important that laboratory assessments are related to in-situ response. Therefore it is desirable that a number of in-service truck roads and motorways in the UK are surveyed to determine the combined effect of age hardening and moisture damage on the fatigue cracking of their asphaltic layers. Both cracking need to consider, bottom-up and top to down cracking. The last one might be more related to age hardening and moisture damage. Nunn et al., 1997 surveyed a number of in-service truck roads and motorways in the UK and found no detrimental effect of age hardening in the lower asphaltic layers. In these pavement, age hardening was shown to reduce pavement deflection over time and reduce the risk of fatigue cracking.

Performing this surveying may help to decide if the designers need to take into account the combined effect of ageing and moisture damage in the relationship of fatigue life prediction when dimensioning the thickness of asphalt layers.

# References

AASHTO, P., 2002. Standard practice for mixture conditioning of hot-mix asphalt (HMA). *American Association of State Highway and Transportation Organization*.

AASHTO, T., 2012. 315-12. Standard Method of Test for Determining the Rheological Properties of Asphalt Binder Using a Dynamic Shear Rheometer (DSR). *American Association of State Highway and Transportation Organization*.

AASHTO, T., 2007. 62-07. Standard Method of Test for Determining Dynamic Modulus of Hot Mix Asphalt HMA. *American Association of State Highway and Transportation Organization*.

Abdullah, M.E., Zamhari, K.A., Buhari, R., Nayan, M.N. and Mohd Rosli, H., 2014. Short term and long term aging effects of asphalt binder modified with montmorillonite. *Trans Tech Publications.* Vol.594, pp.996-1002.

Abojaradeh, M., 2013. Development of fatigue failure criterion for hot-mix asphalt based on dissipated energy and stiffness ratio. *Jordan Journal of Civil Engineering*, *7*(1), pp.54-69.

Abojaradeh, M., Witczak, M., Mamlouk, M. and Kaloush, K., 2007. Validation of Initial and Failure Stiffness Definitions in Flexure Fatigue Test for Hot-Mix Asphalt. *ASTM Journal of Testing and Evaluation*, 35: 95-102.

Adedimila, A.S. and Kennedy, T.W., 1975. Fatigue and resilient characteristics of asphalt mixtures by repeated-load indirect tensile test (No. CFHR-3-9-72-183-5 Res. Rpt.). University of Texas at Austin.

Aglan, H.A. and Figueroa, J.L., 1993. Damage-evolution approach to fatigue cracking in pavements. *Journal of engineering mechanics*, 119(6), pp.1243-1259.

Aguiar-Moya, J.P., Salazar-Delgado, J., García, A., Baldi-Sevilla, A., Bonilla-Mora, V. and Loría-Salazar, L.G., 2017. Effect of ageing on micromechanical properties of bitumen by means of atomic force microscopy. *Road Materials and Pavement Design*, 18(sup2), pp.203-215.

Airey, G., 1997. *Rheological characteristics of polymer modified and aged bitumens* (Doctoral dissertation, University of Nottingham).

Airey, G.D., Collop, A.C., Zoorob, S.E. and Elliott, R.C., 2008. The influence of aggregate, filler and bitumen on asphalt mixture moisture damage. *Construction and building materials*, 22(9), pp.2015-2024.

Airey, G.D. and Choi, Y.K., 2002. State of the art report on moisture sensitivity test methods for bituminous pavement materials. *Road Materials and Pavement Design*, *3*(4), pp.355-372.

Airey, G.D., 2002. Use of black diagrams to identify inconsistencies in rheological data. *Road Materials and Pavement Design*, *3*(4), pp.403-424.

Airey, G.D., 2004. Fundamental binder and practical mixture evaluation of polymer modified bituminous materials. *International Journal of Pavement Engineering*, *5*(3), pp.137-151.

Ajideh, H., Bahia, H. and Earthman, J., 2010. Damage Resistance and Performance Evaluations of Engineered Asphalt Materials and Asphalt-Aggregate Mixtures with High Percentage of RAP. Research Report, City of Los Angeles, the University of California, Irvine and the University of Wisconsin, Madison.

Alfaqawi, R.M.S., 2018. *Investigation into ageing and the effect of hydrated lime on mastics and mixture ageing* (Doctoral dissertation, University of Nottingham).

Al-Swailmi, S. H. and R. L. Terrel, 1992. Evaluation of Water Damage of Asphalt Concrete Mixtures Using the Environmental Conditioning System (ECS). *Journal of the Association of Asphalt Paving Technologists (AAPT)*, Vol.61, pp.405-445.

Al-Khateeb, G. and Shenoy, A., 2004. A distinctive fatigue failure criterion. *Journal of the Association of Asphalt Paving Technologists (AAPT)*, Vol.*73*, pp.585-622.

Anderson, D.A., Christensen, D.W. and Bahia, H., 1991. Physical properties of asphalt cement and the development of performance-related specifications. *Journal of the Association of Asphalt Paving Technologists (AAPT),* Vol. 60, pp. 437-475.

Anderson, M., 2002. Tests to assess the potential for Moisture Damage in Asphalt Mixtures. In Houston, *TX: Asphalt Institute Spring Meeting Report*.

Anderson, D.A., Christensen, D.W., Bahia, H.U., Dongre, R., Sharma, M.G., Antle, C.E. and Button, J., 1994. Binder characterisation and evaluation, volume 3: Physical characterisation. *Strategic Highway Research Program, National Research Council,* Report No. SHRP-A-369.

Al-Qadi, I., Loulizi, A., Lahouar, S., Flintsch, G. and Freeman, T., 2003. Quantitative field evaluation and effectiveness of fine mix under hot-mix asphalt base in flexible pavements. Transportation Research Record: Journal of the Transportation Research Board, (1823), pp.133-140.

Apeagyei, A.K., Buttlar, W.G. and Dempsey, B.J., 2006. Moisture damage evaluation of asphalt mixtures using AASHTO T283 and DC (T) fracture test. *10th International Conference on Asphalt Pavements,* August 12 to 17, 2006, Quebec, Canada, Vol.1, pp.740-751.

Apeagyei, A.K. and Diefenderfer, S.D., 2011. Asphalt material design inputs for use with the mechanistic-empirical pavement design guide in Virginia (No. FHWA/VCTIR 12-R6).

Apeagyei, A.K., Grenfell, J.R. and Airey, G.D., 2014. Observation of reversible moisture damage in asphalt mixtures. *Construction and Building Materials*, *60*, pp.73-80.

Arambula, E. and Kutay, M.E., 2009. Tension-compression fatigue test evaluation using fracture mechanics and field data. *Road Materials and Pavement Design*, *10*(1), pp.83-108.

Artamendi, I. and McHale, M. (2015). Evaluation of EME2 type mixtures incorporating softer grade binders - Phase I progress report. Published Project Report PPR 750. Crowthorne: TRL Limited (PPR750).

ASTM, A., D7460-10 Standard test method for determining fatigue failure of compacted asphalt concrete subjected to repeated flexural bending.

Ayar, P., Moreno-Navarro, F. and Rubio-Gámez, M.C., 2016. The healing capability of asphalt pavements: a state of the art review. *Journal of Cleaner Production*, 113, pp.28-40.

Baaj, H., Di Benedetto, H. and Chaverot, P., 2005. Effect of binder characteristics on fatigue of asphalt pavement using an intrinsic damage approach. *Road Materials and Pavement Design*, *6*(2), pp.147-174.

Baburamani, P. 1999. Asphalt fatigue life prediction models: a literature review. Research Report ARR 334, *ARRB Transport Research*.

Bagampadde, U., Isacsson, U. and Kiggundu, B.M., 2006. Impact of bitumen and aggregate composition on stripping in bituminous mixtures. Materials and structures, 39(3), pp.303-315.

Baladi, G.Y., M. Schorsch, and T. Svasdisant, 2003. Determining the Causes of Top-Down Cracks in Bituminous Pavements. Report No. MDOT-PRCE-MSU-2003-110. *Pavement Research Centre of Excellence, Michigan Asphalt State University.*

Barksdale, R.D. and Miller, I.I., 1977. *Development of equipment and techniques for evaluating fatigue and rutting characteristics of asphalt concrete mixes* (No. GDOT Res Prj No 7305Final Rpt.).

Barra, B., Momm, L., Guerrero, Y. and Bernucci, L., 2012. Fatigue behaviour of dense asphalt mixes in dry and environmental-conditioning states. *Construction and Building Materials*, *29*, pp.128-134.

Bazin, P. and Saunier, J.B., 1967. Deformability, Fatigue and Healing Properties of Asphalt Mixes. Proceedings, *Second International Conference on the Structural Design of Asphalt Pavements*, Ann Arbor, Michigan, (pp. 553-569).

Beeson, J. 2012. Healing and fatigue characteristics of asphalt surface courses. *Master Dissertation*, submitted at the University of Nottingham. May 2012.

Bell, C.A., 1989. *Summary report on aging of asphalt-aggregate systems* (No. SHRP-A-305).

Bennert, T. and Williams, S., 2009. Precision of AASHTO TP62-07 for Use in Mechanistic—Empirical Pavement Design Guide for Flexible Pavements. *Transportation Research Record: Journal of the Transportation Research Board*, (2127), pp.115-126.

Bhasin, A., Castelo Branco, V.T., Masad, E. and Little, D.N., 2009. Quantitative comparison of energy methods to characterise fatigue in asphalt materials. *Journal of materials in civil engineering*, *21*(2), pp.83-92.

Bonnaure, F., Gravois, A. and Udron, J., 1980. A new method for predicting the fatigue life of bituminous mixes. *Journal of the Association of Asphalt Paving* Technologists (AAPT), Vol.49, pp.499-529.

Bonnaure, F., Huibers, A., and Boonders, A., 1982. A Laboratory Investigation of the Influence of Rest Periods on the Fatigue Characteristics of Bituminous Mixes. *Journal of the Association of Asphalt Paving Technologists* (AAPT), Vol.51, pp.104-128.

Bonnot, J., 1986. Asphalt aggregate mixtures. *Transportation Research Record 1096*, Transportation Research Board, Washington, D.C., pp.42-51.

Bonaquist, R. and Christensen, D.W., 2005. Practical procedure for developing dynamic modulus master curves for pavement structural design. *Transportation Research Record*, *1929*(1), pp.208-217.

Branthaver, J.F., Petersen, J.C., Robertson, R.E., Duvall, J.J., Kim, S.S., Harnsberger, P.M., Mill, T., Ensley, E.K., Barbour, F.A. and Scharbron, J.F., 1993. Binder characterization and evaluation. Volume 2: Chemistry (No. SHRP-A-368).

British Board of Agrément (BBA), 2008, BBA Thin Surfacing A.2. Determination of the Water Sensitivity of Bituminous Specimens. WS/PT0037 (BBA-6 No)/Issue 5.

British Standards Institution (2005), Coated macadam (asphalt concrte) for roads and other paved areas – Part 1: Specification for constituent materials and for mixtures, BS 4987-1:2005, London.

British Standards Institution (2004), Bituminous mixtures – Test methods for hot mix asphalt – Part 35: Laboratory mixing, BS EN 12697-35: 2004, London.

British Standards Institution (2003), Bituminous mixtures – Test methods for hot mix asphalt – Part 33: Specimen prepared by roller compactor, BS EN 12697-33: 2003, London.

British Standards Institution (2009), Bituminous mixtures – Test methods for hot mix asphalt – Part 5: Determination of the maximum density, BS EN 12697-5: 2009, London.

British Standards Institution (2003), Bituminous mixtures – Test methods for hot mix asphalt – Part 6: Determination of bulk density of bituminous specimens, BS EN 12697-6: 2003, London.

British Standards Institution (2003), Bituminous mixtures – Test methods for hot mix asphalt – Part 8: Determination of void characteristics of bituminous specimens, BS EN 12697-8: 2003, London.

British Standards Institution (2004), Bituminous mixtures – Test methods for hot mix asphalt – Part 26: Stiffness, BS EN 12697-26: 2004, London.

British Standards Institution (2012), Bituminous mixtures – Test methods for hot mix asphalt – Part 26: Stiffness, BS EN 12697-26: 2012, London.

British Standards Institution (2004), Bituminous mixtures – Test methods for hot mix asphalt – Part 24: Resistance to fatigue, BS EN 12697-24: 2004, London.

British Standards Institution (2012), Bituminous mixtures – Test methods for hot mix asphalt – Part 24: Resistance to fatigue, BS EN 12697-24: 2012, London.

British Standards Institution (2008), Bituminous mixtures – Test methods for hot mix asphalt – Part 12: Determination of the water sensitivity of bituminous specimens, BS EN 12697-12: 2008, London.

British Standards Institution (2015), Bituminous mixtures – Test methods Part 4: Bitumen recovery: Fractionating column, BS EN 12697-4:2015, London.

British Standards Publication (2007), Bitumen and bituminous binders – Determination of needle penetration, BS EN 1426:2007, London.

British Standards Publication (2015), Bitumen and bituminous binders – Determination of the softening point – Ring and Ball method, BS EN 1427:2015, London.

Brown, S.F., Brunton, J.M. and Pell, P.S., 1982, August. The development and implementation of analytical pavement design for British conditions.

In *Proceedings, Fifth International Conference on the Structural Design of Asphalt Pavements*, University of Michigan, Ann Arbor, Michigan (pp. 3-16).

Brown, S.F., 1988. Effect of mix properties on structural design: A review. *Journal of the Association of Asphalt Paving Technologists* (AAPT), Vol.57, pp. 245-261.

Brown, S.F., 1995. Practical test Procedures for Mechanical properties of Bituminous Materials. *In Proceedings of the Institution of Civil Engineers: Transport* (Vol. 111, No. 4, pp.289-297).

Brown, E.R., Kandhal, P.S., Roberts, F.L., Kim, Y.R., Lee, D.Y. and Kennedy, T.W., 2009. Hot mix asphalt materials, mixture design, and construction. *National Asphalt Pavement Association (NAPA): Research and Education Foundation*.

Buss, A., Williams, R.C. and Schram, S., 2016. Evaluation of moisture susceptibility tests for warm mix asphalts. *Construction and Building Materials*, *102*, pp.358-366.

Carpenter, S. and Shen, S., 2006. Dissipated energy approach to study hot-mix asphalt healing in fatigue. *Transportation Research Record: Journal of the Transportation Research Board*, (1970), pp.178-185.

Castro, M. and Sánchez, J.A., 2006. Fatigue and healing of asphalt mixtures: discriminate analysis of fatigue curves. *Journal of transportation engineering*, *132*(2), pp.168-174.

Chen, J.S. and Huang, L.S., 2000. Developing an aging model to evaluate engineering properties of asphalt paving binders. *Materials and Structures*, *33*(9), pp.559-565.

Chiangmai, C.N., 2010. *Fatigue-fracture relation on asphalt concrete mixtures*. (Master dissertation, University of Illinois at Urbana-Champaign).

Cocurullo, A., Airey, G.D., Collop, A.C. and Sangiorgi, C., 2008, November. Indirect tensile versus two-point bending fatigue testing. In *Proceedings of the Institution of Civil Engineers-Transport* (Vol. 161, No. 4, pp. 207-220). Thomas Telford Ltd.

Cumming, G., Fidler, F. and Vaux, D.L., 2007. Error bars in experimental biology. *The Journal of cell biology*, *177*(1), pp.7-11.

Copper, K.E. and Pell, P.S., 1974. *The effect of mix variables on the fatigue strength of bituminous materials* (No. TRRL LR 633).

Corté, J.F. and Goux, M.T., 1996. Design of pavement structures: the French technical guide. *Transportation Research Record: Journal of the Transportation Research Board*, (1539), pp.116-124.

Daniel, J.S., Bisirri, W. and Kim, Y.R., 2004. Fatigue evaluation of asphalt mixtures using dissipated energy and viscoelastic continuum damage approaches (with discussion). *Journal of the Association of Asphalt Paving Technologists* (AAPT), Vol.73, pp.557-583.

Das, P.K., Balieu, R., Kringos, N. and Birgisson, B., 2015. On the oxidative ageing mechanism and its effect on asphalt mixtures morphology. Materials and Structures, 48(10), pp.3113-3127.

Dauzats, M. and R. Linder, 1982. A Method for the Evaluation of the Structural Condition of Pavement with Thick Bituminous Road Bases. *Fifth International Conference on the Structural Design of Asphalt Pavements*, the Delft University of Technology, August 23-26, 1982 Vol.1, p.378.

Dauzats, M., and A. Rampal, 1987. Mechanism of Surface Cracking in Wearing Courses. Proceedings of the *6th International Conference on Asphalt Pavements*, Ann Arbor, pp. 232-247.

Deacon, J., Tayebali, A., Coplantz, J., Finn, F. and Monismith, C., 1994. Fatigue Response of Asphalt-Aggregate Mixes, Part III—Mix Design and Analysis. *Strategic Highway Research Program Report: No. SHRP-A*, *404*.

De Mello, L.G.R., de Farias, M.M. and Kaloush, K.E., 2018. Effect of temperature on fatigue tests parameters for conventional and asphalt rubber mixes. *Road Materials and Pavement Design*, *19*(2), pp.417-430.

De La Roche, C.D., 1996. *Module de rigidité et comportement en fatigue des enrobés bitumineux: expérimentations et nouvelles perspectives d'analyse* (Doctoral dissertation, Châtenay-Malabry, Ecole centrale de Paris).

Devore, J. L., 2012. Probability and Statistics for Engineering and the Sciences, 3rd edition. Brooks/Cole Publishing Company, Pacific Grove, California.

Diab, A., You, Z.P., Othman, A.M. and Ahmed, H.Y., 2013. Fatigue characteristics of hydrated lime modified HMA*. International Journal of Pavement Research and Technology*, 6(1), pp.31-36.

Di Benedetto, H. and De La Roche, C., 1998. State of the art on stiffness modulus and fatigue of bituminous mixtures. RILEM Report 17. *Bituminous Binders and Mixes*, pp.137-180.

Di Benedetto, H., de La Roche, C., Baaj, H., Pronk, A. and Lundstrom, R., 2003. Fatigue of bituminous mixtures: different approaches and RILEM group contribution. In *Sixth International RILEM Symposium on Performance Testing and Evaluation of Bituminous Materials* (pp. 15-38). RILEM Publications SARL.

Di Benedetto, H., De La Roche, C., Baaj, H., Pronk, A. and Lundström, R., 2004. Fatigue of bituminous mixtures. *Materials and structures*, *37*(3), pp.202-216.

Di Benedetto, H., Nguyen, Q.T. and Sauzéat, C., 2011. Nonlinearity, heating, fatigue and thixotropy during cyclic loading of asphalt mixtures. *Road Materials and Pavement Design*, *12*(1), pp.129-158.

Dietmar, G. and Thomson, S., 2006. Fracture Mechanics with an introduction to micromechanics. *New York*.

Doan, T., 1976. Studies of the fatigue of bituminous mixtures at the LCPC. *Bull Liaison Lab Ponts Chauss*, Issue Number: 84, pp.85-100.

Dunford, A., 2013. *Friction and the texture of aggregate particles used in the road surface course* (Doctoral dissertation, University of Nottingham).

Epps, J., and Monismith, C. L. 1972. Fatigue of asphalt concrete mixtures—A summary of existing information. *Fatigue of Compacted Bituminous Aggregate Mixtures*. Rep. No. STP 508, American Society for Testing and Materials, Philadelphia, pp.19-45.

Epps, J.A., Monismith, C.L., Warden, W.B., Pell, P.S., Kallas, B.F., Terrell, R.L., Busching, H.W. and Mcleod, N.W., 1969, February. Influence of mixture variables on the flexural fatigue properties of asphalt concrete. In *Association of Asphalt Paving Technologists (AAPT),* Vol.38, pp.423-464.

Finn, F., Saraf, C.L., Kulkarni, R., Nair, K., Smith, W. and Abdullah, A., 1986. Development of pavement structural subsystems. *NCHRP Report*, (291).

Francken, L. and Clauwaert, C., 1987. Characterisation and structural assessment of bound materials for flexible road structures. *Sixth International Conference, Structural Design of Asphalt Pavements*. University of Michigan, July 13-17, 1987, ANN Arbor, Michigan. Publication of Michigan University. Volume I, pp.130-144.

Francken, L., 1979. Fatigue d'un Enrobé Bitumineux Soumis à des Conditions de Sollicitations Réalistes. *TECH ROUT*, *24*(4).

Goddard, R.T.N., Powell, W.D. and Applegate, M.W., 1978. *Fatigue resistance of dense bitumen macadam: the effect of mixture variables and temperature* (No. SR410 Monograph).

Gibb, J.M., 1996. *Evaluation of resistance to permanent deformation in the design of bituminous paving mixtures* (Doctoral dissertation, University of Nottingham).

Ghuzlan, K. A., and Carpenter, S. H., 2003. Traditional Fatigue Analysis of Asphalt Concrete Mixtures. Presented at the 82nd Annual Meeting of the Transportation Research Board, Washington, D.C.

Glover, C.J., Davison, R.R., Domke, C.H., Ruan, Y., Juristyarini, P., Knorr, D.B. and Jung, S.H., 2005. Development of a new method for assessing asphalt binder durability with field validation. Report FHWA/TX-05/1872-2. *Texas Department of Transportation*, Austin.

Gómez-Meijide, B., Ajam, H., Lastra-González, P. and García, A., 2016. Effect of air voids content on asphalt self-healing via induction and infrared heating. *Construction and Building Materials*, *126*, pp.957-966.

Groenendijk, J., 1998. *Accelerated testing and surface cracking of asphaltic concrete pavements* (Doctoral dissertation, TU Delft, Delft University of Technology).

Harmelink, D. and Aschenbrener, T., 2003. Extent of top-down cracking in Colorado (No. CDOT-DTD-R-2003-7).

Hartman, A.M., Gilchrist, M.D. and Walsh, G., 2001. Effect of mixture compaction on indirect tensile stiffness and fatigue. *Journal of transportation engineering*, 127(5), pp.370-378.

Harvey, J., Eriksen, K., Sousa, J. and Monismith, C.L., 1994. Effects of Laboratory Specimen Preparation on Aggregate-Asphalt Structure, Air-Void

Content Measurement, and Repetitive Simple Shear Test Results. *Transportation Research Record*, (1454).

Harvey, J.T., Deacon, J.A., Tsai, B.W. and Monismith, C.L., 1995. Fatigue performance of asphalt concrete mixes and its relationship to asphalt concrete pavement performance in California. University of California, Berkeley, Institute of Transportation Studies, Asphalt Research Program, CAL/APT Program, Report Number: RTA-65W485-2.

Harvey, J. and Tsai, B.W., 1996. Effects of asphalt content and air void content on mix fatigue and stiffness. Transportation Research Record: *Journal of the Transportation Research Board*, (1543), pp.38-45.

Harvey, J. and Tsai, B.W., 1997. Long-term oven-aging effects on fatigue and initial stiffness of asphalt concrete. *Transportation Research Record: Journal of the Transportation Research Board*, (1590), pp.89-98.

Hofko, B., Cannone Falchetto, A., Grenfell, J., Huber, L., Lu, X., Porot, L., Poulikakos, L.D. and You, Z., 2017. Effect of short-term ageing temperature on bitumen properties. *Road Materials and Pavement Design*, 18(sup2), pp.108-117.

Hofko, B., Alavi, M.Z., Grothe, H., Jones, D. and Harvey, J., 2017. Repeatability and sensitivity of FTIR ATR spectral analysis methods for bituminous binders. Materials and Structures, 50(3), p.187.

Hopman, P.C., Kunst, P.A.J.C. and Pronk, A.C., 1989, October. A renewed interpretation method for fatigue measurements, verification of miner's rule. In 4th Eurobitumen symposium in Madrid (Vol. 1, pp. 557-561).

Houston, W.N., Mirza, M.W., Zapata, C.E. and Raghavendra, S., 2007. Simulating the effects of hot mix asphalt aging for performance testing and pavement structural design. NCHR Research Results Digest, 324.

Hsu, T.W. and Tseng, K.H., 1996. Effect of rest periods on fatigue response of asphalt concrete mixtures. *Journal of Transportation Engineering*, 122(4), pp.316-322.

Huang, C., Najjar, Y.M. and Romanoschi, S.A., 2007. Predicting asphalt concrete fatigue life using artificial neural network approach (No. 07-1607).

Hugo, F., and T.W. Kennedy, 1985. Surface Cracking of Asphalt Mixtures in Southern Africa. Proceedings of the *Association of Asphalt Paving Technologists (AAPT)*, Vol. 54, pp 454-501.

Hveem, F. N., 1955. Pavement Deflections and Fatigue Failures in Design and Testing of Flexible Pavements. HRB Bulletin 114, *Highway Research Board*, pp. 43-87.

Jimenez, R. A., 1972. Fatigue testing of asphaltic concrete slabs. Fatigue of compacted bituminous aggregate mixtures, ASTM STP 508, ASTM, West Conshohocken, pp.3–17.

Judycki, J., 1991. Fatigue of asphalt mixes, Univ. of Oulu, Publications of Road and Transport Laboratory, Oulu, Finland. Issue Number: 11.

Jimenez, R.A. and Gallaway, B.M., 1962, January. Preliminary report of an apparatus for the testing of asphaltic concrete diaphragms. In Meeting of the *Association of Asphalt Paving Technologists* (No. E-68-61).

Jimenez, R.A. and Gallaway, B.M., 1962. Behaviour of asphaltic concrete diaphragms to repetitive loadings. *In International Conference on the Structural Design of Asphalt Pavements*. University of Michigan, Ann Arbor (Vol.203, No.1).

Jaskula, P. and Judycki, J., 2014. Durability of asphalt concrete subjected to deteriorating effects of water and frost. *American Society of Civil Engineers: Journal of Performance of Constructed Facilities*, 30(1), pp.1-10.

Jung, S. H., Walubita, L. F., Martin, A. E. and Glover, C. J. Mixture versus neat-film binder oxidation and hardening and the Impact of Binder Oxidation on Estimated mixture fatigue life. *Transportation Research Board 86th Annual Meeting*, 2007.

Khan, R. and Collop, A.C., 2010. The use of X-ray computed tomography to characterise micro damage in asphalt. *Road Materials and Pavement Design*, 11(sup1), pp.89-109.

Kennedy, T.W., 1977. Characterisation of asphalt pavement materials using the indirect tensile test. In *Association of Asphalt Paving Technologists (AAPT)*, Vol.46, pp.132–150.

Kennedy, T.W., Roberts, F.L. and McGennis, R.B., 1984. Effects of compaction temperature and effort on the engineering properties of asphalt concrete mixtures. *Placement and Compaction of Asphalt Mixtures*, ASTM Special Technical Publication 829. American Society for Testing and Materials, Philadelphia, pp.48-66.

Kim, O.K., Montalvo, J., Bell, C.A., Hicks, R.G. and Wilson, J.E., 1986. Effect of moisture and aging on asphalt pavement life: Part 1-effect of moisture (No. FHWA-OR-RD-86-01). Oregon. Dept. of Transportation.

Kim, O.K., Montalvo, J., Bell, C.A., Hicks, R.G., Wilson, J.E. and Boyle, G.E., 1986. Effect of moisture and aging on asphalt pavement life: Part 2-effect of aging (No. FHWA-OR-RD-86-01-2). Oregon. Dept. of Transportation. Research Unit.

Kim, S. and Coree, B.J., 2005. Evaluation of hot mix asphalt moisture sensitivity using the Nottingham asphalt test equipment (No. IHRB Project TR-483). Iowa State University. Center for Transportation Research and Education.

Kim, Y., Khosla, N. and Kim, N., 1991. Effect of temperature and mixture variables on fatigue life predicted by diametral fatigue testing. *Transportation Research Records 1317*, pp.128-138.

Kim, Y.R. and Little, D.N., 1990. One-dimensional constitutive modelling of asphalt concrete. *Journal of engineering mechanics*, 116(4), pp.751-772.
KIRK, J. Results of fatigue tests on different types of bituminous mixtures. Intl Conf Struct Design Asphalt Pvmts, 1967.

Kirk, J. M., 1967. Results of Fatigue Tests on Different Types of Bituminous Mixes. Proceedings, *Second International Conference on the Structural Design of Asphalt Pavement*, University of Michigan, pp.571-575.

Kumar, A. and Goetz, W.H. (1977). Asphalt hardening as affected by film thickness, voids and permeability in asphaltic mixtures. *Association of Asphalt Paving Technologists (AAPT),* Vol.46, pp.571-605.

Kunst, P.A.J.C., 1989. Surface Cracking on Asphalt Layers, Working Committee B12, Hoevelaken, Holland, 1989.

Lamontagne, J. 2001. Comparison by Fourier transform infrared (FTIR) spectroscopy of different ageing techniques: application to road bitumens. Fuel, 80, 483-488.

Lehman, A., O'Rourke, N., Hatcher, L. and Stepanski, E., 2013. JMP for basic univariate and multivariate statistics: Methods for researchers and social scientists. SAS Institute.

Liang, R.Y. and Zhou, J., 1997. Prediction of fatigue life of asphalt concrete beams. *International journal of fatigue*, 19(2), pp.117-124.

Little, D.N., Lytton, R.L., Williams, D. and Chen, C.W., 2001. Microdamage healing in asphalt and asphalt concrete, Volume 1: microdamage and microdamage healing, project summary report (No. FHWA-RD-98-141). Turner-Fairbank Highway Research Center.

López-Montero, T. and Miró, R., 2016. Differences in cracking resistance of asphalt mixtures due to ageing and moisture damage. *Construction and Building Materials*, 112, pp.299-306.

Lu, X. and Isacsson, U., 2002. Effect of ageing on bitumen chemistry and rheology. Construction and Building materials, 16(1), pp.15-22.

Lu, X., Talon, Y. and Redelius, P., 2008, May. Ageing of bituminous binders-laboratory tests and field data. In Proceedings of the 4th Eurasphalt and Eurobitume Congress, Copenhagen (pp. 21-23).

Lu, Q. and Harvey, J.T., 2008. Inclusion of moisture effect in fatigue test for asphalt pavements. In Transportation and Development Innovative Best Practices 2008 (pp. 498-504).

Liu, H., Hao, P., Wang, H. and Adhikair, S., 2013. Effects of physio-chemical factors on asphalt aging behaviour. Journal of Materials in Civil Engineering, 26(1), pp.190-197.

Lytton, R.L., Uzan, J., Fernando, E.G., Roque, R., Hiltunen, D. and Stoffels, S.M., 1993. Development and validation of performance prediction models and specifications for asphalt binders and paving mixes. Rep. No. SHRP-A-357, *Strategic Highway Research Program*, National Research Council, Washington, D.C.

Ma, T., Huang, X.M., Mahmoud, E. and Garibaldy, E., 2011. Effect of moisture on the aging behavior of asphalt binder. International Journal of Minerals, Metallurgy, and Materials, 18(4), p.460.

Maggiore, C., 2014. *A comparison of different test and analysis methods for asphalt fatigue* (Doctoral dissertation, University of Nottingham).

Majidzadeh, K., Kauffmann, E.M. and Ramsamooj, D.V., 1971. Application of fracture mechanics in the analysis of pavement fatigue. *Association of Asphalt Paving Technologists (AAPT)*, Vol.40, pp.227–246.

Majidzadeh, K., E. M. Kaufmann, and C. L. Saraf. Analysis of Fatigue of Paving Mixtures from the Fracture Mechanics Viewpoint. *In Fatigue of Compacted*

*Bituminous Aggregate Mixtures*, American Society for Testing and Materials, West Conshohocken, 1972, ASTM Spec Tech Publ, 508:67–83.

Malan, G.W., Strauss, P.J., Kleyn, E. and Servas, V.P., 1989. A Field Study of Premature Surface Cracking in Asphalt. Proceedings of the *Association of Asphalt Paving Technologists*, Vol. 58, pp. 142-162.

Mamlouk, M., Souliman, M. and Zeiada, W., 2012, July. Optimum testing conditions to measure HMA fatigue and healing using flexural bending test. In *TRB annual meeting*.

Mandula, J. and Olexa, T., 2017, September. High temperature impact on fatigue life of asphalt mixture in Slovakia. In IOP Conference Series: *Materials Science and Engineering* (Vol.236, No.1, pp.1-8).

Mannan, U.A., Ahmad, M. and Tarefder, R.A., 2017. Influence of moisture conditioning on healing of asphalt binders. *Construction and Building Materials*, 146, pp.360-369.

Marsac, P., Piérard, N., Porot, L., Grenfell, J., Mouillet, V., Pouget, S., Besamusca, J., Farcas, F., Gabet, T. and Hugener, M., 2014. Potential and limits of FTIR methods for reclaimed asphalt characterisation. Materials and structures, 47(8), pp.1273-1286.

Mashaan, N.S., Karim, M.R., Abdel Aziz, M., Ibrahim, M.R., Katman, H.Y. and Koting, S., 2014. Evaluation of fatigue life of CRM-reinforced SMA and its relationship to dynamic stiffness. *The Scientific World Journal*. Volume 2014, Article ID 968075, 11 pages.

Matthews, J.M., Monismith, C.L. and Craus, J., 1993. Investigation of laboratory fatigue testing procedures for asphalt aggregate mixtures. *Journal of transportation engineering*, 119(4), pp.634-654.

Maupin, G.W. and Diefenderfer, B.K., 2006. Design of a high-binder--high-modulus asphalt mixture (No. VTRC 07-R15). Virginia Transportation Research Council.

Mikhailenko, P., Bertron, A. and Ringot, E., 2016. Methods for analyzing the chemical mechanisms of bitumen aging and rejuvenation with FTIR spectrometry. In 8th RILEM International Symposium on Testing and Characterisation of Sustainable and Innovative Bituminous Materials (pp. 203-214). Springer, Dordrecht.

McCarthy, P.F., 1960. *Factors Affecting the Fatigue Characteristics of Bitumen Sand Mixtures* (Doctoral dissertation, Ph. D. Thesis, University of Nottingham, UK).

Mc Elvaney, J. and Pell, P.S., 1973. Fatigue damage of asphalt. Effect of rest periods. *Highways and Road Construction*, 41(1766).

Mehrara, A. and Khodaii, A., 2015. Evaluation of moisture conditioning effect on damage recovery of asphalt mixtures during rest time application. *Construction and Building Materials*, 98, pp.294-304.

Metcalf, J.B., Roberts, F.L., Rasoulian, M., Romanoschi, S., Li, Y. and Djakfar, L., 2001. Construction comparison of Louisiana's conventional and alternative base courses under accelerated loading (No. FHWA/LA-00/347). Louisiana Transportation Research Center.

Miller J.S., Bellinger W.Y., "Distress identification manual for the long-term pavement performance" (fourth revised edition", Report FHWA-RD-03-031, Federal Highway Administration, June 2003.

Molenaar, A.A.A., 1984. Fatigue and Reflection Cracking due to Traffic Loads. Proceedings. *Association of Asphalt Paving Technologies (AAPT)*, Vol.53, pp. 440-474.

Monismith, C. L., "Some Applications of Theory in the Design of Asphalt Pavements," Fifth Annual Nevada Streets and Highway Conference, University of Nevada, March 1970.

Monismith, C.L., Epps, J.A., Kasianchuk, D.A. and McLean, D.B., 1970. Asphalt mixture behaviour in repeated flexure. Report No. TE 70-5, Institute of Transportation and Traffic Engineering, University of California, Berkeley.

Monismith, C. L., J. A. Epps, and F. N. Finn, 1985. Improved Asphalt Mix Design. *Association of Asphalt Paving Technologists (AAPT)*, Vol.54, pp.347–406.

Monismith, C.L., Coplantz, J.S., Deacon, J.A., Finn, F.N., Harvey, J.T. and Tayebali, A.A., 1994. Fatigue Response of Asphalt-Aggregate Mixtures, Strategic Highway Research Program, National Research Council, Washington, DC. SHRP-A-404.

Mouillet, V., Lamontagne, J., Durrieu, F., Planche, J.P. and Lapalu, L., 2008. Infrared microscopy investigation of oxidation and phase evolution in bitumen modified with polymers. *Fuel*, 87(7), pp.1270-1280.

Nadkarni, A., Kaloush, K., Zeiada, W. and Biligiri, K., 2009. Using dynamic modulus test to evaluate moisture susceptibility of asphalt mixtures. Transportation Research Record: *Journal of the Transportation Research Board*, (2127), pp.29-35.

Nunn, M.E., Brown, A., Weston, D. and Nicholls, J.C., 1997. Design of long-life flexible pavements for heavy traffic, TRL report 250, 1997. TRL Limited, London, ISSN 0968- 4107.

Olard, F., Noël, F. and Loup, F., 2006. Modulus testing in indirect tension mode. *Road materials and pavement design*, 7(4), pp.543-554.

Oliveira, J.R.M., 2006. *Grouted macadam: Mechanical characterisation for pavement design* (Doctoral dissertation, Ph. D. thesis, Univ. of Nottingham, Nottingham, UK).

Oliveira, J., Pais, J.C., Thom, N.H. and Zoorob, S., 2009. The effect of using rest periods in 4PB tests on the fatigue life of grouted macadams. *In second Workshop on Four Point Bending* (pp. 277-283). Universidade do Minho.

Ouyang, C., Wang, S., Zhang, Y. and Zhang, Y., 2006. Improving the aging resistance of styrene–butadiene–styrene tri-block copolymer modified asphalt by addition of antioxidants. *Polymer degradation and stability*, 91(4), pp.795-804.

Pamulapati, Y., Elseifi, M.A., Cooper III, S.B., Mohammad, L.N. and Elbagalati, O., 2017. Evaluation of self-healing of asphalt concrete through induction heating and metallic fibers. *Construction and Building Materials*, 146, pp.66-75.

Paris, P. C., and Fazil Erdogan. "A critical analysis of crack propagation laws" *Journal of Fluids Engineering* 85.4 (1963): 528-533.

Pell, P.S., 1962. Fatigue characteristics of bitumen and bituminous mixes. *In International Conference on the Structural Design of Asphalt Pavements*. University of Michigan, Ann Arbor (Vol. 203, No. 1).

Pell, P.S., 1967. Fatigue of Asphalt Pavement Mixes, *Proceeding of the Second international Conference on the Structural Design of Asphalt Pavem*ents, Ann Arbor, Michigan, pp. 577-594.

Pell, P.S. and Cooper, K.E., 1975. The effect of testing and mix variables on the fatigue performance of bituminous materials. Journal of the *Association of Asphalt Paving Technologists*, (AAPT), Vol.44, pp.1-37.

Pell, P.S. and Hanson, J.M., 1973. Behaviour of Bituminous Road Base Materials under Repeated Loading. *Association of Asphalt Paving Technologists (AAPT)*, Vol.42, pp.201-229.

Pell, P.S. and Taylor, I.F., 1969, February. Asphaltic road materials in fatigue. *Association of Asphalt Paving Technologists* (AAPT), Vol.38, pp.371-422.

Pellinen, T., Christensen, D., Rowe, G. and Sharrock, M., 2004. Fatigue-Transfer Functions: How Do They Compare? Transportation Research Record: Journal of the Transportation Research Board, (1896), pp.77-87.

Petersen, J.C., Robertson, R.E., Branthaver, J.F., Harnsberger, P.M., Duvall, J.J., Kim, S.S., Anderson, D.A., Christiansen, D.W., Bahia, H.U., Dongre, R. and Antle, C.E., 1994. SHRP A-370: Binder Characterisation and Evaluation. Volume 4: Test Methods. Strategic Highway Research Program, National Research Council, Washington DC.

Pfeiffer, J.P. and Van Doormaal, P.M., 1936. The rheological properties of asphaltic bitumens. *Journal of the Institute of Petroleum Technologists*, 22, pp.414-440.

Poulikakos, L.D., dos Santos, S., Lee, J. and Partl, M.N., 2014. Moisture susceptibility of recycled asphalt concrete: a multi-scale approach. Transportation Research Board 93rd Annual Meeting, Transportation Research Board, Washington DC, USA. No. 14-0041.

Preston, J. N., 1991. *The design of bituminous concrete mixes* (Doctoral dissertation, University of Nottingham).

Priest, A.L. and Timm, D.H., 2006. Methodology and Calibration of Fatigue Transfer Functions for Mechanistic Empirical Flexible Pavement Design (No. NCAT Report 06-03).

Pronk, A.C. and Hopman, P.C., 1990. Energy dissipation: the leading factor of fatigue. Highway research: "shearing the benefits", Proceedings of the conference of the United States strategic highway research program. London, England, Teldford. October 1990, pp 225-267.

Pronk, A.C. 1995. Evaluation of the dissipated energy concept for the interpretation of fatigue measurement in the crack initiation phase. The Road and Hydraulic Engineering Division (DWW), Netherlands, P-DWW-95-001, 1995.

Raad, L., Saboundjian, S. and Minassian, G., 2001. Field aging effects on fatigue of asphalt concrete and asphalt-rubber concrete. Transportation Research Record: *Journal of the Transportation Research Board*, 1767, 126-134.

Rahman, M., 2004. Characterisation of dry process crumb rubber modified asphalt mixtures (Doctoral dissertation, University of Nottingham).

Raithby, K.D. and Sterling, A.B., 1970. The effect of rest periods on the fatigue performance of a hot-rolled asphalt under reversed axial loading and discussion. *Association of Asphalt Paving* Technologists (AAPT). Vol.39, pp.134-147.

Raithby, K.D. and A.D. Sterling, 1972. Some Effects of Loading History on the Fatigue Performance of Rolled Asphalts. TRRL Report LR 496. Transport and Road Research Laboratory, Department of the Environment, Crowthorne, Berkshire, England, 1972.

Raithby, K.D., Ramshaw, J.T., 1972. Effects of Secondary Compaction on the Fatigue Performance of a Hot-Rolled Asphalt." Crowthorne, England: TRRL-LR 471.

Read, J.M., 1996. *Fatigue cracking of bituminous paving mixtures* (Doctoral dissertation, University of Nottingham).

Read, J. and Whiteoak, D., 2003. *The shell bitumen handbook*. Thomas Telford.

Robertus, C., 1993. Shell multi-grade bitumen: A binder for high stability asphalt. *In Eurobitumen Congress, 5th*, Stockholm, Sweden (Vol.1, 161–165).

Rolt, J., 2000, October. Top-down cracking: myth or reality. *In The World Bank regional seminar on innovative road rehabilitation and recycling technologies*, Amman, Jordan (pp.24-26).

Roque, R. and B.E. Ruth, 1990. Mechanisms of Modelling of Surface Cracking in Asphalt Pavements. *Association of Asphalt Paving Technologists (AAPT)*, Vol. 59, pp.396-421.

Rowe, G.M., 1993. Performance of asphalt mixtures in the trapezoidal fatigue test. *Association of Asphalt Paving Technologists (AAPT)*, Vol. 62, pp.344-344.

Rowe, G.M., 1996. *Application of the dissipated energy concept to fatigue cracking in asphalt pavements* (Doctoral dissertation, University of Nottingham).

Rowe, G., Khoee, S., Blankenship, P. and Mahboub, K., 2009. Evaluation of aspects of $|E^*|$ test by using hot-mix asphalt specimens with varying void contents. Transportation Research Record: *Journal of the Transportation Research Board*, (2127), pp.164-172.

Rowe, G.M., Blankenship, P. and Bennert, T., 2012. Fatigue assessment of conventional and highly modified asphalt materials with ASTM and AASHTO standard specification. Four Point Bending-CRC Press Book, pp.113-122.

Santucci, L. and Schmidt, R., 1969. The effect of asphalt properties on the fatigue cracking of asphalt concrete on the Zaca-Wigmore test project. *Association of Asphalt Paving Technologists (AAPT)*. Vol.38, pp.39-64.

Schmidt, R.J. and Graf, P.E., 1972. Effect of water on resilient modulus of asphalt-treated mixes. Journal of the *Association of Asphalt Paving Technologists*, 41, pp.118-162.

Shen, S. and Carpenter, S.H., 2006. Dissipated energy concepts for HMA performance: fatigue and healing (Vol. 67, No. 11).

Singh, D., Zaman, M. and Commuri, S., 2011. Effect of long term oven aging on dynamic modulus of hot mix asphalt. In *Geo-Frontiers 2011*: Advances in Geotechnical Engineering (pp. 4773-4781).

Si, Z., Little, D. and Lytton, R., 2002. Evaluation of fatigue healing effect of asphalt concrete by pseudo stiffness. *Transportation Research Record: Journal of the Transportation Research Board*, (1789), pp.73-79.

Soenen, H., de La Roche, C. and Redelius, P., 2003. Fatigue behaviour of bituminous materials: from binders to mixes. *Road materials and pavement design*, 4(1), pp.7-27.

Solaimanian, M., Kennedy, T.W. and Elmore, W.E., 1993. Long-term evaluation of stripping and moisture damage in asphalt pavements treated with lime and antistripping agents. Report CTR 0-1286-1F. Texas Department of Transportation, Center for Transportation Research, University of Texas at Austin.

Soliman, M.I., Zeiada, W.A., Kaloush, K.E. and Mamlouk, M.S., 2012. Assessment of different flexure fatigue failure analysis methods to estimate the number of cycles to failure of asphalt mixtures. Paper presented at the 3rd Conference on Four-Point Bending, pp.27-34, DAVIS, CA, USA.

Souliman, M., Zeiada, W., Mamlouk, M. and Kaloush, K., 2013. Laboratory Validation of Healing-Based Fatigue Endurance Limit for Hot-Mix Asphalt. Transportation Research Record*: Journal of the Transportation Research Board*, (2373), pp.1-10.

Sol-Sánchez, M., Moreno-Navarro, F., García-Travé, G. and Rubio-Gámez, M.C., 2015. Laboratory study of the long-term climatic deterioration of asphalt mixtures. *Construction and Building Materials*, 88, pp.32-40.

Soltani, A. and Anderson, D.A., 2005. New test protocol to measure fatigue damage in asphalt mixtures. *Road materials and pavement design*, 6(4), pp.485-514.

Sousa, J.B., 1986. *Dynamic Properties of Pavement Materials*, Ph.D. Thesis, University of California, Berkeley.

Sousa, J. B., Tayebali, A., Harvey, J., Hendricks, P., and Monismith, C. L., 1993. Sensitivity of strategic highway research program A-003A testing equipment to mix design parameters for permanent deformation and fatigue. Transp. Res.

Rec. No. 1384, National Research Council, Transportation Research Board, Washington, D.C., 69–79.

Steiner, D., Hofko, B. and Blab, R., 2016. Effect of Air Void Content and Repeated Testing on Stiffness of Asphalt Mix Specimen. In Civil Engineering Conference in the Asian Region Cecar (Vol. 7).

Subhy, A.T., 2017. *Characterisation and development of rubberised bitumen and asphalt mixture based on performance-related requirements* (Doctoral dissertation, University of Nottingham).

Tangella, S.R., Craus, J., Deacon, J.A. and Monismith, C.L., 1990. Summary report on fatigue response of asphalt mixtures (No. SHRP-A-312).

Tarefder, R.A., Bateman, D. and Swamy, A.K., 2013. Comparison of fatigue failure criterion in flexural fatigue test. *International Journal of Fatigue*, 55, pp.213-219.

Tayebali, A.A., Tsai, B.W. and Monismith, C.L., 1994. *Stiffness of asphalt-aggregate mixes* (No. SHRP-A-388). Washington DC: Strategic Highway Research Program, National Research Council.

López-Montero, T, and Miró, R, 2016. Differences in cracking resistance of 16 asphalt mixtures due to ageing and moisture damage. *Construction and Building Materials*, 112, 299-306.

Thom, N.H. and Brown, S.F., 1987. Effect of moisture on the structural performance of a crushed-limestone road base. *Transportation Research Record: Journal of the Transportation Research Board*, (1121), pp.116-124.

Thom, N., 2006. Asphalt cracking: a Nottingham perspective. Engenharia Civil/Civil Engineering, 26, pp.75-84.

Ugé, P., Gravois, A. and Lemaire, J.N., 1976. Le comportement en fatigue des enrobés bitumineux: influence du liant. *REV GEN ROUTES AERODR*, (521).

Uhlmeyer, J., Willoughby, K., Pierce, L. and Mahoney, J., 2000. Top-down cracking in Washington state asphalt concrete wearing courses. Transportation Research Record: *Journal of the Transportation Research Board*, (1730), pp.110-116.

Vallerga, B.A., Finn, F.N. and Hicks, R.G., 1967, January. Effect of asphalt aging on the fatigue properties of asphalt concrete. *Third International Conference on Asphalt Pavements*, Ann Arbor, Michigan, 1972, pp.595-617.

Van Dijk, W., Moreaud, H., Quedeville, A. and Uge, P., 1972, September. The fatigue of bitumen and bituminous mixes. In *Presented at the Third International Conference on the Structural Design of Asphalt Pavements, Grosvenor House, Park Lane, London, England, Sept. 11-15, 1972.* (Vol. 1, No. Proceeding).

Van Dijk, W., 1975. Practical fatigue characterisation of bituminous mixes. Journal of the *Association of Asphalt Paving Technologists*, 44, pp.38-72.

Van Dijk, W. and Visser, W., 1977. Energy approach to fatigue for pavement design. In *Association of Asphalt Paving Technologists* Proc (Vol. 46).

Verstraeten, J., 1976. Aspects divers de la fatigue des mélanges bitumineux, prévision, rupture, condition de sollicitations. *Rapport de Recherche*, (170/JV/1976).

Verstraeten, J., 1991. Fatigue of bituminous mixes and bitumen thixotropy. In Proc. XIXth World Road Congress (pp. 766-769).

Vieira, J.M., Desmoluin, D. and Pellevoisin, P., 2012. Indirect tensile fatigue test for asphalt mixes commonly used in France. In Proc. 5th Eurasphalt and Eurobitume Congress. 13-15 June 2012 Istanbul, Turkey (p. 16).

Virgili, A., Partl, M.N., Grilli, A. and Santagata, F.A., 2008. Damage model for environmental conditioned fatigue test with CAST. *Fatigue and Fracture of Engineering Materials and Structures*, 31(11), pp.967-979.

Von Quintas, H., Scherocman, J., Kennedy, T.W. and Hughes, C.S., 1988. "Asphalt aggregate mixture analysis system", Final Report to NCHRP.

Wakefield, A., Anderson, R.M., McKay, Z., Tighe, S.L., McLeod, N.W., 2018. A Review of Solvent Extraction-Recovery Procedures and their Effect on Recovered Asphalt Binder Properties. *In proceedings for the 63rd Annual Conference of Canadian Technical Asphalt Association*. Nov. 2018 in Regina, Saskatchewan. Vol. LXIII, pp.475-496.

Walubita, L.F., 2006. *Comparison of fatigue analysis approaches for predicting fatigue lives of hot-mix asphalt concrete (HMAC) mixtures* (Doctoral dissertation, Texas A&M University).

Walubita, L. F., Epps Martin, A., Jung, S. H., Glover, C. J., Park, E. S., Chowdhury, A., and Lytton, R. L. Comparison of Fatigue Analysis Approaches for Two Hot Mix Asphalt Concrete (HMAC) Mixtures, Draft TxDOT Technical Research Report FHWA/TX-05/0-4468-2, College Station, Texas, October 2005.

Walubita, L.F., Simate, G.S., Ofori-Abebresse, E., Martin, A.E., Lytton, R.L. and Sanabria, L.E., 2012. Mathematical formulation of HMA crack initiation and crack propagation models based on continuum fracture-mechanics and work-potential theory. *International Journal of Fatigue*, 40, pp.112-119.

Wasserstein, R.L. and Lazar, N.A., 2016. The ASA's statement on p-values: context, process, and purpose. The American Statistician, 70(2), pp.129-133.

Wen, H., and Ramme, B., 2008. A performance evaluation of asphalt pavement with recycled pavement materials treated by self-cementing Fly Ash and field verification using M-E design guide: A case study. Paper presented at 2008 ASCE pavement conference: Airfield and Highway Pavements, pp.423-433. Bellevue, WA.

Whiteoak, D. and BROWN, S. F. 1990. The shell bitumen handbook, Shell Bitumen UK.

Witczak, M.W., Mamlouk, M. and Abojaradeh, M., 2001. Flexural Fatigue Tests, NCHRP 9-19, Subtask F6 Evaluation Tests, Task F Advanced Mixture Characterisation. Interim Report, Arizona State University, Tempe, Arizona.

Woo, W.J., Chowdhury, A. and Glover, C.J., 2008. Field Aging of Unmodified Asphalt 1 Binder in Three Long-Term Performance Pavements. Transportation Research Record, 2051(1), pp.15-22.

Wu, J., 2009. *The influence of mineral aggregates and binder volumetrics on bitumen ageing* (Doctoral dissertation, University of Nottingham).

Wu, S., 2016. *A mechanistic-empirical model for top-down cracking in asphalt pavement overlay* (Doctoral dissertation, Washington State University).

Xiao, F., Amirkhanian, S. and Juang, C.H., 2007. Rutting resistance of rubberized asphalt concrete pavements containing reclaimed asphalt pavement mixtures. *Journal of Materials in Civil Engineering*, 19(6), pp.475-483.

Yamamoto, M., 2013. Research and Development of Fatigue Issues for Railway Steel Products and Future Prospects. *Environment*, 199(28.6), pp.8-8.

Yang, S.H., Keita, A. and Wang, H., 2014. Comparison of Field Aging Characteristics of Warm Mix Asphalt (No.14-3293). Transportation Research Board 93rd Annual Meeting.

Yu, J.M. and Zou, G.L., 2013. Asphalt pavement fatigue cracking prediction model with mode factor. International *Journal of Pavement Research and Technology*, 6(2), pp.123-129.

Yut, I. and Zofka, A., 2014. Correlation between rheology and chemical composition of aged polymer-modified asphalts. Construction and Building Materials, 62, pp.109-117.

Zaumanis, M., Poulikakos, L.D. and Partl, M.N., 2017. Performance-based design of asphalt mixtures and review of key parameters. *Materials and Design*, 141, pp.185–201.

Zeiada, W. A., 2012. *Endurance limit for HMA based on healing phenomenon using viscoelastic continuum damage analysis*. Ph.D. dissertation, Arizona State University.

Zeiada, W.A., Gudipudi, P.P., Underwood, B.S. and Souliman, M.I., 2018. Effect of Loading Waveform Pattern and Rest Period on Fatigue Life of Asphalt Concrete Using Viscoelastic Continuum Damage Model. *Transportation Research Record*, Paper Number: 18-03274. In print.

Zhang, J., Sabouri, M., Guddati, M.N. and Kim, Y.R., 2013. Development of a failure criterion for asphalt mixtures under fatigue loading. Road Materials and Pavement Design, 14(sup2), pp.1-15.

Zhao, W., 2011. *The effects of fundamental mixture parameters on hot-mix asphalt performance properties*. PhD Dissertation, Clemson University, South Carolina. USA.

http://www.pavementinteractive.org/wp-content/uploads/2011/07/Fatigue cracking.jpg. [Online] Available at: https://www.pavementinteractive.org/. Accessed 12 March 2015.

http://www.pavementinteractive.org/wp-content/uploads/2007/08/Alligator-to-pothole.jpg. [Online] Available at: https://www.pavementinteractive.org/. Accessed 12 March 2015.

http://www.pavementinteractive.org/wp-content/uploads/2011/07/Endurance_limit.jpg. [Online] Available at: https://www.pavementinteractive.org/. Accessed 10 February 2015.

https://www.eng.auburn.edu/research/centers/ncat/files/technicalreports/re 15-05.pdf.[Online] Available at: http://eng.auburn.edu/research/centers/ncat/. Accesses 12 November 2015.

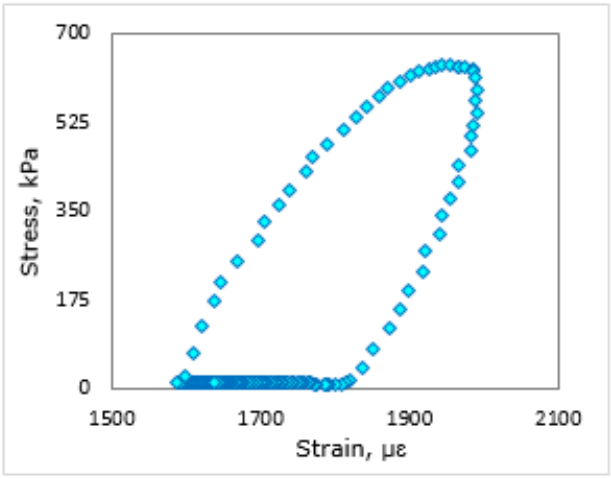
https://www.pavementinteractive.org/reference-desk/materials/aggregate/. [Online] Available at: https://www.pavementinteractive.org/. [Accessed 23 September 2017].

# Appendix

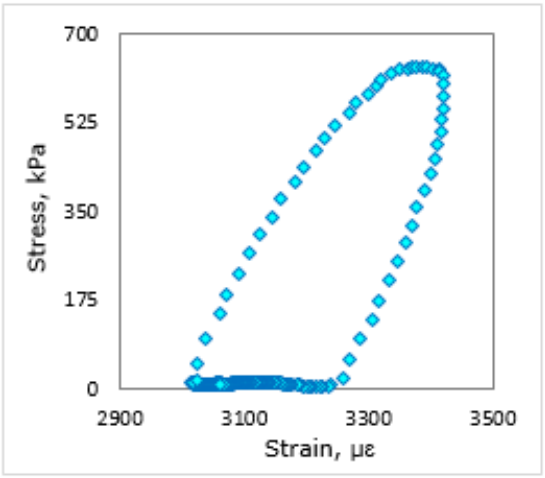
## A-1: Sample of hysteresis loops progress of ITFT.

The hysteresis loop progress was plotted for the ITFT conducted at 400 με and 20˚C of asphalt mixture specimen manufactured using 40/60 Pen. The hysteresis loop index (HLI) was calculated as following:

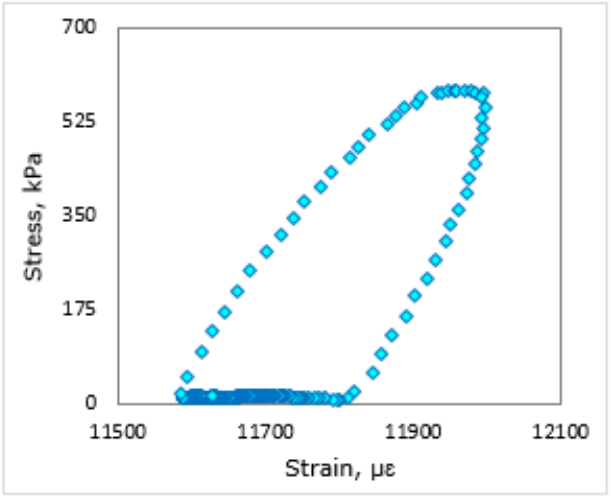
$$HLI = \frac{area\ of\ the\ loop\ at\ \ cycle\ i}{area\ of\ the\ loop\ at\ \ cycle\ 50^{th}} \times 100$$



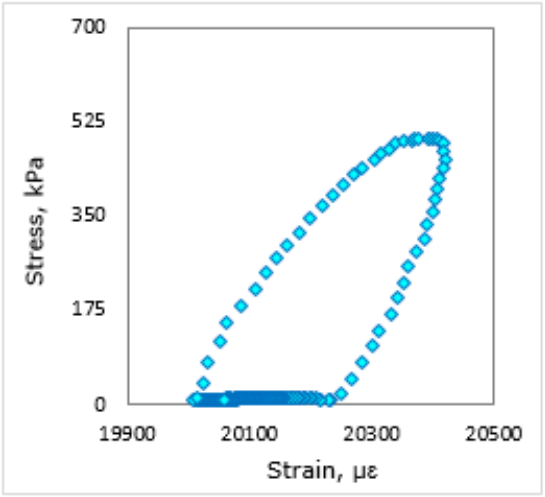

At cycle 50th, HLI=100%




At cycle 100th, HLI=100%

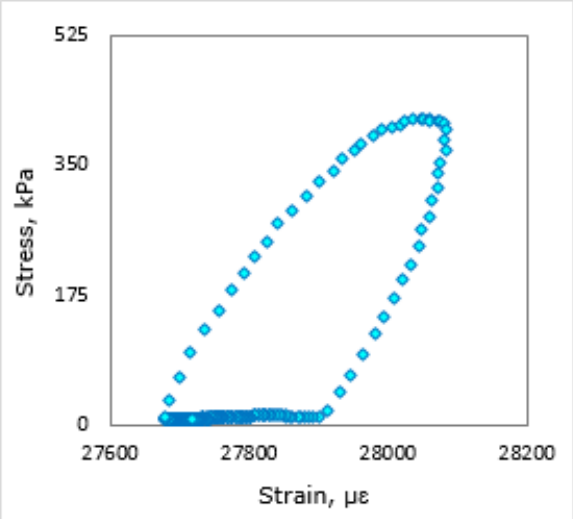



At cycle 500th, HLI=96.3%

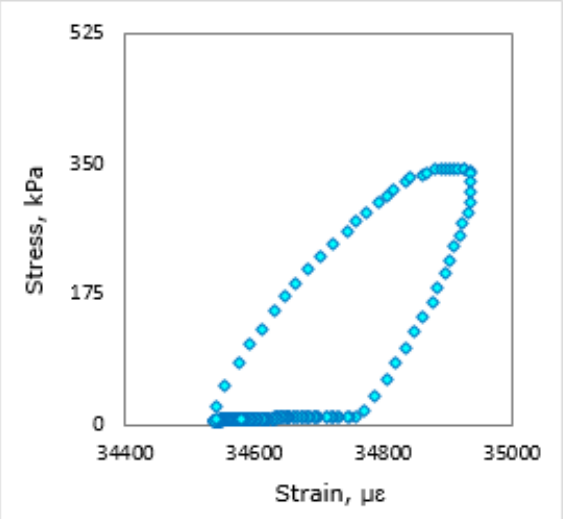



At cycle 1000th, HLI=77.8%

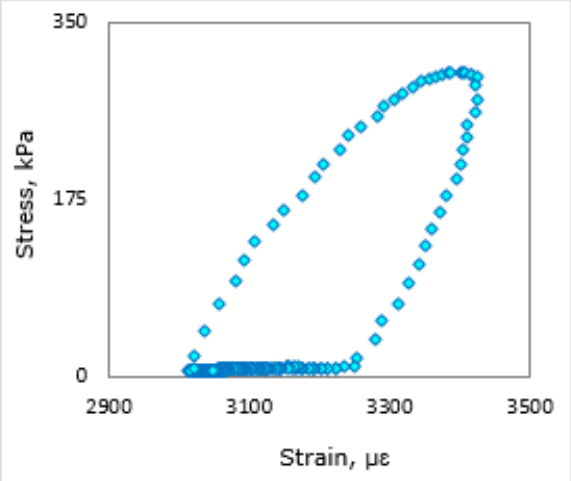
.....continue



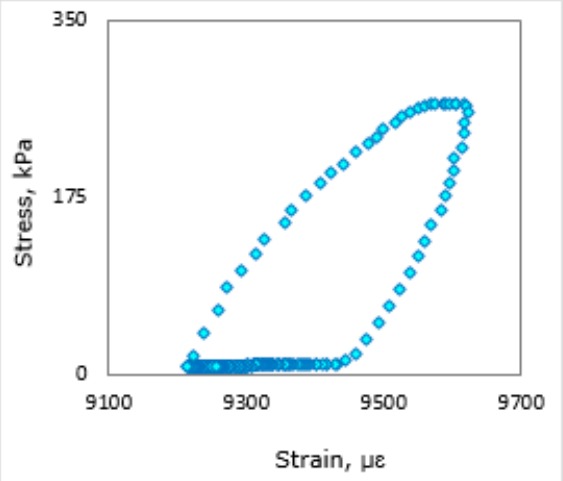

At cycle 1500th, HLI=67.4%



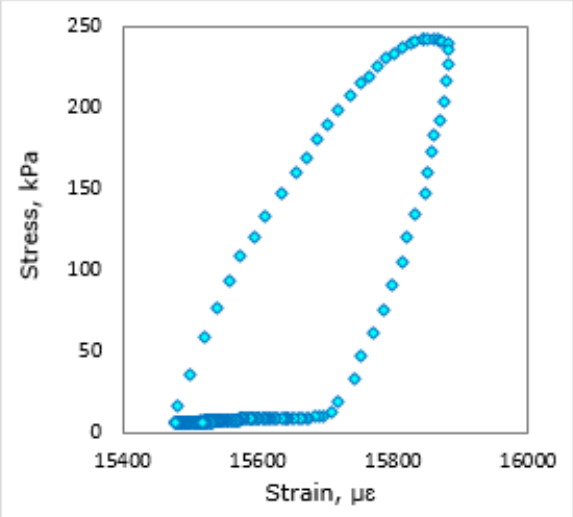

At cycle 2000th, HLI=55.8%



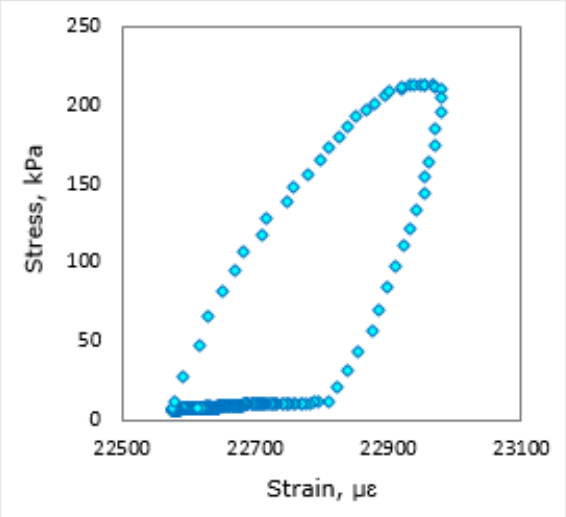

At cycle 2500th, HLI=52.3%




At cycle 3000th, HLI=45.3%

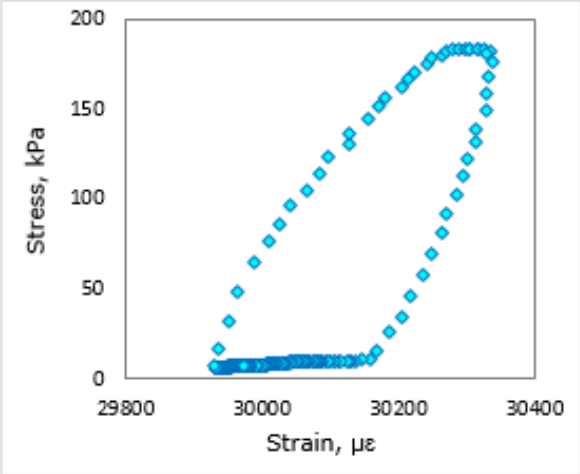



At cycle 3500th, HLI=41.7%

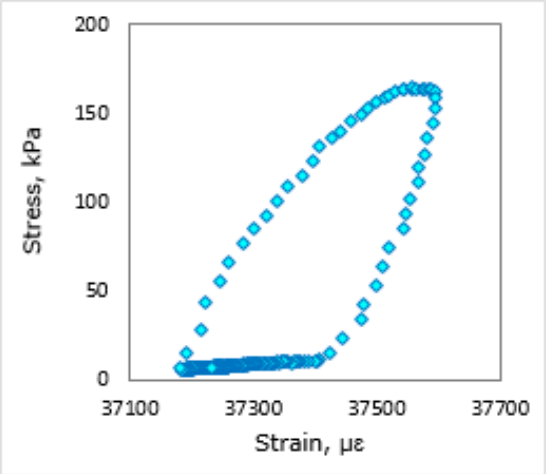



At cycle 4000th, HLI=36.5%

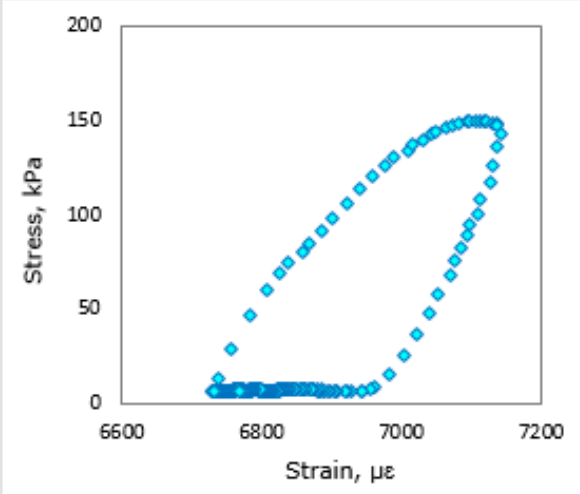
.....continue



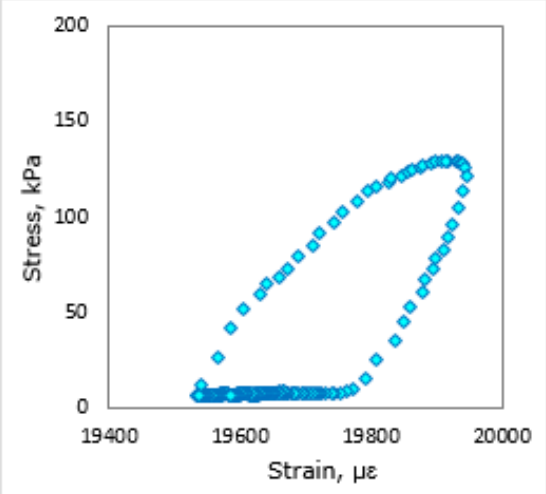

At cycle 4500th, HLI=31.8%



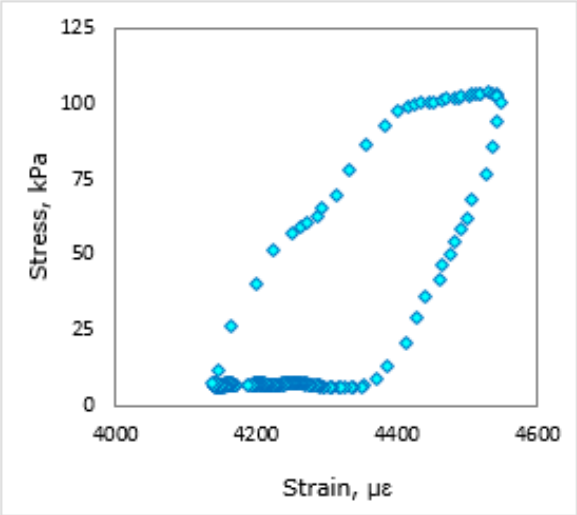

At cycle 5000th, HLI=30.1%



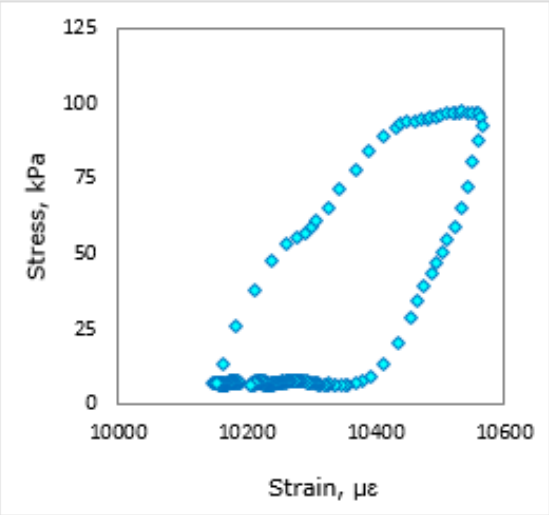

At cycle 5500th, HLI=27.1%




At cycle 6000th, HLI=23.6%




At cycle 6500th, HLI=20.2%




At cycle 6650th, HLI=18.6%

## A-2: Calculations of Chi-Square Goodness-of-Fit Test.

| Observed (O) Log scale | Expected E Log scale | Residual = O-E | (O-E)^2 | (O-E)^2/E |
|---|---|---|---|---|
| 5.345 | 5.419 | -0.073 | 0.005 | 0.001 |
| 4.779 | 5.100 | -0.320 | 0.103 | 0.020 |
| 4.647 | 4.769 | -0.123 | 0.015 | 0.003 |
| 4.332 | 4.595 | -0.262 | 0.069 | 0.015 |
| 4.067 | 4.322 | -0.255 | 0.065 | 0.015 |
| 3.784 | 3.951 | -0.167 | 0.028 | 0.007 |
| 3.398 | 3.729 | -0.331 | 0.109 | 0.029 |
| 5.195 | 5.401 | -0.206 | 0.042 | 0.008 |
| 5.100 | 4.950 | 0.150 | 0.022 | 0.005 |
| 4.429 | 4.779 | -0.350 | 0.122 | 0.026 |
| 4.352 | 4.560 | -0.208 | 0.043 | 0.009 |
| 4.241 | 4.262 | -0.021 | 0.000 | 0.000 |
| 3.717 | 4.009 | -0.292 | 0.085 | 0.021 |
| 3.275 | 3.518 | -0.243 | 0.059 | 0.017 |
| 5.015 | 4.811 | 0.204 | 0.042 | 0.009 |
| 4.295 | 4.474 | -0.179 | 0.032 | 0.007 |
| 3.837 | 4.230 | -0.393 | 0.154 | 0.036 |
| 3.349 | 3.482 | -0.133 | 0.018 | 0.005 |
| 4.911 | 5.369 | -0.458 | 0.210 | 0.039 |
| 4.736 | 5.051 | -0.314 | 0.099 | 0.020 |
| 4.217 | 4.522 | -0.306 | 0.093 | 0.021 |
| 3.613 | 3.950 | -0.338 | 0.114 | 0.029 |
| 3.312 | 3.563 | -0.251 | 0.063 | 0.018 |
| 5.752 | 5.508 | 0.244 | 0.060 | 0.011 |
| 5.275 | 5.155 | 0.120 | 0.014 | 0.003 |
| 4.944 | 4.834 | 0.111 | 0.012 | 0.003 |
| 4.775 | 4.645 | 0.129 | 0.017 | 0.004 |
| 4.444 | 4.318 | 0.126 | 0.016 | 0.004 |
| 3.987 | 4.021 | -0.034 | 0.001 | 0.000 |

| | | | | |
|---|---|---|---|---|
| 3.451 | 3.614 | -0.163 | 0.027 | 0.007 |
| 5.352 | 5.436 | -0.084 | 0.007 | 0.001 |
| 5.102 | 5.031 | 0.071 | 0.005 | 0.001 |
| 4.633 | 4.508 | 0.125 | 0.016 | 0.003 |
| 3.929 | 3.923 | 0.006 | 0.000 | 0.000 |
| 3.301 | 3.583 | -0.282 | 0.080 | 0.022 |
| 4.744 | 5.055 | -0.310 | 0.096 | 0.019 |
| 4.549 | 4.685 | -0.137 | 0.019 | 0.004 |
| 4.379 | 4.399 | -0.020 | 0.000 | 0.000 |
| 4.296 | 4.250 | 0.047 | 0.002 | 0.001 |
| 3.868 | 3.998 | -0.131 | 0.017 | 0.004 |
| 3.699 | 3.638 | 0.061 | 0.004 | 0.001 |
| 3.357 | 3.361 | -0.005 | 0.000 | 0.000 |
| 4.683 | 5.030 | -0.347 | 0.120 | 0.024 |
| 4.399 | 4.634 | -0.235 | 0.055 | 0.012 |
| 4.114 | 4.179 | -0.066 | 0.004 | 0.001 |
| 3.891 | 3.912 | -0.021 | 0.000 | 0.000 |
| 3.698 | 3.616 | 0.082 | 0.007 | 0.002 |
| 3.229 | 3.354 | -0.125 | 0.016 | 0.005 |
| 4.752 | 5.059 | -0.307 | 0.094 | 0.019 |
| 4.574 | 4.594 | -0.020 | 0.000 | 0.000 |
| 4.041 | 4.234 | -0.193 | 0.037 | 0.009 |
| 3.875 | 3.551 | 0.324 | 0.105 | 0.030 |
| 3.398 | 3.317 | 0.081 | 0.007 | 0.002 |
| 4.477 | 5.095 | -0.618 | 0.382 | 0.075 |
| 4.203 | 4.710 | -0.508 | 0.258 | 0.055 |
| 3.892 | 4.280 | -0.388 | 0.150 | 0.035 |
| 3.639 | 3.687 | -0.048 | 0.002 | 0.001 |
| 3.125 | 3.391 | -0.266 | 0.071 | 0.021 |
| 4.820 | 5.067 | -0.247 | 0.061 | 0.012 |
| 4.628 | 4.686 | -0.058 | 0.003 | 0.001 |
| 4.322 | 4.250 | 0.072 | 0.005 | 0.001 |
| 3.813 | 3.662 | 0.150 | 0.023 | 0.006 |

| | | | | |
|---|---|---|---|---|
| 3.447 | 3.358 | 0.089 | 0.008 | 0.002 |
| 4.771 | 4.965 | -0.194 | 0.038 | 0.008 |
| 4.492 | 4.648 | -0.156 | 0.024 | 0.005 |
| 4.146 | 4.255 | -0.109 | 0.012 | 0.003 |
| 3.713 | 3.665 | 0.048 | 0.002 | 0.001 |
| 3.176 | 3.376 | -0.200 | 0.040 | 0.012 |
| 5.177 | 5.260 | -0.083 | 0.007 | 0.001 |
| 4.973 | 4.841 | 0.132 | 0.017 | 0.004 |
| 4.670 | 4.446 | 0.225 | 0.050 | 0.011 |
| 4.330 | 4.421 | -0.091 | 0.008 | 0.002 |
| 4.128 | 4.214 | -0.086 | 0.007 | 0.002 |
| 3.631 | 3.850 | -0.219 | 0.048 | 0.012 |
| 3.282 | 3.430 | -0.148 | 0.022 | 0.006 |
| 5.276 | 5.064 | 0.212 | 0.045 | 0.009 |
| 4.982 | 4.732 | 0.250 | 0.063 | 0.013 |
| 4.606 | 4.534 | 0.072 | 0.005 | 0.001 |
| 4.422 | 4.297 | 0.125 | 0.016 | 0.004 |
| 3.953 | 4.108 | -0.155 | 0.024 | 0.006 |
| 3.721 | 3.792 | -0.071 | 0.005 | 0.001 |
| 3.268 | 3.451 | -0.183 | 0.034 | 0.010 |
| 4.872 | 5.069 | -0.196 | 0.039 | 0.008 |
| 4.519 | 4.694 | -0.175 | 0.031 | 0.007 |
| 4.431 | 4.308 | 0.124 | 0.015 | 0.004 |
| 3.875 | 3.498 | 0.377 | 0.142 | 0.041 |
| 3.477 | 3.166 | 0.311 | 0.097 | 0.031 |
| 4.789 | 5.052 | -0.263 | 0.069 | 0.014 |
| 4.628 | 4.714 | -0.086 | 0.007 | 0.002 |
| 4.462 | 4.313 | 0.149 | 0.022 | 0.005 |
| 3.639 | 3.669 | -0.030 | 0.001 | 0.000 |
| 3.125 | 3.388 | -0.263 | 0.069 | 0.020 |
| 4.957 | 5.194 | -0.237 | 0.056 | 0.011 |
| 4.663 | 4.798 | -0.135 | 0.018 | 0.004 |
| 4.243 | 4.367 | -0.124 | 0.015 | 0.004 |

| | | | | |
|---|---|---|---|---|
| 3.699 | 3.628 | 0.071 | 0.005 | 0.001 |
| 3.398 | 3.431 | -0.034 | 0.001 | 0.000 |
| 4.613 | 4.978 | -0.365 | 0.133 | 0.027 |
| 4.525 | 4.693 | -0.168 | 0.028 | 0.006 |
| 4.279 | 4.279 | -0.001 | 0.000 | 0.000 |
| 3.778 | 3.723 | 0.055 | 0.003 | 0.001 |
| 3.398 | 3.362 | 0.036 | 0.001 | 0.000 |
| 6.103 | 5.388 | 0.715 | 0.511 | 0.095 |
| 5.605 | 5.028 | 0.577 | 0.333 | 0.066 |
| 4.868 | 4.593 | 0.275 | 0.076 | 0.016 |
| 3.902 | 4.019 | -0.117 | 0.014 | 0.003 |
| 3.489 | 3.617 | -0.128 | 0.016 | 0.005 |
| 6.133 | 5.302 | 0.832 | 0.691 | 0.130 |
| 5.397 | 4.977 | 0.420 | 0.176 | 0.035 |
| 4.716 | 4.538 | 0.178 | 0.032 | 0.007 |
| 3.929 | 3.906 | 0.024 | 0.001 | 0.000 |
| 3.602 | 3.523 | 0.079 | 0.006 | 0.002 |
| 5.710 | 5.429 | 0.280 | 0.079 | 0.014 |
| 5.450 | 5.011 | 0.439 | 0.193 | 0.038 |
| 4.836 | 4.595 | 0.241 | 0.058 | 0.013 |
| 3.954 | 4.028 | -0.074 | 0.005 | 0.001 |
| 3.602 | 3.595 | 0.007 | 0.000 | 0.000 |
| 5.701 | 5.476 | 0.225 | 0.051 | 0.009 |
| 5.456 | 5.043 | 0.413 | 0.171 | 0.034 |
| 4.591 | 4.572 | 0.019 | 0.000 | 0.000 |
| 3.845 | 3.995 | -0.150 | 0.022 | 0.006 |
| 3.477 | 3.595 | -0.118 | 0.014 | 0.004 |
| 5.517 | 5.466 | 0.050 | 0.003 | 0.000 |
| 4.820 | 5.078 | -0.258 | 0.067 | 0.013 |
| 4.623 | 4.547 | 0.076 | 0.006 | 0.001 |
| 3.447 | 3.621 | -0.174 | 0.030 | 0.008 |
| 5.368 | 5.388 | -0.020 | 0.000 | 0.000 |
| 4.826 | 5.023 | -0.197 | 0.039 | 0.008 |

| | | | | |
|---|---|---|---|---|
| 4.607 | 4.473 | 0.134 | 0.018 | 0.004 |
| 3.477 | 3.570 | -0.093 | 0.009 | 0.002 |
| 5.911 | 5.463 | 0.448 | 0.200 | 0.037 |
| 5.491 | 5.094 | 0.397 | 0.158 | 0.031 |
| 4.823 | 4.616 | 0.207 | 0.043 | 0.009 |
| 4.041 | 4.000 | 0.041 | 0.002 | 0.000 |
| 3.301 | 3.583 | -0.282 | 0.079 | 0.022 |
| 5.701 | 5.465 | 0.236 | 0.056 | 0.010 |
| 5.332 | 5.027 | 0.305 | 0.093 | 0.019 |
| 4.667 | 4.586 | 0.081 | 0.007 | 0.001 |
| 3.602 | 3.998 | -0.396 | 0.156 | 0.039 |
| 3.301 | 3.538 | -0.237 | 0.056 | 0.016 |
| 5.681 | 5.515 | 0.166 | 0.028 | 0.005 |
| 5.334 | 5.086 | 0.249 | 0.062 | 0.012 |
| 4.531 | 4.584 | -0.053 | 0.003 | 0.001 |
| 3.602 | 3.981 | -0.379 | 0.143 | 0.036 |
| 3.079 | 3.607 | -0.528 | 0.279 | 0.077 |
| 5.429 | 5.402 | 0.027 | 0.001 | 0.000 |
| 4.857 | 5.056 | -0.198 | 0.039 | 0.008 |
| 4.597 | 4.548 | 0.048 | 0.002 | 0.001 |
| 3.477 | 3.967 | -0.490 | 0.240 | 0.061 |
| 3.000 | 3.545 | -0.545 | 0.297 | 0.084 |
| 5.902 | 5.568 | 0.334 | 0.111 | 0.020 |
| 5.642 | 4.925 | 0.717 | 0.514 | 0.104 |
| 4.908 | 4.618 | 0.291 | 0.084 | 0.018 |
| 4.021 | 3.953 | 0.069 | 0.005 | 0.001 |
| 3.740 | 3.620 | 0.120 | 0.014 | 0.004 |
| 5.697 | 5.524 | 0.173 | 0.030 | 0.005 |
| 5.483 | 5.048 | 0.435 | 0.189 | 0.037 |
| 4.860 | 4.433 | 0.428 | 0.183 | 0.041 |
| 3.398 | 3.564 | -0.166 | 0.028 | 0.008 |
| 4.470 | 4.576 | -0.106 | 0.011 | 0.002 |
| 4.279 | 4.438 | -0.159 | 0.025 | 0.006 |

| | | | | |
|---|---|---|---|---|
| 3.926 | 3.993 | -0.068 | 0.005 | 0.001 |
| 3.597 | 3.417 | 0.180 | 0.032 | 0.009 |
| 3.230 | 3.135 | 0.096 | 0.009 | 0.003 |
| 4.301 | 4.614 | -0.313 | 0.098 | 0.021 |
| 4.097 | 4.239 | -0.142 | 0.020 | 0.005 |
| 3.813 | 3.876 | -0.063 | 0.004 | 0.001 |
| 3.342 | 3.432 | -0.090 | 0.008 | 0.002 |
| 3.230 | 3.097 | 0.133 | 0.018 | 0.006 |
| 4.337 | 4.541 | -0.204 | 0.042 | 0.009 |
| 4.217 | 4.305 | -0.088 | 0.008 | 0.002 |
| 3.978 | 3.922 | 0.056 | 0.003 | 0.001 |
| 3.516 | 3.411 | 0.105 | 0.011 | 0.003 |
| 3.197 | 3.110 | 0.086 | 0.007 | 0.002 |
| 4.322 | 4.722 | -0.400 | 0.160 | 0.034 |
| 4.088 | 4.153 | -0.065 | 0.004 | 0.001 |
| 3.964 | 3.964 | 0.000 | 0.000 | 0.000 |
| 3.597 | 3.435 | 0.161 | 0.026 | 0.008 |
| 3.301 | 3.111 | 0.190 | 0.036 | 0.012 |
| 4.579 | 4.596 | -0.017 | 0.000 | 0.000 |
| 4.358 | 4.232 | 0.126 | 0.016 | 0.004 |
| 4.190 | 3.887 | 0.304 | 0.092 | 0.024 |
| 3.748 | 3.351 | 0.397 | 0.158 | 0.047 |
| 3.461 | 3.030 | 0.432 | 0.186 | 0.062 |
| 4.313 | 4.537 | -0.224 | 0.050 | 0.011 |
| 4.165 | 4.305 | -0.140 | 0.020 | 0.005 |
| 4.086 | 3.820 | 0.266 | 0.071 | 0.018 |
| 3.562 | 3.315 | 0.247 | 0.061 | 0.018 |
| 3.266 | 3.069 | 0.197 | 0.039 | 0.013 |
| 4.704 | 4.882 | -0.178 | 0.032 | 0.006 |
| 4.353 | 4.559 | -0.206 | 0.042 | 0.009 |
| 4.174 | 3.976 | 0.198 | 0.039 | 0.010 |
| 3.643 | 3.457 | 0.186 | 0.035 | 0.010 |
| 3.255 | 3.209 | 0.046 | 0.002 | 0.001 |

| | | | | |
|---|---|---|---|---|
| 4.585 | 4.781 | -0.196 | 0.038 | 0.008 |
| 4.352 | 4.509 | -0.157 | 0.025 | 0.005 |
| 4.021 | 4.004 | 0.017 | 0.000 | 0.000 |
| 3.544 | 3.545 | -0.001 | 0.000 | 0.000 |
| 3.301 | 3.177 | 0.124 | 0.015 | 0.005 |
| 4.653 | 4.726 | -0.073 | 0.005 | 0.001 |
| 4.301 | 4.493 | -0.192 | 0.037 | 0.008 |
| 3.966 | 4.161 | -0.195 | 0.038 | 0.009 |
| 3.676 | 3.485 | 0.191 | 0.036 | 0.010 |
| 3.398 | 3.148 | 0.250 | 0.063 | 0.020 |
| 4.431 | 4.798 | -0.367 | 0.135 | 0.028 |
| 4.342 | 4.453 | -0.110 | 0.012 | 0.003 |
| 3.845 | 4.145 | -0.300 | 0.090 | 0.022 |
| 3.477 | 3.559 | -0.081 | 0.007 | 0.002 |
| 3.362 | 3.146 | 0.216 | 0.047 | 0.015 |
| 5.169 | 4.808 | 0.361 | 0.130 | 0.027 |
| 4.708 | 4.567 | 0.140 | 0.020 | 0.004 |
| 4.119 | 4.178 | -0.059 | 0.003 | 0.001 |
| 3.301 | 3.272 | 0.029 | 0.001 | 0.000 |
| 4.832 | 4.797 | 0.035 | 0.001 | 0.000 |
| 4.667 | 4.494 | 0.174 | 0.030 | 0.007 |
| 4.204 | 4.139 | 0.065 | 0.004 | 0.001 |
| 3.256 | 3.229 | 0.027 | 0.001 | 0.000 |
| 4.746 | 4.511 | 0.235 | 0.055 | 0.012 |
| 4.519 | 4.231 | 0.287 | 0.082 | 0.019 |
| 3.697 | 3.712 | -0.015 | 0.000 | 0.000 |
| 3.477 | 3.347 | 0.130 | 0.017 | 0.005 |
| 4.591 | 4.496 | 0.095 | 0.009 | 0.002 |
| 4.217 | 4.128 | 0.089 | 0.008 | 0.002 |
| 3.740 | 3.596 | 0.144 | 0.021 | 0.006 |
| 3.301 | 3.219 | 0.082 | 0.007 | 0.002 |
| 4.845 | 5.069 | -0.224 | 0.050 | 0.010 |
| 4.653 | 4.600 | 0.053 | 0.003 | 0.001 |

| | | | | |
|---|---|---|---|---|
| 4.114 | 4.154 | -0.040 | 0.002 | 0.000 |
| 3.602 | 3.685 | -0.083 | 0.007 | 0.002 |
| 3.351 | 3.243 | 0.108 | 0.012 | 0.004 |
| 4.571 | 4.861 | -0.291 | 0.084 | 0.017 |
| 4.430 | 4.586 | -0.156 | 0.024 | 0.005 |
| 3.993 | 4.154 | -0.162 | 0.026 | 0.006 |
| 3.602 | 3.599 | 0.003 | 0.000 | 0.000 |
| 3.327 | 3.281 | 0.045 | 0.002 | 0.001 |
| 5.157 | 5.139 | 0.018 | 0.000 | 0.000 |
| 4.760 | 4.765 | -0.006 | 0.000 | 0.000 |
| 4.512 | 4.322 | 0.190 | 0.036 | 0.008 |
| 3.892 | 3.705 | 0.187 | 0.035 | 0.009 |
| 3.623 | 3.257 | 0.366 | 0.134 | 0.041 |
| 4.947 | 4.996 | -0.049 | 0.002 | 0.000 |
| 4.698 | 4.655 | 0.043 | 0.002 | 0.000 |
| 4.447 | 4.166 | 0.281 | 0.079 | 0.019 |
| 3.845 | 3.673 | 0.172 | 0.030 | 0.008 |
| 3.477 | 3.295 | 0.182 | 0.033 | 0.010 |
| 5.083 | 4.997 | 0.085 | 0.007 | 0.001 |
| 4.638 | 4.682 | -0.044 | 0.002 | 0.000 |
| 4.352 | 4.160 | 0.193 | 0.037 | 0.009 |
| 3.954 | 3.589 | 0.365 | 0.133 | 0.037 |
| 3.663 | 3.239 | 0.424 | 0.179 | 0.055 |
| 4.914 | 5.035 | -0.121 | 0.015 | 0.003 |
| 4.760 | 4.589 | 0.171 | 0.029 | 0.006 |
| 4.380 | 4.243 | 0.137 | 0.019 | 0.004 |
| 3.954 | 3.600 | 0.355 | 0.126 | 0.035 |
| 3.505 | 3.323 | 0.182 | 0.033 | 0.010 |
| | | | **SUM** | **3.176** |

## A-3: Testing profile for |E*| test using the 4-PB machine.

17-1465 - unaged - dry - Complex Modulus - 20C - Notepad

File Edit Format View Help

```
Cooper Research Technology Ltd - www.cooper.co.uk
Date:23/04/2017

Version V4-2-0

Test Standard:EN 12697-26
**********************************************
Specimen Reference: 17-1465
Total Length: 380.80mm
Width: 50.90mm
Height: 59.70mm
Mbeam: 2584.8g
Mass Of Moving Parts: 16798.0g
Additional Mass Of Moving Parts : 0.0g
Beam Size: Medium Beam
Effective Length: 420.00mm
Mid-Span Length: 140.00mm
**********************************************
Test Method:Constant Strain
Test Temperature:20.0°C
**********************************************
Operator:       Ahmed
Comments:

**********************************************
List of Test Stages:
Stage:  Freq:   Strain: # of Cycles:    Time:
1       1.000   50.000     100         100.000
2       2.000   50.000     100         50.000
3       5.000   50.000     100         20.000
4       8.000   50.000     100         12.500
5       10.000  50.000     100         10.000
6       15.000  50.000     100         6.667
7       20.000  50.000     100         5.000
8       25.000  50.000     100         4.000
9       30.000  50.000     100         3.333
10      40.000  50.000     100         2.500
11      50.000  50.000     100         2.000
12      60.000  50.000     100         1.667

**********************************************
```

## A-4: Testing profile for healing test using the 4-PB machine.

16-4172- un aged - dry - 10C - 6000L-6000R - Notepad

File Edit Format View Help

```
Cooper Research Technology Ltd - www.cooper.co.uk
Date:31/10/2016

Version V4-2-0

Test Standard:EN 12697-26
**********************************************
Specimen Reference: 16-4172- un aged - dry - 10C -  6000L-6000R
Total Length: 379.60mm
Width: 51.50mm
Height: 59.20mm
Mbeam: 2577.5g
Mass Of Moving Parts: 16798.0g
Additional Mass Of Moving Parts : 0.0g
Beam Size: Medium Beam
Effective Length: 420.00mm
Mid-Span Length: 140.00mm
**********************************************
Test Method:Constant Strain
Test Temperature:10.0°C
**********************************************
Operator:       Ahmed
Comments:

**********************************************
List of Test Stages:
Stage:  Freq:   Strain: # of Cycles:    Time:
1       10.000  200.000 6000    600.000
2       10.000  0.000   6000    600.000
3       10.000  200.000 6000    600.000
4       10.000  0.000   6000    600.000
5       10.000  200.000 6000    600.000
6       10.000  0.000   6000    600.000
7       10.000  200.000 6000    600.000
8       10.000  0.000   6000    600.000
9       10.000  200.000 6000    600.000
10      10.000  0.000   6000    600.000
11      10.000  200.000 6000    600.000
12      10.000  0.000   6000    600.000
13      10.000  200.000 6000    600.000
14      10.000  0.000   6000    600.000
15      10.000  200.000 6000    600.000
16      10.000  0.000   6000    600.000
17      10.000  200.000 6000    600.000
18      10.000  0.000   6000    600.000
19      10.000  200.000 6000    600.000

**********************************************
```